UNIVERSITY OF BELGRADE

FACULTY OF MECHANICAL ENGINEERING

Dušan M. Todorović

EFFECT OF BIOMASS CHARACTERISTICS AND COMBUSTION PROCESS ON FLUE GASEOUS COMPOSITION AND ASH RELATED PROPERTIES

Doctoral Dissertation

Belgrade, 2015

УНИВЕРЗИТЕТ У БЕОГРАДУ

МАШИНСКИ ФАКУЛТЕТ

Душан М. Тодоровић

УТИЦАЈ ОДАБРАНИХ ВРСТА БИОМАСЕ И ПРОЦЕСА САГОРЕВАЊА НА САСТАВ И КАРАКТЕРИСТИКЕ ГАСОВИТИХ И ЧВРСТИХ ПРОДУКАТА

Докторска дисертација

Београд, 2015.

Комисија за преглед и одбрану

Ментор: проф. др Александар Јововић, редовни професор, ментор
Универзитет у Београду, Машински факултет

Чланови комисије: проф. др Мирослав Станојевић, редовни професор,
Универзитет у Београду, Машински факултет

проф. др Драгослава Стојиљковић, редовни професор,
Универзитет у Београду, Машински факултет

проф. др Дејан Радић, ванредни професор,
Универзитет у Београду, Машински факултет

проф. др Нико Самец, редовни професор,
Универзитет у Марибору, Машински факултет

Датум одбране:

Title:

Effect of biomass characteristics and combustion process on flue gaseous composition and ash related properties

ABSTRACT:

The growing problem of environmental protection and a decline in reserves of fossil fuels has led to increasing interest in the use of renewable energy in recent decades. Climate change, caused by anthropogenic factors in recent years are also a major driving force in the development of technologies for the utilization of renewable energy sources. Biomass today represents the largest single renewable energy source, with about 10% of total primary energy production in the world. Recent analyzes show that the production of primary energy from biomass from the current 50 EJ increase to 160 EJ by 2050, of which 100 EJ in the power generation sector.

Gases and solid products occurring as biomass combustion process, which could be to a greater or lesser extent, may have different side effects.

The reduction of harmful products of combustion can be achieved by preventing their formation (primary measures) or their removal from flue gas (secondary measures). Overall, the primary measure is a modification of the combustion process and fuel, while the application of secondary measures foreseen after the combustion process. Accordingly, so far a lot of effort was made to identify opportunities and reduction of harmful products.

The subject and the scientific contribution of the doctoral dissertation is an investigation of possible processes to reduce harmful combustion products using the primary methods during combustion of biomass, and experimentally examine the possibilities and the degree of reduction of certain harmful products of combustion of selected types of biomass (wood, demolition wood and coffee waste and selected mixtures of these) using selected primary measures.

As research within this doctoral dissertation included a very detailed analysis of the products of combustion of biomass, this thesis made a significant contribution to the research of the air staged combustion and modifications of fuel composition on the composition of the gaseous products of biomass combustion and ash characteristics.

In order to define the optimum combustion conditions, in terms of emissions of nitrogen oxides, in demolition wood experiments, it was determined that the optimum excess air ratio (λ) in air staging experiments, is in the range from 0.8 to 0.95 of primary air, and 1.6-1.9 for overall λ, which is in good agreement with the available literature data. It was also confirmed that the aforementioned λ value is adequate in terms of CO emissions, as well as air staging leads to higher emissions of CO, comparing to processes without the air staging.

For experiments with mixtures (co-combustion) of above mentioned three different types of biomass with different portions of nitrogen, and bringing the air staging conditions, it was shown that mixinging fuels and increase the share of nitrogen, leading to:

- decreasing of conversion factors fuel-N to NOx and N_2O, while a further reduction could be achieved with air staging; These could be explained by the reaction of nitrogen oxides precursor (NH_3 and HCN), which occur to a greater extent in the fuel with a higher share of nitrogen, with NO leading to higher conversion of fuel-N to N2; correlation of Fuel-N influences on conversion factors for fuel-N to NOx and N2O for staged and non-staged combustion are given in this dissertation.

- the effect that the emission of nitrogen oxides from combustion without air staging, slightly increase exponentially in the range of 0.14, wood biomass, to 1.34%, what is the share of nitrogen in fuel mixture with equal shares of wood biomass and coffee waste, while observing the further growth of the share of nitrogen in the fuel mix (1.34 to 2.80%) is practically not observable changes in emission levels, and emissions are almost constant; in the case with air staging it is a clear trend of reduction of nitrogen oxides, whereby the emission values for different portions of nitrogen in fuel mixtures are as well almost constant, except for wood biomass where emissions are several times lower, due to the extremely low proportion of nitrogen; due to the nitrogen oxide mechanism, N_2O emissions was multiple increased, but, considering the constant reduction in NOx emissions in the environment with air staging, the negative overall impact of nitrogen oxides emissions on the environment is reduced.

The potential for reduction of nitrogen oxides for each of biomass used as well as mixtures thereof is also identified, while in parallel with the potential reduction of NOx increasing potentials of N2O are provided, due to the adverse impact of air staging to this compound.

It was found that the mixing of different biomass may be an efficient method to affect the overall chemistry of specific chemical elements and therewith operational challenges such as fouling, deposition or slagging, pelletisation may enhance the chemical effects of mixing; staging, by influencing aerosols formation (staging leads to a displacement towards larger particles from less than 0.1 mm to over 0.1 mm indicating a change in release behavior and mechanisms), may be a promising way of reducing the problems associated with them, especially corrosion, since the aerosols are the most corrosive fraction of fly ash.

In the present work, the first attempts are made to determine which chemical effects of peat ash addition in demolition wood combustion are detectable on the bottom ash, fly ash and gas composition in carefully controlled combustion experiments. Special emphasis is placed on the behavior of zinc, lead, potassium, sodium, chlorine, and sulfur. The particle size distribution in the flue gas was monitored and dependencies of effects of temperature and ash peat are shown. A method was developed to estimate the composition and speciation of the salt part of fly ash samples based on SEM/EDX analysis.

An experimental attempt was made to understand the behavior of the corrosive chlorine compounds for variations in reactor temperature, combustion air distribution and kaolin addition.

It is shown that the kaolin is very effective in reducing the concentration of chlorine in the fly as well as in the bottom ashes, while the effect of temperature was not clear in terms of the chlorine content in the fly ash.

Kaolin also influenced the melting behavior of the bottom ash in that way that fusion temperature characteristics increased with increased addition of kaolin.

The results, as well as presented correlations between the parameters observed in his doctoral dissertation represent a valuable data for future research in this field. The results achieved in this work are very important for further improvement of facilities for

the thermal conversion of biomass, regardless of their capacity and use, which is a additional contribution to this study.

Key words:

air staging, wood, demolition wood, coffee waste, NOx, N_2O, aerosols, fly ash, bottom ash, deposition, corosion, peat ash, kaolin

General scientific field:	Mechanical Engineering
Particular scientific field:	Process Engineering
UDC:	662.63:662.61(043.3)
	662.613.1(043.3)

Наслов:

Утицај одабраних врста биомасе и процеса сагоревања на састав и карактеристике гасовитих и чврстих продуката

РЕЗИМЕ:

Растући проблем заштите животне средине и константно смањење резерви фосилних горива довео је до све већег интереса за коришћењем обновљивих извора енергије у претходним деценијама. Климатске промене, изазване антропогеним факторима, последњих година такође представљају велику покретачку снагу развоја технологија за искоришћење обновљивих извора енергије. Биомаса данас представља највећи појединачни обновљиви извор енергије, са око 10% од укупне примарне производње енергије у Свету. Последње анализе показују да ће производња примарне енергије из биомасе са садашњих 50 EJ порасти на 160 EJ до 2050. године, од којих 100 EJ у термоенергетском сектору.

Приликом сагоревања биомасе настају гасови и чврсти продукти, који у већој или мањој мери, могу имати различита нежељена дејства.

Редукција штетних продуката сагоревања може се остварити кроз спречавање њиховог настајања (примарне мере) или њиховог уклањања из димног гаса (секундарне мере). Генерално, примарне мере представљају модификацију процеса сагоревања и горива, док је примена секундарних мера предвиђена након самог процеса сагоревања. У складу са тиме, до сада је пуно напора уложено на идентификацију и могућности редукције појединих штетних продуката.

Предмет и научни допринос докторске дисертације представља истраживање могућих процеса смањења штетних продуката сагоревања применом примарних метода при сагоревању биомасе, односно екпериментално испитивање могућности и степена смањења одређених штетних продуката сагоревања одабраних врста биомасе (сировог не третираног дрвета, отпадног дрвета и отпадне биомасе из процеса производње кафе, као и њихових мешавина) применом изабраних примарних мера.

Како су истраживања у оквиру израде докторске дисертације обухватила веома детаљне анализе продуката сагоревања биомасе, овим радом остварио се

допринос проучавању утицаја вишестепеног довођења ваздуха за сагоревање и модификације састава горива на састав гасовитих продуката сагоревања биомасе и карактеристике пепела.

У циљу дефинисања оптималних услова сагоревања, са аспекта емисије азотних оксида, у експериментима у којима је као гориво коришћено отпадно дрво, одређено је да се оптимални коефицијент вишка ваздуха (λ) при двостепеном довођењу ваздуха, креће у опсегу 0,8-0,95 за примарни ваздух, односно 1,6-1,9 када је у питању укупна вредност λ, што се добро слаже са доступним литературним подацима. Такође је потврђено да је поменута вредност λ адекватна и са аспекта емисија CO, као и да довођење вишестепеног ваздуха за сагоревање генерално доводи до виших емисија CO, у односу на процесе без вишестепеног довођења ваздуха.

Приликом експеримената са намешавањем (косагоревањем) већ поменуте три различите врсте биомасе са различитим уделима азота, и вишестепеним довођењем ваздуха за сагоревање, показано је да намешавање горива, односно повећање удела азота у тако новоформираном гориву, доводи до:

- опадања фактора конверзије азота из горива у азотне оксиде и азот субоксид, док се додатно смањење може постићи у условима сагоревања са вишестепеним довођењем ваздуха; овакви резултати су последица реакција прекурсора азотних оксида (NH_3 и HCN), који настају у већој мери код горива са вишим уделом азота, са NO што доводи до веће конверзије азота из горива у N_2; у дисертацији су дате корелационе криве, којима је могуће утврдити вредности фактора конверзије азота у азотне оксиде и азот субоксид у функцији удела азота у биомаси;

- ефекта да емисије азотних оксида, при сагоревању без вишестепеног довођења ваздуха, благо експоненцијално расту у опсегу од 0,14, код чисте дрвне биомасе, до 1,34%, што је удео азота у мешавини са једнаким уделима чисте дрвне биомасе и отпадне биомасе из процеса производње кафе, док посматрајући даљи раст удела азота у мешавини горива (1.34 до 2,80%) практично се не могу уочити промене у вредностима емисија, односно емисије су готово константне; у случају сагоревања са вишестепеним довођењем ваздуха јасан је тренд редукције азотних оксида,

при чему су емисионе вредности за различите уделе азота у намешаном гориву и у овом случају готово константе, осим за чисту дрвну биомасу где су емисије неколико пута ниже, услед изузетно ниског удела азота; услед механизма стварања азотних оксида, уочено је вишеструко повећање емисије N_2O али је, обзиром на константно смањење емисије NOx у условима са вишестепеним довођењем ваздуха, укупни утицај на животну средину емисије азотних оксида смањен.

Утврђени су потенцијали за редукцију азотних оксида за сваку од коришћених биомаса као и за њихове мешавине, док су паралелно са потенцијалима редукције азотних оксуда дати потенцијали повећања азот субоксида, услед супротног утицаја вишестепеног довођења ваздуха за сагоревање на ово једињење.

Утврђено је да мешање различитих врста биомасе може бити ефикасан метод којим се утиче на распоред појединих хемијских елемената у оквиру једињења која улазе у састав пепела, такође се дошло до закључка да процес пелетирања биомасе додатно утиче на ову појаву.

Показано је да сагоревање биомасе при условима вишестепеног довођења ваздуха, својим утицајем на формирање аеросола, односно уоченом тенденцијом њиховог укрупњавања са испод 0,1 µm на преко 0,1 µm, може бити веома корисно у смислу редукције проблема корозије, јер упућује на промене у механизму њиховог настајања и њиховим емисијама, а треба имати на уму да су аеросоли као најситније истовремено и најкорозивније честице летећег пепела;

Радом на овој дисертацији учињен је један од првих покушаја утврђивања свеобухваног утицаја летећег пепела тресета, као адитива, на састав ложишног пепела, летећег пепела и састав димног гаса, при строго контролисаним условима сагоревања отпадног дрвета; посебан акценат је стављен на понашање цинка, олова, калијума, натријума, хлора и сумпора; приказане су и зависности, тј. утицаји температуре и пепла тресета, на гранулометријски састав летећег пепела; развијена је метода за одређивање састава летећег пепела, „сланог дела" аеросола (сулфати и хлориди калијума, натријума, цинка и олова), заснована на примени скенирајућег електронског микроскопа са енергодисперзивним детектором рендгенских зрака (SEM/EDX).

Анализиран је утицај каолина, као адитива, на једињења хлора при различитим температурама, дистрибуцији ваздуха за сагоревање; такође су приказани утицаји на гранулометријски састав летећег пепела.

Показано је да је каолин веома ефикасан у редукцији концентрације хлора како у летећем тако и у ложишном пепелу, док је утицај температуре незнатан.

Анализом експерименталних резултата установљено је да каолин има позитиван утицај на топљивост ложишног пепела, тј. да са уделом каолина расте и температура топљивости пепела.

Добијени резултати као и приказане корелације између посматраних величина у докторској дисертацији представљаће и основу за будућа истраживања у овој области. Резултати остварени у овом раду имаће практичан значај за даља унапређења постројења за термичку конверзију биомасе без обзира на њихов капацитет и употребу, што представља посебни допринос.

Кључне речи:

вишестепено довођење ваздуха за сагоревање, чиста дрвна биомаса, отпадна биомаса, биомаса из процеса производње кафе, NOx, N_2O, аеросоли, летећи пепео, ложишни пепео, зашљакивање, корозија, пепо тресета, каолин

Научна област:	Машинство
Ужа научна област:	Процесна техника
UDK број:	662.63:662.61(043.3)
	662.613.1(043.3)

CONTENTS

NOMENCLATURE

A	flow cross-section area, m^2; particle surface area, $m^2 m^{-3}$; pre-exponent factor, s^{-1}
A_r	pre-exponent factor in char burning rate, $kg\ m^{-2}\ s^{-1}$
A_v	pre-exponent factor in devolatilisation rate, s^{-1}
Bi	Biot number
Bi'	modified Biot number
C	constant; molar fractions of species
C_{fuel}	fuel concentration, $kg\ m^{-3}$
C_{pg}	specific heat capacity of the gas mixture, $J\ kg^{-1}\ K^{-1}$
C_{mix}	mixing-rate constant, 0.5
$C_{w,g}$	moisture mass fraction in the gas phase
$C_{w,s}$	moisture mass fraction at the solid surface
CW	coffee waste
D_g	molecular diffusion coefficient of volatile hydrocarbons in air, $m^2\ s^{-1}$
D_{ig}	dispersion coefficients of the species Yi, $m^2\ s^{-1}$
d_p	particle diameter, m
DW	demolition wood
E	activation energy, $J\ kmol^{-1}$
E_b	black body emission, Wm^{-2}
E_r	activation energy in char burning rate, $J\ kmol^{-1}$
E_v	activation energy in devolatilization rate, $J\ kmol^{-1}$
E^0	effective diffusion coefficient
F_2	fraction of the volume occupied by water replaced by pores during drying
F_3	fraction of the volume occupied by volatile matter replaced by pores during pyrolysis
FT	Flow temperature, $^{\circ}C$
H_{evp}	evaporation heat of the solid material, $J\ kg^{-1}$
H_g	gas enthalpy, $J\ kg^{-1}$
H_s	solid-phase enthalpy, $J\ kg^{-1}$
HT	hemisphere temperature, $^{\circ}C$

h_s	convective mass transfer coefficient between solid and gas, kg m^{-2} s^{-1}
h_s'	convective heat transfer coefficient between solid and gas, W m^{-2} K^{-1}
I_x^+	radiation flux in positive x-direction, W m^{-2}
I_x^-	radiation flux in negative x-direction, W m^{-2}
IDT	Initial deformation temperature, $^\circ$C
k	thermal conductivity of particle material, W m^{-1} K^{-1}; reaction rate constant
k_a	radiation absorption coefficient, m^{-1}
k_d	rate constants of char burning due to diffusion, kg m^{-2} s^{-1}
k_{if}	rate constant (forward), m^3 kmol^{-1} s^{-1}
k_{ir}	rate constant (backward), m^3 kmol^{-1} s^{-1}
k_r	rate constants of char burning due to chemical kinetics, kg m^{-2} s^{-1}
k_v	rate constant of devolatilization, s^{-1}
k_s	radiation scattering coefficient, m^{-1}
K	permeability
L_b	bed top height, m
M	moisture in fuel, wt%
M_b	bound water
M_f	free water
m_s	green or moist mass
m_{sd}	oven-dry mass
NS	nonstage combustion
p_g	gas pressure, Pa
Q_h	heat loss/gain of the gases, W m^{-3}
Q_{sh}	thermal source term for solid phase, W m^{-3}
q_r	radiative heat flux, W m-2
Ri	process rate (i=2,3,4), kg m^{-3} s^{-1}
R	universal gas constant, J mol^{-1} K; reaction rate
R_{mix}	mixing-rate of gaseous phase in the bed, kg m^{-3} s^{-1}
S_{sg}	conversion rate from solid to gases due to evaporation, devolatilisation and char burning, kg m^{-3} s^{-1}
Sy_{ig}	mass sources due to evaporation, devolatilisation and combustion, kg m^{-3} s^{-1}

Sy_{is}	source term, kg m^{-3} s^{-1}
ST	soften temperature, °C
t	time instant, s
T	temperature, K
V	velocity, ms^{-1}; volume of the bed, m^3
V_0	volume of the initial bed, m^3
WP	wood pellets
x	co-ordinate in bed height direction, m
Y_n	Volume fraction of individual species (C, H, O, N, S, O$_2$, Air)
Y_{ig}	mass fractions of individual species (e.g. H$_2$,H$_2$O, CO, CO$_2$, C$_m$H$_n$,.)
Y_{is}	mass fractions of particle compositions (moisture, volatile, fixed carbon and ash)
$Y_{is,0}$	mass fraction of particles components at fresh feed state;
β	temperature exponent
ε_s	system emissivity
σ_b	Stefan–Boltzmann constant, 5.86 X 10^{-8} W m^{-2} K^{-4}
υ	remaining volatile in solid at time t
υ_∞	ultimate yield of volatile
ϕ	void fraction in the bed; equivalence ratio
ρ	density, kg m^{-3}
λ_g	thermal dispersion coefficient, W m^{-1} K^{-1}
λ_g^0	effective thermal diffusion coefficient, W m^{-1} K^{-1}
λ_s	effective thermal conductivity of the solid bed, W m^{-1} K^{-1}
$\varpi_{i,k}$	volume fraction of component i in biomass k

Subscripts

env	environmental
g	gas phase
i	identifier for a component
p	particle
s	solid phase

2	moisture or moisture evaporation
3	volatile matter or devolatilization
4	fixed carbon or char gasification
A	material in its initial state
B	dried material
C	dried and pyrolysed material
D	Dried, pyrolysed and gasified material

1. INTRODUCTON

*"**Biomass** includes a wide range of products and by-products from forestry and agriculture as well as municipal and industrial waste streams. It thus includes: trees, arable crops, algae and other plants, agricultural and forest residues, effluents, sewage sludge, manure, industrial by-products and the organic fraction of municipal solid waste. After a conversion process, the biomass can be used as a fuel to provide heat, electricity or as transport fuel, depending on the conversion technology and the type of primary biomass (EC, 2005c)."*

Due to the consequences caused by anthropogenic activities and the rapid technological progress, which began during the second half of the 19th century and which is still ongoing, the use of renewable energy is no longer a potential for substitution of conventional fuel types, but commitment and cultural norm.

Humankind currently uses 410×10^{18} joules of commercially energy per annum. This is equivalent to the energy content of over 90 000 billion liters of oil [1]. World energy consumption in future will keep increasing trend. Bearing in mind these predictions of energy consumption as well as climate change (global warming) and other environmental issues, it is clear that there is a need for sustainable alternative for fossil fuels.

According the usual definition sustainable development is: *Meeting the needs of the present generation without compromising the ability of future generations to meet their own needs.*

It is well known that any activity related to the energy sector, directly or indirectly, have an impact on the environment, so it is difficult to define some of the technology as a fully sustainable. The physicist C.P. Snow said "Technology brings you great gifts with one hand, and stabs you in the back with the other." Nevertheless, the idea of sustainability is spreading and "green revolution" is slowly moving forward.

To meet the challenges of the rapidly increasing atmospheric levels of carbon dioxide (one of the six major greenhouse gases) resulting mainly from the continued burning of fossil fuels, the use of alternative cleaner energy sources will be necessary, together with energy efficiency and conservation measures. There will not be a single technical or social solution to this hugely complex environmental problem. We shall

need to utilize all possible means of mitigation at our disposal. The use of biomass in a wise, clean and sustainable manner will be one of them [2].

Many countries around the globe have developed a growing interest in the use of biomass as an energy source, and therefore various technological developments in this field are ongoing. Although major technological developments have already been achieved, most bioenergy technologies are not yet commercially feasible without political support. In order to achieve wider application of modern bioenergy technologies, individual countries have set varying targets and implemented promotional policies. As a result of increased support for bioenergy technologies, major progress has been made [3].

The potentials of biomass are determined on the basis of a number of different methodologies, which makes significantly differences in the assessment of current and future potential. Current estimates for Europe are between 40 and 55 Mtoe [4] annually, depending on the applied methodology.

In accordance with the Directive 2009/28/EC and Decision of MC of EnC D/2012/04/MC-EnC is determined an ambitious binding target for Serbia, which is 27 % for the overall share of energy from renewable sources and a 10 % for energy from renewable sources in transport by 2020.

In Serbia, biomass is traditionally used for household cooking, lighting and space-heating. Currently there is no precise, formal monitoring of the use of biomass for energy purposes in Serbia. Available data are mostly the results of scientific research projects and needs of different institutions. According the latest data from National Renewable Energy Action Plan of the Republic of Serbia (In accordance with the template foreseen in the Directive 2008/29/EC- Decision 2009/548/EC) the estimated overall technically usable potential of renewable energy sources are about 5.6 Mtoe per annum, and biomass potential is approximately 3.4 Mtoe per year (2.3 Mtoe per year is unused, and 1.1 Mtoe is used).

Increasing the use of bioenergy offers significant opportunities for reduction of greenhouse gas emissions and other environment impacts as well as security in energy supply. Although generally is known as a *green energy*, the considerable rise in the use of biomass might have substantial impact on environment. Agriculture, forestry and waste for producing energy might put additional pressure on farmland and forest

biodiversity as well as on soil and water resources. As this thesis consider issues related to the thermal conversion of biomass, more precisely combustion, future considerations in this work will focus on emissions to the atmosphere and ash related operational challenges.

Thermal conversion of biomass, including combustion, gasification, and pyrolysis, is the most common method of extracting energy from biomass. Among the three mentioned technologies, combustion, which has been used for a long time as a source of heat for residential purposes, remains the leading technology also in recent years. Life cycle analyses show that the most important environmental issue regarding emissions from wood combustion is NOx, contributing to almost 40% of the total emissions, including NOx, PM10, CO_2, SO_X, NH_3, CH_4, nonmethane volatile organic compounds (NMVOC), residues, and others. Reduction of harmful emissions is generally possible to obtain in two basic methods: primary measures (avoiding creation of such substances) and secondary measures (removing the pollutants from the flue gas). This doctoral thesis considers certain primary measures.

The thesis is wide study which has been carried out in the same reactor, investigating different operating parameters and biomass. This study is focusing on experiments in a lab-scale reactor with a good control and overview of the operational parameters (temperature, feedstock and air inputs) and the combustion products (flue gas, fly and bottom ash) in order to study the influence of the air staging, temperature, additives and mixing of chosen biomass fuels on combustion products.

The objectives of thesis are:

- investigation the effect of staged combustion and temperature on NOx and N_2O formation, as well as the effect on the emission levels of incomplete products of combustion (CO and hydrocarbons (CxHy)), using three types of biomass including coffee waste (CW), demolition wood (DW), wood pellets (WP), or combinations of these;

- the fate of selected element (with focus on the important ones in sense of corrosion i.e. Na, K, Pb, Cl and S) are investigated for three biomasses (wood, demolition wood and coffee waste) and six mixtures of these as pellets both with and without air staging in laboratory reactor. Information are collected about flue gas

composition, particle (fly ash) size distribution and composition, bottom ash composition and melting properties, Cl-conversion, S- conversion;

- in attempt to look at means for reduction of corrosion in boilers, combustion experiments are performed on demolition wood with kaolin and peat-ash as additive. A total characterization of the elemental composition of the fuel, the bottom ash and some particle size stages of fly ash was performed. This was done in order to follow the fate of some problematic compounds in demolition wood as a function of kaolin and peat-ash addition and other combustion – related parameters. A method was developed to estimate composition and speciation of the salt part of aerosols based on SEM/EDX analysis. The characteristic of bottom ash are reported as a function of increased kaolin and peat-ash addition, reactor temperature and air staging.

In order to give information and possibilities for improving the process of biomass combustion, numerous results achieved through this experimental work and results of the relevant literature, primarily papers published in leading international journals, in this thesis are presented as follows:

- Current status of biomass as a renewable energy source;
- Biomass fuel sources, properties and pre-treatment;
- Thermochemical conversation of biomass;
- Environmental Aspects of Biomass Combustion;
- Description of experimental research work;
- Analysis of the results and conclusions about the correlation between the observed parameters.

The results, as well as presented correlations between the parameters observed in his doctoral dissertation represent a valuable data for future research in this field. The results achieved in this work are very important for further improvement of facilities for the thermal conversion of biomass, regardless of their capacity and use, which is a additional contribution to this study.

All experimental studies were performed according to valid international standards and methods. In order to get a precise data and complete overview of the combustion products, both online and offline state of art analytical methods are used.

Belgrade – Trondheim – Belgrade
2009-2015.

2. BIOMASS AS A RENEWABLE ENERGY SOURCE

2.1 State of Renewable Energy

The evolution of the universe can be told as the story of the evolution of energy. Energy is transformed into matter: first subatomic particles (quarks, neutrinos), then atoms and molecules, and subsequently into more complex molecules including what we now call organic molecules (containing carbon). Certain organic molecules can be found even in space, but just because they are organic molecules does not mean that they have been formed by or within living organisms [5].

The continuous growth of global energy consumption raises urgent problems. The larger part of mineral oil and gas reserves (1/3 of the world's energy supply) is located within a small group of countries, forming a vulnerable energy supply. Moreover, this supply is expected to reach its limits. On the other side the use of fossil fuels causes numerous environmental problems, such as local air pollution and greenhouse gases (GHGs) emission [6]. The widespread use of fossil fuels within the current energy infrastructure is considered as the largest source of anthropogenic emissions of CO2, which is largely blamed for global warming and climate change [7]. Total primary energy supply from all sources in 2011 was 590 EJ, with over 80% being from fossil fuels [8]. Various organisations such as the oil companies BP and Shell, the US Energy Information Administration (EIA), the European Commission (EC), the International Energy Agency (IEA), the International Atomic EnergyAgency (IAEA), the International Institute for Applied Systems Analysis (IIASA) and the World Energy Council (WEC) have all projected values for one or more of these future dates. The lowest and highest values for projected primary energy use from each of these organisations are shown in Table 2.1. There is remarkably little spread of values either within or between the various projections up to 2050. By 2050, world energy use is forecast to rise to 800 EJ or more, and the one projection for 2100 envisages that levels as high as 1740 EJ could occur [9].

Current trends in energy supply and use are patently unsustainable – economically, environmentally and socially. Without decisive action, energy-related emissions of carbon dioxide (CO_2) will more than double by 2050 and increased oil demand will heighten concerns over the security of supplies [10].

Table 2.1 Global primary energy projections, 2020-2100 [EJ] [9]

Organisation and year	2020	2030	2050	2100
BP (2011)	565-635	600-760	NA	NA
EC (2006)	570-610	650-705	820-935	NA
EIA (2010)	600-645	675-780	NA	NA
IAEA (2009)	585-650	670-815	NA	NA
IEA (2010)	NA	605-705	NA	NA
IIASA (2007)	555-630	NA	800-1175	985-1740
Shell International (2008)	630-650	690-735	770-880	NA
WEC (2008)	615-675	700-845	845-1150	NA
Tellus Institute (2010)	504-644	489-793	425-1003	243-1200

The supply of sustainable energy is one of the main challenges that mankind will face over the coming decades, particularly because of the need to address climate change [11]. Reducing GHG emissions is an extremely complex problem, and there is no single solution [12]. Fossil fuels are responsible for an estimated 74% of all CO_2 emissions [14]. Global atmospheric levels are now at 390 ppm, and some Earth scientists have argued that this level is already too high, and should be reduced to 350 ppm (a pre-industrial value was about 280 ppm) [9,7].

Enhanced energy efficiency and increased renewable energy production will reduce CO_2 emissions, but energy efficiency and renewable energy do not have the potential to reduce global CO_2 emissions as much as the IPCC target of 50–80% reduction by 2050. However, new sources, not existing sources, will be primarily responsible for global CO_2 emissions in the 21st century, since new sources provide for growth and replace existing sources at the end of their useful lives [7].

Table 2.2 shows the technical potential for the six main form of RE. The world gets about 17–18% of its energy from renewables, including about 9% from "traditional biomass" and about 8% from "modern renewables". The "traditional" share has been relatively stable for many years, while the "modern" share has grown rapidly since the late 1990s. During the 1990s, projections of renewable energy that were considered most credible, for example by the International Energy Agency (IEA), foresaw shares of modern renewables reaching no more than 5–10% into the far future, given the policies and technologies existing at the time.

Table 2.2 Published estimates for RE global technical potential [9]

Study and year of estimate	Solar	Wind	Ocean	Hydro	Biomass	Geothermal Electricity	Heat
Hafele (1981) ('realizable' potential)	NA	95 (32)	33 (16)	95 (47)	189 (161)	3.2 (3.2)	47 (16)
Lightfoot/Green (2002) (range of values)	163 (118–206)	72 (48–72)	0 (1.8–3.6)	19 (16–19)	539 (373–772)	1.5 (1.5)	NA (NA)
Gross et al. (2003)	43–144	72–144[a]	7–14[b]	NA	29–90	NA	14–144[c]
Sims et al. (2007)	1650	600	7	62	250	NA	5000[c]
Field et al. (2008)	NA	NA	NA	NA	27	NA	NA
Resch et al. (2008)	1600	600	NA	50	250	NA	5000[c]
Klimenko et al. (2009) ('economic' potential)	2592 (19)	191 (8.6)	22 (2.2)	54 (29)	NA (NA)	22 (3.6)	NA (NA)
Cho (2010)	>1577	631	NA	50	284	NA	120
Tomabechi (2010)[d]	1600	700	11	59	200	NA	310,000[c]
WEC (2010)	NA	NA	7.6[b]	57.4	50–1500	1.1–4.4	140
All studies range	118–2592	48–600	1.8–33	50–95	27–1500	1.1–22	14–310,000
Earth energy flows	3,900,000	28,400	700	130–160	3000	1300	

NA: not available; [a]Onshore only; [b]Wave only; [c]Includes both electricity and direct heat; [d]Usable maximum'.

As a result of the market, policy, and technology developments of the past 15 years, those early projections have already been reached. Table 2.3 shows global sectoral-share projections for the years 2030 to 2050 from several scenarios. These include two conservative scenarios by oil companies, two moderate scenarios by the IEA (WEO "New Policies" and "450"), and four high-renewables scenarios by IEA ETP, GEA, Greenpeace, and WWF [13].

Table 2.3 Sectorial shares of renewable energy in recent global scenarios [13]

Scenario	By Year	Electricity	Heat	Transport
By 2030-2040				
ExxonMobil *Outlook for Energy: A View to 2040* (2012)		16%	—	—
BP *Energy Outlook 2030* (2012)	2030	25%	—	7%
IEA *World Energy Outlook* (2012) "New Policies"	2035	31%	14%	6%
IEA *World Energy Outlook* (2012) "450"	2035	48%	19%	14%
Greenpeace (2012) *Energy [R]evolution*	2030	61%	51%	17%
By 2050				
IEA *Energy Technology Perspectives* (2012) "2DS"	2050	57%	—	39%
GEA *Global Energy Assessment* (2012)	2050	62%	—	30%
IEA *Energy Technology Perspectives* (2012) "2DS High Renewables"	2050	71%	—	—
Greenpeace (2012) *Energy [R]evolution*	2050	94%	91%	72%
WWF (2011) *Ecofys Energy Scenario*	2050	100%	85%	100%

Although the RE is generally considered as "environmental friendly" and besides all proved positive characteristics it should be discussed about its known and possible negative effects on environment. Table 2.4 presents summarized environmental and social effects of RE.

Table 2.4 Environmental and social effects of RE [9]

RE Type	Environmental and social effects
Solar	Pollution from PV production; adverse effects on fragile semi-arid land ecosystems; competition for fresh water; depletion of scarce materials; albedo decreases.
Wind	Bird and bat deaths; possible habitat loss for other wildlife; noise and vibration pollution for nearby residents; adverse effects on visual amenity; possible adverse effects on marine mammals from offshore wind farms; possible climate changes for large-scale implementation.
Ocean	For OTEC, disruption to marine ecosystems from need to pump vast amounts of seawater; possible adverse effects on marine mammals from wave and current energy devices; shipping disruption.
Hydro	Loss of homes and livelihoods for those displaced; fresh-water biodiversity loss; inundation of farmland or natural forest; possible increases in micro-seismicity and slope instability; loss of heritage sites; increased downstream erosion; coastal land retreat and declining soil fertility from loss of sediment deposition; greenhouse gas emissions from submerged biomass.
Biomass	Competition with other biomass uses (especially food production) for fertile land and water; loss of existing uses for biomass wastes; biodiversity loss.
Geothermal	Land subsidence; increase in micro-seismicity; potential air and water pollution.

The environmental problems of RE operation are thus pitting local environmentalists against major environmental organisations with a more national or even global viewpoint, including awareness of the environmental costs of fossil fuels. RE sources, unlike fossil fuels, are regarded as 'clean fuels'; the public thus find it harder to accept environmental damages from these energy sources. Above all, we must realise that there is a third way; we can reduce the environmental problems of both RE and its alternatives by using less energy, either through more efficient energy-consuming devices or less use of these devices [9].

A portfolio of different policies is needed to reduce GHG emissions by promoting low-carbon technologies, energy efficiency, and conservation [12]. The energy system can be monitored in three principal areas: energy consumption, industry structure that affects both the demand and supply of energy, and energy generation. The instruments the government may use to exercise this influence are: support for research and development, support for demonstration, support for information dissemination, administrative policy instruments, and economic incentives. These instruments may be used separately or in combination [14]. The development of renewable energy - particularly energy from wind, water, solar power and biomass - is a central aim of the European Commission's energy policy. The target for renewable energy in Europe has been laid down in Directive 2009/28/EC of the European Parliament and the Council of the European Union. This Directive is internationally known as the Renewable Energy

Directive (RED). In the light of the positions taken by the European Parliament, the Council and the Commission, it is appropriate to establish mandatory national targets consistent with a 20 % share of energy from renewable sources and a 10 % share of energy from renewable sources in transport in Community energy consumption by 2020. There are several reasons for this: Renewable energy has an important role to play in reducing Carbon Dioxide (CO_2) emissions - a major Community objective. Increasing the share of renewable energy in the energy balance enhances sustainability. It also helps to improve the security of energy supply by reducing the Community's growing dependence on imported energy sources. Renewable energy sources are expected to be economically competitive with conventional energy sources in the medium to long term. Renewable energy is, by definition, local energy. Its development can create new business, bring employment and encourage economic and social cohesion in regions that otherwise lack industrial development. There is a considerable export potential for renewable energy technologies, particularly in the developing world [15, 16].

As the starting point, the renewable energy potential and the energy mix of each Member State vary, it is therefore necessary to translate the Community 20 % target into individual targets for each Member State, with due regard to a fair and adequate allocation taking account of Member States' different starting points and potentials, including the existing level of energy from renewable sources and the energy mix. in order to ensure consistency in transport fuel specifications and availability 10 % target for energy from renewable sources in transport is set at the same level for each Member State.

Annex I of Directive gives National overall targets for the share of energy from renewable sources in gross final consumption of energy in 2020. Republic of Serbia as a non-Member State has target of 27% RES by 2020, which is, beside Sweden (49%), Finland (38%), Latvia (40%), the highest one in Europa.

Another important Policy document for promotion of renewable fuels is DIRECTIVE 2003/30/EC on the promotion of the use of biofuels or other renewable fuels for transport, contributing to objectives such as meeting climate change commitments, environmentally friendly security of supply through use of renewable fuels to replace diesel or petrol for transport purposes in each Member State.

According [17] the transport sector accounts for more than 30 % of final energy consumption in the Community and is expanding, a trend which is bound to increase, along with carbon dioxide emissions and this expansion will be greater in percentage terms in the candidate countries following their accession to the EU.

The EU policies and measures to achieve the Energy 2020 goals and the Energy 2020 strategy are ambitious [18]. The EU is committed to reducing greenhouse gas emissions to 80-95% below 1990 levels by 2050 [19] in the context of necessary reductions by developed countries as a group.

Introducing a price for CO_2 is another important measure to reduce energy-related GHG emissions by promoting the more efficient use of fossil energy and supporting the use of renewable and other low-carbon energy sources. There are various ways to introduce a price on CO_2, some of which have been established under the Kyoto Protocol, such as international emission trading which has been introduced in the European Union and is envisaged for Australia from 2015. Another example is joint implementation of GHG mitigation projects between developed countries, and Clean Development Mechanism (CDM) for joint projects by developed countries in developing countries. The CDM is particularly relevant for attracting investments in bioenergy projects in developing countries: 12% of all CDM projects are related to bioenergy (UNEP, 2012). With the recent (2011) inclusion of CCS in the CDM, accounting for negative emissions is possible (as opposed to current provisions in the EU Emissions Trading Scheme), and BECCS projects could thus also be eligible. Another measure that has proved quite successful is a so-called "carbon tax", which has been introduced for instance in Sweden, Denmark, Finland, and Australia [10].

The need for Community support for renewable energy is clear. While several of the technologies, notably wind energy, small-scale hydro power and energy from biomass, are economically viable and competitive, and others are approaching viability, initial investment costs are high and investors often lack confidence in technologies that are relatively unknown. As a result, development has been limited, and the sector needs help if it is to 'take off' in marketing terms. The main reasons for the growing international interest in utilising renewable fuels are the objectives of promoting the use of renewable fuels in line with the statements in the European Commission's White Paper and of meeting emission limits and targets set by the EU directives. Emission

allowance trading may also pose new challenges to power producers in the future. It can already be stated with great confidence that power producers will have to cope with an increasing number of EU-level regulations concerning emission levels in general, and especially greenhouse gas emissions. Usually these regulatory actions aim at favouring the use of biomass [15].

2.2 Biomass potential for energy purposes

The term bioenergy refers to energy obtained from biomass, which is the biodegradable fraction of products, waste and residues from agriculture (of vegetable and animal origin), forestry and related industries, as well as the biodegradable fraction of industrial and municipal waste [20]. Biomass can make a substantial contribution to supplying future energy demand in a sustainable way. It is presently the largest global contributor of renewable energy, and has significant potential to expand in the production of heat, electricity, and fuels for transport [11]. Biomass is considered the renewable energy source with the highest potential to contribute to the energy needs of modern society for both the industrialized and developing countries worldwide [7].

As it is stated in [21] biomass appears to be an attractive feedstock for three main reasons. First, it is a renewable resource that could be sustainably developed in the future. Second, it appears to have formidably positive environmental properties, resulting in no net releases of carbon dioxide and very low sulfur content. Third, it appears to have significant economic potential provided that fossil fuel prices increase in the future.

Traditional biomass materials, including fuelwood, charcoal and animal dung, continue to be important sources of bioenergy in many parts of the world and, to date, woodfuels represent by far the most common sources of bioenergy. Modern bioenergy relies on efficient conversion technologies for applications at the household, small business and industrial scale. Solid or liquid biomass inputs can be processed to be more convenient energy carriers. These include solid biofuels (e.g. firewood, wood chips, pellets, charcoal and briquettes), gaseous biofuels (biogas, synthesis gas, hydrogen) and liquid biofuels (e.g. bioethanol, biodiesel) [20]. Generally speaking, biofuels are generally considered as offering many benefits, including sustainability, reduction of

greenhouse gas emissions, regional development, social structure and agriculture and security of supply [21].

It provides a diverse source of energy, potentially improving energy security through the substitution of oil and natural gas. The use of domestic bioenergy resources would generally contribute to the diversification of the energy mix. Biomass imports, from widely distributed international sources, also contribute to energy diversification, especially if lignocellulosic resources and bioenergy products derived from them are considered [22].

2.2.1 Global energy biomass potential

The potential supply of biomass for energy purposes is the subject of many assessments with national, regional and global focus, some of which are rather optimistic. These estimates need to be carefully evaluated, as they do not always fully consider all factors involved in mobilising the indicated biomass potential. This is particularly true for the economics of biomass production and transport, which are inevitably subject to uncertainties [10].

As mentioned above numerous estimates have been made of the possible contribution of biomass to future energy supply, especially in the next 30-50 years. Biomass energy annual usage currently represents approximately 8-15% of the world final energy consumption [23, 24, 25, 26, 27, 21, 10, 28, 13, 29]. Despite the current minor contribution of modern bioenergy to the global energy mix, biomass has, in the long run, potential to contribute much more significantly to the global energy supply. As it is presented in Table 2.5 [23] the overall sustainable worldwide biomass energy potential is about 100 EJ/yr. Various studies on global bio-energy potential use a margin spanning from a few hundred to more than 1000 EJ – depending on the assumptions they make on agriculture, yields, population, etc. Most of the biomass resource is located outside Europe and this worldwide resource is relatively unexploited, except for Asia, which uses more biomass than the actual annual regional potential (Table 2.5) [23,7].

Potential vary from region to region and are dependent on geographic location, the climate, the population density and the degree of industrialisation of the country.

Table 2.5 Biomass potential and use distribution between regions [10^3 PJ/year] [23]

Biomass potential	North America	Latin America	Asia	Africa	Europe	Middle East	Former USSR	World
Woody biomass	12.8	5.9	7.7	5.4	4.0	0.4	5.4	41.6
Energy crops	4.1	12.1	1.1	13.9	2.6	0.0	3.6	37.4
Straw	2.2	1.7	9.9	0.9	1.6	0.2	0.7	17.2
Other	0.8	1.8	2.9	1.2	0.7	0.1	0.3	7.6
Total potential	19.9	21.5	21.6	21.4	8.9	0.7	10.0	103.8
Use	3.1	2.6	23.2	8.3	2.0	0.0	0.5	39.7
Use/potential (%)	16	12	107	39	22	7	5	38

Information about the long-term primary biomass potential is essential to understand the prospective role of bioenergy in the global energy mix [22]. Predictions on the future usage of biomass are usually to 2050, and indeed some as far as to 2100. It has been concluded that the contribution from biomass could be raised to 200 EJ/year (4.8 Gtoe) by 2050, but some estimates make it five times greater (24 Gtoe). Because of the competition of land for bioenergy crops versus food, and because of the sustainability requirement, there are advantages in integrated processes, where the primary value products, foodstuffs and oils are produced, and the agricultural residues and biomass wastes are used for energy applications [28]. Since different studies used different approaches to consider determining factors – such as demand for food, soil and water constraints, biodiversity and nature preservation requirements, and a variety of other sustainability issues – they come to diverging conclusions regarding the biomass supply, ranging from roughly the current level of production (about 50 EJ) to levels above the current world primary energy consumption (about 500 EJ). When assessing the biomass potential, one must distinguish between the technical potential, which is the unconstrained production potential limited only by the technology used and the natural circumstances, and the sustainable potential, which further considers a range of environmental and social constraints in order to guarantee sustainable feedstock production [22].

Significant potential to expand biomass use represents large volumes of unused residues and wastes. As well enlargement of conventional crops for energy use is feasible, taking care of land availability and food demand. Lignocellulose crops (herbaceous and woody) could be produced on marginal, degraded and surplus agricultural lands and aquatic biomass (algae) could make a significant contribution.

According [30] bioenergy could provide 3100 TWh of electricity, i.e. 7.5% of world electricity generation by 2050. In addition heat from bioenergy could provide 22

EJ (15% of total) of final energy consumption in industry and 25 EJ (20% of total) in the buildings sector in 2050. As it is presented in Figure 2.1. the technical potential for 2050 indicates the upper bound of biomass technical potential based on integrated global assessment studies using five resource categories indicated on the stacked bar chart, and limitations and criteria with respect to biodiversity protection, water limitations, and soil degradation, assuming policy frameworks that secure good governance of land use. Expert estimates undertaken by the IPCC (2011) indicate potential deployment levels of terrestrial biomass for energy by 2050 in the range of 100 to 300 EJ, with a most likely range of 80-190 EJ/yr, with upper levels in the range of 265-300 EJ/yr.

With increasing economic growth, world electricity demand will grow rapidly, according that predictions shows that share of renewable electricity will increase from 19% in 2009 to almost 60% in 2050, with the remaining 40% coming from nuclear as well as coal, natural gas and other fossil sources. By 2050 total bioenergy electricity generation could provide around 7.5% of world electricity generation, Figure 2.2. The use of biomass for power generation varies between regions, depending on biomass availability, conversion costs, and the availability of alternative low-carbon energy sources.
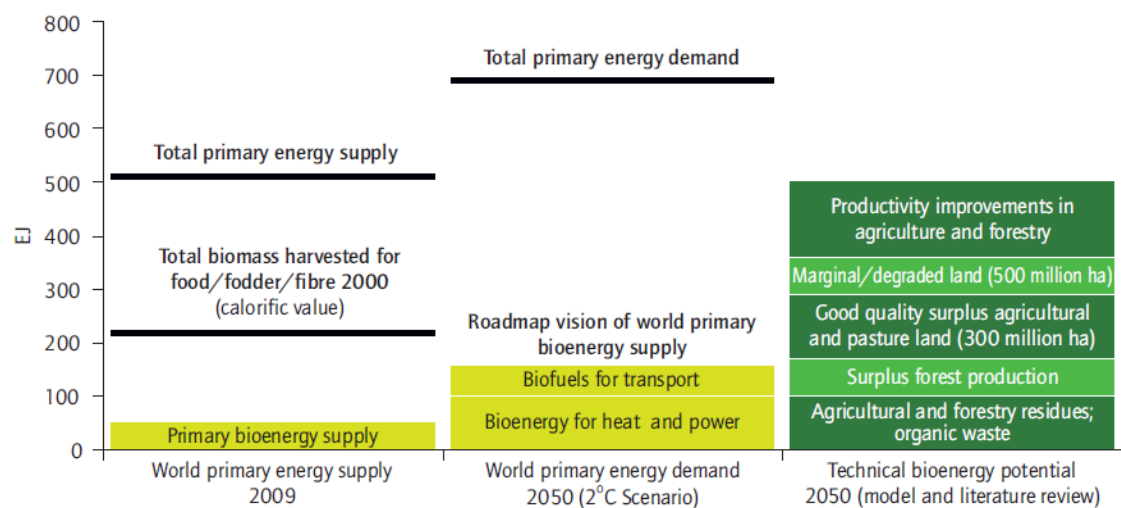
Figure 2.1 Global technical bioenergy potential estimate in 2050 [35]
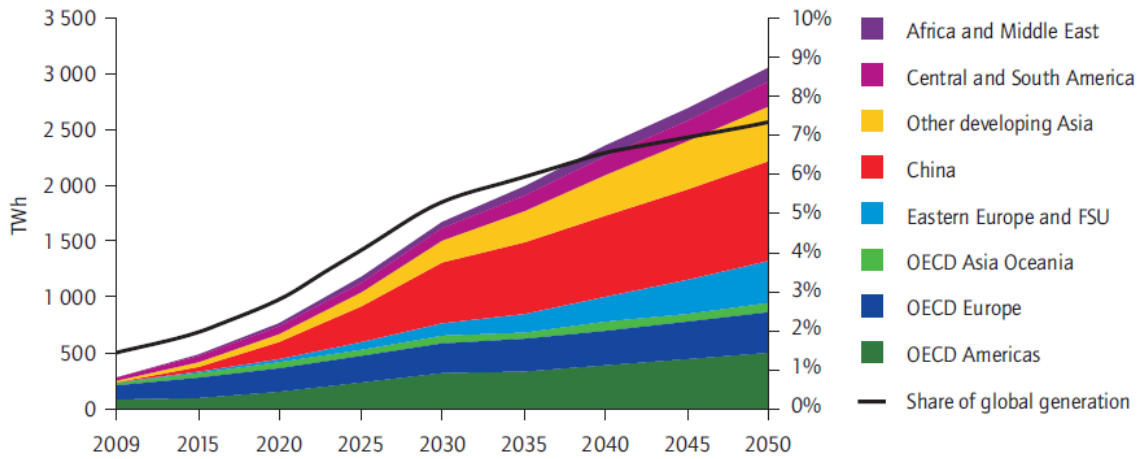
Figure 2.2 Roadmap vision of bioenergy electricity generation by region [30]

Even despite predicted decreasing trend of bioenergy consumption in buildings sector, its use in this sector is expected to remain the largest consumer of biomass throughout the projection period. Decreasing trend of use in Non-OECD countries, is explanting by applying more energy efficient technologies, continued and accelerating shift away from traditional biomass cookstoves to more modern forms of stoves and fuels, including efficient biomass cookstoves and stoves that burn biogas or biofuels. While in OECD countries, Eastern Europe and FSU bioenergy demand in the residential sector will roughly double current consumption by 2050 Figure 2.3, driven by regulations for space heating demand and energy efficiency [30]. Many cities have already reached high levels of heat supply from bioenergy, for example, Växjö (Sweden) supplies 90% of heat demand from renewables, primarily biomass [13].

Figure 2.3 Final bioenergy consumption in the building sector in different world regions [30]

15

The industry sector is definitely the sector with highest potential for increased consumption of bioenergy. And [16] finds that renewables play a relatively small role in industry today, but it finds that over 20% of all final energy use and feedstock in industry in 2050 could come from renewables. This includes contributions from biomass, solar thermal, and heat pumps 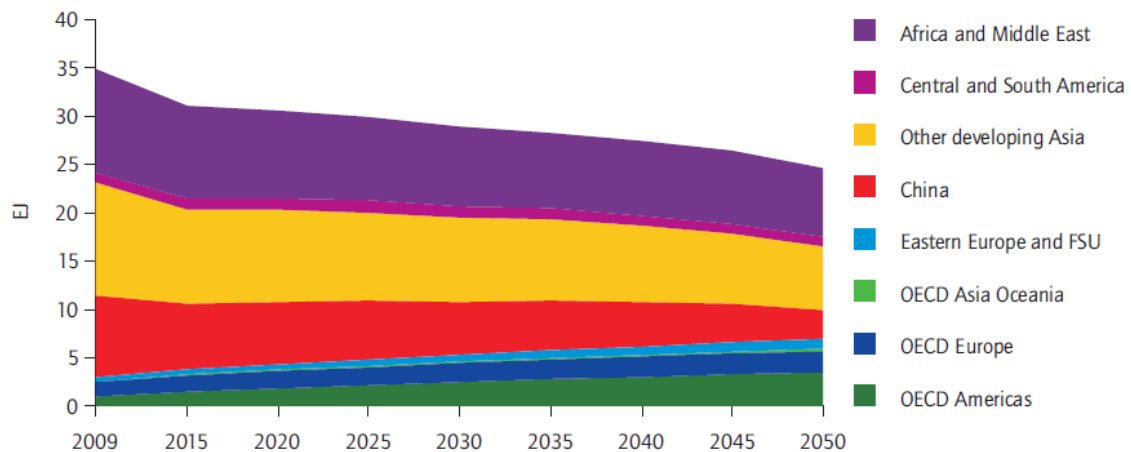by 2050 that together represent almost half of today's level of industrial energy use from all sources. It emphasizes future biomass use in energy-intensive industries such as pulp/paper, wood, cement, chemicals, and petrochemicals. The chemical industry also sees the potential to integrate solid biomass and liquid biofuels as industrial feedstock. As it is presented on Figure 2.4 bioenergy consumption should reach 22 EJ by 2050, which is almost a triple of current use. It will make 15% of the sector total final energy demand.

Generally, biomass has been a marginal source of energy in industry and district heating. However, in countries such as Sweden, Finland, and Austria, which have a large forestry sector, forest-based biomass has a remarkable importance. For example, in Finland, renewable energy sources account for 24% of the total primary energy consumption, and 85% of renewable energy is was derived from wood [25].
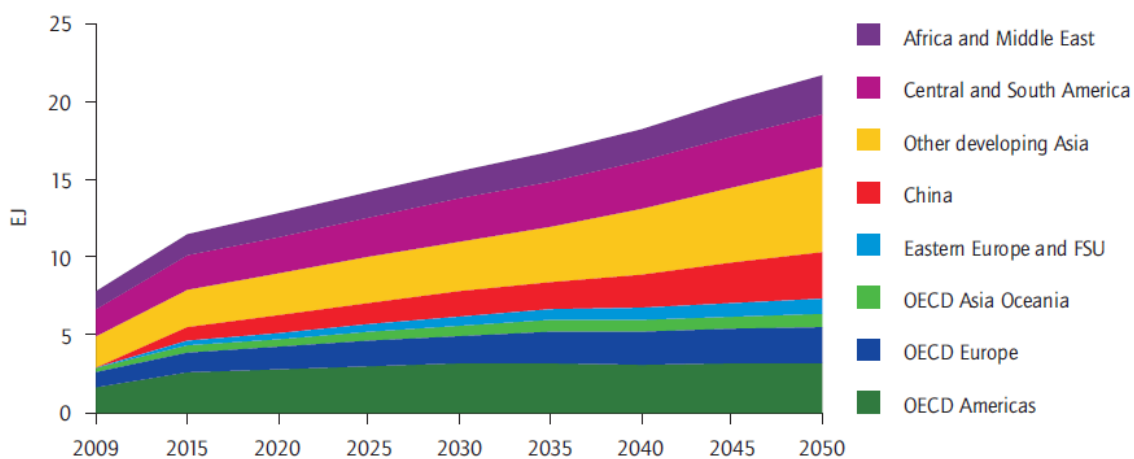
Figure 2.4 Final bioenergy consumption in industry [30]

Transport biofuels are currently the fastest growing bioenergy sector, receiving a great deal of public attention. However, today they represent only 1.5% of total road transport fuel consumption and only 2% of total bioenergy. They are, however, expected to play an increasing role in meeting the demand for road transport fuel, with second generation biofuels increasing in importance over the next two decades. Even under business-as usual scenarios, biofuel production is expected to increase by a factor

16

of 10 to 20 relative to current levels by 2030 (corresponding to a 6 - 8% average annual growth rate) [8].

In [13] the future of biomass is overviewed from four distinct viewpoints:

- **Fuel supplies.** A breakthrough in biomass demand could come as biomass becomes a mainstream commodity in commercial markets in standard forms like pellets or bio-heating oil (from pyrolysis/torrefaction), said experts. In particular, they expected pellets to become a widespread commodity, efficiently transported internationally. And while some experts questioned how much biomass could be produced given competition for land and food, others saw no real limits because of the huge resources available from agricultural and forest wastes, and from new approaches to growing biomass crops on surplus land.

- **Technical conversion pathway/process.** Most biomass used today is simply burned for heat and power. The second most common process is anaerobic conversion to biogas. Experts foresaw increased production of biogas from sewage plants, manure, and organic waste, and cheaper biogas plants made with new materials. Some also saw new applications for the biogas: "Biogas will be used for transport, as it doesn't need to be cleaned for use in a vehicle

engine to the same extent it needs to be clean for a gas turbine," said one expert. Some foresaw much greater use of thermal gasification, while others questioned whether gasification would achieve wide scope.

- **Heating technologies.** Experts envisioned much greater use of biomass heating technologies, including CHP plants, district heating systems, cooling systems for commercial and public buildings, and industrial process heat. Future CHP systems might predominantly fall into the "small or medium scale" of 5–10 MW, but also at smaller sizes of 1 MW, or larger sizes up to 100 MW.

- **Integration into agricultural and forestry industries through integrated "bio-refineries."** The future would see fewer stand-alone bioenergy production sites, and rather would trend toward multi-purpose co-production systems, which co-produce biofuels, sugar, electricity, and biogas, and also utilize leftover waste for fertilizer, chemicals, biofuels, animal feed, and other chemicals. These "integrated bio-refineries" could become part of the food system by 2020, and lead to integrated "bio-based" industries for food, fuels, chemicals, textiles, paper, and other products.

Whatever is actually realised will depend on the cost competitiveness of bioenergy and on future policy frameworks, such as greenhouse gas emission reduction targets. Growth in the use of biomass resources in the mid-term period to 2030 will depend on many demand and supply side factors. Strong renewable energy targets being set at regional and national level (e.g. the European Renewable Energy Directive) are likely to lead to a significant increase in demand. This demand is likely to be met through increased use of residues and wastes, sugar, starch and oil crops, and increasingly, lignocellulosic crops. Drivers for increased bioenergy use (e.g. policy targets for renewables) can lead to increased demand for biomass, leading to competition for land currently used for food production, and possibly (indirectly) causing sensitive areas to be taken into production. This will require intervention by policy makers, in the form of regulation of bioenergy chains and/or regulation of land use, to ensure sustainable demand and production. Development of appropriate policy requires an understanding of the complex issues involved and international cooperation on measures to promote global sustainable biomass production systems and practices. To achieve the bioenergy potential targets in the longer term, government policies and industrial efforts need to be directed at increasing biomass yield levels and modernising agriculture in regions such as Africa, the Far East and Latin America, directly increasing global food production and thus the resources available for biomass. This can be achieved by technology development and by the diffusion of best sustainable agricultural practices. The sustainable use of residues and wastes for bioenergy, which present limited or zero environmental risks, needs to be encouraged and promoted globally [8].

2.2.2 Energy biomass potential of Republic of Serbia

As a country with large areas of agricultural and forested lands, Serbia has strong potential for the production of biomass. Biomass sources represent 63 % of the total renewable energy sources (RES). Forests cover about 30 % of the territory and approximately 55 % is arable land. In addition to residues from crop farming for food production, there is a strong presence of, targeted crop farming for production of biomass fuel without competition with food production [31].

According to numerous studies, the most promising options for biomass utilization in Serbia are:

- space heating in households and buildings using biomass pellets or briquettes,
- co-fi ring or total replacement in district heating plants that currently burn heavy oil or coal,
- production of electricity utilizing agricultural and wood residues and,
- production of biofuels for transport.

The technically feasible, annual energy biomass potential in the Republic of Serbia is approximately 2.7 Mtoe. The energy potential of wood biomass (tree felling and wood residues produced during primary and/or industrial wood processing) is estimated at approximately 1.0 Mtoe, while about 1.7 Mtoe could be generated from agriculture biomass (agricultural waste and crop farming residues, including liquid manure) [31]. The detailed analysis of biomass sources and potentials is given in Table 2.5.

Table 2.5 Biomass energy potential [31]

Biomass source		Potential (toe)
Wood biomass		*1,527,678*
Fuel wood		1,150,000
Forest residue		163,760
Wood processing residue		179,563
Wood from trees outside the forest		34,355
Agricultural biomass		*1,670,240*
Crop residue		1,023,000
Residue from fruit growing, viniculture and fruit processing		605,000
Liquide manure (for biogas production)		42,240
Biofuels for transport		*191,305*
Total Biomass	without transportation fuel	**3,197,918**
	with transportation fuel	**3,389,223**

Ethanol Production in Serbia between 2006 and 2011 was almost non-existent. The small amounts of Ethanol produced in 2008, 2009, and 2010 were undenatured and most likely were used in beverages, although accurate data is not available. It is projected that there will be small-scale production at the existing facility as new renewable energy policies come online in the future. There are no accurate statistics on biodiesel production in Serbia, but the Serbian Ministry of Energy estimates that the consumption of biodiesel accounts for less than 0.5 percent of all diesel consumption in

Serbia. Due to the significant potential for production of biodiesel in Serbia, the Ministry estimates that the Serbian transport fuel system could substitute 13-15 percent of its domestic consumption of diesel (by energy content) [32].

2.3 Clasification of Biofuels

Among many energy alternatives, biofuels, hydrogen, natural gas and syngas (synthesis gas) may likely emerge as the four strategically important sustainable fuel sources in the foreseeable future. Within these four, biofuels are the most environment friendly energy source [33]. Biofuels are referred to liquid, gas and solid fuels predominantly produced from biomass. A variety of fuels can be produced from biomass such as ethanol, methanol, biodiesel, Fischer –Tropsch diesel, hydrogen and methane [34].

Because of its widespread noncommercial use in developing countries, biomass is by far the greatest source of renewable energy. Approximately two-thirds of biomass is used for cooking and heating in developing countries. The remaining energy use of biomass takes place in industrialised countries where biomass is utilized both in industrial applications within the heat, power, and road transportation sectors and for heating purposes in the private sector [25].

According [35, 36] biofuels are classified as primary and secondary biofuels. The primary biofuels are used in natural and an unprocessed form, primarily for heating, cooking or electricity production such as fuelwood, wood chips and pellets, etc. and are mainly those where the organic material is utilised essentially in its natural and original chemical form. In contrast to primary, the secondary biofuels are modified and produced by processing of biomass e.g. ethanol, biodiesel, DME, etc. that can be used in vehicles and various industrial processes. The secondary biofuels are further divided in to first, second and third generation biofuels on the basis of raw material and technology used for their production (Figure 2.5).

Biofuels are also classified according to their source and type. They may be derived from forest, agricultural or fishery products or municipal wastes, also including by-products and wastes originated from agro-industry, food industry and food services.

Biofuels can be solid, such as fuelwood, charcoal, and wood pellets; or liquid, such as ethanol, biodiesel and pyrolysis oils; or gaseous, such as biogas (methane).
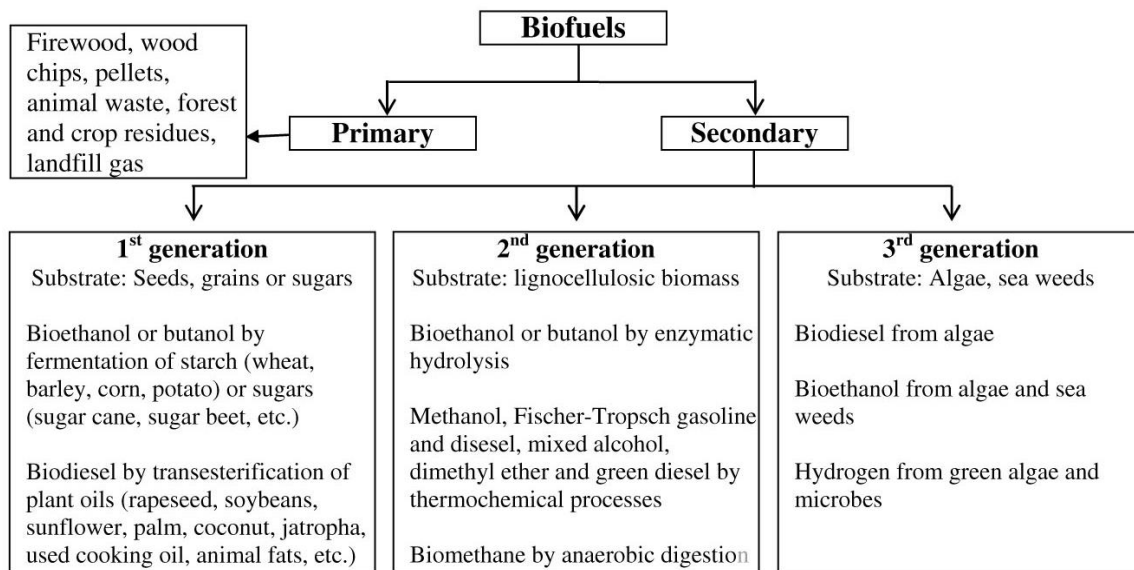
Figure 2.5 Classification of biofuels [35]

As is stated in [37], due to some technological and economic consequences, practical experiences of biofuel-energy do have wide applications neither in the richest countries nor in the poorest countries at present. For the developed countries, active involvement in biofuel research and development, especially through collaborative international programs, could facilitate the introduction of new biofuel technologies as they become competitive. A major dilemma now faced by the developing countries is how to invest in biofuel research and development for the transition to biofuel economy. Most developing countries will probably rather than developers of cutting-edge technologies. Developing countries have at least as much to gain from a move towards the biofuel economy as industrialized ones, since they generally suffer more from urban pollution and their economies tend to be more energy intensive.

2.4 Policy Framework

Over the past decades, the use of bioenergy has increased rapidly in many parts of the world. In order to comply with Kyoto greenhouse gas reduction targets, many

countries have set goals for the utilization of biomass, intensifying its production and consumption for energy purposes [24].

Policymakers are increasingly aware of renewable energy's wide range of benefits-including energy security, reduced import dependency, reduction of greenhouse gas (GHG) emissions, prevention of biodiversity loss, improved health, job creation, rural development, and energy access—leading to closer integration in some countries of renewable energy with policies in other economic sectors. Policy development and implementation were stimulated in some countries by the Fukushima nuclear catastrophe in Japan and by the UN Secretary-General's announced goal to double the share of renewables in the energy mix by 2030. Some countries are beginning to tap the synergies between renewable and energy efficiency improvements. Successful policies depend on predictable, transparent, and stable framework conditions and on appropriate design. Although many policy developments have helped to expand renewable energy markets, encourage investments, and stimulate industry developments, not all policies have been equally effective or efficient at achieving these goals. [38]

The deployment of RES is one of the core components of the EU's energy and climate policies. The Directive on the promotion of electricity produced from RES 2001/77/EC gave EU Member States (MS) indicative goals and the requirement to implement national support schemes for RES based electricity. Mandatory RES target of 20% in final energy consumption and a minimum of 10% for biofuels by 2020 were implemented via the Renewable Energy Directive 2009/28/EC. Furthermore, the Directive 2009/28/EC defines sustainability requirements for the production of liquid biofuels and bioliquids. Solid (and gaseous) biofuels are so far excluded from these requirements [39].

Drivers for increased bioenergy use (e.g. policy targets for renewables) can lead to increased demand for biomass, leading to competition for land currently used for food production, and possibly (indirectly) causing sensitive areas to be taken into production. This will require intervention by policy makers, in the form of regulation of bioenergy chains and/or regulation of land use, to ensure sustainable demand and production. Development of appropriate policy requires an understanding of the complex issues involved and international cooperation on measures to promote global sustainable biomass production systems and practices [22].

EU policy framework is the leading bioenergy promotion tool. Within which there are numerous legal acts dealing with the use of biomass as fuel and driving force for future development of this energy source. Surely the most important are Renewable Energy Directive 2009/28/EC, Biomass action plan {SEC (2005) 1573} and the Biofuels for Transport Directive 2003/30/EC.

Republic of Serbia as an EU candidate country has an obligation to harmonize all its legal acts into line with EU legislation. In 2006, the Republic of Serbia ratified the Treaty that established the Energy Community, also known as the Energy Community South East Europe Treaty or ECSEE (signed between the EU and South East Europe countries). According to Article 20 of the Treaty, one year after ratification, the Republic of Serbia was obliged to prepare a program of implementation of Directive 2001/77/EC on the promotion of electricity produced from renewable energy sources on the internal electricity market as well as Directive 2003/30/EC on the promotion of the use of biofuels or other renewable fuels for transport. In order to foster the investment in RES Serbia has adopted several energy related legislations and sub-legislations [31].

2.4.1 Renewable Energy Directive 2009/28/EC

By this Directive a common framework for the use of energy from renewable sources in order to limit greenhouse gas emissions and to promote cleaner transport is established. For that purpose, national action plans are defined, as well as procedures for use of biofuels.

Mandatory RES target of 20% in final energy consumption and a minimum of 10% for biofuels by 2020 are implemented through the Renewable Energy Directive 2009/28/EC. According this Directive Each Member State has a target calculated according to the share of energy from renewable sources in its gross final consumption for 2020. This target is in line with the overall '20-20-20' goal for the Community. Directive stipulates that Member States should establish national action plans that set out the share of energy from renewable sources consumed in transport, as well as in the production of electricity and heating, for 2020. Effects of other energy efficiency measures on final energy consumption (the higher the reduction in energy consumption, the less energy from renewable sources will be required to meet the target) must be

taken into account within action plans. National action plans should as well establish procedures for the reform of planning and pricing schemes and access to electricity networks, promoting energy from renewable sources.

The origin of electricity, heating and cooling produced from renewable energy sources has to be guaranteed by each Member State. These guarantees must be standadised and should be recognised by all Member States.

Regarding biofuels and bioliquids Directive stipulates their production using raw materials coming from outside or within the Community. They should not be produced using raw materials from land with high biodiversity value or with high carbon stock. To benefit from financial support, they must be qualified as "sustainable" in accordance with the criteria of this Directive. Bioliquids should contribute to a reduction of at least 35 % of greenhouse gas emissions in order to be taken into account. Their share in emissions savings should be increased to 50 %, from 1 January 2017.

2.4.2 Biomass action plan {SEC (2005) 1573}

To promote the use of biomass energy, a renewable source of energy with a huge potential, the Commission has decided to propose an ambitious action plan. The action plan was the first coordinating step and set measures to promote the biomass in three sectors: heating, electricity and transport, affecting biomass supply, financing and research.

Fundamental elements of this policy are: the need to reduce energy demand; increase reliance on renewable energy sources, given the potential to produce them domestically and their sustainability; diversify energy sources; and enhance international cooperation.

In order to increase the development of biomass energy from wood, wastes and agricultural crops, this action plan set out measures (listed in Annex 1) by creating market-based incentives to its use and removing barriers to the development of the market. At the moment of adoption of this plan, the aim was that Europe could reduce greenhouse gas emissions and use of fossil fuels, as well stimulation of economy in rural areas.

The plan includes recommendations of improvements for biomass usage for transport, heating and electricity generation; investment in research, particularly in making liquid fuels from wood and waste materials; and a initiative to inform farmers and forest owners about energy crops.

The Commission estimated that the measures in the plan would increase the use of biomass to about 150 Mtoe by 2010 (compared with 69 Mtoe in 2003) without increasing the intensity of agriculture or significantly affecting domestic food production. As well plan should lead to reduction of oil imports by 8%, greenhouse gas emissions by 209 million tons CO2-equivalent per year; provided direct employment for up to 300,000 people, in the agricultural and forestry sector.

2.4.3 Biofuels for Transport Directive 2003/30/EC

The EU adopted Directive 2003/30 EC to promote the use of renewable fuels and biofuels in transport. A directive is binding on the Member States, by 2003, set indicative targets for the minimum proportion of biofuels to be placed on the market: 2% in 2005 and 5.75% in 2010. The Directive has set a minimum percentage of biofuels to replace diesel or petrol for transport purposes in each Member State, in order to reduce conventional emissions of CO_2 (carbon dioxide), CO (carbon monoxide), NOx (nitrogen oxides), VOC (volatile organic compounds) and other particles which are toxic for health and the environment.

According Directive Member States have ensured that a minimum proportion of biofuels and other renewable fuels is placed on their markets, and, to that effect, shall set national indicative targets. Calculated on the basis of energy content, a reference value for these targets shall be 2 %, of all petrol and diesel for transport purposes placed on their markets by 31 December 2005. Directive stipulated specific labelling at the sales points for percentages of biofuels, blended in mineral oil derivatives, exceeding the limit value of 5 % of fatty acid methyl ester (FAME) or of 5 % of bioethanol. This directive required from Member States annually reporting on measures taken to promote biofuels and quantifiable progress. Directive thought provisions provided a stimulus to the rural economy through the creation of new sources of income and employment. In

many cases in the agri-food and forestry industries, biofuels could turn problematical waste production into a sustainable product.

Directive 2003/30/EC is repealed by Directive 2009/28/EC with effect from 1 January 2012.

2.4.4 National Renewable Energy Action Plan of the Republic of Serbia in accordance with the template as per Directive 2009/28/EC (Decision 2009/548/EC)

National Renewable Energy Action Plan (NREAP) is the document presenting the framework policy of the Republic of Serbia and setting the pathway in the field of RES until 2020. Its aim is to enhance and encourage investments into green energy field. The Action Plan is prepared in accordance with the EU methodology and standards EU, on the basis of all relevant data in the field of energy and renewable energy sources in the Republic of Serbia.

In compliance with the Directive 2009/28/EC and the Decision of the Ministerial Council of the Energy Community of 18 October 2012, binding target for the Republic of Serbia was defined, amounting to 27 % of renewable energy sources in gross final energy consumption in 2020. At the same time, it was defined that the National action plan for renewable energy sources of the Republic of Serbia should be prepared, in compliance with the adopted template for the preparation of this document (Decision 2009/548/EC).

Since until 2020, the Republic of Serbia should increase the share of RES to 27,0 %. In compliance with the envisaged gross final energy consumption, the quantity of renewable energy sources should amount to 2.563,6 ktoe in 2020, meaning that in the period from 2009 to 2020 the increase of RES amount to 621,0 ktoe should be achieved. Having in mind the available potential of renewable energy sources and unused potentials, the Republic of Serbia can achieve the target set for 2020 from the domestic sources, except regarding the binding share of biofuels of 10 % in the transport sector in 2020. Taking into account the currently available capacities for the production of second generation biofuels from biomass which meets the parameters regarding GHG emissions, as well as the non-existence of the legislation and the relevant infrastructure

for its application in the field of biofuels, the Republic of Serbia will have to plan import of biofuels in 2018.

NREAP includes list of detail list of measures for achieving the targets as well all relevant sectorial information and projections. Within the prescribed measures are given, as well, specific measures for the promotion of the use of energy from biomass, that includes biomass supply and measures to increase biomass availability, taking into account other biomass users. Estimated contribution of biomass energy use in 2015 and 2020. are 1.106 ktoe as primary energy production and 1.673 ktoe as expected amount of domestic resource, respectively.

Estimations of total contribution expected from each renewable energy technology in Republic of Serbia to meet the binding 2020 targets and the indicative interim trajectory for the shares of energy from renewable resources in period 2010-2020. are given for electricity, heating and cooling, as well for transport sector. According those estimations in 2020 bioenergy will reach:

- total installed capacity (gross electricity generation): 143 MW (983 GWh),
- heating and cooling: 1.102 ktoe,
- transport: 246 ktoe.

2.4.5 Biomass Action Plan for The Republic of Serbia 2010 – 2012

The aim of the BAP is to define a strategy for biomass utilization as RES, within the framework of actual potentials, current national strategies, as well as national and European directives. At the same time, one of the most important tasks of the BAP is to identify the problems/bottlenecks in the process of biomass utilization as well as the actions required to overcome them. In some cases, a specific timeframe for actions will be defined and some long-term activities will be suggested. It is important to underscore that cooperation among the numerous stakeholders (from governmental institutions to the private and non-governmental sector) is essential for the successful implementation of the BAP. The actions outlined in BAP include legislative, economic, policy and technical aspects. This document covers all types of biomass and different possibilities for their use (electricity and heat generation, transport) and it will facilitate greater biomass utilization in the Republic of Serbia. The BAP is a dynamic policy document

which can be modified, updated and extended according to the future development of the country, the energy sector strategy and all other relevant strategies (agricultural, rural development, forestry and environment). As already indicated the BAP was focused on short term activities (through the end of 2012), but some recommendations for long term actions are also laid out. The BAP for Serbia was drafted in accordance with the Energy Community Treaty and in the spirit of Directive 2009/28/EC. The implementation of Directive 2009/28/EC in the Republic of Serbia and other countries signatories of the Treaty will be determined and harmonized within the community in the future.

2.5 Bioenergy trade

Beside the strong policy support and sustainable use, trade presents the main precondition for successful bioenergy chain.

Traditionally, all biomass fuels are used more or less in the same geographical region in which they are produced. In recent years, this pattern has been changed, especially in Northern Europe, by large-scale use of re-cycled wood, forest and wood residues and densified biofuels for district heating. Solid biofuels like wood residues (e.g. industrial by-products: bark and sawdust, re-cycled wood), upgraded biofuels (e.g. wood pellets, briquettes) and wood chips are today traded, e.g. in Europe and North America. In several countries there is growing interest in international biomass trade because this can provide biomass fuels at lower prices [23]. International bioenergy trade can also offer opportunities for economic growth and socio-economic development for exporting countries, and may enable countries with few domestic biomass resources to meet their renewable energy targets, gain more fuel diversity and improve security of supply [40]. Beside exchange opportunities of goods and services between the countries, international bioenergy trade is essential to fully utilize available biomass. Favorable policies and other commercial driving factors will continuously bring increased demand for bioenergy, with a resultant expansion in biomass and bioenergy markets [24].

Major drivers for international bioenergy trade in general are the large resource potentials and relatively low production costs in producing countries such as Canada and Brazil, and high fossil fuel prices and various policy incentives to stimulate biomass

use in importing countries. However, also barriers are somewhat hindering the market development: (i) developing the required logistic infrastructure both in exporting and importing countries is required to access larger physical biomass volumes and to reach other (i.e. smaller) end-consumers, (ii) better statistics and methods have to be developed to chart the growing trade volumes, (iii) policy measure still determine large parts of the trade flows, and sudden changes in policy can result in quickly changing trade patterns, (iv) safeguards are required to ensure the sustainable production of biomass [41].

Wood pellets, ethanol, vegetable oils, charcoal and fuel wood are the most important products that currently are internationally traded for energy purposes. In Table 2.6, a brief overview of the production and trade of the major biomass commodities is presented.

Bioethanol is a commodity which has been produced and traded globally in large volumes for decades. The bioethanol market is well-developed, as is its infrastructure and logistics in many countries. The USA and Brazil are the world's largest bioethanol producers and consumers, covering almost 90% of the 40 million m^3 produced globally in 2006. Estimates indicate that bioethanol trade has steadily grown from about 3 million m^3 in 2000 to 6 million m^3 in 2005. Presuming that the rise in recent years was mostly due to increasing fuel ethanol trade, about 10% of the fuel ethanol consumed in 2005 was imported. The world's largest exporter by far is Brazil (48% of the total traded volume in 2005), followed by the USA (6%) and France (6%) [22].

Table 2.6 Overview of global production and trade of the major biomass commodities in 2008 [40]

	Bioethanol	Biodiesel	Wood pellets
Global production	52.4	13.1	11.5
Global net trade	2.8 (min) – 3.1 (max)	2.4	Approx. 4
Main exporters	Brazil	United States, Argentina, Indonesia and Malaysia	Canada, USA, Baltic countries, Russia
Main importers	USA, Japan, European Union	European Union	Belgium, Netherlands, Sweden, Italy

Overall solid biomass trade has grown from about 56 to 300 PJ between 2000 and 2010. Wood pellets grew strongest, i.e. from 8.5 to 120 PJ. Other relevant streams by 2010 included wood waste (77 PJ), fuel wood (76 PJ), wood chips (17 PJ), residues

(9 PJ), and round wood (2.4 PJ). Intra-EU trade covered two thirds of global trade by 2010 [39].

According [22] biomass imports contribute substantially to the overall biomass use in developed countries, e.g. 21-43% in North-West Europe and Scandinavia. In the longer term, significant amounts (up to over 100 EJ) of biomass commodities might be traded internationally, with Latin America and Sub-Saharan Africa having the potential to become large net exporters and North America, Europe and South-East Asia large net importers. As it stated in [40] experts believed in ''local for local'', i.e. that biomass should first and foremost produced be before any biomass imported (possibly even if available at lower costs). To achieve this some proposed that policies should in first instance stimulate local production before any support is given to imported biomass. Strong policy support for liquid biofuels (for ethanol and biodiesel) and for electricity and heat from biomass (for pellets) was also deemed very important conditions for further growth of international bioenergy trade. Global or country-specific initiatives (not initiated by governments) aimed at GHG emissions reductions were deemed less important drivers for biomass trade.

As bioenergy trade is expected to increase strongly, reliable bioenergy trade figures are of use for industry actors, policymakers, and scientists alike, and, on account of its expected pivotal role in developing biomass production potential in the future, it is recommended to increase efforts to collect and publish coherent bioenergy trade statistics, which is currently often unavailable [25].

3. BIOMASS PROPERTIES

The characteristics of biomass greatly influence the performance of biomass utilization. A proper understanding of the physical and the chemical properties of biomass feedstock is essential for the design of biomass appliances to be reliable. This chapter discusses some important properties of biomass that are relevant for biomass thermal utilization.

Biomass is the name given to any organic matter which is derived from plants. That is plant and animal materials such as wood from forests, crops, seaweed, material left over from agricultural and forestry processes, and organic industrial, human and animal wastes. Biomass is a general term which includes phytomass or plant biomass and zoomass or animal biomass. The sun's energy when intercepted by plants and converted by the process of photosynthesis into chemical energy, is 'fixed' or stored in the form of terrestrial and aquatic vegetation. The vegetation when grazed (used as food) by animals gets converted into zoomass (animal biomass) and excreta. The excreta from terrestrial animals, especially dairy animals, can be used as a source of energy, while the excreta from aquatic animals gets dispersed as it is not possible to collect it and process it for energy production [42].

Two fundamental aspects related to biomass use as fuel are: (1) to extend and improve the basic knowledge on composition and properties; and (2) to apply this knowledge for the most advanced and sustainable utilisation of biomass. The systematic identification, quantification and characterisation of chemical and phase composition of a given solid fuel are the initial and most important steps during the investigation and application of such fuel. This composition is a fundamental code that depends on various factors and definite properties, quality and application perspectives, as well as technological and environmental problems related to any fuel [43].

3.1 Biomass sources

Biomass resources that can be used for energy production cover a wide range of materials [2]. According [44] biomass could be defined in four main types:

- woody plants,

- herbaceous plants/grasses,

- aquatic plants,

- manures.

Within this categorization, herbaceous plants can be further subdivided into those with high- and low-moisture contents. Apart from specific applications or needs, most commercial activity has been directed towards the lower moisture-content types. Aquatic plants and manures are intrinsically high-moisture materials and as such, are more suited to 'wet' processing techniques.

```
                        ┌─────────────────────┐
                        │  Biomass resources  │
                        └─────────────────────┘
              ┌───────────────────┐   ┌────────────────────────┐
              │ The woody biomass │   │ The non-woody biomass  │
              └───────────────────┘   └────────────────────────┘
        ┌──────────────────┐        ┌──────────────────────────┐
        │ Forest residues  │        │ Agricultural crop residues│
        └──────────────────┘        └──────────────────────────┘
  ┌───────────────────────────────────┐   ┌─────────────┐
  │ Short - rotation energy forest     │   │  Rice husk  │
  │ plantations                        │   └─────────────┘
  └───────────────────────────────────┘   ┌─────────────┐
  ┌──────────────────────┐                │   Bagasse   │
  │ Municipal greenwaste │                └─────────────┘
  └──────────────────────┘                ┌─────────────┐
                                          │ Cereal straw│
                                          └─────────────┘
                                      ┌───────────────┐
                                      │ Energy crops  │
                                      └───────────────┘
                                      ┌───────────────┐
                                      │ Animal wastes │
                                      └───────────────┘
                                      ┌───────────────┐
                                      │     Waste     │
                                      └───────────────┘
                                      ┌───────────────┐
                                      │Aquatic biomass│
                                      └───────────────┘
```
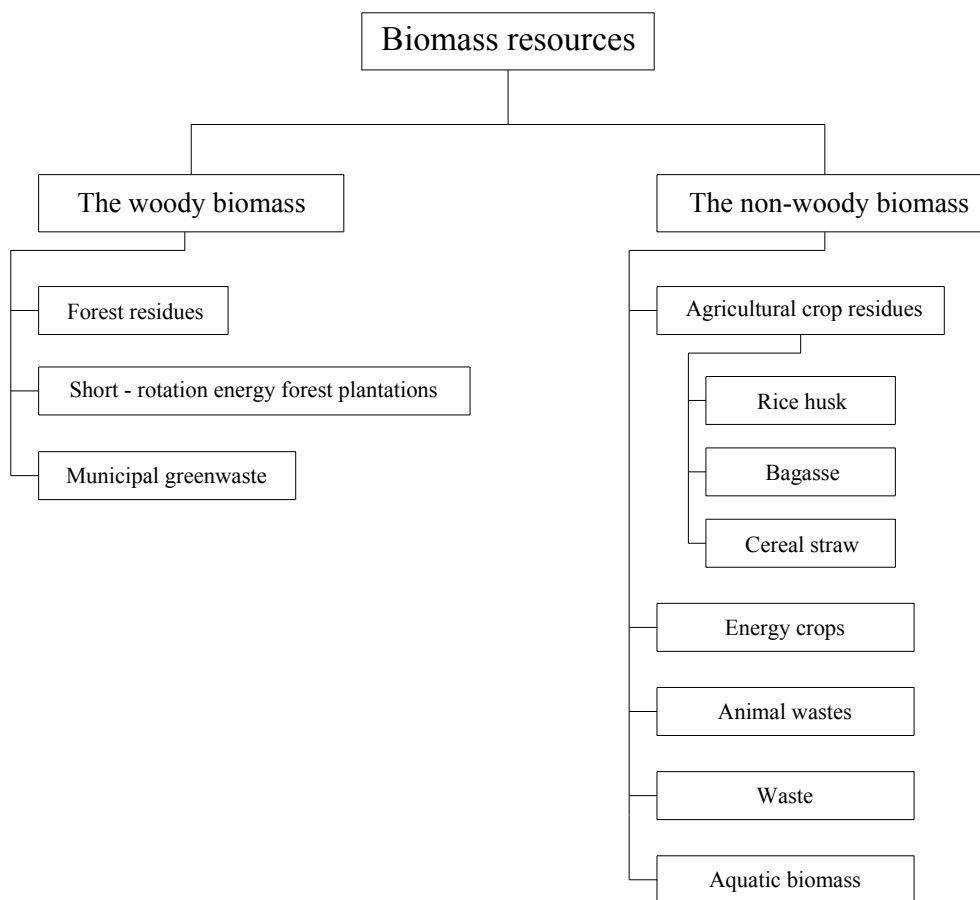
Figure 3.1 Biomass resources

Further [45] brings two types of biomass characterization. The first one named as *Common sources of biomass* groups biomass as:

- *Agricultural:* food grain, bagasse (crushed sugarcane), corn stalks, straw, seed hulls, nutshells, and manure from cattle, poultry, and hogs;

- *Forest:* trees, wood waste, wood or bark, sawdust, timber slash, and mill scrap;
- *Municipal:* sewage sludge, refuse-derived fuel (RDF), food waste, waste paper, and yard clippings;
- *Energy:* poplars, willows, switchgrass, alfalfa, prairie bluestem, corn, and soybean, canola, and other plant oils;
- *Biological:* animal waste, aquatic species, biological waste.

And the second one that divides biomass into two broad groups:
- *Virgin biomass* includes wood, plants, and leaves (ligno-cellulose); and crops and vegetables (carbohydrates).
- Waste includes solid and liquid wastes (municipal solid waste (MSW)); sewage, animal, and human waste; gases derived from landfilling (mainly methane); and agricultural wastes.

Primary or virgin biomass comes directly from plants or animals. Waste or derived biomass comes from different biomass-derived products lists a range of biomass types, grouping them as virgin or waste.

According to their distinct biological diversity and similar source and origin biomass as fuel resources, based on [46], could be divided preliminary and roughly into several groups and sub-groups (Table 3.1).

The two main sources of biomass are the purpose-grown energy crops and wastes. Energy crops include woody crops and agricultural crops. Wastes include wood residues, forestry residues; temperate crop wastes, tropical crop wastes, sewage, municipal solid wastes and animal wastes [42].

These crops are ligno-cellulosic. They typically have a short growing period and high yields, and require little or no fertilizer, so they provide quick return on investment. Energy crops are densely planted. For energy production, woody crops such as *Miscanthus*, willow, switchgrass, and poplar are widely utilized. These plants have high energy yield per unit of land area and require much less energy for cultivation [45]. Both woody and herbaceous plant species have specific growing conditions, based on the soil type, soil moisture, nutrient balances and sunlight, which will determine their suitability and productive growth rates for specific, geographic locations [44].

In general, according [10] the characteristics of the ideal energy crop are:

- high yield (maximum production of dry matter per hectare),

- low energy input to produce,

- low cost,

- composition with the least contaminants,

- low nutrient requirements.

Table 3.1 General classification of biomass varieties as solid fuel resources according to their biological diversity, source and origin [46]

Biomass groups	Biomass sub-groups, varieties and species
1.Wood and woody biomass	Coniferous or deciduous; angiospermous or gymnospermous; soft or hard; stems, branches, foliage, bark, chips, lumps, pellets, briquettes, sawdust, sawmill and others from various wood species
2.Herbaceous and agricultural biomass	Annual or perennial and field-based or processed-based such as: 2.1. Grasses and flowers (alfalfa, arundo, bamboo, bana, brassica, cane, cynara, miscanthus, switchgrass, timothy, others) 2.2. Straws (barley, bean, flax, corn, mint, oat, rape, rice, rye, sesame, sunflower, wheat, others) 2.3. Other residues (fruits, shells, husks, hulls, pits, pips, grains, seeds, coir, stalks, cobs, kernels, bagasse, food, fodder, pulps, cakes, others)
3.Aquatic biomass	Marine or freshwater algae; macroalgae (blue, green, blue-green, brown, red) or microalgae; seaweed, kelp, lake weed, water hyacinth, others
4.Animal and human biomass wastes	Bones, meat-bone meal, chicken litter, various manures, others
5.Contaminated biomass and industrial biomass wastes (semi-biomass)	Municipal solid waste, demolition wood, refuse-derived fuel, sewage sludge, hospital waste, paper-pulp sludge, waste papers, paperboard waste, chipboard, fibreboard, plywood, wood pallets and boxes, railway sleepers, tannery waste, others
6.Biomass mixtures	Blends from the above varieties

Wastes are secondary biomass, as they are derived from primary biomass (trees, vegetables, meat) during different stages of their production or use. MSW is an important source of waste biomass, and much of it comes from renewables like food scraps, lawn clippings, leaves, and papers. Nonrenewable components of MSW like plastics, glass, and metals are not considered biomass. The combustible part of MSW is at times separated and sold as refuse-derived fuel (RDF). Sewage sludge that contains human excreta, fat, grease, and food wastes is an important biomass source. Another waste is sawdust, produced in sawmills during the production of lumber from wood [45].

Reasonably, two fundamental aspects related to biomass use as fuel are: (1) to extend and improve the basic knowledge on composition and properties; and (2) to apply this knowledge for the most advanced and environmentally safe utilization. Numerous studies have been conducted worldwide and extensive data for biomass and its conversion products have been generated, particularly during the last two decades.

These results provide a sound foundation for an initial database that can be used for characterization and subsequent classification and sustainable exploitation of biomass [46].

3.2 Composition of biomass

The identification and characterization of chemical and phase compositions of a given solid fuel is the initial and most important step during the investigation and application of such fuel. These compositions are a unique fundamental code that characterizes and determines the properties, quality, potential applications and environmental problems related to any fuel. For that purpose, well-known physical, chemical, petrographic, mineralogical and geochemical studies were used for characterization of solid fuels. Authors used data from: (1) structural analysis, (2) proximate analysis, (3) ultimate analysis, (4) ash analysis, (5) petrographic analysis, (6) mineralogical analysis, (7) separation procedures, and (8) other analyses of fuel, low-temperature ash (LTA) or high-temperature ash (HTA) to characterize specific solid fuels. Identical or similar analyses are also applicable for biomass characterization despite some peculiarities and limitations [42].

3.2.1 Structural composition

Photosynthesis results in the production of structural and non-structural carbohydrates comprising the plant tissues [47]. Typically photosynthesis converts less than 1% of the available sunlight to stored, chemical energy. The solar energy driving photosynthesis is stored in the chemical bonds of the structural components of biomass. If biomass is processed efficiently, either chemically or biologically, by extracting the energy stored in the chemical bonds and the subsequent 'energy' product combined with oxygen, the carbon is oxidised to produce CO_2 and water. The process is cyclical, as the CO_2 is then available to produce new biomass. The biomass resource can be considered as organic matter, in which the energy of sunlight is stored in chemical bonds. When the bonds between adjacent carbon, hydrogen and oxygen molecules are broken by

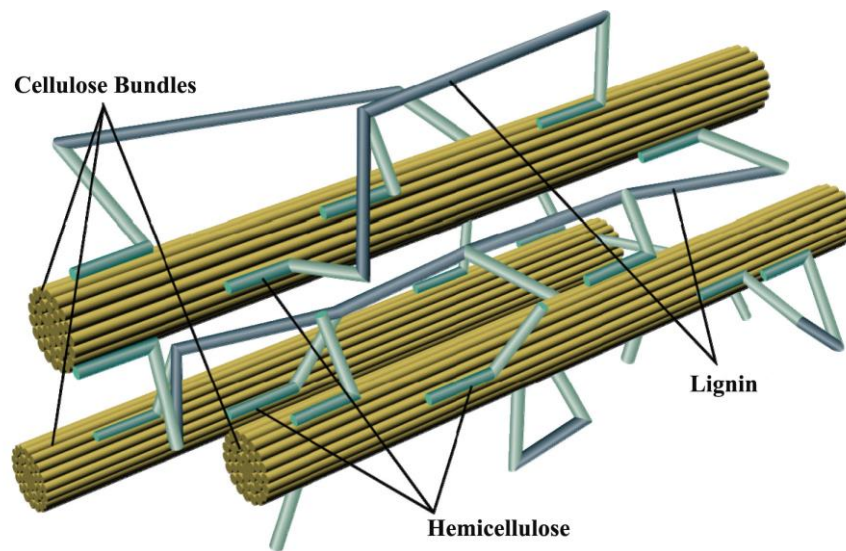digestion, combustion, or decomposition, these substances release their stored, chemical energy [44].

Figure 3.2 Arrangement of cellulose, hemicellulose and lignin in biomass matrix [48]

Biomass is a complex mixture of organic materials such as carbohydrates, fats, and proteins, along with small amounts of minerals such as sodium, phosphorus, calcium, and iron. The main components of plant biomass are extractives fiber or cell wall components, and ash.

- Extractives include protein, oil, starch, sugar etc. Those substances present in vegetable or animal tissue that can be separated by successive treatment with solvents and recovered by evaporation of the solution.

- Cell wall provides structural strength to the plant, allowing it to stand tall above the ground without support. A typical cell wall is made of carbohydrates and lignin. Carbohydrates are mainly cellulose or hemicellulose fibers, which impart strength to the plant structure; the lignin holds the fibers together.

- Ash presents the inorganic component of the biomass.

- Cellulose, hemicellulose, and lignin are the three main constituents, among these compounds. Depending on species, type of plant tissue, stage of growth, and growing conditions the concentration of each class of compound varies [45]. Figure 3.2 shows the arrangement of cellulose, hemicellulose, and lignin in a biomass matrix [48].

According results that are presented in [43], which taking in consideration contents of structural components of 93 varietes of biomass, in Table 3.2 is presented minimum, maximum and mean values of cellulose, hemicellulose and lignin of these on dry ash-free basis and mormalised to 100.0%. Given results clearly represent high variations in contents, even within the same type of biomass.

Table 3.2 Contents of structural components (cellulose, hemicellulose, lignin) of different biomass [43]

Biomass	Cellulose			Hemicellulose			Lignin		
	Min	Max	Avg.	Min	Max	Avg.	Min	Max	Avg.
Wood and woody biomass	12.4	65.5	39.5	6.7	65.6	34.5	10.2	44.5	26
Herbaceous and agricultural biomass	23.7	87.5	46.1	12.3	54.5	30.2	0.0	54.3	23.7
Animal biomass*		32.7			24.5			42.8	
Contaminated biomass**	45.6	92.5	68.1	0.0	31.3	17.1	7.5	23.1	14.8
All varieties of biomass	12.4	92.5	44.4	0.0	65.6	31.2	0.0	54.3	24.4
Natural biomass	12.4	87.5	43.3	6.7	31.8	65.6	0.0	54.3	24.9

* Only one sample of cattle manure has been considered.

** Different types of paper and RDF have been considered.

3.2.1.1 Lignin

Lignin $[C_9H_{10}O_3(OCH_3)_{0.9–1.7}]_n$ [49] is a complex, irregular, highly branched polymer of phenylpropane and is an integral part of the secondary cell walls of plants, as well it could be regarded as a group of amorphous, high molecular-weight, chemically related compounds (Figure 3.3) [44, 45, 47].

The building blocks of lignin are believed to be a three carbon chain attached to rings of six carbon atoms, called phenyl-propanes. These may have zero, one or two methoxyl groups attached to the rings, giving rise to three structures, termed I, II and III, respectively. The proportions of each structure depend on the source of the polymer i.e. structure I is found in plants such as grasses; structure II in the wood of conifers; while structure III is found in deciduous wood [44].
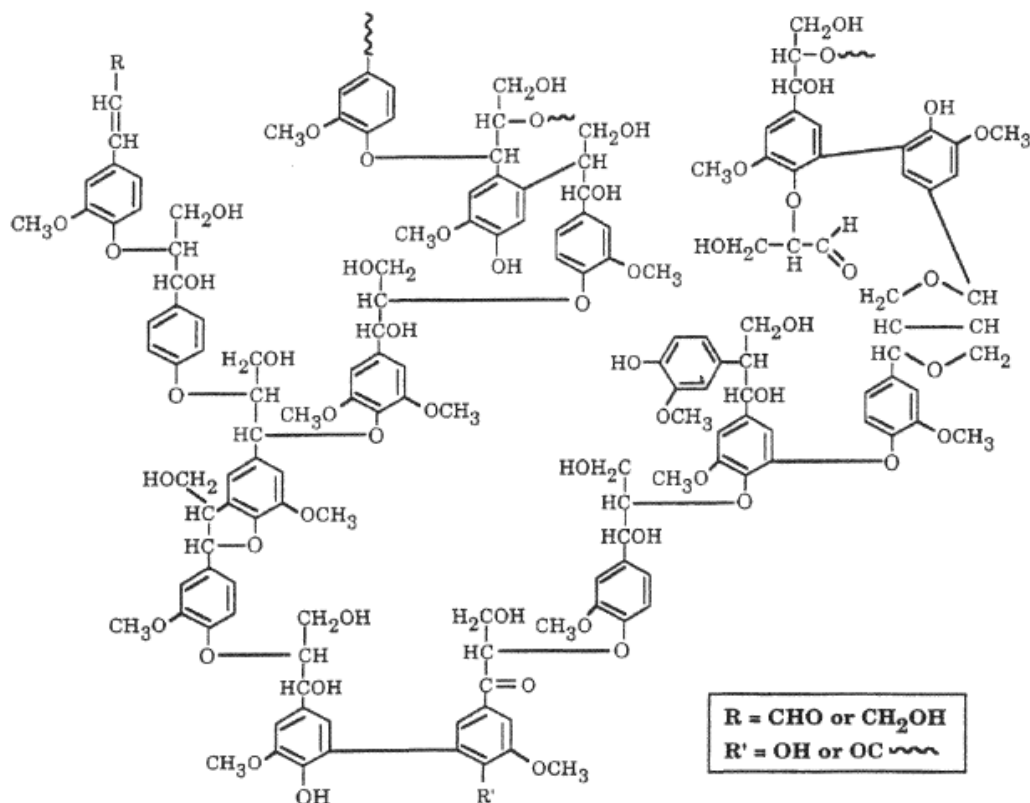
Figure 3.3 Partial structure of lignin [50]

It is one of the most abundant organic polymers on Earth (exceeded only by cellulose). It is the third important constituent of the cell walls of woody biomass. Lignin is the cementing agent for cellulose fibers holding adjacent cells together. The dominant monomeric units in the polymers are benzene rings. It is similar to the glue in a cardboard box, which is made by gluing together papers in special fashion. Lignin is highly insoluble, even in sulphuric acid [45]. The polymeric lignin that one isolates from wood is chemically altered, which means that many lignin bonds are broken in order to separate the lignin from the wood, and the resultant lignin is often called by the name of the process ("Kraft lignin", "Klason lignin", "Thermomechanical lignin", …) [51]. A typical hardwood contains about 18 to 25%, while softwood contains 25 to 35% by dry weight [45]. The order of decreasing Lignin contents is normally: softwoods > hardwoods > herbaceous and agricultural biomass or non-woody biomass. The annual biomass species have commonly lower lignin value than perennial biomass species. However, it was also found that the lignin concentrations are normally higher in leaves and young shoots than in stems for different woods [43]. As is stated in [49] the lignin,

as well, largely controls the viscoelastic properties of the wood. According [52] in the process of biomass densification at elevated temperatures lignin softness and helps the binding process.

3.2.1.2 Cellulose

Cellulose is generally the largest fraction, representing about 40–50% of the biomass by weight (Figure 3.3) [44].Cellulose, the most common organic compound on Earth, is the primary structural component of cell walls in biomass. Its amount varies from 90% (by weight) in cotton to 33% for most other plants [45]. Represented by the generic formula $(C_6H_{10}O_5)_n$, cellulose is a long chain polymer with a high degree of polymerization and a large molecular weight, consisting of linear chains of (1,4)-D-glucopyranose units, in which the units are linked 1–4 in the β-configuration [44, 45]. Cellulose forms long chains that are bonded to each other by a long network of hydrogen bonds (Figure 3.4) [53]. This carbohydrate has fibrous structure with smooth surface [54] and it is occasionally protected by a waxy outer surface as in the case for the cellulose structural tubes in straws [55]. It has a crystalline structure of thousands of units, which are made up of many glucose molecules. This structure gives it high strength, permitting it to provide the skeletal structure of most terrestrial biomass [45], and makes is insoluble in most solvents [51]. Cellulose is primarily composed of d-glucose, which is made of six carbons or hexose sugars [45].
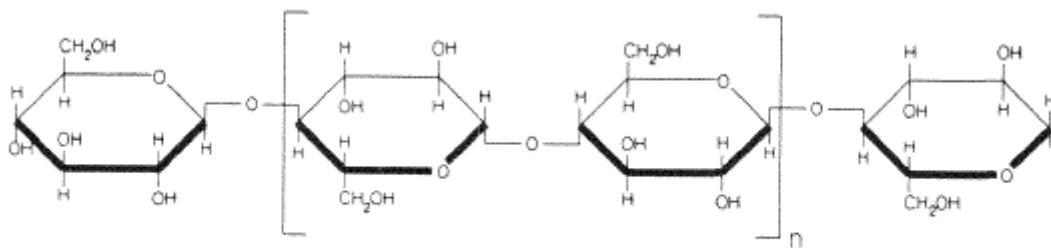
Figure 3.4 Structural formula of cellulose [51]

Biomass contains various proportions of two distinct crystalline polymorph phases of cellulose, namely: (1) the form Ia which is triclinic, metastable and dominant

for lower plants; and (2) the form Ib which is monoclinic, stable and dominant for higher plants [43].

3.2.1.3 Hemicelluloses

Hemicellulose is another constituent of the cell walls of a plant. While cellulose is of a crystalline, strong structure that is resistant to hydrolysis, hemicellulose has a random, amorphous structure with little strength, which contain 50 to 200 monomer units and exhibit a branched rather than a linear structure, and it represents 20–40% of the biomass material by weight [44, 45, 51].

Hemicelluloses, represented by the generic formula $(C_5H_8O_4)_n$ [45], are polysaccharides of variable composition including both five and six carbon monosaccharide units, plus glucuronic and galacturonic acids [43, 47]. In contrast to cellulose, hemicellulose is a heterogeneous branched polysaccharide that binds tightly, but non-covalently, to the surface of each cellulose microfibril. Hemicellulose differs from cellulose, in consisting primarily of xylose and other five-carbon monosaccharides [44].

The reference investigations show that hemicellulose is commonly described as xylan, pentosan or polyose [43]. Figure 3.5 shows the molecular arrangement of a typical hemicellulose molecule, xylan.
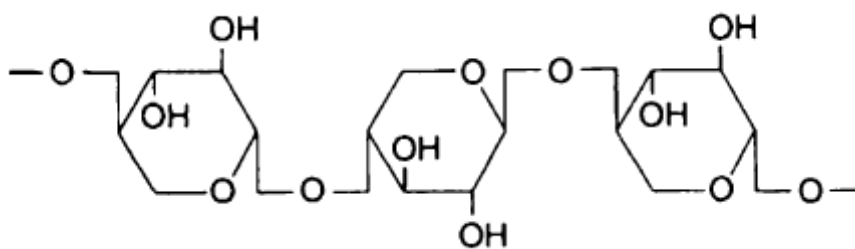
Figure 3.5 Molecular structure of a typical hemicelluloses, xylan. [45]

There is significant variation in the composition and structure of hemicellulose among different biomass. Most hemicelluloses, however, contain some simple sugar residues like d-xylose (the most common), d-glucose, d-galactose, l-ababinose, d-glucurnoic acid, and d-mannose. Hemicellulose tends to yield more gases and less tar

than cellulose. It is soluble in weak alkaline solutions and is easily hydrolyzed by dilute acid or base. It constitutes about 20 to 30% of the dry weight of most wood [45].

3.2.2 Proximate composition

Proximate analysis helps to assess the percentage of moisture content, volatile matter, fixed carbon and ash contents. This analysis is very important to study the combustion phenomenon of biomass. For instance, ash contents in biomass fuels can cause ignition and combustion problems. The melting point of the dissolved ash can be low, this causes fouling and slagging problems. High volatility of the biomass offers many advantages as a combustion feedstock. Moreover, high fixed carbon and volatile matter increase the heating value of any biomass fuels [42].

There are large variations for the characteristics determined by the proximate analyses of biomass samples. However, these variations are mostly due to the moisture contents and ash yields, which vary in the greatest intervals. When the measured parameters are recalculated on dry and dry ash-free basis their variations are in more narrow ranges for biomass groups and sub-groups. Therefore, it is better to use dry, dry ash-free or ash basis for comparative chemical characterization of biomass varieties. The moisture content and ash yield are important parameters of the biomass system and require a more detail discussion [46].

According results that are presented in [46], which taking in consideration contents of structural components of numerous varietes of biomass, in Table 3.3 is presented minimum, maximum and mean values of volatile matter, fixed carbon, moisture content and ash yeald, for wood and woody biomass (28 different speaces), herbaceous and agricultural biomass (10 different speaces) and contaminated biomass (7 different speaces). Given results clearly represent high variations in contents, even within the same type of biomass.

Table 3.3 Proximate analysis of different types of biomass [46]

Biomass group	Volatile Matter	Fixed Carbon	Moisture content	Ash yield
Wood and woody biomass				
Average	*62.9*	*15.1*	*19.3*	*2.7*
Minimum	*30.4*	*6.5*	*4.7*	*0.1*
Maximum	*79.7*	*24.1*	*62.9*	*8.4*
Herbaceous and agricultural biomass				
Average	*66.0*	*16.9*	*12.0*	*5.1*
Minimum	*41.5*	*9.1*	*4.4*	*0.8*
Maximum	*76.6*	*35.3*	*47.9*	*18.6*
Contaminated biomass				
Average	*63.7*	*8.0*	*11.6*	*16.7*
Minimum	*40.9*	*0.5*	*2.5*	*3.2*
Maximum	*79.0*	*14.5*	*38.1*	*43.3*

3.2.2.1 Ash content

The composition of biomass ash is strongly dependent on the species and part of the biomass plant [42].

Biomass has highly variable composition and properties, especially with respect to moisture, structural components and inorganic constituents. These characteristics are more changeable and differ significantly in comparison with those of coal and a good understanding is critical for proper use of biomass and/or co-processing with coal and other fuels. The major and minor elements in biomass, in decreasing order of abundance, are commonly C, O, H, N, Ca, K, Si, Mg, Al, S, Fe, P, Cl and Na, plus Mn, Ti and other trace elements. In comparison with coal, natural biomass is normally: (1) highly enriched in Mn > K > P > Cl > Ca > (Mg,Na) > O > moisture >volatile matter; (2) slightly enriched in H; and (3) depleted in ash, Al, C, Fe, N, S, Si and Ti [56]. The available nutrients, soil quality, fertilizers and weather conditions have significant impact on the contents of potassium, sodium, chlorine and phosphorus especially in agro-biomass ashes [42].

The ash yield (db) determined at 550–600 °C for biomass varies in the interval of 0.1–46% and normally decreases in the order: Animal Biomass > Contaminated

Biomass > Herbaceous and agricultural biomass > Wood and woody biomass. In contrast, the ash content (815 °C) in peat and coal (db) is in the relatively more narrow range of 4–52% (commonly 4–30%). The ash normally shows much lower value in biomass than in solid fossil fuels, excluding Animal biomass and some Contaminated Biomass and Herbaceous and agricultural biomass samples. The ash in Wood and woody biomass decreases in the order: foliage > bark > wood. The high ash yields of some wood fuels such as chemically treated wood and waste wood are an indication for increased amounts of mineral and metallic impurities and other contaminants due to the manufacturing process. Hence, there is agreement between the present and reference data, but some additional elucidation of this important parameter is required. The ash is one of the most studied characteristics of biomass, but unfortunately with the poorest understanding. The complex character of this parameter is the reason for such a problem because ash originates simultaneously from natural and technogenic inorganic, organic and fluid matter during biomass combustion [46].

3.2.2.2 Moisture content

Moisture content (M), the water mass per unit mass of dry or wet material, is an important fuel characteristic and related to physical properties and flow characteristics (e.g. bulk density and cohesion strength) [57].

High moisture is a major characteristic of biomass [58]. Moisture in solid fuels can exist in two forms, as free water within the pores of the fuel, and as bound water which is absorbed in the interior surface structure of the fuel [3].

Bound water (M_b) is found in the cell wall and is believed to be hydrogen bonded to the hydroxyl groups of primarily the cellulose and hemicelluloses, and to a lesser extent also to the hydroxyl groups of lignin [51]. The moisture in biomass is mineralized aqueous solution containing cations (Al, Ca, Fe, K, Mg, Mn, Na, Ti), anions (Br, Cl, CO_3, F, HCO_3, H_2PO_4, I, NO_3, OH, PO_4, SO_4) or non-charged species (H_4SiO_4). This fluid plays a key role for the composition of biomass because of: (1) high water content in the living cells; (2) variable total mineralization of water (dissolved solid matter); and (3) different chemical specification (predominant anions, cations and their ratios) of these water solutions [46].

Free water (M_f) in liquid from is found in the lumens or voids of the wood. The amount of free water which wood may hold is limited by the fraction void space or porosity of the wood. There is no hydrogen bonding and therefore is held only by weak capillary forces and cannot cause swelling or shrinking or changes in most other physical properties because the cell wall is already saturated.

The moisture content is the quantity of moisture in the wood expressed as a percentage of oven-dry mass. The latter is defined as the constant mass obtained after wood has been dried in an air oven maintained at $102 \pm 3°C$ [51].

$$M = \frac{m_s - m_{sd}}{m_{sd}} = M_b - M_f$$

(3.1)

where: $\qquad$ m_s= green or moist mass

$\qquad$ m_{sd}= oven-dry mass.

The moisture content in biomass as measured (at different basis, but normally as received, air-dried and oven-dried basis) varies in the interval of 3–63% and it can reach even 80% for raw wood species [46].

The maximum moisture content of raw materials for thermochemical processes can be up to 65%. As the moisture content increases, so does the cohesive strength of the particulate material. Increasing moisture content therefore usually accentuates the tendency to bridge and block biomass feeding systems, especially for long thin particles [57].

3.2.2.3 Volatile matter

The volatile matter (VM) of a fuel is the condensable and noncondensable vapor released when the fuel is heated. Its amount depends on the rate of heating and the temperature to which it is heated [45]. The volatiles are that part of the organic content of the fuel that is released in 7 minutes at a temperature of 900°C under exclusion of air (according to EN 15148) [49]. The volatile matter yield of biomass commonly includes light hydrocarbons, CO, CO_2, H_2, moisture and tars [46].

The amount of volatile matter in biomass fuels is higher than in coals, and usually varies between 70 and 86wt% (d.b.). As a result of this high amount of volatiles, the major part of a biomass fuel is vaporized before homogeneous gas phase combustion reactions take place; the remaining char then undergoes heterogeneous combustion reactions. Therefore, the amount of volatile matter strongly influences the thermal decomposition and combustion behavior of solid fuels [3].

3.2.2.4 Fixed carbon

The fixed carbon content (FC), is the mass remaining after the releases of volatiles, excluding the ash and moisture contents [44].

$$FC = 1 - M - VM - ASH \qquad (3.2)$$

Biomass carbon comes from photosynthetic fixation of CO_2 and thus all of it is organic. During the determination of VM, a part of the organic carbon is transformed into a carbonaceous material called pyrolytic carbon [45].

The fixed carbon content (db) in biomass varies in the interval of 1–38% and normally decreases in the order: HAR > HAB > WWB > HAS > HAG > AB > CB. In contrast, the fixed carbon value in peat and coal (db) is commonly in the larger range of 20–72%. This parameter typically reveals lower content in biomass than in SFFs. The extremely high fixed carbon content is characteristic of some wood barks and HAB residues. Furthermore, biomass commonly has a volatile matter/fixed carbon ratio >3.5, while this ratio for peat and coal is normally in the interval 0.6–2.4 [46].

The plotted mean proximate composition (db) of solid fuel types in Figure 3.6 illustrates:

(1) the differentiations between the biomass and coals; (2) the relatively closer position of peat to biomass than coals; and (3) the similarities among various biomass groups and sub-groups, excluding only AB and CB biomass groups. The distinctions for the last groups are evidenced by their plots in Fig. 1 and maximum or minimum values in the above-listed orders for the proximate characteristics. Both AB and CB groups

commonly have intermediate positions between SFFs and other biomass groups and sub-groups [46].
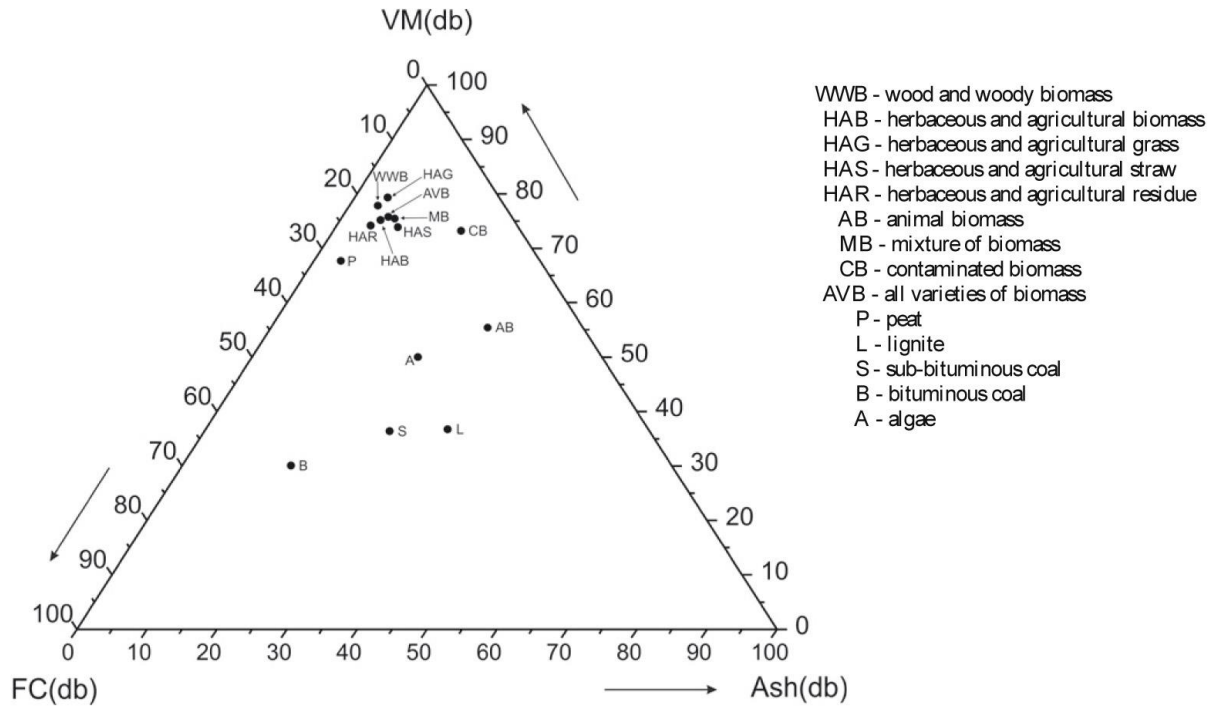
Figure 3.6 Mean proximate composition of solid fuel types, wt.% [46]

3.2.3 Ultimate composition

Ultimate analysis provides the chemical composition of the biomass in elemental terms, and is used to determine combustion air requirements, flue losses and likely emission levels [2]. Inorganic material in biomass can be divided into two fractions, one of which is inherent in the fuel and the other of which is added to the fuel through processing steps [47]. Ultimate analysis is one of the important factors when studying biomass fuels properties. It helps to assess the percentage of N, S and Cl to study the environmental impact of biomass. Moreover, it helps to calculate the percentage of C, H, O to estimate the heating value of these fuels. Table 3.4 shows ultimate analysis of different types of biomass [42].

Beside the experimental analysis in order to determinate the ultimate composition of biomass, published literature [60, 61, 62] gives correlation between elemental composition and proximate analysis. According [60] there is a correlation for

calculating the elemental composition based on proximate analysis of biomass. The correlations are given as: C = 0.635FC + 0.460VM - 0.095ASH, H = 0.059FC + 0.060VM + 0.010ASH, O = 0.340FC + 0.469VM - 0.023ASH, where 9.2% ≤ FC ≤ 32.79%, 57.2% ≤ VM ≤ 90.6%, 0.1% ≤ ASH ≤ 24.6%, 36.2% ≤ C ≤ 53.1%, 4.7% ≤ H ≤ 6.61%, and 31.37% ≤ O ≤ 48.0% in wt.% on dry basis, where FC, VM, C, H and O represent fixed carbon, volatile matter, carbon, hydrogen and oxygen content of biomass, respectively.

Table 3.4 Ultimate analysis of different types of biomass, wt%. [42]

Biomass group	C	O	H	N	S
Wood and woody biomass					
Average	52.1	41.2	6.2	0.4	0.08
Minimum	48.7	32.0	5.4	0.1	0.01
Maximum	57	45.3	10.2	0.7	0.42
Herbaceous and agricultural biomass					
Average	49.9	42.6	6.2	1.2	0.15
Minimum	42.2	34.2	3.2	0.1	0.01
Maximum	58.4	49.0	9.2	3.4	0.60
Contaminated biomass*					
Average	53.6	37.0	7.3	1.7	0.46
Minimum	45.4	16.4	6.0	0.2	0.01
Maximum	70.9	46.1	11.2	6.1	2.33

* Contaminated biomass here includes: Currency shredded, Demolition wood, Furniture waste, Mixed waste paper, Greenhouse-plastic waste, Refuse-derived fuel, Sewage sludge, Wood yard waste.

Decreasing order of mean values for the chemical characteristics of the biomass groups and sub-groups is given in Table 3.5.

Table 3.5 Decreasing order of mean values for the chemical characteristics of the biomass groups and sub-groups specified [46]

Symbol	Order for groups and sub-groups
M (am)	WWB > HAG > HAR > HAB > CB > HAS > AB
VM (db)	HAG > WWB > HAB > HAS > HAR > CB > AB
FC (db)	HAR > HAB > WWB > HAS > HAG > AB > CB
A (db)	AB > CB > HAS > HAB > HAR > HAG > WWB
C (daf)	AB > CB > WWB > HAR > HAB > HAS > HAG
O (daf)	HAG > HAS > HAB > HAR > WWB > CB > AB
H (daf)	AB > CB > HAR > (WWB, HAB) > (HAG, HAS)
N (daf)	AB > CB > HAR > (HAB, HAS) > HAG > WWB
S (daf)	AB > CB > HAR > (HAB, HAS) > HAG > WWB
Cl (db)	AB > HAS > CB > HAG > HAB > HAR > WWB
SiO_2	HAG > HAS > CB > HAB > HAR > WWB > AB
CaO	AB > WWB > CB > HAR > HAB > HAS > HAG
K_2O	HAR > HAB > HAG > HAS > WWB > AB > CB
P_2O_5	AB > HAR > HAG > HAB > HAS > CB > WWB
Al_2O_3	CB > WWB > HAR > HAB > HAS > AB > HAG
MgO	HAR > WWB > HAB > HAS > HAG > CB > AB
Fe_2O_3	CB > HAR > WWB > HAB > HAS > HAG > AB
SO_3	AB > HAR > HAG > HAB > CB > HAS > WWB
Na_2O	AB > HAR > WWB > HAB > CB > HAS > HAG
TiO_2	CB > WWB > HAR > HAB > HAS > HAG > AB
Mn	WWB > HAG > HAR > CB > HAB > HAS > AB

Abbreviations: AB, animal biomass; CB, contaminated biomass; HAB, herbaceous and agricultural biomass; HAG, herbaceous and agricultural grass; HAR, herbaceous and agricultural residue; HAS, herbaceous and agricultural straw; WWB, wood and woody biomass.

3.2.3.1 Carbon (C), hydrogen (H) and oxygen (O)

C, H and O are the main components of solid biofuels. C and H are oxidized during combustion by exothermic reactions (formation of CO_2 and H_2O). The content of C and H contributes positively to the gross calorific value (GCV), the content of O negatively. H also influences the net calorific value (NCV) due to the formation of water. The C contents of wood fuels (including bark) are higher than those of herbaceous biofuels, which explains the slightly higher GCV of wood fuels [63]. This element typically shows lower content in biomass than in SFFs. The extremely high C content is characteristic of some wood barks and high-ash greenhouse-plastic waste, chicken litter, meat-bone meal, and refuse-derived fuel [46].

On a dry ash-free basis all wood types are similar, with a relatively high oxygen content compared with fossil fuels. This is typical of lower-ranked fuels in terms of energy content [2].

The O content in biomass is mostly calculated by difference and this element typically shows much higher content in biomass than in SFFs [46]. The organically bound O released through the thermal decomposition of biomass fuels covers a part of the overall O needed for the combustion reactions taking place; the rest is supplied by air injection [3].

The H commonly shows higher content in biomass than in SFFs. The extremely high H content is characteristic of greenhouse-plastic waste, tamarack bark, mustard and cotton husks, meat-bone meal, refuse-derived fuel, and groundnut shells. The H value normally decreases in the order: AB > CB > HAR > (WWB, HAB) > (HAG, HAS) (Table 3.5). The similar order of H and C indicates their association (occurrence and behavior) in biomass probably as hydrocarbons and carbohydrates. It is well-known that photosynthesis results in the production of structural and non-structural carbohydrates comprising the plant tissues [46]. The molar ratios of oxygen and hydrogen to carbon for a wide range of biomass fuels are shown in Figure 3.7. The amount of variation is not particularly large considering the range of different materials examined [47].
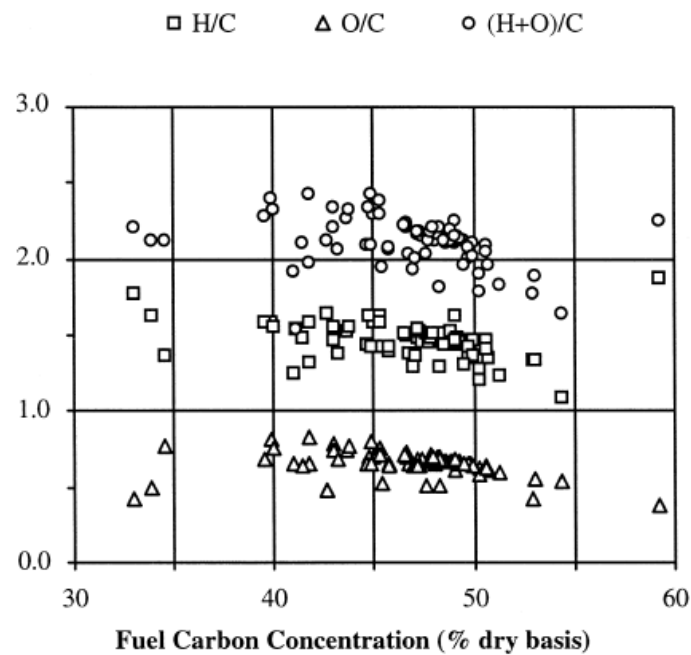
Figure 3.7 Molar ratios of hydrogen and oxygen to carbon in biomass [47]

3.2.3.2 Nitrogen (N)

The fuel N content is responsible for NOx formation. NOx emissions belong to the main environmental impact factors of solid biofuel combustion [63]. The N content in biomass varies in the interval of 0.1–6.1% (Table 3.4) and normally decreases in the order: AB > CB > HAR > (HAB, HAS) > HAG > WWB (Table 3.5). In contrast, the N value in peat and coal is in the narrow range of 1–3% [46]. Coniferous and deciduous wood has the lowest N content. Higher concentrations are found in bark, logging residues, short rotation coppice (willow and poplar) and straw from wheat, rye and barley. The concentrations are usually still higher in rape straw (wheat, rye and barley straw can also have N contents in this range), miscanthus and fruit residues (e.g. olive or grape cakes, kernels, shells). Grains and grasses usually show the highest values [63].

This mobile element normally has slightly lower content in biomass than in SFFs, excluding AB and some varieties from CB and HAB groups. The extremely high N content is characteristic of meat-bone meal, chicken litter, sewage sludge, pepper residues, alfalfa and mint straws, palm kernels, and buffalo gourd grass. [46].

3.2.3.3 Sulphur (S)

The sulphur content of biomass is usually very 1ow compared with that of coal, excluding AB and some varieties from CB and HAB groups [2, 46]. It should not therefore lead to emission problems of SO_x (thought to contribute to acid rain), or to corrosion of the conversion plant components outside the combustion zone owing to high acid dew points, when sulphuric acid can be formed as the gases cool and then eventually condense [2].

The S content in biomass varies in the interval of 0.01–2.33% (Table 3.4) and normally decreases in the order: AB > CB > HAR > (HAB, HAS) > HAG > WWB (Table 3.5). This order is identical to N and indicates the close association of both N and S. It was noted that bark and straw have a higher S content than wood, but some wood products (pellets and briquettes) can also contain S-bearing additives [46].

The plotted mean ultimate composition (daf) of solid fuel types in Figure 3.8 illustrates: (1) the differentiations between the biomass and coals; (2) the closer position of peat to biomass than coals; and (3) the similarities among various biomass groups and sub-

groups, excluding again (like the proximate composition) only the AB and CB biomass groups. Both AB and CB groups have intermediate positions between SFFs and other biomass groups and sub-groups [46].
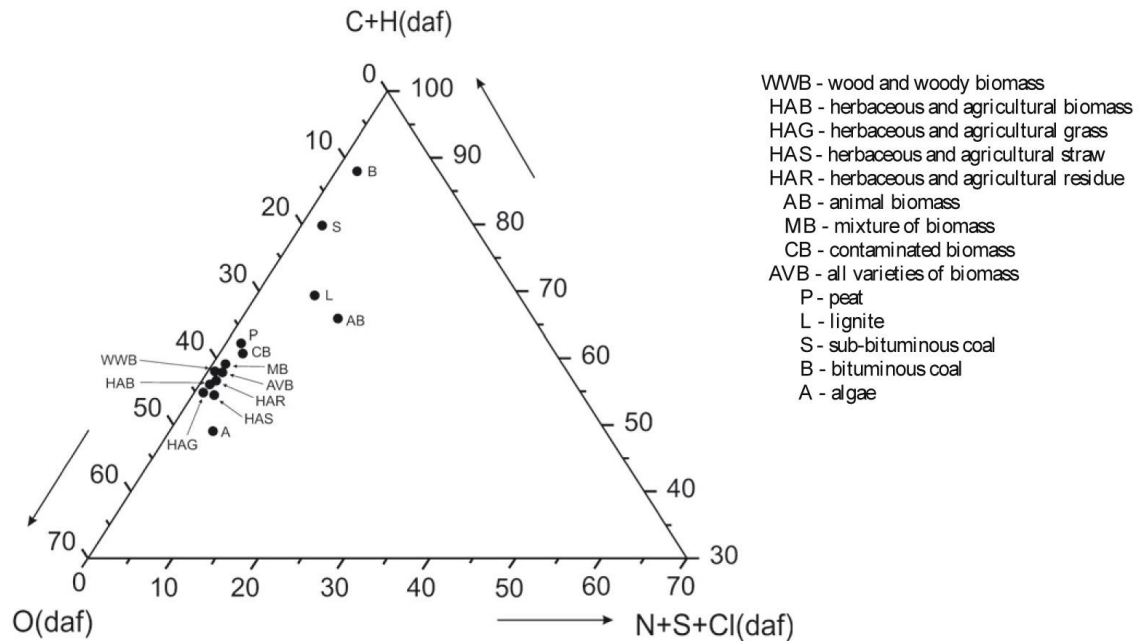
Figure 3.8 Mean ultimate composition of solid fuel types, wt.% [46]

3.3 Densification of biomass

In order to utilize biomass in the most energy efficient way and from the perspective of techno-economic analysis, biomass has to pass through a series of interlinking procedures. The summation of these procedures or path from planting to the point at that the chemical energy of biomass as a fuel is converted into heat is called the *supply chain*.

The fuel supply chain (Figure 3.9) consists of a series of sequential steps such as planting, growing, harvesting, comminution, densification, drying, storage, transport and handling. The combination of these steps depends on the kind of biomass as well as on the needs of the combustion plant and determines feedstock form and costs. The aim is to have the whole chain functioning smoothly and cost-effectively with a minimum of losses along the way for a given system. The sequence of steps in the chain can be

varied (alternative supply strategies) to meet the needs of a given conversion technology and cost structure [3].
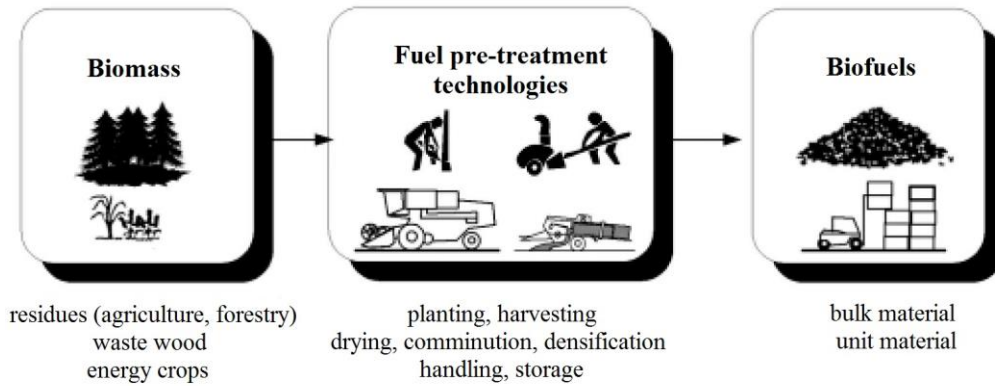
Figure 3.9 Fuel supply chain for woody biomass [3]

Liquids and gases are relatively easy to handle because they continuously deform under shear stress—they easily take the shape of any vessel they are kept in and flow easily under gravity if they are heavier than air. For these reasons, storage, handling, and feeding of gases or liquids do not generally pose a major problem [58].

Since the objective of this thesis is combustion of pelletized three types of biomass and their mixtures, in this subchapter the focus will be on densification process.

In order to make the biomass materials available for a variety of applications, the challenges with the use of biomass materials in their original form must be resolved. Because of high moisture content, irregular shape and sizes, and low bulk density, biomass is very difficult to handle, transport, store, and utilize in its original form. One solution to these problems is densification of biomass materials into pellets, briquettes, or cubes [64]. As well, as it stated in [65], when biomass is co-fired with coal, the difference in density between biomass and coal makes the energy density of the two fuels different, and causes difficulties in feeding the fuel into the boiler, densified biomass fuel can ease these problems.

Densification increases the bulk density of biomass from an initial bulk density (including baled density) of 40–200 kgm^{-3} [64], 80 – 150 kgm^{-3} for herbaceous and 150 – 200 kgm^{-3} for woody biomass [48], to a final bulk density of 600 – 800 kgm^{-3}. Thus, densification of biomass materials could reduce the costs of transportation (the low bulk

density of fresh biomass as compared to coal restricts the economic transportation distance less than 200 km [66]), handling, and storage. Because of uniform shape and sizes, densified products can be easily handled using the standard handling and storage equipment, and can be easily adopted in direct-combustion or co-firing with coal, gasification, pyrolysis, and in other biomass-based conversions [64].

According to [42] densification of biomass is a very important factor to increase its density and thus improve biomass quality. Densification has the following advantages:

- Densification raises the energy density (kJ/m^3 Fuel) which makes combustion in boilers more efficient;
- Densification reduces costs associated with the handling, storage and transportation of the biomass fuel;
- Densification improves biomass stability and durability.

Before entering into any densification equipment, feed is ground to a desired particle size, subjected to pretreatments such as mixing with additives or fats, and conditioned with steam or expander to increase the temperature and/or moisture level [67]. Pretreatment of herbaceous and woody biomass increases both its physical and chemical properties, thereby making the material easy to densify and helping minimize the costs of transport, handling, and storage [48].

Pretreatment methods include:
- Grinding;
- Preheating;
- Steam conditioning and explosion;
- Torrefaction.

Densification of lignocellulosic material is a complex process and no coherent theory exists. Besides material specific factors, compaction pressure, compaction temperature, compaction velocity, moisture content (binding agent and a lubricant) and distribution of particle size determine the outcome of press agglomeration [68].

Several studies showed that strength and durability of the densified products increased with increasing moisture content until an optimum is reached [48]. Moisture addition to dry bulk solids increases adhesion forces between particles, and against

adjacent surfaces. An increase in moisture content over an optimum limit does not improve production [69].

Pretreatment using high temperatures makes the material more energy dense, opens up the cell-wall structure, and makes the material easy to densify and transport [48]. The temperature of the feed is usually increased to activate the inherent binders or added binders (i.e., additives). Elevated temperatures also promote plastic deformation of thermoplastic particles. Plastic deformation of particles is important for making permanent bonding. Feed temperature can be increased by either direct or indirect heating. Direct heating includes friction, fluidized bed heating, and steam conditioning. Indirect heating includes conduction-based heating systems such as band-electrical resistance heaters, and hot-oil circulation heat exchangers. Preheating temperature is limited to 300 °C to avoid decomposition of biomass materials [70].

The temperature of the densified products after leaving the densification equipment is generally higher than the conditioned feed due to frictional heat developed in the pressing systems and, therefore, densified products are cooled using ambient air before storing/packaging [67].

Torrefaction involves the heating of biomass at moderate temperatures (220–300 °C) under an inert atmosphere. Torrefaction is influenced by many parameters that include the composition of the biomass and operation conditions [71]. The process is also called a mild pyrolysis as most of the smoke-producing compounds and other volatiles are removed resulting in a final product that has approximately 70% of the initial weight and 80–90% of the original energy content. Thus, treatment yields a solid uniform product with lower moisture content and higher energy content compared to the initial biomass [48]. As it stated in [58] after the process of torrefaction biomass stop to absorbing moisture. Torrefied biomass is brown to blackish brown in colour, it has a smoky smell and properties similar to coal [59].

The binding forces that act between the individual particles in densified products have been categorized into five major groups. They are (i) solid bridges, (ii) attraction forces between solid particles, (iii) mechanical interlocking bonds, (iv) adhesion and cohesion forces, and (v) interfacial forces and capillary pressure [64].

According [72] there are three stages during densification of biomass. In the first stage, particles rearrange themselves to form a closely packed mass where most of the

54

particles retain their properties and the energy is dissipated due to inter-particle and particle-to-wall friction. In the second stage, the particles are forced against each other and undergo plastic and elastic deformation, which increases the inter-particle contact significantly; particles become bonded through van der Waal's electrostatic forces. In the third phase, a significant reduction in volume at higher pressures results in the density of the pellet reaching the true density of the component ingredients. Figure 3.10 presents the deformation mechanism of the powder particles under compression.

Due to the application of high pressures and temperatures, solid bridges may be developed by diffusion of molecules from one particle to another at the points of contact. Solid bridges may also be formed between particles due to crystallization of some ingredients, chemical reaction, hardening of binders, and solidification of melted components. Solid bridges are mainly formed after cooling/drying of densified products [64].

The attraction between the particles is due to van der Waal's electrostatic or magnetic forces. The attraction is inversely proportional to the distance between the particles, where larger distances have less attraction. Electrostatic forces' influence on particle bonding is negligible, and these are commonly encountered in dry fine powders where inter-particle friction can also contribute to particle bonding when magnetic forces exist. Closed bonds or interlocking occurs in fibers, platelets, and bulk particles, where particles interlock or fold about each other, thereby causing the bonding. Interlocking of the particles can help provide sufficient mechanical strength to overcome the destructive forces caused by elastic recovery after compression [48].
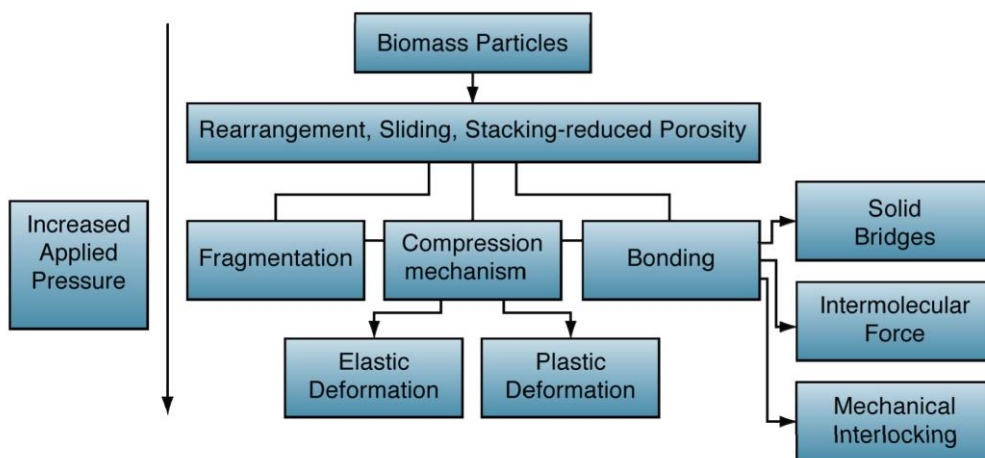
Figure 3.10 Deformation mechanisms of powder particles under compression [48]

Densification of biomass can be categorized into 5 types: (1) Baling, (2) Extrusion, (3) Pelletizing, (4) Briquetting roller press, and (5) Punch and die press [42].

3.3.1 Balers

Baler uses ram mechanism to compress biomass in a specifically designed steel chamber, then the compressed biomass is banded or tied prior to being released and hauled away in a uniform size and shape. Commonly, balers are used to reduce storage space and transportation cost [42].

Herbaceous biomass fuels such as straw, hay or cereals are pressed into bales to increase their energy density and to ease handling. Baling of straw is usually done as an extra process step after grain harvesting or feedstock cutting. For energy crops such as miscanthus or cereals, one-step combined harvesting and baling is possible. Baling of forest residues before transport, in combination with centralized chipping, is a comparatively new approach to reduce the production costs of forest woodchips. Initial activities in this direction were reported in the mid 1990s. The bales are similar to round straw bales, with a diameter of 1.2 m and 1.2 m high [3].

3.3.2 Extrusion

The aim of compaction using an extruder is to bring the smaller particles closer so that the forces acting between them become stronger, providing more strength to the densified bulk material. During extrusion, the material moves from the feed port, with the help of a rotating screw, through the barrel and against a die, resulting in significant pressure gradient and friction due to biomass shearing [48]. The diameter of extrusion products may range from 20 to 100 mm [64]. Figure 3.11 shows the typical extruder.

There are various types of extrusion such as:

- Ram-type extrusion (this type uses a reciprocating ram (piston or rod) that forces raw material falling from the feed hopper through a tapered die),

- Screw extrusion (this type uses a screw to force a feedstock under high pressure into a die, thereby forming large cylinders 2.5–10 cm in diameter) [42].
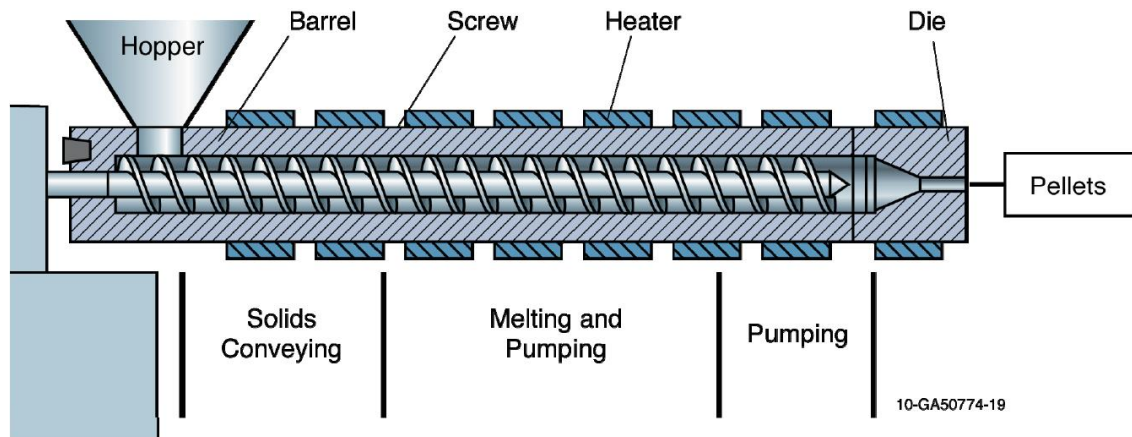
Figure 3.11 Extruder for biomass processing [48]

3.3.3 Pelleting (pelletizing)

Pellets are a solid biomass fuel with consistent quality – low moisture content, high energy density and homogeneous size and shape. Consistent fuel quality makes pellets a suitable fuel type for all areas of application, from stoves and central heating systems to large-scale plants. [59]. Compared to traditional firewood, pellets provide possibilities for automation and optimization similar to oil, with high combustion efficiency and low combustion residues [73].

Pelletizing process consists of few interconnected steps (Figure 3.12), which could be classified as:

- **Drying**: The moisture content of the raw material is an important parameter for the pelletizing (compaction) process because moisture facilitates the heat transfer and friction [74]. Moisture acts as one of the binding agents in the pelleting process [75]. Depending on the kind of wood used, the moisture content of the raw material before entering the pellet press must be between 8 and 15wt% [3, 75, 76] or even 17–20% wb for high pelletising temperatures (up to 180 °C) [75]. Due to the fact that the stability of the pressings is influenced by the friction between gooseneck and raw material, constant moisture content is essential. If the material is too dry, the surface of the particle may carbonize and binders will get burned before the process is finished. If the wood is too wet, moisture contained in the pressings cannot escape and enlarges the product volume, making it mechanically weak [3].

57
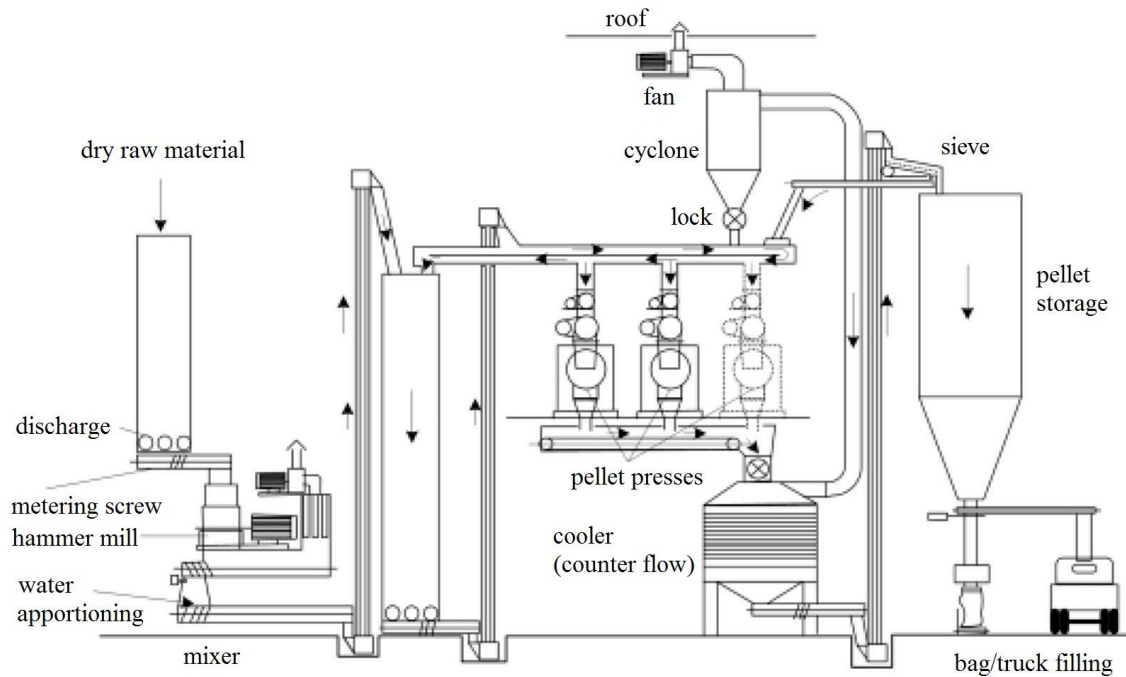
Figure 3.12 Pelletizing plant [3]

- **Size reduction (Grinding)**: After drying, or of course as a primary step when the material is dry already, the raw material is ground up to the required particle size. The particle size of the raw material must be reduced and homogenized depending

  on the diameter of the pellets produced, sawdust is ground to a particle size usually less than 4 mm [3, 59, 76]. Grinding of raw material is generally done by hammer mills because they achieve the right fineness and homogenization [59].

- **Conditioning**: Conditioning denotes the addition of steam or water to the prepared materials just before pelletising [59]. By the addition of steam, the particles are covered with a thin liquid layer in order to improve adhesion [3]. Another way of conditioning is the utilisation of biological additives. It too takes place just before pelletising inside a mixer, in order to achieve thorough mixing of the biological additive and raw material, which ensures it can work as it should [59].

- **Pelletizing**: This sequence of process is achieving by extruding of already prepared feedstock through die holes (Figure 3.13). The pelleting press consists of a drum-shaped hard steel die which is perforated in the perimeter with a dense

array of holes 0.3–1.3cm in diameter [42], mostly 0.6 cm [59]. The die rotates against an inner pressure roller, forcing the biomass feedstock into the die holes, as the pellets are extruded through the die holes, they broke off at a specified length (normally less than 3 cm, and according) [42]. Important parameters of pelletising are the press ratio, the quantity of bore holes and the resulting open area of holes (without considering the inlet cones) [59].

a)   b)
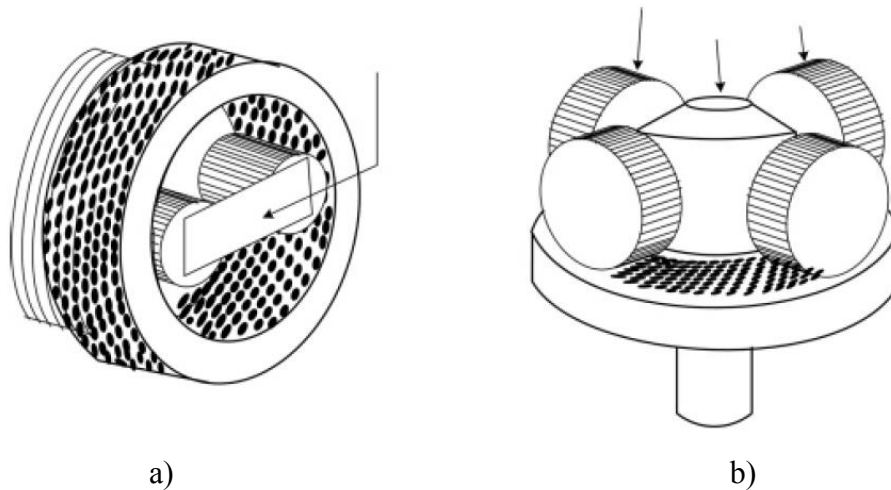
Figure 3.13 Ring die pelletizer (a) and flat die pelletizer (b) [3]

The dimensions of the pellets, both diameter and length, are important factors with respect to combustion. Experience has shown that thinner pellets allow a more uniform combustion rate than thicker ones, especially in small furnaces. The length of the pellets affects the fuel feeding properties, the shorter the pellets the easier the continuous flow can be arranged [75]. According [75] the pellets had higher ash content and lower calorific heating value than the raw materials, probably due to loss of volatiles during drying. The friction between the wood material and the die during the forced passage results in a rise in temperature. This in combination with the moisture content of the raw material softens the wood components and is assumed to have a crucial influence on the self-bonding processes. Because no adhesives are used in the process, wood pellets should be considered as a specific kind of binder less wood particle product [76]. Bearing that in mind, abrasion is one of the most important pellet parameters. The main reason for this is the fact that a high share of fines in the storage system of the end user can cause failures in the feeding system. A low

share of fines in the storage system is therefore essential for a high reliability of the equipment and for end user convenience. In addition a high share of fines also increases dust emissions during combustion [77].

With bulk density between 550 and 700 kg (w.b.)/m³, pellets are used in all areas ranging from small-scale furnaces with nominal capacities of up to 100 kWth and medium-scale furnaces with 100 to 1,000 kWhth to large-scale furnaces with nominal capacities of more than 1,000 kWhth. In addition, pellets are used in CHP as well as in co-firing in fossil fuel furnaces [59].

- **Cooling**: the temperature of the pellets increases during the densification process. Therefore, careful cooling of the pellets leaving the press is necessary to guarantee high durability [3]. Pellets leave the pellet press at temperatures of 60–95 _C and moisture contents of 12–18% (w.b.). The excess heat and moisture should be removed from the pellet for safe storage. Pellets are cooled (mostly using forced air) immediately after the die to within 5 _C of ambient temperature, and to within 0.5% of the original moisture content of the feed ahead of the conditioner. In general, the final moisture content of the pellets should be less than 13% (w.b.) [64].

3.3.4 Briquetting

The biofuel briquette is a clean and green fuel that can ideally be used in furnaces, boilers, or open fires. In the biomass briquetting process, the material is compressed under high pressure and temperature [48]. Briquetting of biomass can be done through various techniques [68]. During briquetting the biomass particles self-bond to form a briquette due to thermoplastic flow. Lignin, which is a natural binder, is made available from high temperatures and pressures resulting in the formation of high-density briquettes [48].

The technologies used for binderless biomass briquetting include machines based on screw and piston-pressed technology. Biomass in screw-pressed technology is extruded continuously by a screw through a taper die, which is externally heated to reduce friction. With piston-press technology, biomass is punched or pushed (corresponding to impact or hydraulic technology, respectively) into a die by a

reciprocating ram or plunger by high pressure. In both cases, application of high pressure increases the temperature of the biomass, and existing lignin in the biomass is fluidized and acts as a binder [68].

The basic technologies for briquetting are shown in Figure 3.14. A constant moisture content of the raw material (12–14wt% w.b.), a constant back-pressure in the briquette press and sufficient cooling are essential for the stability of the briquettes produced [3].
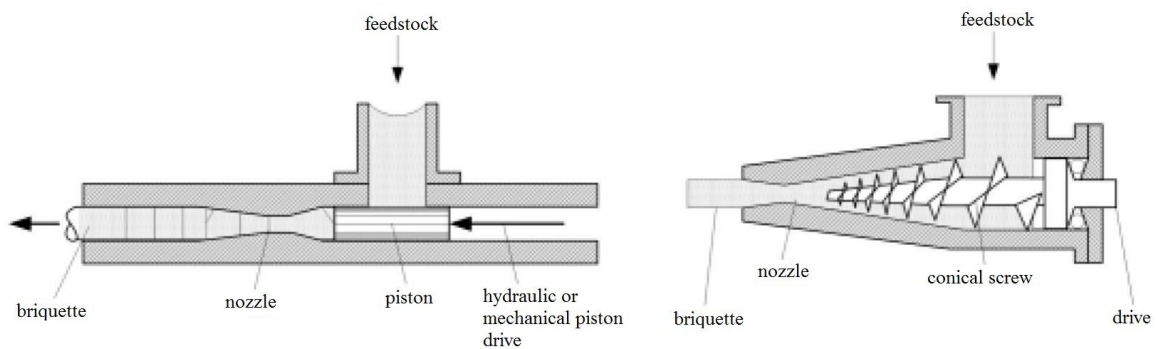
Figure 3.14 Briquetting technologies [3]

The briquettes' densities generally range from 900 to 1300 kg/m^3. Unlike pellet mills, briquetting machines can handle larger-sized particles and wider moisture contents without the addition of binders. Advantages of briquettes are the ease of charging the furnace, increased calorific value, improved combustion characteristics, reduced entrained particulate emissions, and uniform size and shape. In addition, furnaces that use other solid fuels can use briquettes also. The main disadvantage of using biomass briquettes or pellets in industrial furnaces is ash slagging due to the alkali content in briquettes made from biomass [48].

3.3.5 Punch and die

Punch and die (piston-and-mold) process can achieve high and uniform pressure so that dense and strong logs can be produced under normal temperature without having to use binder or heat [65]. Punch and die press uses two opposing pistons inside a cylinder to compress the material in the mold. Once compressed, the product in the form of a slug, log or tablet is pushed out of the mold by one of the two pistons. Due to this

method, the material can compacted under very high pressure even when the material is relatively wet [42].

During compaction, as the pressure becomes high, the displacement of the piston becomes less and less. At the final stage of compaction with very high pressure, the displacement becomes negligible. Therefore, the work done in the compaction process is much less than that for the pelletizing or extrusion process in which the ram is always geared up to the highest pressure when pushing the material forward. The compaction process (punch-and-die) also does not require preheating of materials. Materials can be compacted rapidly at room temperature to form good-quality products logs or slugs [65].

4. THERMOCHEMICAL CONVERSION OF BIOMASS

In order to maximize utilization of all the benefits offered by the use of biomass for energy purposes, must take into account the selection of appropriate conversion method, depending on the needs, as well as the impact of the overall process on the environment.

Biomass is used to meet a variety of energy needs, including generating electricity, heating homes, fueling vehicles and providing process heat for industrial facilities [78].

In order to benefit from the chemical energy contained in biomass, this energy has to be transformed into more convenient energy forms (heat or electricity) [79] or convert into more calorific fuel (Figure 4.1).
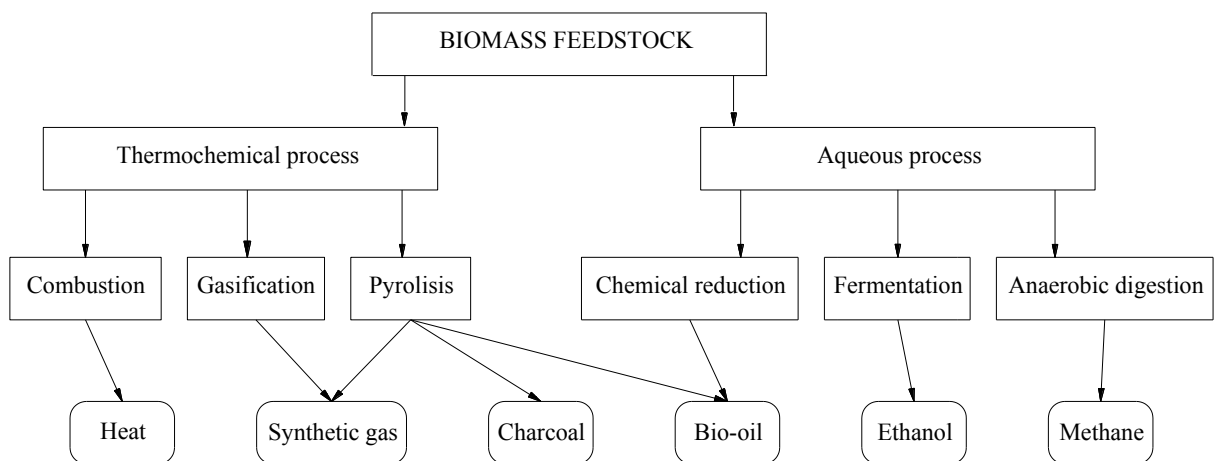
Figure 4.1 Biomass conversion paths

As this Ph.D. work concentrates only on the thermochemical conversion processes, this chapter focuses only on:

- Pyrolysis
- Gasification
- Combustion

Some of them are endothermic and others exothermic and often they take place simultaneously inside the same reactor. The products from any thermochemical process are [79]:

63

- a solid residue, called char;

- a gas product;

- a tarry liquid of complex composition, known as "tar", often present in vapour phase at process temperature.

4.1 Pyrolysis

Pyrolysis can be defined as thermal degradation (devolatilization) in the absence of an externally supplied oxidizing agent [3]. It is always also the first step in combustion and gasification processes where it is followed by total or partial oxidation of the primary products [80]. Pyrolysis of biomass starts at 350–550 °C and goes up to 700 °C. This leads to the production of useful liquid oil, gases and solid products. Different condition leads to formation of products in different proportions [81]. Chemical decomposition through pyrolysis is the same technology used to refine crude fossil fuel oil and coal. Pyrolysis produces energy fuels with high fuel-to-feed ratios, making it the most efficient process for biomass conversion and the method most capable of competing with and eventually replacing non-renewable fossil fuel resources [78].

In all thermo-chemical conversion processes, pyrolysis plays a key role in the reaction kinetics and hence in reactor design and determining product distribution, composition, and properties [82]. The biomass polymer fragments (volatiles) formed are driven out of the biomass particle due to the pressure that is being built up inside the particle. The intrinsic pyrolysis reactions are very fast, but in practice heating of the biomass particles and mass transfer limitation delays the pyrolysis process significantly [83]. The pyrolysis reactions and products are non-equilibrium and therefore hard to predict, the simplified pyrolytic reaction to convert the complex ligno-cellulose molecules of biomass to oils is [2]:

$$\left(C_xH_yO_z\right)+O_2+\text{heat} \rightarrow C+CO_2+CO+H_2O+\text{hydrocarbons}+\text{heat} \qquad (4\text{-}1)$$
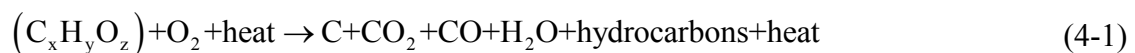
Some authors [3, 78, 84, 85, 81, 79] presents liquefaction as process separate from pyrolysis. Both are thermochemical processes in which feedstock organic compounds are converted into liquid products. In the case of liquefaction, feedstock macromolecule compounds are decomposed into fragments of light molecules in the

64

presence of a suitable catalyst. At the same time, these fragments, which are unstable and reactive, repolymerize into oily compounds having appropriate molecular weights. With pyrolysis, on the other hand, a catalyst is usually unnecessary, and the light decomposed fragments are converted to oily compounds through homogeneous reactions in the gas phase [78].

Thermogravimetric analysis (TGA) is a method by which the weight loss of a sample is recorded against temperature under controlled heating rate and gas atmosphere. Differential thermogravimetric analysis (DTG) curves are derived from TG curves, and they have been widely applied to biomass to evaluate pyrolysis kinetics [86]. Figure 4.2 illustrates thermogravimetric analysis (TGA) of biomass. When the temperature is raised, drying of the sample occurs.
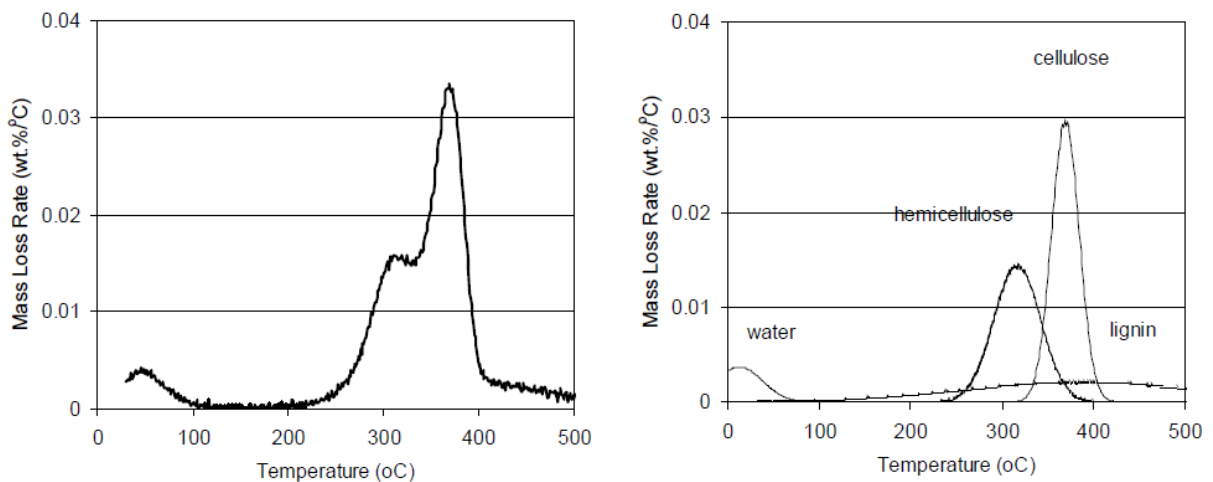
Figure 4.2 Thermographic analysis of biomass [83]

At 473K, devolatilization starts and the devolatilization rate increases as the temperature is raised. There are two areas of weight loss producing a single peak with a plateau or shoulder located at the lower temperature region. The lower temperature shoulder represents the decomposition of hemicellulose and the higher temperature peak represents the decomposition of cellulose. At 673K, most of the volatiles are gone and the devolatilization rate decreases rapidly. However, a low devolatilization rate can be observed in the temperature range of 673–773K. This is caused by lignin decomposition, which occurs throughout the whole temperature range, but the main area

of weight loss occurs at higher temperatures, it means that the lignin is mainly responsible for the flat tailing section [3].

4.1.1 Pyrolysis process types

Quality and quantity of resulting products obtained from biomass pyrolysis depend mainly on the chemical composition of the feedstock and the operating temperature [84]. Mainly depending on operating temperature, heating rate and reaction time pyrolysis process could be classified as:

- Slow pyrolysis,
- Fast pyrolysis,
- Flash pyrolysis.

4.1.1.1 Slow pyrolysis

Conventional pyrolysis, in other words slow pyrolysis, is applied for thousands of years when charcoal production is aimed [87].

Operating temperature in slow pyrolysis process usually in the range of 550–950 K and at slow heating rates (5–7 K/min) [84, 81]. Lower process temperature and longer vapour residence times favour the production of charcoal and pyrolysis gas composed of H_2 and CO, via secondary coking and repolymerisation reactions. [80, 88, 89]. However, if the heating rate is increased to between about 20 and 100 min^{-1} with maximum temperatures of 600 °C, than the liquid and gas yields are markedly increased [89].

In slow pyrolysis, the reactions taking place are always in equilibrium. The heating period is sufficiently slow to allow equilibration during the pyrolysis process. In this case the ultimate yield and product distribution are limited by the heating rate. The products residence time in the reactor is also important since their presence can influence both the primary and secondary reactions [90].

Slow pyrolysis is well known and usually appears in traditional charcoal kiln [81]. Modern process often takes place in continuous reactors, e.g., drum pyrolysers,

rotary kilns, or screw pyrolysers. These plants, which, besides charcoal, collect bio-oil and syngas, are highly energy efficient compared to traditional kilns [91].

4.1.1.2 Fast pyrolysis

Fast pyrolysis occurs in a time of few seconds or less. Therefore, not only chemical reaction kinetics but also heat and mass transfer processes, as well as phase transition phenomena, play important roles. As the fast pyrolysis is used to obtain high-grade bio oil, liquid mixture of numerous organic molecules with water [92, 93], the critical issue is to bring the reacting biomass particle to the optimum process temperature and minimise its exposure to the intermediate (lower) temperatures that favour formation of charcoal [80].

In the fast pyrolysis process biomass is thermolys at elevated temperature (577–977 °C) in the inert atmospheric conditions [84]. Heating rate is somewhere about 300 °C/min [81].

In fast pyrolysis, biomass decomposes very quickly to generate mostly vapours and aerosols and some charcoal and gas. After cooling and condensation, a dark brown homogenous mobile liquid is formed which has a heating value about half that of conventional fuel oil. A high yield of liquid is obtained with most biomass feeds low in ash [94].

Yield of fast pyrolysis processes is 60–75 wt.% of liquid bio-oil, 15–25 wt.% of solid char, and 10–20 wt.% of noncondensable gases, depending on the feedstock used [95]. According [94] the essential features of a fast pyrolysis process for producing liquids are:

- Very high heating rates and very high heat transfer rates at the biomass particle reaction interface usually require a finely ground biomass feed of typically less than 3 mm as biomass generally has a low thermal conductivity,
- Carefully controlled pyrolysis reaction temperature of around 500 °C to maximise the liquid yield for most biomass,
- Short hot vapour residence times of typically less than 2 s to minimise secondary reactions,
- Rapid removal of product char to minimise cracking of vapours,

- Rapid cooling of the pyrolysis vapours to give the bio-oil product.

Fast pyrolysis is successful with most of fluidized bed reactors as it offers high heating rates, rapid de-volatilization, easy control, easy product collection, etc.. Various reactors (some of them presented in Figure 4.3) like entrained flow reactor, wire mesh reactor, vacuum furnace reactor, vortex reactor, rotating reactor, circulating fluidized bed reactor, etc. were designated for performing fast pyrolysis [81].
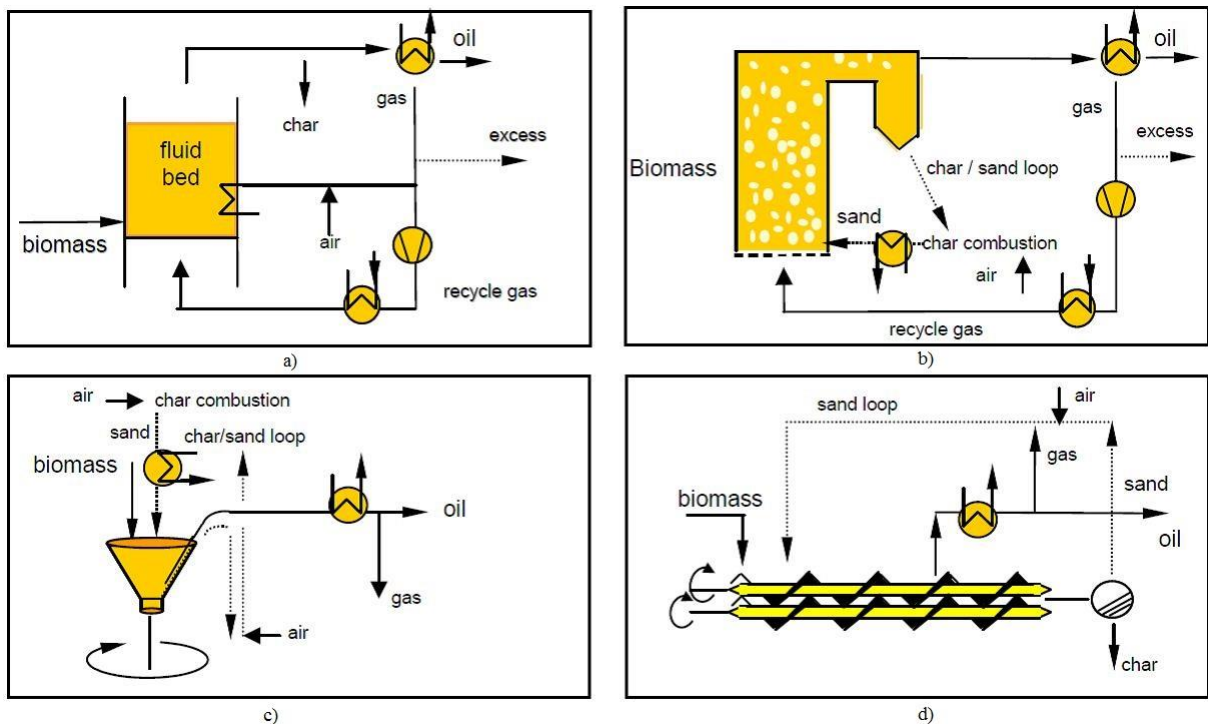
Figure 4.3 Fast pyrolysis reactors: a) Fluidised bed, b) Circulated fluidized bed,
c) Rotating cone, d) Twin screw [83]

4.1.1.3 Flash pyrolysis

Process condition in which the reaction time is of only several seconds or even less and high heating rates of up to 10^4 K s^{-1} at temperatures < 650 °C and with rapid quenching, favour the formation of liquid products and minimize char and gas formation, are often referred as 'flash pyrolysis' [81, 96]. Rapid heating and rapid quenching produced the intermediate pyrolysis liquid products, which condense before further reactions break down higher molecular-weight species into gaseous products.

High reaction rates minimize char formation. Under some conditions, no char is formed [84].

This requires special reactor configuration in which biomass residence times are only of few seconds. Two of appropriate designs are entrained flow reactor and the fluidized bed reactor. Flash pyrolysis of any kind of biomass requires rapid heating and therefore the particle size should be fairly small [81]. Analysis of flash pyrolysis results is complicated by instrumental inadequacies which make uniform heating rates difficult to control and even following which make uniform heating rates difficult to control and even following sample temperature closely seems to be an insurmountable task [97].

According [81] flash pyrolysis is of following types:

(a) Flash hydro-pyrolysis

(b) Rapid thermal process

(c) Solar flash pyrolysis

(d) Vacuum flash pyrolysis

The conversion of biomass to crude oil can have efficiency up to 70% for flash pyrolysis processes. The so-called bio-crude can be used in engines and turbines. Its use as feedstock for refineries is also being considered. Some problems in the conversion process and use of the oil need to be overcome. These include poor thermal stability and corrosivity of the oil. Upgrading by lowering the oxygen content and removing alkalis by means of hydrogenation and catalytic cracking of the oil may be required for certain applications [84].

4.1.2 Composition of pyrolysis products

Depending of process conditions (heating rate, operating temperature, reaction time, pressure and biomass type) previously is presented that pyrolysis products could be in liquid, gas and solid state. Despite of state, product have very complex composition.

Pyrolysis gas comprises of CO, CO_2 (formed in considerable quantities, especially from oxygen-rich fuels) and CH_4. The other components present are H2, propane, propylene, butane, butenes, C_5, ethane, etc [3, 81].

Char contains elemental carbon along with hydrogen. In addition, char also comprises various inorganic species [81]. This solid product is more thermally instable than peat or coal, especially from grass biomass. Low heating rates and long residence times will decrease the reactivity of the char. On the contrary, high heating rates contribute to increase the reactivity of the resulting char, making it more suitable for further thermal treatment like gasification or combustion. The characteristics of the remaining char depend enormously on the pyrolysis conditions, namely heating rate and final pyrolysis temperature. Therefore, the pyrolysis conditions are one of the most important parameters when studying char reactivity and char pore structure. The char produced during pyrolysis can be upgraded to activated carbon (metallurgical industry use), domestic cooking fuel or barbecuing [79].

The liquid product from pyrolysis consists mainly of polyaromatic hydrocarbons (PAH), oxygenated aromatic compounds such as phenol and water (due to the moisture content of the fuel). It is also called pyrolysis oil or bio-oil and can be upgraded to hydrocarbon liquid fuels for combustion engines, or directly used for power generation or heat. Calorific value of the pyrolysis oils varies between 5-30 MJ/kg although they are physically and chemically unstable products [79]. As it is presented in [81] oil obtained from the pyrolysis of biomass contains several organic as well as inorganic species. Some of the organic groups present in the bio-oil are mentioned below:

- Acids: Formic, acetic, propanoic, hexanoic, benzoic, etc.
- Esters: Methyl formate, methyl propionate, butyrolactone, methyl n-butyrate, velerolactone, etc.
- Alcohols: Methanol, ethanol, 2-propene-1-ol, isobutanol, etc.
- Ketones: Acetone, 2-butanone, 2-butanone, 2-pentanone, 2-cyclopentanone, 2,3 pentenedione, 2-hexanone, cyclo-hexanone, etc.
- Aldehydes: Formaldehyde, acetaldehyde, 2-butenal, pentanal, ethanedial, etc.
- Phenols: Phenol, methyl substituted phenols.
- Alkenes: 2-methyl propene, dimethylcyclopentene, alpha-pinene, etc., Aromatics: Benzene, toluene, xylenes, nphthalenes, phenanthrene, fluoranthrene, chrysene, etc.
- Nitrogen compounds: Ammonia, methylamine, pyridine, methylpyridine, etc.
- Furans: Furan, 2-methyl furan, 2-furanone, furfural, furfural alcohol, etc.

- Guaiacols: 2-methoxy phenol, 4-methyl guaiacol, ethyl guaiacol, eugenol, etc.
- Syringols: Methyl syringol, 4-ethyl syringol, propyl syringol, etc.
- Sugars: Levoglucosan, glucose, fructose, D-xylose, D-arabinose, etc.
- Miscellaneous oxygenates: Hydroxyacetaldehyde, hydroxyacetone, dimethyl acetal, acetal, methyl cyclopentenolone, etc.

Inorganics present in the bio oil comprises of Ca, Si, K, Fe, Al, Na, S, P Mg, Ni, Cr, Zn, Li, Ti, Mn, Ln, Ba, V, Cl, etc.

4.2 Gasification

Gasification is a form of pyrolysis, carried out at high temperatures with the presence of an externally supplied oxidizing agent in order to optimize the gas production [3, 88]. In general terms, the gasification process is the total or partial transformation of solid fuel components into gases. This is usually accomplished by thermal treatments or chemical reactions, or a combination of both. Therefore, devolatilization is part of the gasification process, as well as combustion or the reaction of carbonaceous fuel and oxygen. However, in the usual context of thermal sciences, gasification reactions are the ones taking place between the char-or devolatilized solid fuel-and gases excluding oxygen. In addition, one should be aware that in a real process, devolatilization, gasification, and combustion reactions might occur simultaneously, at least during part of the time taken by these processes [98].

Gasification is a subject for extensive R&D activities almost worldwide, although the use of gasification is not a new phenomenon. Gasification was in use for gas production from 1800 to about 1950. The gasifier fuel was mainly coal and the producer gas (or city gas, town gas, etc.) was stored in gas tanks and distributed in pipelines for both domestic use and industrial processes [99].

Biomass gasification is an efficient and environmentally friendly way to produce energy. Gasification process is nothing but it is a conversion of solid fuel into gaseous fuel for wide applications. This whole process completed at elevated temperature range of 800–1300℃ with series of chemical reaction that is why it come under thermo chemical conversion [84]. Biomass gasification is considered one of the most promising routes for syngas or combined heat and power production because of the potential for

higher efficiency cycles. Instead of utilizing biomass in traditional low-efficient systems (steam cycles), high-efficient as engines or combined gas and steam turbine cycles can be applied. Good technical progress has been made in the field of biomass gasification but at a commercial level good achievements still have to be attained [100].

The manufacture of combustible gases from solid fuels is an ancient art, as it is mentioned before, but by no means a forgotten one. In its widest sense the term *gasification* covers the conversion of any carbonaceous fuel to a gaseous product with a useable heating value. This definition excludes combustion, because the product flue gas has no residual heating value. It does include the technologies of pyrolysis, partial oxidation, and hydrogenation. Early technologies depended heavily on pyrolysis (i.e., the application of heat to the feedstock in the absence of oxygen), but this is of less importance in gas production today. The dominant technology is partial oxidation, which produces from the fuel a synthesis gas (otherwise known as syngas) consisting of hydrogen and carbon monoxide in varying ratios, whereby the oxidant may be pure oxygen, air, and/or steam. Partial oxidation can be applied to solid, liquid, and gaseous feedstocks, such as coals, residual oils, and natural gas, and despite the tautology involved in "gas gasification," [101]

Gasification adds value to low- or negative-value feedstock by converting them to marketable fuels and products. Gasification of fossil fuels like coal and oil for syngas production is well-known and commercially available, but gasification of biomass faces several problems, which are a.o. related to the characteristics of biomass. Important differences are the much higher volatile matter content in biomass and the morphology. Gasification is also called "staged combustion", since usually the gas is produced with the intent to burn it later. This raises the question why first gasifying and then burning the gas over direct combustion of the biomass [100]. The advantages of biomass gasification compared to direct combustion include [99, 100]:

- Possibility to transport in pipelines;
- Diversities in power production. Product gas can be used in gas engines, gas turbines, Stirling engines, and as basis for suitable fuel for fuel cells whilst direct combustion is limited to steam processes (steam turbine and steam engine), Stirling engines and indirectly fired gas turbines, which generally operate with low efficiencies.

- Combustion control. Combustion of gaseous fuels is easier to control and optimize compared to solid fuel combustion.

- Low emission. Emission components can be removed either in the gasifier or in the gas cleaning system. since impurities can be removed from the producer gas, and the volume of producer gas is much smaller compared to flue gas;

- Integration. By gasification, biomass can be integrated into existing power plants based on natural gas or coal, with a resulting reduction of CO_2 and other emissions.

- Production of hydrogen. The gasification process is found very suitable for production of high-yield hydrogen gas mixtures. In view of a future increase in the use of hydrogen, biomass gasification thus represents a solution for a hydrogen production step with no net CO_2 emission.

- Chemical synthesis. The product gas from indirect biomass gasification can be a basis for synthesis gas, which is used for production of nitrogen fertilizers and other chemicals.

Actually, is almost impossible to have combustion without other reactions typical of gasification. This is because almost all fuels have, for instance, hydrogen as a component, forming water during combustion, which in turn reacts with carbon. As a rough rule, gasification reactions are endothermic. That is why the great majority of gasification processes use partial combustion of the solid fuel to provide the energy necessary [98].

4.2.1 Gasification processes

The process of synfuels from biomass will lower the energy cost, improve the waste management and reduce harmful emissions. The molecules in the biomass (primarily carbon, hydrogen and oxygen) and the molecules in the steam (hydrogen and oxygen) reorganize to form this syngas [102].

Air, oxygen, steam or a mixture of them could be used as a oxidizing agent (Table 4.1).

Air gasification produces a low calorific value gas (gross calorific value (GCV) of 4–7 megajoules per normal cubic metre (MJ/Nm^3 dry), while oxygen gasification

produces a medium calorific value gas (GCV of 10–18MJ/Nm^3 dry) [3]. However, oxygen gasification is a very expensive procedure. Some researchers have also experimented gasification with an oxygen-enriched atmosphere what could be more reasonable. Pure steam gasification can also produce a MCV gas. Both oxygen and steam gasification produce a nitrogen free gas [79].

Through synthesis, the fuel gas can be upgraded to methanol, burned externally in a boiler for producing hot water or steam, in a gas turbine for electricity production or in internal combustion engines, such as diesel and spark ignition engines. Before the fuel gas can be used in gas turbines or internal combustion engines, the contaminants (tar, char particles, ash and alkali compounds) have to be removed. The hot gas from the gas turbine can be used to raise steam to be utilized in a steam turbine (IGCC – integrated gasification combined cycle) [3].

Table 4.1 Comparison of gasification agents [79].

Gasification agent	Advantages	Disadvantages	Heating value of product gas [MJ/Nm^3]
Air	Inexpensive	Low heating value	4-7
Oxygen	N2 free product gas Medium heating value	Expensive	10-18
Steam	N2 free product gas Medium heating value Enhanced H$_2$ content	Very endothermic process	10-18

In the discussion of the theoretical background to any chemical process, it is necessary to examine both the thermodynamics (i.e., the state to which the process will move under specific conditions of pressure and temperature, given sufficient time) and the kinetics (i.e., what route will it take and how fast will it get there) [101].

From a chemical point of view, the process of biomass gasification (Figure 4.4) is quite complex. It includes a number of steps like [100]:

- thermal decomposition to gas, condensable vapors and char (pyrolysis);
- subsequent thermal cracking of vapors to gas and char;
- gasification of char by steam or carbon dioxide;
- partial oxidation of combustible gas, vapors and char.
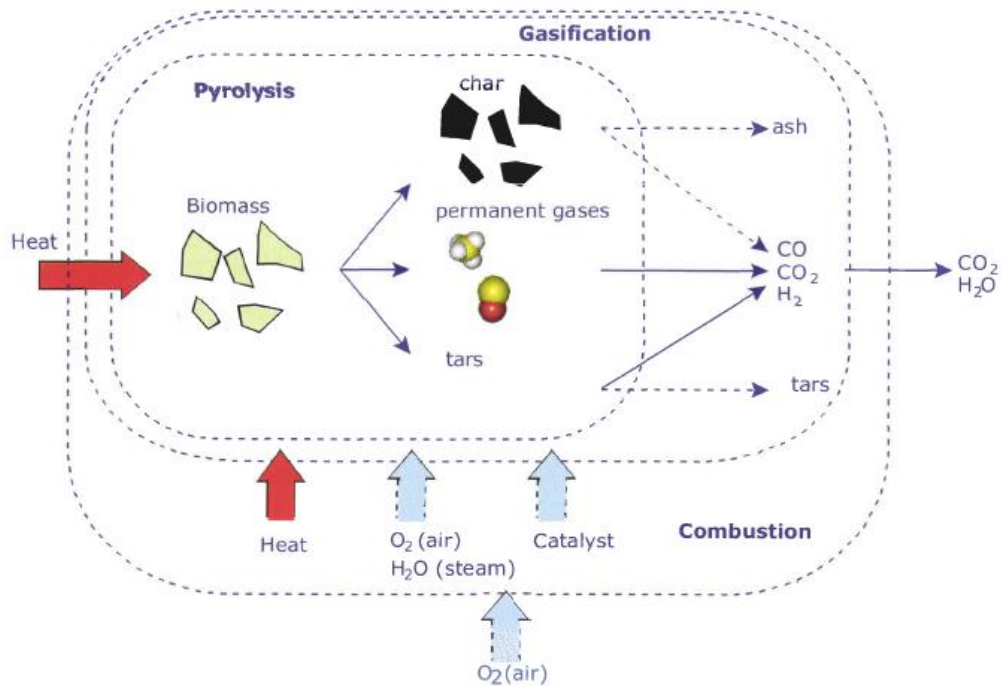
Figure 4.4 Schematic presentation of gasification [100]

The kinetics of gasification is as yet not as developed as is its thermodynamics. Homogeneous reactions occurring, for example, in the gas phase can often be described by a simple equation, but heterogeneous reactions are intrinsically more complicated. This is certainly the case with the gasification of solid particles such as coal, (pet) coke, or biomass because of their porous structure. The latter complication causes mass transfer phenomena to play an important role in the gasification of solids. During the process of gasification of solid carbon whether in the form of coal, coke, or char, the principle chemical reactions are those involving carbon, carbon monoxide, carbon dioxide, hydrogen, water (or steam), and methane. These reactions are [101]:

Combustion reactions,

$$C + \tfrac{1}{2}\,O_2 = CO \qquad\qquad \text{-111 MJ/kmol} \qquad\qquad (4\text{-}2)$$

$$CO + \tfrac{1}{2}\,O_2 = CO_2 \qquad\qquad \text{-283 MJ/kmol} \qquad\qquad (4\text{-}3)$$

$$H_2 + \tfrac{1}{2}\,O_2 = H_2O \qquad\qquad \text{-242 MJ/kmol} \qquad\qquad (4\text{-}4)$$
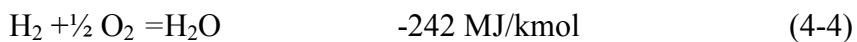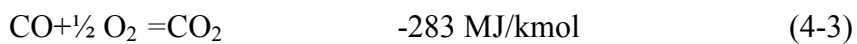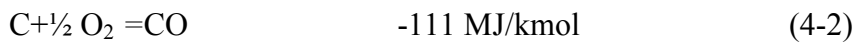
These reactions are exothermic and provide – autotermal gasification – the heat necessaty for the the endothermic reactions in the drying, pyrolysis and the reduction zone [100].

The slowest reactions in gasification, and therefore those that govern the overall conversion rate, are the heterogeneous reactions with carbon, namely the water gas, Boudouard, and hydrogenation reactions. The rates of reaction for the water gas and Boudouard reactions with char are comparable and are several orders of magnitude faster than for the hydrogenation reaction [101].

The water gas reaction,

$$C+H_2O \leftrightarrow CO+H_2 \qquad +131 \text{ MJ/kmol} \qquad (4-5)$$
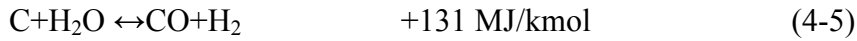
The water vapor introduced with the air and production by the drying and pyrolysis of the biomass reacts with the hot carbon according to the heterogeneous reversible water gas reaction [100].

The Boudouard reaction,

$$C+CO_2 \leftrightarrow 2 \text{ CO} \qquad +172 \text{ MJ/kmol} \qquad (4-6)$$
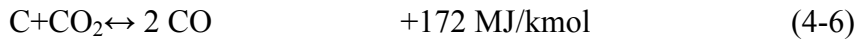
The water gas and Boudouard reaction are the most important reduction reactions. These heterogeneous endothermic reactions increase the gas volume of CO and H_2 at higher temperatures and lower pressures (a high pressure suppresses the gas volume) [100].

The methanisation reaction,

$$C+2H_2 \leftrightarrow CH_4 \qquad -75 \text{ MJ/kmol} \qquad (4-7)$$
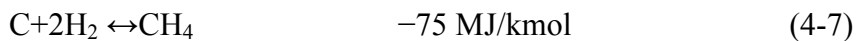
As reactions with free oxygen are all essentially complete under gasification conditions, reactions 4-2, 4-3, and 4-4 do not need to be considered in determining an equilibrium syngas composition. The three heterogeneous (i.e., gas and solid phase) reactions 4-5, 4-6, and 4-7 are sufficient. In general, we are concerned with situations where also the carbon conversion is essentially complete. Under these circumstances we can reduce equations 4-5, 4-6, and 4-7 to the following two homogeneous gas reactions:

CO shift reaction:

$$CO+H_2O \leftrightarrow CO_2+H_2 \qquad -41 \text{ MJ/kmol} \qquad (4\text{-}8)$$
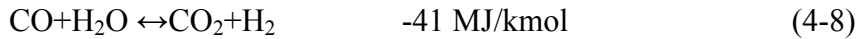
and the steam methane reforming reaction:

$$CH_4+H_2O \leftrightarrow CO_2+3H_2 \qquad +206 \text{ MJ/kmol} \qquad (4\text{-}9)$$
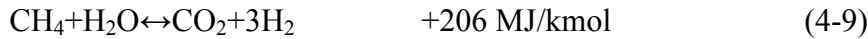
By subtracting the moles and heat effects from reaction 4-6 from those in reaction 4-5 one obtains reaction 4-8, and by subtracting reaction 4-7 from 4-5 one obtains reaction 4-9. Thus reactions 4-8 and 4-9 are implicit in reactions 4-5, 4-6, and 4-7. But not the other way around! Three independent equations always contain more information than two.

Reactions 4-2, 4-5, 4-6, and 4-7 describe the four ways in which a carbonaceous or hydrocarbon fuel can be gasified. Reaction 4-6 plays a role in the production of pure CO when gasifying pure carbon with an oxygen/CO_2 mixture. Reaction 4-5 takes a predominant role in the water gas process. Reaction 4-7 is the basis of all hydrogenating gasification processes. But most gasification processes rely on a balance between reactions 4-2 (partial oxidation) and 4-5 (water gas reaction) [100].

4.2.2 Gasification reactors designs

In the practical realization of gasification processes a broad range of reactor types has been and continues to be used [101]. Depending of operational parameters gasifiers could be classified in different ways [100]:

According to the gasification agent

- Air-blown gasifiers
- Oxygen gasifiers
- Steam gasifiers

According to heat for gasification

- Autothermal or direct gasifiers: heat is provided by partial combustion of the biomass

- Allothermal or indirect gasifiers: heat is supplied from an external source through heat exchanger or indirect process, i.e. separation of gasification and combustion zone

According to pressure in the reactor:

- Atmosphric
- Pressurised

And the most common, reactors are grouped based on design as:

- Fix bed gasifiers
- Fluidised bed gasifiers

The choice of one type of gasifier over other is dictated by the fuel, its final available form, its size, moisture content and ash content [103].

4.2.2.1 Fixed bed gasifiers

The fixed bed (or moving bed [101]) type gasifier simply consisting of cylindrical reactor in which solid biomass fuel gasifying and moves slowly downward under gravity and produced gas move either upward or downward. These types of gasifier are simple in construction and generally operate with high carbon conversion, long solid residence time; low gas velocity and low ash carry over [84]. Depending on the relative direction of the producer gas or flow of biomass and gases, fixed bed gasifiers could be divided into updraft (concurrent), downdraft (concurrent) and crossdraft gasifiers (crosscurrent) (Figure 4.5). Table 4.2 lists the advantages and disadvantages generally found for various classes of these gasifiers [103].
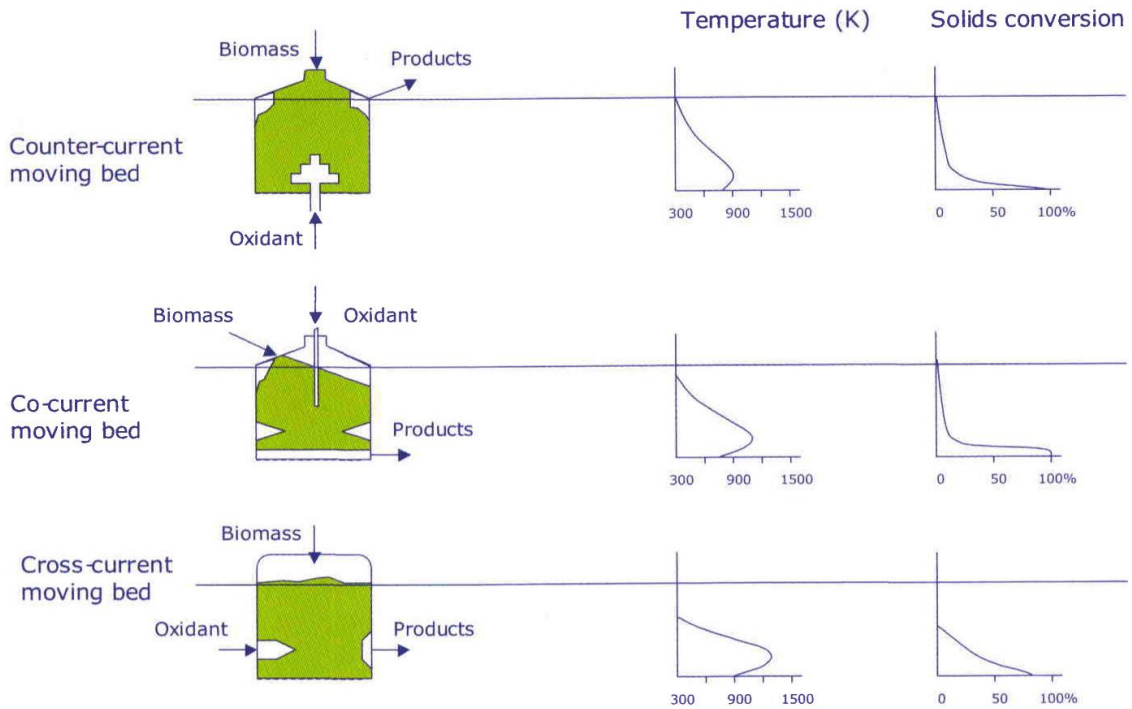
Figure 4.5 Characteristics of different fixed bed gasifier configurations [100]

In fixed gasification, countercurrent or concurrent flow of gas and solids creates distinct temperature zones in the gasifier (or in one stage of multizone gasifier) that assist in the conversion of fixed carbon to gas. Zones frequently found in countercurrent, downflow fixed bed gasification include drying/devolatilizing at the top (low temperature); the steam decomposition and stem-carbon reducing reaction zone; the high temperature carbon oxidation zone where hot oxidizing gases are generated by carbon combustion; and the ash collection and discharge zone (the ash may be dry or slagged depending on the technology under consideration). Fixed bed gasifiers are sensitive to fines in the feed material since these may cause bed plugging and channeling. Tars and liquid products in addition to gaseous hydrocarbons heavier than methane can be produced in fixed bed gasifier [104]. An advantage of fixed bed gasifiers is the low particle content of the product gas, since the bed of char itself acts as a filter [79].

Table 4.2 Advantage and Disadvantages of various fixed bed gasifiers [103]

Gasifier Type	Advantage	Disadvantages
Updraft	• Small pressure drop; • Good thermal efficiency; • Little tendency towards slag formation;	• Great sensitivity to tar and moisture and moisture content of fuel; • Relatively long time required for startup of IC engine; • Poor reaction capability with heavy gas load;
Downdraft	• Flexible adaptation of gas production to load; • Low sensitivity to charcoal dust and tar content of fuel;	• Design tends to be tall; • Not feasible for very small particle size of fuel;
Crossdraft	• Short design height; • Very fast response time to load; • Flexible gas production;	• Very high sensitivity to slag formation • High pressure drop

4.2.2.2 Fluidised bed gasifiers

The fluidized bed reactors represent the most promising gasifier design for directly heated biomass gasification. They present higher throughput capabilities and greater fuel flexibility than fixed beds and can accept low-density feedstock, as well they required minimal pre-processing of feedstock [79]. This feature is especially attractive for biomass fuels, such as agricultural residues and wood, that may be available for gasification at different times of the year [105]. Limitations are mostly with respect to fuel particle size, typically less than 0.1 m and moisture content, typically less than 65% (wt) [99].

Fluidised bed gasifiers for biomass originate from the technology for coal gasification and are usually suitable for large scale operation. The reactors are built with porous grate in the bottom where sand or other fluidization medium lies above. Air or other types of gasification agent such as steam, oxygen or a combination of theses pass through the porous grate at an enough speed so the bed particles become suspended [106]. The fuel particles are introduced at the bottom of the reactor as well, very quickly mixed with the bed material and almost instantaneously heated up to the bed temperature. As a result of this treatment the fuel is pyrolyzed very fast, resulting in a component mix with a relatively large amount of gaseous materials [84]. The thermal degradation and the gasification reactions of the fuel take place at high speed in an environment that is well mixed due to turbulence [106]. Such extremely good mixing, between feed and oxidant, promotes both heat and mass transfers [101]. Because of the

intense mixing, the heat transport to the fuel happens at a high rate so that the different zones found in fixed bed reactors are not distinguished in fluidized beds [106].

The fluidized bed reactors that are commonly used in gasification are: bubbling fluidized bed and circulating fluidized bed (Figure 4.6) [106]. Both systems include use of a bed material that can be the fuel itself or inert material such as sand, dolomite or alumina. In a bubbling bed, the bed material and fuel are well mixed due to the fluidisation caused by the gas flowing through the reactor. Circulating bed gasifiers are operated with high gas velocities and particles, bed material and unreacted fuel are separated in a cyclone and led back to the bed [99]. Circulating fluidized bed gasifiers have advantages over BFBGs such as higher carbon conversion efficiency and smaller size [105].
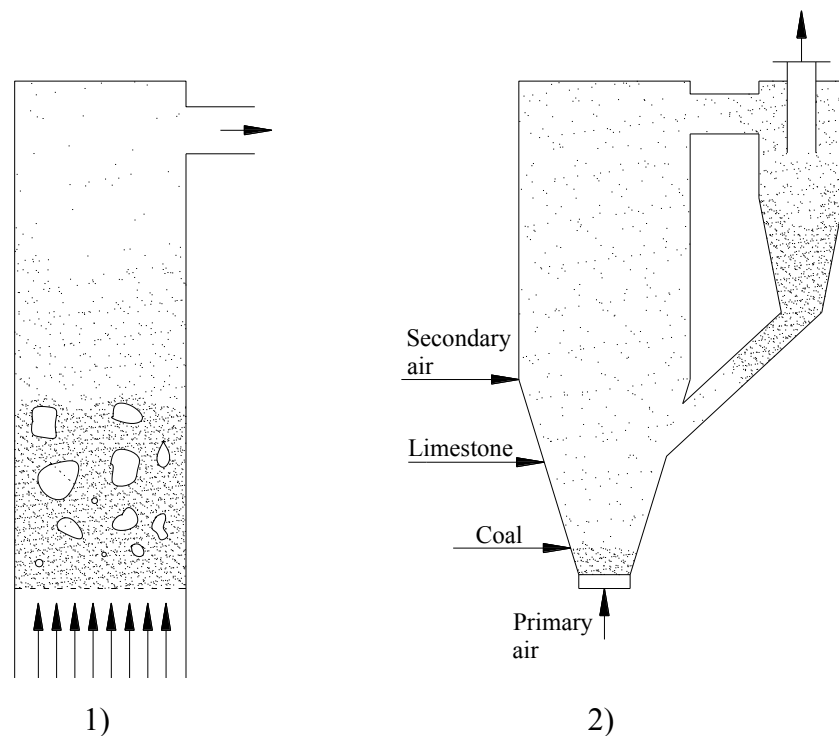
Figure 4.6 Fluidized bed reactors 1) Bubbling bed, 2) Circulating bed [107]

Fluidised bed gasifiers accept a wide size distribution of feed solids and achieve a reasonably uniform bed temperature distribution through rapid fluid-solids mixing. Ash and unconverted carbon exit the bed in product gas stream or are withdrawn at the gasifier base. Temperatures at the gasifiers base control carbon loss [104]. Tar components are cracked by contact with hot bed material, and the tar content in the products gas is generally relatively low [99]. Sizing of the particles in the feed is

critical; material that is too fine will tend to become entrained in the syngas and leave the bed overhead. This is usually partially captured in a cyclone and returned to the bed. The lower temperature operation of fluid-bed processes means that they are more suited for gasifying reactive feedstocks, such as low-rank coals and biomass [101].

4.3 Combustion

Biomass combustion is the main technology route for bioenergy, responsible for over 90 per cent of the global contribution to bioenergy [3]. In the ideal case, combustion represents the complete oxidation of the solid organic part of the fuel into the gases CO_2 and H_2O [63]. The burning of biomass in air, i.e. combustion, is used over a wide range of outputs to convert the chemical energy stored in biomass into heat, mechanical power, or electricity using various items of process equipment, e.g. stoves, furnace s, boilers, steam turbines, turbo-generators, etc. Combustion of biomass produces hot gases at temperatures around 800–1000 °C. It is possible to burn any type of biomass but in practice combustion is feasible only for biomass with a moisture content <50%,unless the biomass is pre-dried [85]. Biomass rarely arises naturally in an acceptable form of burning. In most of the cases it requires some pretreatment like drying, chopping, grinding, etc., which in turn is associated with financial costs and energy expenditure [81].

This conversion occurs in three steps: drying of the fuel (vaporising of water), pyrolysis/gasification (thermal degradation (devolatilisation) in the absence or presence of externally supplied oxygen (air), respectively) and the final oxidation of the charcoal and the flue gases (Figure 4.7). After drying, the main controlling parameter of the combustion process is the ratio between the amount of air added and the amount of air (oxygen) necessary for a complete combustion of the combustible parts of the fuel, the lambda (λ, excess air) factor [63]. Several parameters in the combustion zone are quite crucial to the combustion process; among these are reactor technology, combustion temperature, size and moisture content of the fuel [106].
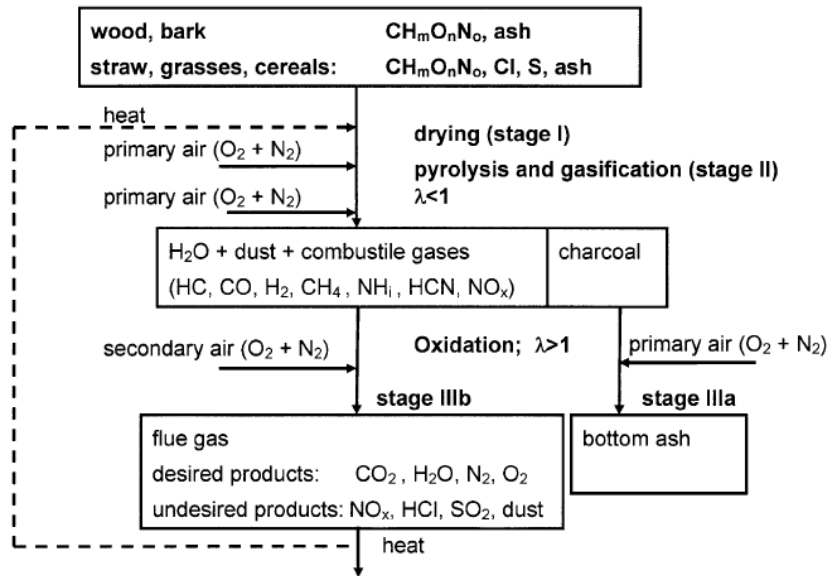
Figure 4.7 Process of biomass combustion – principle [63]

Drying and pyrolysis/gasification will always be the first steps in a solid fuel combustion process. The relative importance of these steps will vary, depending on the combustion technology implemented, the fuel properties and the combustion process conditions. A separation of drying/pyrolysis/gasification and gas and char combustion, as in staged-air combustion, may be utilized. In large-scale biomass combustion applications with continuous fuel feeding, such as moving grates, these processes will occur in various sections of the grate. However, in batch combustion applications there will be a distinct separation between a volatile and a char combustion phase, in both position and time. Figure 4.8 shows qualitatively the combustion process for a small biomass particle. For larger particles, there will be a certain degree of overlap between the phases, while in batch combustion processes, as in wood log combustion in wood-stoves and fireplaces, there will be a large degree of overlap between the phases [3].

The combustion process may be defined as an interaction between fuel, energy, and the environment rather than merely a chemical reaction of fuel with oxygen to release energy, or a physical reaction of the fuel with the environment involving heat and mass transfer. The process is enormously complex even with relatively simple or homogenous fuels [104].
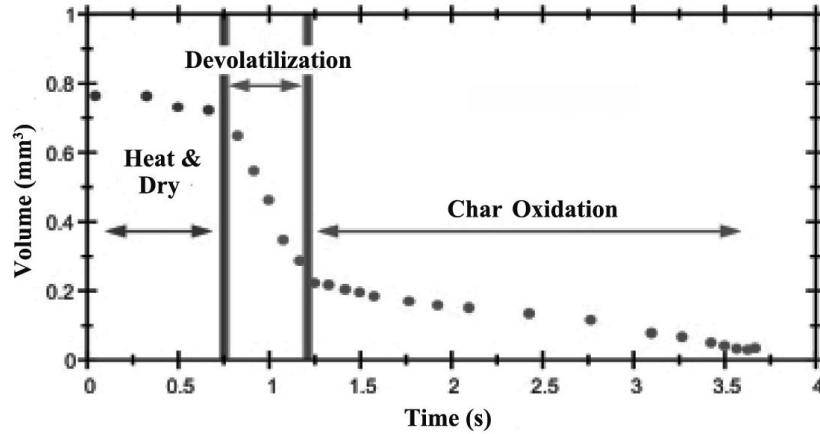
Figure 4.8 The combustion of small biomass particle proceeds in distinct stages [3]

4.3.1 Combustion chemistry

Wood fuels never burn directly: wood fuels are thermally degradable and under the influence of a sufficiently strong energy source they break down into a mixture of volatiles and carbonaceous char. The two modes of combustion (solid char and gaseous volatiles) have completely different chemical mechanisms and kinetics [88]. In order to understand wood combustion, it is important to understand the properties of wood which determine its behavior as a fuel for combustion. Influencing properties include anatomical structure and pathways for movement of moisture, moisture content, specific gravity, and holocellulose and lignin. Main combustion reactions are:

Non-reacting solid → Heat, drying → Pyrolysis (Volatiles; Steam) → Precombustion reactions → Primary gas phase combustion → Secondary combustion → Effluent stack gas [102].

A detailed understanding of combustion processes requires a detailed knowledge of chemical kinetics, fluid mechanics, turbulence phenomena, etc. This is also the case for biomass combustion. A combustion process can – in a simplified manner – be described by an overall combustion reaction:

$$a \cdot \left(Y_C Y_H Y_O Y_N Y_S \right) + n \cdot \left(\frac{1 - Y_{O_2, Air}}{Y_{O_2, Air}} \cdot N_2 + O_2 \right)$$

$$\Rightarrow b \cdot CO_2 + c \cdot H_2O + d \cdot O_2 + e \cdot N_2 + f \cdot CO + g \cdot NO$$

$$+ h \cdot NO_2 + i \cdot C_x H_y + j \cdot SO_2 + m \cdot N_2O$$

(4-10)
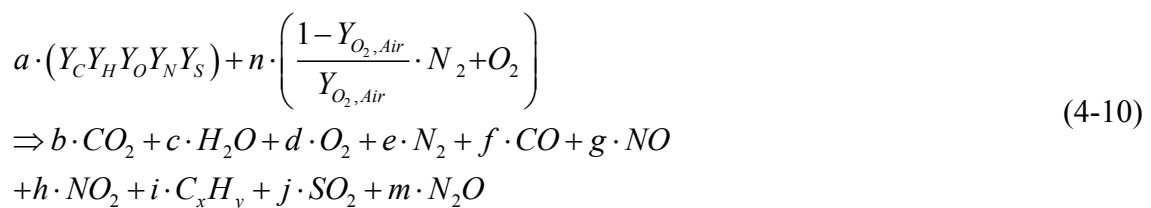
where Y_i is the volume fraction of carbon (C), hydrogen (H), oxygen (O), nitrogen (N) and sulphur (S) in the fuel. O_2, *Air* is the volume fraction of oxygen in air and the coefficients *a*, n, *b*, *c*, *d*, *e*, *f*, *g*, *h*, *i*, *j* and *m* can be found partly by applying element balances (C, H, O, N, S) and partly by making assumptions regarding product composition (e.g. chemical equilibrium). By assuming complete combustion, neglecting dissociation effects at high temperatures and formation of NO, NO_2 and N_2O, the product composition can be found directly from the elemental balances [3].

However, in reality several hundreds of reversible elementary reactions are needed to describe in detail the combustion process of even light hydrocarbons, such as methane, which is an important intermediate in biomass combustion. The reaction rate of the elementary reactions depends on mixing through the availability of reactants in the flame zone, and temperature and residence time through the reaction rate constant, *k*. This is shown in equation 4-11:

$$a \cdot \text{Fuel} + b \cdot \text{Oxidant} \rightarrow c \cdot \text{Product}$$

$$\Downarrow$$

$$\frac{d[\text{Product}]}{dt} = k \cdot [\text{Fuel}]^a \cdot [\text{Oxidant}]^b \quad \left[\frac{mole}{m^3 s} \right] \tag{4-11}$$

$$where \quad k = A \cdot T^\beta \cdot \exp\left(-\frac{E}{\text{R}_u \cdot T} \right)$$

where *A*, *b* and *E* are the pre-exponential factor, the temperature exponent, and the activation energy, respectively. These are constants for a given elementary reaction and are found experimentally. *Ru* is the universal gas constant and *T* is the temperature [3]. Burning the solid coke adds a new dimension to the combustion process. Coke is largely carbon; it has a low vapour pressure, so that evaporation followed by gas-phase oxidation is not a major reaction path. Instead, the surface carbon is oxidized to CO by gas phase CO_2 (and O_2), that collide with, and/or stick to, the surface. This reaction of CO_2 is $C(s) + CO_2(g) = 2 \, CO(s)$. The carbon is now strongly attached to the oxygen and weakly attached to the surface. Thus, the nascent CO does have a high vapor pressure and leaves the surface to the gas phase where CO can be further oxidized to CO_2 [108]. Heterogeneous reactions involving carbon are usually slower than gas phase reactions, as for charcoal combustion. However, in some cases, the heterogeneous reactions may

be significantly faster than the equivalent gas phase reactions. This is the case for catalytic converters [3].

Since this thesis presented results achieved during the grate firing of biomass, in this subsection the focus will be on packed bed solid combustion.

According [109] a packed bed consists of a number of solid particles which are piled up upon a support grate with a characteristic porosity. Primary air is supplied from underneath the grate and flows upward. For ordinary packed bed combustion, ignition starts at the bed top layer heated up by over-bed radiation from the over-bed flame and hot walls. Once the bed is ignited, the flame front travels downwards at a speed depending on fuel type and operating parameters, until it arrives at the bed bottom or the support grate. In ideal conditions, three reacting waves travel down the bed successively: moisture evaporation, devolatilisation and char combustion (Figure 4.9).
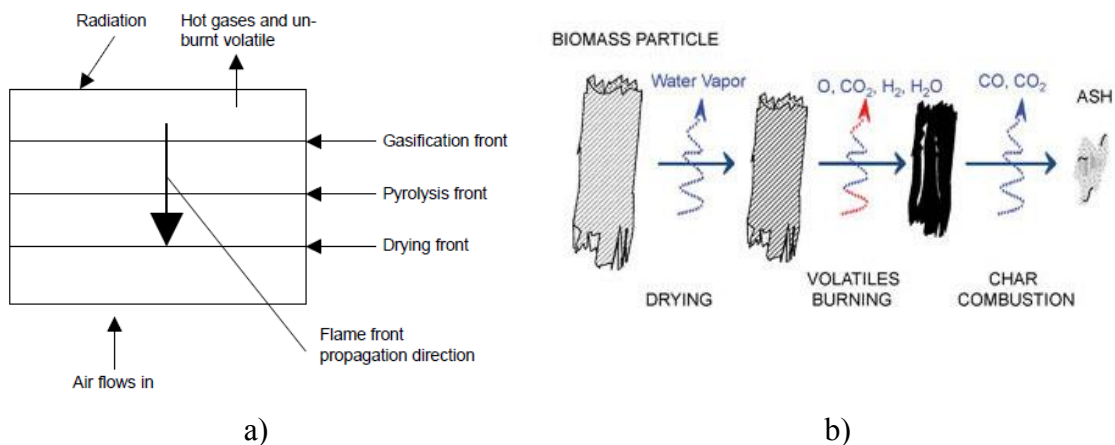
Figure 4.9 a) Propagation of flame front in a packed bed, b) Combustion occurs in three stages [109, 110]

They may overlap each other, depending upon particle size or the Biot number. The Biot number is a measure of uniformity of temperature distribution inside a particle and for a single particle heated uniformly at the external surface, it is defined as

$$\text{Bi} = h_s' d_p / k \tag{4-12}$$

When Bi>>1.0 particles are considered thermally thick and there exists a significant temperature gradient inside the particles under an external heating source. Otherwise,

the particles can be viewed as thermally thin, and the temperature gradient inside the particle is small.

The above definition of Biot number for a single particle, however, has to be modified to account for the changed heating conditions for the situation of a packed bed. Radiation from the flame front can only penetrate the bed through voids; therefore the actual external heated area of a particle in a packed bed is proportional to the local bed voidage. So we add an extra parameter, the void fraction to the original Biot number and the modified Biot Number is thus as follows:

$$\text{Bi}' = \phi h_s' d_p / k \tag{4-13}$$

It means that, according above equation, particles smaller than 30 mm can be roughly regarded as thermally thin in the situation of packed bed combustion. The assumption of thermally thin particles eliminates the need for a separate solution for temperature profile inside the particles. Instead, the whole bed can be viewed as a continuous porous medium with two phases (solid and gases), and continuous conservation or transport equations can be applied to both phases in a much simpler way.

Table 4.3 summarises the equations employed for packed-bed biomass combustion as it is presented in [109]. The whole set of equations consists of bed volume change, individual process rates, gaseous phase and solid phase conservation equations and radiation heat transfer in the bed. The conservation equations for the gas-phase in the packed bed include continuity, momentum, species and energy conservation equations. It was found that burning rate is mostly influenced by fuel size and smaller fuels result in higher combustion rate due to increased reacting surface area and enhanced gas-phase mixing in the bed; combustion stoichiometry is equally influenced by fuel LCV and size as a consequence of variation in burning rate as well as the mass ratio of combustible elements to the oxygen in the fuel; for the solid-phase temperature, material density has the strongest influence and a denser material has a higher maximum bed temperature as it results in a less fuel-rich combustion condition; while CO concentration in the flue gases is mostly affected by both fuel calorific value and size, CH4 in the exiting flow is greatly affected by material density due to change in reaction zone thickness [109].

Table 4.3 Summary of the equations employed for packed-bed biomass combustion [109]

Bed volume change		$\frac{dV}{V_0\,dt} = \frac{R_2}{\rho_2\omega_{2A}}\left[\frac{(\phi_B-\phi_A)-(1-\phi_A)(1-F_2)\omega_{2A}}{(1-\phi_B)(1-\phi_A)}\right] + \frac{R_3}{\rho_3\omega_{3,B}}\left[\frac{(\phi_C-\phi_B)-(1-\phi_B)(1-F_3)\omega_{2,B}}{(1-\phi_C)(1-\phi_B)}\right] + \frac{R_4}{\rho_4\omega_{4,C}}\left[\frac{(\phi_D-\phi_C)}{(1-\phi_D)(1-\phi_C)}\right]$
Process rate equations	Moisture evaporation	$R_2 = A_p h_s (C_{w,s} - C_{w,g})$ when $T_s < 100\,°C$
		$R_2 = \frac{A_p[h_c'(T_g-T_s)+\varepsilon_s\sigma_b(T_{env}^4-T_s^4)]}{H_{evp}}$ when $T_s = 100\,°C$
	Devolatilisation	$R_3(1-\phi)\rho_s k_v(v_\infty - v)$ $k_v = A_v \exp\left(-\frac{E_v}{RT_s}\right)$
	Combustion of volatiles	$C_mH_n + \frac{m}{2}O_2 \rightarrow mCO + \frac{n}{2}H_2$ $R_{C_mH_n} = 59.8T_g P^{0.3} \exp(-12200/T_g) C_{C_mH_n}^{0.5} C_{O_2}$
		$CO + \tfrac{1}{2}O_2 \rightarrow CO_2$ $R_{CO} = 1.3\times10^{11} \exp(-62700/T_g)C_{CO}C_{H_2O}^{0.5}C_{O_2}^{0.5}$
		$H_2 + \tfrac{1}{2}O_2 \rightarrow H_2O$ $R_{H_2} = 3.9\times10^{17} \exp(-20500/T_g)C_{H_2}^{0.85}C_{O_2}^{1.42}$
		$R_{mix} = C_{mix}\rho_g\left[150\frac{D_g(1-\phi)^{2/3}}{d_p^2\phi} + 1.75\frac{V_g(1-\phi)^{1/3}}{d_p\phi}\right]\min\left[\frac{C_{fuel}}{S_{fuel}}, \frac{C_{O_2}}{S_{O_2}}\right]$ $R = \min[R_{kinetic}, R_{mix}]$
		$C(s) + \alpha O_2 \rightarrow 2(1-\alpha)CO + (2\alpha-1)CO_2$ $\frac{CO}{CO_2}2500 \exp\left(-\frac{6420}{T}\right)$
	Char gasification	$R_4 = A_p C_{O_2}\left(\frac{1}{k_r}+\frac{1}{k_d}\right)$ $k_r = A_r \exp\left(-\frac{E}{RT_s}\right)$
Gas phase conservation equations	Continuity	$\frac{\partial(\rho_g\phi)}{\partial t} + \frac{\partial(\rho_g V_g\phi)}{\partial x} = S_{sg}$
	Momentum	$\frac{\partial(\rho_g V_g\phi)}{\partial t} + \frac{\partial(\rho_g V_g V_g\phi)}{\partial x} = -\frac{\partial p_g}{\partial x} + F(V_g)$ $F(V_g) =$
		$\begin{cases} -\dfrac{\alpha}{K}V_g, & \text{if } Re < 10 \\ -\dfrac{\alpha}{K}V_g - \rho_g C V_g V_g, & \text{if } Re \geq 10 \end{cases}$
	Species	$\frac{\partial(\rho_g Y_{i,g}\phi)}{\partial t} + \frac{\partial(\rho_g V_g Y_{i,g}\phi)}{\partial x} = \frac{\partial}{\partial x}\left(D_{ig}\frac{\partial(\rho_g Y_{i,g}\phi)}{\partial x}\right) + S_{Y_{i,g}}$
		$D_{ig} = E^0 + 0.5d_p V_g$
	Energy	$\frac{\partial(\rho_g H_g\phi)}{\partial t} + \frac{\partial(\rho_g V_g H_g\phi)}{\partial x} = \frac{\partial}{\partial x}\left(\lambda_g\frac{\partial T_g}{\partial x}\right) + Q_h$
		$\lambda_g = \lambda^0 + 0.5d_p V_g\rho_g C_{pg}$
Solid phase conservation equations	Continuity	$\frac{\partial((1-\phi)\rho_s)}{\partial t} + \frac{\partial((1-\phi)\rho_s V_s)}{\partial x} = -S_{sg}$
		$V_s = \frac{dV}{A\,dt}$
	Species	$\frac{\partial((1-\phi)\rho_s Y_{i,s})}{\partial t} + \frac{\partial((1-\phi)\rho_s V_s Y_{i,s})}{\partial x} = -S_{Y_{i,s}}$
	Energy	$\frac{\partial((1-\phi)\rho_s H_s)}{\partial t} + \frac{\partial((1-\phi)\rho_s V_s H_s)}{\partial x} = \frac{\partial}{\partial x}\left(\lambda_s\frac{\partial T_s}{\partial x}\right) + \frac{\partial q_r}{\partial x} Q_{sh}$
Radiation heat transfer		$\frac{dI_x^+}{dx} = -(k_a + k_s)I_x^+ + \tfrac{1}{2}k_a E_b + \tfrac{1}{2}k_s(I_x^+ + I_x^-)$ $-\frac{dI_x^-}{dx} = -(k_a + k_s)I_x^- + \tfrac{1}{2}k_a E_b + \tfrac{1}{2}k_s(I_x^+ + I_x^-)$
		$k_s = 0$ $k_a = -\frac{1}{d_p}\ln(\phi)$

4.3.2 Combustion technologies

Combustion is widely used on various scales to convert biomass energy to heat and/or electricity with the help of a steam cycle (stoves, boilers and power plants). Production of heat, power and (process) steam by means of combustion is applied for a

wide variety of fuels and from very small scale (for domestic heating) up to a scale in the range of 100 MW$_e$. Co-combustion of biomass in (large and efficient) coal fired power plants is an especially attractive option as well because of the high conversion efficiency of these plants. It is a proven technology, although further improvements in performance are still possible. Net electrical efficiencies for biomass combustion power plants range from 20% to 40%. The higher efficiencies are obtained with systems over 100 MW$_e$ or when the biomass is co-combusted in coal fired power plants [78].

Combustion installations, depending of its characteristics, could be classified in several categories:

According scale and application:

- Domestic burning appliances,
- Combusting technologies for industrial and district heating systems.

Whereas domestic burning appliances are based on batch combustion, industrial and district heating systems combusting technologies could be distinguished as:

- fixed bed combustion;
- fluidized bed combustion; and
- pulverized fuel combustion.

4.3.2.1 Fixed bed combustion

Fixed bed combustion systems include grate furnaces and underfeed stokers. Primary air passes through a fixed bed, in which drying, gasification and charcoal combustion take place (Figure 4.10). The combustible gases produced are burned after secondary air addition has taken place, usually in a combustion zone separated from the fuel bed [3]. The grate, which is at the bottom of the combustion chamber in a grate-fired boiler, has two main functions: lengthwise transport of the fuel, and distribution of the primary air entering from beneath the grate. The grate may be air-cooled or water-cooled. The water-cooled grate requires little air to cool (primary air confined to combustion requirement) and is flexible with the use of an advanced secondary air system [111].

There are various grate furnace technologies available: fixed grates, moving grates, travelling grates, rotating grates and vibrating grates. All of these technologies have specific advantages and disadvantages, depending on fuel properties, so careful selection and planning is necessary. Grate furnaces are appropriate for biomass fuels with a high moisture content, varying particle sizes (with a downward limitation concerning the amount of fine particles in the fuel mixture) and high ash content. Mixtures of wood fuels can be used, but current technology does usually not allow for mixtures of wood fuels and straw, cereals and grass, due to their different combustion behavior, low moisture content and low ash-melting point. Only special grate constructions are able to cope with woody and herbaceous biomass fuel mixtures, e.g. vibrating grates or rotating grates. Such grates have to ensure a mixture of the fuels across the grate.
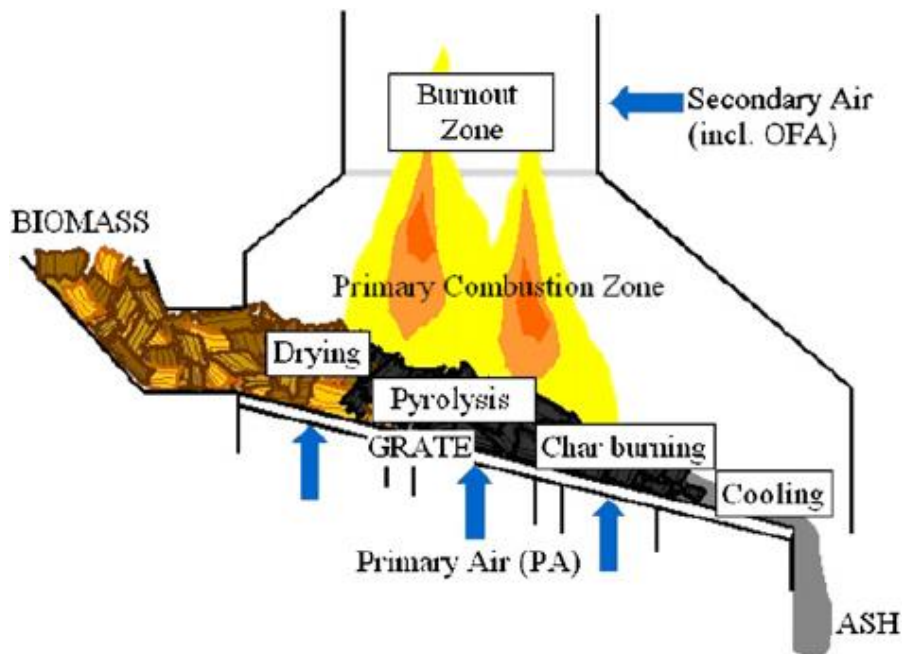
Figure 4.10 Comustion process in fixed fuel beds [111]

A well-designed and well-controlled grate guarantees a homogeneous distribution of the fuel and the bed of embers over the whole grate surface. This is very important in order to guarantee an equal primary air supply over the various grate areas. Inhomogeneous air supply may cause slagging, higher fly-ash amounts and may increase the excess oxygen needed for a complete combustion, resulting in boiler heat

losses. Furthermore, the transport of the fuel over the grate has to be as smooth and homogeneous as possible in order to keep the bed of embers calm and homogeneous, to avoid the formation of 'holes' and to avoid the release of fly ash and unburned particles as much as possible [3].

Grate firing is one of the main technologies that are currently used in biomass combustion for heat and power production. Grate-fired boilers can fire a wide range of fuels of varying moisture content and show great potential in biomass combustion. Though grate firing of biomass has been tried and tested over many years, there are still some problems to be further studied, for instance, conversion of biomass in the fuel bed on the grate, mixing in both the fuel bed and the freeboard, deposit formation and corrosion and their control, pollutant formation and control [111].

4.3.2.2 Fluidized bed combustion

The use of the fluidized bed combustor (FBC) has increased. It began in the 20th century as coal combustion and gasification, which then developed into catalytic reactions. Only recently, the application field has been extended to the incineration of biomass and pretreated waste, for either power generation or waste disposal. The success of fluidized bed combustion is due to high combustion efficiency, great flexibility when it comes to the heating value of the fuel and reduction in pollutants emitted with the flue gas [112].

In FB furnaces (Figure 4.11), an initially stationary bed of solid particles (usually silica sand), located in the bottom part of the furnace, is brought to a fluidized state by the primary air which is supplied through a nozzle distributor plate. In BFB, the bed particles are kept in suspension by the primary air at comparatively lower fluidization velocities (~1.0–3.0 m/s) while in CFBC, higher gas velocities (~ 3.0–6.0 m/s) are employed, more and more solids are carried out of the bed, the well-defined surface of the bed (prominent in BFB) disappears, and the solids concentration decreases continuously with increasing height above the distributor plate [113]. At this stage, the fuel with a (optional) sorbent (mainly limestone or dolomite) can be injected into the boiler. All bed particles are now in a 'liquid state' [114].
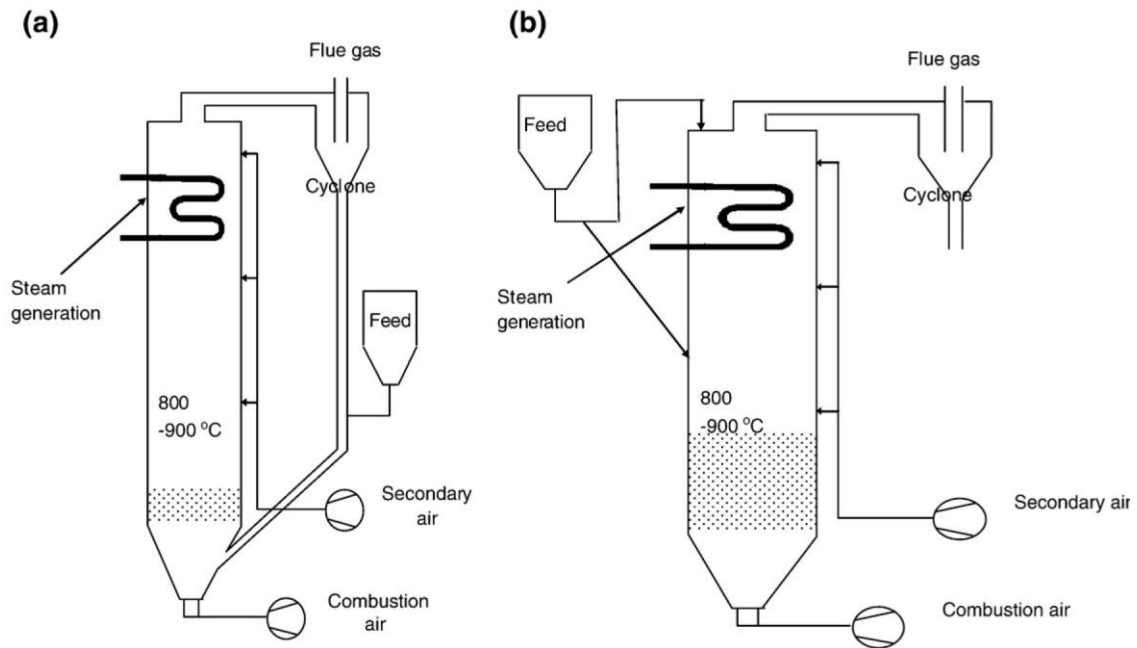
Figure 4.11 (a) Circulating fluidized bed boiler (CFBB) (b) bubbling fluidized bed boiler (BFBB) [113]

In the fluidized state, bed material and fuel is mixed in a highly turbulent suspension. This allows rapid transfer of combustion heat to the bed material, thereby reducing peak flame temperatures. In circulating fluidized beds, bed material is carried over with the gas stream, separated from it after leaving the combustor and reintroduced into the furnace. In bubbling fluidized beds, fluidizing air velocities also provide for proper mixing of bed material and fuel, but are not high enough to carry over much bed material. Reduced peak flame temperatures and increased residence times of the fuel in the combustion zone are favorable for improved environmental performance of fluidized bed combustors compared to other combustion systems [115]. The most important process characteristics are given in Table 4.4.

The success of fluidized bed combustion is due, above all, to the great flexibility as regards the quality of the fuel. In fact, low-heating value fuels can be used thanks to the high mixing rate of solids and the absence of temperature gradients in the bed. Also the reduction in pollutants emitted with flue gas is one of the most relevant advantages of fluidized bed combustion: the low combustion temperature (700–850 °C) guarantees the NOx abatement while sulphur and halogen capture is achieved by limestone or dolomite injection in the bed. Limestone, within the temperature range 700–850 °C, not

only reacts with SO_2 to form calcium sulphite and calcium sulphate, but also captures hydrogen chloride to form liquid- or solid-phase calcium chloride. Furthermore, the gas mixing in the combustor restrains the formation of CO and unburned hydrocarbon in such a way that high combustion efficiency is obtained [112].

Table 4.4 Design parameters BFB and CFB [114]

Design parameter	BFB	CFB
Combustion temperature (1°C)	760–870	800–900
Fuel particle size (mm)	0–50	0–25
Fluidization velocities (m/s)	1–3	3–10
Solids circulation	No[a]	Yes
Particle concentration	High in bottom, low in freeboard	Gradually decreasing along furnace height
Limestone[b] particle size (mm)	0.3–0.5	0.1–0.2
Average steam parameters[c]		
Steam flow (kg/s) (range)	36 (13–139)	60 (12–360)
Steam temperature (1°C) (range)	466 (150–543)	506 (180–580)
Steam pressure (bar) (range)	72 (10–160)	103 (10–275)

[a]Circulation of (large) unburned particles is possible in the case of bad burnout. However, solid circulation in BFB is compared to CFB a less integrated part of the combustion process. [b]Applicable in the case when limestone is used for in bed sulphur removal. [c]Data on steam parameters is collected for ca. 400 FBC installations.

Despite its broad application, solid fuel conversion in fluidized bed processes still has some technical difficulties. Agglomeration is a major operational problem. Usually, the conversion of the solid fuel is carried out with silica sand and ash as bed material. Inorganic alkali components from the fuel, mainly potassium (K) and sodium (Na), can be a source for agglomeration by the formation of low-melting silicates with the silica from the sand. The content of this critical inorganic material can vary much between fuels; especially in the case of certain types of biomass as well as some low-rank coal types the content is often rather high. When both alkalis and silica are present in the bed they can form low-melting silicates, characterized by a lower melting point than the individual components. As a consequence, the sand particles become coated with an adhesive layer. Sand particles with a sticky surface then grow towards larger agglomerates due to the formation of permanent bonds upon collisions. If this process is not recognized, it eventually propagates to partial or total defluidization of the reactor, which in turn results in a lengthy and expensive unscheduled shutdown [116].

4.3.2.3 Pulverized fuel combustion

Globally, there is an increasing interest in the co-firing of biomass with coal in order to reduce net CO_2 emissions and the dependence of foreign fossil fuel resources [117]. Since the most of the existing boilers in thermal-electric power generation units work with suspension combustion of pulverized coal [98], the pulverized combustion (co-combustion) is the most appropriate way to achieve this goal.

In pulverized fuel combustion systems, fuels such as sawdust and fine shavings are pneumatically injected into the furnace [3]. The transportation air is used as primary air. Startup of the furnace is achieved by an auxiliary burner. When the combustion temperature reaches a certain value, biomass injection starts and the auxiliary burner is shut down. Fuel quality in pulverized fuel combustion systems has to be quite constant. A maximum fuel particle size of 10–20mm has to be maintained (in practice, in pulverized fuel combustion the coal is milled to give the particles between 5 and 400 μm in diameter [118]) and the fuel moisture content should normally not exceed 20wt% (w.b.). Due to the explosion-like gasification of the fine biomass particles, the fuel feeding needs to be controlled very carefully and forms a key technological unit within the overall system. Fuel/air mixtures are usually injected tangentially into the cylindrical furnace muffle to establish a rotational flow (usually a vortex flow). The rotational motion can be supported by flue gas recirculation in the combustion chamber. Due to the high energy density at the furnace walls and the high combustion temperature, the muffle should be water-cooled. Fuel gasification and charcoal combustion take place at the same time because of the small particle size. Therefore, quick load changes and an efficient load control can be achieved [3].

The main features of commercial designs for pulverized fuel burners (p-f) (Figure 4.12) are amount of secondary air is controlled through a cylinder that can slide and therefore vary the entrance area or the flow rate of air into the chamber. At the end of the smaller tube, which carries the primary air and the pulverized fuel, there is an impeller. This last device promotes a swirl in the injected stream and diverts the coal into the secondary air stream. In this way, the impeller also provokes a partial backward circulation of the suspended burning particles, which is essential for the flame stability. Through the center of the small tube, an oil burner is installed and is used for the

ignition of the pulverized fuel. Moreover, a gas torch is employed to ignite the oil. The impeller may be advanced or retracted from the firing position by pneumatic control of the position of the tube that carries the fuel [98].
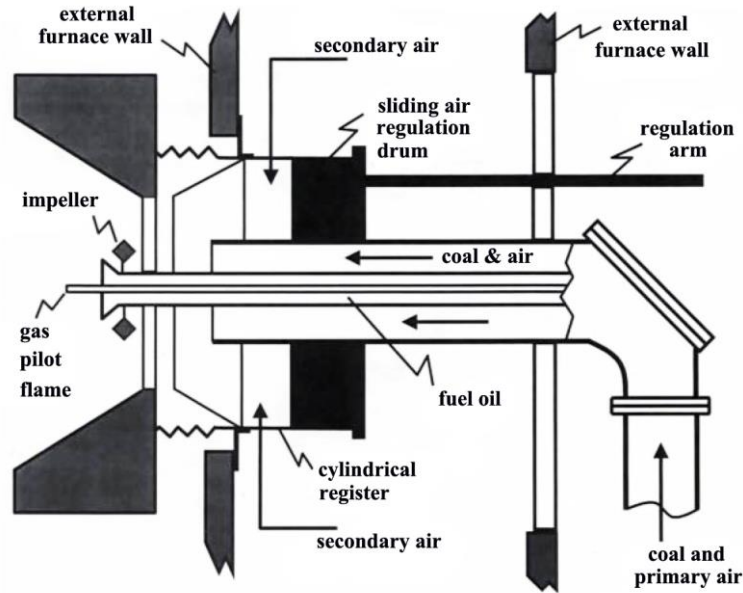
Figure 4.12 Schematic view of a typical pulverized fuel burner [98]

Certain technical issues appear when pulverized biomass/coal is used, for example, emissions of NO_x was found to be sensitive to the burner configuration and the injection position of the fuel particles. For a given pulverized biomass combustion boiler, ignition of the fuel particles, flame stabilization, particle burnout and emission of carbon monoxide as well as particulate matters (soot, ash, condensed tar/oils) depend on the boiler operation conditions and the fuel particle characteristics such as the moisture content and the maximum particle size [119]. The interaction of the airflow patterns and heat release by combustion determine the rate of chemical reaction of the p.f. particles, the stoichiometry of both the primary and secondary reaction zones and thus their temperatures. This in turn determines flame stability, the rate of char burnout, which in turns controls the formation of NO_x, and the unburnt carbon ash. Not only the temperature field and reaction time determine the reaction rates but also the level of turbulent mixing of the volatiles with free radicals and hot combustion products and the influence of turbulence on char burnout. There is an additional influence of turbulence that results in permitting the escape of rich turbulent pockets of gases containing

95

volatile organic compounds (VOC) and super-equilibrium amounts of CO in the flue gas [118].

4.3.2.4 Summary of combustion technologies

Given combustion technologies gives different opportunities and its use mostly depend of the application size and fuel type. In order to achieve the best possible results, it should be taken into account the adequate choice of combustion technology, operating conditions as well as maintenance. Table 4.5 gives review of the advantages and disadvatages of presented combustion technologies.

Table 4.5 Advantages and disadvantages of given combustion technologies [3, 120]

Advantages	Disadvantages
Grate applications	
Low investment costs for plants <10 MW Low operating costs Low dust load in the flue gas Good burn-out of fly ash particles Good operation at partial load possible Less sensible to slagging than BFB and CFB furnaces	No mixtures of wood fuels and straw / cereals possible Efficient NOx reduction requires special technology Higher excess oxygen decreases the efficiency Combustion conditions not as homogeneous as in BFB and CFB furnaces
BFB applications	
Low investment costs for plants >10MW No moving parts in the hot combustion chamber NOx reduction by air staging works well High flexibility concerning particle size, moisture Content and mixtures of biomass fuels Lower excess oxygen raises the efficiency	High operating costs Higher dust load in the flue gas than grate furnaces Good operation at partial load requires special technology Medium sensibility concerning ash slagging Medium erosion of heat exchanger tubes
CFB applications	
No moving parts in the hot combustion chamber NOx reduction by air staging works well	High investment costs (interesting only for plants

High flexibility concerning moisture content and mixtures of biomass fuels	>30 MW)
	High operating costs
Homogeneous combustion conditions in the furnace if several fuel injectors are used	High dust load in the flue gas
	Partial-load operation requires a second bed
High specific heat transfer capacity due to high turbulence	Loss of bed material with the ash
	High sensibility concerning ash slagging
Addition of additives easy	Medium erosion of heat exchanger tubes
Efficient S fixation in the ash if enough Ca available	Low flexibility concerning particle size of the fuel
Pulverized fuel applications	
Low excess oxygen (4–6vol%) increases efficiency	Particle size of biomass fuel is limited (< 10–20mm)
High NOx reduction by efficient air staging and mixing possible if cyclone or vortex burners are used	High wear rate of the insulation brickwork if cyclone or vortex burners are used
Very good load control and fast alteration of load possible	An extra start-up burner is necessary

5. IMPACTS OF BIOMASS COMBUSTION

While biomass possesses the advantage of CO_2 neutrality, or nearly so, there are potential problems concerned with the environmental pollution. As well that it causes and the influence on food production. In many of the small combustion appliances there is significant atmospheric pollution - indeed it is estimated that many millions of people are exposed to the effects of wood smoke and 1.6 million people/annum die as a result of pollution. Biomass feedstock expansion can have adverse impacts on the environment; particularly where there has been a major change of land-use (such as deforestation) when there can be little or no saving in Greenhouse Gas emissions. In this respect, economic and life cycle analyses are helpful. These can identify the benefit, if at all, of various strategies, but they are sensitive to the weightings set to the pollutants and particularly to carbon dioxide and the other greenhouse gases such as CH_4 and N_2O [121].

Pollutants are formed alongside the main combustion reactions from the N, S, Cl, K as well as other trace elements contained in the volatiles and char. CO, PAH and soot, together with characteristic smoke markers of biomass combustion such as levoglucosan, guaiacols, phytosterols and substituted syringols are released if the combustion is incomplete, due to factors such as local stoichiometry (mixing), temperature, residence time etc. Thus, the atmospheric emissions can contain tar aerosols and soot, which together with fine char particles and metal-based aerosols such as KCl, form smoke. The nitrogen compounds are partially released with the volatiles, whilst some forms a C-N matrix in the char and is then released during the char combustion stage forming NOx and the NOx precursors, HCN and HNCO. Sulphur is released as SO_2 during both volatile and char combustion. KCl, KOH and other metal containing compounds together the sulphur compounds form a range of gas phase species, which can be released as aerosols, but importantly also deposit in combustion chambers [121].

Life cycle analyses show that the most important environmental issue regarding emissions from wood combustion is NOx, contributing to almost 40% of the total emissions, including NOx, PM10, CO_2, SO_X, NH_3, CH_4, nonmethane volatile organic compounds (NMVOC), residues, and others (Table 5.1). The basis for this comparison

is in relation to expected environmental impact points (EIP) of the specific emission according to the ecological scarcity method, applied for heating with wood chips. However, it is evident that the given data from any LCA analysis depends strongly on the valuation of the greenhouse gas effect since the ranking changes significantly as a result of the different CO_2 impacts of the fuels. In this respect, much effort has been done to characterize biomass and reduce NOx emissions from the combustion of biomass and other solid fuels [122].

Table 5.1 Environmental Impact Points (EIP) according to the Ecological Scarcity Method for heating with wood chips (base case for greenhouse effect) [123]

	[EIP/GJ]	[%]
NOx	13 030	38.6
PM 10	12 600	36.5
CO_2	670	2.0
SOx, NH_3, CH_4, NMVOC, primary energy, residues, and others	8 200	22.9
Total	34 500	100

On the other hand, in case of poor combustion conditions in manually operated wood stoves or boilers, PM emissions can be higher than assumed in the cited LCA by a factor of 10 thus leading to a far higher environmental impact than described here. In addition, at excessively high emissions of unburnt hydrocarbons including methane, even the greenhouse gas effect can be higher than from light fuel oil or natural gas due to the higher impact of methane (Figure 5.1). Hence wood combustion can only be assessed as being environmentally friendly in case of low airborne emissions [123].

According the [43] the biomass energy can be not only carbon–neutral, but also with some extra carbon-capture and storage effect due to fixation of CO_2 in the combustion residues. For example, the mineral composition of biomass ashes (500 °C) clearly shows the intensive formation of various newly formed carbonates. These carbonates are a result of solid–gas reaction between the volatile CO_2 (released from biomass or occurring naturally in the atmosphere) and alkaline-earth and alkaline oxyhydroxides formed during biomass combustion. Such carbonates are relatively stable during weathering and thermal treatment up to 900 °C.
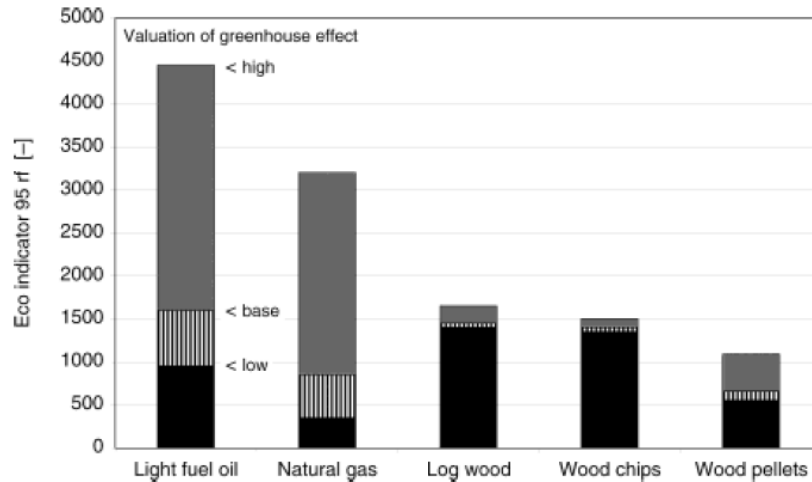
Figure 5.1 Enivironmental impact points (EIP) for different valuations of the greenhouse effect [124]

Ash related problems resulting in unscheduled and expensive shutdown periods in power plants (corrosion, deposit buildup, slagging/fouling). In fixed bed combustors, the alkali metals in particular can become volatile and stick on heat transfer surfaces downstream in the process. This process has been found in many cases to be accelerated by the presence of zinc and lead in the fuel, which both are even more volatile than alkali metal compounds. Such depositions are difficult to remove and cause lower efficiencies due to a decrease in heat transfer. They can also bridge between the tubes and cause flue gas flow restriction which results in higher pressure drops. The deposits themselves have a composition which make them quite aggressive resulting in attacks on the metallic surface of the heating tubes.

Variety of methods exist to mitigate ash-related problems, including use of corrosion-resistant alloys and coatings, improved design, improved combustion process and control, better cleaning methods and the use of additives [125, 126]

As the amount of pollutants emitted to the atmosphere is highly dependent on the combustion technology implemented, the fuel properties and the combustion process conditions, reduction of harmful emissions through flue gases and effluents can be obtained by either avoiding creation of such substances (primary measures) or removing the substances from the flue gas (secondary measures). In general we distinguish these two basic methods by stating that a primary measure is a modification of the combustion process (e.g. limestone injection in the furnace), and a secondary measure

100

takes places after the combustion process (e.g. ammonia injection in the flue gas channel).

- modification of the fuel composition;
- modification of the moisture content of the fuel;
- modification of the particle size of the fuel;
- selection of the type of combustion equipment;
- improved construction of the combustion application;
- combustion process control optimization;
- staged-air combustion;
- staged fuel combustion and reburning; and
- catalytic converters.

Secondary measures can be applied to remove emissions from the flue gas once it has left the boiler. For virgin wood combustion, particle removal is of particular relevance. For other types of biomass, additional secondary measures may be necessary, depending on the elementary composition and the fuel characteristics of the selected biomass fuel, and the combustion technology [3].

The basic features of biomass combustion and resultant pollutant formation are understood but much of the detail is lacking. It seems that if biomass is to be more widely used as a major energy source then a greater understanding of the detailed processes is necessary. This needs to be across all aspects of the combustion and pollution processes [121].

This chapter gives a theoretical description of topics covered throughout the work on this thesis. It includes details on NOx formation as well as mechanisms for its reduction with focus on air staging and combustion conditions as a primary measures. Additionally in order to get complete overview of the combustion product, ash related problems, as a one of the major issues of biomass combustion, are presented as well as the mitigation potentials.

5.1 Nitrogen oxides

For energy production, the most common energy carriers are solid fuels (coal, biomass, wastes, etc.). However, it is a concern that combustion of biomass will lead to

high levels of nitrogen oxides emissions (NOx; collective term for NO and NO_2) from oxidation of nitrogen in the fuel (fuel nitrogen) or potentially conversion of nitrogen in the air (air nitrogen). NOx are contributing to environmental problems such as acid rain, photochemical smog formation and depletion of stratospheric ozone [127].

5.1.1 Mechanisms of nitrogen oxides formation

Formation mechanism of oxides of nitrogen has been a topic of intensive research for many decades. The importance of this mechanism stems from the fact that nitrogen oxides are one of the principal contaminants emitted by combustion processes.

Oxides of nitrogen damage the environment severely; thus, government agencies are passing stringent laws to control the emissions of pollutants. An in-depth understanding of the mechanism of formation of the oxides of nitrogen is essential when automotive and other industrial devices are designed. Suitable schemes must be developed for controlling the amount of NOx generated from combustion products of various engines and other energy-conversion systems.

Therefore, knowledge of the NOx formation mechanism is essential for understanding combustion of energetic materials. The first major work on the kinetics of NOx was performed by Zel'dovich in 1946, who postulated the thermal NO mechanism, now known as the Zel'dovich NO mechanism. Later on, Fenimore in 1979 proposed the prompt NO mechanism to explain the additional NO being produced over and above the Zel'dovich thermal NO in hydrocarbon flames. Recently, researchers identified some additional routes through which NO and other oxides of nitrogen are formed [128]. Also nitrous oxide (N_2O) may be formed, having a strong greenhouse gas effect. The formation of NOx happens through four main routes:

(1) Thermal mechanism (Zeldovich).

(2) Prompt mechanism (Fenimore).

(3) Nitrous oxide mechanism.

(4) Fuel-N conversion (Fuel-N mechanism).

The first three mechanisms are contributing to the conversion of air nitrogen to NOx. Theoretical and experimental studies have shown that these three mechanisms are

contributing much less to NOx formation in biomass combustion than fuel-N conversion.

Regarding the first route, this is because the Zel'dovich mechanism is predominant at temperatures greater than 1500 °C [127,129], while the temperatures during biomass combustion for power production are typically lower. Contributions from the prompt mechanism are mainly found for fuel rich and high temperature conditions which are also not relevant in biomass combustion. The nitrous oxide mechanism is of relative importance in very fuel lean and low temperature conditions. However, it has been shown that more than 80% of NOx emissions in pulverized coal combustion systems are coming from fuel-N conversion, where the remaining emissions are a result of the thermal mechanism [130].

In biomass combustion systems, fuel-N conversion is even more dominant due to the unfavorable temperature conditions in typical biomass furnaces for other than fuel-N conversion. The combustion of biomass is normally carried out in grate or fluidized bed combustors, with relatively low temperature, which increase the importance of fuel-NOx, while pressurized combustion and high temperature in coal combustion can enhance the other NOx formation mechanism. Hence, the other mechanisms can be neglected from further studies of such biomass fired systems. As a conclusion, one should concentrate on fuel-N conversion to NOx in order to effectively control NOx formation in biomass combustion.

Their individual mechanisms are described in the following sections [128].

5.1.1.1 Thermal NO Mechanism (Zel'dovich Mechanism)

In the combustion of clean fuels (which do not contain nitrogen compounds) with air (which contains atmospheric N_2) NO is formed mainly by the Zel'dovich mechanism. This mechanism consists of three principal reactions as follows:

$$O + N_2 \underset{k_{1r}}{\overset{k_{1f}}{\rightleftharpoons}} NO + N \tag{5.1}$$

$$k_{1f} = 1.8 \times 10^{11} \exp(-38,370 / T) \ m^3 /(kmol \cdot s)$$
$$k_{1r} = 3.8 \times 10^{10} \exp(-425 / T) \ m^3 /(kmol \cdot s)$$

$$N+O_2 \underset{k_{2r}}{\overset{k_{2f}}{\rightleftarrows}} NO+O \tag{5.2}$$

$$k_{2f} = 1.8 \times 10^{10} \exp(-4,680/T) \; m^3/(kmol \cdot s)$$
$$k_{2r} = 3.8 \times 10^{9} \exp(-20,820/T) \; m^3/(kmol \cdot s)$$

$$N+OH \underset{k_{3r}}{\overset{k_{3f}}{\rightleftarrows}} NO+H \tag{5.3}$$

$$k_{3f} = 7.1 \times 10^{10} \exp(-450/T) \; m^3/(kmol \cdot s)$$
$$k_{3r} = 1.7 \times 10^{11} \exp(-24,560/T) \; m^3/(kmol \cdot s)$$

The chain nature of this mechanism can be observed in Figure 5.2. The Zel' dovich mechanism is also known as the "thermal" mechanism, because reaction (5.1) has very high activation energy (319 kJ/mol) due to the strong triple bond in the N_2, and so it is sufficiently fast only at high temperatures. Because of the low reaction rate constant, reaction (5.2) is the rate-determining step in the Zel'dovich reaction mechanism. As a rule-of-thumb, the thermal mechanism is usually unimportant at temperatures below 1800 K. NO is generally considered to be formed in the post-flame gases.
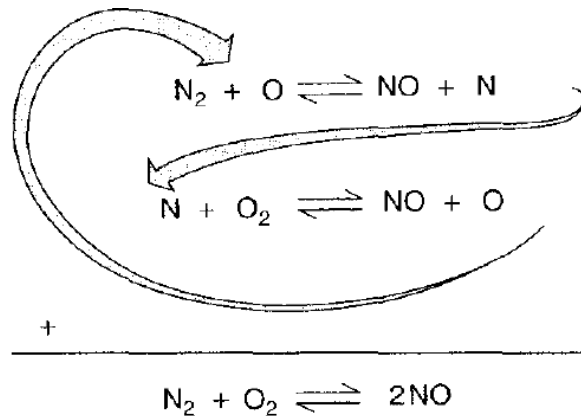
Figure 5.2 Chain nature of the thermal NO formation mechanism [128]

In general, this mechanism is coupled with the fuel combustion chemistry through the O_2, O, and OH species. Since the overall rate of NO formation by the thermal mechanism generally is slow compared with the fuel oxidation reactions, it often is assumed, following the suggestion of Zel'dovich, that the NO formation reactions can be decoupled from the fuel oxidation process. The concentration of NO

cannot be predicted well by considering it to be in equilibrium in reaction (5.1), because the reaction (5.1) is so slow that equilibrium is reached only for times that are much longer than typical residence times in the high-temperature range.

Quasi-steady-state assumption for N atom can be used to simplify the rate expression of NO formation. If the assumption that the NO concentrations are much less than the equilibrium values is made, the reverse reactions can be neglected. These assumptions greatly simplify the calculation of NO formation rate. Using reactions (5.l), (5.2), and (5.3), we have

$$\frac{dC_{NO}}{dt} = k_{1f}C_O C_{N_2} + k_{2f}C_N C_{O_2} + k_{3f}C_N C_{OH} \tag{5.4}$$

Assuming N atoms to be in quasi steady state [because of fast reactions (5.2) and (5.3)], $dC_N/dt = 0$; thus,

$$\frac{dC_N}{dt} = k_{1f}C_O C_{N_2} - k_{2f}C_N C_{O_2} - k_{3f}C_N C_{OH} \tag{5.5}$$

Solving Eq. (5.5) for C_N and substituting it into Eq. (5.4), we get

$$\frac{dC_{NO}}{dt} = k_{1f}C_O C_{N_2} \tag{5.6}$$

Hence, it can be observed that NO formation rate depends on the concentrations of N_2 and O. The concentration of N_2 can be accurately measured with a probe or can be estimated assuming equilibrium in the burnt gases. If the relevant timescales are sufficiently long, one can assume that the N_2, O_2, O, and OH concentrations are at their equilibrium values and N atoms are in quasi steady state. In flame zone proper and in certain short-timescale post-flame processes, the equilibrium assumption is not truly valid. *Super-equilibrium concentrations* of O atoms, up to several orders of magnitude greater than equilibrium, can greatly increase NO formation. *Partial-equilibrium* assumption for O atoms gives better estimate of O atom concentration as has been verified from experiments. Consider partial equilibrium for the following reactions:

$$H + O \underset{k_{i,r}}{\overset{k_{i,f}}{\rightleftharpoons}} OH + O \tag{5.7}$$

$$O + H_2 \xrightleftharpoons[k_{ii,r}]{k_{ii,f}} OH + H \tag{5.8}$$

$$OH + H_2 \xrightleftharpoons[k_{iii,r}]{k_{iii,f}} H_2O + H \tag{5.9}$$

For each of the reactions, the forward and backward reaction rates are equal. Therefore, we get

$$k_{i,f} C_H C_{O_2} = k_{i,r} C_{OH} C_O \tag{5.10}$$

$$k_{ii,f} C_O C_{H_2} = k_{ii,r} C_{OH} C_H \tag{5.11}$$

$$k_{iii,f} C_{OH} C_{H_2} = k_{iii,r} C_{H_2O} C_H \tag{5.12}$$

Solving for O-atom concentration, we obtain,

$$C_O = \frac{k_{i,f} k_{iii,f} C_{O_2} C_{H_2}}{k_{i,r} k_{iii,r} C_{H_2O}} \tag{5.13}$$

Therefore, the 0 atom concentration can be calculated from the concentrations of H_2O, O_2, and H_2, which can be measured or estimated easily, since they are stable species.

5.1.1.2 Prompt NO Mechanism (Fenimore Mechanism)

Fenimore discovered that some NO was promptly produced in the flame zone of laminar premixed flames long before there would be time to form NO by the thermal mechanism, and he termed this rapidly formed NO the "prompt" NO, Numerous studies have shown that prompt NO in hydrocarbon flames is formed primarily by a reaction sequence that is indicated by the rapid reaction of hydrocarbon radicals (CH, CH_2, C_2, C_2H, C) with molecular nitrogen, leading to formation of amines or hydrocyanic acid (HCN) that subsequently reacts to form NO, Therefore, prompt NO reaction mechanism is of paramount importance in hydrocarbon fuels, especially in fuel-rich conditions.

The following reactions are considered principal reactions, although there might also be other reactions:

$$CH + N_2 \xrightleftharpoons[k_{4r}]{k_{4f}} HCN + N \tag{5.14}$$

$$CH_2 + N_2 \xrightleftharpoons[k_{5r}]{k_{5f}} HCN + NH \tag{5.15}$$

$$CH_2 + N_2 \xrightleftharpoons[k_{6r}]{k_{6f}} H_2CN + N \tag{5.16}$$

$$C + N_2 \xrightleftharpoons[k_{7r}]{k_{7f}} CN + N \tag{5.17}$$

Reaction (5.14) is the primary path and is the rate-limiting step in the sequence. The rate constant k_{4f} correlated from many sets of experimental data can be expressed as

$$k_{4f} = 4.4 \times 10^{12} \exp(-11{,}060K / T) \ \text{cm}^3/(\text{kmol} \cdot \text{s}) \tag{5.18}$$

Reaction (5.14) leads to prompt NO. There have been indirect measurements of $k4$ from flame, shock-tube, and stirred-reactor data and one direct shock-tube measurement. The estimated accuracy of k_4 from Eq. (5.18) is about a factor of 2 at the present time. The activation energy for reaction (5.14) is between 75 and 92 kJ/mol, which is much lower than 319 kJ/mol for the formation of thermal NO. Thus, reaction (5.14) is very important for NO formation through the production of HCN species.

Overall, prompt-NO formation involves three separate kinetic issues, including (1) the CH concentration and how it is established; (2) the rate of molecular nitrogen fixation (i.e., value of k_4); and (3) the rate of interconversion among fixed nitrogen fragments. it was found that reaction (5.14) is an important rate-limiting step for NO, HCN, and TFN (total fixed nitrogen, TFN=NO+ HCN + NH$_3$) production under all conditions investigated. The reaction has sensitivity coefficients for these species approaching unity in rich mixtures. Even under lean conditions ($\phi < 0.8$), it plays a major role in NO formation. The thermal NO mechanism is the dominant source of NO only in the equivalence-ratio range ($\phi = 0.8$-1.0). For $\phi < 0.8$, the temperature becomes sufficiently low and the following reactions become an important source of NO formation:

$$O + N_2 + M \xrightleftharpoons[k_{8r}]{k_{8f}} N_2O + M \tag{5.19}$$

$$O + N_2O \xrightleftharpoons[k_{10r}]{k_{10f}} NO + NO \tag{5.20}$$

CH is formed as an intermediate at the flame front only. The mechanism of CH formation depends slightly on the fuel. In all cases, CH is formed from methylene (CH_2) by reaction with H and OH, i.e.,

$$H+CH_2 \underset{k_{11r}}{\overset{k_{11f}}{\rightleftharpoons}} CH+H_2 \tag{5.21}$$

$$OH+CH_2 \underset{k_{12r}}{\overset{k_{12f}}{\rightleftharpoons}} CH+H_2O \tag{5.22}$$
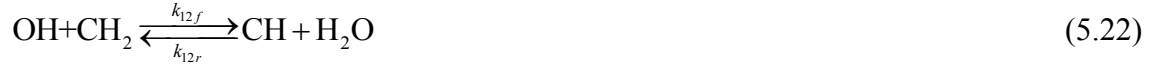
The CH_2 can be formed either from methyl radical (CH_3) or from acetylene. For $\phi < 1.5$, the CH_3 is the dominant source.

$$CH_3+OH \underset{k_{13r}}{\overset{k_{13f}}{\rightleftharpoons}} CH_2+H_2O \tag{5.23}$$

$$CH_3+H \underset{k_{14r}}{\overset{k_{14f}}{\rightleftharpoons}} CH_2+H_2 \tag{5.24}$$
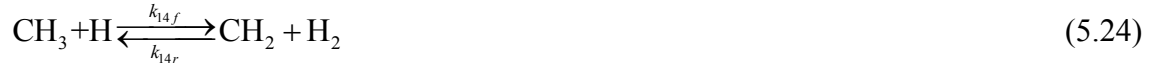
The most important CH-consuming steps are the following reactions:

$$CH+H \underset{k_{15r}}{\overset{k_{15f}}{\rightleftharpoons}} C+H_2 \tag{5.25}$$

$$CH+H_2O \underset{k_{16r}}{\overset{k_{16f}}{\rightleftharpoons}} CH_2O+H \tag{5.26}$$

$$CH+CO_2 \underset{k_{17r}}{\overset{k_{17f}}{\rightleftharpoons}} HCO+CO \tag{5.27}$$

Up to an equivalence ratio of approximately $\phi = 1.2$, the HCN and N produced by reaction (5.14) are converted rapidly to NO, primarily by the following reactions:

$$HCN+O \underset{k_{18r}}{\overset{k_{18f}}{\rightleftharpoons}} NCO+H \tag{5.28}$$

$$NCO+H \underset{k_{19r}}{\overset{k_{19f}}{\rightleftharpoons}} NH+CO \tag{5.29}$$

$$NH+H \underset{k_{20r}}{\overset{k_{20f}}{\rightleftharpoons}} N+H_2 \tag{5.30}$$

$$N+OH \underset{k_{21r}}{\overset{k_{21f}}{\rightleftharpoons}} NO+H \tag{5.31}$$

Beyond $\phi = 1.2$, several factors combine to cause the NO concentration to decrease relative to HCN:

1. The conversion of HCN to NO by the above mechanism is no longer rapid.

2. The "recycle" of NO to HCN by the mechanism discussed below begins to inhibit NO production.

3. The reaction $N + NO \leftrightarrow N_2 + O$ shifts direction from reverse to forward.

A decrease in the 0 atom concentration contributes to all three of the above occurrences. Under rich conditions, reactions that convert CH_3 to CH_2 become more competitive with the oxidation reaction of CH_3 according to $CH_3 + O \leftrightarrow CH_2O + H$, thereby producing the radicals C, CH, and CH_2 and allowing the following recycle reactions to be more effective:

$$C + NO \underset{k_{22r}}{\overset{k_{22f}}{\rightleftharpoons}} CN + O \tag{5.32}$$

$$CH + NO \underset{k_{23r}}{\overset{k_{23f}}{\rightleftharpoons}} HCN + O \tag{5.33}$$

$$CH_2 + NO \underset{k_{24r}}{\overset{k_{24f}}{\rightleftharpoons}} HCNO + H \tag{5.34}$$

It has been found that at $\phi = 1.4$ the peaks in the CH and TFN (total fixed nitrogen) concentrations occur simultaneously. Beyond $\phi = 1.4$, the fixed nitrogen concentration is limited by the availability of the chain carriers (H and OH) required for producing CH from methane. The following chain-branching reactions occur

$$H + O_2 \underset{k_{25r}}{\overset{k_{25f}}{\rightleftharpoons}} OH + O \tag{5.35}$$

$$OH + CH_3 \underset{k_{26r}}{\overset{k_{26f}}{\rightleftharpoons}} CH_2OH + H \tag{5.36}$$

$$CH_2OH + M \underset{k_{27r}}{\overset{k_{27f}}{\rightleftharpoons}} CH_2O + H + M \tag{5.37}$$

In this regime, the following reaction

$$CH_3 + N \underset{k_{28r}}{\overset{k_{28f}}{\rightleftharpoons}} H_2CN + H \tag{5.38}$$

appears as a competitor for nitrogen atoms, competing with

$$N+OH \underset{k_{29r}}{\overset{k_{29f}}{\rightleftharpoons}} NO+H \qquad (5.39)$$

The dissociation of H_2CN following reaction (5.38) results in the formation of hydrogen cyanide, rather than nitric oxide, from the N atom in reaction (5.38).

From experiments and calculations, it has been found that at low temperatures (T < 2000 K) the hydrocarbon-nitrogen prompt-NO channel dominates the rate of NO formation. As the temperature increases, the relative importance of the hydrocarbon-nitrogen prompt-NO channel decreases, so that for temperatures above 2500 K, NO formation is controlled mainly by the thermal mechanism. For a series of premixed methane/air flames ($1.37 \geq \phi > 1.06$), the transition from the hydrocarbon-nitrogen prompt NO mechanism to the thermal mechanism occurs as conditions become leaner.

5.1.1.3 NO Production from Fuel-Bound Nitrogen

In fossil fuels (coal and coal-derived fuels), nitrogen is present as the chemically bound nitrogen. It is the primary source of production of nitrogen oxides formed on their combustion. From different experiments, it has been found that the extent of conversion of fuel-bound nitrogen (FN) into NO is strongly dependent on the local combustion environment (temperature and stoichiometric conditions) and on the initial level of nitrogen compounds in the fuel-air mixture. Available data suggest that the gas-phase fuel-nitrogen reaction sequence is initiated by a rapid conversion of the fuel nitrogen compounds to hydrogen cyanide (HCN) and ammonia (NH_3). HCN appears to be the principal product when the fuel nitrogen is bound in an aromatic ring, NH_2 when the fuel nitrogen is in the form of amines. Thus, the mechanism of NO production is essentially the mechanism of oxidation of HCN and NH_3. The important paths are shown in Figure 5.3, along with the prompt mechanism.

5.1.1.3.1 The Oxidation of HCN

The removal of HCN is controlled by the reaction of HCN with O atoms, even in rich flames.

$$HCN + O \xrightleftharpoons[k_{18r}]{k_{18f}} NCO + H \qquad (5.28)$$

$$HCN + O \xrightleftharpoons[k_{30r}]{k_{30f}} NH + CO \qquad (5.40)$$
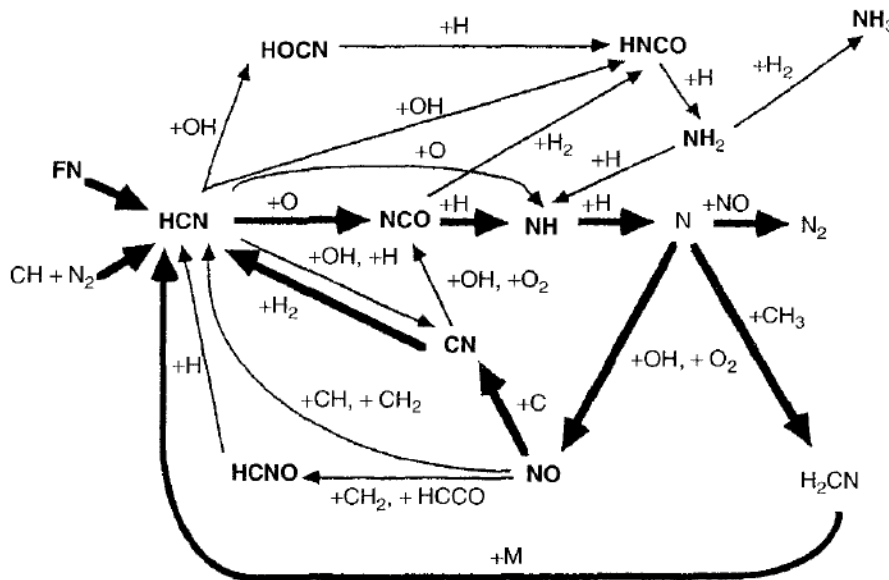
Figure 5.3 Reaction path diagram showing the major steps in prompt NO and conversion of fuel nitrogen to NO [128]

The subsequent reactions of NCO and NH with hydrogen atoms, producing N, are relatively fast and have little influence on the observed species profiles. The distribution of NO and N_2 in the flame is governed by the N atom reactions,

$$N + OH \xrightleftharpoons[k_{3r}]{k_{3f}} NO + H \qquad (5.3)$$

$$N + NO \xrightleftharpoons{} N_2 + O \qquad (5.1)$$

In the post-flame gases of very rich atmospheric-pressure flames, HCN is removed primarily by reaction with OH. Two routes have been suggested one that is first order in OH,

$$OH + HCN \xrightleftharpoons[k_{31r}]{k_{31f}} HOCN + H \qquad (5.41)$$

111

and one that is second order,

$$OH + HCN \underset{k_{32r}}{\overset{k_{32f}}{\rightleftharpoons}} CN + H_2O \tag{5.42}$$

$$CN + OH \underset{k_{33r}}{\overset{k_{33f}}{\rightleftharpoons}} NCO + H \tag{5.43}$$

under the partially equilibrated conditions prevalent in the post-flame gases of atmospheric-pressure flames. The first route is dominant below 2300 K and the second route above 2300 K.

Accumulated experience by chemists in modeling a variety of flames, stirred reactors, and flow reactors indicates that the O + HCN sequence shown in Figure 5.4 always plays a major role in the conversion to NO and N_2 . The OH+ HCN reactions normally come into play only under conditions that are both rich and nearly equilibrated. If HCN conversion takes place in a highly nonequilibrated reaction zone, even under very rich conditions, the O + HCN sequence still is likely to be dominant.
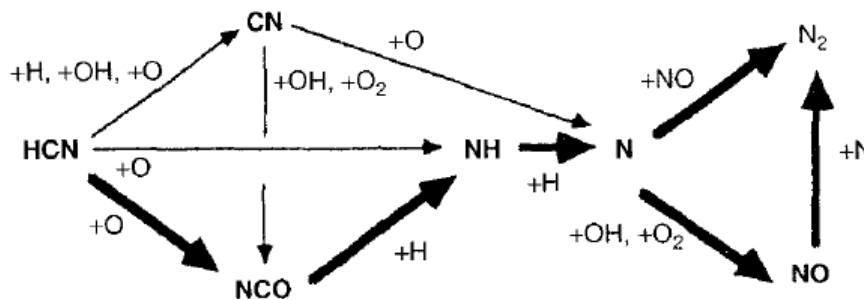
Figure 5.4 Reaction path diagram illustrating the reaction mechanism by which HCN is converted to NO and N_2 [128]

5.1.1.3.2 The NO → HCN → N₂ Mechanism

In rich combustion systems, there is the possibility of reaction of NO with hydrocarbon free radicals, leading to the formation of HCN and, eventually, of molecular nitrogen N_2. The main reaction paths involved in converting NO to N_2 through HCN and CN is shown in Figure 5.5. As shown in this figure, there is no direct interaction between hydrocarbon and nitrogen chemistry. There are different routes of production of HCN. Based on experiments conducted on low-pressure premixed flames (ϕ = 1.5, $H_2/O_2/Ar$ flames), to which small quantities of acetylene, HCN, and NO were

added in various combinations, researchers found that CN concentration has a sharp peak at a few millimeters above the flame. From such observations, it can be concluded that CN is produced and destroyed in this region of the flame by the sequence

$$C + NO \underset{k_{22r}}{\overset{k_{22f}}{\rightleftharpoons}} CN + O \tag{5.32}$$

$$CN + H_2 \underset{k_{34r}}{\overset{k_{34f}}{\rightleftharpoons}} HCN + H \tag{5.44}$$
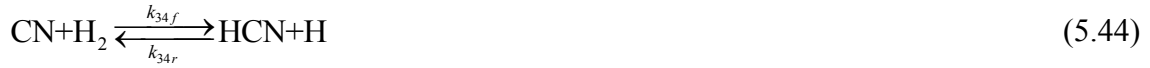
Another sequence for HCN production is the following reaction:

$$CH + NO \underset{k_{23r}}{\overset{k_{23f}}{\rightleftharpoons}} HCN + O \tag{5.33}$$

HCN is partially converted to N_2 in the flame by the following sequence of reactions:

$$HCN + O \underset{k_{18r}}{\overset{k_{18f}}{\rightleftharpoons}} NCO + H \tag{5.28}$$

$$NCO + H \underset{k_{19r}}{\overset{k_{19f}}{\rightleftharpoons}} NH + CO \tag{5.29}$$

$$NH + H \underset{k_{20r}}{\overset{k_{20f}}{\rightleftharpoons}} N + H_2 \tag{5.30}$$

$$N + NO \rightleftharpoons N_2 + O \tag{5.1}$$

It has been shown that in atmospheric-pressure, fuel-rich $H_2/O_2/Ar$ flames to which small amounts of NO were added, significant removals of NO ($\sim$ 40%) occurs by the following reaction sequence:

$$H + NO + M \underset{k_{35r}}{\overset{k_{35f}}{\rightleftharpoons}} HNO + M \tag{5.45}$$

$$HNO + H \underset{k_{36r}}{\overset{k_{36f}}{\rightleftharpoons}} NH + OH \tag{5.46}$$

$$NH + H \underset{k_{37r}}{\overset{k_{37f}}{\rightleftharpoons}} N + H_2 \tag{5.47}$$

$$N + NO \rightleftharpoons N_2 + O \tag{5.1}$$
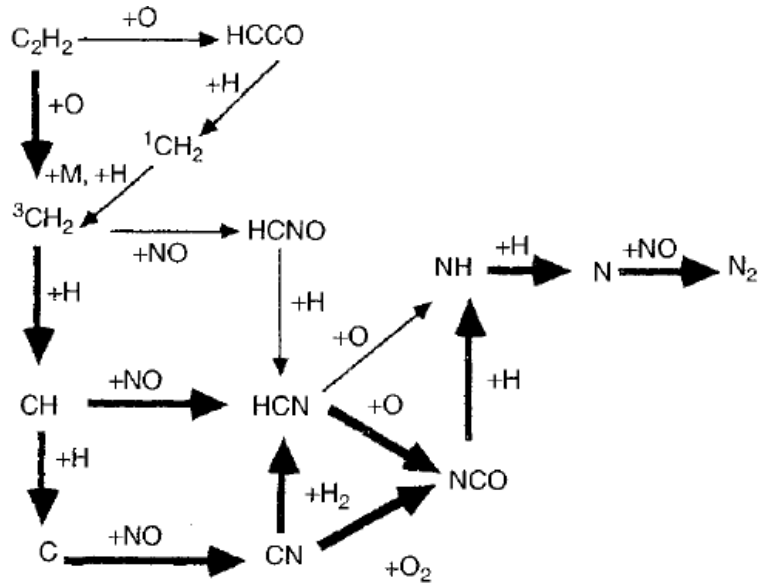
Figure 5.5 Reaction path diagram illustrating the NO→HCN→N$_2$ conversion mechanism for NO added flames [128]

5.1.1.3.3 The Oxidation of NH$_3$

Figure 5.6 shows the principal reactions through which ammonia is oxidized to NO and then NO is converted to molecular nitrogen in NH$_3$/O$_2$ flames. Ammonia is converted to NH$_2$ by hydrogen abstraction. The primary abstraction reaction is

$$NH_3 + OH \underset{k_{38r}}{\overset{k_{38f}}{\rightleftharpoons}} NH_2 + OH_2 \qquad (5.48)$$

The NH$_3$ reaction with O atom under fuel-lean conditions and the NH$_3$ reaction with H atom under fuel-rich conditions are both significant for NH$_2$ formation:

$$NH_3 + O \underset{k_{39r}}{\overset{k_{39f}}{\rightleftharpoons}} NH_2 + OH \qquad (5.49)$$

$$NH_3 + H \underset{k_{40r}}{\overset{k_{40f}}{\rightleftharpoons}} NH_2 + H_2 \qquad (5.50)$$
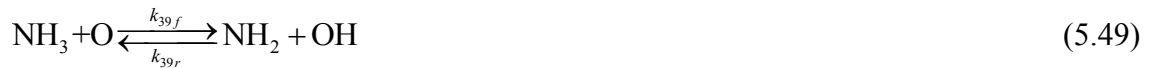
Successive smaller amine free radicals are formed by reaction with H atoms and to a lesser extent by reaction with OH,

$$NH_i + H(OH) \underset{k_{41r}}{\overset{k_{41f}}{\rightleftharpoons}} NH_{i-1} + H_2 (H_2O) \qquad (5.51)$$

$i = 1, 2$

114
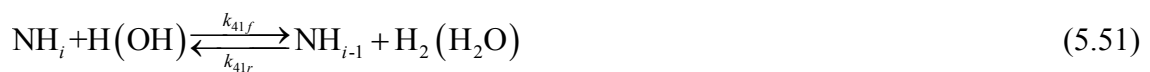
Each NH; free radical can undergo subsequent reaction by one of two mechanisms:

1. oxidation leading to NO formation;

2. reaction with NO leading to the formation of molecular nitrogen.
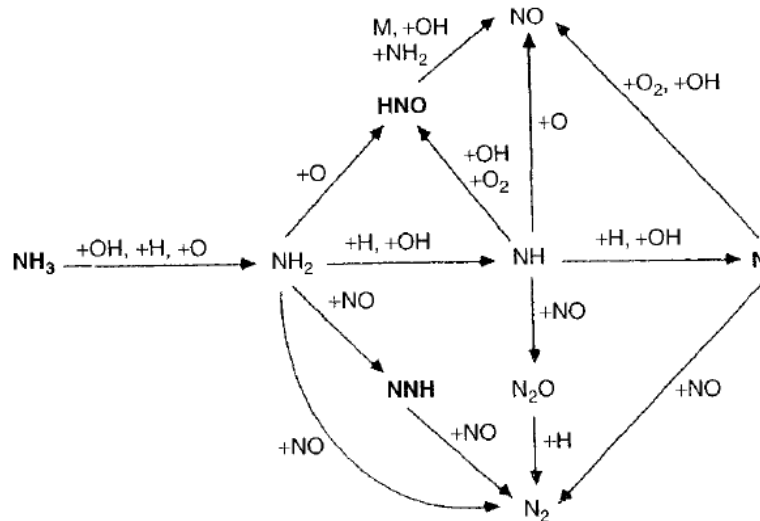
Figure 5.6 Reaction path diagram showing the major routes for the oxidation of NH_3 [128]

Whether N, NH, or NH2 is the primary radical in determining NO/N_2 product distribution depends on the equivalence ratio (ϕ). For very lean flames, NH_2 is the critical amine radical. As ϕ increases, the greater availability of H atoms results in a shift in the critical radical species from NH_2 to NH to N. Normally all three radicals play same role. However, in rich flames the N atom is more dominant. It is interesting to note that there are reactions other than those shown in Figure 5.6 that form N_2 but do not involve NO.

5.1.1.4 NO$_2$ Mechanism

It has been observed that NO_2 can have significant concentration in certain combustion conditions, especially near the flame zone. Kinetic calculations have indicated that the NO_2 formation and destruction in flames can occur according to the following sequence.

$$NO+HO_2 \underset{k_{42r}}{\overset{k_{42f}}{\rightleftharpoons}} NO_2 + OH \tag{5.52}$$

$$NO_2 + H \xrightleftharpoons[k_{43r}]{k_{43f}} NO + OH \tag{5.53}$$

$$NO_2 + O \xrightleftharpoons[k_{44r}]{k_{44f}} NO + O_2 \tag{5.54}$$

In the low-temperature regions of flames, significant HO_2 concentrations are found that can react with NO formed in the high-temperature regions and transported by diffusion to the low-temperature region. The NO_2 removal reactions are rapid, and in the presence of high radical concentrations, NO_2 will be converted rapidly back to NO. The most important reaction for NO_2 formation is reaction (5.52). Since the rate of this reaction depends on the HO_2 concentration, NO_2 formation is also sensitive to reactions forming and removing HO_2. The following is the principal HO_2 formation reaction in the low-temperature region of the flame.

$$H + O_2 + M \xrightleftharpoons[k_{45r}]{k_{45f}} HO_2 + M \tag{5.55}$$

The H atoms needed for this reaction are transported from the high-temperature regions by molecular diffusion. Since H atoms play an important role in HO_2 production, NO_2 formation is also sensitive to reaction (5.35). The principal NO_2 removal step is reaction (5.53), while reaction (5.54) is not so important.

5.1.1.5 N_2O Mechanism

N_2O is an important nitrogen oxide under fuel-lean conditions. Studies indicate that N_2O is a very short-lived species in hot combustion gases and that the principal N_2O formation reactions involve NO and various nitrogen-containing radicals such as

$$NH + NO \xrightleftharpoons[k_{46r}]{k_{46f}} N_2O + H \tag{5.56}$$

$$NCO + NO \xrightleftharpoons[k_{47r}]{k_{47f}} N_2O + CO \tag{5.57}$$
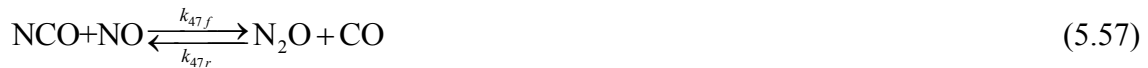
The principal N_2O formation reaction is reaction (5.56). For rich mixtures, both reactions (5.56) and (5.57) are important in N_2O formation. The forward reaction rate coefficient for reaction (5.56) is estimated to be $k_{46f} = 2.46 \times 10^{15}\ T^{-0.8}\ cm^3/mol\text{-}s$ and

that of reaction (5.57) is $k_{47f} = 1.0 \times 10^{13}$ (390 cal/R_uT) cm^3/mol-s. The N$_2$O formed in these reactions rapidly reacts with H atoms to form N$_2$:

$$N_2O+H \underset{k_{48r}}{\overset{k_{48f}}{\rightleftharpoons}} N_2 + OH \qquad (5.58)$$

In fuel-lean flames, the primary N$_2$O removal reaction is reaction (5.58). While the removal is done by reaction (5.58), there is another mechanism for the formation of N$_2$O and subsequent conversion to NO. This mechanism is analogous to the thermal mechanism in that O atom attacks N$_2$. In the presence of a third body, *M,* the outcome of this reaction is N$_2$O.

$$N_2+O+M \rightarrow N_2O + M \qquad (5.59)$$

The N$_2$O may subsequently react with O atoms to form NO

$$N_2O+O \rightarrow NO + NO \qquad (5.60)$$

The activation energy of this reaction is around 97 kJ/mol. Under fuel-lean conditions, CH formation is suppressed, leading to less Fenimore prompt NO, and at low-temperatures, Zel'dovich thermal NO is also less. What remains is NO generated via N$_2$O, which is promoted at high pressures because of the three-body reaction. Since the activation energy for the three-body reaction is low, low temperature does not affect the formation rate of NO. Due to the characteristic of the reaction mechanism, this route is the major source of NO in lean premixed combustion in gas turbine engines.

5.1.2 Reduction of nitrogen oxides

Two major approaches exist for NOx reduction, primary measures and secondary measures. Primary measures focus on preventing the formation of NOx during the combustion stage whereas secondary measures aim to reduce NOx after its formation. Modifications to fuel properties and the combustion chamber and improvements to combustion technologies are examples of primary measures. One of the most important and widely used measures to reduce NOx in solid fuels combustion is staged combustion. Staged combustion, including staged air combustion and staged fuel combustion, can give a NOx reduction in the range of 50-80% [124,131-134, 135, 136].

5.1.2.1 Air staging

Concerning the applications, air staging was first used in pulverized coal and oil fired boilers, but with time the technique was adjusted and renamed for a variety of other applications, e.g., "late air-staging" for fluidized bed combustors and "rich-lean combustion" for gas turbines. As for the fuels, air staging has been applied mainly to fossil fuels, biomass, gasified coal and biomass and waste [134]. Staged-air combustion is applied also in small scale biomass combustion applications. However, the possibilities for an accurate control of the combustion air are usually limited in small-scale applications, which may result in higher emission levels [3].

The general principle of air staging (Figure 5.7) is to create a distinct fuel rich (oxygen deficient) zone and a subsequent fuel lean zone inside the furnace. The primary zone stoichiometric ratio (SR1, actual air/ stoichiometric air) is kept less than 1, creating a fuel-rich zone or pockets in the primary combustion zone and leading to less intensive primary combustion flame. A portion of the secondary air (over-fire air) is injected later in the furnace a creating fuel lean zone to complete the combustion. The region downstream of the over-fire air ports is the burnout zone. Air staging reduces NOx formation mainly by two mechanisms: (1) air staging allows deprivation of oxygen, and less mixing of fuel and air in the primary combustion zone, inhibiting the conversion of fuel-N to NOx and hence reducing fuel-NOx and (2) air staging results in a cooler primary combustion flame and hence less thermal-NOx [137, 135]. By applying staged-air combustion, a simultaneous reduction of both emissions from incomplete combustion and NOx emissions is possible through a separation of devolatilization and gas phase combustion. These results in improved mixing of fuel gas and secondary combustion air, which reduces the amount of air needed, providing a lower local and overall excess air ratio and higher combustion temperatures. Hence, emissions from incomplete combustion are reduced by a temperature increase, which speeds up the elementary reaction rates, and by an improved mixing which reduces the residence time needed for the mixing of fuel and air [3].
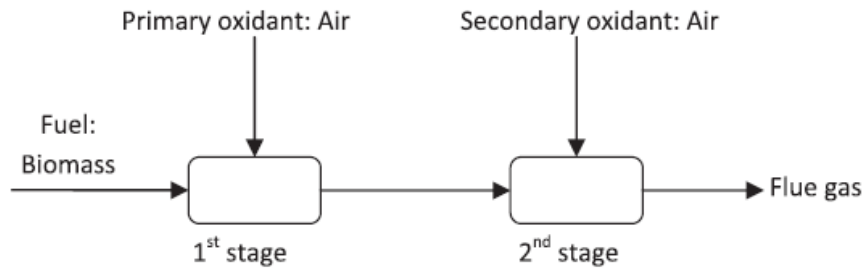
Figure 5.7 Principal sketch of air staging in solid fuel combustion [132]

Add primary air at a less than stoichiometric ratio, in order to devolatilize the volatile fraction of the fuel, resulting in a fuel gas consisting mainly of CO, H_2, C_xH_y, H_2O, CO_2, and N_2 and also small amounts of NH_3, HCN, and NOx from the fuel nitrogen content. If sufficient oxygen exists in the first stage, the fuel nitrogen intermediates will be converted to NOx (mainly NO), but shortage of oxygen will cause NO to act as an oxidant for CO, CH_4, HCN, and NH_i (with $i = 0, 1, 2, 3$) in the reduction zone, hence to reduce the nitrogen in NO and NH_i to molecular nitrogen, i.e., N_2, in reactions such as $NO + NH_2 = N_2 + H_2O$ or $NO + CO = CO_2 + 0.5N_2$ [124,138-140]. NH_3 and HCN form in the pyrolysis stage of combustion depending on the temperature and fuel type, where ammonia is believed to be the most important N-species in the combustion of biomass, while HCN is more important for high-rank coals [141-143]. Ammonia that is formed in this stage is converted to radicals of NH_i. At high temperatures and fuel lean combustion, these radicals will be converted to NO, while at fuel rich conditions, N_2 will be the main product [144]. In the second stage, sufficient secondary air is supplied to ensure a good burnout and low emission levels from incomplete combustion [3]. As illustrated in Figure. 5.8, NO_X reduction may also occur by char and NO interactions. It is a complex process affected by a variety of factors involving several fuel and technology parameters and is not completely understood yet. It is believed that the NO-char reaction is affected by physical structure and chemical composition of char. Concerning the latter, an important catalytic effect is mainly attributed to concentration of potassium; however, its effect is very temperature dependent because of the formation of K-silicates [145].

Fuel-N content and the conversion rate of NOx precursors (NH_3 and HCN) to NOx have been experimentally and numerically investigated for different solid biomass [146-149].
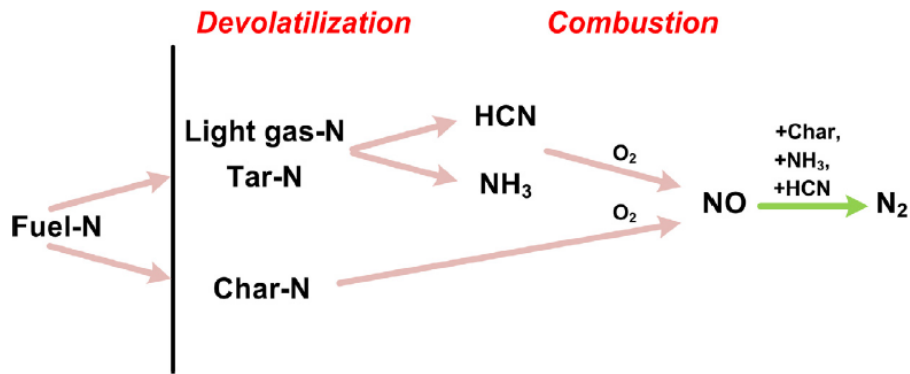
Figure 5.8 Simplified schematic description for the Fuel-N conversion paths based on literature. Main products related to each step are indicated.

According to the GRI-mechanism [150], the decomposition of HCN and NH_3 follows the reactions [132]:

$$HCN + O = NCO + H \tag{5.61}$$

$$HCN + O = NCO + H \tag{5.62}$$

$$HCN + OH = CN + H_2O \tag{5.63}$$

$$HCN + O = CN + CO \tag{5.64}$$

$$HCN + OH = HNCO + H \tag{5.65}$$

$$NH3 + OH = NH_2 + H_2O \tag{5.66}$$

$$NH3 + H = NH_2 + H_2 \tag{5.67}$$

$$NH3 + O = NH_2 + OH \tag{5.68}$$

In [151, 152, 153] it has been showed that the primary excess air ratio, number of air stages, temperature, and residence time all affect the NOx reduction level. However, the most important variable is the primary excess air ratio. The primary air ratio possibly varies depending on the grate system and biomass fuel used. Generally, increasing the excess air ratio increases the NOx emission level. Decreasing primary air ratio leads to higher temperature peaks at the transition between the first and the second combustion chamber due to a higher concentration of unburned flue gas compounds released from the biomass fuel bed. The primary air ratio should not be too low without additional measures, because this would lead to higher concentrations of combustible

flue gases released from the fuel bed, resulting in higher furnace temperature and CO concentrations despite the higher stagnation momentum of the secondary air jets (if the total excess air ratio is kept constant). Yet an optimum primary excess air ratio exists (0.7-1[3, 136, 137, 145, 153, 154, 155, 156] but due to furnace design sometimes it is not possible to achieve this optimal stoichiometric ratio [135]). Increasing the number of air stages will decrease the potential fuel-N to NOx conversion, but the effect of additional air stages may be very small. Large and modern grate fired boilers are generally operated with an appropriate excess air ratio, and consequently under favorable combustion conditions, which result in low unburnt emissions [147, 153]. The position of the secondary air inlets above the fuel bed was shown to greatly affect the NOx emissions, with a higher position leading to lower NOx emissions [135, 137, 145, 157, 158]. But in domestic/small-scale biomass boilers, injecting the secondary air at the higher position increases the residence time in the primary combustion zone due to the fixed and relatively small furnace space, the reduced residence time in the secondary combustion zone inevitably leads to higher CO emissions [135]. Concerning the optimal number of stages, the literature is somewhat controversial, but it appears that 3 to 5 stages is a favorable option [134]. Also, previous work showed the effect of fuel type and cocombustion of biomass with natural gas on NO emissions when using two-stage combustion [159].

Temperature can decrease, increase, or has no effect on the NOx emission level, depending on the temperature range applied to the reactor [147]. The temperature impact on NO_x emission depends on the flue gas atmosphere. Whereas in air-rich proportions the NO_x emission increases with higher temperatures, the trend is reversed under reducing conditions: in air staging, high temperatures cause lower NO_x emissions. The reason for the decreasing NO_x emission with increasing temperature may be an increase in the release of volatile nitrogen or accelerated decomposition of gaseous nitrogen and a reduced amount of char-N which may be converted to NO_x. The analysis of the simulations indicates that at high burnout temperature NH_3 and HCN are destroyed leading only to a weak increase of the NO_x emission. N_2O which is formed at low temperatures in the reduction zone is also reduced to a negligible amount at this burnout temperature. A comparison of the temperature effects for air staging and reburning suggests that accelerated decomposition is the dominant effect for the lower

NO_x emissions. The temperature has also a distinct influence on the reaction velocities. Regarding the nitrogen species forming and consuming reactions, the characteristic reaction time at 800 °C is about 10 times slower than at 1300 °C [132, 157]. Increased temperature in the exit duct has a clear effect on the CO emissions and allows a more radical mode of operation of the combustor to reduce NO [145].

5.1.2.2 Other primary measures for nitrogen oxides reduction

Fuel staging (and reburning) uses the principal of NO reduction in the second stage by adding more fuel or even a different fuel, e.g., more of the same solid fuel for fuel staging or hydrocarbons, such as natural gas for reburning. In the first stage, NOx is formed because of lean combustion. In the second fuel stage, NO reduction occurs at reducing conditions, where air is added for complete combustion. Low NOx levels can be achieved by fuel staging at lower temperatures than what is needed for air staging and the secondary fuel properties affect the NOx emission level (better efficiency with smaller particle size and higher amount of volatile matter) [132, 133].

Another technique of primary measures for NOx reduction in biomass combustion is flue gas recirculation (FGR) which basically increases the total mass flux of the gases and decreases the temperature and the partial pressure of oxygen in the mixture [160]. It is proposed that in fixed-bed combustion of straw, the effect of FGR on NO reduction could be considerable [161]. Whereas at combustion of demolition wood employing FGR is not so considerable and can reduce the NOx emissions by an additional 5%−10% [128] comparing to staged air combustion. The results of the same study show that the NOx reduction level depends heavily on the stoichiometric conditions in the primary (reduction) zone and the effectiveness of FGR is higher outside of the optimum range of excess air ratios.

Fuel staging or reburning has first been tested on coal fired utilities using natural gas as reburn fuel. In fuel staging the first stage of the combustion process operates slightly fuel lean, whereby the NO_X production is high (Figure 5.9). Then, additional fuel is added which creates fuel-rich conditions in the reburn zone. When hydrocarbons are used as reburn fuel, the hydrocarbon radicals entering the reburn zone can initialize the NO reduction mechanisms. The major reaction path found from research studying

the reburning mechanism through elementary chemical reactions under fuel rich conditions is the formation of HCN.

$$C, CH, CH_2, CH_i + N \rightarrow HCN... \tag{5.69}$$

$$HCN+O, OH \rightarrow N_2 +... \tag{5.70}$$

Because the volatile content of wood is high (80-85%), wood is highly reactive and therefore well suited as reburn fuel. Also the nitrogen content may be beneficial since it leads to additional reducing species [132].

$$NH_i + NO \rightarrow N_2 +... \tag{5.71}$$
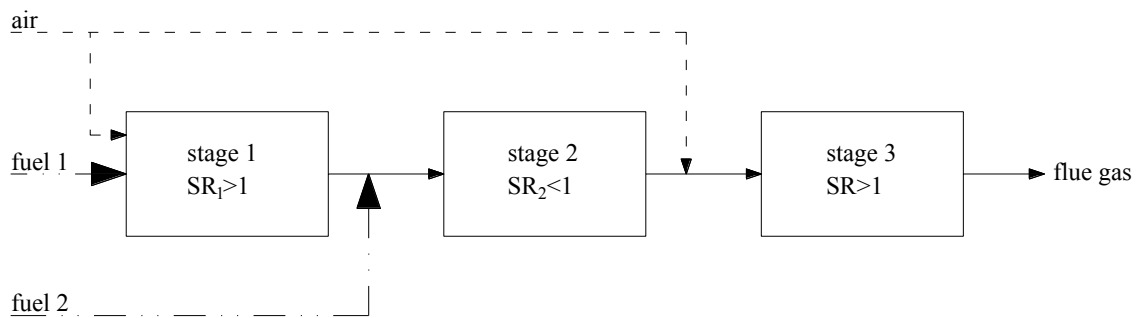
Figure 5.9 Principles of fuel staging [132]

Combined staged (CS) technology [134] is a method of NOx reduction including reburning, staged air combustion (AS), staged fuel combustion (FS), and selective noncatalytic reduction (SNCR) [162-164]. Combined staged technology starts to reduce NOx emissions where the other methods are not sufficient. Studies showed that CS is more effective for NOx reduction, especially in the temperature range of 1000-1400 °C [134]. For temperatures below 850 °C, higher N_2O, lower NOx, and slightly higher CO emissions are reported for cocombustion of coal and woody biomass [165].

5.2 Ash related properties

The ash formation during biomass combustion under grate firing conditions is illustrated in Figure 5.10. Part of the inorganic elements contained in the fuel may be released and form inorganic gas species and particulate matter (fly ash particles and aerosols), whilst the remaining part forms bottom ash. It can be seen, from the figure, that the particulate matter can be formed by two different modes, which lead to a characteristic bimodal particle size distribution. One is the fine mode, in which the main route of particle formation is nucleation and condensation from the gas phase. The fine mode usually consists of aerosols with particle diameters between 30 and 300 nm. The other is the coarse mode, which mainly consists of non-volatilized ash residuals and results in fly ash particles with diameters of 1 μm $< d_p <$ 10 μm. Amongst all the ash streams, bottom ash represents the majority, in terms of mass fractions, for grate-fired boilers burning biomass. The mass fraction of the bottom ash varies with different factors, e.g., the type of grate-fired boilers, the operation, and the fuel properties [111].
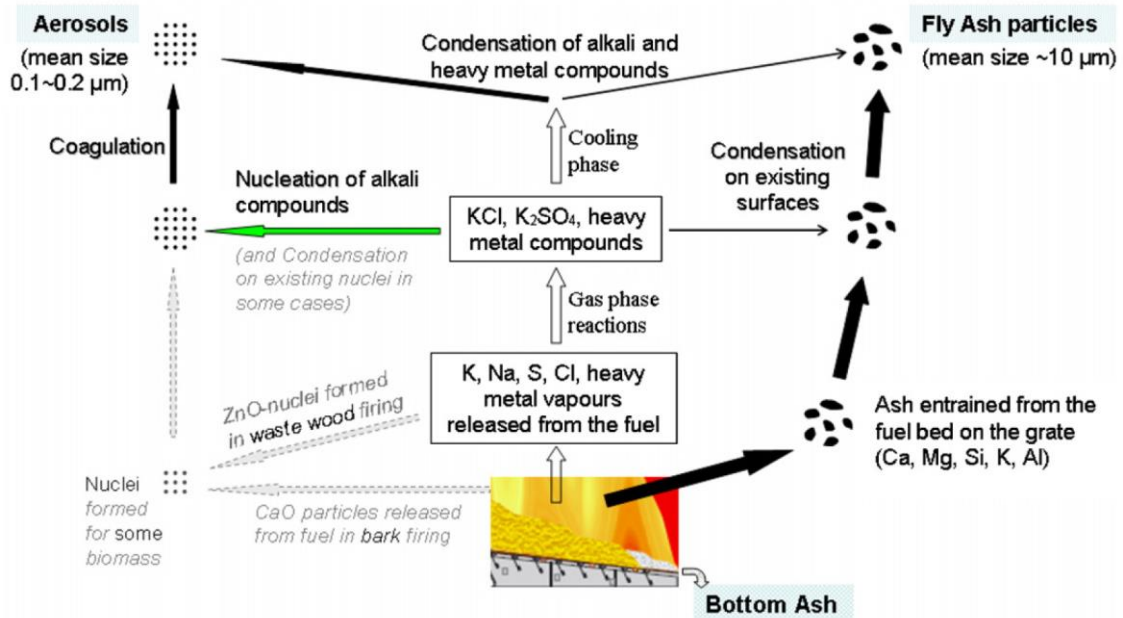
Figure 5.10 Schematic illustration of ash formation routines during grate-firing of biomass [111]

Beside the environmental impact issues, ash related problems (deposition and corrosion) represent the great challenge in process of biomass utilization. Additional, the increased biomass consumption has resulted in higher prices of virgin wood up to a range where it is no longer profitable to operate power stations based on combustion of wood alone [166]. This has led to increased utilization of alternative fuels that are cheaper but have different properties compared to virgin wood, which can make combustion more problematic. This is also true for small power units that usually rely on indigenous fuel supply delivered at a minimal transport costs. Alternative fuels that are solely combusted or co-combusted such as peat, agricultural waste, different grass types and fast growing species all have one thing in common, a high ash content compared to wood.

Among variety of existing methods for ash related problems mitigation, additives represents very important and effective instrument. Additives are chemicals that can mitigate corrosion and deposition. Extensive tests, both lab- and full-scale, and calculations have been performed on several classes of chemicals, especially AlSi-, Ca-, S- and P-containing substances [167-173]. Some additives are part of patented systems [174], however, it is a disputed field because of often inconclusive or installation-specific results. Furthermore, even though some additives show good abilities, far from everything is understood about their action.

Corrosion is mainly associated with alkali (Na, K) and Cl but also Pb and Zn [175]. Rather than using expensive additives, wastes or by-products containing high enough concentrations of corrosion-fighting chemical elements can be added. These materials are cheaper than standard additives and it can allow the combustion of an otherwise low-quality and/or unused fuel. A possible problem is that, contrary to dedicated chemicals, these materials have a complex chemical make-up which may include chemical elements interfering with and diluting the action of the corrosion-fighting elements. One example is the reaction of Ca with S which would otherwise prevent the formation of corrosive alkali chlorides by forming alkali sulphates. They may contain problematic elements (trace metals) when it comes to final disposal. On the other hand, the complex structure of these fuels might also lead to synergy effects. The literature concerning "additional" fuels focuses on three materials: coal [171,176], ash [177] and sludge [177-179].

The reactions involved are complex and only partly identified but a general consensus is that three mechanisms may take place (M is Na or K) [167, 168, 173, 180, 181]:

- Chemical sorption:
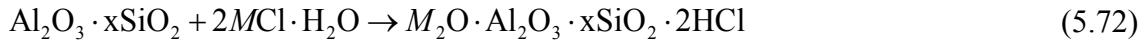
$$Al_2O_3 \cdot xSiO_2 + 2MCl \cdot H_2O \rightarrow M_2O \cdot Al_2O_3 \cdot xSiO_2 \cdot 2HCl \qquad (5.72)$$

- Physical sorption: Cl and alkalis are bound to $Al_2O_3 \cdot xSiO_2$ by Van der Waals forces

- Chemical reaction: MCl + S (as sulphate or dioxide) $\rightarrow M_2SO_4$

Experimental studies have shown that the predominating mechanism is dependent on the additive but also on temperature [167, 168, 173, 180, 181]. During chemical sorption, the alkali is strongly associated to the aluminosilicate while Cl is released as harmless HCl. The strong association means that the aluminosilicate cannot be recycled and reused but also that there is no risk of the alkali to be released because of, for example, concentrations or temperature variations as might happen with physical adsorption. However, physical adsorption has a higher capture capacity (several layers of alkali chlorides may be captured) and the additive may be reused after washing.

Beside NOx reduction effect, reducing conditions (air staging) may also affect the ash components speciation and partitioning and therewith corrosion and deposition. Little attention has been given to alkalis and reducing conditions in thermal systems, except for a few theoretical results [182, 183]. Trace metals have been studied to a larger extent [184-189]. These studies show that advanced air distribution can modify the phase distribution and speciation of chemical elements [190, 191].

During combustion of fuels with high alkali content, the mobility of present chlorine is greatly enhanced. These alkali-chlorine compounds leave the bottom ash as different gaseous volatiles passing through the process along with the reacting gas and finally the flue gas. However, the capture of alkalis (and/or alkali chlorides in some cases) through the use of additives has helped lowering the alkali chlorides concentration in the flue gas and by that decreasing substantially corrosion in boilers. Similar possibilities to capture zinc and lead are highly interesting. When additives are

used, chlorine is usually released as HCl, a compound that is corrosive on its own but lacks the sticky property that metal chlorides have. In addition, HCl is easily cleaned from the flue gas in a post-combustion stage by scrubbing it with lime stone or by dry-sorption with $Ca(OH)_2$ [111].

Additives can be either mixed with the fuels prior to combustion, they can be added to the bed material in case of fluidized bed or they can be sprayed at critical stages directly into the flue gas. Depending on their elemental composition, additives can be separated into groups containing calcium, phosphorous, sulfur, aluminum or aluminumsilicate [192]. For liquid-based additives, the so-called ChlorOut system developed by Vattenfall has shown good results in substantially decreasing the alkali chlorides and possibly also trace metal chlorides in the flue gas [193,194]. ChlorOut is based on spraying a solution of ammonium sulfate prior to the superheater section in the boiler. Other sulfate solutions like aluminum and ferric sulfates have also shown to have a similar effect to the ChlorOut system [195]. Additives in the form of solid particles can also be mixed with the bio-fuel prior to combustion. Sulfur rich additives such as peat or pure sulfur are expected to chemically react with potassium, sodium, zinc and lead to form $MxSO_4$. Sulfur addition to agricultural waste has shown promising results in decreasing the potential of corrosion in boilers [178,196]. Calcium–phosphorous and Aluminum–silicate based additives were tested in a full scale straw pellet boiler at the Amager power station in Denmark [197]. Among the tested additives were sand, dicalciumfosfat, chalk and bentonite. In addition, kaolin as an additive is studied in this PhD thesis.

A special group is addition of fuel ash from other fuels or by cocombustion [177, 198]. Dedicated chemicals are not the only possible additives, other materials/fuels such as biomass, sludge, coal or coal ash may also have a positive effect on alkali chemistry. For example, fly ash from peat may potentially absorb alkali and possibly some trace elements (Pb, Zn). The chemistry of peat ash is complicated due to its complex and varying composition. Many studies, mainly from co-combustion of peat with problematic fuels show the many possible reactions between peat ash and other ash constituents [199–202]. Peat also contains inert ash components like silicate and oxides which do not interact chemically with other components. The physical effect of this inert ash may, however, be significant. It has been shown to have a cleaning effect on

superheater deposits by mechanical wearing effects. Part of the oxide ash has been found to have an alkali absorbing ability and high calcium content may promote formation of Ca-compounds which dissolve potassium and possibly also zinc and lead. Peat is also relatively rich in sulfur and promotes the formation of alkali sulfates instead of chlorides, which lowers both deposition and corrosion risks.

In fluidized bed combustion systems, agglomeration (Figure 5.11) can become a serious problem for fuels containing high amounts of potassium oxides (K_2O). The K_2O and other alkali oxides react with silicate (Si) found in the sand that is usually used as bed material and form compounds with low melting points (760–875 °C) [203]. Furthermore, in such cases the role of additives has been shown to have a positive effect on abating agglomeration by forming compounds that can withstand the high temperature environment [204 - 211].

a)   b)

Figure 5.11 Molten ash agglomerations formed during the combustion of herbaceous fuels (a) and Hard super heater deposits in a waste wood fired boiler (b) [212]

In this thesis, kaolin was chosen as the additive to demolition wood in order to study in detail its effectiveness in capturing the alkalis from the gas phase. Kaolin reactivity with gaseous alkalis has already been shown to be quite effective [213, 214] and many publications applying kaolin as additive in fullscale applications have shown good tendencies towards benefits in preventing agglomeration, fouling and corrosion [177, 205, 211]. However, in this thesis a laboratory-scale reactor with good control over temperature, fuel and air inputs in addition to gas and particle measurement was used to study some parameter variations on the reactivity of kaolin. The aluminium

128

silicates in kaolin can react with alkalis and form compounds with higher melting point [206]. The reactions between alkali chlorides and aluminium silicates are expected to follow mechanisms presented in Equation (5.73) and Equation (5.74) [177].
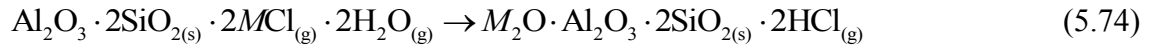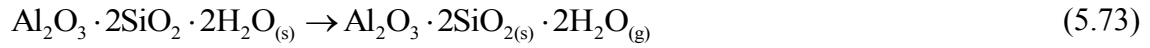
$$Al_2O_3 \cdot 2SiO_2 \cdot 2H_2O_{(s)} \rightarrow Al_2O_3 \cdot 2SiO_{2(s)} \cdot 2H_2O_{(g)} \tag{5.73}$$

$$Al_2O_3 \cdot 2SiO_{2(s)} \cdot 2MCl_{(g)} \cdot 2H_2O_{(g)} \rightarrow M_2O \cdot Al_2O_3 \cdot 2SiO_{2(s)} \cdot 2HCl_{(g)} \tag{5.74}$$

where M can be either K or Na.

As reactions in Equation (1) and (2) show the alkalis are captured by the kaolin while the chlorine is released as HCl.

6. EXPERIMENTAL WORK

All experimental research within this PhD thesis has been done at NTNU/SINTEF Energy research laboratory, with exception of some offline analysis of fuel and ash, which have been done by external laboratories.

This chapter gives an overview of equipment that has been used, and as well as describes the experimental procedures carried out within work on this thesis.

6.1 Multifuel reactor

Combustion experiments were carried out in an electrically heated high temperature (up to 1300 °C) multi-fuel reactor with small diameter reaction tube (Monika I), presented in Figure 6.1 and 6.2. The reactor incorporates a fuel inlet tube, a primary gas inlet tube, a flue gas outlet tube, a flue gas sampling tube, 2 secondary gas inlet tubes and 2 tertiary gas inlet tubes and a view glass tube (inspection hole).
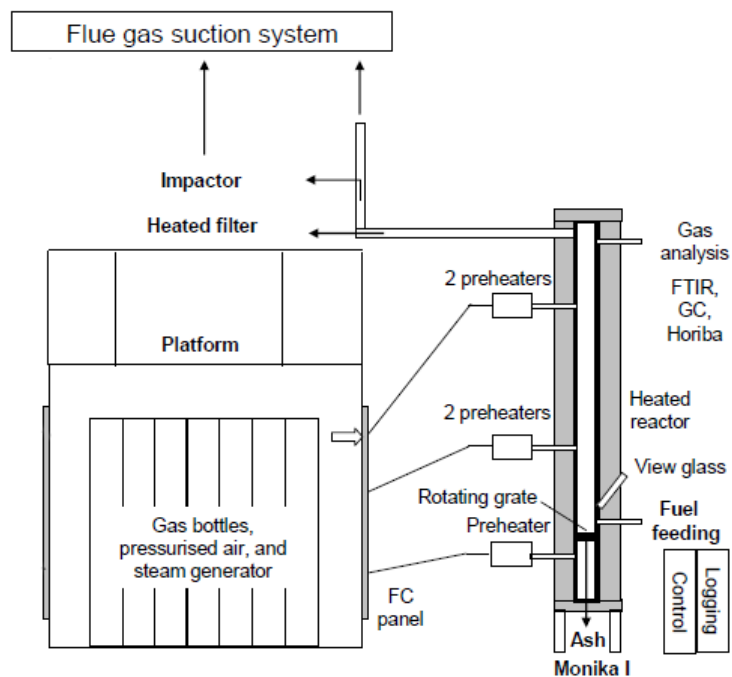
Figure 6.1 Overview of the multi-fuel reactor system

This reactor is flexible reactor for fuel testing, and it is designed to be as flexible as possible with respect both to fuels and reaction conditions. The reactor has next characteristics and possibilities:

- Gas type and amount selection for the reactions,
- Gas mixing,
- Gas preheating to desired temperature (up to 1300 °C),
- Preheated secondary (tertiary) gas addition,
- Combustion, gasification or pyrolysis,
- 4 temperature zones in the reactor,
- Computer regulated temperature programs both in the reactors and preheaters,
- Continuous feed,
- Continuous ash removal from the grate,
- Bottom ash sampling,
- Fly ash sampling,
- Flue gas analysis: GC, FTIR, conventional analyzers,
- Data logging: temperatures, gas flows, flue gas composition,
- Inspection hole.

Key operational data are given below:

- Fuel feeding rate: up to 0.5 kg/h
- Max inlet gas flow (using air) demand: 120 Nl/min
- Max gas flow (using air) in reactor after fuel conversion: 130 Nl/min
- Max residence time in reactor (section above grate, 1.6 m high): 10 s
- Minimum residence time in reactor (section above grate, 1.6 m high): 1 s
- Max gas flow speed: 1.6 m/s, corresponding to a Reynolds number of about 800
- Minimum gas flow speed: 0.16 m/s, corresponding to a Reynolds number of about 150
- Max net inlet gas flow preheating effect in external preheater (using air, 1300°C): 3.5 kW
- Max energy release, from fuel, due to reactions: 2.5 kW
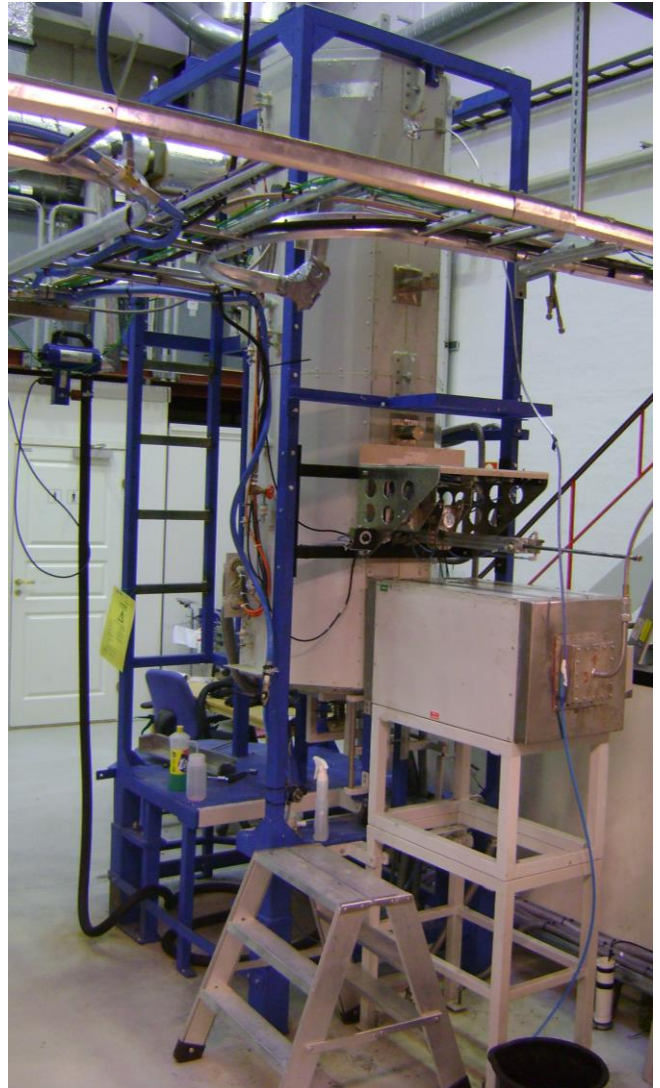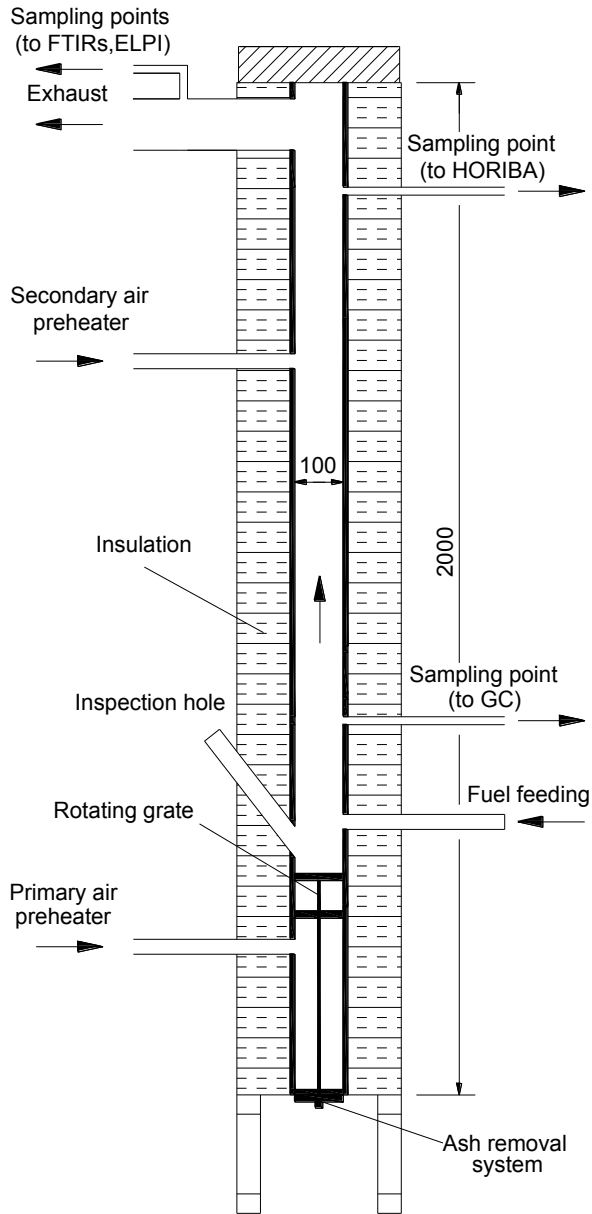
Figure 6.2 Multi-fuel reactor

6.1.1 Combustion chamber

Reactor combustion chamber (Figure 6.3) consists of two vertical ceramic tubes with 100mm diameter, which are each 1000 mm long and connected with a ceramic socket. The ceramic tubes are made of non-porous and non-catalytic alumina, with follows composition:

a)

b)

Figure 6.3 Reactor tube

a) without insolation, b) bottom view

The reactor body is divided in two vertical parts connected with hinges (Figure 6.4). Half of the furnace body is fixed and the other half can be opened approximately 90° rolling over a wheel installed in the bottom, allowing access to the reactor furnace for inspection and/or reparation.

The section above the grate, the reaction section, is 1.6 m long, while the section below the grate is 0.4 m long. The reactor preheating temperature is up to 1300°C. The reactor heating system is fitted inside the insulation shell and consists of four separate heating zones, with elements of 4 kW each (16 kW in total) that enclose the ceramic tube (four separate heating sections, 0.5 m high each) (Figure 6.4). The limiting heating rate of the furnace is 600 °C/hour.

Figure 6.4 Heating system

6.1.2 Air addition

Air for the combustion process is added through the preheaters. The gas flow is controlled by two high-precision digital mass flow controllers (Alicat Scientific) presented in Figure 6.5.

Those controllers are used as well, during the reactor leakage test. Namely, in the final stage of reactor setting up phase and before the first experiment, it was necessary to conduct the reactor check in order to detect the eventual leaking spots. For that purpose helium has been used. Helium was introduced from bottles through flow controller to the reactor, and leaks have been detected by portable helium sniffer. Leaking spots have been sealed with silicon.

The air was preheated up to the reactor temperature in external preheaters (Figure 6.6). The primary air is added under the grate (underfire air) and the secondary air is added over the grate (overfire air).
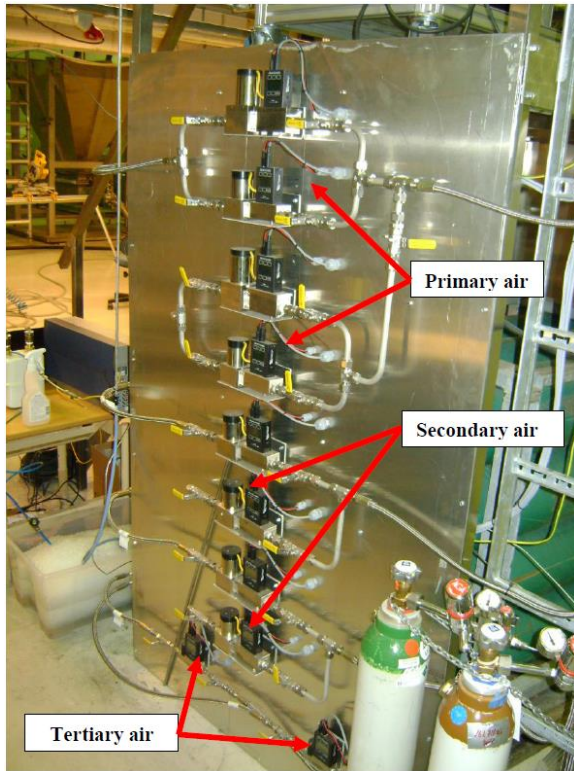
Figure 6.5 Flow controllers   Figure 6.6 Air preheaters
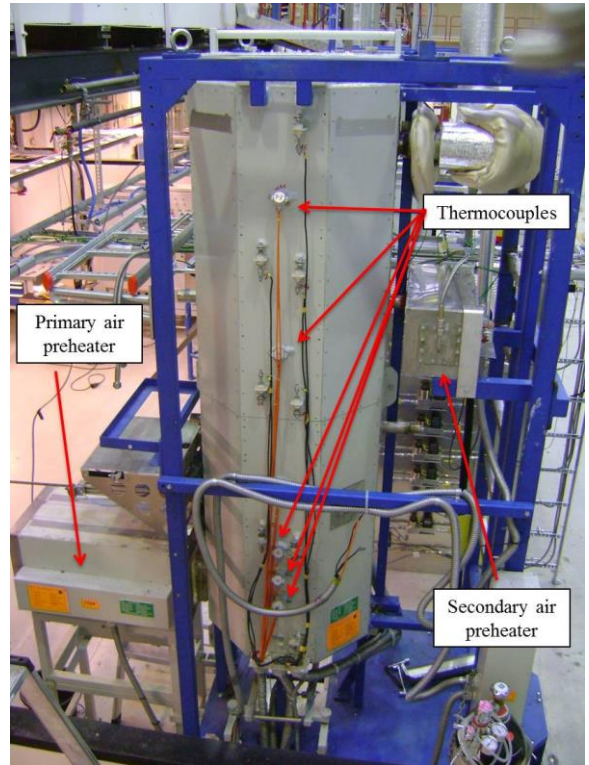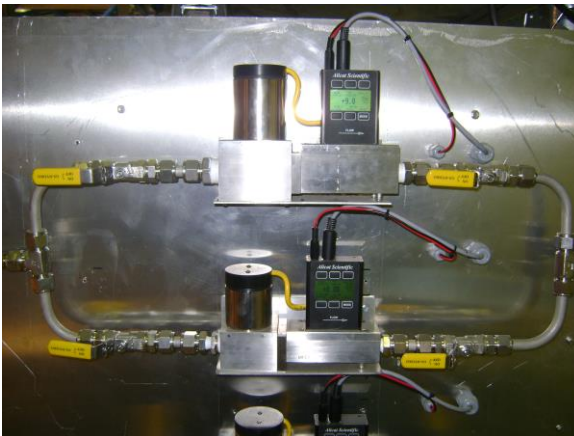
6.1.3 Feeding system

The fuel-feeding system is based on a water-cooled piston (Figure 6.7). The fuel is fed from a rotating battery of fuel containers to the piston through a slot. The piston is pneumatically driven quickly into the reactor where the fuel falls onto the grate. After feeding the reactor, the piston quickly returns to its starting position and the same process starts again. The feeding interval has been chosen with a regulator.
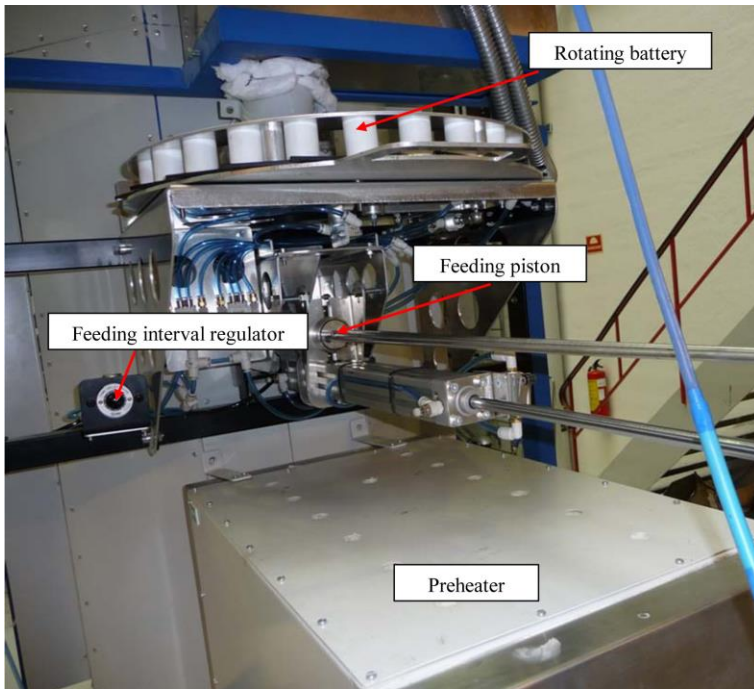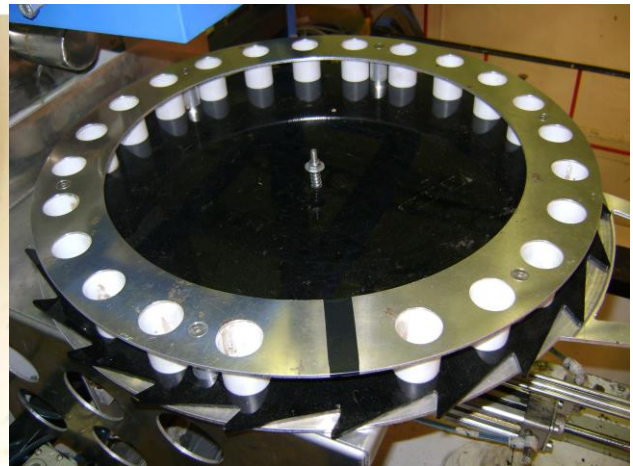
Figure 6.7 Fuel-feeding system

a) Elements of feeding system in work position; b) Feeding piston; c) Feeding piston into reactor (final feeding position); d) Rotating battery

The rotating battery is located above the piston and contains 23 fuel containers. The battery rotates after each time the piston feeds, continuously replacing an emptied fuel container with one containing fuel, allowing the piston to introduce new fuel into the reactor. The fuel containers were filled manually.

6.1.4 Grate and ash removal

The lower part of the multi-fuel reactor is the section containing the grate, the final burnout grate and the bottom ash collection system with an ash bin (Figure 6.8). Both grates and the ash bin are made of inconel. Two levels of the grate have a distance of 10 cm. The fuel that is fed onto the upper grate is primarily combusted there. The fuel is gradually moved from the fuel-feeding inlet to a slot leading to the second grate by rotating blades. The system has two rotating blades which rotational speed was adjusting.
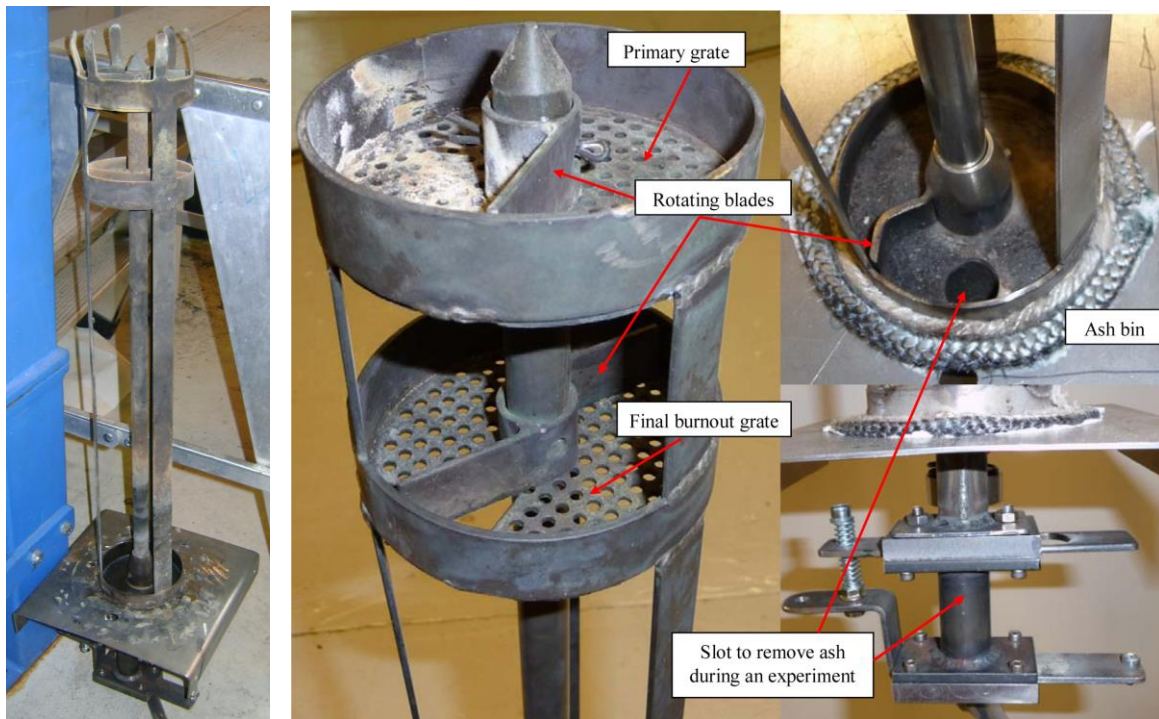
Figure 6.8 Cascade grate and ash removal system

Final burnout takes place on the second grate before the ash is moved by rotating blades to a slot from where it falls to the ash bin. At the bottom of the ash bin there is a rotating blade which moves the ash into an ash tube. From the ash tube the ash is removed through slots during the experiments.

6.1.5 Temperature control and logging

Temperature measurements, with thermocouples type P, are available in the reactors at several heights (Figure 6.6). Furthermore, additional thermocouples were used to control and protect the heating elements of the reactor from overheating. 6 (logging) + 4 (control) + 4 (protect) thermocouples are installed in the reactor furnaces. The preheating units have separate control systems. The control cabinet is shown in Figure 6.10 and the logging software interface is shown in Figure 6.11.
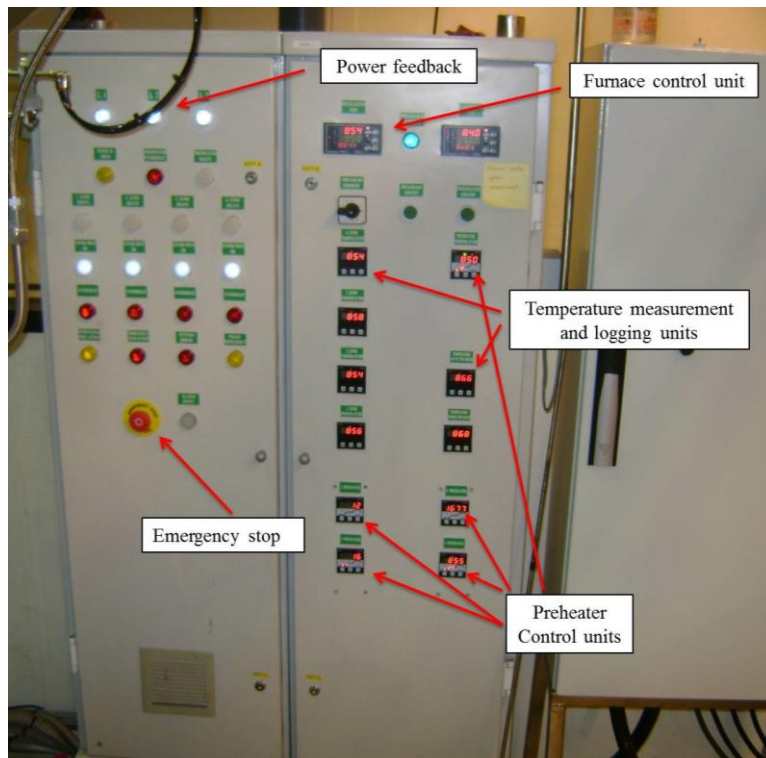
Figure 6.10 Temperature control cabinet
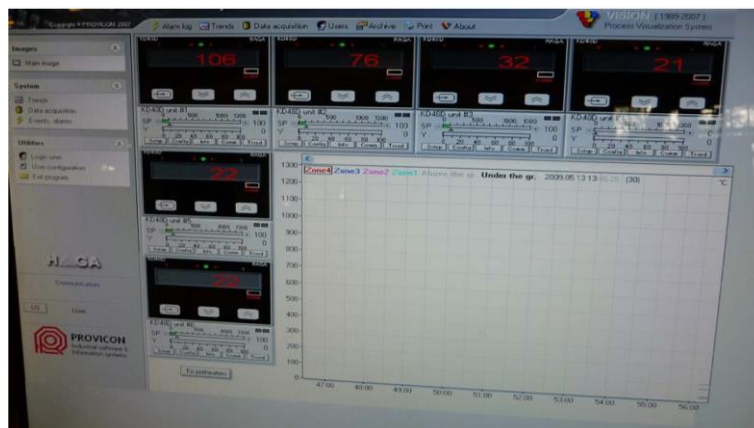
Figure 6.11 Software interface of the temperature logging system

6.2 Gas and particle analysis

The reactor flue gas composition and the particle emission size distribution were continuously monitored during the experiments. A schematic diagram of the sampling line is shown in Figure 6.12 and positions of sampling points in Figure 6.1 and Figure 6.2. As shown in Figure 6.12, gas is extracted in four places to carry out analysis and further measurements. The flue gas composition is measured by means of three gas analyzers. In case of staged air combustion, a gas chromatograph (GC) is used to measure the gases in the primary section.
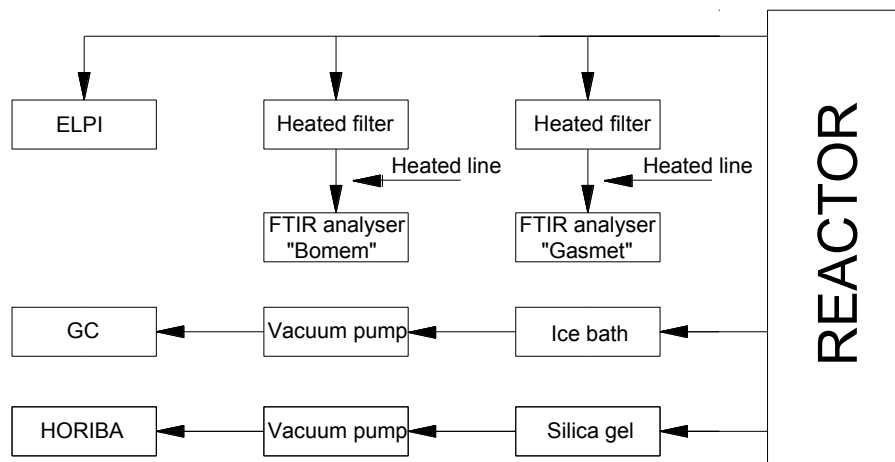
Figure 6.12 Schematic diagram of the sampling line

For gas analysis in the primary zone a Varian CP-4900 micro gas chromatography (GC) was used (Figure 6.13). A stainless steel probe with an outside diameter of 10 mm and an inside diameter of 8 mm was used for the gas sampling. The sampled gas was passing first through a tar, water and particle ice-cooled trap consisting of a steel container filled with glass wool and glass microfiber paper filter on the top.

The sampling gas flow was about 1 l/min. The GC is equipped with two dual-channel micromachined thermal conductivity detectors TCD detectors, with detection limit of 1 ppm, and double injectors, each connected to a separate column. The first column is a 10 m long PoraPLOT Q type, with an internal diameter of 0.25 mm and 10 μm film thickness produced by Varian Inc., and uses helium as carrier gas. This column is used for the separation of CO_2, CH_4, C_2H_2 plus C_2H_4 and C_2H_6. The second column is a 20 m long CP-MolSieve 5A PLOT, with an inner diameter of 0.25 mm and 30 μm

film thickness produced by Varian Inc., and uses argon as a carrier gas. Argon was used to be able to detect hydrogen. This column is able to quantify H_2, O_2, N_2, CH_4 and CO. The GC has a sampling time of approximately two minutes.

Figure 6.13 Varian CP-4900 micro gas chromatography (GC)

The exhausts gases were quantified online with two different devices which work at Fourier transform infrared spectroscopy principle (FTIRs), ABB-Bomem 9100 and Gasmet DX-4000 (Figure 6.14 and 6.15). Extracted gases were passing through heated filters and heated lines, before they were led to the FTIRs. Stainless steel probes with an outside diameter of 10 mm and an inside diameter of 8 mm were used for the gas sampling. Both sampling positions were located in the flue gas stack. They do sampling at the same point, which allows for comparing different measurements for these species: H_2O, CO_2, CO, NO, N_2O, NO_2, SO_2, NH_3, HCl, HF, CH_4, C_2H_6, and C_3H_8.

The ABB-Bomem 9100 FTIR has two cells that operate at 176 ºC, which ensures that the sample stays in the gaseous phase even with high concentrations of condensable hydrocarbons. This device is used to measure mentioned common mutual species and C_4H_{10}. The measurement time is typically 80 s. The large cell has an optical path length of 6.4 m and is equipped with a TGS (TriGlycine Sulfate) detector, with maximum instrument resolution of 1 cm^{-1}. The small cell has an optical path length of

140

19 cm and is equipped with a MCT (Mercury Cadmium Telluride, liquid-N_2 cooled) detector. The small cell wasn't used in this study.

The Gasmet DX-4000 has an integrated (zirconium oxide) O_2 analyzer. The instrument is equipped with a cooled Peltier MCT detector at has a maximum resolution of 4 cm^{-1} at a scan frequency of 10 scans/s and The measurement time is typically 60 s. The sampling line and cell are heated, at 180 ºC. The cell volume is 0.4 l and the optical path length is 5 m. To measure O_2, an optional oxygen sensor, based on a ZrO_2 cell, is attached to the analyzer.

Beside common species and O_2, using this FTIR device it is possible to measure in addition next components: C_2H_4, C_6H_{14}, CHOH, HCN.

Generally FTIR measurements of NO may introduce significant uncertainties. However, the NOx emissions reported in the results part are based on the Horiba analyzer, which is using the chemiluminescence technique. The N_2O measurements were made by the FTIR analyzers, and the reported values were measured by the Gasmet FTIR. The Bomem FTIR showed N_2O values close to the values measured by the Gasmet FTIR.

Figure 6.14 ABB-Bomem 9100 FTIR
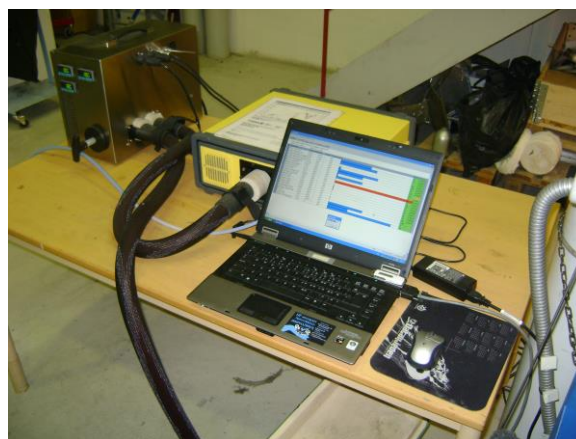
Figure 6.15 Portable FTIR (Gasmet DX-4000)

A partial flow for gas analysis was taken through a sampling point near the top of reactor. An inconel probe with an outside diameter of 6 mm and an inside diameter of 4 mm is used for the gas sampling. The gas first passed through silica gel and was thereafter led to a HORIBA analyzer by vacuum pump. The sampling rate was 0.4

l/min. The HORIBA PG-250 (Figure 6.16) is a portable stack gas analyzer that can simultaneously measure up to five separate gas components. The HORIBA PG-250 uses Non-Dispersive Infrared (NDIR) absorption method for CO, SO_2, and CO_2, cross-modulation ordinary pressure chemiluminescence method for NO_x, and a Zirconium method using a galvanized cell for O_2 measurements. The response time (T90) of the analyzer is less than 45 s for NOx, CO, O2, and CO2 and less than 240 s for SO2. The sampling unit has a filter, mist catcher, pump, electronic cooling unit, and NO_X to NO converter built in.

Particles size distribution and concentration from the flue gas were estimated by Electrical Low Pressure Impactor (ELPI) Figure 6.17. A partial stream of flue gas was collected by stainless steel probe at a sampling position which is located in the flue gas stack. The flue gas is then led through the double diluter system to the particle size analyzer

The Dekati Standard ELPI is a real-time particle size analyzer for real-time monitoring of aerosol particle size distribution. The ELPI measures airborne particle size distribution in the size range of 0.03−10 μm with 13 stages and a time resolution of 2-3 s. Electrical detection is applied to 12 stages while the first stage of the impactor is a pre-selector stage. All stages are electrically insulated from each other using teflon insulators. With a filter stage the size range can be extended down to 7 nm. The nominal air flow is 10 l/min, and the lowest stage pressure is 100 mbar.

a)   b)

Figure 6.16 a) Portable gas analyzer HORIBA PG-250; b) Part of HORIBA's sampling line (silica gel and vacuum pump)
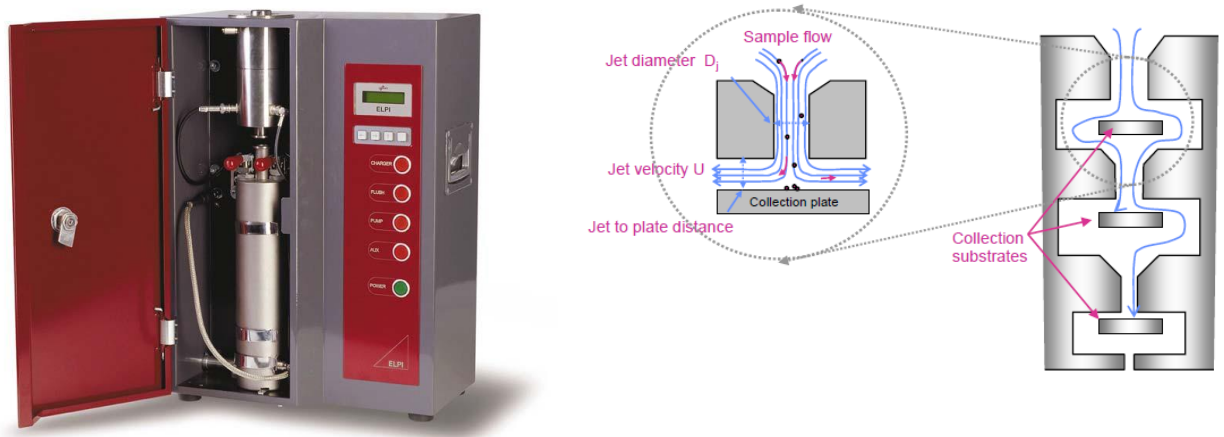
Figure 6.17 Electrical Low Pressure Impactor (ELPI) [215]

The double diluter setup is shown in Figure 6.18. The system consists of two diluters (6.19). The first diluter incorporates a heating unit to avoid nucleation and condensation of volatile compounds. The flue gas is then cooled in the second diluter (which operates at ambient temperature) before entering the ELPI. When the flue gas reaches the second stage condensation is no longer an issue since the flue gas has already been diluted once.
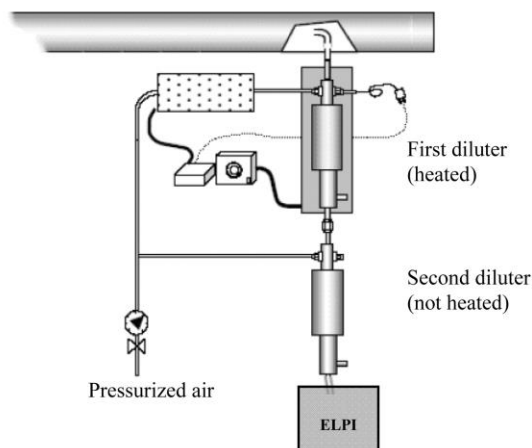
Figure 6.18 Double diluter setup [215]   Figure 6.19 Dilution chamber [215]
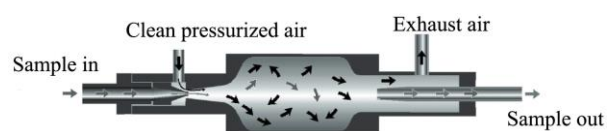
The experimental set-up with its advanced monitoring and control systems as well as the online and offline analytical methods gives a very accurate picture of the thermal process all its products

6.3 Procedure for preparation of fuel used in experiments

Depending of experiment, staged and non-staged experiments are carried out with six kinds of pellets:

(1) wood pellets (WP),

(2) demolition wood pellets (DW),

(3) coffee waste pellets (CW), and

(4) six mixtures of these fuels:

- 1/2 WP-1/2 DW
- 1/2 WP-1/2CW
- 1/2 DW-1/2CW
- 2/3 WP-1/3CW
- 1/3 WP-2/3CW
- 1/3 WP-1/3DW-1/3CW.

(5) three mixtures of demolition wood and kaolin as an additive:

- 1% of kaolin,
- 5% of kaolin,
- 10% of kaolin,

(6) three mixtures of demolition wood and peat-ash:

- 1% of peat-ash,
- 5% of peat-ash,
- 10% of peat-ash.

The WP is a Norwegian mixed timber of pine and spruce obtained through Felleskjøpet, Norway. DW is from houses/buildings in Sweden, provided by Vattenfall from the combustion plant at Nyköping, Sweden. CW was received from Kjeldsberg Kaffe, Norway. This substance consists of skin, silverskin, pulp, parchment, and broken beans that are lost during the roasting process. The beans used were almost exclusively from Brazil. All the samples were collected in 2009-2010.

The peat ash originates from the combustion plant owned by Vattenfall in Uppsala. The peat ash was mixed with lime from the plant's deSOx stage. The lime addition was unavoidable since it is part of the gas cleaning system at the Vattenfall plant in Uppsala.

The received biomass was ground in a mill to produce a maximum particle size of 2–3 mm (Figure 6.20). For mixture of fuels and DW with additives, components were mixed manually while spraying approximately 8% water relative to the total mass into the blend.
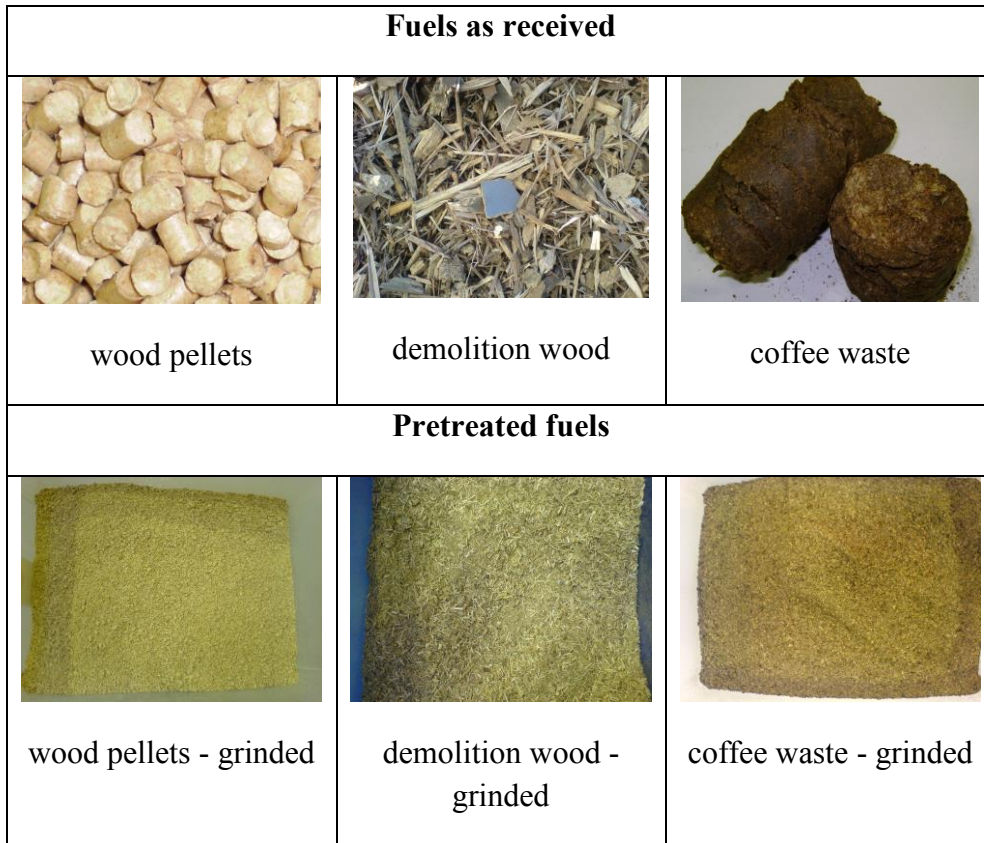
Figure 6.20 Biomass as received and pretreated for the pellet production

The water was necessary in order to produce pellets of adequate quality which was performed in a laboratory scale pellet machine (Figure 6.21 and 6.22). The received biomass is pelletized with a pellet machine to get a similar shape and composition for all the experimental runs. To ensure a homogeneous distribution, a large volume of biomass was shredded to sawdust size, followed by thorough mixing. Pellets were then made from these fine pieces.

Figure 6.21 Pellet machine

Figure 6.22 Steel matrix

Pellets were obtained as cylindrical extrudates, with a diameter of 6 mm and a variable length of 5–15 mm and were only air-dried to an average moisture content of 12 wt.% before they were used in experiments. Some of pellets produced and used in this research work are presented in Figures 6.23-26.

Figure 6.23 Wood pellets

Figure 6.24 Coffee waste pellets

Figure 6.25 1/3 DW-2/3CW pellets   Figure 6.26 DW+10% Kaolin pellets

6.4 Experimental procedure and data treatment

Two types of experiments are carried out: (1) experiments with air staging and (2) experiments without air staging. Depending of experiment five different temperatures are selected, 800, 850, 900, 950, and 1000 °C. During each experiment, only isothermal experiments were performed, primary air, and secondary air at the mentioned values. The primary air and secondary air were also preheated to the same temperature. All the sampling devices are calibrated each day, before starting the experiments. Also the Gasmet FTIR calibration was performed daily by means of background spectra. Each experiment has been carried out for at least 2 h at stable operating conditions, or in experiments with fly ash sampling until a 90% fill signal of aerosols in the impactor.

For the staged air combustion experiments, the total excess air ratio is also set to 1.6, while the primary excess air ratio is set to 0.8, which means that 50% of the total air is fed at each stage. The air flow has been held constant during the experiments. However, the variation in the fuel feeding rate allows capturing a total excess air ratio range of 1.2-3, making it possible to see emission trends as a function of total excess air ratio, since the fuel was fed as pellets and, depending on the length of the pellets and the position of the pellets on the grate after feeding, natural variations in the excess air ratio occurred.

The total excess air ratio for nonstaged combustion is set to 1.6.

Pellets with a diameter of 6 mm and a length of 10-15 mm are fed by the automatic feeding system. The fuel feeding rate is set to 400 g/h. The pellets are mainly combusted on the upper (primary) grate. The pellets are gradually moved from the fuel-feeding inlet to a slot leading to the second (final burnout) grate by rotating blades. Each grate has two rotating blades with a rotational speed of 3 min. Final burnout takes place on the second grate before the ash is moved by the rotating blades to a slot from where it falls into the ash bin. At the bottom of the ash bin another rotating blade is placing the ash into an ash tube.

The residence time of the fuel in the reactor is high, and the gas in the reactor has very low flow velocity (0.04-0.07 m/s). The secondary combustion zone ensures a residence time of several seconds and is hence in fact comparable to conventional combustion systems. According to the given reactor dimensions and velocity, the residence time for the primary zone (90 cm) is 13-23 s and for the secondary zone (70 cm) 10-18 s, giving a total residence time of 23-41 s. The gas residence time between the grate levels is in the range of 1–2 s.

To have a precise composition of the fuel, during each run, three different samples at three different times are taken from the fuel feeding system to analyze the moisture content. Hence, variation in the N-content is not regarded as a challenge in these experiments. The type of biomass, the origin of it, and the pretreatment technology applied to it are important parameters influencing the ultimate and proximate analysis of the biomass. For example, drying can reduce the moisture content from 65% in virgin wood down to below 10% in wood pellets. Moisture content is measured during each experimental run. Moisture, VM, ash content, ash fusion temperatures are measured using ASTM E871 (50 g, 103 ± 2 °C, 24 h), ASTM E872 (1 g, 950 °C, 7 min), and ASTM D1102 (2 g, 580-600 °C, 4 h), ASTM 1857 and ISO 540:2008 standards, respectively, and the fixed carbon is calculated by the difference to 100%. Three samples are analyzed from different parts of the pellets to get repeatable analyses, showing that the fuel was homogeneous.

The heating value is calculated based on the elemental composition.

All the samples have been dried in a vacuum exsiccator over phosphorus pentoxide prior to analysis. The determination of C/H/N/S is performed using the "EA 1108 CHNS-O" by Carlo Erba Instruments elemental analyzer. The method is adjusted

148

for sample amounts of 2-10 mg and performs with an uncertainty within 0.3 wt % as required for confirmation of assumed chemical composition. The operation range covers the content from 100 to 0.1 wt %; sulfur determination is in the concentration range of 1.0 down to 0.01 wt % and the uncertainty is estimated to be 0.02 wt % for C/N/S/Cl.

A chemical analysis of the ash content of the primary fuel and all the blends was determined by the inductive coupled plasma equipped with an atomic emission spectrometry analyser (ICP-AES) and inductive coupled plasma equipped a mass spectrometry analyser (ICP-SFMS) methods.

The ash fusion temperature for the bottom ash was determined in an oxidizing atmosphere in a carbolite ash fusion analyser according to the international test standard (ISO 540:2008). The ash samples from each experiment were shaped into three duplicates of cube pellets with a size of 3 mm. The ash cubes were put on a tile and placed inside the furnace that was programmed to increase the temperature at a rate of 8 °C min^{-1} and up to 1500 °C.

The changes of the shape of the ash cubes were recorded with a high resolution video system. The initial deformation temperature (IDT), the softening temperature (ST), the hemisphere temperature (HT), and the fluid temperature (FT) were determined after a visual observation of the recorded video. As this method for determining the fusion characteristics for ash depends on visual observation of the ash deformation, some uncertainties can be expected due to the human error factor.

The fly ash samples measured by means of a 13 stage low-pressure impactor, in a particle size range of 0.03-10 mm, where collected on aluminum plates (Figure 6.27). The plates were covered by a thin layer of Vaseline to provide a sticky surface. The chemical analysis of the samples was made by energy-dispersive X-ray analysis connected to a scanning electron microscope, SEM/EDX. The particles on each plate formed a pattern of piles as seen in Figure 6.28.

Figure 6.27 ELPI – plates/samples
after experiment
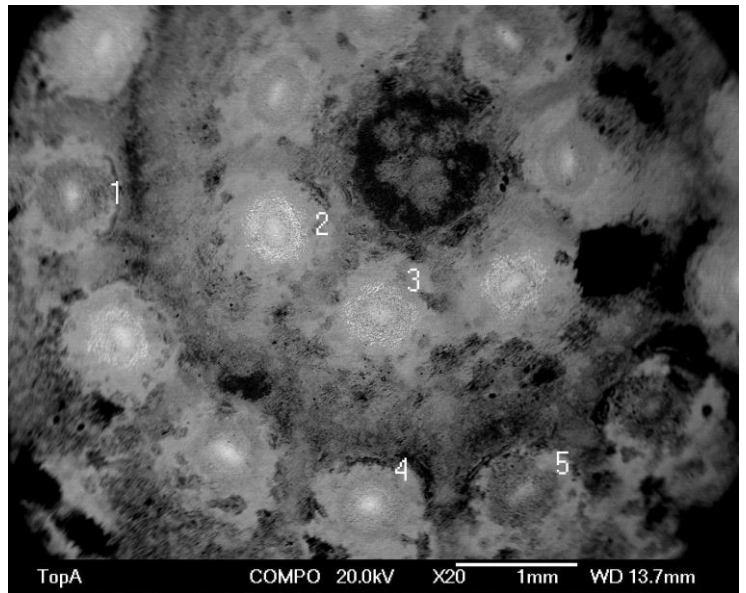
Figure 6.28 SEM image of the pattern on particles
collected on the ELPI-plates

The total mass of the particles on each plate was around 10–100 μg. For each run, four plates with the particle sizes (D50%) 0.093, 0.26, 0.611 and 1.59 μm were chosen for SEM/EDX analysis. Five EDX spot analyzes were taken from different locations on each plate (see Figure 6.28). After standard ZAF-correction the analysis was normalized to 100% by weight. The analysis of the aluminum plates was made directly on the foil. The signals for carbon, oxygen and aluminum cannot be used for quantitative information due to several reasons. The carbon signal can originate from possible unburned residue in the samples, but also from the adhering Vaseline. The oxygen signal can come from, besides the particles, from the Vaseline and from the oxide layer covering the aluminum plate. The aluminum signal comes mainly from the plate beneath the samples. It was seen that the aluminum signal was stronger for bigger particles, probably due a lower coverage of the aluminum than with small particles. Peat ash and kaolin contains aluminum so the effect of those additions on the fly ash could not be studied. The assumptions made for the data treatment of the aerosol concentrations will be explained later.

6.5 Data treatment

All data from HORIBA and FTIRs gas analyzers have been processed and treated by Fuelsim – Average tool. Fuelsim - Average is a relatively simple, but useful, mass, volume and energy balance spreadsheet for continuous combustion applications, but can also be used for other thermal conversion processes where solid fuel is converted to a fuel gas mixture of O_2, CO, NO, NO_2, UHC (unburned hydrocarbons), SO_2, N_2O, H_2, NH_3, HCN, Tar, CO_2, N_2, Ar and H_2O. Fuelsim - Average uses thermodynamic data on CHEMKIN format for all gas species and also liquid water, while the specific heat capacity of a solid or liquid fuel is user defined. Fuelsim - Average calculates emissions in various denominations based on the user input. However, also a separate emission conversion section is included, where emission values in various denominations can be inserted and converted between the various denominations. The corresponding emission levels in volume fractions can be inserted into the Fuelsim - Average main calculations and additional useful information are then calculated. The emission conversion procedure is based directly on the combustion equation, no simplified expressions are applied. When converting emission levels between different oxygen concentrations, the defined oxidant is added to, or removed from, the given flue gas composition until the calculated oxygen concentration equals the reference oxygen concentration.

Procedure for treatment of experimental results within Fuelsim - Average included the following steps:
- Converting log files to proper input data in pre-prepared Excel spreadsheet;
- Removing data points that does not belong there (not necessarily easy);
- Inserting the useful log files data in the proper place in the pre-prepared Excel spreadsheet;
- Inserting the fuel composition;
- Performing the calculations;
- Selected pre-prepared graphs can be viewed directly in sheet "Figures" when the calculations have finished;
- Checking the figures for:

- Calculated CO_2 versus measured CO_2 and calculated H_2O versus measured H_2O;
- Errors or unexpected results.

Data treatment has been carried out in a cautious manner to avoid nonreliable data. Significant transient effects are effectively eliminated by a filtering procedure while treating the experimental data. It should be noted that the first and very last section of the data has not been considered in the final data for further treatment, since these parts are typical transient periods, outside of the stable run period. This filtering procedure requires that the change in the excess air ratio per second is less than 0.01; otherwise, the complete measured data set at the current time is omitted in the final results.

All experiments were checked with respect to carbon and hydrogen balance using both the Horiba analyzer and FTIR. Data points which (1) did not satisfy a maximum deviation between the calculated and measured levels of CO_2 and (2) were clearly influenced by fast transient conditions were removed from the results. This is because these data points were not reliable or not representative respectively for a close to continuous and constant combustion process.

The experimental reproducibility was tested by reruns of the experiments, showing good reproducibility capability of the experimental setup.

Assumptions made for aerosol characterization, previously mentioned, included few steps. The first step of the data treatment was to recalculate the analysis to 100 wt.% discarding C, O and Al-signals. The variation among the five analyses of each plate was fairly small, indicating that the particles in the piles are homogeneous. This is illustrated in Figure 6.29 which shows the normalized analyzes for the smallest (0.1 μm) and the biggest (1.6 μm) particle fraction analyzed. Note the significantly higher concentrations of Si, Ca and Fe in the bigger fractions. In the following calculations arithmetical average for the five analyzes are used.
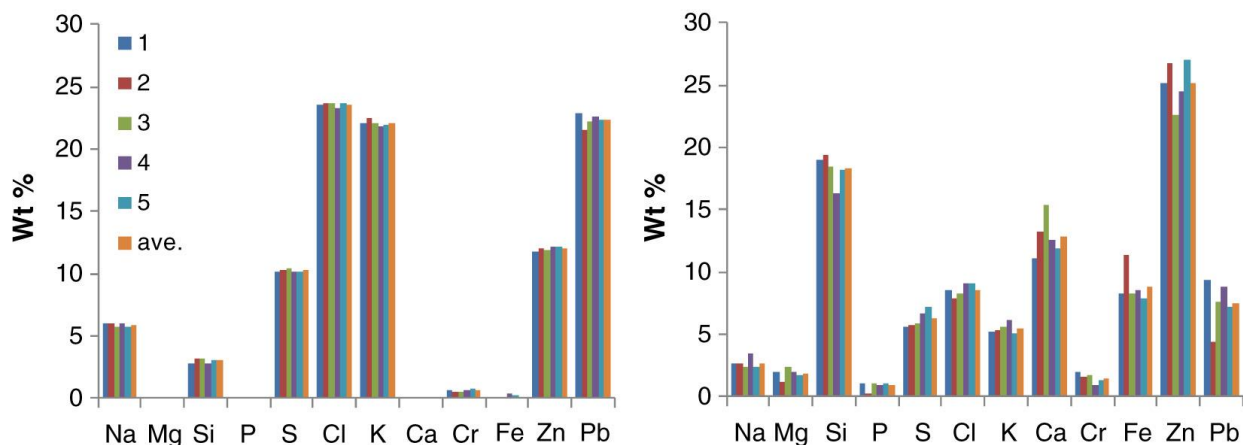
Figure 6.29 Normalized concentrations (wt-%) calculated from C-O-Al free SEM/EDX analyzes of the five spots of the ELPI-samples for the reference run with demolition wood at 850 °C. Left: 0.1 μm plate. Right: 1.6 μm plate.

The second step of the data treatment was to estimate in which compounds the elements studied are in the samples. This consideration is based on several recently published studies on aerosol formation in combustion, as well as on thermodynamic considerations and own field experience. The following assumptions regarding the speciation are made: (i) Potassium and sodium are as chlorides or sulfates, (ii) Silicon, calcium, iron, magnesium and chromium are as oxides, (iii) Zinc and lead can be both as oxides and/or chlorides and sulfates. The first assumption is well established for fuels containing sulfur and chlorine. Alkali is volatilized as hydroxides or chlorides. Some of the alkali is sulfated at high temperatures and the first aerosol particles to form are sulfate. At lower temperatures alkali chlorides start to condense, probably mainly by a heterogeneous nucleation mechanism on sulfate or other submicron particles. The second assumption is based on the fact that Si, Ca, Fe, Mg and Cr are non-volatile. All these elements, except Ca, do not form sulfates or chlorides at higher temperatures. Thus they are transported downstream mainly as particles with a somewhat uncertain formation mechanism. Some of them may act as seed particles for alkali compound nucleation. Ca forms easily sulfate, but in the present case the calcium content in the samples are so low that this formation is not critical. Probably the non-sulfated part of Ca is in the form of carbonate at lower temperatures. Ca can also form phosphates at high temperatures, usually calcium hydroxyapatite. However, the content of P is so low in the present samples that this reaction can be neglected.

153

The third assumption is the most critical one. In combustion conditions zinc and lead are partly volatile depending on the local chlorine content. These metals do not have similar chemistry although they are often treated together. Lead is much more volatile than zinc, but mainly in the form of gaseous PbO, which condensates at temperatures around 400 °C. Partly the oxide can react with chlorine and condensates as $PbCl_2$ at temperatures below 300 °C. At higher SO_2 concentrations lead can condensate as sulfates or as oxy-sulfate. Several sulfate-oxide compounds are possible. Solid zinc oxide is very stable in combustion conditions, but at lower temperatures both chlorides and sulfate can form. Probably zinc oxide is transported as small solid particles. It has been suggested that zinc inside the reducing fuel particle can form Zn gas which rapidly oxidizes to ZnO particles when it reaches oxygen rich location in an around the burning fuel particle [188,216]. This can explain the submicron size of the ZnO particles. We define two chemical different fractions in the fly ash samples: an "inert" part which constitutes of SiO_2, CaO, Fe_2O_3, MgO, P_2O_5, Cr_2O_3, ZnO and PbO, and a "salt" part consisting of sulfates and chlorides of potassium, sodium, zinc and lead. The inert part is assumed not to chemically interact with the salt part. It consists of high melting oxides and may be silicates as well as free oxides. The portion of the inert part increases with particles size indicating that these particles have their origin in the fuel ash. The salt part can be denoted (K, Na, Zn, Pb)(Cl2, SO4) and all its constituents are probably formed via the gas phase in a condensation/sublimation process. In this chemical system both solid and liquid solubility can exist between the components. Potassium and sodium chloride can form a solid solution, as can the sulfates of the two metals. Several double salts exist, both Zn and Pb form compounds with potassium chlorides. All four metals form a common chloride and sulfate melt with its lowest first melting point at around 200 °C [217]. The definition "salt" is somewhat inaccurate, but refers here to a low-melting water soluble fraction in contrast to the high melting insoluble inert oxide fraction. The salt fraction is the one causing deposition problems in the superheater area of steam boilers. The submicron particles which are transported to the heat transfer surfaces by thermophoresis can both initiate and further promote deposit build up if they contain a molten fractions above 15 wt-% [217]. The water solubility as such is not important for the deposition mechanisms, but it indicates an important property that can be used to determine the portion of Zn and Pb present in the salt part. It is evident that

154

the salt part must have a balance between cations and anions. Thus, because we know, based on the chemical analysis of the fly-ash samples, the amount of Cl, S (as SO_4), K and Na, we can determine by difference the portion of Zn and Pb. It is not possible to distinguish in which form the specific metals are (chloride or sulfate), only the sum of metals can be balanced against the sum of anions. Figure 6.30 shows as plot of the equivalent cations vs. equivalent anions (molar basis) for fly-ash samples from a run with kaolin addition.
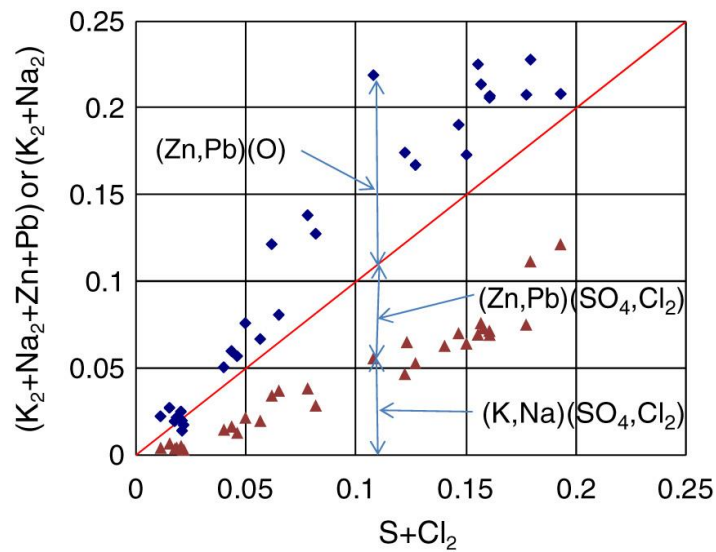
Figure 6.30 Equivalent cations plotted against equivalent anions for fly ash samples from runs with kaolin addition. The upper points are for $K_2+Na_2+Zn+Pb$ and the lower for K_2+Na_2. Indicated with arrows are the portions of different compounds in a certain sample.

The notation K_2, Na_2 and Cl_2 are used for consistency with $ZnCl_2$ and $PbCl_2$. "S" should be read as "SO_4". It can be seen that the amount of K_2 and Na_2 cannot fill up all sulfate and chloride in the samples. Thus, a part of Zn and Pb are expected to be present as sulfate and chloride, too.

Subsequently a diagram with normalized equivalent fractions of the cations and anions are used to compare the compositions of the salt part of fly-ash samples taken in different running conditions.

7. RESULTS AND DISCUSSION

This chapter presents the results achieved within research work on thesis. In order to on clear way present the results this chapter is organized in five subchapters, the first two deals with NOx emission reduction while the other three are dedicated to ash related properties.

7.1 NO$_X$ emission reduction by staged air combustion of biomass fuels and fuel mixtures

Two types of experiments are carried out: (1) experiments with staged air addition and (2) experiments without air staging. Only isothermal experiments were performed with a reactor temperature of 850 ºC. The primary air and secondary air were also preheated to the same temperature. The total excess air ratio was about 1.6, and the primary excess air ratio was about 0.8 in the staged air experiments.

Staged and non-staged experiments are carried out with four kinds of pellets: (1) wood (WP), (2) demolition wood (DW), (3) coffee waste (CW) and (4) six mixtures of these fuels. The proximate analysis of the pellet samples are shown in Table 7.1. The ultimate analyses of the pellets are shown in Table 7.2, where the nitrogen content in the fuel will be important in the following discussion. The heating value is calculated based on the elemental composition.

7.1.1 Combustion quality, measurement accuracy and experimental reproducibility

Due to the relatively long reactor residence time (19-35 s) and the chosen reactor temperature (850 °C) the amount of unburnt gases were low (typically below 50 ppm CO at 11% O_2 in dry flue gas). However, an initial stabilization period and fuel feeding fluctuations during close to constant operating conditions introduced also periods with significantly lower excess air ratios than the target value of 1.6, where the CO emission level increased to typically 200 ppm at 11% O_2 in dry flue gas.

Table 7.1 Proximate analysis of pellets (wt%)

Pellets:	Ash (dry basis)	Volatile (dry basis)	Fixed carbon (dry basis)	Moisture (as received)	HHV MJ/kg, dry basis
Wood (WP)	0.2	85.43	14.37	6.5	20.63
Demolition wood (DW)	3.73	77.27	19	8.1	20.54
Coffee waste (CW)	5.8	76.17	18.07	17.53	22.20
Mixtures of pellets (calculated, except for moisture):					
1/2 WP-1/2 DW	1.97	81.35	16.69	6.78	20.62
1/2 WP-1/2 CW	3.00	80.80	16.22	8.76	21.36
1/2 DW-1/2 CW	4.77	76.72	18.54	12.72	21.24
2/3 WP-1/3 CW	2.07	82.34	15.60	11.35	21.08
1/3 WP-2/3 CW	3.93	79.26	16.84	8.02	21.55
1/3 WP-1/3 DW-1/3 CW	3.24	79.62	17.15	24.53	21.04

Table 7.2 Ultimate analysis of pellets (wt% dry ash free basis)

Pellets:	C	H	O	N	S	Cl
Wood (WP)	51.22	6.07	42.54	0.14	0.03	0.02
Demolition wood (DW)	50.59	6.09	41.65	1.59	0.075	0.113
Coffee waste (CW)	52.9	6.47	37.64	2.8	0.187	0.038
Mixtures of pellets (calculated):						
1/2 WP-1/2 DW	50.91	6.08	42.11	0.85	0.052	0.065
1/2 WP-1/2 CW	51.98	6.25	40.33	1.34	0.101	0.028
1/2 DW-1/2 CW	52.01	6.06	39.21	2.58	0.137	0.085
2/3 WP-1/3 CW	51.93	6.06	40.8	1.14	0.08	0.027
1/3 WP-2/3 CW	52.79	6.04	38.68	2.35	0.141	0.036
1/3 WP-1/3 DW-1/3 CW	51.72	6.07	40.45	1.67	0.097	0.061

Figure 7.1 shows the CO emission level as a function of excess air ratio for the non-staged experiment with demolition wood pellets. The trend shown is typical for all the experiments presented in this PhD thesis. The combined emission levels of hydrocarbons, C_xH_y, were typically below 5 ppm at 11% O_2 in dry flue gas, with the highest values found at the highest excess air ratios, also shown in Figure 7.1. The trend shown is also here typical for all the experiments. Levels of NH_3, HCN and HF were within the measurement uncertainty level of the two FTIR analyzers, and will not be considered further.

All essential gas species for this study could be measured with good measurement accuracy. The two FTIR analyzers also showed good correspondence with regards to all essential gas species for this study.

The experimental reproducibility was tested by reruns of the wood pellets and the demolition wood pellets experiments with and without staged air combustion, showing good reproducibility capability of the experimental setup, including the NO_X and the N_2O emission levels.
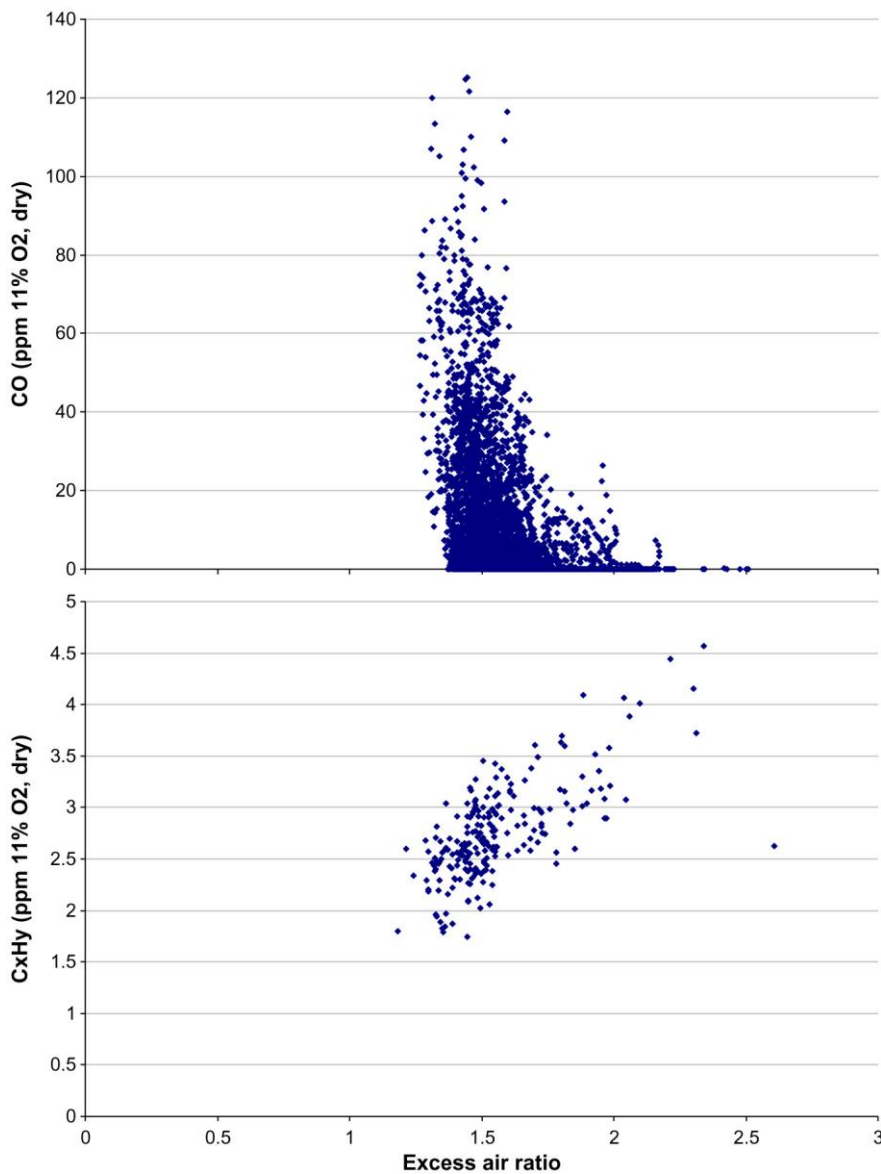
Figure 7.1 Typical CO and hydrocarbons (C_xH_y) emission trends as a function of excess air ratio (results from non-staged DW combustion)

All experiments were checked with respect to carbon and hydrogen balance using both the Horiba analyzer and the Gasmet FTIR. Figure 7.2 shows the carbon and hydrogen balance as a function of excess air ratio for the non-staged experiment with demolition wood pellets.
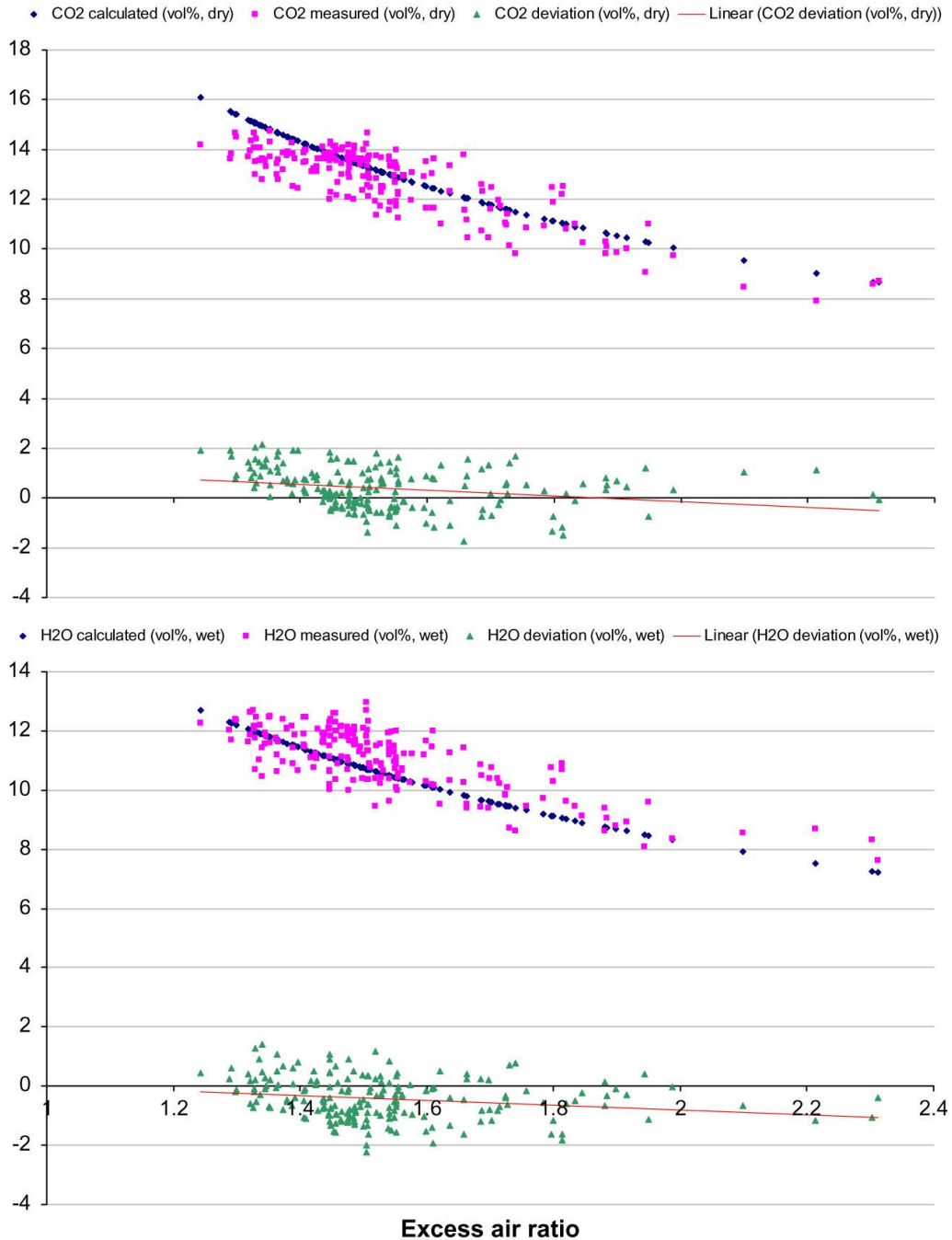
Figure 7.2 Carbon and hydrogen balance check (results from non-staged DW combustion)

7.1.2 NOx emissions – staged versus non-staged

Mean, minimum, and maximum NOx emissions as a function of the fuel-N content (ppm at 11% O2 in dry flue gas) are shown in Figure 7.3 for both staged and non-staged combustion. The NO2 fraction of the NOx was found to be insignificant at all conditions.
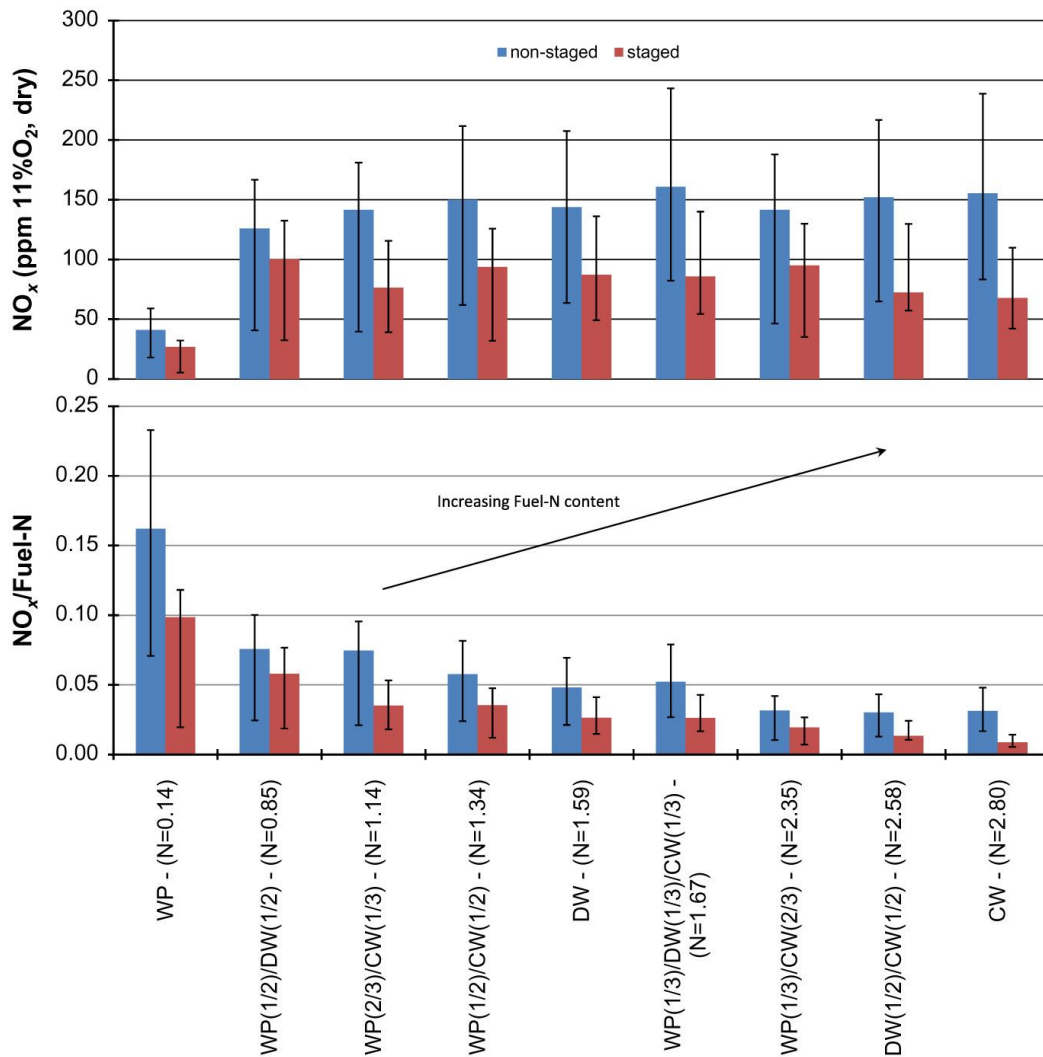
Figure 7.3 Mean, minimum, and maximum NOx emissions and NOx/Fuel-N for staged and non-staged combustion (mixture fractions and fuel-N content (daf) in brackets).

A large NOx reduction potential can be seen for staged combustion. An average NOx reduction of 20–56% was found for the different fuels and fuel mixtures. The optimum NOx reduction is significantly higher, at the optimum primary excess air ratio,

as will be discussed later. In addition, the fuel-N to NOx conversion factor is shown in Figure 7.3.

A clear trend can be seen in this figure which shows considerable decrease in the total fuel-N conversion factor toward NOx with increased fuel-N content. The lower conversion of fuel nitrogen in the fuels with higher amount of nitrogen (e.g., coffee waste) can be explained by formation and reduction of NOx precursors. NH3 is preliminary formed from the conversion of volatile nitrogen. Afterwards, the formed NH_i radicals (NH_3, NH_2, or NH) can be oxidized to form NO or react with NO (which is also created in the conversion of volatile nitrogen) to form molecular nitrogen, N_2. It should be noted that the latter reaction is the reaction which happens in staged combustion technology and SNCR to reduce NOx. The same procedure can happen for HCN as the second NOx precursor. Combustion of fuels with high nitrogen content, results in high concentrations of NH3 and HCN [218,219]. This environment will strengthen the second reaction path (i.e., reaction of precursors with NO) and hence higher fuel-N conversion to N_2, which corresponds to a lower NOx/Fuel-N ratio. On the other side, heterogeneous reactions in the conversion of char nitrogen to NO should be taken into account, even though it has less effect on the total NOx.

7.1.3 N_2O emissions – staged versus non-staged

Mean, minimum, and maximum N_2O emissions as a function of the fuel-N content (ppm at 11% O_2 in dry flue gas) are shown in Figure 7.4 for both staged and non-staged combustion. As in the previous case, the fuel-N to N_2O conversion factor is also shown. For N_2O, no emission reduction potential can be seen for staged combustion. On the contrary, an increase in the N_2O emission level was observed. An average N_2O increase of 18–288% was found for the different fuels and fuel mixtures. The increase in N_2O at optimum NOx reduction conditions (optimum primary excess air ratio) is significantly higher, as will also be discussed later. The N_2O formation and reduction in biomass combustors are discussed and investigated earlier [218, 220–222]. The major global reaction pathways for fuel nitrogen conversion toward NO and N_2O depend on operating conditions [223, 224].
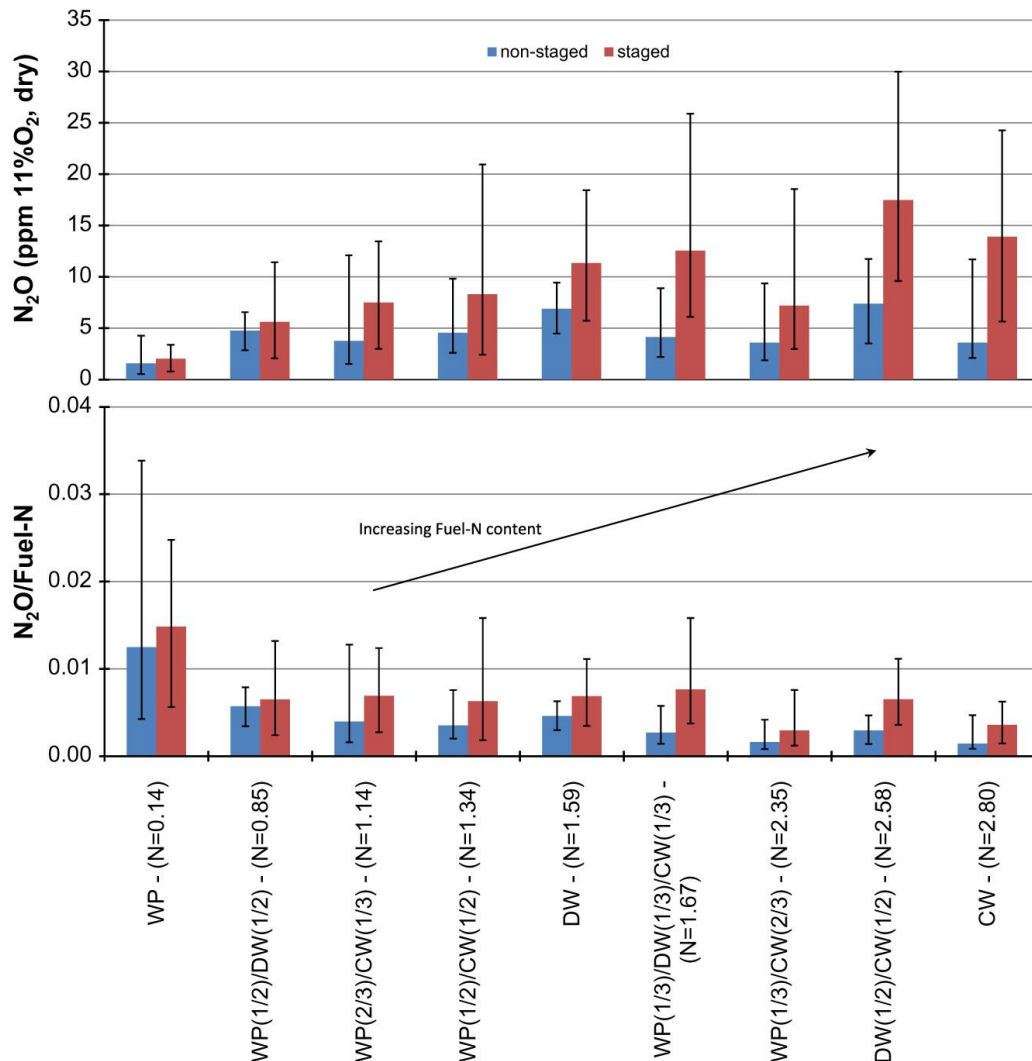
Figure 7.4 Mean, minimum, and maximum N2O emissions and N2O/Fuel-N for staged and non-staged combustion (mixture fractions and fuel-N content (daf) in brackets).

7.1.4 Fuel influence on NOx and N2O emission levels

As Figures 7.3 and 7.4 shows, there is a significant fuel influence on the NOx and N_2O emission levels and the conversion factor for fuel-N to NOx and N2O, both for staged and non-staged combustion. This is at otherwise similar conditions mainly due to the N-content in the fuel. Increasing fuel-N content will increase the NOx emission level. However, the conversion factor for fuel-N to NOx will decrease with increasing fuel-N content, as shown in Figure 7.5. This effect is due to gas phase chemical kinetics, i.e., the reduction of fuel-NOx precursors mainly through reaction between two intermediate nitrogen species, forming molecular nitrogen [97]. The N_2O emission level

is also significantly dependent on the fuel-N content, as also can be seen in Figure 7.5. The shape of the curves means that NOx emissions increase, but not linearly, with increasing fuel-N content. An example is the first and second point for non-staged combustion where the fuel-N content increases from 0.14 to 0.85 (6 times), while NOx/Fuel-N decrease from about 0.24 to 0.10 (about 2.4 times). For higher fuel-N content, the decrease becomes less exponential.

7.1.5 Fuel mixing effect on NO_X and N_2O emission levels and fuel-N conversion factors

Fuel mixing has a positive influence on the NO_X and N_2O emission level, but a negative influence on the overall conversion factor for fuel-N to NO_X and N_2O. The average conversion factor for fuel-N to NO_X and N_2O trends shown in Figure 7.3 and Figure 7.4, respectively, can be modeled by simple exponential functions, as a function of the fuel-N content. From these trends one can estimate the NO_X and N_2O emission level for various fuel mixtures. A mixture of e.g. wood and coffee waste will get an increased conversion factor compared to the fuel with the highest fuel-N content (coffee waste), while it will be lowered even more for the fuel with the lowest fuel-N content (wood). However, when comparing the option of combusting the fuels in separate boilers compared to mixing them in one boiler, the total NO_X and N_2O emission level will theoretically always increase in the case of fuel mixing, due to the exponential increase in the fuel-N to NO_X and N_2O conversion factors with decreasing fuel-N content.
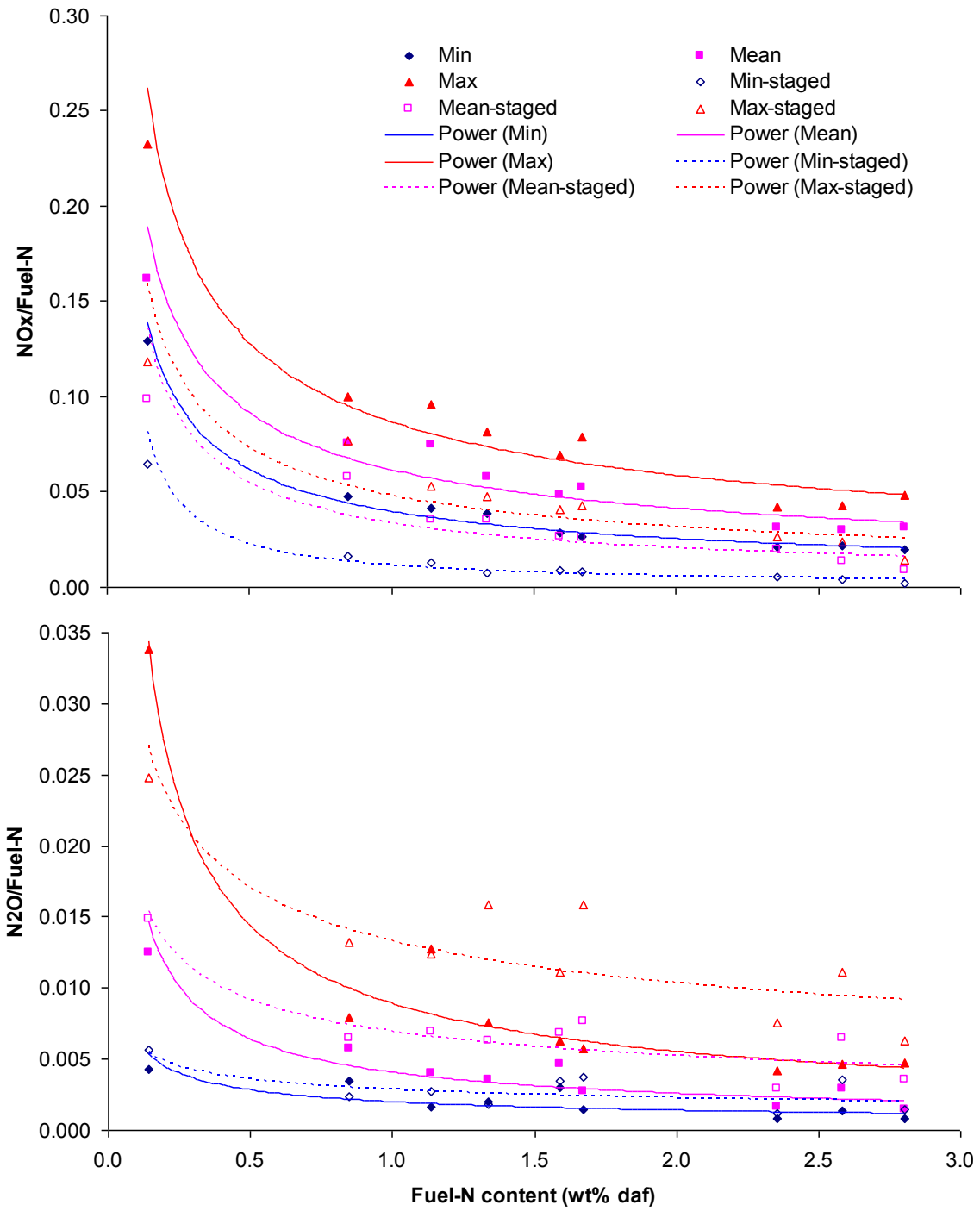
Figure 7.5 Fuel-N influences on conversion factors for fuel-N to NO_X and N_2O

for staged and non-staged combustion

7.1.6 Primary excess air ratio influence on NO_X and N_2O emission levels

Figure 7.6 shows the primary excess air ratio, represented by the O_2 need of the measured unburnt primary gas species (H_2, CO, CH_4, C_2H_2, C_2H_4 and C_2H_6) for

stoichiometric combustion, influence on NO_X and N_2O emission levels for staged combustion of CW. Clearly, there is a correlation between the amount of unburnt primary gas species and the conversion of fuel-N to NO_X.
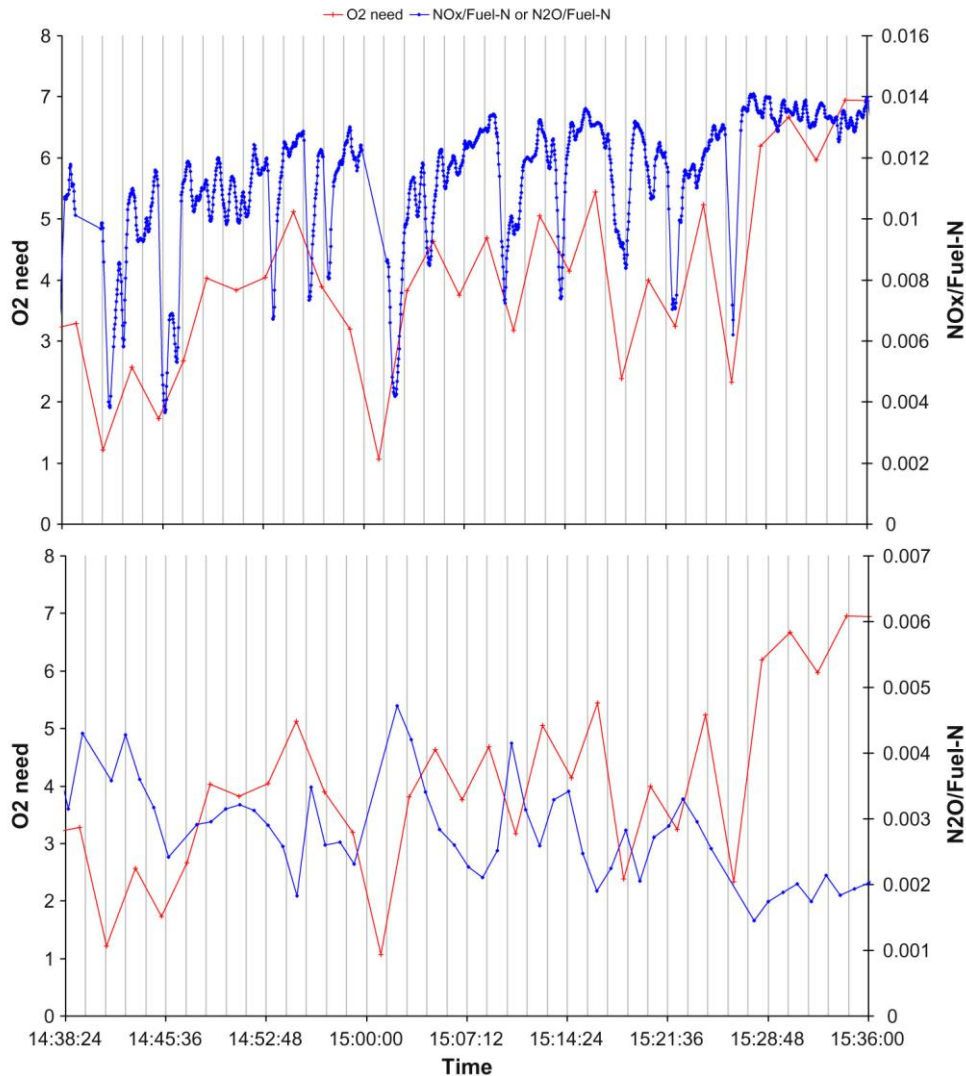
Figure 7.6 Primary excess air ratio influences on NO_X and N_2O emission levels for staged combustion of CW. O_2 need as vol% O_2 needed for stoichiometric combustion of the measured primary gas composition

Decreasing O_2 need gives until a certain point a decreasing fuel-N to NOx conversion factor. Hence, there must exist and optimum primary excess air ratio for minimum conversion of fuel-N to NO_X. This optimum is related to chemical kinetics effects, i.e. the radical pool in the primary gas zone [97, 151] which is also dependent on the mixing conditions. For perfectly stirred reactor conditions the optimum primary

165

excess air ratio will be close to unity, while for plug flow reactor conditions the optimum primary excess air ratio will be significantly lower than unity [151]. At the optimum primary excess air ratio, the highest conversion of fuel-N to N_2O is also found. However, the increased N_2O emission level does not significantly influence the optimum primary excess air ratio for minimum conversion of fuel-N to fixed nitrogen species.

7.1.7 Overall excess air ratio influence on NO_X and N_2O emission levels

Figure 7.7 shows the typical total excess air ratio influence on NOx and N2O emission levels for staged and non-staged combustion, for coffee waste pellets. The corresponding primary excess air ratio is also shown for staged air combustion. As stated above, there exists an optimum overall/primary excess air ratio for minimum conversion of fuel-N to NOx, which is directly visible also in Figure 7.7. The residence time in such generic studies is not relevant once the reactor design and the experimental conditions yield sufficiently long residence times for NOx reduction [169]. In this work the highest possible NOx reduction is positively reached. The direct influence of the total excess air ratio is clearly seen in the non-staged experiments, with increasing NOx emission level with increasing total excess air ratio. Increasing NOx with increasing excess air ratio in conventional burners (non-staged combustion) is due to the higher availability of oxygen at higher excess air ratios. This promotes the reaction of nitrogen containing species with O2 and O and OH radicals and hence formation of NO. The effect on N2O is less clear, but with a trend of increasing N2O emission levels with increasing total excess air ratio. The N2O emission levels are significantly higher for the staged experiments.

Figure 7.7 Overall excess air ratio influence on NO_X and N_2O emission levels for staged and non-staged combustion of CW

Figure 7.8 shows the optimum NOx reduction potential of staged combustion compared to the non-staged combustion, at the optimum primary/total excess air ratio for staged combustion. It can be explained as follows: In the first stage, primary air is added for devolatilization of the volatile fraction of the fuel, resulting in a fuel gas consisting mainly of CO, H_2, CxHy, H_2O, CO_2 and N_2. In addition to the major species, small amounts of NH3, HCN and NO will be formed from the fuel-N content. The key factor here is the distribution of nitrogen containing species, which is regulated by the level of oxygen in the primary zone, and a sufficient residence time in the primary (reduction) zone. In the second stage, sufficient secondary air is supplied to ensure a good burnout and low emission levels from incomplete combustion. If the primary excess air ratio is very low, i.e., very low availability of oxygen, just HCN and NH_i will appear in the first stage and NO will not be formed, i.e., little reduction will take place in the primary zone. Therefore HCN and NH_i will react with added O_2 in the second stage to produce NOx. On the other hand, a very high primary excess air ratio will result in the oxidation of all pyrolysis gases due to high O_2 concentration. Therefore, much more NO will appear while no NH_i exist in the primary stage to go through the

167

reduction path. As can be seen, a NOx reduction of 54–91% is achieved for staged combustion.

Figure 7.8 Optimum NO_X reduction potential for staged combustion compared to non-staged combustion, and the adverse effect on N_2O emissions at the optimum primary excess air ratio for NO_X reduction

These are very good NOx emission reduction results, and is a result of air staging and potentially to some extent fuel staging due to the two level design of the grate. However, at the optimum primary excess air ratio for NOx reduction, emissions of N_2O are adversely affected, increasing the N_2O emission levels with 138–635%.

7.2 Effect of temperature, excess air ratio and staged air combustion on NOx emission

Experiments are performed for non-staged and staged air combustion. Four different temperatures were selected; 850, 900, 950 and 1000 °C. During each experiment, the temperature is kept constant for the reactor and the fuel feeding rate was about 400 g/h. The biomass that has been used for the present work is classified as demolition wood (DW). The proximate analysis of the chosen biomass is given in Table 7.3, while Table 7.4 shows DW ultimate analysis. Combustion of DW as a type of residue wood, represents a large source of alternative energy, in addition to the fact that a waste disposal problem will also be solved. DW comes from many sources, therefore it contains normally different undesirable component such as metals, paints, plastics, etc. which will raise the environmental impact of DW. Especially the high nitrogen content, compared to wood, is the focus in this part of research work. The nitrogen content, which is the most important element in this study is 1.06%, while for wood, straw, peat, sewage sludge and coal it is 0.03-1, 0.3-1.5, 0.5-2.5, 2.5-6.5 and 0.5-2.5 wt%, respectively [89].

Table 7.3 Proximate analysis of DW pellets (wt%).

Pellets	Ash (dry basis)	Volatile (dry basis)	Fixed Carbon (dry basis)	Moisture
Demolition Wood (DW)	2.49	75.97	21.54	9.68 - 14.97

The total excess air ratio for non-staged combustion was around 1.6, where the variation in the fuel feeding rate allows capturing a total excess air ratio range of 1-3, making it possible to see emission trends as a function of total excess air ratio. Each experiment has been carried out for at least two hours at stable operating conditions. For the staged air combustion experiments, the total excess air ratio was also 1.6, while the primary excess air ratio is set to 0.8, which means that 50% of the total air is fed at each stage.

169

Table 7.4 Ultimate analysis of DW pellets (wt% dry ash free basis).

Pellets	C	H	O	N	S	Cl
Demolition Wood (DW)	48.45	6.37	44.11	1.06	0.02	0.05

7.2.1 Accuracy of the results and Combustion Quality (emissions of CO and C_xH_y)

In order to establish the accuracy of the measured results, the total carbon balance is needed to quantify the measured values compared to expected analytical values. The carbon balance for one of the experiments, at 1000 °C for staged air combustion, is shown in Figure 7.9.
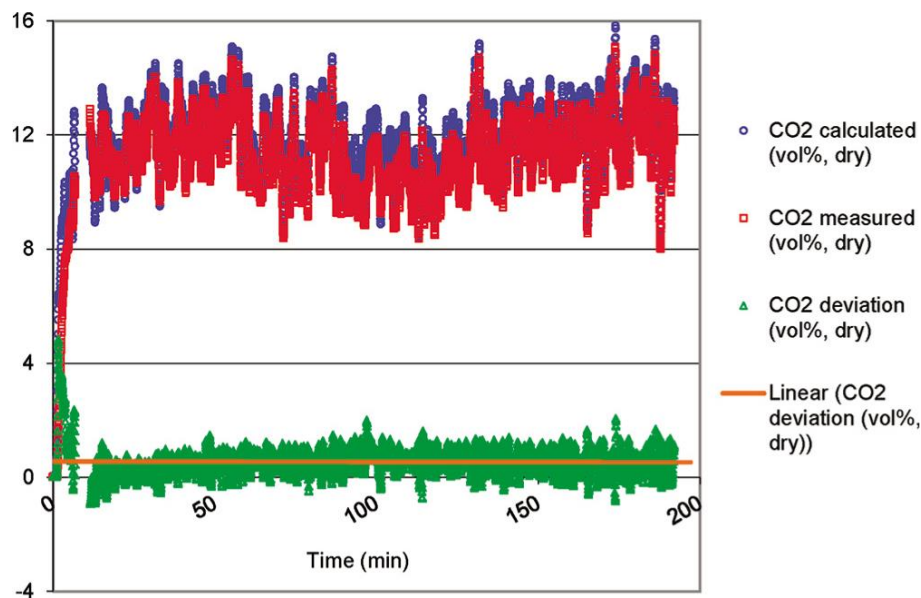
Figure 7.9 CO_2 deviation based on calculated and measured values from the Horiba gas analyzer for one set of the experiments; 1000 °C, staged air combustion

This figure shows the results from the start time until the end of the experiment. However,

it should be noted that the first and very last section of the data has not been considered in the final data for further treatment, since these parts are typical transient periods, outside of the stable run period. The calculated values for CO_2, based on the carbon content in the fuel and the measured volume percentage of oxygen and CO in the flue gas, is very close to the measured values for CO2 for each sampling interval and hence the deviation is sufficiently close to zero. In the case of a large deviation between

measured and calculated values, the data set is removed from further treatment, since it could be from an unstable or transient period. Therefore the carbon balance for the presented set of results is in good order. All the experiments at the different temperatures, with and without staging air, show the same good results for the CO_2 deviation. Emission level of C_xH_y and CO for both staged and nonstaged combustion is shown in Figure 7.10. For C_xH_y, both staged air combustion and nonstaged combustion show the same emission level, typically below 4 ppm at 11% O_2 in dry flue gas. Here, low values for C_xH_y and CO emissions, respectively, below 5 and 50 ppm show good mixing conditions and residence times in line with modern industrial scale boilers [225]. Emissions of gaseous hydrocarbon compounds and CO are a result of incomplete combustion. Favorable combustion leads to small emissions of hydrocarbons because the organic material burns out. Large emissions of hydrocarbons indicate unsatisfactory combustion conditions and probably soot emissions. Large boilers are generally operated at an appropriate oxygen concentration, temperature, and residence time and consequently are under favorable combustion conditions. Particles originating from incomplete combustion are few or none and can be decreased in modern boiler types by 180 times [147, 156, 226] and in the advanced wood furnaces, CO emissions of 10-20 mg/m3 can be reached, depending on the temperature and selection of the optimum excess air ratio [124]. At 900 and 950 °C, some values up to 10 ppm C_xH_y are visible for nonstaged combustion, which originate from the sets of data from the period where the actual stable experiment had not been started, which means that in the stable run, the C_xH_y for both 900 and 950 °C still is 1 to 3 ppm. The C_xH_y emission level is slowly increasing with excess air ratio for both staged air combustion and nonstaged combustion. The influence of excess air ratio is small, but the C_xH_y emission level is a direct function of the excess air ratio, and the minimum C_xH_y emission is taking place at the lowest total excess air ratio.

For nonstaged combustion, the temperature has an inverse effect on the CxHy emission levels. The lowest emissions occur at 850 °C, while at 900, 950, and 1000 °C the temperature has no effect.
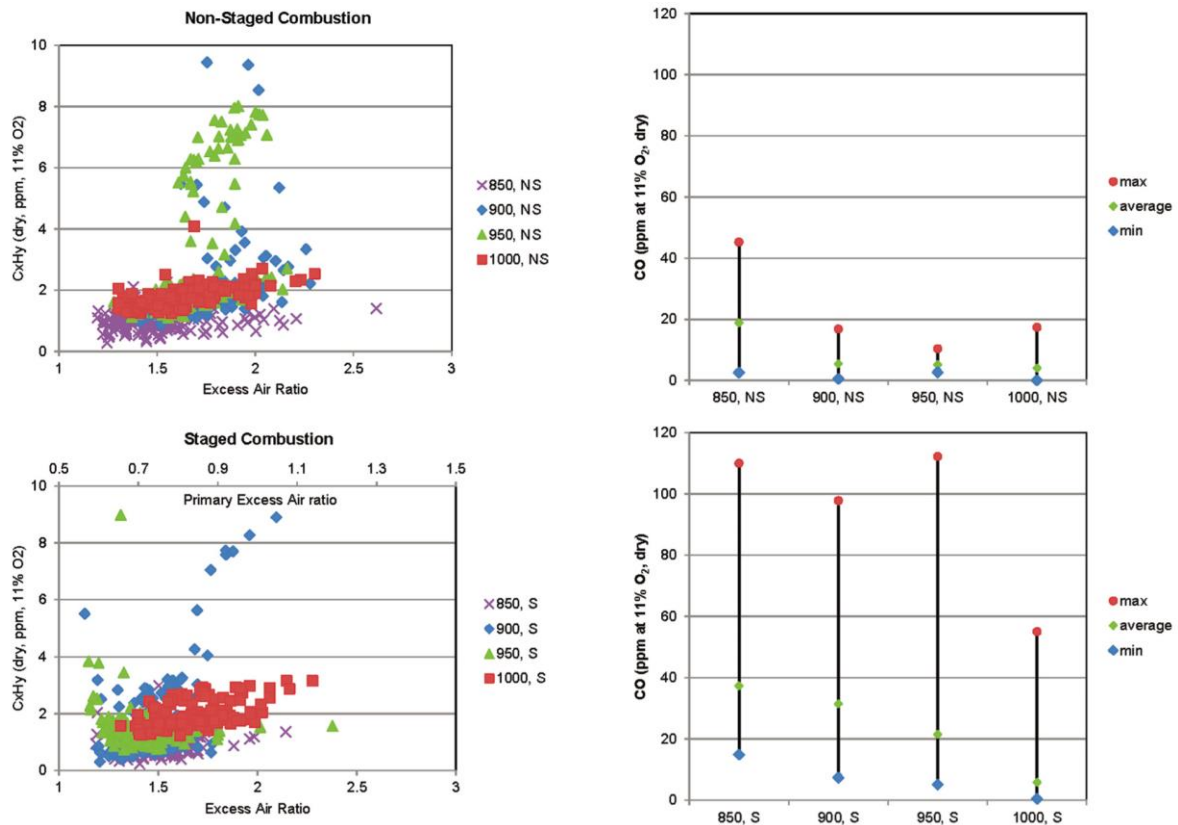
Figure 7.10 (Left) CxHy as ppm corrected to 11%O2 in dry flue gas for staged air combustion and nonstaged combustion as a function of excess air ratio at the different temperature levels. (Right) Average, minimum, and maximum value of CO as ppm corrected to 11% O2 in dry flue gas for staged air combustion (S) and nonstaged combustion (NS) at the different temperature levels

For staged air combustion, the effect of temperature is more visible than for nonstaged combustion. Here the effect of temperature is still low, but it is clearly possible to observe an increase in emission levels with increasing temperature in the lower graph. The observed increase of C_xH_y may be due to a higher release of gaseous hydrocarbons from the fuel at higher temperatures, where the pyrolysis process is intensified by temperature and the formation of hydrocarbons are increased [227].

Detailed experimental and thermodynamic studies on particulate emissions from this multifuel reactor to investigate particle size distribution and chemical composition of fly/bottom ash is extensively discussed later. The effect of temperature on CO is the same as for N_2O. As shown in Figure 7.10, increasing temperature decreases the CO level, while staged air combustion has a negative effect on CO. The former effect is due

172

to a more complete oxidation of CO, forming CO_2. However, with air staging, the low stoichiometric ratio in the first stage cause the oxidation route to be less effective, so the emission of CO rises. The staged air combustion results indicate an increase of 99-482% for CO for staged air combustion, while the mean CO levels are about a factor of two increased.

Emissions of gaseous hydrocarbon compounds and CO are a result of incomplete combustion. Large emissions of CO indicate unsatisfactory combustion conditions. In the present case, higher excess air ratio (more oxygen available) will lead to an almost complete combustion (heated reactor, i.e., temperature not influenced by the excess air ratio). Consequently, the maximum CO level corresponds to the lowest excess air ratio or the more fuel rich condition. In the staged combustion experiments, because of the under-stoichiometric condition in the first stage, a large amount of unburnt species (including CO) will be formed in the primary stage. The burnout of the unburnt species should take place in the second stage. If necessary air is available in the burnout zone, the CO level will be very low; if not the CO level will be high. So the higher deviation for CO emission in the staged combustion is a result of the variations in secondary excess air ratio, where more fuel rich conditions in the secondary stage can, combined with not perfect mixing of fuel gas and secondary air, cause higher fluctuations in the CO level.

7.2.2 NOx emissions: Effect of excess air ratio and air staging

In [228] has been showed that the fuel-N conversion to NOx is strongly dependent on the excess air ratio and that it increases with increasing excess air. However, in this study we investigate further the effect of temperature on this dependency. Figure 7.11 shows the effect of temperature on the NOx emission level (ppm at 11% O_2 in dry flue gas) for both staged air combustion and nonstaged combustion of DW at 850, 900, 950, and 1000 °C.

NO_2 was typically below 1 ppm for the staged and nonstaged experiments which is within the measurement error ranges for the analyzers (Gasmet and Bomem FTIRs) for NO2, except for one case at 900 °C for staged-air combustion, where a NO_2 level of up to 3 ppm is measured. Consequently, we have not found any clear relation between NO_2 and temperature in the investigated temperature range. The upper graph for

173

nonstaged combustion shows an increasing trend for NOx when the excess air ratio is increasing. This corresponds with the findings in [228]. The NOx level for these cases, at all temperatures, varies from 75 to 200 ppm at 11% O_2 in dry flue gas. However, this graph also indicates that temperature variations have almost no effect on the NOx emission level. All the data for the different temperatures are included, showing that they are in the same range for the same excess air ratio and temperature. This indicates that the temperatures are, as expected, too low for thermal NOx formation. According to the literature, thermal NOx formation in different biomass combustion systems starts at temperatures above 1400 ℃ [132,229].

The lower graph, which shows the same information for staged air combustion of DW, is distinctively different from that of nonstaged combustion. Here an optimum excess air ratio exists for each combustion temperature. The NOx results are here plotted as a function of overall excess air ratio while the corresponding primary excess air ratio (half of the overall excess air ratio) is given on the upper x-axis for staged combustion. GC measurements were carried out to analyze the composition of the primary gas, but they can only provide an indicative value for the primary excess air ratio and not with a sufficient time resolution. The main point is to use total excess air ratio as an indicative value to show the effect of variations in the primary excess air ratio on the NOx reduction degree, and this was effectively achieved with the experimental setup, the measurements carried out, and the data treatment procedures employed. The NOx emission level is ranging from 25 to 120 ppm at 11% O_2 in dry flue gas. This range points out that the emission level by staged air combustion of DW decreases by a factor of 2-4, corresponding to 50-75% NOx reduction compared to nonstaged combustion. In the optimum case, i.e., at an excess air ratio of 1.6-1.9, the NOx reduction is 85%. This corresponds to an optimum primary excess air ratio of
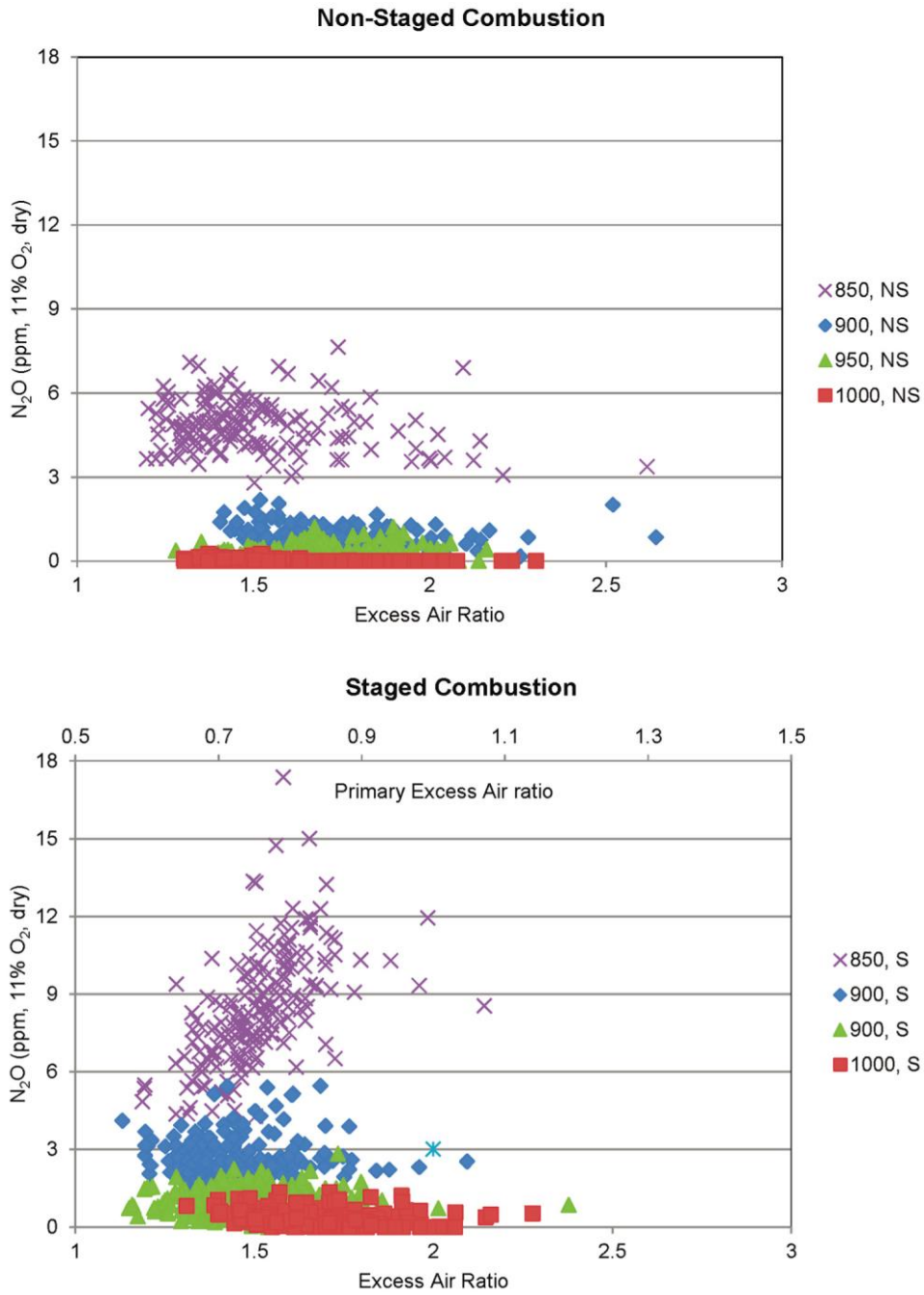
Figure 7.11 NOx as ppm corrected to 11%O2 in the dry flue gas for staged air combustion and nonstaged combustion as a function of excess air ratio at the different temperature levels

0.8-0.95. Again, the effect of temperature is very low, as was the case for nonstaged combustion, and all temperatures show the same trend. First an increase occurs in the NOx level with an increasing excess air ratio up to approximately 1.5, and from this point the NOx level is decreasing until the excess air ratio approaches 2. A further increase in the excess air ratio will cause the NOx level to start increasing again. This

effect is due to the increase of available air both in the primary and secondary zone, which causes the first stage not to be in a fuel rich condition, as was explained in the Introduction. This will increase the TFN/Fuel-N ratio, hence lowering the NOx reduction potential, where total fixed nitrogen (TFN) is the total mass of nitrogen in the flue gas (all N containing gases coming out from the reactor except for N_2), and Fuel-N is the total mass of nitrogen in the fuel [151]. The concentration of NH_3 and HCN was very low in the flue gas after a long residence time, typically below 1 ppm, which was within the measurement error range of the analyzers for these species.

Figure 7.12 shows the effect of temperature on N_2O emissions at different excess air ratios. The upper graph clearly shows that in the case of nonstaged combustion, the N_2O emission level is not a function of the excess air ratio. However, the effect of temperature on the N_2O emission level is significant in nonstaged combustion. The maximum N_2O emission level is seen at the lowest temperature, i.e., 850 °C. Increasing the temperature with just 50 °C will decrease N_2O from 4.8 to 0.9 ppm (mean value), which corresponds to 80% reduction. The same trend has been found for N_2O formation for temperatures above 750 °C in the literature, where reduction of NO has a significant effect on the production of N_2O [230, 231]. The production of N_2O is mainly from the reaction of NO + NCO and NO + NH, so N_2O is mainly reduced by thermal decomposition.HCNandNH$_3$ either can reduce to N_2O and N_2 or oxidize to NO. At the higher temperature, the oxidation route becomes more dominant; therefore, having a low amount of N_2O is predicted [11, 42]. The staged air combustion experiments show higher values of N_2O for the same conditions. At the optimum excess air ratio for NOx reduction, the increase in N_2O emission compared to nonstaged combustion is almost 120%.

Figure 7.12 N_2O as ppm corrected to 11% O_2 in the flue gas for staged air combustion and nonstaged combustion as a function of excess air ratio at the different temperature levels

7.2.3 Temperature Influence on NOx and N2O Emission Levels

As discussed earlier, the effect of temperature on the NOx emission level is small in the investigated temperature range of 850-1000 °C. However, with the extraction of the maximum and minimum levels for each temperature, some important trends can be established. Figure 7.13 shows mean, maximum, and minimum NOx emission level (ppm at 11% O_2 in dry flue gas) for nonstaged (NS) and staged air (S) combustion of DW in the mentioned temperature range. The average (mean value for different excess air ratios over a period of time) is remaining constant at the different temperatures, at almost 150 ppm for nonstaged combustion. The maximum, mean, and minimum values are at the highest level for 900 °C in the nonstaged experiments. NOx at staged air combustion seems not to be a function of temperature either. The average value is on the order of 80 ppm at 11% O_2 in dry flue gas and the highest mean value is seen at 900 and 950 °C. It is interesting to note that in both cases the spread between the highest and lowest values are higher in the lower end of the temperature range. The lower amount of NOx at 1000 °C needs more clarification.

Considering the optimum primary excess air ratio as the key point for minimizing the NOx emission, we can see that at 1000 °C most of the time the reactor was running in the optimum excess air ratio range (see Figure 11). This resulted in a lower average NOx value (for a complete run). At 900 and 950 °C, in spite of our efforts to operate at optimum conditions, the primary excess air ratio has also been slightly lower than the optimum range (0.8-0.95) for the experiment. Hence, the higher average value at 900 and 950 °C corresponds to a lower average primary excess air ratio.

N_2O has a different behavior in relation to temperature, showing similar values for staged air combustion and nonstaged combustion. However, temperature has a great influence on mean, maximum, and minimum N_2O levels, shown in Figure 7.14. They decrease significantly with increasing temperature, and for high temperatures the N_2O level is almost negligible. Yet again the spread between maximum and minimum values are higher in the lower end of the temperature range. Previous studies shows that the main precursor for N_2O formation is HCN oxidation [139, 232] while N_2O destruction is mainly by the reaction of $N_2O+H=N_2+OH$ [218]. At the high temperatures, the

destruction reaction with H radicals is faster and also the HCN oxidation reaction tends to NO formation instead of N_2O. This mechanism causes the N_2O level to be very low at higher temperatures.
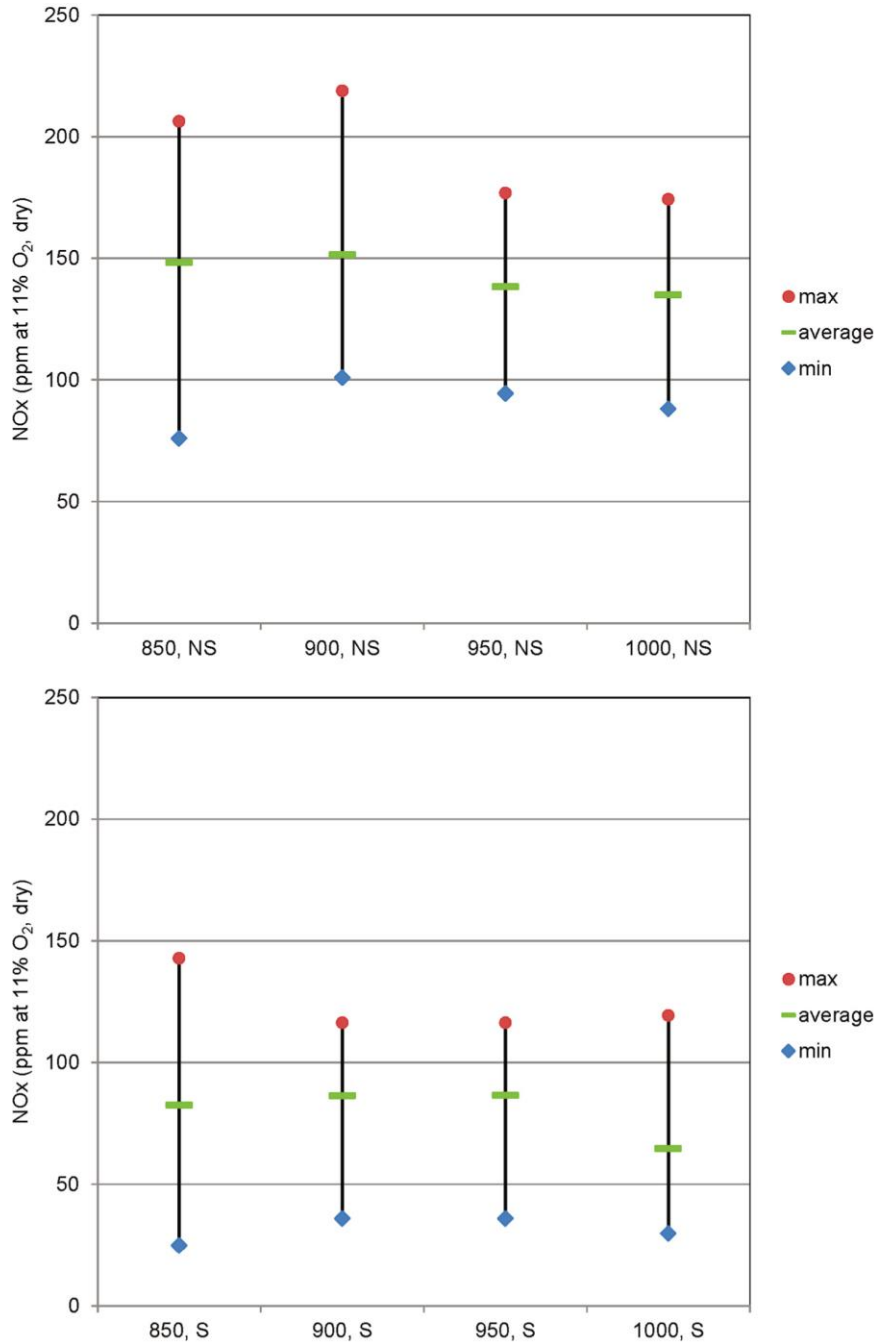
Figure 7.13 Average, minimum and maximum value of NOx as ppm corrected to 11% O2 in dry flue gas for staged air combustion (S) and nonstaged combustion (NS) at the different temperature levels.
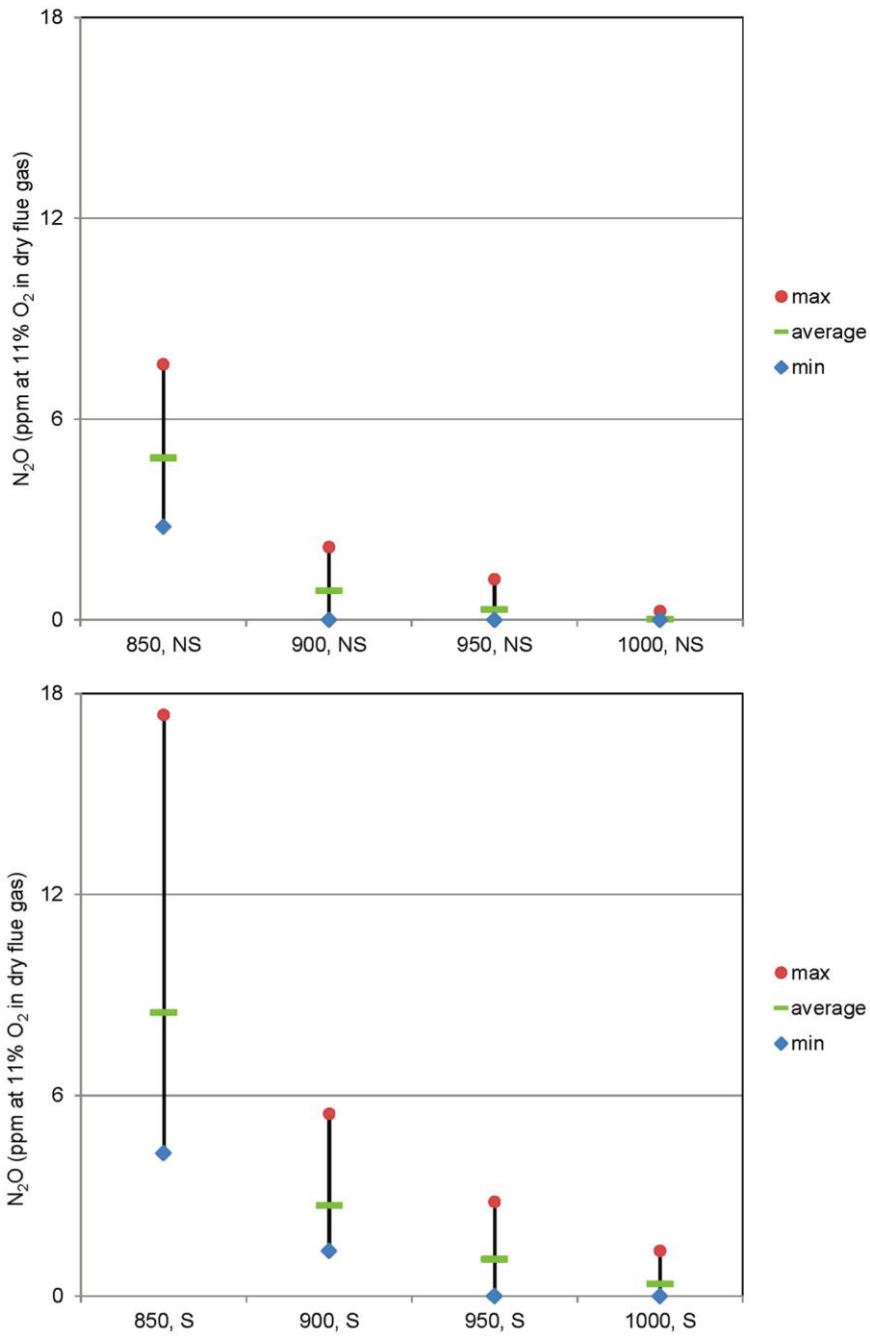
Figure 7.14 Average, minimum and maximum value of N_2O as ppm corrected to 11% O2 in dry flue gas for staged air combustion (S) and nonstaged combustion (NS) at the different temperature levels

7.2.4 Effect of Stoichiometry, Temperature, and Residence Time on TFN/Fuel-N

In addition to the reactor temperature, primary excess air ratio, fuel-N content, differences in residence times and mixing conditions may also have an effect on the fuel

nitrogen conversion. The optimum condition for maximum conversion of fuel-N to molecular nitrogen, N_2, is highly affected by the mentioned parameters. However, since only one fuel was tested, the primary excess air ratio is the only important variable in addition to the potential temperature effect regarding the NOx emission level. The NOx/Fuel-N and TFN/Fuel-N ratios, as shown in Figure 7.15, were checked and showed good consistency, always well below unity [132], since the values for TFN (TFN = NO+ NO_2 + $2N_2O$ + HCN + NH_3) is calculated after complete burnout where the residence time has been several seconds.
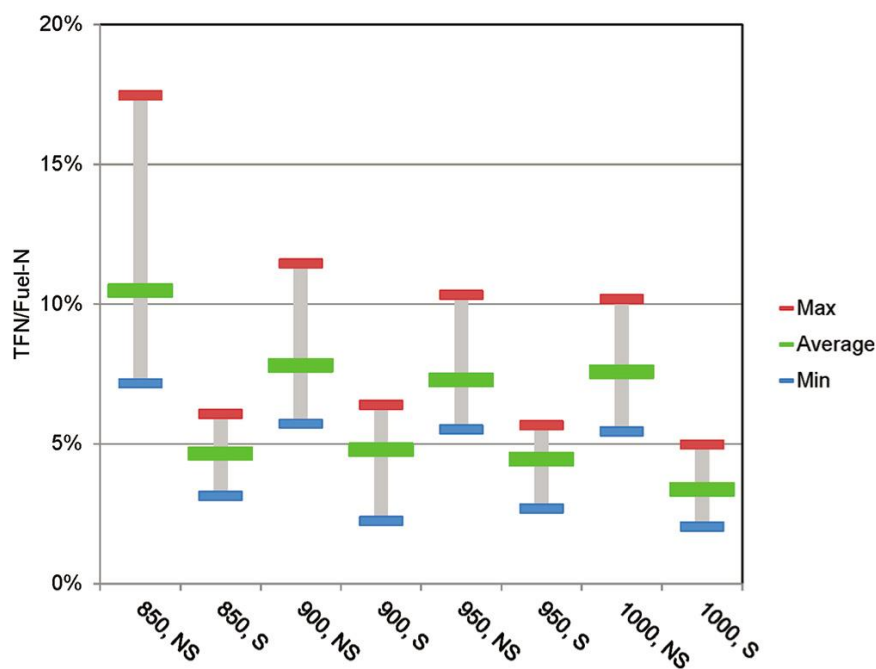
Figure 7.15 Average, minimum and maximum values of TFN/Fuel-N for staged air combustion (S) and nonstaged combustion (NS) at the different temperature levels

Residence time in the reduction zone is of importance for nitrogen conversion, however up to a certain value, beyond which it does not significantly influence TFN/Fuel-N [112, 233]. In this work, the residence time is well above the expected needed time (below 2 s) and, hence, the results are not influenced by the residence time. After the reduction zone, the combustion is completed by injection of the secondary air. Of course, good mixing of secondary air and the combustible gases are important. In average, a large amount of the TFN is composed of NOx (96%) and is varying between 81 and 100% depending on the temperature and the combustion scenario. Therefore the

mentioned values in the last figure, Figure 7.15, can be regarded as approximate values for NOx/Fuel-N.

7.3 Ash related behavior in staged and non-staged combustion of biomass fuels and fuel mixtures

This part of research work on PhD thesis is focusing on the influence of (a) the mixing of biomass fuels in pellets; (b) air staging. Seven parameters have been chosen to evaluate the effects of mixing and staging: (1) HCl & SO_2 emissions; (2) fly ash size distribution; (3) bottom ash composition; (4) bottom ash fusion properties; (5) fly ash composition; (6) Cl-conversion; (7) S-conversion.

Two types of experiments are carried out: (1) experiments with air staging and (2) experiments without air staging. Only isothermal experiments were performed with a reactor temperature of 850 °C. The primary air and secondary air were also preheated to this temperature. The total excess air ratio was about 1.6, and the primary excess air ratio was about 0.8 in the staged air experiments. Pellets feeding rate were 400 g/h.

Staged and non-staged experiments are carried out with four kinds of pellets: (1) wood (WP), (2) demolition wood (DW), (3) coffee waste (CW) and (4) six mixtures of these fuels. The proximate analysis of the pellet samples are shown in Table 7.5.

Table 7.5 Proximate analysis and heating value of pellets (wt%)

Pellets:	Ash (dry basis)	Volatile (dry basis)	Fixed carbon (dry basis)	Moisture (as received)	HHV MJ/kg, dry basis
Wood (WP)	0.2	85.43	14.37	6.5	20.63
Demolition wood (DW)	3.73	77.27	19	8.1	20.54
Coffee waste (CW)	5.8	76.17	18.07	17.53	22.20
Mixtures of pellets (calculated, except for moisture):					
1/2 WP-1/2 DW	1.97	81.35	16.69	6.78	20.62
1/2 WP-1/2 CW	3.00	80.80	16.22	8.76	21.36
1/2 DW-1/2 CW	4.77	76.72	18.54	12.72	21.24
2/3 WP-1/3 CW	2.07	82.34	15.60	11.35	21.08
1/3 WP-2/3 CW	3.93	79.26	16.84	8.02	21.55
1/3 WP-1/3 DW-1/3 CW	3.24	79.62	17.15	24.53	21.04

182

The ultimate analyses of the pellets, including ashes are shown in Table 7.6. The heating value is calculated based on the elemental composition. Mixing has an effect on elemental and ultimate analyses but the fuels also have different chemical structures [79].

Table 7.6 Ultimate analysis of pellets (wt% dry ash free basis) including ash composition

Pellets:	C	H	O	N	S	Cl
Wood (WP)	51.22	6.07	42.54	0.14	0.03	0.02
Demolition wood (DW)	50.59	6.09	41.65	1.59	0.075	0.113
Coffee waste (CW)	52.9	6.47	37.64	2.8	0.187	0.038
Mixtures of pellets (calculated):						
1/2 WP-1/2 DW	50.91	6.08	42.11	0.85	0.052	0.065
1/2 WP-1/2 CW	51.98	6.25	40.33	1.34	0.101	0.028
1/2 DW-1/2 CW	52.01	6.06	39.21	2.58	0.137	0.085
2/3 WP-1/3 CW	51.93	6.06	40.8	1.14	0.08	0.027
1/3 WP-2/3 CW	52.79	6.04	38.68	2.35	0.141	0.036
1/3 WP-1/3 DW-1/3 CW	51.72	6.07	40.45	1.67	0.097	0.061

ELEMENT	SAMPLE	WP	DW	CW	WP/DW	WP/CW	DW/CW	WP(2/3)/CW(1/3)	WP(1/3)/CW(2/3)	WP(1/3)/DW(1/3)/CW(
Si	% TS	0.0394	1.2333	0.1933	0.896	0.0831	1.7	0.358	0.698	0.797
Al	% TS	0.0085	0.1937	0.0803	0.113	0.0399	0.416	0.214	0.485	0.291
Ca	% TS	0.1195	0.7003	1.6367	0.399	0.808	1.02	0.461	0.819	0.657
Fe	% TS	0.0064	0.5490	0.1263	0.296	0.12	0.504	0.209	0.75	0.532
K	% TS	0.0579	0.1130	1.9800	0.0886	0.947	1.46	0.948	2.01	1
Mg	% TS	0.0251	0.1107	0.6453	0.0677	0.308	0.382	0.219	0.44	0.25
Mn	% TS	0.0135	0.0142	0.0099	0.0135	0.0114	0.0142	0.0135	0.014	0.0143
Na	% TS	0.0093	0.1320	0.0168	0.0691	0.011	0.0908	0.0136	0.0147	0.0582
P	% TS	0.0120	0.0367	0.2030	0.0242	0.0986	0.173	0.109	0.227	0.12
Ti	% TS	0.0003	0.2227	0.0082	0.122	0.0029	0.196	0.0327	0.0696	0.122
As	mg/kg TS	0.0900	3.9800	0.0983	3.02	0.1	2.09	0.15	0.135	2.54
Ba	mg/kg TS	10.4500	318.6667	87.2000	175	42.5	263	27.8	38.3	136
Be	mg/kg TS	0.0040	0.0420	0.0500	0.0204	0.02	0.0522	0.02	0.0458	0.0371
Cd	mg/kg TS	0.0635	1.3133	0.0738	0.361	0.0611	1.13	0.0633	0.0588	0.309
Co	mg/kg TS	0.0288	1.3633	0.3603	0.848	0.183	2.23	0.867	1.93	1.37
Cr	mg/kg TS	0.3765	59.3000	28.4000	37.9	11.1	37.7	8.16	45.9	44.1
Cu	mg/kg TS	0.5875	166.0333	66.0333	15.5	31.4	39.5	17.9	33.3	27
Hg	mg/kg TS	0.0100	0.0959	0.0208	0.0631	0.0162	0.0541	0.02	0.0186	0.0373
Mo	mg/kg TS	0.0400	0.8930	1.2533	0.93	0.442	1.15	0.2	0.4	0.608
Nb	mg/kg TS	0.0400	0.6023	0.5000	0.297	0.2	1.16	0.519	1.29	0.686
Ni	mg/kg TS	0.0639	2.6800	1.0047	2.43	0.499	4.94	2.39	4.6	2.82
Pb	mg/kg TS	0.0923	426.3333	4.9933	300	0.474	331	11.5	2.26	95.9
Sc	mg/kg TS	0.0080	0.1055	0.0957	0.0555	0.05	0.481	0.292	0.656	0.336
Sn	mg/kg TS	0.0267	1.8900	0.2530	1.46	0.0626	0.956	0.115	0.119	0.601
Sr	mg/kg TS	4.1200	25.4667	81.3000	15.2	39.3	45.8	20.9	38.5	28.4
V	mg/kg TS	0.0420	1.5667	1.0480	1.01	0.503	4.52	2.4	5.51	3.13
W	mg/kg TS	0.4000	12.3667	5.0000	9.56	2	8.64	2	4	3.75
Y	mg/kg TS	0.0150	0.4917	0.2000	0.273	0.09	0.713	0.265	0.61	0.488
Zn	mg/kg TS	8.7700	679.3333	26.4667	390	15.3	265	19.3	16.7	135
Zr	mg/kg TS	0.0947	9.3567	2.2700	5.99	0.473	12.3	3.45	6.58	6.15

CW has the highest ash content but it is still relatively low (5.8 wt% ddb.). DW has the highest Cl-content while CW has the highest S-content. DW has the highest Si and Al but also Na contents. CW has both the highest Ca and K concentrations.

7.3.1 HCl & SO$_2$ emission levels

For pure biomass fuels, staging leads to a reduction in HCl emissions while no clear trend is observed for the mixtures (three are unaffected, two display increasing emissions and one a decrease). This might be due to accuracy issues as HCl is difficult to quantify. However the somewhat consistent results (all pure fuels exhibit a decrease in HCl while mixtures exhibit varying trends) might reveal complex synergies between mixed fuels.

The experimental results (both staged and non-staged) show that increasing fuel-Cl lead to increasing HCl emissions during combustion. The resulting emissions for the mixtures indicate an unexpected effect of mixing on HCl emissions: in most cases, the resulting emissions are lower than the average of the pure biomass emissions, including for the ternary mixtures. No explanation can be given except synergy effects between the mixed fuels. Such complex (i.e. non-linear) interactions between chemical elements are actually not uncommon in biomass combustion [234].

Increasing S-fuel is leading to increasing SO$_2$ emissions. Contrary to HCl, the mixing effect can generally be described "as expected" with the resulting mixtures emissions in between those of the involved pure biomass samples. For DW and DW/WP (WP has a very low S concentration) no effect from staging is visible while the other fuels and mixtures show a little increase of SO$_2$ with staging.

The opposite effects of mixing and staging on the chemistries of S and Cl show that the same methods cannot be used to reduce the circulation of both S and Cl.

Figure 7.16 presents the SO$_2$ and HCl emission levels during staged and non-staged incineration for the three biomass fuels and their mixtures.
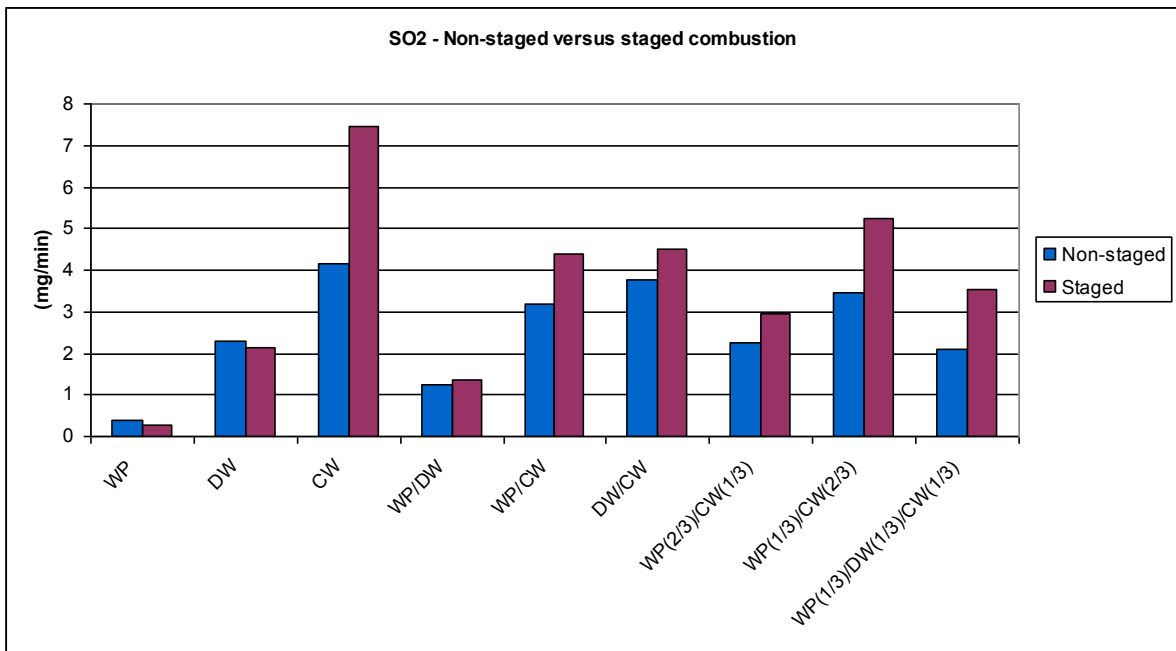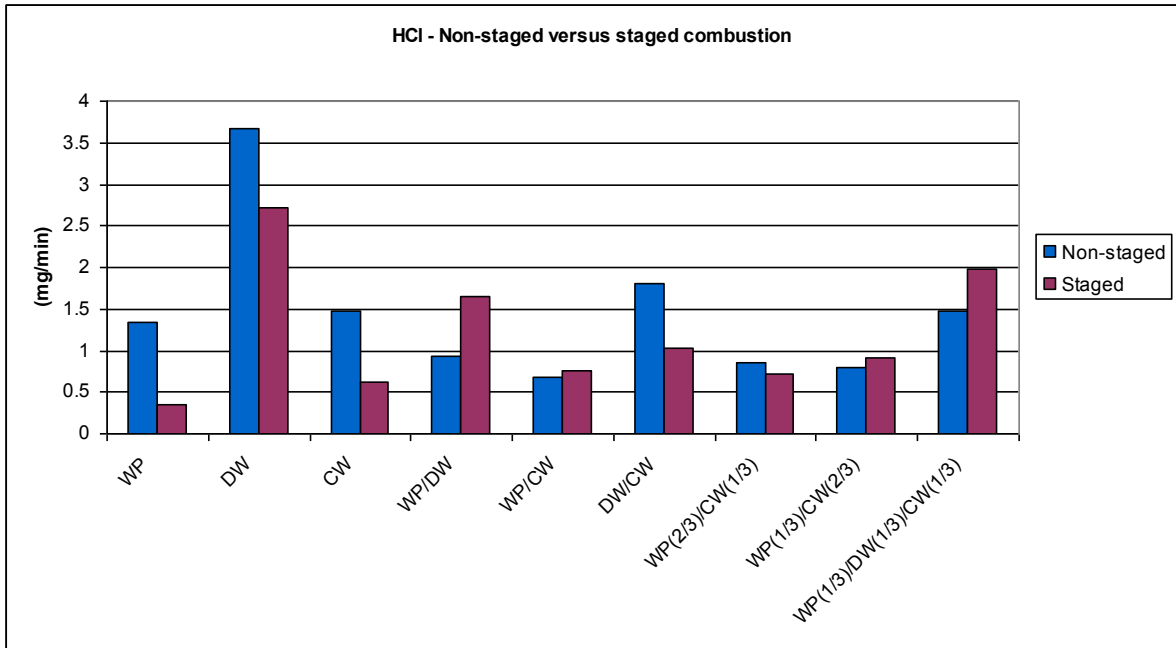
Figure 7.16 HCl and SO_2 emission levels for staged and non-staged combustion conditions

7.3.2 Particle size distribution

The particles formed during fixed bed biomass incineration are of two groups [235]: (a) coarse fly ash particles with a diameter comprised between 1 and 250 µm (mainly between 10 and 100 µm); (b) aerosols with a diameter under 1 µm (sub-micron particles mainly between 0.1 and 1 µm). Together they constitute the fly ash. The particle size distribution from fixed bed combustion of biomass is therefore bimodal. While the large particles are physically entrained from the bed by the flue gas, the aerosols are originating from the release of volatiles compounds (such as alkali chlorides) from the fuel followed by nucleation, and condensation of these vapors and subsequent coagulation of particles [235]. Other processes (condensation of vapors onto large particles) may also occur. The release behavior and governing mechanisms are not well known yet and are affected by a variety of operating and feedstock parameters [235].

Figure 7.17 presents the particle size distribution of the fly ash up to 10 µm, i.e. mainly the aerosols, as they are the most corrosive, for the pure fuels and mixtures for non-staged and staged experiments.
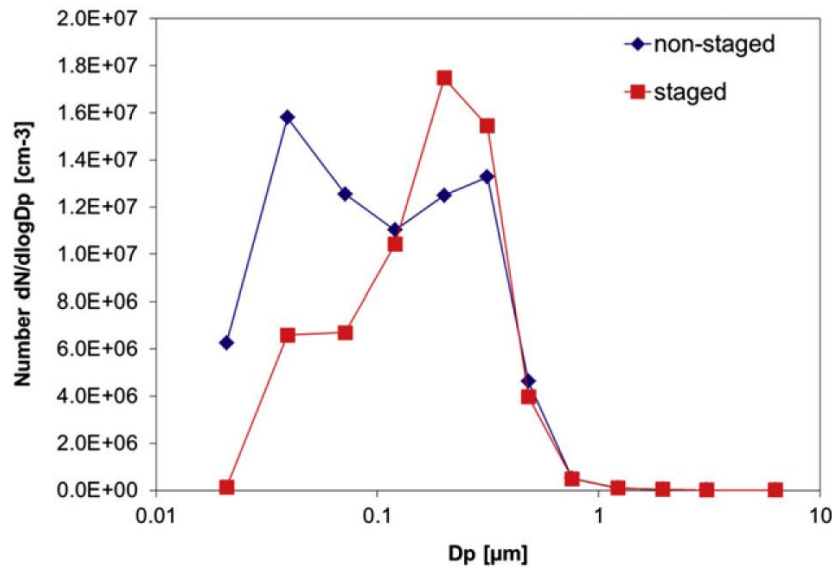
Figure 7.17 Comparison of particle size distribution for staged and non-staged combustion conditions

The curves are an average of all experiments as the same trend is observed for all fuels and mixtures. Staging leads to a displacement towards larger particles from less

than 0.1 μm to over 0.1 μm (but under 1 μm) indicating a shift in release behavior and mechanisms. The total number of particles emitted appears little affected by staging meaning that the total weight of particles emitted is increased by staging.

7.3.3 Bottom ash composition

Figure 7.18 summarizes the main elements constituting bottom ash in the experiments. The main constituents of the bottom ash for all biomass and mixtures are Si, Al, Ca, Fe, K and Mg with variations between the fuels in relation with the elemental composition of the fuels (see Table 7.7). The main components of fly ash are K, S, Cl and Na but also significant levels of Pb and Zn (more details will be given later). These compositional differences directly translate the different processes involved in the formation of these two categories of ashes as discussed before: bottom ash is mainly made of non-volatile inorganic matrix left over after the release of volatiles, such as Si, Al, Ca and Fe while aerosols (submicron fly ash particles) are mainly made of volatiles such as alkali chlorides [235]. Two very interesting results concerning bottom ash (staging and non-staging as there is no major difference) are:

(a) The high concentrations of K for most biomass and mixtures (exception: DW and its mixtures). This might be due to the formation of potassium (alumino) silicates [236] or to the fact that K is part of non-volatile chemical compounds in the fuel (such as aluminosilicates). It is also believed that pellets, more compact and denser than loose biomass, might also contribute to a more intimate contact and therewith promote reactions between inorganic compounds.

(b) The most interesting result concerning the effect of staging is that K is (relatively) more retained in the bottom ash than Na when staging is used with pure biomass fuels while staging has no measurable effect on Na and K chemistries in mixtures. This strongly infers that mixed fuels in pellets interact together and that these interactions lead to nonlinear effects on overall chemistry. This is not uncommon as indicated earlier and in [234].
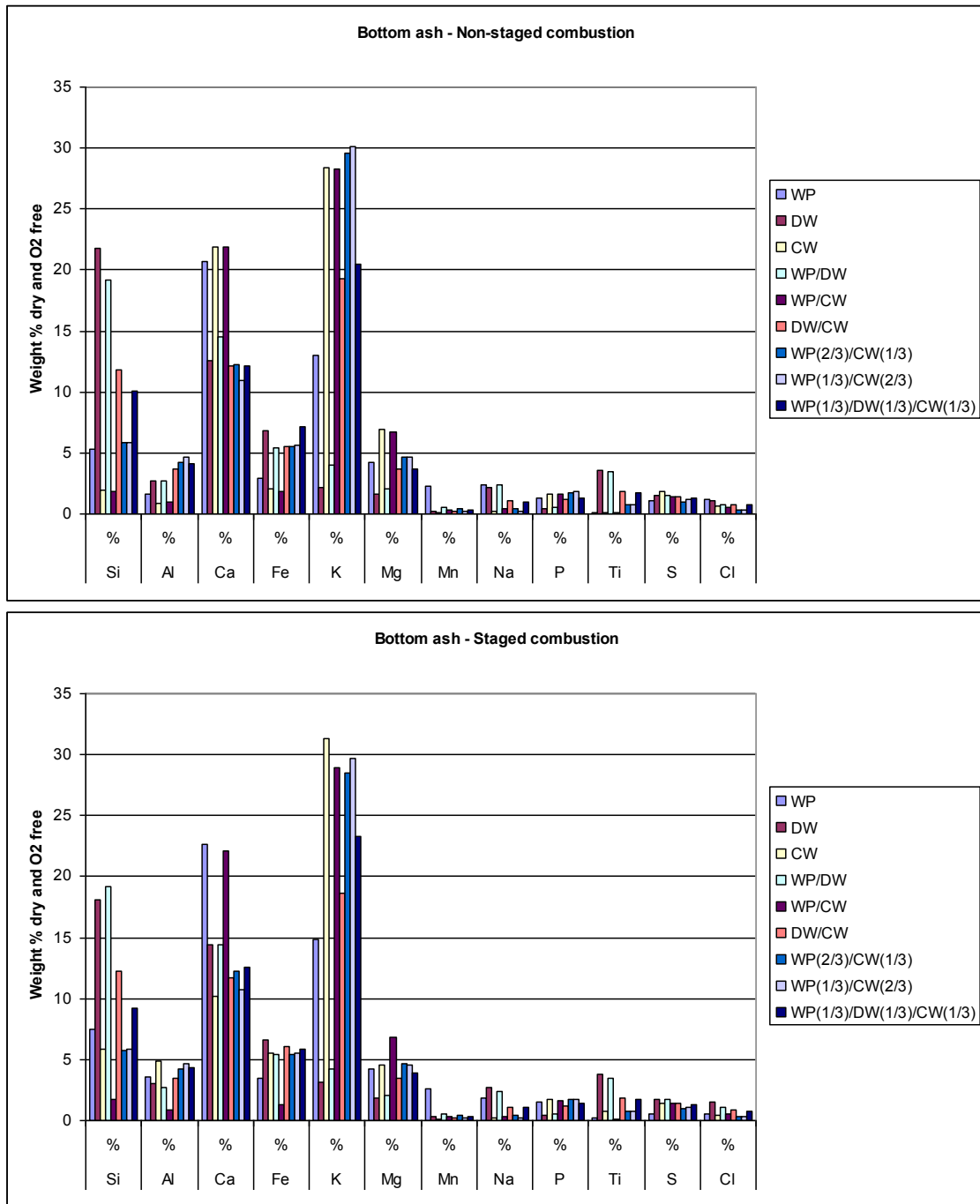
Figure 7.18 Comparison of bottom ash composition for staged and non-staged combustion conditions

A single fuel significantly deviates from these two observations: coffee waste (CW). CW does not have high bottom ash K concentrations and the two alkalis are found at the same (weight) concentrations in the bottom ash even though much less Na is present in the fuel than K. This unique behavior also affects the chemistry of alkalis

in the mixtures involving CW (decrease in K in bottom ash, see Figure 6). Several parameters may contribute to the peculiar behavior of CW compared to the other fuels such as chemical makeup (very high N-content, high S-content) including ash (high Ca content) but no more detailed explanation can be given at the present time.

7.3.4 Bottom ash fusion properties

The four ash fusion temperatures represent transitional states between solid and fluid ash. These temperatures give an indication of the softening and melting behavior of the ash. Despite the shortcomings inherent to this empirical method and a relatively weak record of correlation with slagging and fouling (especially for fuels other than coal), fusion temperatures are valuable guides to the high temperature behavior of the fuel inorganic elements and can give useful information regarding the fouling and slagging propensities of ashes [237]. The initial deformation temperature (IDT) is for example a guidance criterion for the prevention of severe superheater fouling: plant design should limit the temperature of the flue gas entering the superheater section to a value below IDT. The fusion temperatures may be related to the composition but also structure of the ashes. Figure 7.19 presents the ash fusion temperatures (ASTM 1857 Standard) for the bottom ash of the three pure biomass and the six mixtures.

For the non-staged experiments, the IDT of the pure fuels are all around 1100°C (+/- 50°C). This is also true for the mixtures except for WP (1/3)/CW (2/3) and the ternary mixture. Wood pellets (WP) and demolition wood pellets (DW) fusion temperatures are almost not affected by staging, while CW fusion temperatures are increasing from under 1100 to over 1200°C. The four transitional temperatures are very close for DW.
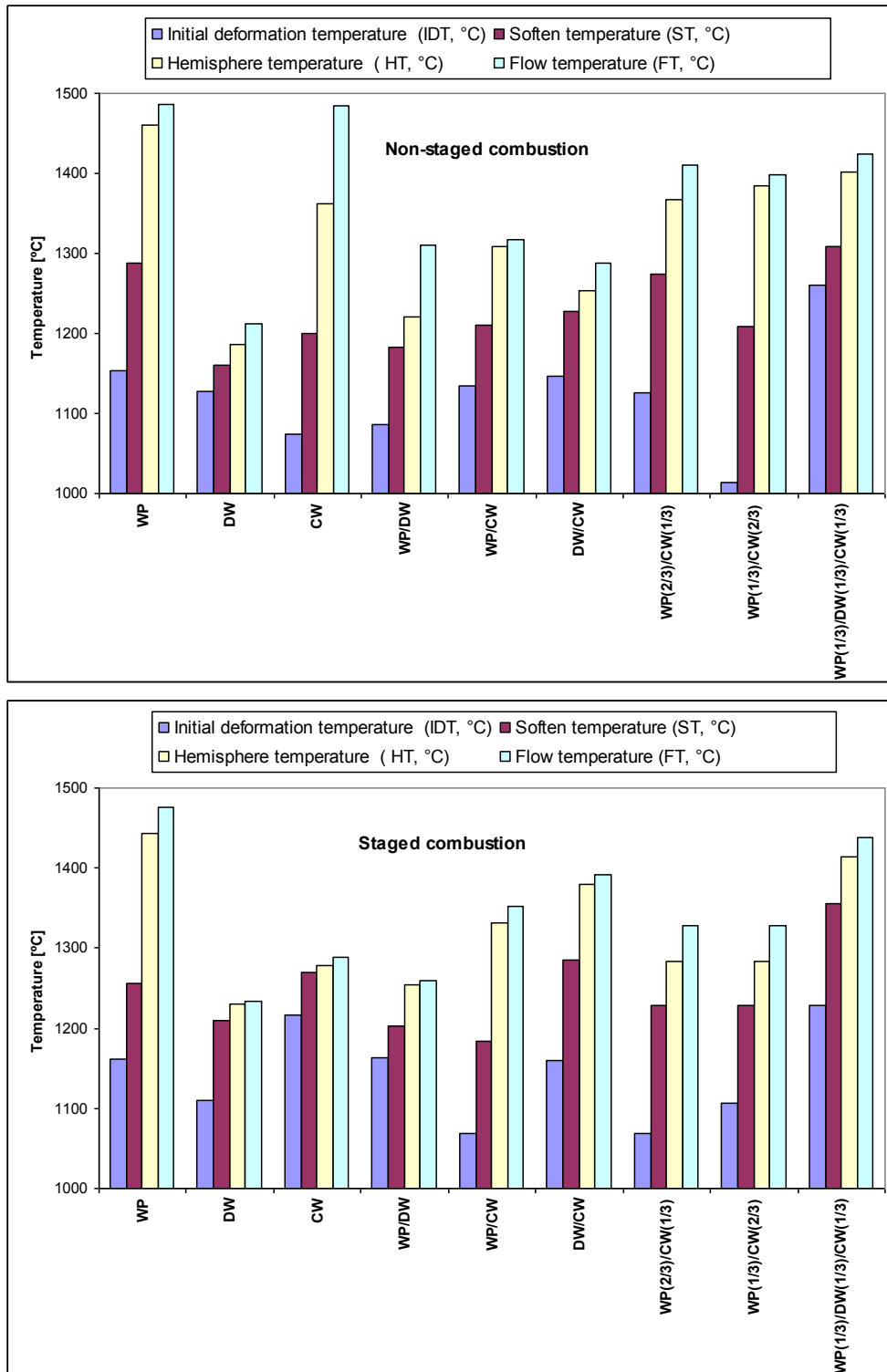
Figure 7.19 Comparison of ash fusion properties of bottom ash for staged and non-staged combustion conditions

No obvious trends concerning the influence of mixing and staging are observed as presented in Figure 7.20.
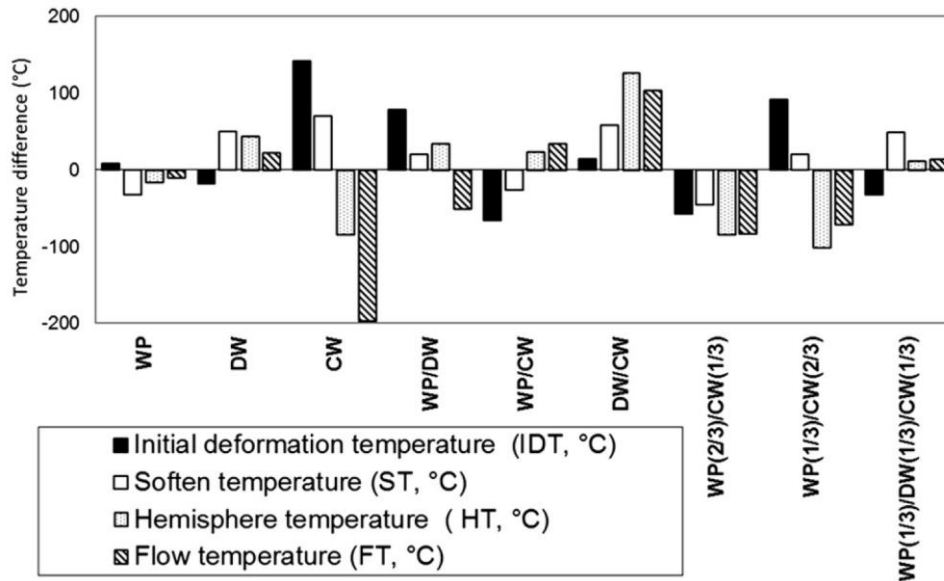
Figure 7.20 Temperature difference between non-staged and staged experiments for four characteristic temperatures in the various fuels and fuel mixtures

However, two main behaviors may be envisioned:

(a) there are interactions between the chemical elements of the fuels during incineration therewith forming an ash with a new structure (having ash properties difficult to predict and/or correlate). As already mentioned, this might be promoted by the use of pellets in which ash compounds are more intimately in contact than in loose biomass;

(b) the resulting ash might be a mixture of the two pure fuels ash (no interactions).

The largest effect observed is for CW for which staging leads to a narrowing of all the bottom ash fusion temperatures, concentrated within about 70°C, implying that the softening-melting of the ashes is happening almost simultaneously.

7.3.5 Fly ash composition

The main components in the fly ash are K, S, Cl and Na (see Figure 7.21 (a) and (b)). In average 70 wt% of the oxygen-free samples (excluding C and Al) consisted of these four elements. Zn and Pb represent on average 20 wt-% whereas the portion of the inert oxide forming elements Si, Ca, Fe, P, Mg and Cr is 10 wt%. P and Mg compositions are very low in all samples.

191

The portion of inert metals is generally higher in the bigger particle size fractions than in the smaller fractions, indicating that the compounds of these metals (oxides) originate from the original fuel ash and have not been vaporized during combustion.

Pb and Zn are partly in oxide form, partly in salt form. The oxides are most probably ZnO and PbO. The salt part is made of sulfate and chloride of K, Na, Zn and Pb.

The Cl content of the salt part of the WP sample is 5-20 % with the staged samples showing slightly higher values than the non-staged samples. The DW sample has 50-60 % Cl in both non-staged and staged samples, whereas the CW samples have no Cl .

CW composition shows no trends as a function of particle size. K constitutes some 70 % of the metals, Zn 25 % and Na 5 %. Non-staged and staged samples are similar except for significantly higher Zn in the staged samples.

In the WP samples, K decreases with increasing particles size. Zn is low in the smaller fractions and higher in the bigger particles. The staged samples have significantly higher Na than the non-staged.

The DW samples show significant trends in the metal content as a function of particle size. In the staged runs, K decreases from 40 % in the 0.1 μm sample to 20 % in the 1.5 μm sample. In the non-staged sample, K is 20 % in the small particles and 15 % in the larger ones. Zn increases correspondingly from smaller to bigger particles. Pb shows a slight decrease. There is significantly higher Na in the non-staged samples, but in neither runs Na showed any trend as a function of particle size.

The salt part of the mixture WP/DW consists of 60 % Cl both in non-staged and staged runs. Some 50 % of the metals are Zn and Pb with a slight increase of Zn as a function of particle size.

The WP/CW samples show very small amounts of Cl, almost no in the non-staged samples and below 10 % in the staged samples. K is the dominating metal with 70 % in the non-staged samples and around 50 % in the staged samples. In the staged samples, Zn increases with increasing particle size while there are no trends in composition of the non-staged samples.
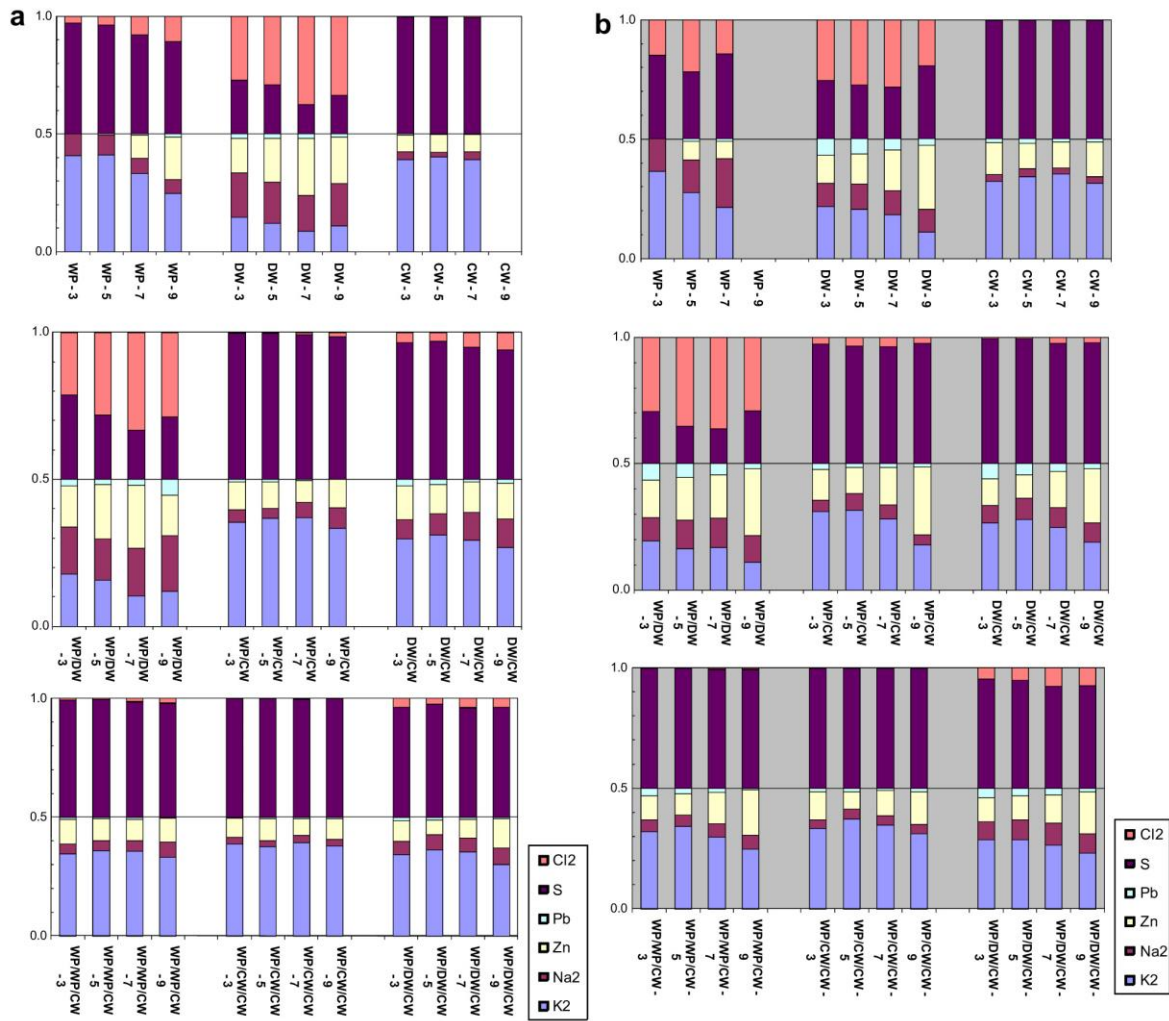
Figure 7.21 (a) Calculated composition (mass fraction) of the salt part of fly ash samples from the runs with different fuel mixtures at non-staged primary air conditions. Upper: Pure fuels. Middle: Binary mixtures. Lower: Ternary mixtures. (b) Calculated composition (mass fraction) of the salt part of fly ash samples from the runs with different fuel mixtures at staged primary air conditions. Upper: Pure fuels. Middle: Binary mixtures. Lower: Ternary mixtures.

The DW/CW samples contain very small amounts of Cl, slightly more in the non-staged samples. In the staged run, K shows a small decreasing trend with particle size and Zn a corresponding increase. This trend is not seen in the non-staged run.

The samples from runs with mixtures of WP and CW (2/3WP+1/3CW) and (1/3WP+2/3CW) are very similar. The non-staged samples show no compositional changes as a function of particle size, while K is decreasing and Zn is increasing in the two air-staged runs. Na shows no trend as function of particle size.

The samples from the run with mixture WP/DW/CW show higher Cl-content than the other ones. The staged samples have some 10 % and the non-staged some 5 %

193

Cl. The Zn content is somewhat higher in the staged samples and increases in bigger particles. K shows a corresponding decrease. Na is, again, not affected by particle size.

7.3.6 Cl-chemistry

Figure 7.22 presents the phase distribution of Cl in the three biomass samples and six biomass mixtures both for nonstaged and staged combustion experiments. Experimental challenges make it difficult to reach satisfying mass balances in some experiments but the interpretation of the overall trends, i.e. qualitative rather than quantitative results, still brings valuable knowledge.

The three biomass samples (non-staged combustion experiments) can be said to belong to two groups: (1) fuels in which most of Cl is converted to HCl represented here by wood pellets (WP); (2) fuels in which Cl is distributed equally in both phases. Such grouping has also been reported in thermodynamic equilibrium calculations for waste fractions (including biomass) [238].

Staging has the same effect on all fuels (but with different relative strengths): it displaces Cl from the gas to the solid phase. For example, the proportion of Cl in the bottom ash is increasing from about 57% to about 80% in CW. The differences in the magnitude of the effect are partly attributable to the fuel-Cl content but the chemical makeup of the fuels (modes of occurrence) is most probably another important factor.

When looking at the (non-staged) results for the three 50/50 mixtures (see Figure 7.22), it appears that the resulting retention in the bottom ash is at the high end of the values of the respective mixed fuels (WP/DW: 50%; WP/CW: 56%; DW/CW: 60%; WP: 15%; DW: 40%; CW: 57%). This behavior cannot be explained but seems to prove that complex interactions between the mixed fuels are occurring. Air staging does not have a significant effect for WP/DW and WP/CW.

Mixtures in which one fuel is dominating (WP(2/3)/CW(1/3) and WP(1/3)/CW(2/3)) offer clearer trends when it comes to Cl-distribution (for non-staging experiments): increasing the share of CW increases the share of Cl in bottom ash. This result is in good correlation with the results for the single-fuel pellets. As observed previously, the effect of air staging is almost non-existent in mixtures.
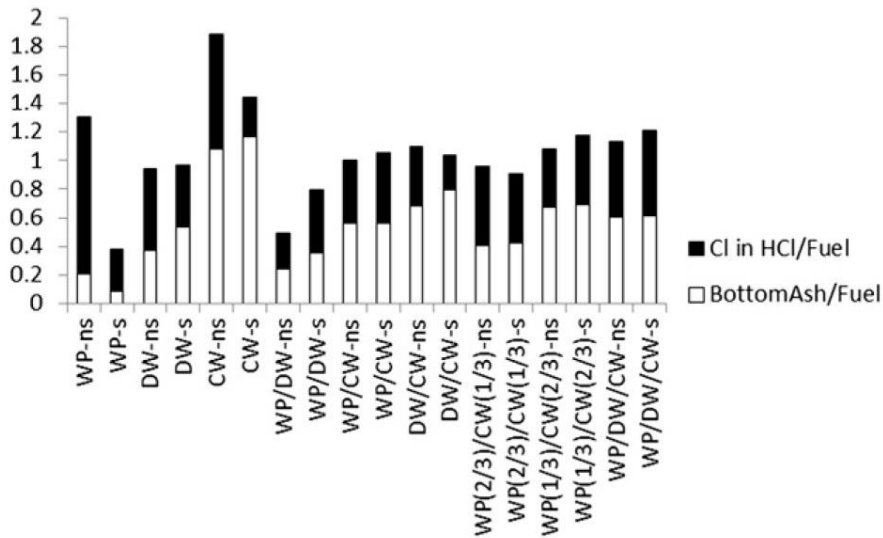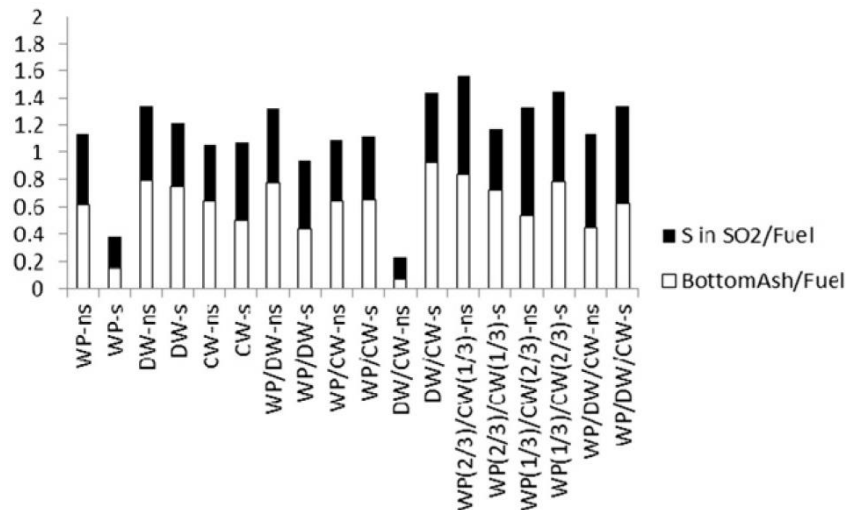
Figure 7.22 Cl-phase distribution (conversion factors) for staged (s) and non-staged (ns) combustion conditions.

7.3.7 S-chemistry

Figure 7.23 shows the phase distribution of S in the three pure biomass fuels and the biomass mixtures. S partitioning is between the gas phase (as SO_2) and the solid phase (bottom ash). An important experimental issue is the S-mass balances which are not really satisfactory for some of the experiments, but the interpretation of the overall trends, i.e. qualitative rather than quantitative results, still brings valuable knowledge.

Overlooking this issue, which trends may be extracted? In non-staged experiments, it appears that for all fuels and fuel mixtures studied, slightly more than half of S is to be found in the bottom ash (except for WP and WP(2/3)/CW(1/3) where slightly more than half of S is to be found as SO_2). Distribution does not seem to be affected by S-concentration or its modes of occurrence which most certainly vary in the different fuels. This is in good accordance with both experimental results [189] where it is measured that 25-55% of S is released to the gas phase from 500°C for woody biomass and with thermodynamic calculations [238] which predict that about 45% of biomass-S is released to the gas phase (average at 600-1200 °C).

Staging does not appear to have an influence on S-phase distribution apart from a minor increase in S-conversion to SO_2 for most of the mixtures.

Figure 7.23 S-phase distribution (conversion factors) for staged (s) and non-staged (ns) combustion conditions

7.4 The effect of peat ash addition on the combustion of demolition wood

In the present work, the first attempts are made to determine which chemical effects of peat ash addition in demolition wood combustion are detectable on the bottom ash, fly ash and gas composition in carefully controlled combustion experiments. All experiments in this work were carried out with demolition wood and demolition wood with peat ash employing staged air combustion. Demolition wood has high contents of zinc and lead and has been shown to be quite problematic from a corrosion point of view. The results of both the proximate and ultimate analysis are presented in Table 7.7. The metal composition of the ash for the different fuel mixtures are presented in Table 7.8 recalculated on dry fuel basis.

Table 7.7 Ultimate and proximate analysis of the demolition wood

Proximate analysis			
Volatiles (dry basis)	Fixed carbon (dry basis)	Ash (dry basis)	Moisture (as received)
77.13	19.00	3.87	7.98

Ultimate Analysis (Oxygen calculated by difference)					
C	H	N	O	S	Cl
50.53	6.09	1.59	41.60	0.08	0.11

Table 7.8 Chemical composition (dry basis) of the ash of demolition wood and the generated mixtures

Peat ash %	0	1	5	10
Ash content [%]	3.9	5.2	8.9	13.4
Si [%]	1.2	1.9	2.4	3.6
Al [%]	0.2	0.3	0.3	0.5
Ca [%]	0.7	1.1	1.7	3.7
Fe [%]	0.5	0.4	2.5	1.2
K [%]	0.1	0.1	0.1	0.1
Mg [%]	0.1	0.3	0.7	1.8
Mn [%]	0.01	0.02	0.03	0.03
Na [%]	0.1	0.1	0.1	0.1
P [%]	0.04	0.05	0.05	0.10
Ti [%]	0.2	0.3	0.2	0.2
As [mg/kg]	4	3	4	5
Ba [mg/kg]	319	367	274	379
Be [mg/kg]	0.04	0.06	0.13	0.25
Cd [mg/kg]	1.31	1.02	0.97	0.55
Co [mg/kg]	1.36	2.21	1.37	1.46
Cr [mg/kg]	59	50	55	96
Cu [mg/kg]	166	275	29	29
Mo [mg/kg]	0.89	1.43	0.82	2.56
Nb [mg/kg]	0.60	0.68	0.60	0.90
Ni [mg/kg]	2.7	2.3	3.1	2.8
Pb [mg/kg]	426	447	637	258
Sc [mg/kg]	0.11	0.19	0.21	0.54
Sn [mg/kg]	1.89	2.99	5.40	2.11
Sr [mg/kg]	25	30	28	45
V [mg/kg]	1.57	2.12	3.14	3.57
W [mg/kg]	12	75	12	15
Y [mg/kg]	0.49	1.05	2.11	5.10
Zn [mg/kg]	679	606	421	346
Zr [mg/kg]	9	12	10	13

Only isothermal experiments were performed, the reactor was preheated to the required temperature which was held constant during the experiment. The total excess air ratio was about 1.6, and the primary air stoichiometry was about 0.8 for most of the experiments but was also varied in order to study the effect of lean O_2 condition in the primary zone on the volatility of chlorine and other alkali compounds.

The reference experiment was run at a reactor temperature of 850 °C and with no addition of peat ash. Three other experiments were run at the same operational conditions with the exception of the peat ash addition of respectively 1, 5 and 10% to the demolition wood. Another two were run with 5% peat ash addition at different reactor temperatures of 800 and 900 °C. And finally two experiments were performed with lower (marked as LP) and higher (HP) air supply to the primary zone compared to the reference experiment. The secondary air combustion was changed respectively in order to obtain a total air excess ratio of 1.6.

7.4.1 Bottom ash analysis

To determine the fate of some of the ash elements during combustion and the effect of peat ash, the chemical composition of the bottom ash was determined by the ICP-AES and ICP-SFMS methods. The concentrations of the main elements for all the experiments are shown graphically in Figure 7.24.

The figure shows that the peat ash is richer in calcium and magnesium than the demolition wood (DW) ash, which, hold more silicon, potassium, sodium, aluminum and titanium. The ash content of DW is around 4%, i.e. an addition of 5% peat ash would approximately double the amount of incoming ash. The results show a clear trend of decreasing Si, K, Na, Al and Ti with increasing peat ash addition as expected. Similarly Ca and Mg increase with peat ash addition. No clear trends are seen between the samples for the other major elements. Differences between the samples at different temperatures (800–900 °C) are small, as are they for the samples taken during different air staging at 850 °C and 5% peat ash addition. As seen in Figure 7.25, the concentration of both lead and zinc decrease linearly with peat ash addition. The decrease corresponds fairly well with the dilution effect due to added peat ash. It was not possible to close the mass balance for lead and zinc accurately enough to determine

if there is an enrichment or depletion of these metals in the bottom ash due to peat ash addition. On the other hand, a clear trend for both lead and zinc can be seen in the samples at different temperatures with 5% peat ash addition. The concentration of both metals decrease as a function of temperature indicating higher devolatilization at higher temperatures.
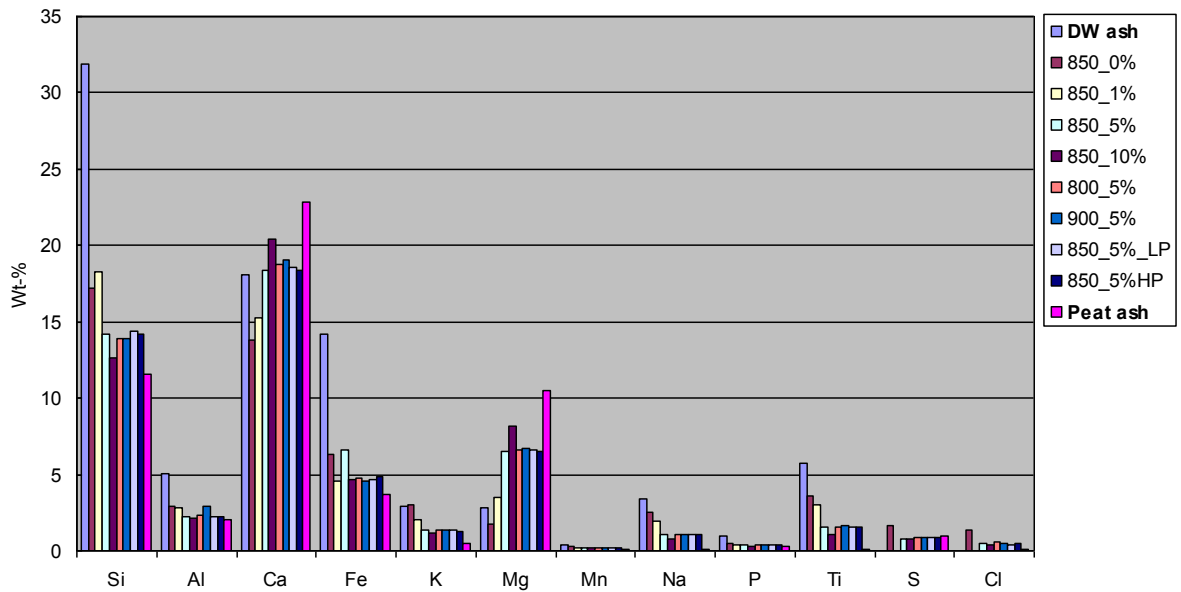
Figure 7.24 Major element composition of bottom ash samples from all experiments. In the first column the composition of the demolition wood ash and in the last column the composition of the peat ash added are given
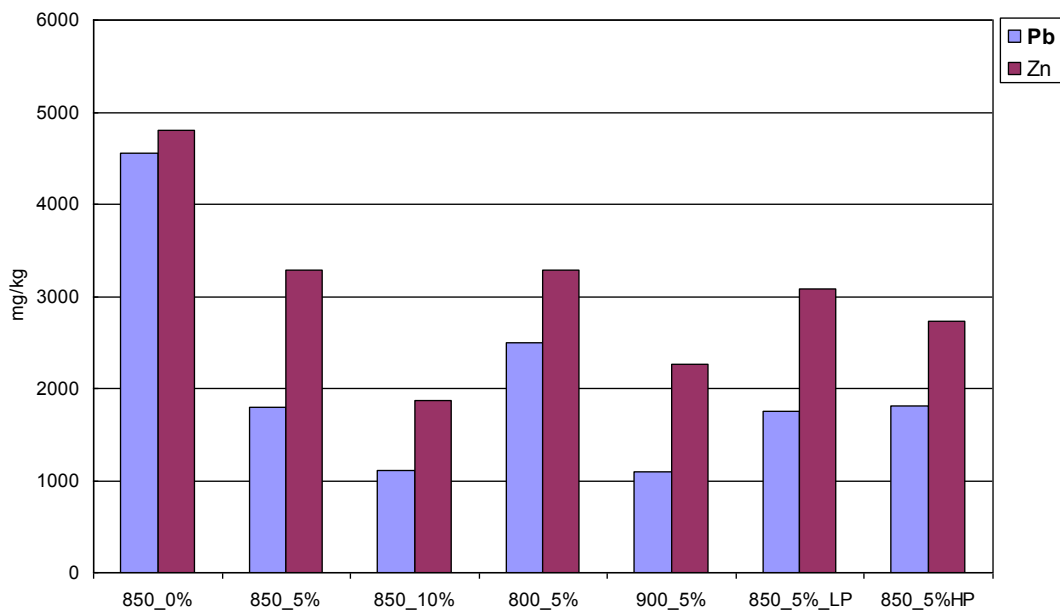
Figure 7.25 Lead and zinc concentrations in the bottom ash samples

7.4.2 Aerosol size distribution and composition

The particle size distribution in the flue gas was monitored with an ELPI for the aerosols
in the range of 0.03−10 μm. It is acknowledged by the authors that larger particles belonging to the coarse fly ash range might exist in addition to the size range discussed in this study. It is however believed that these particles are most likely found in moderate quantities because of a low probability of entrained particles. This is due to the straight reactor geometry and the extremely low flow velocity (0.03 – 0.07 m/s). The results of the particle size distribution are shown in Figures 7.26-7.28. There is not a clear trend showing how increasing addition of peat ash influences the particle size distribution (Figure 7.26).
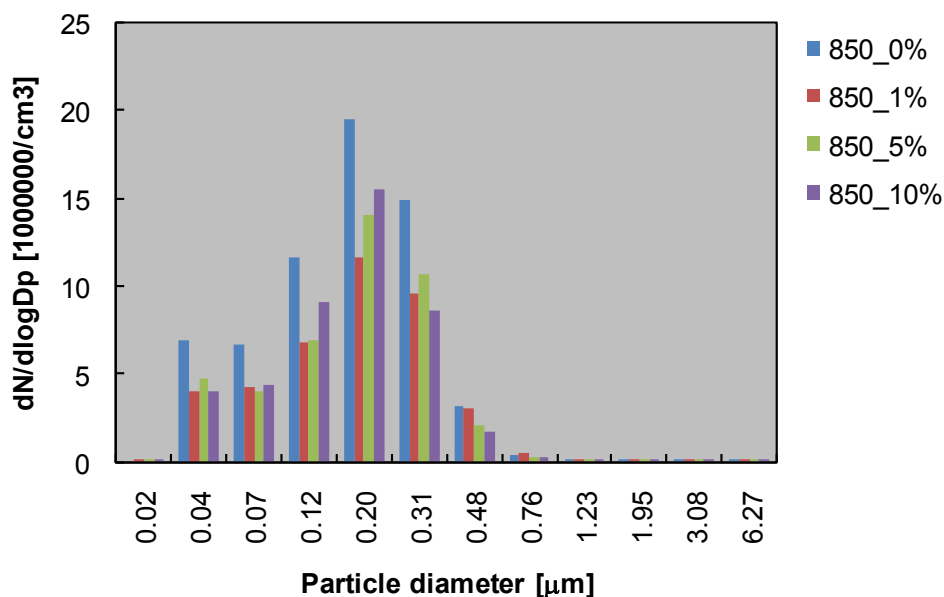
Figure 7.26 The particle size distribution in the fly ash for different peat ash additions at 850°C

In the reference sample without ash addition, the amount of smaller particles are considerably higher than in the experiments with peat ash addition, which show a slight increase of particles smaller than 0.2 with increased peat ash addition. For bigger particles a decrease in the amount of particles is seen. Higher temperatures give increased amount of all particle fractions (Figure 7.27). The load of 0.04 μm particles is exceptionally high at 900°C. For the other size fractions the amount of particles is 50-

100% higher at 900°C that at 800°C. The results indicate that a low level primary air-staging give higher particle loads, especially for smaller particles (Figure 7.28), whereas the high level air-staging seems to promote formation of particles in the range 0.3 - 1.2 μm.
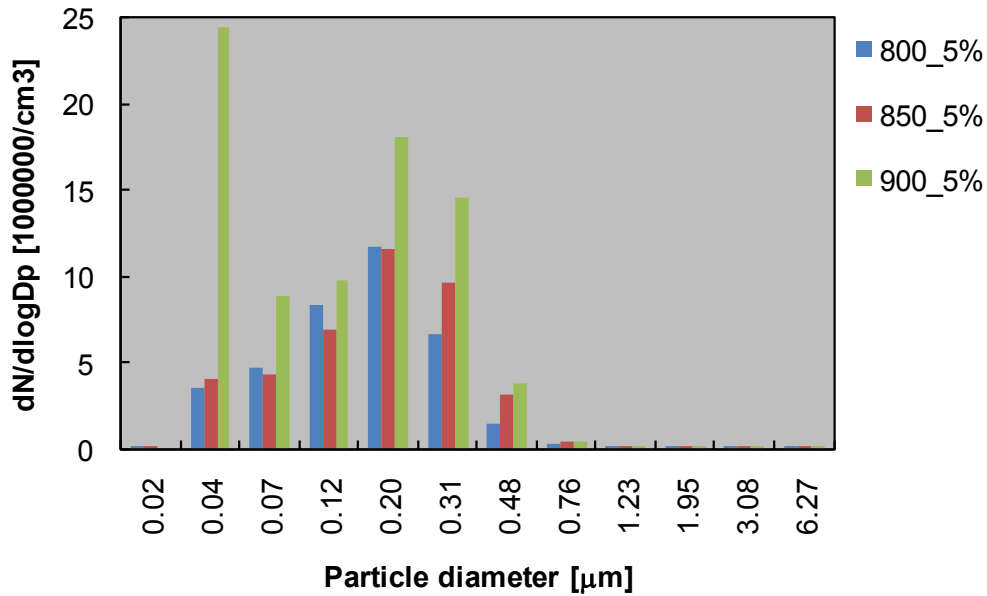
Figure 7.27 The particle size distribution in the fly ash for different reactor temperatures, 5 % peat ash addition
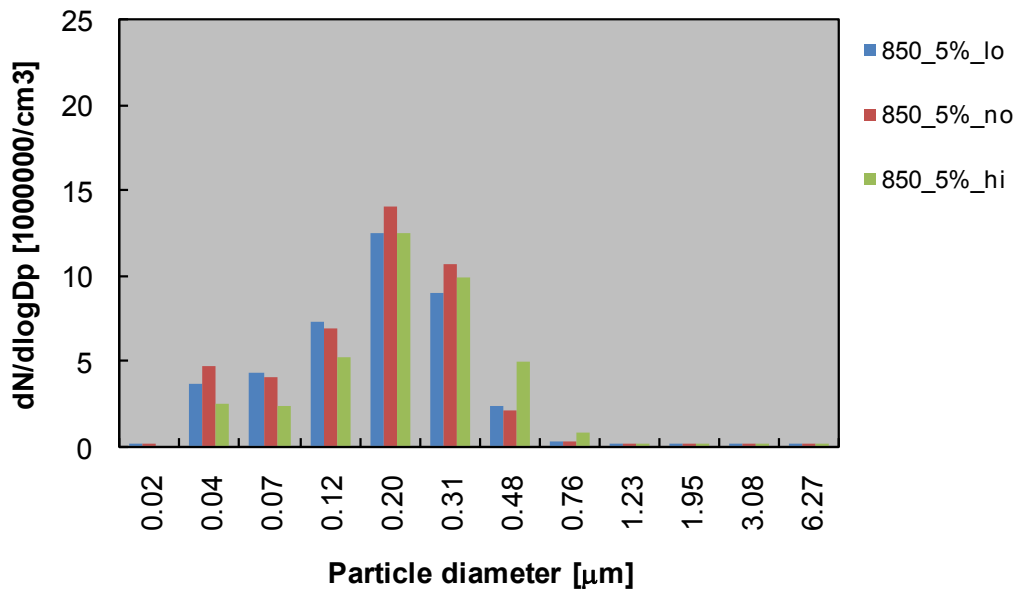
Figure 7.28 The particle size distribution in the fly ash for different primary air amounts, 850°C and 5 % peat ash addition

7.4.3 Chemical composition of particles

The composition of the salt part of the samples collected in the ELPI measurements are given in Figures 7.29–7.31. The samples are dominated by Zn and Pb. In average 50 wt.% of the oxygen-free samples (excluding carbon and aluminum) consisted of these elements. The portion of K, S, Cl and Na where in average 35 wt.%, whereas the portion of the inert oxide forming elements Si, Ca, Fe, P, Mg and Cr was 15 wt.%. P and Mg were very low in all samples. The portion of inert metals was generally higher in the bigger particle size fractions than in the smaller fractions, indicating that the compounds of these metals (oxides) originate from the original fuel ash and have not been devolatilized.

Lead and zinc are partly in oxide form, partly in salt form. The oxides are most probably ZnO and PbO. The salt part constitutes of sulfate and chloride of K, Na, Zn and Pb. For peat ash addition at 850 °C (Figure 7.29),

Figure 7.29 The chemical composition of the impactor stages 3, 5, 7 and 9 corresponding to the sizes 0.093; 0.26; 0.611; 1.59 μm of the fly ash taken by the ELPI in the exhaust of the reactor as a function of peat ash + lime addition

the salt part was richest in chloride for the reference run (50%) and decreased at peat ash addition to 20–30% chloride at 1%, and to 5–10% chloride at 5 and 10% ash addition, respectively, the latter two being very similar in composition. Potassium decreased significantly with increasing peat ash addition, being 40–50% in the reference run and 5–10% at 10% ash addition. A corresponding decrease in the Na content is not observed. Zinc increased with increasing ash addition, indicating formation of zinc sulfate. The zinc content was higher in big particles compared to smaller particles.

Lead, again, showed the opposite trend decreasing with particle size. The composition of the salt part for the different temperatures is very similar for the runs at 800 °C and 850 °C, chloride being some 20% in all samples (Figure 7.30).
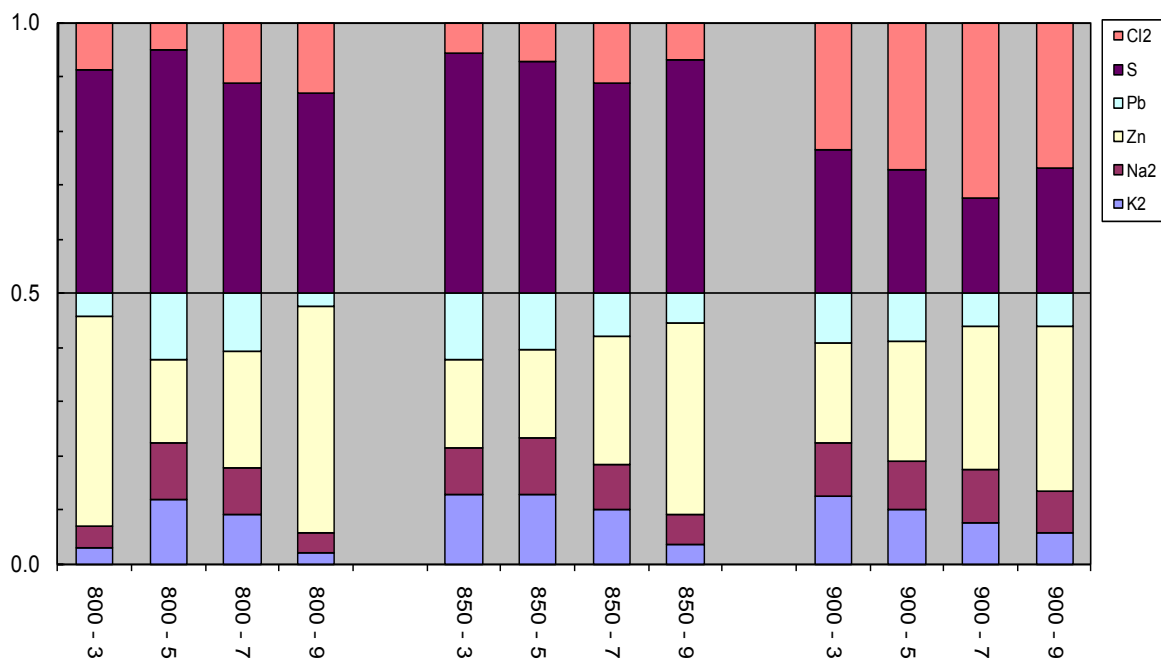
Figure 7.30 The chemical composition of the impactor stages 3, 5, 7 and 9 corresponding to the sizes 0.093; 0.26; 0.611; 1.59 μm of the fly ash taken by the ELPI in the exhaust of the reactor as a function of temperature, at 5% peat ash addition

At all three temperatures the zinc content is dominating. The concentrations of zinc (and lead) account for about 40–50% of the salts produced for the small particles (0.093 μm) and up to 90% for the larger particles (1.59 μm). It shows an increasing trend with increasing particle size. In contrast, both potassium and lead decrease with particle size while the trends in sodium content are weak. No clear trend can be seen in

203

the composition of the salt part as a function of primary air level (Figure 7.31). Low and normal primary air are very similar. They have a chloride content of 10–20% and show all an increase of zinc and decrease of potassium and lead with increasing particle size. The high primary air sample has slightly higher chloride content (20–40%) for all size fractions. To sum up, lower alkali chloride concentrations could have an inhibiting effect on corrosion, but high Zn and especially Pb concentrations may lead to a lower first melting point of the aerosol particles. This, again, may promote deposition on heat transfer surfaces in the flue gas channel.
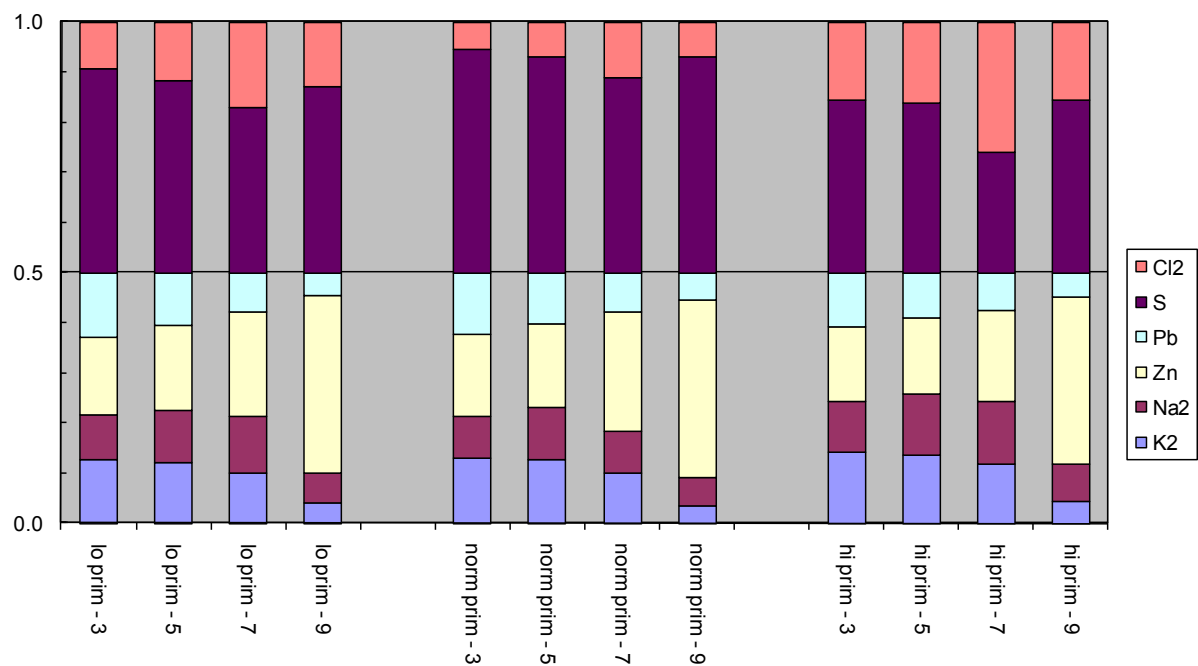
Figure 7.31 The chemical composition of the impactor stages 3, 5, 7 and 9 corresponding to the sizes 0.093; 0.26; 0.611; 1.59 μm of the fly ash taken by the ELPI in the exhaust of the reactor as function of different air distribution between primary and secondary stages (lo prim/hi prim; low/high primary air amounts compared to the reference experiment), at 5% peat ash addition

7.4.4 The fate of chlorine and sulfur

The chlorine distribution between the bottom ash and the gas phase relative to the chlorine input in the fuel is shown in Figure 7.32. Note that bottom ash analysis could not be made for the sample with 1% peat ash addition. The figure does not include the chlorine in the fly ash because not all of the impactor stages were chemically analyzed. However, the chlorine in the fly ash is assumed to have a minor influence on the total mass balance due to the relatively small amounts of fly ash compared to bottom ash. It can be noticed that the chlorine distribution is somewhat unbalanced probably due to uncertainties in the chemical analysis of the raw fuel, the bottom ash and measurements in the gas phase.
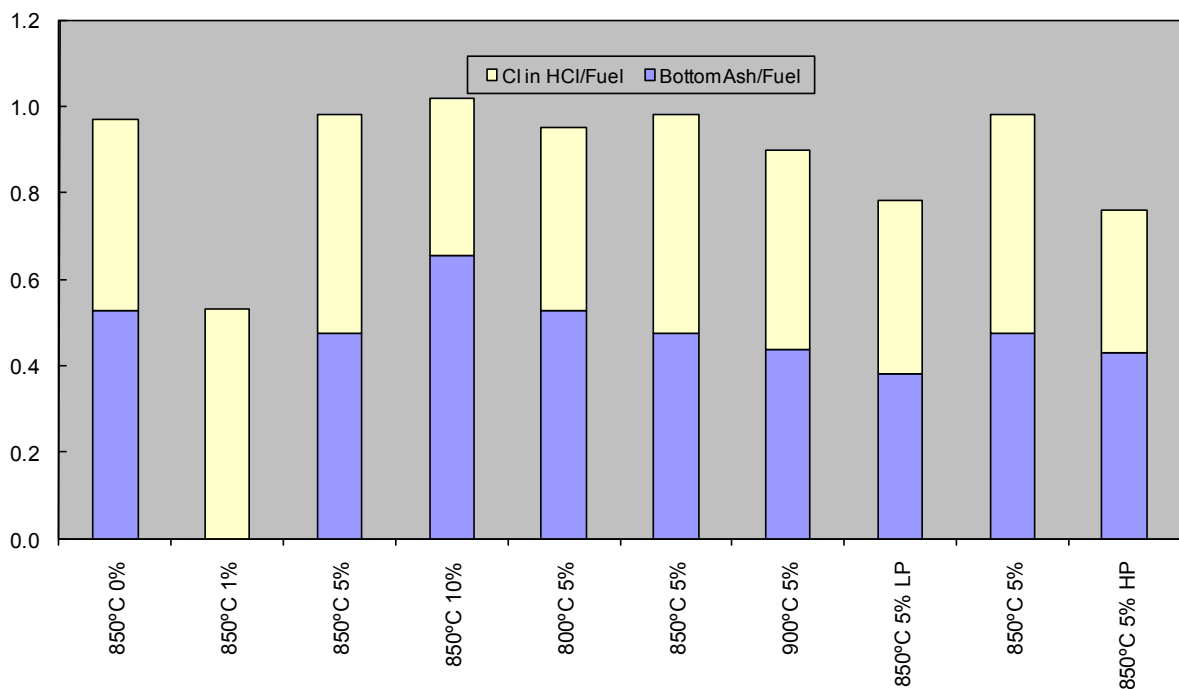
Figure 7.32 Distribution of chlorine between gas phase (as measured HCl) and bottom ash.

However, some interesting trends can be extracted from the results. Generally, the portion of chlorine in the bottom ash is 40–50% of total chlorine. This is a high value, which may be due to the relatively high amount of unburned char in the bottom ash samples. It is expected based on thermodynamic considerations and experience that

the chlorine is in the form of alkali chlorides in completely burned ash fractions. Some chlorine can probably dissolve into molten silicates but the amount of this is expected to be low compared to alkali chlorides. The chlorine in the bottom ash seems to increase with increased peat ash addition.

Comparing the 5% and 10% additions at 850 °C, show considerably higher Cl in the bottom ash at 10% addition. This indicates that the retention of Cl is strongly affected by the presence of peat ash in the fuel pellet. The calcium content of the peat ash used is rather high, which could promote $CaCl_2$ formation, but taking into consideration the high sulfur content in the bottom ash, the stable form of calcium not bound to silicate, should be calcium sulfate. The peat ash seems to be facilitating chlorine mobility at higher temperatures. A slight trend in seen for the different reactor temperatures with less chlorine in the bottom ash at higher temperatures, However, a clear corresponding increase of HCl is not seen in these samples. No clear trends on the Cl-distribution of different air-staging could be detected.

The distribution of sulfur between bottom ash and SO_2 in the gas is shown in Figure 7.33.
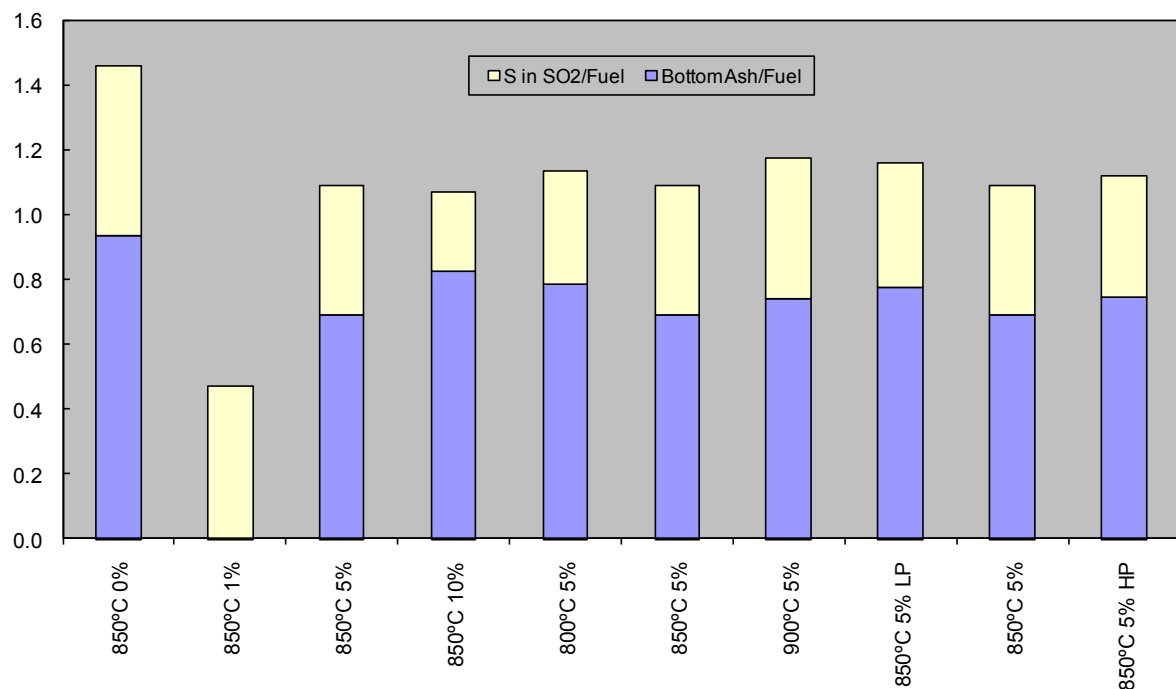
Figure 7.33 Distribution of sulfur between gas phase (as measured SO2) and bottom ash

The ratios for sulfur in gas to total sulfur and the ratio in bottom ash to total sulfur are rather near to unity, indicating that the mass balance for sulfur is fairly well

closed based on these two fractions. Thus, the amount of sulfur of the fly ash is small compared to the total amount. Some 60–80% of the total sulfur is found in the bottom ash for all samples. No clear trends can be detected between the different running conditions indicating that the sulfur chemistry for the demolition wood is not significantly affected by the ash addition. This could be expected due to the rather low sulfur content in the peat ash used.

7.5 The effect of kaolin on the combustion of demolition wood

Kaolin was chosen as the additive to demolition wood in order to study in detail its effectiveness in capturing the alkalis from the gas phase. All experiments in this work were carried out with demolition wood and demolition wood with kaolin employing staged air combustion and isothermal conditions. The results of both the proximate and ultimate analysis for demolition wood are already presented in Table 7.7, while the element composition of the ash for the different fuel mixtures is presented in Table 7.9.

The total excess air ratio was about 1.6, and the primary air stoichiometry was about 0.8 for most of the experiments but was also varied in order to study the effect on the volatility of chlorine and other alkali compounds of a lean O_2 condition in the primary zone. The reference experiment was run first at a reactor temperature of 850 °C and with no addition of kaolin. Three other experiments were run under the same conditions with the exception of the kaolin addition of 1, 5 and 10% of weight, respectively, to the demolition wood. Another two were run with 5% of kaolin addition but with different reactor temperatures of 800 and 900 °C. Finally two experiments were performed with lower (marked as LP) and higher (HP) air supply to the primary zone in comparison with the reference experiment. The secondary air combustion was changed, respectively, in order to obtain a total air excess ratio of 1.6. The feeding frequency was set to ensure a feeding rate of 400 g/h.

Table 7.9 Chemical composition (dry basis) of the ash of demolition wood and the generated mixtures

Kaolin %	0	1	5	10
Ash content [%]	3.9	4.3	7.9	11.7
Si [%]	1.2	1.7	3.7	5.5
Al [%]	0.2	0.7	1.9	3.2
Ca [%]	0.7	0.7	0.7	0.7
Fe [%]	0.5	0.3	0.5	0.5
K [%]	0.1	0.1	0.2	0.2
Mg [%]	0.1	0.1	0.1	0.1
Mn [%]	0.01	0.01	0.01	0.01
Na [%]	0.1	0.1	0.1	0.1
P [%]	0.04	0.04	0.04	0.04
Ti [%]	0.2	0.2	0.3	0.3
As [mg/kg]	4	4	10	3
Ba [mg/kg]	319	332	285	336
Be [mg/kg]	0.04	0.20	0.69	1.25
Cd [mg/kg]	1.31	0.78	1.22	0.88
Co [mg/kg]	1.36	1.20	1.37	1.86
Cr [mg/kg]	59	33	39	56
Cu [mg/kg]	166	358	40	81
Mo [mg/kg]	0.89	0.70	0.67	0.94
Nb [mg/kg]	0.60	0.90	2.47	3.38
Ni [mg/kg]	2.7	13.0	2.0	17
Pb [mg/kg]	426	233	361	415
Sc [mg/kg]	0.11	0.14	0.35	0.57
Sn [mg/kg]	1.89	1.81	1.76	2.20
Sr [mg/kg]	25	26	26	28
V [mg/kg]	1.57	1.93	3.35	4.86
W [mg/kg]	12	21	11	55
Y [mg/kg]	0.49	0.63	1.36	2.15
Zn [mg/kg]	679	1030	333	908
Zr [mg/kg]	9	10	16	20

7.5.1 Bottom ash analysis

The concentrations of the most important elements for all the experiments are shown graphically in Figure 7.34. The increase of silicon and aluminum due to increased kaolin content is noticeable in the bottom ash. The potassium and chlorine also decrease as kaolin increases, although from this figure alone it is difficult to conclude whether this is due to chemical reactions or a dilution effect.

The average values of the four characteristic ash fusion temperature for the bottom ash are showed in Figure 7.35. With the exception of the experiment with 10% kaolin, all the different temperature characteristics seemed to increase with increasing kaolin share in the bottom ash. Increasing kaolin share also resulted in greater scatter among the different characteristics. Some irregular tendencies were also found, mostly for the initial deformation temperature and to some extent for the soften temperature. These two ash temperature characteristics were the most difficult to determine by visual observation. The results of these temperatures could vary by a 100 °C depending on the person interpreting the deformation of ash cube pellets.
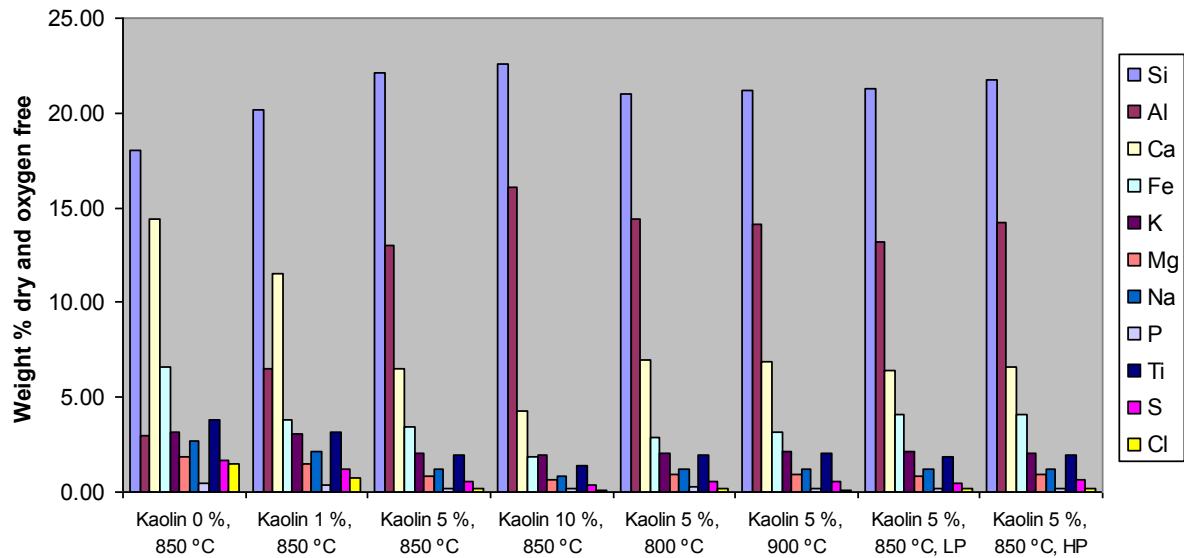
Figure 7.34 Major composition of bottom ash from all experiments of Si, Al, Ca, Fe, K, Mg, Na, P, Ti, S, and Cl using ICP-AES, recalculated on dry ash. Oxygen not included in the analysis.
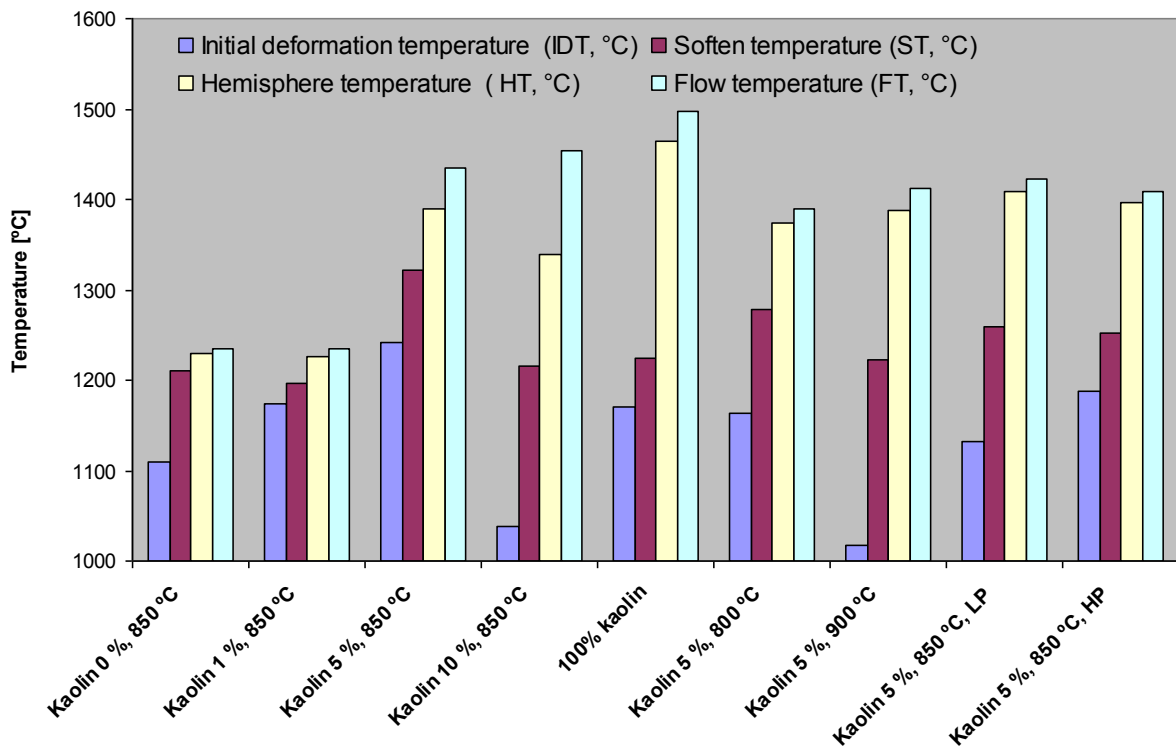
Figure 7.35 The bottom ash fusion temperature

7.5.2 Aerosol size distribution

The particle size distribution in the flue gas was monitored with an ELPI for the aerosols in the range of 0.03−10 μm. Larger particles belonging to the coarse fly ash range might exist in addition to the size range discussed in this study. It is however believed that these particles are most likely found in moderate quantities because of a low probability of entrained particles. This is due to the straight reactor geometry and the extremely low flow velocity (0.03 – 0.07 m/s). The results of the particle size distribution are shown in Figures 7.36, 7.37 and 7.38.

In general, it can conclude that the addition of kaolin to demolition wood is decreasing the particle load in the flue gas (Figure 7.36). This holds true for all the particle size ranges with the exception of the range 0.07 – 0.12 μm for which the trends are more or less constant. Compared to the work performed in [192] on oat grain in a residential boiler with a kaolin addition of 2 and 4 %, the particle size distribution range and shape is quite similar to the ones shown in this study. The only exception is a higher particle load for the smallest particles for experiments with kaolin. This difference could

210

be attributed to totally different reactor geometry and air flow pattern between the two reactors. The reactor temperature influence on the fly ash load in the flue gas can be studied in Figure 7.37. For particles smaller than 0.2 μm the particle load is highest for a reactor temperature of 850 ºC. For higher particle sizes, increasing temperature is giving increased particle load. The same trends can also be found for the experiment with different primary air conditions (Figure 7.38). For particles smaller than 0.31 μm, the highest particle load is obtained for air excess ratio of 0.8 after the primary zone (the middle series). The particle load for larger particles is increasing with increased combustion air through the primary zone.
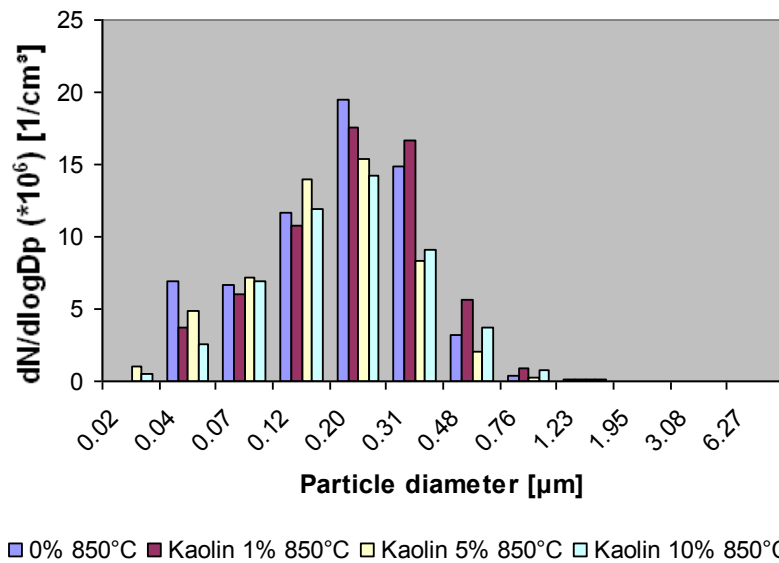
Figure 7.36 The particle size distribution of the fly ash for increasing kaolin addition
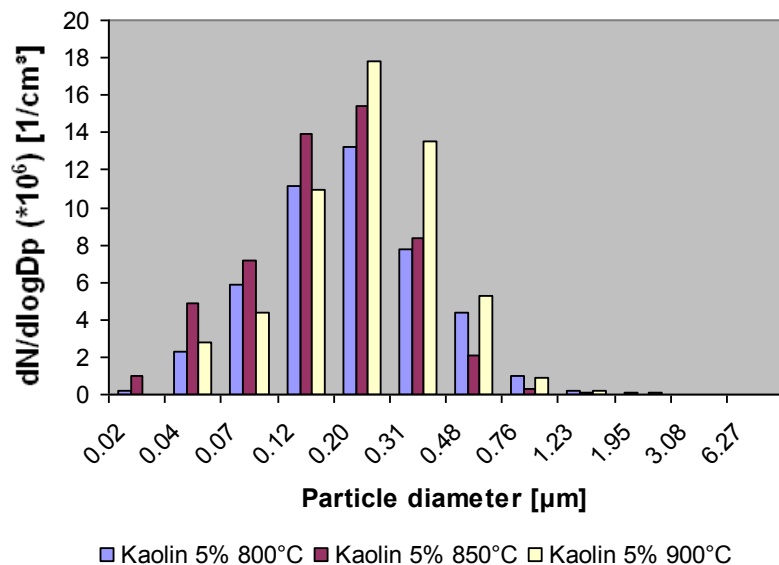
Figure 7.37 The particle size distribution of the fly ash for different reactor temperatures

211
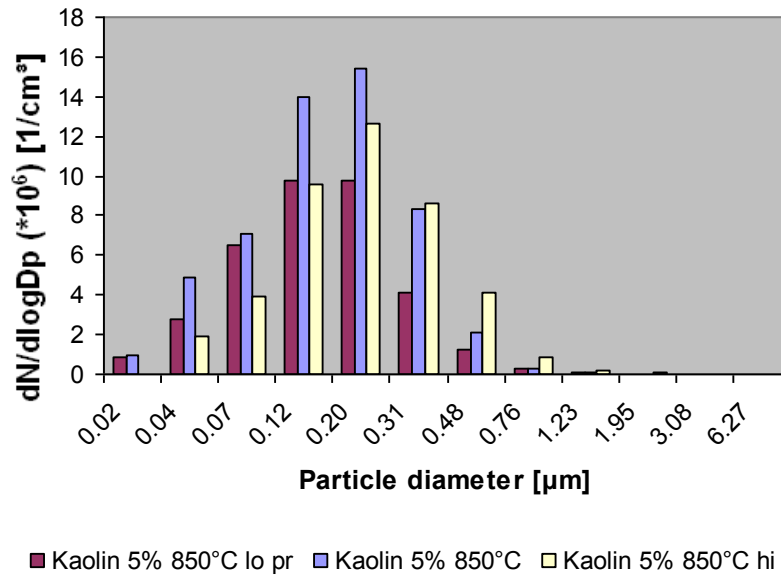
Figure 7.38 The particle size distribution of the fly ash for different primary air amounts

7.5.3 Aerosol composition

The main components in the analyzed particles were K, S, Cl and Na. In average 50 wt-% of the oxygen-free samples (excluding carbon and aluminium) consisted of these elements. Zn and lead constituted on average 35 wt-% whereas the portion of the inert oxide forming elements Si, Ca, Fe, P, Mg and Cr was 15 wt-%. P and Mg were very low in all samples. The portion of inert metals were generally higher in the bigger particle size fractions than in the smaller fractions, indicating that the compounds of these metals (oxides) originate from the original fuel ash and have not been devolatilized. Lead and zinc are partly in oxide form, partly in salt form. The oxides are most probably ZnO and PbO. The salt part constitutes of sulfate and chloride of K, Na, Zn and Pb and calculated from the elemental composition according to the following assumptions: (i) potassium and sodium are as chlorides or sulfates; (ii) silicon, calcium, iron, magnesium and chromium are as oxides; (iii) zinc and lead can be both as oxides and/or chlorides and sulfates. Only the salt formation in the aerosols is shown in Figures 3.39, 3.40 and 3.41.

For kaolin addition at 850 ºC (Figure 7.39), the salt part was richer in chloride for the reference run and at 1 % kaolin addition (30-40 % as chloride) than for the runs with higher kaolin addition (5-10 % chloride), the rest being sulfate. There is no big differences between smaller (0.1 μm) and bigger (1.6 μm) particles. The ratio between

212

sodium and potassium is rather constant (1:2). However, in the reference sample the portion of potassium decreases with increasing particle size and zinc increases. A similar trend can be observed in the samples with 5 % and 10 % kaolin addition. Pb decreases slightly with increasing particle size.
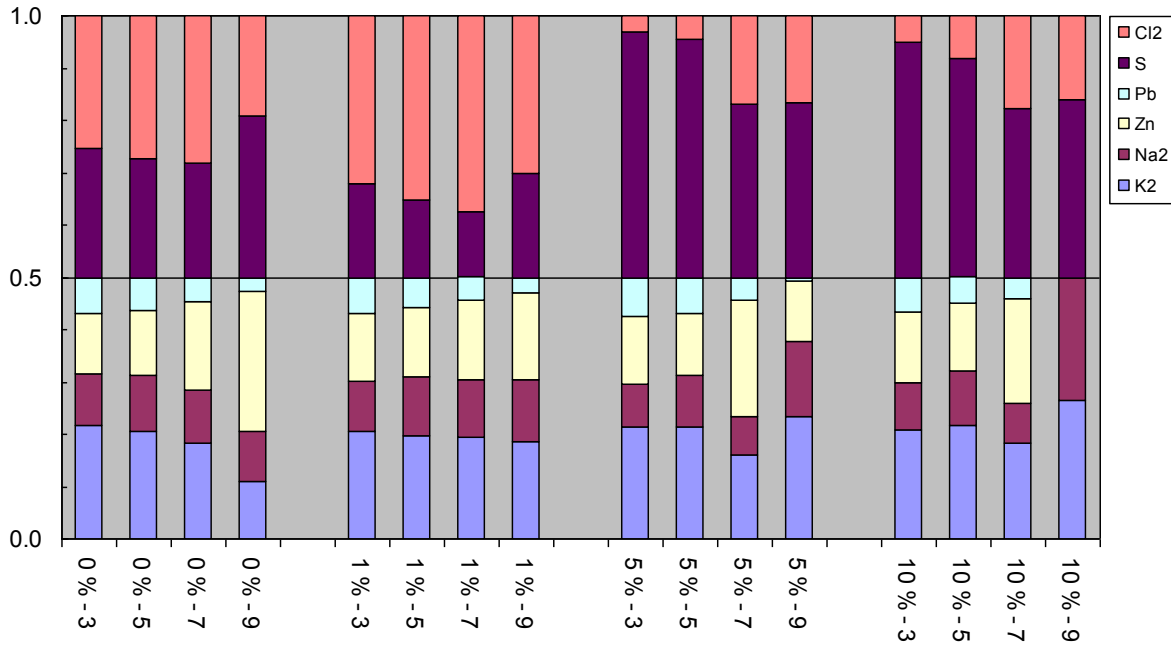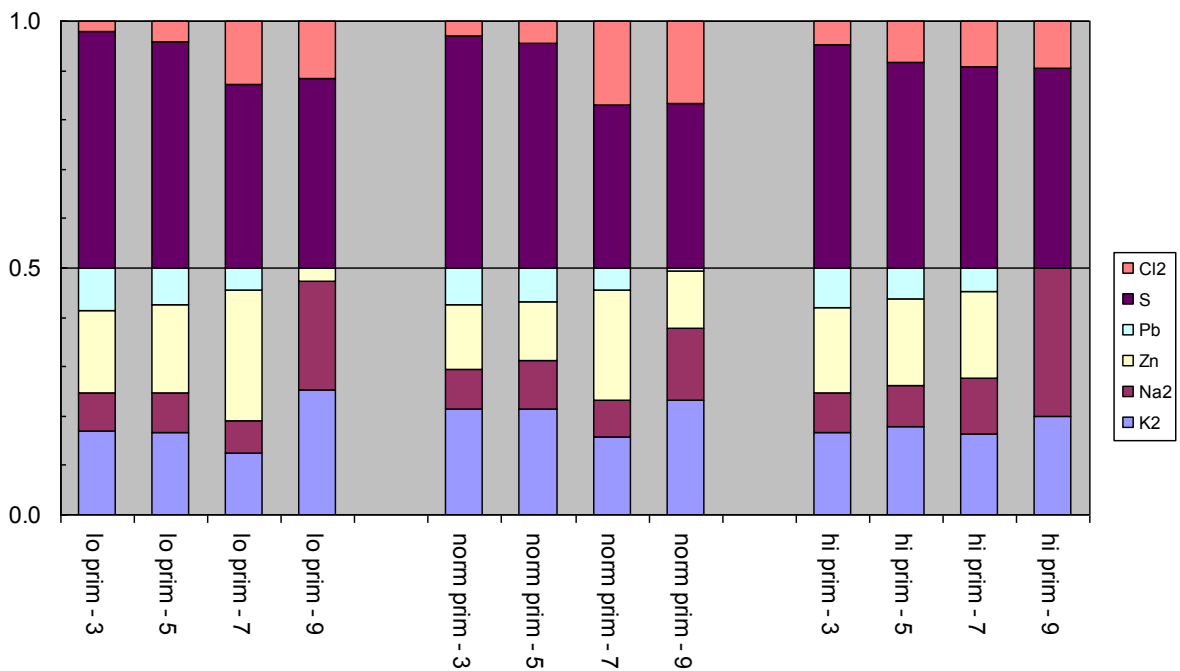

Figure 7.39 The chemical composition impactor stages 3, 5, 7 and 9 corresponding to the sizes 0.093; 0.26; 0.611; 1.59 µm of the fly ash taken by the ELPI in the exhaust of the reactor as a function of kaolin addition

For the temperature effect at 5 % kaolin addition (Figure 7.40), the portion of chloride is higher at 900 ºC (20 – 50 %) than at 800 ºC and 850 ºC (10 – 20 %). A slight decrease in both Zn and Pb is observed with increasing particle size. The results indicate that the smaller particles have less chloride than the larger ones.

For primary air variations (Figure 3.41), no clear trends can be seen in the composition of the salt part as a function of primary air level. Low and normal primary air are very similar. They have a chloride content of 5 – 10 % and show a slight increase of zinc and decrease of lead with increasing particle size. The high primary air sample has constant chloride content (10 %) for all size fractions.
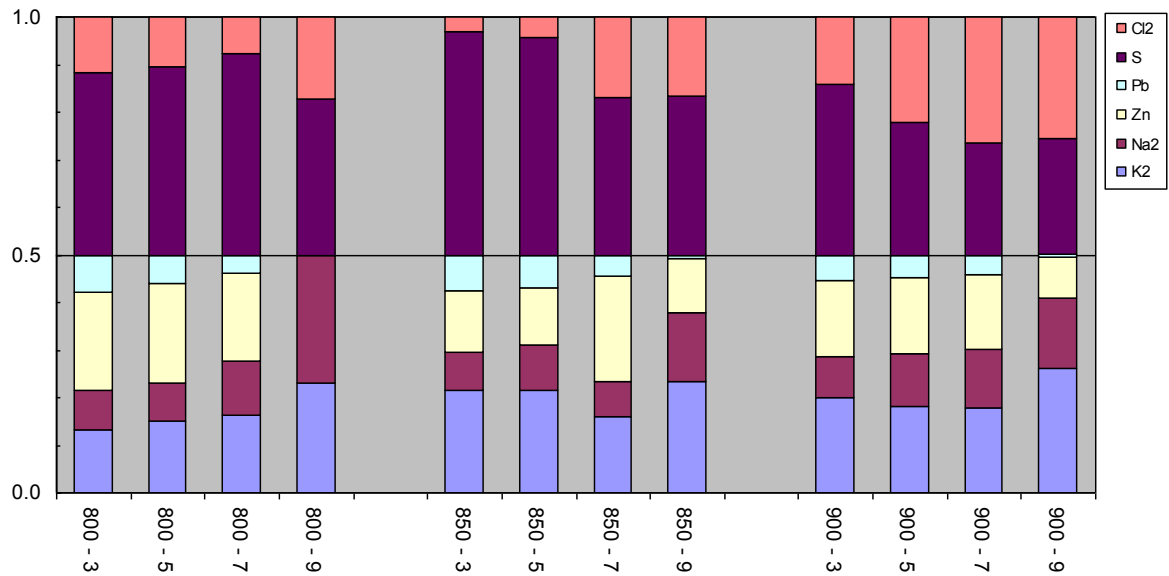
Figure 7.40 The chemical composition impactor stages 3, 5, 7 and 9 corresponding to the sizes 0.093; 0.26; 0.611; 1.59 μm of the fly ash taken by the ELPI in the exhaust of the reactor as a function of temperature

Figure 7.41 The chemical composition impactor stages 3, 5, 7 and 9 corresponding to the sizes 0.093; 0.26; 0.611; 1.59 μm of the fly ash taken by the ELPI in the exhaust of the reactor as a function of different air distribution between primary and secondary stages.

7.5.4 The fate of chlorine

      The chlorine distribution among the bottom ash phase and the gas phase relative to the chlorine input in the fuel is shown in Figure 7.42. This figure does not include the chlorine part found in the fly ash because not all of the impactor stages were chemically analyzed. However, the chlorine part belonging to the fly ash is assumed to have a minor influence on the total mass balance due to the relatively small amounts of fly ash compared to bottom ash.
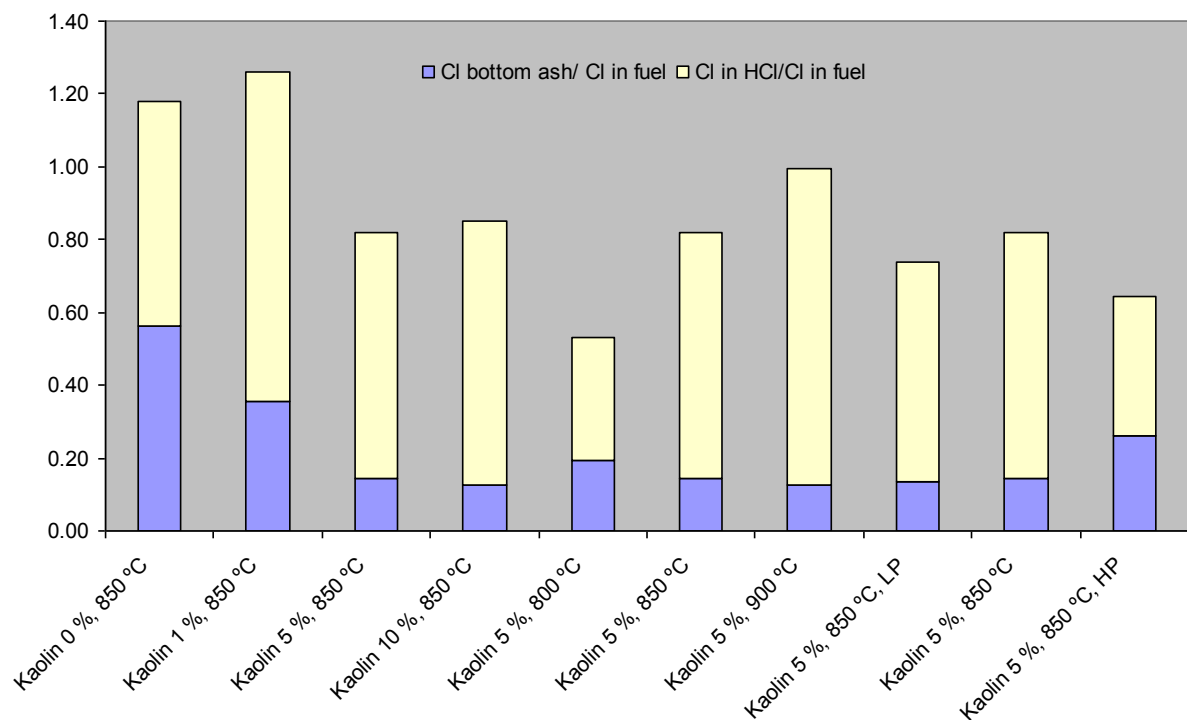
Figure 7.42 Distribution of chlorine between gas phase (as measured HCl) and bottom ash.

      From Figure 7.42 it can been seen that the chlorine distribution is somewhat unbalanced due to uncertainties in the chemical analysis of the raw fuel, the bottom ash and measurements in the gas phase. Nevertheless, the figure gives important information about trends that influence the chlorine distribution as a function of increased kaolin, temperature, and combustion air distribution. The chlorine in the bottom ash is decreasing with increased kaolin amounts and reactor temperature. Leaner conditions in the primary zone seem also to decrease the chlorine content in the bottom

215

ash. The kaolin seems to be facilitating the chlorine mobility although this is not detected as increased amounts in the gas phase throughout the entire range of the kaolin addition. The trends are clearer for the different reactor temperatures where less chlorine in the bottom ash, due to increased temperature, is translated into more HCl release.

As it has been described earlier (equations (5.73) and (5.74)), the effect of kaolin on abating the chlorine release in the fly ash is done by capturing the potassium and sodium in the bottom ash. This should translate into increased potassium and sodium for increased amounts of the additive in the raw fuel. However this is not the case as a similar mass balance as for chlorine shows that the ratios for K and Na (bottom ash to input fuel) are close to unity for all experiments.

8. CONCLUSION

In order to observe the most problematic products of biomass combustion and possibilities for their reduction very complex research work has been done within this PhD thesis.

Combustion experiments were performed in a multi-fuel reactor with continuous feed of pellets by applying staged air combustion. The gas phase was monitored with several gas analyzers both in the primary zone and in the stack. Complete characterization of the raw fuel and the bottom ash was performed for all the experiments. The fly ash particle size distribution was monitored and in addition a chemical analysis of the fly ash from four impactor stages was performed. The experimental set-up with its advanced monitoring and control systems as well as the online and offline analytical methods gives a very accurate picture of the thermal process and all its products.

Presented results, achieved within work on this PhD thesis, are grouped in five topics, aiming that whole research work with its results could be observed in the clearest way. Conclusion is organized in same manner.

(I)

NOx, and N_2O, emissions have been investigated for different biomass fuels and fuel mixtures thereof as pellets both with and without air staging at a constant reactor set point temperature of 850 °C. The fuels investigated are wood, demolition wood, and coffee waste, and selected mixtures of these. Based on analissies of achieved results the next conclusions could be unederlined:

- A large NOx reduction potential, up to 91% and corresponding to less than 20 ppm NOx at 11% O_2 for a fuel containing about 3 wt.% fuel-N, using air staging was found at the optimum primary excess air ratio.
- The effect on N_2O, however, is adverse at the selected set point temperature and optimum primary excess air ratio for NOx reduction, with an increase in the N_2O emission level of up to 635%.

- The NOx emission level increases with increasing fuel-N content, while the conversion factor for fuel-N to NOx decreases with increasing fuel-N content.
- Fuel mixing has a positive influence on the NOx emission level, but a negative influence on the overall conversion factor for fuel-N to NOx and N_2O.

(II)

Temperature range of 850-1000 °C is applied both for staged air combustion and nonstaged combustion of biomass to investigate the effects of these parameters on the emission levels of NOx, N_2O, CO, hydrocarbons (CxHy) and different other components.

From the experimental studies carried out in the present work, using demolition wood pellets as fuel, the following conclusions can be drawn:

- The primary excess air ratio is the most important parameter which can be optimized for maximum conversion of fuel-N to N_2, hence reducing the NOx level.
- The effect of two stage combustion of biomass is significant for reduction of NOx emission levels. Staged air combustion, in this case, can reduce the emission level by 50-75% and even up to 85% at the optimum conditions.
- The maximum NOx reduction happens when the primary air is injected at a primary excess air ratio of 0.8-0.95 and the total excess air ratio is 1.6-1.9 for staged air combustion.
- The experiments show that also the total excess air ratio has an important effect on the NOx emission.
- The N_2O level has an inverse effect for staged air combustion, i.e., increasing for staged air combustion.
- The average N_2O level increase for the different temperatures is 75-1660% but with a low amount of N_2O at high temperatures.
- The experimental results show that the NOx emission level is not affected significantly by temperature neither in nonstaged or staged air combustion when temperatures are kept below 1000 °C in the reactor.

- Yet, the effect of temperature on the N_2O level is considerable. This study shows, as expected, that at high temperatures, N_2O emissions almost disappear.The results point to that the effects of temperature and staged air combustion are counteractive for N_2O, meaning a negative influence on N_2O for staged air combustion and a desirable N_2O reduction effect with increasing temperature. Therefore to minimize N_2O emissions and reduce emissions of unburnt, temperatures of above 900 °C are beneficial.

- Hydrocarbons emission, CxHy, is almost independent of the combustion condition whether it is staged air combustion or nonstaged combustion. In both cases, the emission levels of hydrocarbons are below 4 ppm at 11% O_2 in dry flue gas.

- CO emissions increase for staged air combustion compared to nonstaged combustion by a factor of about 1.5 at a given temperature. Increasing temperature decreases the CO emission level in the whole temperature range of 850-1000 °C.

(III)

The fate of selected ash elements are investigated for three biomasses (wood, demolition wood and coffee waste) and six mixtures of these as pellets both with and without air staging. Data is collected about: flue gas composition, fly ash size distribution and composition, bottom ash composition and melting properties. A very large quantity of data is presented and discussed. The main overall findings are:

- Experimental results (see the effect of staging on Na and K in bottom ash) indicate that complex interactions are taking place between the mixed fuels;

- The same ash-forming element may react differently to staging and/or mixing in different fuels, indicating the importance of the mode of the overall structure of the fuel;

- Several results infer that pelletisation, by bringing chemical elements into more intimate contact than in loose biomass, affects their overall chemistry (partitioning and speciation);

- Staging and mixing might simultaneously have positive and negative effects;
- Staging affects the governing mechanisms of fly ash (aerosols) formation.

The central practical implications of the aforementioned findings may be summarized as such:

- Mixing of different biomass may be an efficient method to affect the overall chemistry of specific chemical elements and therewith operational challenges such as fouling, deposition or slagging;
- Pelletisation may enhance the chemical effects of mixing;
- Staging, by influencing aerosols formation, may be a promising way of reducing the problems associated with them, especially corrosion.

(IV)

Experiments were made to understand how an addition of peat ash affects the composition of ash fractions and gas in combustion of demolition wood with variations in reactor temperature, combustion air distribution and amount of peat ash addition. The following conclusions were made base on the interpretations of the measured data:

- The bottom ash composition changed as peat ash was added. Enrichment of the main elements more abundant in the peat ash (Ca and Mg) was observed indicating that the added ash generally followed the bottom ash.
- Zinc and lead which originate from the demolition wood showed the same behavior, i.e. their concentration in the bottom ash decreased with peat ash addition. As a function of temperature Zn and Pb decrease in the bottom ash indicating more extensive mobility of these metals at higher temperatures. 60–80% of the total sulfur and 40–50% of the total chlorine retain in the bottom ash.
- A method was developed to estimate the composition and speciation of the salt part of fly ash samples based on SEM/EDX analysis. The results show that the concentrations of zinc and lead are very high in the fly ash samples. A considerable part of these metals are chemically bound to chlorides and sulfates together with potassium and sodium indicating extensive volatilization of both zinc and lead.

- Potassium volatilization decreased with peat ash addition, which may be due to reactions between peat ash and alkali. The zinc content was higher in big particles (0.4–1.3 μm) compared to smaller particles. Lead, again, showed the opposite trend decreasing with particle size.

- Although it was not possible to determine quantitatively the effect of peat addition, the experiments show that the inorganic reactions are influenced in several ways. Potassium, zinc and lead are the metals most affected. Probably an absorption effect of potassium gives rise to higher concentrations of zinc and lead in the aerosols. Simultaneously the chloride content in the aerosols decreases with increased peat ash addition.

(V)

An experimental attempt was made to understand the behavior of the corrosive chlorine compounds for variations in reactor temperature, combustion air distribution and kaolin addition.

- Kaolin was found to facilitate the mobility of chlorine by decreasing its concentration in the bottom ash by 37, 74 and 78%, respectively, for 1, 5, and 10% kaolin addition.

- The fly ash particle size distribution was also monitored and in addition a chemical analysis of the fly ash from four impactor stages was performed.

- Kaolin was found to be effective at reducing the chlorine concentration in the fly ash. The optimal addition was 5% and a further increase to 10% did not result in a noticeable chlorine reduction (Figure 7.39). The addition of 5% has almost eliminated the chlorine content for the impactor stages 3 and 5. For fuels with high chlorine content, one can conclude that an addition of 5% kaolin could lead to reduced corrosion potential due to a significant reduction of chlorine in the fly ash.

- The effect of reactor temperature was not clear in terms of the chlorine content in the fly ash (Figure 7.40). This is probably because the reactor temperature does not influence the temperature close to the combusting fuel greatly. On the other hand, leaner air conditions in the primary stage, which should mean lower

temperature in the reacting region between the solid and the gas phase, resulted in decreased chlorine content in the fly ash (Figure 7.41).

- The addition of kaolin clearly changed the composition of the bottom ash as well. The chlorine content in the bottom ash decreased as kaolin increased (Figure 7.42).

- Kaolin also influenced the melting behaviour of the bottom ash as can be seen in Figure 7.35 in which the fusion temperature characteristics increased with increased addition of kaolin.

9. REFERENCES

[1]   Davide A. Coley, Energy and climate change: creating a sustainable future, John Wiley & Sons Ltd, 2008.

[2]   Ralph E H Sims, The Brilliance of Bioenergy In Business and in Practice, James & James (Science Publishers) Ltd, 2002.

[3]   Sjaak van Loo and Jaap Koppejan, The Handbook of Biomass Combustion and Co-firing, Earthscan, 2008.

[4]   Dragoslava Stojiljković, Perspective use of biomass and municipal solid waste, Scientific Meeting Energy and Environment, pp. 325-345., Serbian Academy of Science and Arts, 2013.

[5]   Paul O'Connor, A General Introduction to Biomass Utilization Possibilities, BIOeCON BV and ANTECY BV, Hoevelaken, The Netherlands, 2013

[6]   Carlo N. Hamelinck_, Roald A.A. Suurs, Andre´ P.C. Faaij, International bioenergy transport costs and energy balance, Biomass and Bioenergy 29 (2005) 114–134

[7]   M. Fatih Demirbas , Mustafa Balat, Havva Balat, Potential contribution of biomass to the sustainable energy development, Energy Conversion and Management 50 (2009) 1746–1760

[8]   World Energy Resources 2013 Survey, World Energy Council, 2013.

[9]   Patrick Moriarty, Damon Honnery, What is the global potential for renewable energy?, Renewable and Sustainable Energy Reviews 16 (2012) 244– 252

[10]   Technology Roadmap Bioenergy for Heat and Power, International Energy Agency – IEA, 2012

[11]   2010 Survey of Energy Resources, World Energy Council, 2010.

[12]   Melisa Pollak, Bryn Meyer, Elizabeth Wilson, Reducing greenhouse gas emissions: Lessons from state climate action plans, Energy Policy 39 (2011) 5429–5439

[13]   RENEWABLES GLOBAL FUTURES REPORT 2013, REN21 Secretariat, Paris, France, 2013

[14]   Bengt Hillring, The impact of legislation and policy instruments on the utilisation of wood fuels, Ecological Engineering 16 (2000) S17–S23

[15]   BIOMASS   CO-FIRING   -   AN   EFFICIENT   WAY   TO   REDUCE
         GREENHOUSE GAS EMISSIONS, EUBIONET - European Bioenergy
         Networks, Finland, March 2003.

[16]   BioEnergy status Document 2010, NL Agency, NL Energy and Climate change,
         2011.

[17]   DIRECTIVE 2003/30/EC on the promotion of the use of biofuels or other
         renewable fuels for transport

[18]   Energy Roadmap 2050,IEP

[19]   Energy 2020 A strategy for competitive, sustainable and secure energy

[20]   John Ruane , Andrea Sonnino, Astrid Agostini, Bioenergy and the potential
         contribution of agricultural biotechnologies in developing countries, Biomass
         and Bioenergy 34 (2010) 1427-1439

[21]   Ayse Hilal Demirbas, Imren Demirbas, Importance of rural bioenergy for
         developing countries, Energy Conversion and Management 48 (2007) 2386–
         2398

[22]   BIOENERGY – A SUSTAINABLE AND RELIABLE ENERGY SOURCE
         A review of status and prospects, IEA BIOENERGY: ExCo: 2009:06.

[23]   Matti Parikka, Global biomass fuel resources, Biomass and Bioenergy 27 (2004)
         613–620

[24]   Surya Bahadur Magar, Paavo Pelkonen, Liisa Tahvanainen, Ritva Toivonen,
         Anne Toppinen, Growing trade of bioenergy in the EU: Public acceptability,
         policy harmonization, European standards and certification needs, Biomass and
         Bioenergy 35 (2011) 3318-3327

[25]   J. Heinim, M. Junginger, Production and trading of biomass for energy – An
         overview of the global status, Biomass and Bioenergy 33 (2009) 1310 – 1320

[26]   Bengt Hillring, World trade in forest products and wood fuel, Biomass and
         Bioenergy 30 (2006) 815–825

[27]   N.N.A.N. Yusuf, S.K. Kamarudin, Z. Yaakub, Overview on the current trends in
         biodiesel production, Energy Conversion and Management 52 (2011) 2741–
         2751

[28]   A. Williams, J.M. Jones, L. Ma, M. Pourkashanian, Pollutants from the
         combustion of solid biomass fuels, Progress in Energy and Combustion Science

38 (2012) 113-137

[29]   Bioenergy Project Development & Biomass Supply, Good Practice Guidelines, International Energy Agency (IEA), 2007

[30]   IEA Bioenergy Roadmap

[31]   Biomass Action Plan for The Republic of Serbia 2010 - 2012

[32]   Biofuels report, Gain report Number:RB1212, USDA Foreign Agricultural Service, 2012.

[33]   Dennis JS, Scott SA, Stephenson AL. Improving the sustainability of the production of biodiesel from oilseed rape in the UK. Process Saf Environ Protect 2008; 86:427-40.

[34]   Demirbas A. Comparison of transesterification methods for production of biodiesel from vegetable oils and fats. Energy Convers Manage 208; 49:125-130.

[35]   Poonam Singh Nigam, Anoop Singh, Production of liquid biofuels from renewable resources, Progress in Energy and Combustion Science 37 (2011) 52-68

[36]   The state of food and agriculture. BIOFUELS: prospects, risks and opportunities; 2008.

[37]   Ayhan Demirbas, Competitive liquid biofuels from biomass, Applied Energy 88 (2011) 17–28

[38]   RENEWABLES 2012 GLOBAL STATUS REPORT, REN21 Secretariat, Paris, France, 2012

[39]   Patrick Lamers, Martin Junginger, Carlo Hamelinck, André Faaij, Developments in international solid biofuel trade—An analysis of volumes, policies, and market factors, Renewable and Sustainable Energy Reviews 16 (2012) 3176– 3199

[40]   Martin Junginger, Jinkevan Dame, Simonetta Zarrilli, Fatin Ali Mohamed, Didier Marchal, Andre Faai, Opportunities and barriers for international bioenergy trade, Energy Policy 39 (2011) 2028–2042

[41]   Martin Jungingera, at all. Developments in international bioenergy trade, Biomass and Bioenergy 32 (2008)

[42] R. Saidura, E.A. Abdelaziza, A. Demirbasb, M.S. Hossaina, S. Mekhilef, A review on biomass as a fuel for boilers, Renewable and Sustainable Energy Reviews, 15 (2011) 2262–2289

[43] Stanislav V. Vassilev, David Baxter, Lars K. Andersen, Christina G. Vassileva, Trevor J. Morgan, An overview of the organic and inorganic phase composition of biomass, Fuel 94 (2012) 1–33.

[44] Peter McKendry, Energy production from biomass (part 1): overview of biomass, Bioresource Technology 83 (2002) 37–46

[45] Prabir Basu, Biomass Gasification and Pyrolysis, Elsevier Inc., 2010.

[46] Stanislav V. Vassilev, David Baxter, Lars K. Andersen, Christina G. Vassileva, An overview of the chemical composition of biomass, Fuel 89 (2010) 913–933

[47] B.M. Jenkins, L.L. Baxter, T.R. Miles Jr., T.R. Miles, Combustion properties of biomass, Fuel Processing Technology 54, 1998. 17–46.

[48] Jaya Shankar Tumuluru, Christopher T. Wright, Kevin L. Kenny, J. Richard Hess, A Review on Biomass Densification Technologies for Energy Application, Idaho National Laboratory Biofuels and Renewable Energy Technologies Department Energy Systems and Technologies Division, Idaho Falls, 2010.

[49] M. Fatih Demirbas, Mustafa Balat, Havva Balat, Biowastes-to-biofuels, Energy Conversion and Management 52 (2011) 1815–1828.

[50] Mette Stenseng, Pyrolysis and Combustion of Biomass, Ph.D.-thesis, Department of Chemical Engineering Technical University of Denmark. 2001.

[51] Morten G. Gronli, A THEORETICAL AND EXPERIMENTAL STUDY OF THE THERMAL DEGRADATION OF BIOMASS, Doctoral Thesis, 1996., Norges Teknisk-Naturvitenskapelig Universitet.

[52] Bradfield J, Levi MP. Effect of species and wood to bark ratio on pelleting of southern woods. Forest Products Journal 1984; 34 :61–3.

[53] Mohan D, Pittman JCU, Steele PH. Pyrolysis of wood/biomass for bio-oil: a critical review. Energy Fuels 2006; 20: 848–89.

[54] Raveendran K, Ganesh A. Adsorption characteristics and pore-development of biomass-pyrolysis char. Fuel 1998; 77: 769–81.

[55] Werther J, Saenger M, Hartge E-U, Ogada T, Siagi Z. Combustion of

agricultural residues. Prog Energy Combust Sci 2000; 26: 1–27.

[56]   Stanislav V. Vassileva, David Baxter, Lars K. Andersena, Christina G. Vassileva,

An overview of the composition and application of biomass ash. Part 1. Phase–mineral and chemical composition and classification, Fuel 105 (2013) 40–76

[57]   Jianjun Dai*, Heping Cui, John R. Grace, Biomass feeding for thermochemical reactors, Progress in Energy and Combustion Science 38 (2012) 716-736.

[58]   Prabir Basu, Biomass Gasification, Pyrolysis and Torrefaction, Elsevier Inc., 2013.

BIOMASS HANDLING

[59]   Ingwald Obernberger, Gerold Thek: The Pellet Handbook The production and thermal utilisation of biomass pellets, BIOS BIOENERGIESYSTEME GmbH, 2010.

[60]   Jianfeng Shen, Shuguang Zhu, Xinzhi Liu, Houlei Zhang, Junjie Tan, The prediction of elemental composition of biomass based on proximate analysis, Energy Conversion and Management 51 (2010) 983–987.

[61]   Parikh J, Channiwala SA, Ghosal GK. A correlation for calculating elemental composition from proximate analysis of biomass materials. Fuel 2007;86: 1710–9.

[62]   Vakkilainen EK. Estimation of elemental composition from proximate analysis of black liquor. Paper JA PUU – Paper Timber 2000;82: 450–4.

[63]   Ingwald Obernberger, Thomas Brunner, Georg Barnthaler, Chemical properties of solid biofuels—significance and impact, Biomass and Bioenergy 30 (2006) 973–982

[64]   Nalladurai Kaliyan, R. Vance Morey, Factors affecting strength and durability of densified biomass products, Biomass and Bioenergy 33 (2009) 337 – 359

[65]   Yadong Li, Henry Liu, High-pressure densi_cation of wood residues to form an upgraded fuel, Biomass and Bioenergy 19 (2000) 177-186.

[66]   Saumen Poddar a, Mohammed Kamruzzaman a, S.M.A. Sujan b, M. Hossain b, M.S. Jamal b,⇑, M.A. Gafur c,Mahfuza Khanam b, Effect of compression pressure on lignocellulosic biomass pellet to improve fuel properties: Higher heating value, Fuel 131 (2014) 43–48

[67]   Thomas M, van der Poel AFB. Physical quality of pelleted animal feed. 1. Criteria for pellet quality. Animal Feed Science and Technology 1996;61: 89–112.

[68]   E. Granada , L.M. Lopez Gonzalez , J.L. Mıguez , J. Moran, Fuel lignocellulosic briquettes, die design and products study, Renewable Energy 27 (2002) 561–573

[69]   Sylvia H. Larsson, Mikael Thyrel, Paul Geladi, Torbjorn A. Lestander, High quality biofuel pellet production from pre-compacted low density raw materials, Bioresource Technology 99 (2008) 7176–7182.

[70]   Grover PD, Mishra SK. Biomass briquetting: technology and practices. Regional wood energy development program in Asia, field document no. 46. Bangkok, Thailand: Food and Agriculture Organization of the United Nations; 1996.

[71]   Influence of torrefaction on the grindability and reactivity of woody biomass, Fuel Processing Technology 89 (2008) 169 – 175

[72]   Mani, S., L. G. Tabil, and S. Sokhansanj, 2002, "Compaction Characteristics of Some Biomass Grinds," AIC 2002 Meeting, CSAE/SCGR Program, Saskatoon, Saskatchewan, July 14–17, 2002.

[73]   Christofer Rhen, Marcus Ohman, Rolf Gref, Iwan Wasterlund, Effect of raw material composition in woody biomass pellets on combustion characteristics, Biomass and Bioenergy 31 (2007) 66–72

[74]   Mehrdad Arshadia,∗, Rolf Gref b, Paul Geladia, Sten-Axel Dahlqvistc, Torbjörn Lestandera, The influence of raw material characteristics on the industrial pelletizing process and pellet quality, Fuel Processing Technology 89 (2008) 1442 – 1447

[75]   Paivi Lehtikangas, Quality properties of pelletised sawdust, logging residues and bark, Biomass and Bioenergy 20 (2001) 351–360

[76]   Christofer Rhen, Rolf Gref , Michael Sjostrom , Iwan Wasterlund, Effects of raw material moisture content, densification pressure and temperature on some properties of Norway spruce pellets, Fuel Processing Technology 87 (2005) 11 – 16.

[77]   Ingwald Obernberger, Gerold Thek, Physical characterisation and chemical composition of densified biomass fuels with regard to their combustion

behavior, Biomass and Bioenergy 27 (2004) 653–669

[78] Ayhan Demirbas, Biomass resources facilities and biomass conversion processing for fuels and chemicals, Energy Conversion and Management 42 (2001) 1357-1378.

[79] Maria Bario, Experimental investigation of small-scale gasification of woody biomass, Doctoral thesis, The Norwegian University of Science and Technology, 2002.

[80] Bridgwater AV. Renewable fuels and chemicals by thermal processing of biomass. Chem Eng J 2003;91: 87–102.

[81] H.B. Goyal, Diptendu Seal, R.C. Saxena, Bio-fuels from thermochemical conversion of renewable resources: A review, Renewable and Sustainable Energy Reviews 12 (2008) 504–517.

[82] Sensoz S, Can M. Pyrolysis of pine (pinus brutia ten.) chips. 1. Effect of pyrolysis temperature and heating rate on the product yields. Energy Source Part A, 2002;24: 347–55.

[83] Frederik Ronsse, Robert Nachenius, Dane Dickinson and Wolter Prins, Biomass Pyrolysis Overview, 1st Int. Summer School on Biochar, Potsdam, Sept 9 – 16, 2012.

[84] N.L. Panwar, Richa Kothari, V.V. Tyagi, Thermo chemical conversion of biomass – Eco friendly energy routes, Renewable and Sustainable Energy Reviews 16 (2012) 1801– 1816

[85] Peter McKendry, Energy production from biomass (part 2): conversion technologies, Bioresource Technology 83 (2002) 47–54

[86] Serdar Yaman, Pyrolysis of biomass to produce fuels and chemical feedstocks, Energy Conversion and Management 45 (2004) 651–671

[87] Esin Apaydin-Varol, Ersan Putun, Ayse E. Putun, Slow pyrolysis of pistachio shell, Fuel 86 (2007) 1892–1899

[88] Ayhan Demirbas, Potential applications of renewable energy sources, biomass combustion problems in boiler power systems and combustion related environmental issues, Progress in Energy and Combustion Science 31 (2005) 171–192.

[89] Paul T. Williams and Serpil Besler, The influence 0f temperature and heating

rate on the slow pyrolisis of biomass, Renewable Energy , Vol. 7 No. 3, pp. 233-250, 1996.

[90] Ozlem Onay, O. Mete Kockar, Slow, fast and flash pyrolysis of rapeseed, Renewable Energy 28 (2003) 2417–2433

[91] Esben W. Bruun, Per Ambus, Helge Egsgaard, Henrik Hauggaard-Nielsen, Effects of slow and fast pyrolysis biochar on soil C and N turnover dynamics, Soil Biology & Biochemistry 46 (2012) 73-79

[92] Luo Z, Wang S, Liao Y, Zhou J, Gu Y, Cen K. Research on biomass fast pyrolysis for liquid fuel. Biomass Bioenergy 2004;26:455–62.

[93] Güray Yildiz , Tom Lathouwers , Hilal Ezgi Toraman , Kevin Van Geem , Guy Marin , Frederik Ronsse , Ruben van Duren, Sascha RA Kersten and Wolter Prins , Catalytic fast pyrolysis of pine wood: effect of
 successive catalyst regeneration, Energy Fuels 2014, 28, 4560−4572.

[94] A.V. Bridgwater, Review of fast pyrolysis of biomass and product upgrading, Biomass and Bioenergy 38 (2012) 68 - 94

[95] Mohan D, Pittman CU, Steele PH. Pyrolysis of wood/biomass for bio-oil: a critical review. Energy Fuels 2006; 20: 848–89.

[96] Patrick A. Horne and Paul T. Williams, Influence of temperature on the products from the flash pyrolysis of biomass, Fuel Vol. 75, No. 9, pp. 1051-1059, 1996

[97] T. Funazukuri . R.R. Hudgins and P.L. Silveston , Product distribution for flash pyrolysis of cellulose in a coil pyrolyzer, JournaI of Analytical and Applied Pyrolysis, 10 (1987) 225-249

[98] Marcio L.de Souza-Santos, Solid Fuels Combustion and Gasification, Modeling, Simulation, and Equipment Operation, MARCEL DEKKER, Inc., 2004.

[99] Morten E. N. Fossum, Biomass gasification combustion of gas mixtures, Doctoral thesis, The Norwegian University of Science and Technology, 2002.

[100] Harrie Knoef, Handbook Biomass Gasification, BTG biomass technology group BV, 2005.

[101] Chris Higman, Maarten van der Burgt, GASIFICATION, Elsevier Science (USA), 2003

[102] Ayhan Demirbas, Combustion characteristics of different biomass fuels, Progress in Energy and Combustion Science 30 (2004) 219–230.

[103] Ed. D. Yogi Goswami, Alternative Energy in Agriculture, CRC Press, 1986.

[104] Samir S. Sofer, Oskar R. Zaborski, Biomass Conversion Processes for Energy and Fuels, Plenum Press, 1981.

[105] Prabir Basu, Combustion and Gasification in Fluidized Beds, Taylor & Francis, 2006.

[106] Roger A. Khalil, Thermal conversation of biomass with emphasis on product distribution, reacton kinetics and sulfur abatement, PhD thesis, NTNU, 2009.

[107] Ragnar Warnecke, Gasification of biomass: comparison of fixed bed and fluidized bed gasifier, Biomass and Bioenergy 18 (2000) 489-497.

[108] J.Warnatz, U. Maas, R.W. Dibble, Combustion, Springer, 2006.

[109] Yao Bin Yang, Changkook Ryu, Adela Khor, Nicola E. Yates, Vida N. Sharifi, Jim Swithenbank, Effect of fuel properties on biomass combustion. Part II. Modelling approach—identification of the controlling factors, Fuel 84 (2005) 2116–2130

[110] Arie Verloopa, Combustion Troubleshooting, Canadian Biomass Magazine, January-February 2010.

[111] Chungen Yin, Lasse A. Rosendahl, Søren K. Kær, Grate-firing of biomass for heat and power production, Progress in Energy and Combustion Science 34 (2008) 725– 754

[112] S. Ravelli, A. Perdichizzi, G. Barigozzi, Description, applications and numerical modelling of bubbling fluidized bed combustion in waste-to-energy plants, Progress in Energy and Combustion Science 34 (2008) 224–253.

[113] A.A. Khan, W. de Jong, P.J. Jansens, H. Spliethoff, Biomass combustion in fluidized bed boilers: Potential problems and remedies, Fuel Processing Technology 90 (2009) 21 – 50.

[114] Joris Koornneef, Martin Junginger, Andre Faaij, Development of fluidized bed combustion—An overview of trends, performance and cost, Progress in Energy and Combustion Science 33 (2007) 19–55.

[115] Stefan W. Grass and Bryan M. Jenkins, Biomass fueled fluidized bed combustion: atmospheric emissions, emission control devices and environmental regulations, Biomass and Bioenergy Vol. 6, No. 4, pp. 243-260. 1994.

[116] Malte Bartels, Weigang Lin, John Nijenhuis, Freek Kapteijn, J. Ruud van Ommen, Agglomeration in fluidized beds at high temperatures: Mechanisms, detection and prevention, Progress in Energy and Combustion Science 34 (2008) 633– 666.

[117] M. Mandø, L. Rosendahl, C. Yin, H. Sørensen, Pulverized straw combustion in a low-NOx multifuel burner: Modeling the transition from coal to straw, Fuel 89 (2010) 3051–3062.

[118] A. Williams, M. Pourkashanian, J.M. Jones, Combustion of pulverised coal and biomass, Progress in Energy and Combustion Science 27 (2001) 587-610.

[119] A. Elfasakhany, L. Tao, B. Espenas, J. Larfeldt, X.S. Bai, Pulverised wood combustion in a vertical furnace: Experimental and computational analyses, Applied Energy 112 (2013) 454–464.

[120] Ingwald Obernberger, Decentralized biomass combustion: state of the art and future development, Biomass and Bioenergy Vol. 14, No. 1, pp. 33-56, 1998.

[121] A. Williams, J.M. Jones, L. Ma, M. Pourkashanian, Pollutants from the combustion of solid biomass fuels, Progress in Energy and Combustion Science 38 (2012) 113-137.

[122] Ehsan Houshfar, Øyvind Skreiberg, Terese Løvas, Dusan Todorovic, Lars Sørum, Effect of Excess Air Ratio and Temperature on NOx Emission from Grate Combustion of Biomass in the Staged Air Combustion Scenario, Energy Fuels 2011, 25, 4643–4654.

[123] Thomas Nussbaumer, Overview on Technologies for Biomass Combustion and Emission Levels of Particulate Matter, Zürich, 2010.

[124] Nussbaumer, T. Combustion and co-combustion of biomass: fundamentals, technologies, and primary measures for emission reduction.
Energy Fuels 2003, 17 (6), 1510–1521.

[125] Michael Becidan, Dusan Todorovic, Øyvind Skreiberg, Roger A. Khalil, Rainer Backman, Franziska Goile, Alexandra Skreiberg, Aleksandar Jovovic, Lars Sørum, Ash related behavior in staged and non-staged combustion of biomass fuels and fuel mixtures, Biomass and Bioenergy 41 (2012) 86-93.

[126] Roger A Khalil, Dusan Todorovic, Øyvind Skreiberg, Michael Becidan, Rainer Backman, Franziska Goile, Alexandra Skreiberg, Lars Sørum, The effect of

kaolin on the combustion of demolition wood under well-controlled conditions, Waste Management & Research, 30(7) 672–680.

[127]   Tariq AS, Purvis MRI. NOx emissions and thermal efficiencies of small scale biomass-fuelled combustion plant with reference to process industries in a developing country. Int J Energy Res 1996; 20(1):41–55.

[128]   Kenneth K. Kuo, Principles of Combustion, John Wiley & Sons, 2005.

[129]   Wünning JA, Wünning JG. Flameless oxidation to reduce thermal NO formation. Prog Energy Combust Sci 1997;23 (1):81–94.

[130]   Glarborg P, Jensen AD, Johnsson JE. Fuel nitrogen conversion in solid fuel fired systems. Prog Energy Combust Sci 2003;29 (2):89–113.

[131]   Houshfar, E.; Løvas, T.; Skreiberg, Ø. Detailed chemical kinetics modeling of NOx reduction in combined staged fuel and staged air combustion of biomass. 18th European Biomass Conference & Exhibition (EU BC&E), Lyon, France, 2010; pp 1128_1132.

[132]   Salzmann, R.; Nussbaumer, T. Fuel Staging for NOx Reduction
in Biomass Combustion: Experiments and Modeling. Energy Fuels 2001,
15 (3), 575–582.

[133]   Kicherer, A.; Spliethoff, H.; Maier, H.; Hein, K. R. G. The effect of different reburning fuels on NOx-reduction. Fuel 1994, 73 (9), 1443–1446.

[134]   Zabetta, E. C.; Hupa, M.; Saviharju, K. Reducing NOx Emissions Using Fuel Staging, Air Staging, and Selective Noncatalytic Reduction in Synergy. Ind. Eng. Chem. Res. 2005, 44 (13), 4552–4561.

[135]   Hao Liu, Joel Chaney, Jinxing Li, Chenggong Sun, Control of NOx emissions of a domestic/small-scale biomass pellet boiler by air staging, Fuel 103 (2013) 792–798.

[136]   Ehsan Houshfar, Terese Løvås and Øyvind Skreiberg, Experimental Investigation on NO*x* Reduction by Primary Measures in Biomass Combustion: Straw, Peat, Sewage Sludge, Forest Residues and Wood Pellets, *Energies* 2012, *5*, 270-290;

[137]   S. Munir, W. Nimmo, B.M. Gibbs, The effect of air staged, co-combustion of pulverised coal and biomass blends on NOx emissions and combustion efficiency, Fuel 90 (2011) 126–135.

[138] Skreiberg, Ø.; Kilpinen, P.; Glarborg, P. Ammonia chemistry below 1400 K under fuel-rich conditions in a flow reactor. Combust. Flame 2004, 136 (4), 501–518.

[139] Kilpinen, P.; Hupa, M. Homogeneous N2O chemistry at fluidized bed combustion conditions: A kinetic modeling study. Combust. Flame 1991, 85 (1_2), 94–104.

[140] Kilpinen, P.; Glarborg, P.; Hupa, M. Reburning chemistry: a kinetic modeling study. Ind. Eng. Chem. Res. 1992, 31 (6), 1477–1490.

[141] Hamalainen, J. P.; Aho, M. J.; Tummavuori, J. L. Formation of nitrogen oxides from fuel-N through HCN and NH3: a model-compound study. Fuel 1994, 73 (12), 1894–1898.

[142] Becidan, M.; Skreiberg, Ø.; Hustad, J. E. NOx and N2O Precursors (NH3 and HCN) in Pyrolysis of Biomass Residues. Energy Fuels 2007, 21 (2), 1173–1180.

[143] Hansson, K.-M.; Samuelsson, J.; Tullin, C.; Åmand, L.-E. Formation of HNCO, HCN, and NH3 from the pyrolysis of bark and nitrogen-containing model compounds. Combust. Flame 2004, 137 (3), 265–277.

[144] Nussbaumer, T. Primary and secondary measures for the reduction of nitric oxide emissions from biomass combustion. In Developments in Thermochemical Biomass Conversion, Banff, Canada, 1996; Bridgwater, A. V.; Boocock, D. G. B., Eds. Blackie Academic & Professional: 1997; pp 1447-1461

[145] A. Lyngfelt, B. Leckner, Combustion of wood-chips in circulating fluidized bed boilers — NO and CO emissions as functions of temperature and air-staging, Fuel 78 (1999) 1065–1072

[146] Stubenberger, G.; Scharler, R.; Zahirovic, S.; Obernberger, I. Experimental investigation of nitrogen species release from different solid biomass fuels as a basis for release models. Fuel 2008, 87 (6), 793–806.

[147] Johansson LS, Leckner B, Gustavsson L, Cooper D, Tullin C, Potter A. Emission characteristics of modern and old-type residential boilers fired with wood logs and wood pellets. Atmos Environ 2004; 38(25):4183–95.

[148] Dagaut, P.; Glarborg, P.; Alzueta, M. U. The oxidation of hydrogen cyanide and related chemistry. Prog. Energy Combust. Sci.2008, 34 (1), 1–46.

[149] Sørum, L.; Skreiberg, Ø.; Glarborg, P.; Jensen, A.; Dam-Johansen, K.

Formation of NO from combustion of volatiles from municipal solid wastes. Combust. Flame 2001, 124 (1-2), 195–212.

[150] http://combustion.berkeley.edu/gri-mech/

[151] Skreiberg Ø, Becidan M, Hustad JE, Mitchell RE. Detailed chemical kinetics modelling of NOx reduction by staged air combustion at moderate temperatures. In: Bridgwater AV, Boocock DGB, editors. The science in thermal and chemical biomass conversion conference, 2004; Victoria, BC, Canada. Newbury, Berkshire, UK: CPL Press; 2006. p. 40–54.

[152] Skreiberg Ø, Glarborg P, Jensen AD, Dam-Johansen K. Kinetic NOx modelling and experimental results from single wood particle combustion. Fuel 1997; 76(7):671–82.

[153] Robert Scharler, Ingwald Obernberger, Gunter Langle, Josef Heinzel, CFD analysis of air staging and flue gas recurculation in biomass grate furnaces, Proceedings of the 1st World Conference on Biomass for Energy and Idustry, pp. 1935-1939, June 2000, Sevilla, Spain.

[154] Ehsan Houshfar, Roger A. Khalil, Terese Løvas and Øyvind Skreiberg, Enhanced NOx Reduction by Combined Staged Air and Flue Gas Recirculation in Biomass Grate Combustion, Energy Fuels 2012, 26, 3003−3011.

[155] Maryori Díaz-Ramírez, Fernando Sebastián, Javier Royo, Adeline Rezeau, Influencing factors on NO_X emission level during grate conversion of three pelletized energy crops, Applied Energy 115 (2014) 360–373.

[156] Eskilsson D, Ronnback M, Samuelsson J, Tullin C. Optimisation of efficiency and
emissions in pellet burners. Biomass Bioenergy 2004;27:541–6.

[157] Hartmut Spliethoff, Ulrich Greul, Helmut R0diger and Klaus R. G. Hein, Basic effects on NOx emissions in air staging and reburning at a bench-scale test facility, Fuel Vol. 75, No. 5, pp. 560-564, 1996.

[158] Sen Li, Tongmo Xu, Shien Hui, Xiaolin Wei, NOx emission and thermal efficiency of a 300 MWe utility boiler retrofitted by air staging, Applied Energy 86 (2009) 1797–1803.

[159] Lin, W.; Jensen, P. A.; Jensen, A. D. Biomass Suspension Combustion: Effect of Two-Stage Combustion on NOx Emissions in a Laboratory-Scale Swirl

Burner. Energy Fuels 2009, 23 (3), 1398–1405.

[160]   Bauer, R.; Golles, M.; Brunner, T.;Dourdoumas, N.;Obernberger, I. Modelling of grate combustion in a medium scale biomass furnace for control purposes. Biomass Bioenergy 2010, 34 (4), 417–427

[161]   Zhou, H.; Jensen, A. D.; Glarborg, P.; Kavaliauskas, A. Formation and reduction of nitric oxide in fixed-bed combustion of straw. Fuel 2006, 85 (5_6), 705–716.

[162]   Wendt, J. O. L.; Sternling, C. V.; Matovich, M. A. Reduction of sulfur trioxide and nitrogen oxides by secondary fuel injection. Symp. (Int.) Combust. 1973, 14 (1), 897–904.

[163]   Chen, S. L.; McCarthy, J. M.; Clark, W. D.; Heap, M. P.; Seeker, W. R.; Pershing, D. W. Bench and pilot scale process evaluation of reburning for in-furnace NOx reduction. Symp. (Int.) Combust. 1988, 21 (1), 1159–1169.

[164]   Pershing, D, W.; Berkau, E, E., The Chemistry of Nitrogen Oxides and Control through Combustion Modifications. In Pollution Control and Energy Needs, Jimeson, R. M.; Spindt, R. S., Eds.; American Chemical Society: Washington, DC, 1974; Vol. 127, pp 218-240

[165]   Svoboda, K.; Poho_rel_y, M.; Hartman, M. Effects of Operating Conditions and Dusty Fuel on the NOx, N2O, and CO Emissions in PFB Co-combustion of Coal and Wood. Energy Fuels 2003, 17 (4), 1091–1099.

[166]   L.L. Baxter, T.R. Miles, T.R. Miles, B.M. Jenkins, T. Milne, D. Dayton, R.W. Bryers, L.L. Oden, The behavior of inorganic material in biomass-fired power boilers: field and laboratory experiences, Fuel Process. Technol. 54 (1998) 47–78.

[167]   Punjak WA, Uberoi M, Shadman F. High-temperature adsorption of alkali vapors on solid sorbents. AIChE J 1989; 35 (7): 1186-94.

[168]   Turn SQ, Kinoshita CM, Ishimura DM, Zhou J, Hiraki TT, Masutani SM. "An experimental Investigation of alkali removal from biomass Producer gas using a fixed bed of solid Sorbent. J I Energy 1998; 71 (9):163-77.

[169]   Aho M. Reduction of chlorine deposition in FB boilers with aluminium-containing additives. Fuel 2001; 80 (13): 1943-51.

[170]   Iisa K, Salmenoja YL. Sulfation of potassium chloride at combustion conditions.

Energ Fuel 1999; 13 (6): 1184-90.

[171] Aho M, Ferrer E. Importance of coal ash composition in protecting the boiler against chlorine deposition during combustion of chlorine-rich biomass. Fuel 2005; 84 (2-3): 201-12.

[172] Punjak WA, Shadman F. Aluminosilicate sorbents for control of alkali vapors during coal combustion and gasification. Energ Fuel 1988; 2 (5): 702-8.

[173] Kyi S, Chadwick BL. Screening of potential mineral additives for use as fouling preventatives in Victorian brown coal combustion. Fuel 1999; 78 (7): 845-55.

[174] Andersson C, inventor; Vattenfall AB, applicant. A method for operating a heat-producing plant for burning chlorinecontaining fuels. Worldwide patent WO 2002059526. 2002 Jan 24.

[175] Nielsen HP, Frandsen FJ, Dam-Johansen K, Baxter LL. The implications of chlorine-associated corrosion on the operation of biomass-fired boilers. Prog Energ Combust 2000; 26 (3): 283-98.

[176] Ferrer E, Aho M, Silvennoinen J, Nurminen RV. Fluidized bed combustion of refuse-derived fuel in presence of protective coal ash. Fuel Process Technol 2005; 87 (1): 33-44.

[177] Coda B, Aho M, Berger R, Hein KRG. Behavior of chlorine and enrichment of risky elements in bubbling fluidized bed combustion of biomass and waste assisted by additives,.Energ Fuel 2001; 15 (3): 680-90.

[178] Aho M, Silvennoinen J. Preventing chlorine deposition on heat transfer surfaces with aluminiumesilicon rich biomass residue and additive. Fuel 2004; 83 (10): 1299-305.

[179] Johansson L, Leckner B, Tullin C, Amand L, Davidsson K. Properties of particles in the fly ash of a biofuel-fired Circulating Fluidized Bed (CFB) boiler. Energy Fuel 2008; 22 (5): 3005-15.

[180] Escobar I, Oleschko H, Wolf KJ, Mü̈ller M. Alkali removal from hot flue gas by solid sorbents in pressurized pulverized coal combustion. Powder Technology 2008; 180 (1-2): 51-6.

[181] Uberoi M, Punjak W, Shadman F. The kinetics and mechanism of alkali removal from flue gases by solid sorbents. Prog Energ Combust 1990; 16 (4): 205-11.

237

[182] Nielsen HP. Deposition and high-temperature corrosion in biomass-fired boilers [dissertation]. Lyngby: Technical University of Denmark; 1998.

[183] Knudsen J, Jensen P, Lin W, Frandsen F, Dam-Johansen K., Sulfur transformations during thermal conversion of herbaceous biomass. Energ Fuel 2004;18 (3): 810-9

[184] Elled A-L, Amand L-E, Leckner B, Andersson B-A. The fate of trace elements in fluidised bed combustion of sewage sludge and wood. Fuel 2007;86(5-6):843-52.

[185] Sørum L, Frandsen FJ, Hustad JE. On the fate of heavy metals in municipal solid waste combustion Part I: devotalisation of heavy metals on the grate. Fuel 2003;
82 (18): 2273-83.

[186] Boman C, Ohman M, Nordin A. Trace element enrichment and behavior in wood pellet production and combustion processes. Energ Fuel 2006; 20 (3): 993-1000.

[187] Elled A-L, Amand L-E, Eskilsson D. Fate of zinc during combustion of demolition wood in a fluidized bed boiler. Energ Fuel 2008; 22 (3): 1519-26.

[188] Abanades S, Flamant G, Gagnepain B, Gauthier D. Fate of heavy metals during municipal solid waste incineration. Waste Manage Res 2002; 20 (1): 55-68

[189] Van Lith S. Release of inorganic elements during wood-firing on a grate.[dissertation]. Lyngby: CHEC Research Centre, Technical University of Denmark; 2005.

[190] Dahl J, Obernberger I, Brunner T, Biedermann F. Results and evaluation of a new heavy metal fractionation technology in grate-fired biomass combustion plants as a basis for an improved ash utilisation. In: ETA-renewable energy, editor. Proceedings of the 12th European conference and technology exhibition on biomass for energy, industry and climate protection; 2002 Jun 17-21. Amsterdam; The Netherlands: ETA-Florence; 2002. p. 690-4. Italy and WIP-Munich, Germany.

[191] European Commission. Integrated pollution prevention and control reference document on the best available techniques for waste incineration. Seville, Spain: Directorate-General JRC Joint Research Centre Institute for Prospective

Technological Studies; 2006 Aug. 638 pp.

[192] L.S. Bäfver, M. Rönnbäck, B. Leckner, F. Claesson, C. Tullin, Particle emission from combustion of oat grain and its potential reduction by addition of limestone or kaolin, Fuel Process. Technol. 90 (2009) 353–359.

[193] M. Broström, H. Kassman, A. Helgesson, M. Berg, C. Andersson, R. Backman, A. Nordin, Sulfation of corrosive alkali chlorides by ammonium sulfate in a biomass fired CFB boiler, Fuel Process. Technol. 88 (2007) 1171–1177.

[194] P. Henderson, P. Szakálos, R. Pettersson, C. Andersson, J. Högberg, Reducing superheater corrosion in wood-fired boilers, Mater. Corros. 57 (2006) 128–134.

[195] M. Aho, P. Vainikka, R. Taipale, P. Yrjas, Effective new chemicals to prevent corrosion due to chlorine in power plant superheaters, Fuel 87 (2008) 647–654.

[196] B.J. Skrifvars, T. Laurén, M. Hupa, R. Korbee, P. Ljung, Ash behaviour in a pulverized wood fired boiler - a case study, Fuel 83 (2004) 1371–1379.

[197] L. Tobiasen, R. Skytte, L.S. Pedersen, S.T. Pedersen, M.A. Lindberg, Deposit characteristic after injection of additives to a Danish straw-fired suspension boiler, Fuel Process. Technol. 88 (2007) 1108–1117.

[198] M. Theis, B.J. Skrifvars, M. Zevenhoven, M. Hupa, H.H. Tran, Fouling tendency of ash resulting from burning mixtures of biofuels. Part 2: Deposit chemistry, Fuel 85 (2006) 1992–2001.

[199] L. Pommer, M. Öhman, D. Broström, J. Burvall, R. Backman, I. Olofsson, A. Nordin, Mechanisms behind the positive effects on bed agglomeration and deposit formation combusting forest residue with peat additives in fluidized beds, Energ Fuel 23 (2009) 4245–4253.

[200] B.J. Skrifvars, R. Backman, M. Hupa, G. Sfiris, T. Abyhammar, A. Lyngfelt, Ash behaviour in a CFB boiler during combustion of coal, peat or wood, Fuel 77 (1998) 65–70.

[201] B.J. Skrifvars, M. Zevenhoven, R. Backman, M. Hupa, Predicting the ash behavior of different fuels in fluidized bed combustion, Proceedings of the 16th International Conference on Fluidized Bed Combustion Paper No. FBC01-113, 2001.

[202] M. Zevenhoven-Onderwater, J.P. Blomquist, B.J. Skrifvars, R. Backman, M. Hupa, The prediction of behaviour of ashes from five different solid fuels in

239

fluidised bed combustion, Fuel 79 (2000) 1353–1361.

[203]   Werther J, Sänger M, Hartge EU, et al. (2000) Combustion of agricultural residues, Progress in Energy and Combustion Science 26; 1–27.

[204]   Bartels M, Lin WG, Nijenhuis J, et al. (2008) Agglomeration in fluidized beds at high temperatures: mechanisms, detection and prevention. Progress in Energy and Combustion Science 34: 633–666.

[205]   Davidsson KO, Steenari BM and Eskilsson D (2007) Kaolin addition during biomass combustion in a 35 MW circulating fluidized-bed boiler. *Energy & Fuels* 21: 1959–1966.

[206]   Davidsson KO, Åmand LE, Steenari BM, et al. (2008) Countermeasures against alkali-related problems during combustion of biomass in a circulating fluidized bed boiler. Chemical Engineering Science 63: 5314–5329.

[207]   Khan AA, de Jong W, Jansens PJ, et al. (2009) Biomass combustion in fluidized bed boilers: Potential problems and remedies. Fuel Processing Technology 90: 21–50.

[208]   Llorente MJF, Cuadrado RE, Laplaza JMM, et al. (2006) Combustion in bubbling fluidised bed with bed material of limestone to reduce the biomass ash agglomeration and sintering. Fuel 85: 2081–2092.

[209]   Pettersson A, Åmand LE and Steenari BM (2009) Chemical fractionation for the characterisation of fly ashes from co-combustion of biofuels using different methods for alkali reduction. Fuel 88: 1758–1772.

[210]   Vamvuka D, Pitharoulis M, Alevizos G, et al. (2009) Ash effects during combustion of lignite/biomass blends in fluidized bed. Renewable Energy 34: 2662–2671.

[211]   Vamvuka D, Zografos D and Alevizos G (2008) Control methods for mitigating biomass ash-related problems in fluidized beds. Bioresource Technology 99: 3534–3544.

[212]   http://www.bios-bioenergy.at/en/working-field/research-development.html

[213]   Tran KQ, Iisa K, Hagström M, et al. (2004) On the application of surface ionization detector for the study of alkali capture by kaolin in a fixed bed reactor. *Fuel* 83: 807–812.

[214]   Tran KQ, Iisa K, Steenari BM, et al. (2005) A kinetic study of gaseous alkali

capture by kaolin in the fixed bed reactor equipped with an alkali detector. *Fuel* 84: 169–175.

[215]   ELPI User Manual, Dekati Ltd. 2006

[216]   I. Obernberger, Ash related problems in biomass combustion plants, Inaugural lecture presented on May 20, 2005 at Technische Universiteit Eindhoven, 2005, available at, www.alexandria.tue.nl/extra2/redes/obernberger2005.pdf.

[217]   R. Backman, B.J. Skrifvars, P. Yrjas, The influence of aerosol particles on the melting behaviour of ash deposits in biomass fired boilers, Aerosols in Biomass Combustion Series Thermal Biomass Utilization, Graz, Volume 6, 2005, pp. 119–132.

[218]   Winter F, Wartha C, Hofbauer H. NO and N2O formation during the combustion of wood, straw, malt waste and peat. Bioresour Technol 1999; 70(1):39–49.

[219]   Abelha P, Gulyurtlu I, Cabrita I. Release of nitrogen precursors from coal and biomass residues in a bubbling fluidized bed. Energy Fuel 2007; 22(1):363–71.

[220]   Hämäläinen JP, Aho MJ. Effect of fuel composition on the conversion of volatile solid fuel-N to N2O and NO. Fuel 1995; 74(12):1922–4.

[221]   Hao WM, Scharffe D, Lobert JM, Grutzen PJ. Emissions of N2O from the burning of biomass in an experimental system. Geophys Res Lett 1991; 18(6): 999–1002.

[222]   Gutierrez MJF, Baxter D, Hunter C, Svoboda K. Nitrous oxide (N_2O) emissions from waste and biomass to energy plants. Waste Manage Res 2005;23(2):133–47.

[223]   Goel SK, Morihara A, Tullin CJ, Sarofim AF. Effect of NO and O_2 concentration on N2O formation during coal combustion in a fluidized-bed combustor: modeling results. Symp (Int) Combust 1994; 25(1):1051–9.

[224]   Tullin CJ, Goel S, Morihara A, Sarofim AF, Beer JM. Nitrogen oxide (NO and N_2O) formation for coal combustion in a fluidized bed: effect of carbon conversion and bed temperature. Energy Fuel 1993; 7(6):796–802.

[225]   Nussbaumer, T. Biomass Combustion in Europe Overview on Technologies and Regulations; Report 08-03; prepared by Verenum Switzerland for New York State Energy Research and Development Authority: Albany, NY, 2008.

[226] Johansson, L. S.; Tullin, C.; Leckner, B.; Sj€ovall, P. Particle emissions from biomass combustion in small combustors. Biomass Bioenergy 2003, 25 (4), 435–446.

[227] Kozinski, J. A.; Saade, R. Effect of biomass burning on the formation of soot particles and heavy hydrocarbons. An experimental study. Fuel 1998, 77 (4), 225–237.

[228] Skreiberg, Ø.;Hustad, J. E.; Karlsvik, E. Empirical NOx-modelling and experimental results from wood stove combustion. In Developments in Thermochemical Biomass Conversion, Banff,Canada, 1996; Bridgwater, A. V.; Boocock, D. G. B., Eds. Blackie Academic & Professional: London, UK, 1997; pp 1462-1478.

[229] Mahmoudi, S.; Baeyens, J.; Seville, J. P. K. NOx formation and selective non-catalytic reduction (SNCR) in a fluidized bed combustor of biomass. Biomass Bioenergy 2010, 34 (9), 1393–1409.

[230] Kristensen, P. G.; Glarborg, P.; Dam-Johansen, K. Nitrogen chemistry during burnout in fuel-staged combustion. Combust. Flame 1996, 107 (3), 211–222.

[231] Liu, H.; Gibbs, B. M. Modelling of NO and N2O emissions from biomass-fired circulating fluidized bed combustors. Fuel 2002, 81 (3), 271–280.

[232] Aho, M. J.; Hamalainen, J. P.; Tummavuori, J. L. Importance of solid fuel properties to nitrogen oxide formation through HCN and NH3 in small particle combustion. Combust. Flame 1993, 95 (1_2), 22–30.

[233] Padinger, R.; Leckner, B.; Åmand, L.-E.; Thunman, H.; Ghirelli, F.; Nussbaumer, T.; Good, J.; Hassler, P.; Salzmann, R.; Winter, F.; Wartha, C.; L€offler, G.; Wargadalam, V. J.; Hofbauer, H.; Saastamoinen, J.; Oravainen, H.; Heiskanen, V. P.; H€am€al€ainen, J. P.; Taipale, R.; Bilbao, R.; Alzueta, M. U.; Millera, A.; Oliva, M.; Ib_a~nez, J. C.; Kilpinen, P. Reduction of nitrogen oxide emissions from wood chip grate furnaces, Final report for the EU-JOULE III project JOR3-CT96-0059, 1st World Conference on Biomass for Energy and Industry, Sevilla, Spain, 2000, Kyritsis, S., Beenackers, A. A. A. M., Helm, P., Grassi, A., Chiaramonti, D., Eds.; James & James (Science Publishers) Ltd.: Sevilla, Spain, 2000; pp 1457-1463.

[234] Hupa M. Interaction of fuels in co-firing in FBC. Fuel 2005; 84(10):1312-9.

[235] Obernberger I. Fly ash and aerosol formation in biomass combustion processes an introduction. International seminar on aerosols in biomass combustion, Graz, Austia, 2005 Mar 18, www.ieabcc.nl/meetings/task32_Graz_aerosols/01_Obernberger.pdf. Cited 2011 Dec 20.

[236] Nielsen, HP; Baxter, LL; Sclippab, G; Morey, C; Frandsen, FJ; Dam-Johansen, K. *Fuel* 2000, *79*, 131-139.

[237] Raask, E. Mineral impurities in coal combustion: behaviour, problems, and remedial measures 1985. Hemisphere Publishing Corporation.

[238] Becidan, M; Lindberg, D; Sørum, L. Influence of MSW quality in the behaviour of alkali metals and selected trace elements during combustion − A thermodynamic equilibrium analysis. Submitted to Energy & Fuels.

10. APPENDIX (Papers)

NO$_x$ emission reduction by staged combustion in grate combustion of biomass fuels and fuel mixtures

Ehsan Houshfar [a], Øyvind Skreiberg [b,*], Dušan Todorović [c], Alexandra Skreiberg [b], Terese Løvås [a], Aleksandar Jovović [c], Lars Sørum [b]

[a] Norwegian University of Science and Technology (NTNU), Department of Energy and Process Engineering, Kolbjørn Hejes vei 1B, NO-7491 Trondheim, Norway
[b] SINTEF Energy Research, Postboks 4761 Sluppen, NO-7465 Trondheim, Norway
[c] University of Belgrade, Faculty of Mechanical Engineering, Kraljice Marije 16, 11000 Belgrade, Serbia

ARTICLE INFO

ABSTRACT

NO$_x$ and N$_2$O emissions have been investigated for different pelletized biomass fuels and fuel mixtures thereof both with and without air staging in a grate fired multi-fuel reactor. The fuels investigated are wood, demolition wood and coffee waste, and selected mixtures of these. The multi-fuel reactor was operated at close to constant operating conditions due to impactor (ELPI) measurements, with a total excess air ratio of about 1.6, and a primary excess air ratio of about 0.8 in the air staging experiments. The reactor set point temperature was held constant at 850 °C. NO$_x$ emission levels as a function of air supply mode and fuel nitrogen content are reported, showing a large NO$_x$ reduction potential, up to 91% and corresponding to less than 20 ppm NO$_x$ at 11% O$_2$ for a fuel containing about 3 wt.% fuel-N, using air staging. The effect on N$_2$O, however, is adverse at the selected set point temperature and optimum primary excess air ratio for NO$_x$ reduction. The effect of fuel mixing and fuel nitrogen content on the conversion of fuel nitrogen to NO$_x$ is also reported and discussed. Fuel mixing has a positive influence on the NO$_x$ emission level, but a negative influence on the overall conversion factor for fuel-N to NO$_x$ and N$_2$O.

© 2012 Elsevier Ltd. All rights reserved.

1. Introduction

As a response to continuously increasing levels of carbon dioxide release to the atmosphere, there has in recent years been considerable interest in renewable bioenergy sources from both research communities and the public. Biomass can be regarded as a close to CO$_2$ neutral alternative to fossil fuels if efficient and sustainable production and utilization of such fuels are secured [1].

For energy production, the most common energy carriers are solid fuels (coal, biomass, wastes, etc.). However, it is a concern that combustion of biomass will lead to high levels of nitrogen oxides emissions (NO$_x$; collective term for NO and NO$_2$) from oxidation of nitrogen in the fuel (fuel nitrogen) or potentially conversion of nitrogen in the air (air nitrogen). NO$_x$ are contributing to environmental problems such as acid rain, photochemical smog formation and depletion of stratospheric ozone [2]. Also nitrous oxide (N$_2$O) may be formed, having a strong greenhouse gas effect.

The formation of NO$_x$ happens through four main routes:

(1) Thermal mechanism (Zeldovich).
(2) Prompt mechanism (Fenimore).
(3) Nitrous oxide mechanism.
(4) Fuel-N conversion (Fuel-N mechanism).

The first three mechanisms are contributing to the conversion of air nitrogen to NO$_x$. Theoretical and experimental studies have shown that these three mechanisms are contributing much less to NO$_x$ formation in biomass combustion than fuel-N conversion. Regarding the first route, this is because the Zeldovich mechanism is predominant at temperatures greater than 1500 °C [2,3], while the temperatures during biomass combustion for power production are typically lower. Contributions from the prompt mechanism are mainly found for fuel rich and high temperature conditions which are also not relevant in biomass combustion. The nitrous oxide mechanism is of relative importance in very fuel lean and low temperature conditions. However, it has been shown that more than 80% of NO$_x$ emissions in pulverized coal combustion systems are coming from fuel-N conversion, where the remaining emissions are a result of the thermal mechanism [4]. In biomass combustion systems, fuel-N conversion is even more dominant due to the unfavorable temperature conditions in typical biomass furnaces for other than fuel-N conversion. The combustion of biomass is normally carried out in grate or fluidized bed combustors, with relatively low temperature, which increase the importance of fuel-NO$_x$, while pressurized combustion and high temperature in coal combustion can enhance the other NO$_x$ forma-

* Corresponding author. Tel.: +47 735 93993; fax: +47 735 92889.
E-mail address: oyvind.skreiberg@sintef.no (Ø. Skreiberg).

tion mechanism. Hence, the other mechanisms can be neglected from further studies of such biomass fired systems. As a conclusion, one should concentrate on fuel-N conversion to NO_x in order to effectively control NO_x formation in biomass combustion.

Fuel staging and air staging are two primary methods for decreasing the NO_x level from fuel-N conversion in biomass combustion. Fuel staging (and reburning) uses the principal of NO reduction in the second stage by adding more fuel or even a different fuel, e.g., more of the same solid fuel for fuel staging or hydrocarbons, such as natural gas for reburning. In the first stage, NO_x is formed because of lean combustion. In the second fuel stage, NO reduction occurs at reducing conditions, where air is added for complete combustion. Low NO_x levels can be achieved by fuel staging at lower temperatures than what is needed for air staging and the secondary fuel properties affect the NO_x emission level (better efficiency with smaller particle size and higher amount of volatile matter) [5,6].

Regarding air staging the mechanisms for reduction are different. Fig. 1 shows the principal idea of air staging [6]. Skreiberg et al. [7,8] showed that the primary excess air ratio, number of air stages, temperature, and residence time all affect the NO_x reduction level. However, the most important variable is the primary excess air ratio. Generally, increasing the excess air ratio increases the NO_x emission level. Yet an optimum primary excess air ratio exists. Increasing the number of air stages will decrease the potential fuel-N to NO_x conversion, but the effect of additional air stages may be very small. Temperature can decrease, increase, or has no effect on the NO_x emission level, depending on the temperature range applied to the reactor, and finally there is an optimum/sufficient residence time for optimum fuel-N conversion to N_2. Large and modern grate fired boilers are generally operated with an appropriate excess air ratio, and consequently under favorable combustion conditions, which result in low unburnt emissions [9].

The objective of this study is to investigate the effect of staged combustion on NO_x formation, as well as the effect on N_2O formation, in an air staged combustion process using three types of biomass including coffee waste (CW), demolition wood (DW), wood

pellets (WP), or combinations of these using a temperature controlled multi-fuel reactor. Only air staging is considered in the present study in order to focus on the effect of the fuel-N content on the air staging effect. Important additional parameters affecting the air staging effect are primary excess air ratio and temperature, whereof primary excess air ratio variations are the focus in this study, while temperature variations was the focus of another study
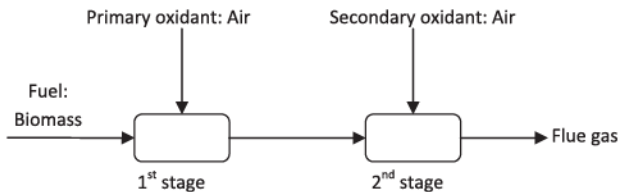
Fig. 1. Principal sketch of air staging in solid fuel combustion.
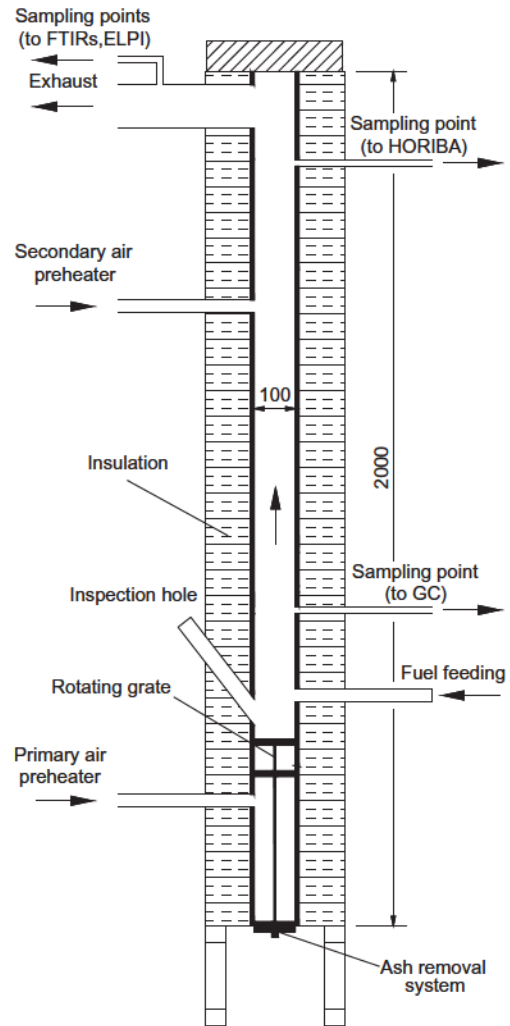
Fig. 2. Schematic drawing of the reactor.
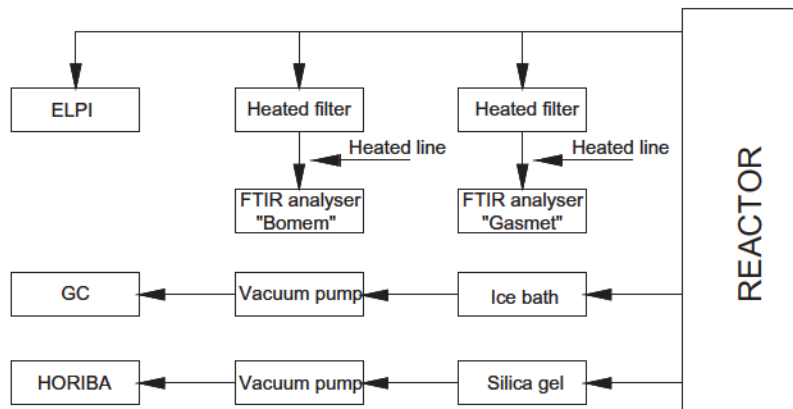
Fig. 3. Schematic diagram of the sampling line.

[10]. However, it should be noted that the results retrieved are generic, and making an experimental study based on scaling laws for a specific full-scale application has not been the intention. In this work the highest possible NO_x reduction is reached, however, the results obtained for the optimum point, etc. are general and can be used for commercial scale grate fired boilers.

2. Experimental apparatus and procedures

2.1. The multi-fuel reactor

The experiments were carried out in an electrically heated high temperature multi-fuel reactor. Its schematic drawing is presented in Fig. 2. The reactor has a ceramic inner tube with a diameter of 100 mm. The altogether 2 m high vertical tube consists of two such ceramic tubes, each 1 m long, which are connected with a ceramic socket. The ceramic tubes are made of non-porous and non-catalytic alumina.

The reaction section, located above the grate, is 1.6 m long, while the section below the grate is 0.4 m long. The reactor heating system is fitted inside the insulation shell and consists of four separate 0.5 m high heating zones of 4 kW each (16 kW in total) that enclose the ceramic tube.

The inlet air is preheated to the reactor temperature in external pre-heaters. The primary air is added under the grate (underfire air) and the secondary air is added above the grate (overfire air). The air flow is controlled by two high-precision digital mass flow controllers.

In addition, the combustion process on the grate can be observed through an inspection hole. The top and bottom of the reactor are insulated, but not heated, and both include detachable and insulated plates. The lower part of the multi-fuel reactor is the section containing the grate, which has two levels (10 cm apart), a primary grate and a final burnout grate, and an ash collection system with an ash bin. Both grates and the ash bin are made of Inconel. The two level design of the grate gives a potential fuel staging effect.

2.2. Experimental procedures

Two types of experiments are carried out: (1) experiments with air staging and (2) experiments without air staging. Only isothermal experiments were performed with a reactor temperature of 850 °C. The primary air and secondary air were also preheated to the same temperature. The total excess air ratio was about 1.6, and the primary excess air ratio was about 0.8 in the air staging experiments. The air flow has been held constant during the experiments. However, since the fuel was fed as pellets of different sizes and the position of the pellets on the grate after feeding varied, natural variations in primary and secondary excess air ratios are achieved. Consequently, the mentioned situation makes it possible to experimentally derive the effect of primary excess air ratio on the NO_x reduction potential by staged air combustion. It should be noted that data treatment has been carried out in a cautious manner to avoid non-reliable data. Significant transient effects are effectively eliminated by a filtering procedure while treating the experimental data.

Pellets are fed from a rotating battery of fuel containers using a water-cooled piston. The piston swiftly moves the fuel into the reactor where it falls onto the grate. Thereafter, the piston quickly returns to its starting position and the process is repeated. The feeding frequency was set to ensure a feeding rate of 400 g/h.

The pellets are mainly combusted on the upper (primary) grate. The pellets are gradually moved from the fuel-feeding inlet to a slot leading to the second (final burnout) grate by rotating blades.

Each grate has two rotating blades with a rotational speed of 3 min. Final burnout takes place on the second grate before the ash is moved by the rotating blades to a slot from where it falls into the ash bin. At the bottom of the ash bin another rotating blade is placing the ash into an ash tube. The gas residence time between the grate levels is in the range of 1–2 s. The residence time of the fuel in the reactor is high due to the low inlet air flow velocity (ca. 0.04–0.07 m/s). According to the given dimensions and flow velocity, the total gas residence time in the primary zone (90 cm) and the secondary zone (60 cm) is about 19–35 s.

2.3. Gas sampling and analysis

Both the reactor flue gas composition and the composition of the fuel gas in the primary zone as well as the particle emission size distribution are continuously monitored. A schematic diagram of the sampling lines is shown in Fig. 3.

For gas analysis in the primary zone, a Varian CP-4900 microgas chromatograph (GC) is used. A stainless steel probe with an outer diameter (OD) of 10 mm and an inner diameter (ID) of 8 mm is used for the gas sampling. The sampled gas passes first through a tar, water, and particle ice-cooled trap consisting of a steel container filled with glass wool and with a glass microfiber paper filter. The sampling gas flow rate is about 1 L/min. The GC is

Table 1
Proximate analysis of pellets (wt.%).

Pellets	Ash (dry basis)	Volatile (dry basis)	Fixed carbon (dry basis)	Moisture (as received)	HHV (MJ/kg, dry basis)
Wood (WP)	0.2	85.43	14.37	6.5	20.63
Demolition wood (DW)	3.73	77.27	19	8.1	20.54
Coffee waste (CW)	5.8	76.17	18.07	17.53	22.20
Mixtures of pellets (calculated, except for moisture)					
1/2 WP-1/2 DW	1.97	81.35	16.69	6.78	20.62
1/2 WP-1/2 CW	3.00	80.80	16.22	8.76	21.36
1/2 DW-1/2 CW	4.77	76.72	18.54	12.72	21.24
2/3 WP-1/3 CW	2.07	82.34	15.60	11.35	21.08
1/3 WP-2/3 CW	3.93	79.26	16.84	8.02	21.55
1/3 WP-1/3 DW-1/3 CW	3.24	79.62	17.15	24.53	21.04

Table 2
Ultimate analysis of pellets (wt.% dry ash free basis).

Pellets	C	H	O	N	S	Cl
Wood (WP)	51.22	6.07	42.54	0.14	0.03	0.02
Demolition wood (DW)	50.59	6.09	41.65	1.59	0.075	0.113
Coffee waste (CW)	52.9	6.47	37.64	2.8	0.187	0.038
Mixtures of pellets (calculated)						
1/2 WP-1/2 DW	50.91	6.08	42.11	0.85	0.052	0.065
1/2 WP-1/2 CW	51.98	6.25	40.33	1.34	0.101	0.028
1/2 DW-1/2 CW	52.01	6.06	39.21	2.58	0.137	0.085
2/3 WP-1/3 CW	51.93	6.06	40.8	1.14	0.08	0.027
1/3 WP-2/3 CW	52.79	6.04	38.68	2.35	0.141	0.036
1/3 WP-1/3 DW-1/3 CW	51.72	6.07	40.45	1.67	0.097	0.061

equipped with two TCDs (Thermal Conductivity Detector) with a detection limit of 1 ppm, and double injectors, each connected to a separate column. The first column is a 10 m long PoraPLOT Q type, with an inner diameter of 0.25 mm, and 10 μm film thickness produced by Varian Inc., and uses helium as carrier gas. This column is used for the separation of CO_2, CH_4, $C_2H_2 + C_2H_4$, and C_2H_6. The second column is a 20 m long CP-Molsieve 5A PLOT, with an inner diameter of 0.25 mm and 30 μm film thickness produced by Varian Inc., and uses argon as carrier gas in order to be able to detect H_2. This column is able to quantify H_2, O_2, N_2, CH_4, and CO. The GC has a sampling time of approximately 2 min.

The exhaust gases are quantified online with two Fourier transform infrared (FTIR) analyzers: a Bomem 9100 and a Gasmet DX-4000. The FTIRs are used to quantify H_2O, CO_2, CO, NO, N_2O, NO_2, SO_2, NH_3, HCl, HF, CH_4, C_2H_6, C_2H_4, C_3H_8, C_6H_{14}, CHOH, HCN, and O_2 (Gasmet) and CO, NO, NO_2, N_2O, SO_2, NH_3, HCl, HF, CH_4, C_2H_6, C_3H_8, C_4H_{10}, H_2O, and CO_2 (Bomem). Extracted gases are passing through heated filters and heated lines, before reaching the FTIRs. Stainless steel probes with an OD of 10 mm and an ID of 8 mm are used for sampling. Sampling positions are located in the stack.

The Bomem 9100 FTIR has two cells which operate at 176 °C. Only the larger cell is used; it has an optical path length of 6.4 m and is equipped with a TGS (Triglycine Sulfate) detector with a maximum resolution of 1 cm^{-1}.

The Gasmet DX-4000 FTIR has an integrated zirconia O_2 analyzer. The instrument is equipped with a cooled MCT detector (Mercury Cadmium Telluride, liquid-N_2 cooled) and has a maximum resolution of 4 cm^{-1}. The sampling line and cell are heated at 180 °C. The cell volume is 0.4 L and the optical path length is 5 m.

Some flue gas is also extracted through a sampling point near the top of the reactor. An Inconel probe with a 6 mm OD and a 4 mm ID is used for sampling. The gas first passes through silica gel and is thereafter led to a HORIBA analyzer using a vacuum pump. The sampling rate is 0.4 L/min. The HORIBA PG-250 is a portable stack gas analyzer that can simultaneously measure up to five separate gas components. The HORIBA PG-250 uses non-dispersive infrared (NDIR) absorption to quantify CO, SO_2, and CO_2, cross-modulation ordinary pressure chemiluminescence to measure NO_x, and a galvanized Zr cell for O_2 measurements. The sampling
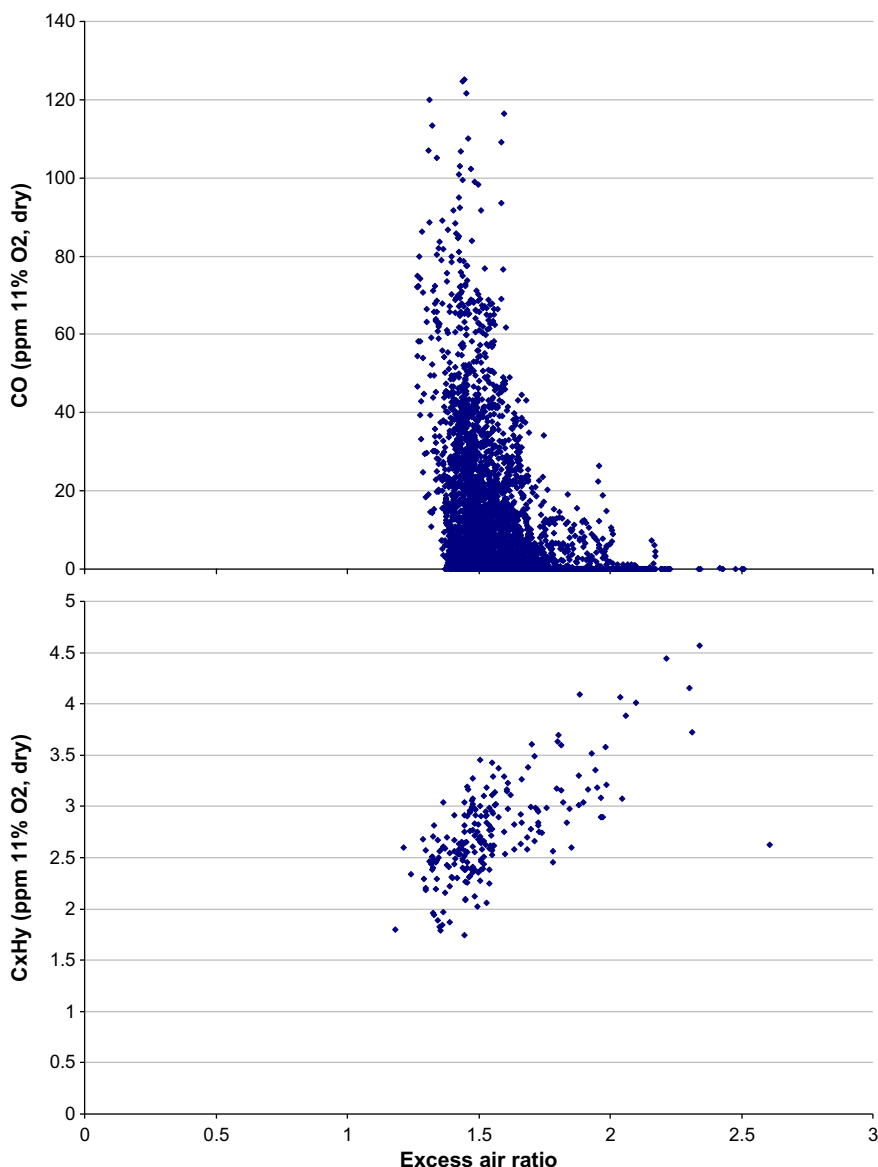
Fig. 4. Typical CO and hydrocarbons (C_xH_y) emission trends as a function of total excess air ratio (results from non-staged DW combustion).

unit comprises a filter, a mist catcher, a pump, an electronic cooling unit, and a NO_2 to NO converter.

Bottom ash sampling and analysis were also carried out. These measurements and results are in this work only used for carbon burnout control and will not be further explained or discussed here.

Temperature is measured in the reactor at several heights. Furthermore, additional thermocouples are used to control and protect the heating elements of the reactor from overheating. Six (logging) + four (control) + four (protection) type S thermocouples are installed in the reactor furnaces. The preheating units have separate control systems. The temperatures are also monitored in the flue gas channel with four type K thermocouples. Two are situated on the outer channel surface, between the insulation and the outside wall of the channel, and two inside the channel.

The experimental setup with its advanced monitoring and control systems as well as the online and offline analytical methods gives a good picture of the thermal process and its products.

2.4. Biomass characteristics and experimental matrix

Staged and non-staged experiments are carried out with four kinds of pellets: (1) wood (WP), (2) demolition wood (DW), (3) coffee waste (CW), and (4) six mixtures of these fuels. The proximate analysis of the pellet samples are shown in Table 1. Moisture, VM, and ash content are measured using ASTM E871 (50 g, 103 ± 2 °C, 24 h), ASTM E872 (1 g, 950 °C, 7 min), and ASTM D1102 (2 g, 580–600 °C, 4 h) standards, respectively, and the fixed carbon is calculated by difference to 100%. Three samples are analyzed from different parts of the pellets to get repeatable analyses, showing that the fuel was homogenous. The ultimate analyses of the pellets are shown in Table 2, where the nitrogen content in the fuel will be important in the following discussion. For ultimate analysis, all the samples have been dried in a vacuum exsiccator over phosphorus pentoxide prior to analysis. The determination of C/H/N/S is performed using the "EA 1108 CHNS-O" method provided by the Carlo Erba Instruments elemental analyzer. The method is adjusted for sample amounts of 2–10 mg and performs with an uncertainty within 0.3 wt.% as required for confirmation of assumed chemical composition. The operation range covers the content from 100 to 0.1 wt.%; sulfur determination is in the concentration range of 1.0–0.01 wt.% and the uncertainty is estimated to be 0.02 wt.% for C/N/S/Cl. The heating value is calculated based on the elemental composition.

Pellets were obtained as cylindrical extrudates, with a fixed diameter of 6 mm and a variable length of 5–15 mm and they were only air-dried before they were used for experiments.
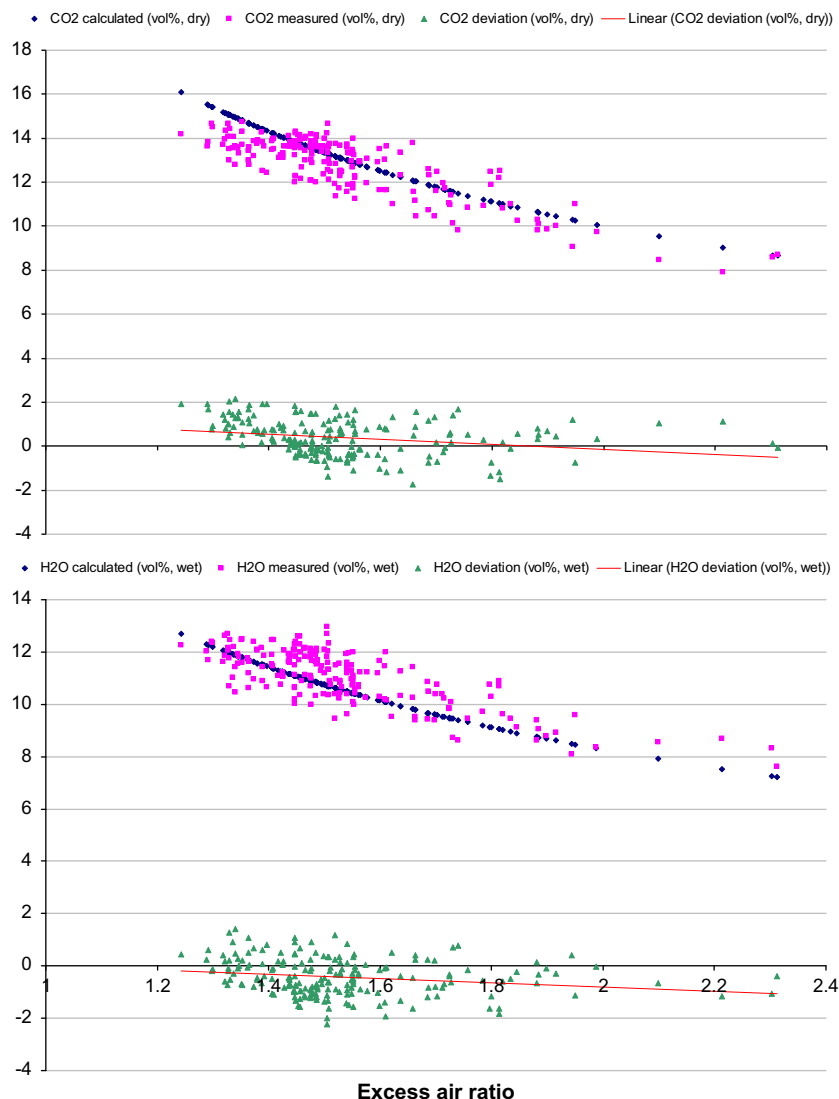
Fig. 5. Carbon and hydrogen balance check (results from non-staged DW combustion).

3. Results and discussion

3.1. Combustion quality, measurement accuracy, and experimental reproducibility

Because of the relatively long reactor residence time (19–35 s) and the chosen reactor temperature (850 °C), the amount of unburnt gases was low (typically below 50 ppm CO at 11% O_2 in dry flue gas). However, an initial stabilization period and fuel feeding fluctuations during close to constant operating conditions introduced also periods with significantly lower excess air ratios than the target value of 1.6, where the CO emission level increased to typically 200 ppm at 11% O_2 in dry flue gas. Fig. 4 shows the CO and C_xH_y emission levels as a function of total excess air ratio for the non-staged experiment with demolition wood pellets. As shown in the upper graph of Fig. 4, at low total excess air ratios, the probability of CO emission is high while at total excess air ratios greater than about 1.6, the CO emission is negligible. The explained behavior was typical for all the experiments regardless of fuel. The combined emission levels of hydrocarbons, C_xH_y, were typically below 5 ppm at 11% O_2 in dry flue gas, with the highest values found at the highest total excess air ratios, as shown in Fig. 4. The increasing trend of C_xH_y emission with total excess air ratio here is again typical for all fuels. The increase in C_xH_y emissions can in principle originate from several sources. Affecting parameters on the hydrocarbons emissions from a reactor are not only temperature, but also residence time, mixing condition and excess air ratio. In many cases, there exists an optimum excess

air ratio at a sufficient temperature to minimize hydrocarbon emissions. The increased C_xH_y emissions with increasing excess air ratio are most probably related to a combination of decreased local combustion temperature and residence time on the fuel bed. Additionally, a high level of air could result in the quenching of combustion reactions and hence increases the hydrocarbon emissions [11]. Levels of NH_3, HCN, and HF were within the measurement uncertainty level of the two FTIR analyzers, and will not be considered further.

All essential gas species for this study could be measured with good measurement accuracy. The two FTIR analyzers also showed good correspondence with regards to all essential gas species for this study.

The experimental reproducibility was tested by reruns of the wood pellets and the demolition wood pellets experiments with and without air staging, showing good reproducibility capability of the experimental setup, including the NO_x and the N_2O emission levels.

All experiments were checked with respect to carbon and hydrogen balance using both the Horiba analyzer and the Gasmet FTIR. Data points which (1) did not satisfy a maximum deviation between the calculated and measured levels of CO_2 and (2) were clearly influenced by fast transient conditions were removed from the results. This is because these data points were not reliable or not representative respectively for a close to continuous and constant combustion process. Fig. 5 shows the carbon and hydrogen balance as a function of total excess air ratio for the non-staged experiment with demolition wood pellets.
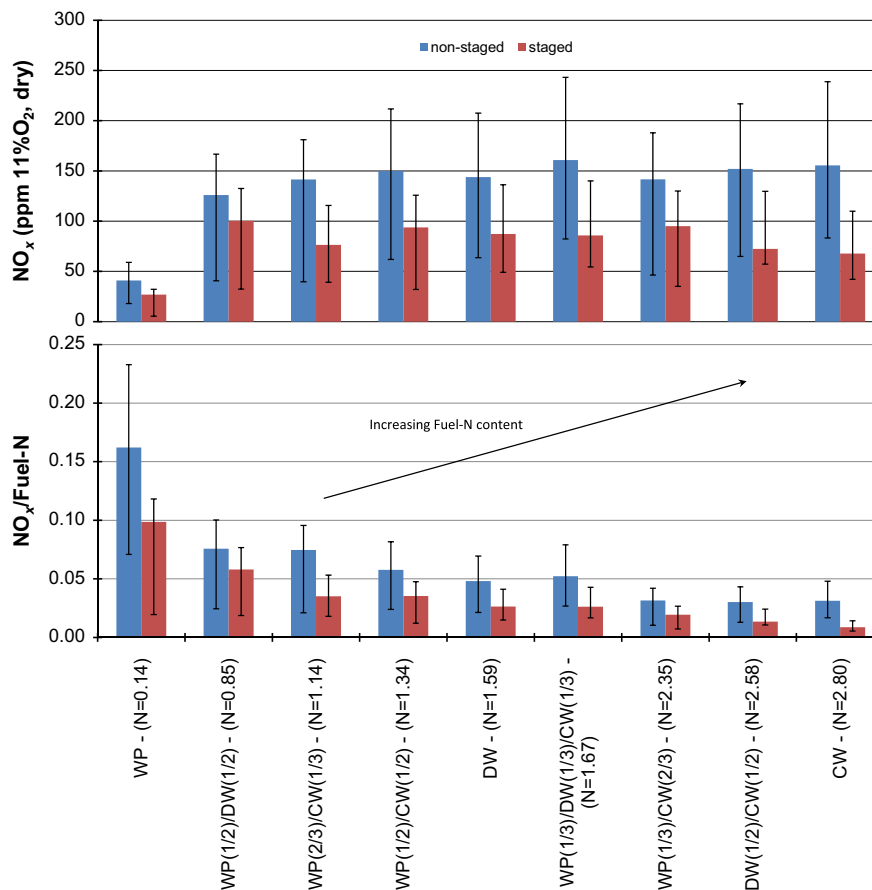
Fig. 6. Mean, minimum, and maximum NO_x emissions and NO_x/Fuel-N for staged and non-staged combustion (mixture fractions and fuel-N content (daf) in brackets).

3.2. NO_x emissions – staged versus non-staged

Mean, minimum, and maximum NO_x emissions as a function of the fuel-N content (ppm at 11% O_2 in dry flue gas) are shown in Fig. 6 for both staged and non-staged combustion. The NO_2 fraction of the NO_x was found to be insignificant at all conditions. A large NO_x reduction potential can be seen for staged combustion. An average NO_x reduction of 20–56% was found for the different fuels and fuel mixtures. The optimum NO_x reduction is significantly higher, at the optimum primary excess air ratio, as will be discussed in Sections 3.6 and 3.7. In addition, the fuel-N to NO_x conversion factor is shown in Fig. 6. A clear trend can be seen in this figure which shows considerable decrease in the total fuel-N conversion factor toward NO_x with increased fuel-N content. The lower conversion of fuel nitrogen in the fuels with higher amount of nitrogen (e.g., coffee waste) can be explained by formation and reduction of NO_x precursors. NH_3 is preliminary formed from the conversion of volatile nitrogen. Afterwards, the formed NH_i radicals (NH_3, NH_2, or NH) can be oxidized to form NO or react with NO (which is also created in the conversion of volatile nitrogen) to form molecular nitrogen, N_2. It should be noted that the latter reaction is the reaction which happens in staged combustion technology and SNCR to reduce NO_x. The same procedure can happen for HCN as the second NO_x precursor. Combustion of fuels with high nitrogen content, results in high concentrations of NH_3 and HCN [12,13]. This environment will strengthen the second reaction path (i.e., reaction of precursors with NO) and hence higher fuel-N conversion to N_2, which corresponds to a lower NO_x/Fuel-N ratio. On the other side, heterogeneous reactions in the conversion of char nitrogen to NO should be taken into account, even though it has less effect on the total NO_x.

3.3. N_2O emissions – staged versus non-staged

Mean, minimum, and maximum N_2O emissions as a function of the fuel-N content (ppm at 11% O_2 in dry flue gas) are shown in Fig. 7 for both staged and non-staged combustion. As in the previous case, the fuel-N to N_2O conversion factor is also shown. For N_2O, no emission reduction potential can be seen for staged combustion. On the contrary, an increase in the N_2O emission level was observed. An average N_2O increase of 18–288% was found for the different fuels and fuel mixtures. The increase in N_2O at optimum NO_x reduction conditions (optimum primary excess air ratio) is significantly higher, as will also be discussed in Sections 3.7 and 3.8. The N_2O formation and reduction in biomass combustors are discussed and investigated earlier [12,14–16]. The major global reaction pathways for fuel nitrogen conversion toward NO and N_2O depend on operating conditions [17,18].

3.4. Fuel influence on NO_x and N_2O emission levels

As Figs. 6 and 7 show, there is a significant fuel influence on the NO_x and N_2O emission levels and the conversion factor for fuel-N to NO_x and N_2O, both for staged and non-staged combustion. This is at otherwise similar conditions mainly due to the N-content in the fuel. Increasing fuel-N content will increase the NO_x emission level. However, the conversion factor for fuel-N to NO_x will decrease with increasing fuel-N content, as shown in Fig. 8. This effect is due to gas
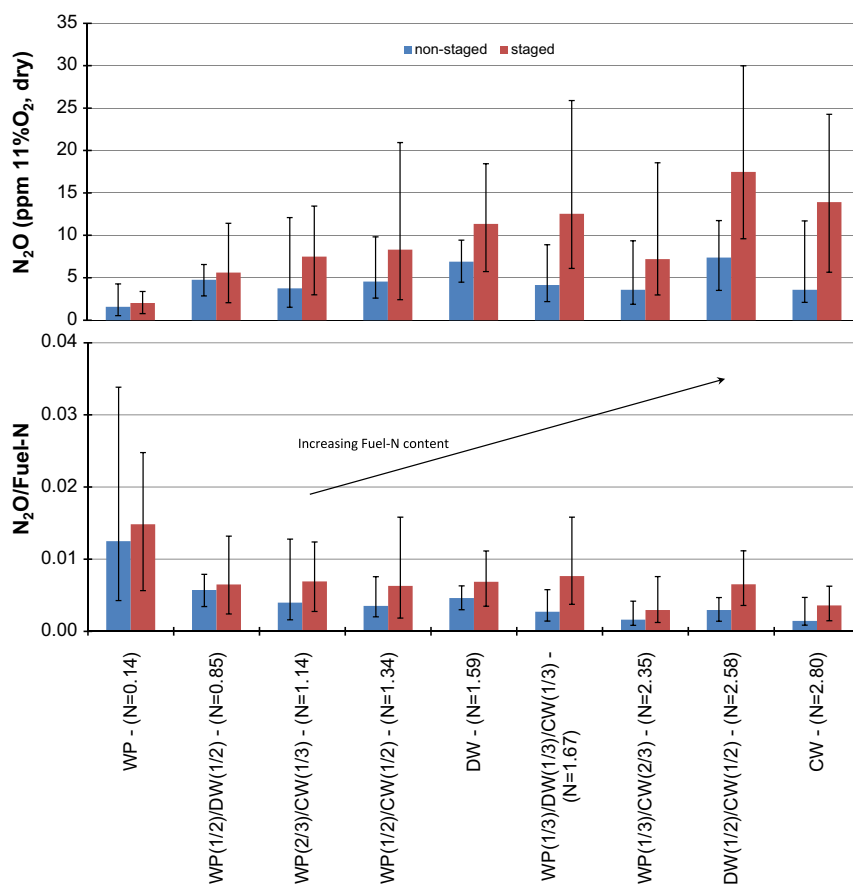
Fig. 7. Mean, minimum, and maximum N_2O emissions and N_2O/Fuel-N for staged and non-staged combustion (mixture fractions and fuel-N content (daf) in brackets).
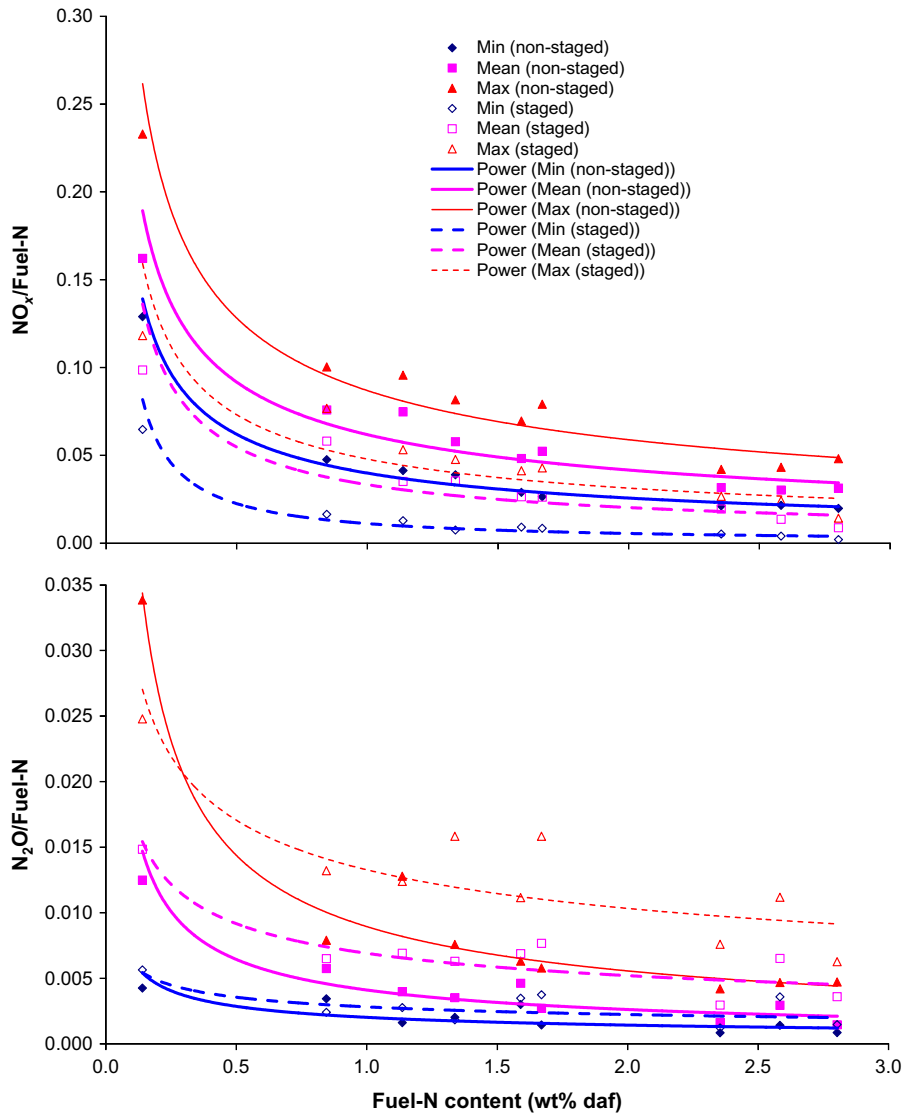
Fig. 8. Fuel-N influences on conversion factors for fuel-N to NO_x and N_2O for staged and non-staged combustion.
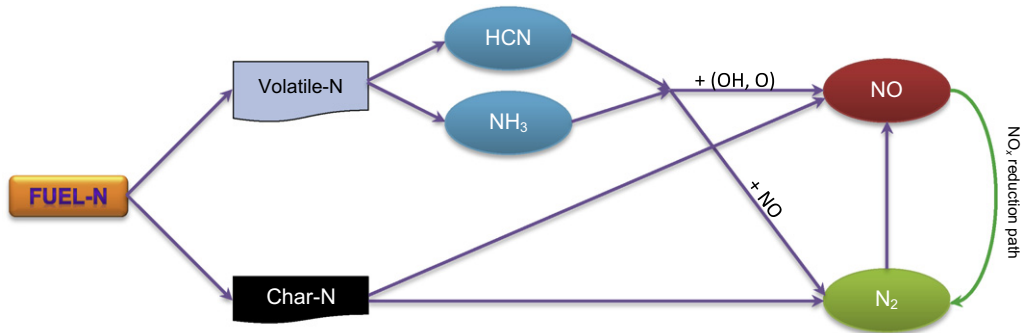

Fig. 9. Simplified diagram of fuel-N conversion (NO formation and reduction).

phase chemical kinetics, i.e., the reduction of fuel-NO_x precursors mainly through reaction between two intermediate nitrogen species, forming molecular nitrogen [19]. A simplified reaction path diagram for NO_x formation and reduction in biomass combustion is presented in Fig. 9. The N_2O emission level is also significantly

dependent on the fuel-N content, as also can be seen in Fig. 8. The shape of the curves means that NO_x emissions increase, but not linearly, with increasing fuel-N content. An example is the first and second point for non-staged combustion where the fuel-N content increases from 0.14 to 0.85 (6 times), while NO_x/Fuel-N decrease

from about 0.24 to 0.10 (about 2.4 times). For higher fuel-N content, the decrease becomes less exponential.

3.5. Fuel mixing effect on NO$_x$ and N$_2$O emission levels and fuel-N conversion factors

Fuel mixing has a positive influence on the NO$_x$ and N$_2$O emission levels (ppm), but a negative influence on the overall conversion factor for fuel-N to NO$_x$ and N$_2$O. The average conversion factor for fuel-N to NO$_x$ and N$_2$O trends shown in Figs. 6 and 7, respectively, can be modeled by simple exponential functions, as a function of the fuel-N content. From these trends one can estimate the NO$_x$ and N$_2$O conversion factors for various fuel mixtures. A mixture of e.g., wood and coffee waste will get an increased conversion factor compared to the fuel with the highest fuel-N content (coffee waste), while it will be lowered even more for the fuel with the lowest fuel-N content (wood). However, when comparing the option of combusting the fuels in separate boilers compared to mixing them in one boiler, the total NO$_x$ and N$_2$O emission level (kg) will theoretically always increase in the case of fuel mixing because of the exponential increase in the fuel-N to NO$_x$ and N$_2$O conversion factors with decreasing fuel-N content.

3.6. Temperature influence on NO$_x$ and N$_2$O emission levels

The experiments were run at constant reactor temperature. However, earlier experiments in a similar reactor [20] showed no significant temperature dependency on the NO$_x$ emission level for non-staged conditions in the temperature range 750–900 °C, but as expected a strong temperature dependency on the N$_2$O emission level, with maximum N$_2$O emission levels at about 850 °C. Hence, the N$_2$O emission levels reported in this study can be expected to be close to the maximum values, considering the temperature influence.

3.7. Primary excess air ratio influence on NO$_x$ and N$_2$O emission levels

Fig. 10 shows the primary excess air ratio, represented by the O$_2$ need of the measured unburnt primary gas species (H$_2$, CO, CH$_4$, C$_2$H$_2$, C$_2$H$_4$, and C$_2$H$_6$) for stoichiometric combustion, influence on NO$_x$ and N$_2$O emission levels for staged combustion of CW. Clearly, there is a correlation between the amount of unburnt primary gas species and the conversion of fuel-N to NO$_x$. Decreasing O$_2$ need until a certain point gives a decreasing fuel-N to NO$_x$ conversion factor. Hence, these results show that there must exist an optimum primary excess air ratio for minimum conversion of fuel-N to NO$_x$. This optimum is related to chemical kinetics effects,
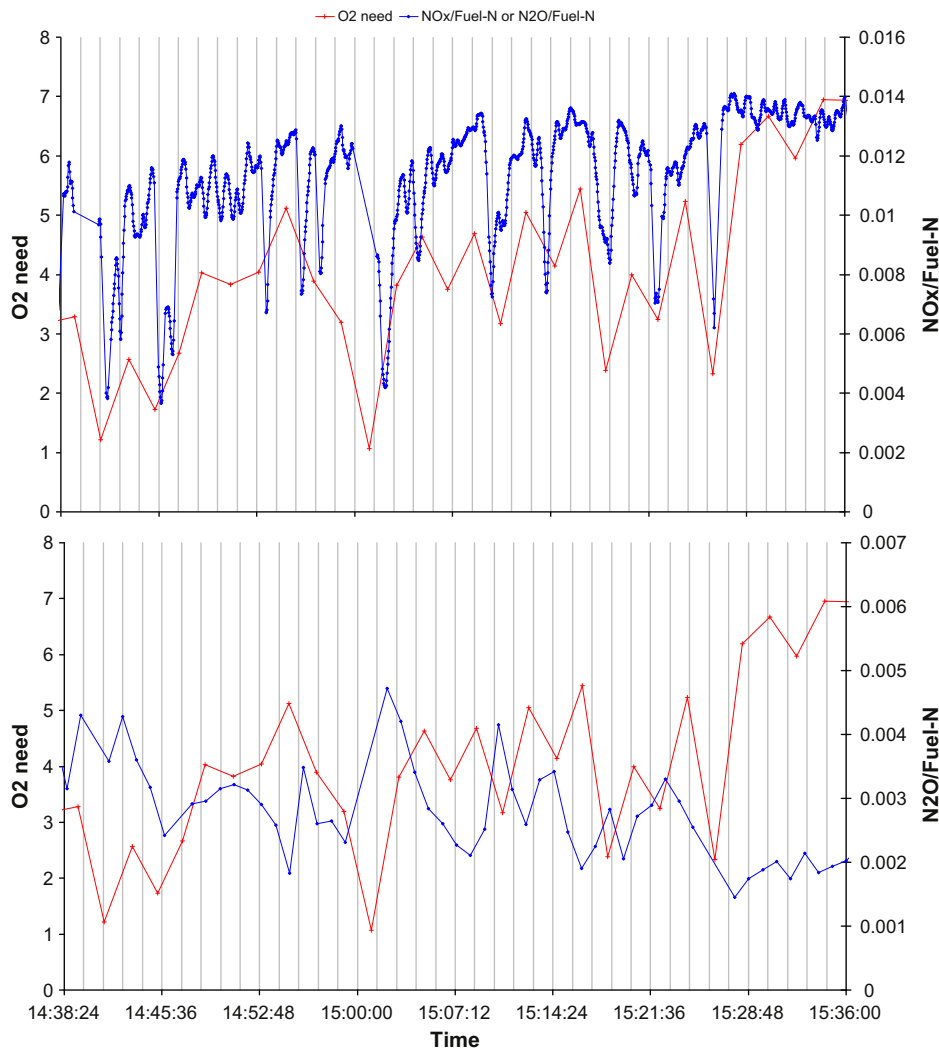
Fig. 10. Primary excess air ratio influences on NO$_x$ and N$_2$O emission levels for staged combustion of CW. O$_2$ need as vol.% O$_2$ needed for stoichiometric combustion of the measured primary gas composition.

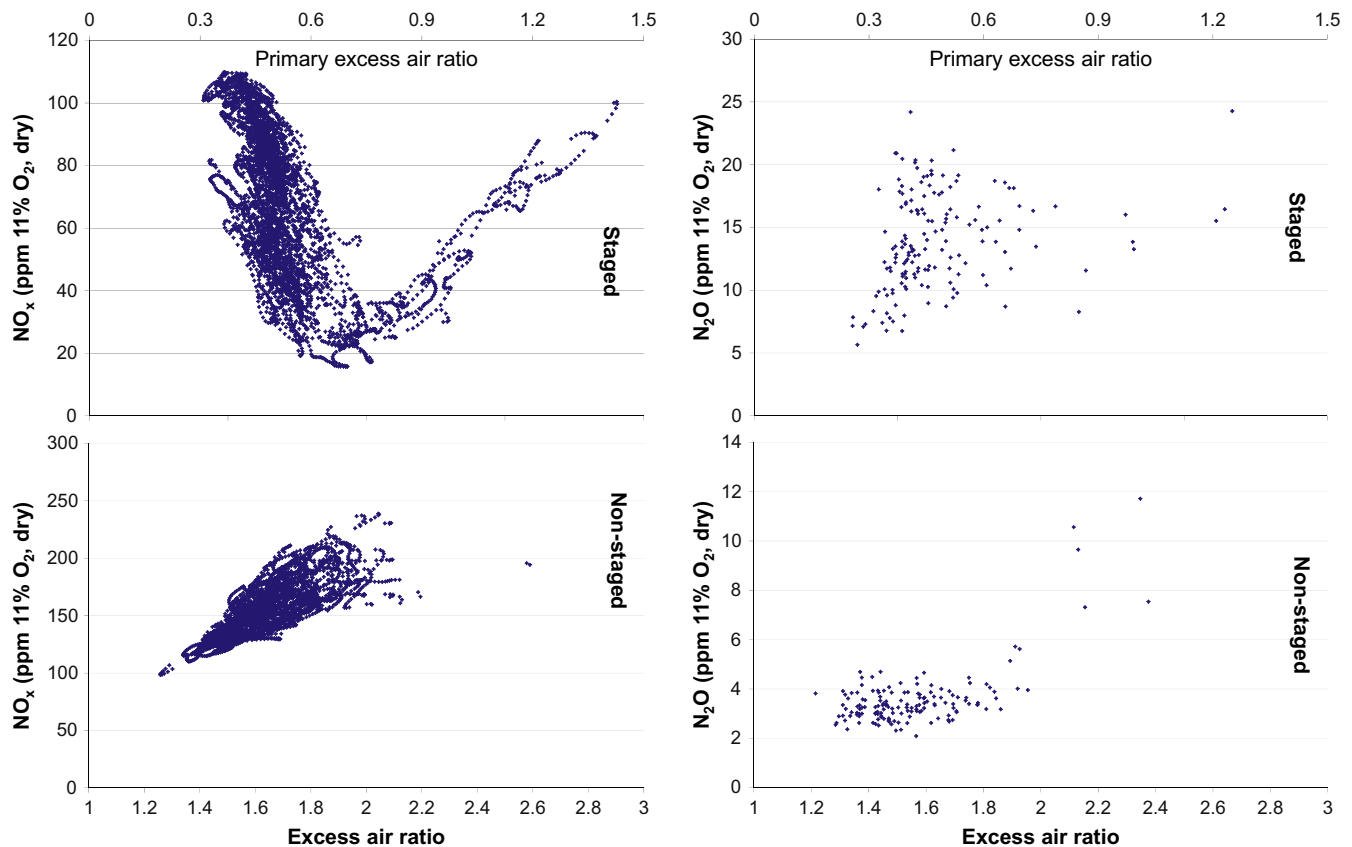**Fig. 11.** Total excess air ratio influence on NO_x and N_2O emission levels for staged and non-staged combustion of CW.

i.e., the radical pool in the primary gas zone [7,19] which is also dependent on the mixing conditions. For perfectly stirred reactor conditions, the optimum primary excess air ratio will be close to unity, while for plug flow reactor conditions, the optimum primary excess air ratio will be significantly lower than unity [7]. At the optimum primary excess air ratio, the highest conversion of fuel-N to N_2O is also found. However, the increased N_2O emission level does not significantly influence the optimum primary excess air ratio for minimum conversion of fuel-N to fixed nitrogen species.

3.8. Total excess air ratio influence on NO_x and N_2O emission levels

Fig. 11 shows the typical total excess air ratio influence on NO_x and N_2O emission levels for staged and non-staged combustion, for coffee waste pellets. The corresponding primary excess ratio is also shown for staged air combustion. As stated above, there exists an optimum overall/primary excess air ratio for minimum conversion of fuel-N to NO_x, which is directly visible also in Fig. 11. The residence time in such generic studies is not relevant once the reactor design and the experimental conditions yield sufficiently long residence times for NO_x reduction [7]. In this work the highest possible NO_x reduction is positively reached. The direct influence of the total excess air ratio is clearly seen in the non-staged experiments, with increasing NO_x emission level with increasing total excess air ratio. Increasing NO_x with increasing excess air ratio in conventional burners (non-staged combustion) is due to the higher availability of oxygen at higher excess air ratios. This promotes the reaction of nitrogen containing species with O_2 and O and OH radicals and hence formation of NO. The effect on N_2O is less clear, but with a trend of increasing

N_2O emission levels with increasing total excess air ratio. The N_2O emission levels are significantly higher for the staged experiments.

Fig. 12 shows the optimum NO_x reduction potential of staged combustion compared to the non-staged combustion, at the optimum primary/total excess air ratio for staged combustion. It can be explained as follows: In the first stage, primary air is added for devolatilization of the volatile fraction of the fuel, resulting in a fuel gas consisting mainly of CO, H_2, C_xH_y, H_2O, CO_2 and N_2. In addition to the major species, small amounts of NH_3, HCN and NO will be formed from the fuel-N content. The key factor here is the distribution of nitrogen containing species, which is regulated by the level of oxygen in the primary zone, and a sufficient residence time in the primary (reduction) zone. In the second stage, sufficient secondary air is supplied to ensure a good burnout and low emission levels from incomplete combustion. If the primary excess air ratio is very low, i.e., very low availability of oxygen, just HCN and NH_i will appear in the first stage and NO will not be formed, i.e., little reduction will take place in the primary zone. Therefore HCN and NH_i will react with added O_2 in the second stage to produce NO_x. On the other hand, a very high primary excess air ratio will result in the oxidation of all pyrolysis gases due to high O_2 concentration. Therefore, much more NO will appear while no NH_i exist in the primary stage to go through the reduction path. As can be seen, a NO_x reduction of 54–91% is achieved for staged combustion. These are very good NO_x emission reduction results, and is a result of air staging and potentially to some extent fuel staging due to the two level design of the grate. However, at the optimum primary excess air ratio for NO_x reduction, emissions of N_2O are adversely affected, increasing the N_2O emission levels with 138–635%.
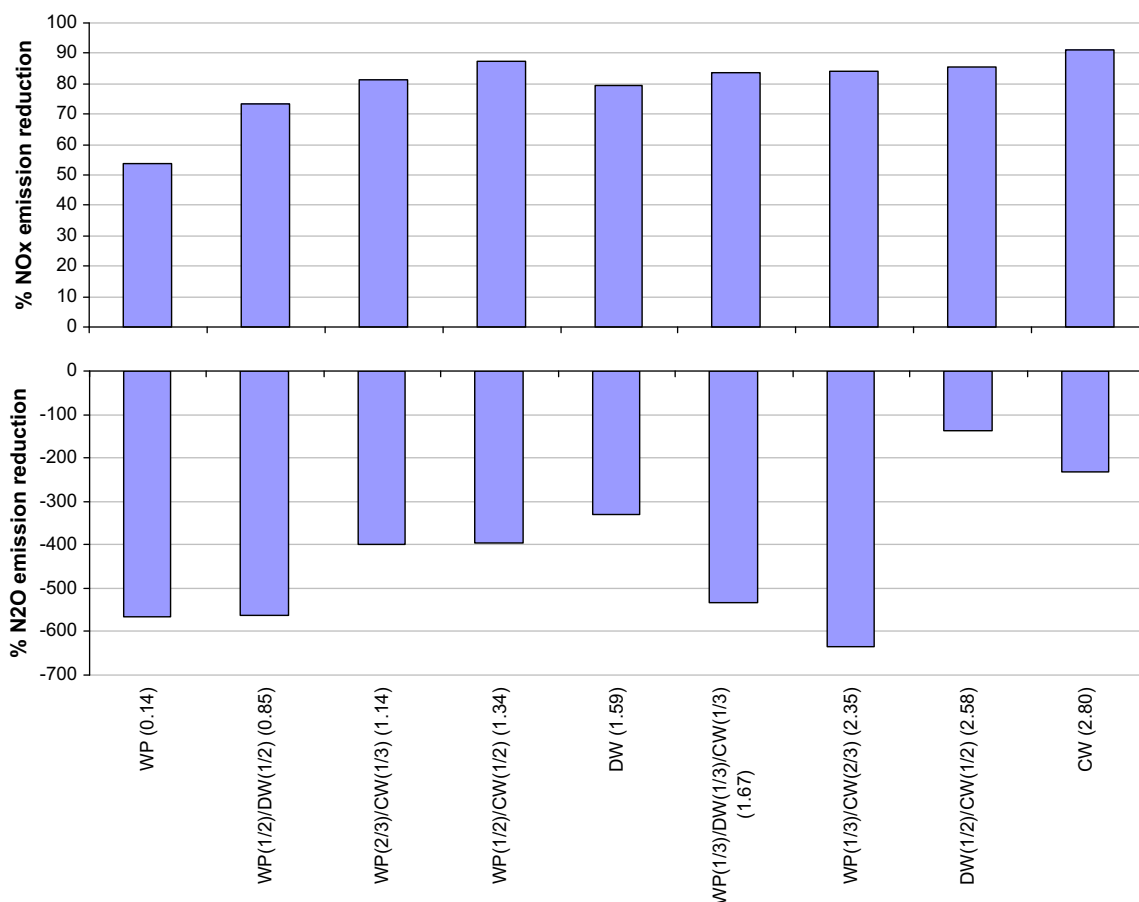
Fig. 12. Optimum NO$_x$ reduction potential for staged combustion compared to non-staged combustion, and the adverse effect on N$_2$O emissions at the optimum primary excess air ratio for NO$_x$ reduction.

4. Conclusions

NO$_x$, and N$_2$O, emissions have been investigated for different biomass fuels and fuel mixtures thereof as pellets both with and without air staging in a grate fired multi-fuel reactor at a constant reactor set point temperature of 850 °C. The fuels investigated are wood, demolition wood, and coffee waste, and selected mixtures of these. A large NO$_x$ reduction potential, up to 91% and corresponding to less than 20 ppm NO$_x$ at 11% O$_2$ for a fuel containing about 3 wt.% fuel-N, using air staging was found at the optimum primary excess air ratio. The effect on N$_2$O, however, is adverse at the selected set point temperature and optimum primary excess air ratio for NO$_x$ reduction, with an increase in the N$_2$O emission level of up to 635%. The NO$_x$ emission level increases with increasing fuel-N content, while the conversion factor for fuel-N to NO$_x$ decreases with increasing fuel-N content. Fuel mixing has a positive influence on the NO$_x$ emission level, but a negative influence on the overall conversion factor for fuel-N to NO$_x$ and N$_2$O.

Acknowledgements

References

[1] Berndes G, Baxter L, Coombes P, Delcarte J, Evald A, Hartmann H, et al. In: van Loo S, Koppejan J, editors. The handbook of biomass combustion and co-firing. London: Earthscan; 2008.

[2] Tariq AS, Purvis MRI. NO$_x$ emissions and thermal efficiencies of small scale biomass-fuelled combustion plant with reference to process industries in a developing country. Int J Energy Res 1996;20(1):41–55.

[3] Wünning JA, Wünning JG. Flameless oxidation to reduce thermal NO-formation. Prog Energy Combust Sci 1997;23(1):81–94.

[4] Glarborg P, Jensen AD, Johnsson JE. Fuel nitrogen conversion in solid fuel fired systems. Prog Energy Combust Sci 2003;29(2):89–113.

[5] Kicherer A, Spliethoff H, Maier H, Hein KRG. The effect of different reburning fuels on NO$_x$-reduction. Fuel 1994;73(9):1443–6.

[6] Salzmann R, Nussbaumer T. Fuel staging for NO$_x$ reduction in biomass combustion: experiments and modeling. Energy Fuel 2001;15(3):575–82.

[7] Skreiberg Ø, Becidan M, Hustad JE, Mitchell RE. Detailed chemical kinetics modelling of NO$_x$ reduction by staged air combustion at moderate temperatures. In: Bridgwater AV, Boocock DGB, editors. The science in thermal and chemical biomass conversion conference, 2004; Victoria, BC, Canada. Newbury, Berkshire, UK: CPL Press; 2006. p. 40–54.

[8] Skreiberg Ø, Glarborg P, Jensen AD, Dam-Johansen K. Kinetic NO$_x$ modelling and experimental results from single wood particle combustion. Fuel 1997;76(7):671–82.

[9] Johansson LS, Leckner B, Gustavsson L, Cooper D, Tullin C, Potter A. Emission characteristics of modern and old-type residential boilers fired with wood logs and wood pellets. Atmos Environ 2004;38(25):4183–95.

[10] Houshfar E, Skreiberg Ø, Løvås T, Todorović D, Sørum L. Effect of excess air ratio and temperature on NO$_x$ emission from grate combustion of biomass in the staged air combustion scenario. Energy Fuel 2011;25(10):4643–54.

[11] Mastral AM, Callén MS. A review on polycyclic aromatic hydrocarbon (PAH) emissions from energy generation. Environ Sci Technol 2000;34(15):3051–7.

[12] Winter F, Wartha C, Hofbauer H. NO and N$_2$O formation during the combustion of wood, straw, malt waste and peat. Bioresour Technol 1999;70(1):39–49.

[13] Abelha P, Gulyurtlu I, Cabrita I. Release of nitrogen precursors from coal and biomass residues in a bubbling fluidized bed. Energy Fuel 2007;22(1):363–71.

[14] Hämäläinen JP, Aho MJ. Effect of fuel composition on the conversion of volatile solid fuel-N to N$_2$O and NO. Fuel 1995;74(12):1922–4.

[15] Hao WM, Scharffe D, Lobert JM, Grutzen PJ. Emissions of N$_2$O from the burning of biomass in an experimental system. Geophys Res Lett 1991;18(6):999–1002.

[16] Gutierrez MJF, Baxter D, Hunter C, Svoboda K. Nitrous oxide (N_2O) emissions from waste and biomass to energy plants. Waste Manage Res 2005;23(2):133–47.
[17] Goel SK, Morihara A, Tullin CJ, Sarofim AF. Effect of NO and O_2 concentration on N_2O formation during coal combustion in a fluidized-bed combustor: modeling results. Symp (Int) Combust 1994;25(1):1051–9.
[18] Tullin CJ, Goel S, Morihara A, Sarofim AF, Beer JM. Nitrogen oxide (NO and N_2O) formation for coal combustion in a fluidized bed: effect of carbon conversion and bed temperature. Energy Fuel 1993;7(6):796–802.
[19] Skreiberg Ø, Kilpinen P, Glarborg P. Ammonia chemistry below 1400 K under fuel-rich conditions in a flow reactor. Combust Flame 2004;136(4):501–18.
[20] Skreiberg Ø, Sandquist J. Initielle multibrensel reaktor forsøk i KRAV prosjektet. Trondheim: SINTEF Energy Research, Energiprosesser; 2008. Report No.: TR A6766. Norwegian.

Effect of Excess Air Ratio and Temperature on NOx Emission from Grate Combustion of Biomass in the Staged Air Combustion Scenario

Ehsan Houshfar,[*,†] Øyvind Skreiberg,[‡] Terese Løvås,[†] Dušan Todorović,[§] and Lars Sørum[‡]

[†]Norwegian University of Science and Technology (NTNU), Department of Energy and Process Engineering, Kolbjørn Hejes vei 1B, NO-7491 Trondheim, Norway

[‡]SINTEF Energy Research, Postboks 4761 Sluppen, NO-7465 Trondheim, Norway

[§]University of Belgrade, Faculty of Mechanical Engineering, Kraljice Marije 16, 11000 Belgrade, Serbia

ABSTRACT: The combustion of biomass, in this case demolition wood, has been investigated in a grate combustion multifuel reactor. In this work a temperature range of 850−1000 °C is applied both for staged air combustion and nonstaged combustion of biomass to investigate the effects of these parameters on the emission levels of NOx, N_2O, CO, hydrocarbons (C_xH_y) and different other components. The composition of the flue gas is measured by four advanced continuous gas analyzers including gas chromatograph (GC), two Fourier transform infrared (FTIR) analyzers, and a conventional multispecies gas analyzer with fast response time. The experiments show the effects of staged air combustion, compared to nonstaged combustion, on the emission levels clearly. A NOx reduction of up to 85% is reached with staged air combustion. An optimum primary excess air ratio of 0.8−0.95 is found as a minimizing parameter for the NOx emissions for staged air combustion. Air staging has, however, a negative effect on N_2O emissions. Even though the trends show a very small reduction in the NOx level as temperature increases in nonstaged combustion, the effect of temperature is not significant for NOx and C_xH_y, neither in staged air combustion or nonstaged combustion, while it has a great influence on the N_2O and CO emissions, with decreasing levels with increasing temperature.

1. INTRODUCTION

Because of environmental problems and a significant decrease in the reserves of fossil fuels, the interest in using renewable energy carriers has become more and more widespread in recent decades. Figure 1 shows the share of different energy resources used by end users in the world in 2008.[1] Biomass, which is almost a CO_2-neutral carbon-based renewable energy source, is cheaper to utilize compared to the other sources of renewable energy, especially in the case of cofiring and combined heat and power (CHP) applications.[2] Thermal conversion of biomass, including combustion, gasification, and pyrolysis, is the most common method of extracting energy from biomass. Among the three mentioned technologies, combustion, which has been used for a long time as a source of heat for residential purposes, remains the leading technology also in recent years.

Life cycle analyses show that the most important environmental issue regarding emissions from wood combustion is NOx, contributing to almost 40% of the total emissions, including NOx, PM10, CO_2, SO_X, NH_3, CH_4, nonmethane volatile organic compounds (NMVOC), residues, and others.[3] The basis for this comparison is in relation to expected environmental impact points (EIP) of the specific emission according to the ecological scarcity method, applied for heating with wood chips. However, it is evident that the given data from any LCA analysis depends strongly on the valuation of the greenhouse gas effect since the ranking changes significantly as a result of the different CO_2 impacts of the fuels.[4] In this respect, much effort has been done to characterize biomass and reduce NOx emissions from the combustion of biomass and other solid fuels.[5,6] Two major approaches exist for NOx reduction, primary measures and secondary measures. The main difference is that primary measures prevent formation of NOx emissions, while secondary measures clean these emissions after their formation. Modifications to fuel properties and the combustion chamber and improvements to combustion technologies are examples of primary measures. One of the most important and widely used measures to reduce NOx in solid fuels combustion is staged combustion. Staged combustion, including staged air combustion and staged fuel combustion, can give a NOx reduction in the range of 50−80%.[4,7−10] The purpose of staged air combustion is to add primary air at a less than stoichiometric ratio, in order to devolatilize the volatile fraction of the fuel, resulting in a fuel gas consisting mainly of CO, H_2, C_xH_y, H_2O, CO_2, and N_2 and also small amounts of NH_3, HCN, and NOx from the fuel nitrogen content. If sufficient oxygen exists in the first stage, the fuel nitrogen intermediates will be converted to NOx (mainly NO), but shortage of oxygen will cause NO to act as an oxidant for CO, CH_4, HCN, and NH_i (with $i = 0, 1, 2, 3$) in the reduction zone, hence to reduce the nitrogen in NO and NH_i to molecular nitrogen, i.e., N_2, in reactions such as NO + NH_2 = N_2 + H_2O or NO + CO = CO_2 + $0.5N_2$.[4,11−13] NH_3 and HCN form in the pyrolysis stage of combustion depending on the temperature and fuel type, where ammonia is believed to be the most important N-species in the combustion of biomass, while HCN is more important for high-rank coals.[14−16] Ammonia that is formed in this stage is converted to radicals of NH_i. At high temperatures and fuel lean combustion, these radicals will be converted to NO, while at fuel rich conditions, N_2 will be the main product.[17] Thereafter sufficient air is added in the second

4643   dx.doi.org/10.1021/ef200714d | Energy Fuels 2011, 25, 4643–4654
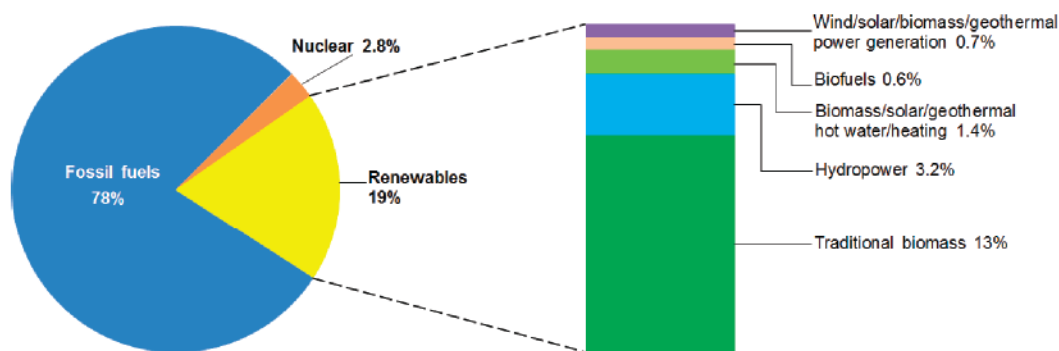
Figure 1. Renewable energy share of global final energy consumption, 2008.[1]

stage to ensure a good burnout and low emission levels from incomplete combustion.

The effect of excess air ratio, residence time, and temperature has previously been studied for a single wood particle in batch combustion, showing dependency of the NO level with excess air ratio and temperature simultaneously.[18] Also, previous work showed the effect of fuel type and cocombustion of biomass with natural gas on NO emissions when using two-stage combustion.[19] Fuel-N content and the conversion rate of NOx precursors (NH_3 and HCN) to NOx have been experimentally and numerically investigated for different solid biomass.[20−23]

Combined staged (CS) technology[10] is a method of NOx reduction including reburning, staged air combustion (AS), staged fuel combustion (FS), and selective noncatalytic reduction (SNCR).[24−26] Combined staged technology starts to reduce NOx emissions where the other methods are not sufficient. Studies showed that CS is more effective for NOx reduction, especially in the temperature range of 1000−1400 °C.[10] For temperatures below 850 °C, higher N_2O, lower NOx, and slightly higher CO emissions are reported for cocombustion of coal and woody biomass.[27] Another technique of primary measures for NOx reduction in biomass combustion is flue gas recirculation (FGR) which basically increases the total mass flux of the gases and decreases the temperature and the partial pressure of oxygen in the mixture.[28] It is proposed that in fixed-bed combustion of straw, the effect of FGR on NO reduction could be considerable.[29]

The present study aims to investigate the effect of temperature on the emission level, especially NOx, for a selected type of biomass, demolition wood (DW). Combustion of DW as a type of wood residue represents a large source of alternative energy, in addition to the fact that a waste disposal problem will also be solved. DW originates from many sources; therefore, it contains normally different undesirable components such as metals, paints, plastics, etc., which will raise the environmental impact of DW. Especially, the high nitrogen content, compared to wood, is the focus in this study. A series of experiments have been carried out for conventional combustion (nonstaged) and staged air combustion to study the effect of temperature variations, combustion technology, and excess air ratio. The work is a part of a wider study which has been carried out in the same reactor, investigating different operating parameters and fuels.[30]

In the next section a brief explanation of the experimental setup and test procedures is presented and the sampling devices and methodologies are described. Thereafter, the results are presented and discussed with respect to different variables, and finally conclusions are given.
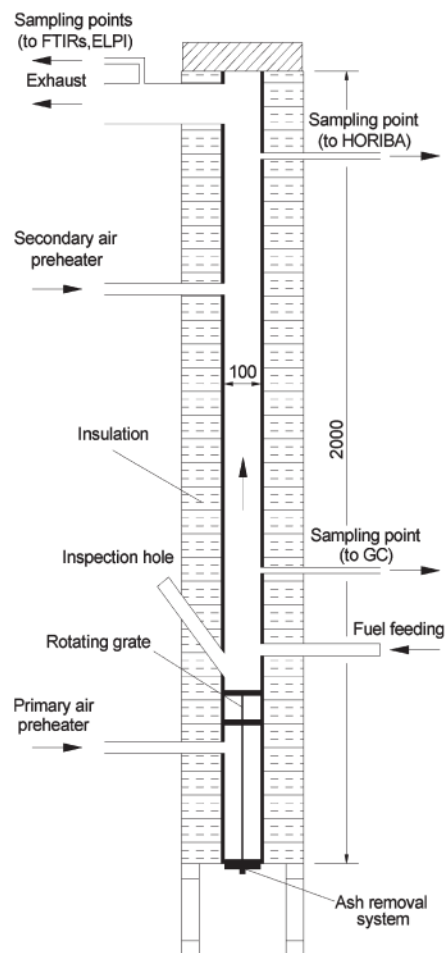

Figure 2. Schematic drawing of the reactor (the sizes are given in millimeters).

2. EXPERIMENTAL SECTION

2.1. Reactor Specifications. The reactor is shown in Figure 2. The reactor is installed vertically and has a total height of 2 m. The inner diameter is 100 mm. The reactor is made of ceramic material (alumina based) and has two reactor tube sections, each 1 m high. A rotating grate, with two grate levels, is placed 0.4 m from the bottom of the reactor, which means that the combustion zone is 1.6 m high. The two grate levels are 10 cm apart and there are rotating blades on each level that moves the unburnt fuel particles on the grates and from the upper grate to the second grate and from the second grate to the ash bin through a
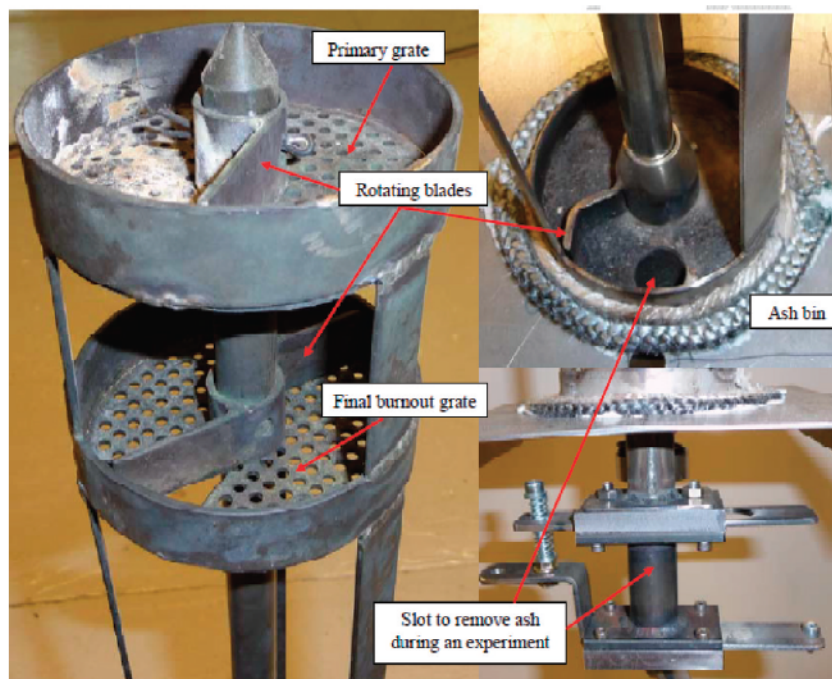
Figure 3. Design of two grates and ash bin.

slot in the grates. The rotational speed of the blades is about 3 min per revolution, which means that the residence time of each pellet on the grates is up to about 6 min, totally. This ensures complete burnout of the particles/char at the lower grate and that the ashes can be collected in the bottom of the reactor, i.e., in the ash bin. The grates and the ash bin are shown in Figure 3. A view glass is located just above of the upper grate to be able to see the combustion zone from the outside. The residence time of the fuel in the reactor is high, and the gas in the reactor has very low flow velocity (0.04−0.07 m/s). The secondary combustion zone ensures a residence time of several seconds and is hence in fact comparable to conventional combustion systems. According to the given reactor dimensions and velocity, the residence time for the primary zone (90 cm) is 13−23 s and for the secondary zone (70 cm) 10−18 s, giving a total residence time of 23−41 s. The outer surface of the reactor is insulated, and the reactor heating system has an effect of 16 kW, composed of four identical electric heaters with a height of 0.5 m.

The reactor can be heated up to 1300 °C, and the fuel feeding rate can be up to 0.5 kg/h. A pneumatic-vibration based feeding system is installed to ensure automatic fuel feeding at a set rate. Pellets are fed by a water-cooled moving piston into the reactor and immediately fall down on the upper grate. Air can be fed to the reactor in three stages (below the lower grate, above the upper grate (two inlets), and at one level higher up (two inlets)), up to 120 NL/min, totally. Five preheaters are installed, one for each air inlet stream, to heat the feeding air to the reactor temperature before entering the reactor. The air flow rate is controlled by mass flow controllers via a PC.

2.2. Sampling and Measurements. As shown in Figure 4, gas is extracted in four places to carry out analysis and further measurements. The flue gas composition is measured by means of three gas analyzers. In case of staged air combustion, a gas chromatograph (GC) is used to measure the gases in the primary section. The GC is sampling between the first and the second combustion stage and is a Varian CP-4900 Micro-GC. Sampling for the GC is made through an 8 mm diameter stainless steel probe, and the gas is passed through an ice bath to ensure removal of water, particles, and tars, in addition to reducing the temperature to an acceptable level for the GC. The sampling condition
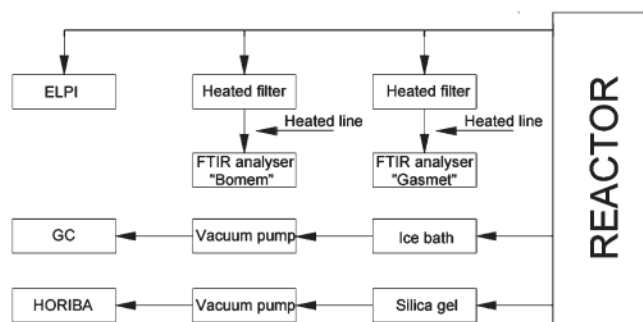

Figure 4. Schematic diagram of the sampling line.

is noncondensing gas of 0−40 °C and the maximum sample pressure is 200 kPa. The GC is equipped with two dual-channel micromachined thermal conductivity detectors (TCD), with a detection limit of 1 ppm for WCOT (wall-coated open-tubular) columns. The WCOT column is a column in which the liquid stationary phase is coated on the essentially unmodified smooth inner wall of the tube. The sample flow rate is 1 L/min and the sampling time interval is 2 min. Argon and helium are used in two columns, 10 and 20 m long, respectively. The first column measures CH_4, CO_2, C_2H_2 + C_2H_4, and C_2H_6 while the second column measures H_2, O_2, N_2, CH_4, and CO.

A Horiba multispecies gas analyzer PG-250 is sampling from the top of the reactor. It is capable of measuring five components, NOx, SO_2, CO, CO_2, and O_2, with the same methods used by a permanent continuous emissions monitoring system (CEMS). These include pneumatic nondispersive infrared (NDIR) for CO and SO_2, pyrosensor NDIR for CO_2, chemiluminescence (crossflow modulation) for NOx, and a galvanic cell for O_2 measurements. A vacuum pump is used to extract the sample gas at a flow rate of 0.4 L/min from the top of the reactor and passes it through a silica gel box and a filter to remove moisture and particles. The response time (T_{90}) of the analyzer is less than 45 s for NOx, CO, O_2, and CO_2 and less than 240 s for SO_2. The

Horiba analyzer is equipped with a drain separator unit (DS-200) and an electronic cooler unit.

Two Fourier transform infrared spectroscopy (FTIR) analyzers are also used to measure the gas composition in the exhaust gas. They do sampling at the same point, which allows for comparing different measurements for these species: H_2O, CO_2, CO, NO, N_2O, NO_2, SO_2, NH_3, HCl, HF, CH_4, C_2H_6, and C_3H_8. The Gasmet DX-4000 FTIR analyzer incorporates a spectrometer, a temperature controlled sample cell, and signal processing electronics. The sample cell is heated up to 180 °C which ensures that the sample stays in the gaseous phase even with high concentrations of condensable hydrocarbons. The measurement time is typically 60 s ,and the spectrometer resolution is 4 cm^{-1} at a scan frequency of 10 scans/s. The sample cell has a multipass fixed path length of 5 m and a volume of 0.4 L. To measure O_2, an optional oxygen sensor, based on a ZrO_2 cell, is attached to the analyzer. In total it can measure C_2H_4, C_6H_{14}, $CHOH$, HCN, and O_2 in addition to the above-mentioned 13 gases.

A Bomem MB 9100 FTIR analyzer is also used to measure common mutual species and C_4H_{10}. The measurement time is typically 80 s. A large cell, operating at 176 °C and equipped with a 1 cm^{-1} spectral resolution detector, was handling the analyses. Generally FTIR measurements of NO may introduce significant uncertainties. However, the NOx emissions reported in the results part are based on the Horiba analyzer, which is using the chemiluminescence technique. The N_2O measurements were made by the FTIR analyzers, and the reported values were measured by the Gasmet FTIR. The Bomem FTIR showed N_2O values close to the values measured by the Gasmet FTIR.

The temperatures at different levels in the reactor are measured by means of thermocouples and are monitored continuously to control and protect the furnace operation. These thermocouples are used to set and control the temperatures of the air preheaters and the reactor wall heaters during heat-up and during the experiment.

2.3. Experimental Procedures. Experiments are performed for nonstaged and staged air combustion. Four different temperatures are selected, 850, 900, 950, and 1000 °C. During each experiment, the temperature is kept constant for the reactor, primary air, and secondary air at the mentioned values. All the sampling devices are calibrated each day, before starting the experiments. Also the Gasmet FTIR calibration was performed daily by means of background spectra.

Pellets with a diameter of 6 mm and a length of 10−15 mm are fed by the automatic feeding system. The fuel feeding rate is set to 400 g/h. To have a precise composition of the fuel, during each run, three different samples at three different times are taken from the fuel feeding system to analyze the moisture content.

The total excess air ratio for nonstaged combustion is set to 1.6; however, the variation in the fuel feeding rate allows capturing a total excess air ratio range of 1.2−3, making it possible to see emission trends as a function of total excess air ratio. Each experiment has been carried out for at least 2 h at stable operating conditions.

For the staged air combustion experiments, the total excess air ratio is also set to 1.6, while the primary excess air ratio is set to 0.8, which means that 50% of the total air is fed at each stage. The air flow has been held constant during the experiments. However the variations in the fuel feeding rate cause natural variations in primary and secondary excess air ratios, since the fuel was fed as pellets and, depending on the length of the pellets and the position of the pellets on the grate after feeding, natural variations in the excess air ratio occurred. Therefore the mentioned situation makes it possible to experimentally derive the effect of variations in the primary excess air ratio on the NOx reduction potential by staged air combustion. Data treatment has been carried out in a cautious manner to avoid nonreliable data. Significant transient effects are effectively eliminated by a filtering procedure while treating the experimental data. This filtering procedure requires that the change in the excess air ratio per second is less than 0.01; otherwise, the

Table 1. Proximate Analysis of DW Pellets (wt %)

pellets	ash (dry basis)	volatile (dry basis)	fixed carbon (dry basis)	moisture (wet basis)
demolition wood (DW)	2.49	75.97	21.54	9.68−14.97

Table 2. Ultimate Analysis of DW Pellets (wt % Dry Ash Free Basis)

pellets	C	H	O	N	S	Cl
demolition wood (DW)	48.45	6.37	44.11	1.06	0.02	0.05

complete measured data set at the current time is omitted in the final results.

2.4. Fuel Characteristics. The biomass that has been used for the present work is classified as demolition wood (DW). The received biomass is pelletized with a pellet machine to get a similar shape and composition for all the experimental runs. To ensure a homogeneous distribution, a large volume of demolition wood was shredded to sawdust size, followed by thorough mixing. Pellets were then made from these fine pieces. Hence, variation in the N-content is not regarded as a challenge in these experiments. The type of biomass, the origin of it, and the pretreatment technology applied to it are important parameters influencing the ultimate and proximate analysis of the biomass. For example, drying can reduce the moisture content from 65% in virgin wood down to below 10% in wood pellets. The proximate analysis of the present fuel is shown in Table 1, where the moisture content is measured during each experimental run. Moisture, VM, and ash content are measured using ASTM E871 (50 g, 103 ± 2 °C, 24 h), ASTM E872 (1 g, 950 °C, 7 min), and ASTM D1102 (2 g, 580−600 °C, 4 h) standards, respectively, and the fixed carbon is calculated by the difference to 100%. Three samples are analyzed from different parts of the pellets to get repeatable analyses, showing that the fuel was homogeneous. Volatile matters for wood chips, bark, and straw are normally in the range of 76−86, 70−77, and 70−81 wt %, respectively,[31] while for the DW it was 75.97%, as shown in Table 1.

Table 2 shows the DW ultimate analysis (dry ash free). All the samples have been dried in a vacuum exsiccator over phosphorus pentoxide prior to analysis. The determination of C/H/N/S is performed using the "EA 1108 CHNS-O" by Carlo Erba Instruments elemental analyzer. The method is adjusted for sample amounts of 2−10 mg and performs with an uncertainty within 0.3 wt % as required for confirmation of assumed chemical composition. The operation range covers the content from 100 to 0.1 wt %; sulfur determination is in the concentration range of 1.0 down to 0.01 wt % and the uncertainty is estimated to be 0.02 wt % for C/N/S/Cl. The nitrogen content, which is the most important element in this study is 1.06%, while for wood, straw, peat, sewage sludge, and coal it is 0.03−1, 0.3−1.5, 0.5−2.5, 2.5−6.5, and 0.5−2.5 wt %, respectively.[32]

3. RESULTS AND DISCUSSION

3.1. Accuracy of the Results and Combustion Quality. In order to establish the accuracy of the measured results, the total carbon balance is needed to quantify the measured values compared to expected analytical values. The carbon balance for one of the experiments, at 1000 °C for staged air combustion, is shown in Figure 5. This figure shows the results from the start time until the end of the experiment. However, it should be noted that the first and very last section of the data has not been considered in the final data for further treatment, since these parts are typical transient periods, outside of the stable run

period. The calculated values for CO_2, based on the carbon content in the fuel and the measured volume percentage of oxygen and CO in the flue gas, is very close to the measured values for CO_2 for each sampling interval and hence the deviation is sufficiently close to zero. In the case of a large deviation between measured and calculated values, the data set is removed from further treatment, since it could be from an unstable or transient period. Therefore the carbon balance for the presented
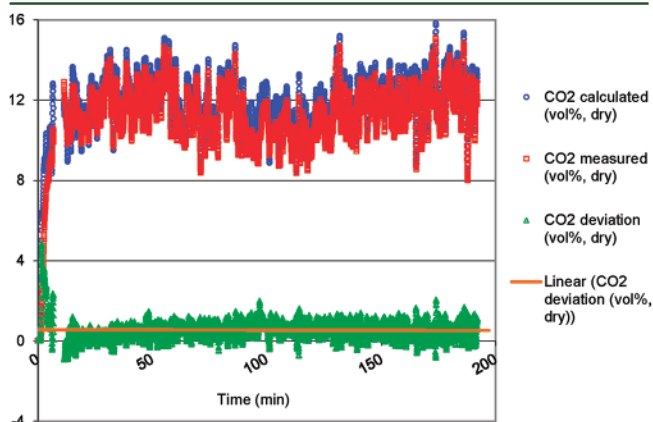
set of results is in good order. All the experiments at the different temperatures, with and without staging air, show the same good results for the CO_2 deviation. Emission level of C_xH_y and CO for both staged and nonstaged combustion is shown in Figure 6. For C_xH_y, both staged air combustion and nonstaged combustion show the same emission level, typically below 4 ppm at 11% O_2 in dry flue gas. Here low values for C_xH_y and CO emissions, respectively, below 5 and 50 ppm shows good mixing conditions and residence times in line with modern industrial scale boilers.[33] Emissions of gaseous hydrocarbon compounds and CO are a result of incomplete combustion. Favorable combustion leads to small emissions of hydrocarbons because the organic material burns out. Large emissions of hydrocarbons indicate unsatisfactory combustion conditions and probably soot emissions. Large boilers are generally operated at an appropriate oxygen concentration, temperature, and residence time and consequently are under favorable combustion conditions. Particles originating from incomplete combustion are few or none and can be decreased in modern boiler types by 180 times,[21,34,35] and in the advanced wood furnaces, CO emissions of 10−20 mg/m^3 can be reached, depending on the temperature and selection of the optimum excess air ratio.[4] At 900 and 950 °C, some values up to 10 ppm C_xH_y are visible for nonstaged combustion, which originate from the sets of data from the period where the actual stable experiment had not been started, which means that in the stable run, the C_xH_y for both 900 and 950 °C still is 1 to 3 ppm. The C_xH_y emission level is slowly increasing with excess air ratio

Figure 5. CO_2 deviation based on calculated and measured values from the Horiba gas analyzer for one set of the experiments; 1000 °C, staged air combustion.

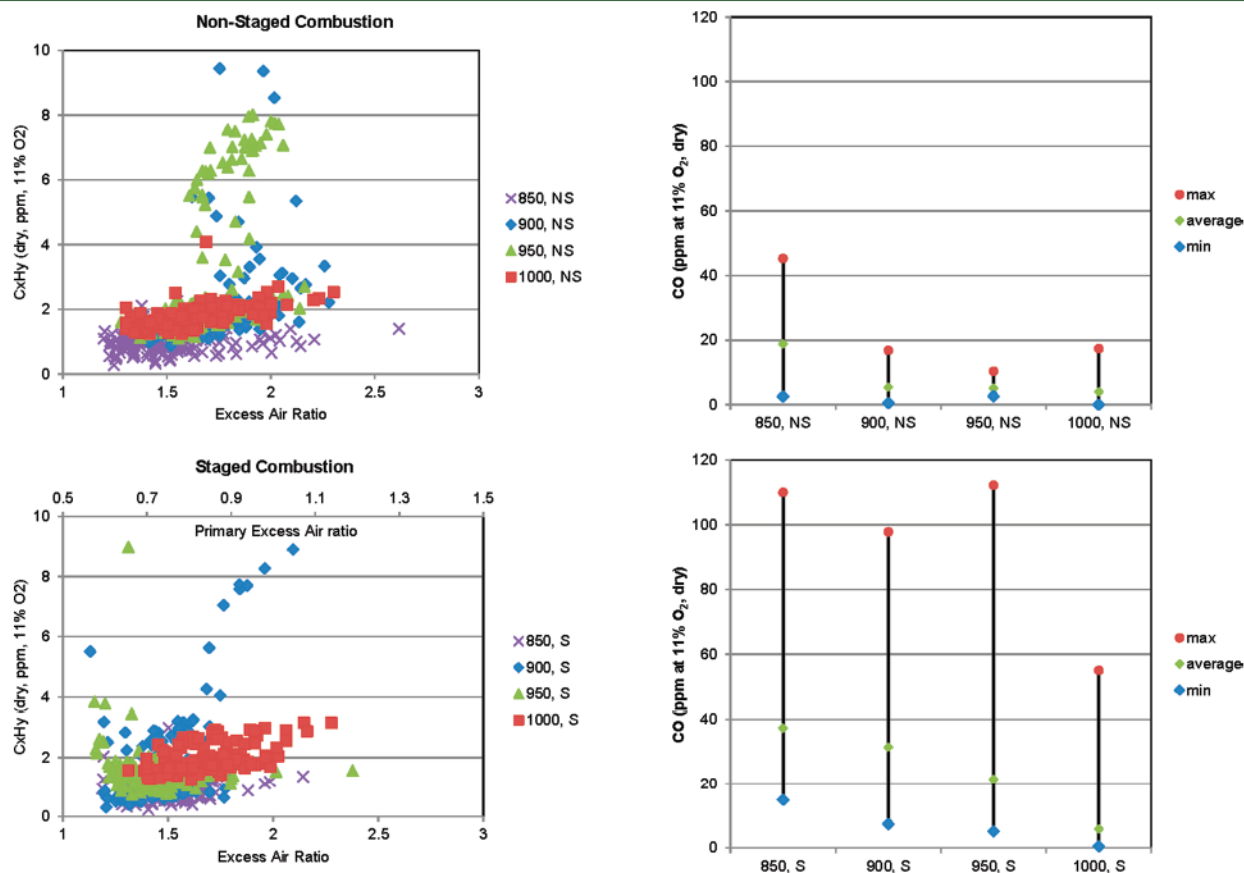**Figure 6.** (Left) C_xH_y as ppm corrected to 11% O_2 in dry flue gas for staged air combustion and nonstaged combustion as a function of excess air ratio at the different temperature levels. (Right) Average, minimum, and maximum value of CO as ppm corrected to 11% O_2 in dry flue gas for staged air combustion (S) and nonstaged combustion (NS) at the different temperature levels.

for both staged air combustion and nonstaged combustion. The influence of excess air ratio is small, but the C_xH_y emission level is a direct function of the excess air ratio, and the minimum C_xH_y emission is taking place at the lowest total excess air ratio.

For nonstaged combustion, the temperature has an inverse effect on the C_xH_y emission levels. The lowest emissions occur at 850 °C, while at 900, 950, and 1000 °C the temperature has no effect. For staged air combustion, the effect of temperature is more visible than for nonstaged combustion. Here the effect of temperature is still low, but it is clearly possible to observe an increase in emission levels with increasing temperature in the lower graph. The observed increase of C_xH_y may be due to a higher release of gaseous hydrocarbons from the fuel at higher temperatures, where the pyrolysis process is intensified by temperature and the formation of hydrocarbons are increased.[36] Detailed experimental and thermodynamic studies on particulate emissions from this multifuel reactor to investigate particle size distribution and chemical composition of fly/bottom ash is extensively discussed recently.[37,38] The effect of temperature on CO is the same as for N_2O. As shown in Figure 6, increasing temperature decreases the CO level, while staged air combustion has a negative effect on CO. The former effect is due to a more complete oxidation of CO, forming CO_2. However, with air staging, the low stoichiometric ratio in the first stage cause the oxidation route to be less effective, so the emission of CO rises. The staged air combustion results indicate an increase of 99−482% for CO for staged air combustion, while the mean CO levels are about a factor of two increased.

Emissions of gaseous hydrocarbon compounds and CO are a result of incomplete combustion. Large emissions of CO indicate unsatisfactory combustion conditions. In the present case, higher excess air ratio (more oxygen available) will lead to an almost complete combustion (heated reactor, i.e., temperature not influenced by the excess air ratio). Consequently, the maximum CO level corresponds to the lowest excess air ratio or the more fuel rich condition. In the staged combustion experiments, because of the under-stoichiometric condition in the first stage, a large amount of unburnt species (including CO) will be formed in the primary stage. The burnout of the unburnt species should take place in the second stage. If necessary air is available in the burnout zone, the CO level will be very low; if not the CO level will be high. So the higher deviation for CO emission in the staged combustion is a result of the variations in secondary excess air ratio, where more fuel rich conditions in the secondary stage can, combined with not perfect mixing of fuel gas and secondary air, cause higher fluctuations in the CO level.

3.2. NOx Emissions: Effect of Excess Air Ratio and Air Staging. Skreiberg et al.[39] showed that the fuel-N conversion to NOx is strongly dependent on the excess air ratio and that it increases with increasing excess air. However, in this study we investigate further the effect of temperature on this dependency. Figure 7 shows the effect of temperature on the NOx emission level (ppm at 11% O_2 in dry flue gas) for both staged air combustion and nonstaged combustion of DW at 850, 900, 950, and 1000 °C. NO_2 was typically below 1 ppm for the staged and nonstaged experiments which is within the measurement error ranges for the analyzers (Gasmet and Bomem FTIRs) for NO_2, except for one case at 900 °C for staged-air combustion, where a NO_2 level of up to 3 ppm is measured. Consequently, we have not found any clear relation between NO_2 and temperature in the investigated temperature range. The upper graph for nonstaged combustion shows an increasing trend for NOx when

the excess air ratio is increasing. This corresponds with the findings of Skreiberg et al.[39] The NOx level for these cases, at all temperatures, varies from 75 to 200 ppm at 11% O_2 in dry flue gas. However, this graph also indicates that temperature variations have almost no effect on the NOx emission level. All the data for the different temperatures are included, showing that they are in the same range for the same excess air ratio and temperature. This indicates that the temperatures are, as expected, too low for thermal NOx formation. According to the literature, thermal NOx formation in different biomass combustion systems starts at temperatures above 1400 °C.[8,40]

The lower graph, which shows the same information for staged air combustion of DW, is distinctively different from that of nonstaged combustion. Here an optimum excess air ratio exists for each combustion temperature. The NOx results are here plotted as a function of overall excess air ratio while the corresponding primary excess air ratio (half of the overall excess air ratio) is given on the upper x-axis for staged combustion. GC measurements were carried out to analyze the composition of the primary gas, but they can only provide an indicative value for the primary excess air ratio and not with a sufficient time resolution. The main point is to use total excess air ratio as an indicative value to show the effect of variations in the primary excess air ratio on the NOx reduction degree, and this was effectively achieved with the experimental setup, the measurements carried out, and the data treatment procedures employed. The NOx emission level is ranging from 25 to 120 ppm at 11% O_2 in dry flue gas. This range points out that the emission level by staged air combustion of DW decreases by a factor of 2−4, corresponding to 50−75% NOx reduction compared to nonstaged combustion. In the optimum case, i.e., at an excess air ratio of 1.6−1.9, the NOx reduction is 85%. This corresponds to an optimum primary excess air ratio of 0.8−0.95. Again, the effect of temperature is very low, as was the case for nonstaged combustion, and all temperatures show the same trend. First an increase occurs in the NOx level with an increasing excess air ratio up to approximately 1.5, and from this point the NOx level is decreasing until the excess air ratio approaches 2. A further increase in the excess air ratio will cause the NOx level to start increasing again. This effect is due to the increase of available air both in the primary and secondary zone, which causes the first stage not to be in a fuel-rich condition, as was explained in the Introduction. This will increase the TFN/Fuel-N ratio, hence lowering the NOx reduction potential, where total fixed nitrogen (TFN) is the total mass of nitrogen in the flue gas (all N containing gases coming out from the reactor except for N_2), and Fuel-N is the total mass of nitrogen in the fuel.[41] The concentration of NH_3 and HCN was very low in the flue gas after a long residence time, typically below 1 ppm, which was within the measurement error range of the analyzers for these species.

Figure 8 shows the effect of temperature on N_2O emissions at different excess air ratios. The upper graph clearly shows that in the case of nonstaged combustion, the N_2O emission level is not a function of the excess air ratio. However, the effect of temperature on the N_2O emission level is significant in nonstaged combustion. The maximum N_2O emission level is seen at the lowest temperature, i.e., 850 °C. Increasing the temperature with just 50 °C will decrease N_2O from 4.8 to 0.9 ppm (mean value), which corresponds to 80% reduction. The same trend has been found for N_2O formation for temperatures above 750 °C in the literature, where reduction of NO has a significant effect on the production of N_2O.[42,43] The production of N_2O is mainly

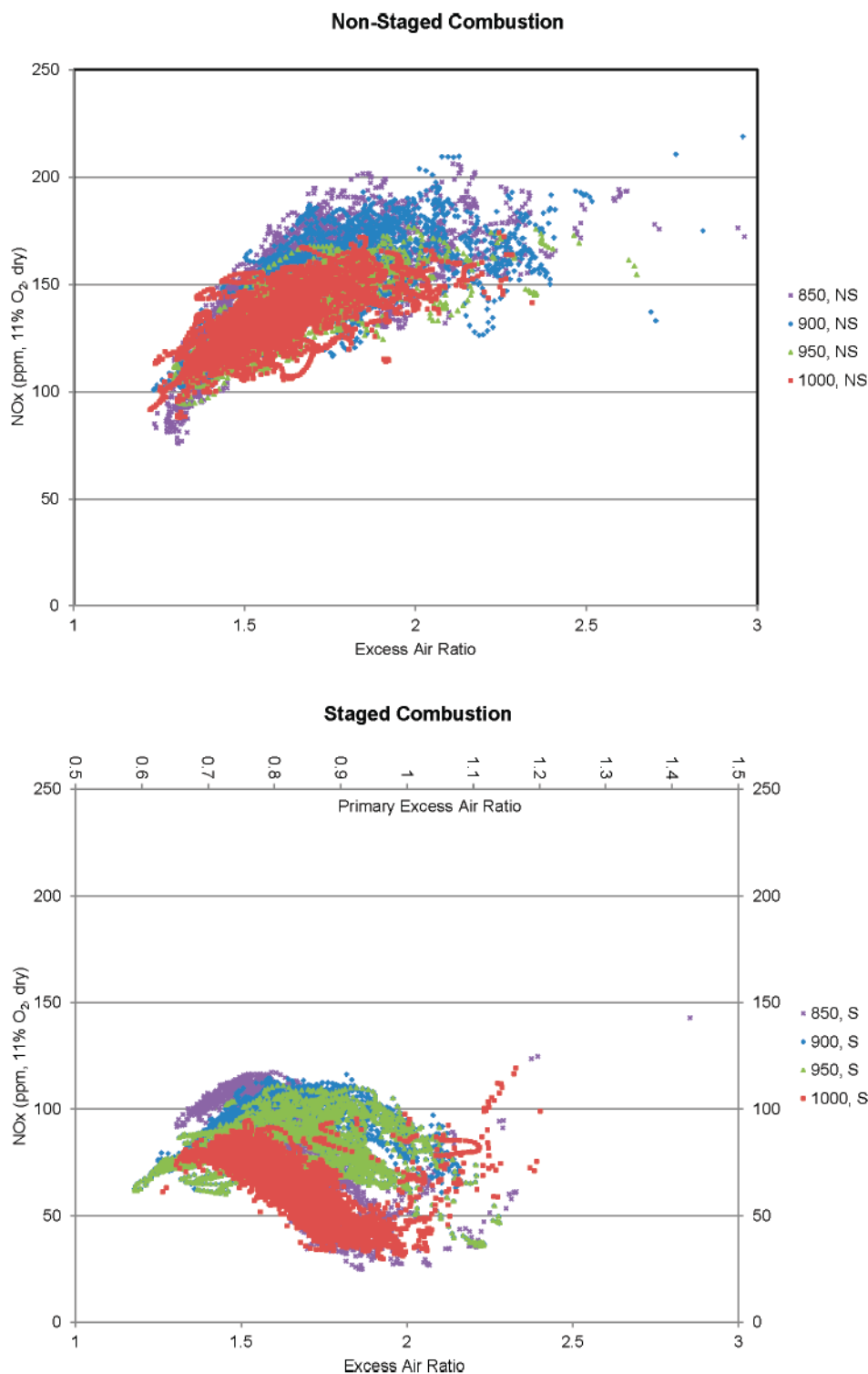**Non-Staged Combustion**

Staged Combustion

Figure 7. NOx as ppm corrected to 11% O_2 in the dry flue gas for staged air combustion and nonstaged combustion as a function of excess air ratio at the different temperature levels.

from the reaction of NO + NCO and NO + NH, so N_2O is mainly reduced by thermal decomposition. HCN and NH_3 either can reduce to N_2O and N_2 or oxidize to NO. At the higher temperature, the oxidation route becomes more dominant; therefore, having a low amount of N_2O is predicted.[11,42] The staged air combustion experiments show higher values of N_2O for the same conditions. At the optimum excess air ratio for NOx

reduction, the increase in N_2O emission compared to nonstaged combustion is almost 120%.

3.3. Temperature Influence on NOx and N_2O Emission Levels. As discussed in sections 3.2 and 3.3, the effect of temperature on the NOx emission level is small in the investigated temperature range of 850−1000 °C. However, with the extraction of the maximum and minimum levels for each
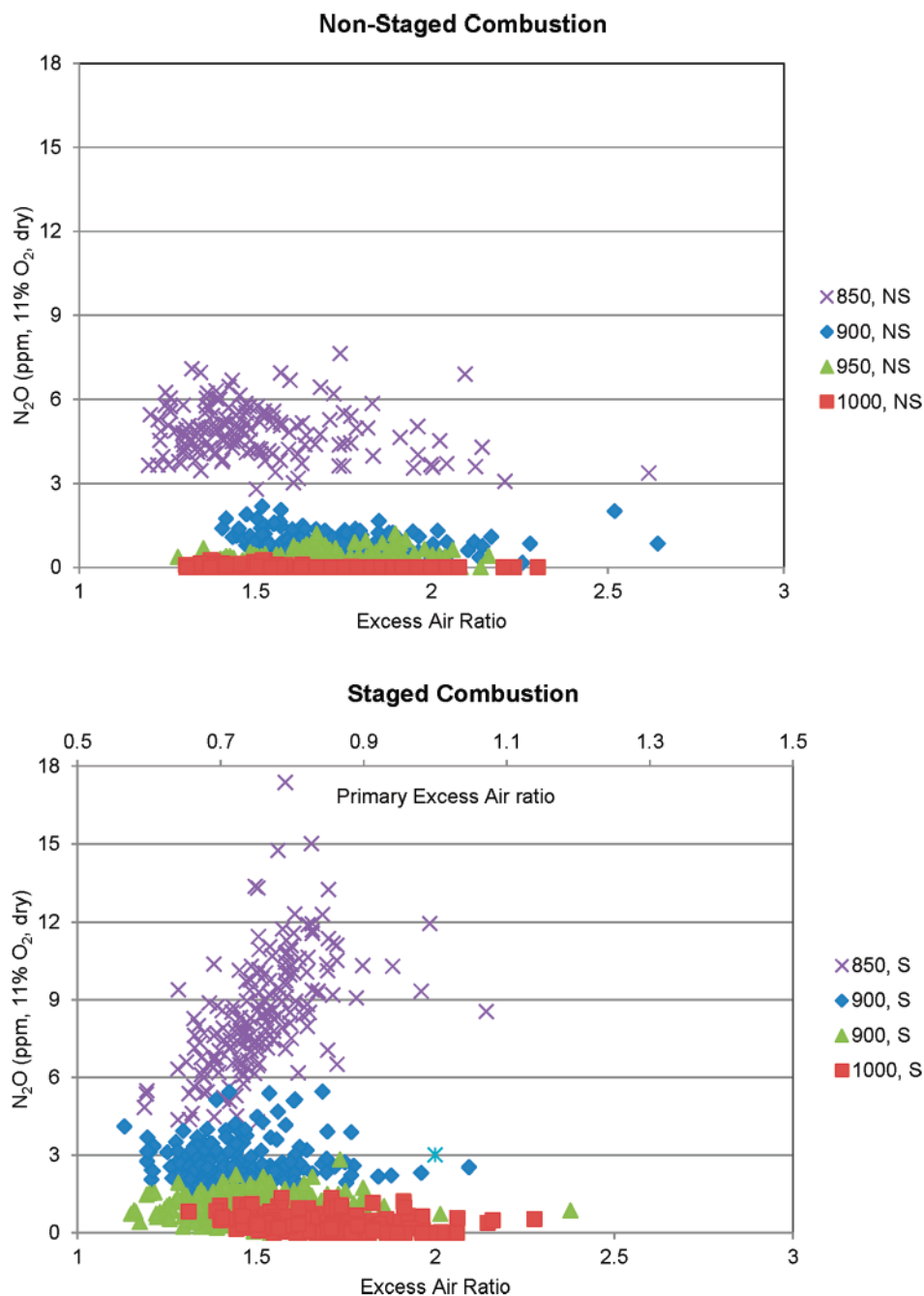
Non-Staged Combustion

Staged Combustion

Figure 8. N_2O as ppm corrected to 11% O_2 in the flue gas for staged air combustion and nonstaged combustion as a function of excess air ratio at the different temperature levels.

temperature, some important trends can be established. Figure 9 shows mean, maximum, and minimum NOx emission level (ppm at 11% O_2 in dry flue gas) for nonstaged (NS) and staged air (S) combustion of DW in the mentioned temperature range. The average (mean value for different excess air ratios over a period of time) is remaining constant at the different temperatures, at almost 150 ppm for nonstaged combustion. The maximum, mean, and minimum values are at the highest level for 900 °C in the nonstaged experiments. NOx at staged air combustion seems not to be a function of temperature either. The average value is on the order of 80 ppm at 11% O_2 in dry flue gas and the highest mean value is seen at 900 and 950 °C. It is interesting to

note that in both cases the spread between the highest and lowest values are higher in the lower end of the temperature range. The lower amount of NOx at 1000 °C needs more clarification. Considering the optimum primary excess air ratio as the key point for minimizing the NOx emission, we can see that at 1000 °C most of the time the reactor was running in the optimum excess air ratio range (see Figure 7). This resulted in a lower average NOx value (for a complete run). At 900 and 950 °C, in spite of our efforts to operate at optimum conditions, the primary excess air ratio has also been slightly lower than the optimum range (0.8–0.95) for the experiment. Hence, the higher average value at 900 and 950 °C corresponds to a lower average primary excess air ratio.
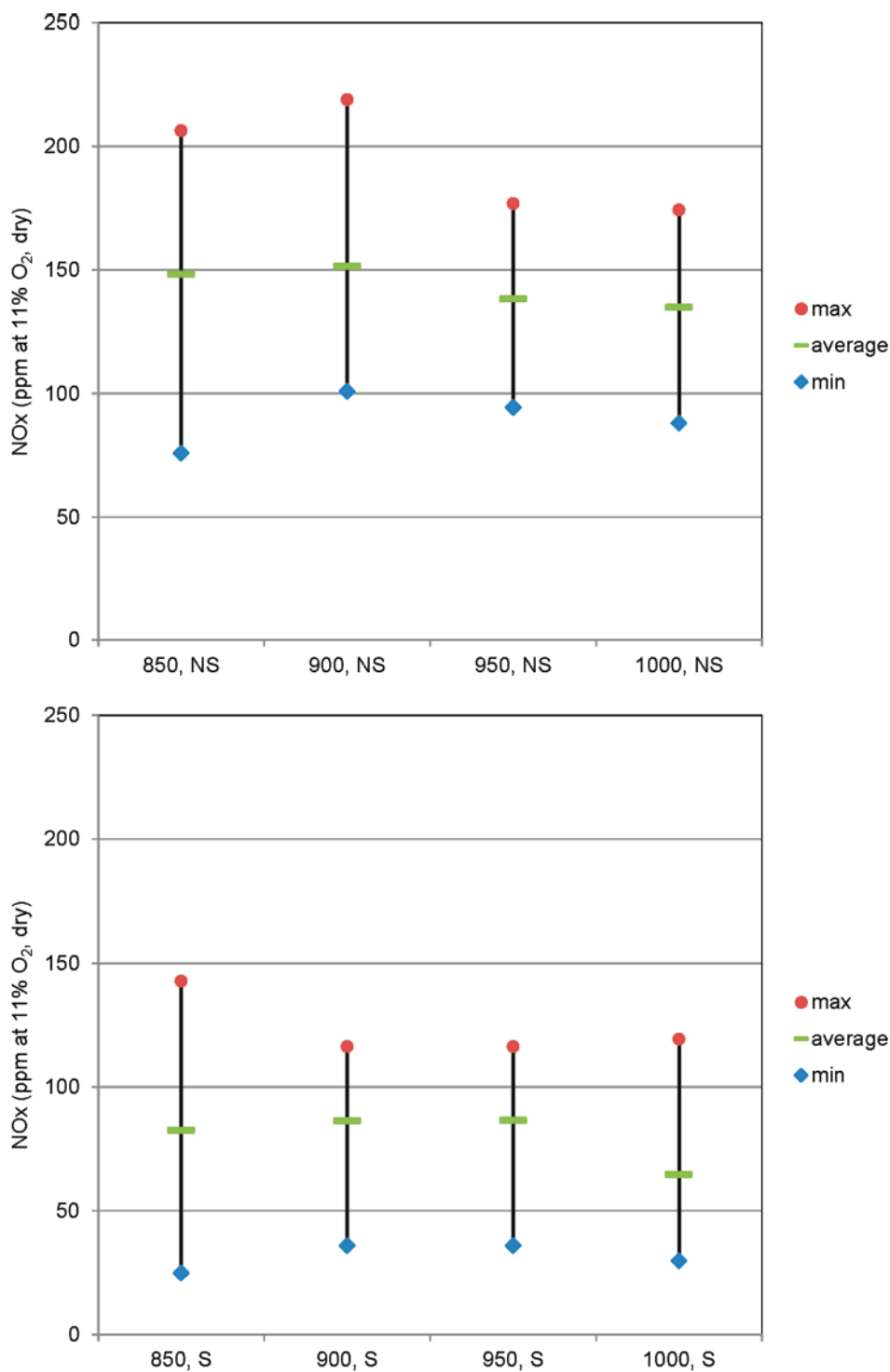
Figure 9. Average, minimum, and maximum value of NOx as ppm corrected to 11% O_2 in dry flue gas for staged air combustion (S) and nonstaged combustion (NS) at the different temperature levels.

N_2O has a different behavior in relation to temperature, showing similar values for staged air combustion and nonstaged combustion. However, temperature has a great influence on mean, maximum, and minimum N_2O levels, shown in Figure 10. They decrease significantly with increasing temperature, and for high temperatures the N_2O level is almost negligible. Yet again the spread between maximum and minimum values are higher in the lower end of the temperature range. Previous studies shows that the main precursor for N_2O formation is HCN oxidation,[12,44] while N_2O destruction is mainly by the reaction of $N_2O + H = N_2 + OH$.[45] At the high temperatures, the destruction reaction with H radicals is faster and also the HCN oxidation reaction tends to NO formation instead of N_2O. This mechanism causes the N_2O level to be very low at higher temperatures.

3.4. Effect of Stoichiometry, Temperature, and Residence Time on TFN/Fuel-N. In addition to the reactor temperature,
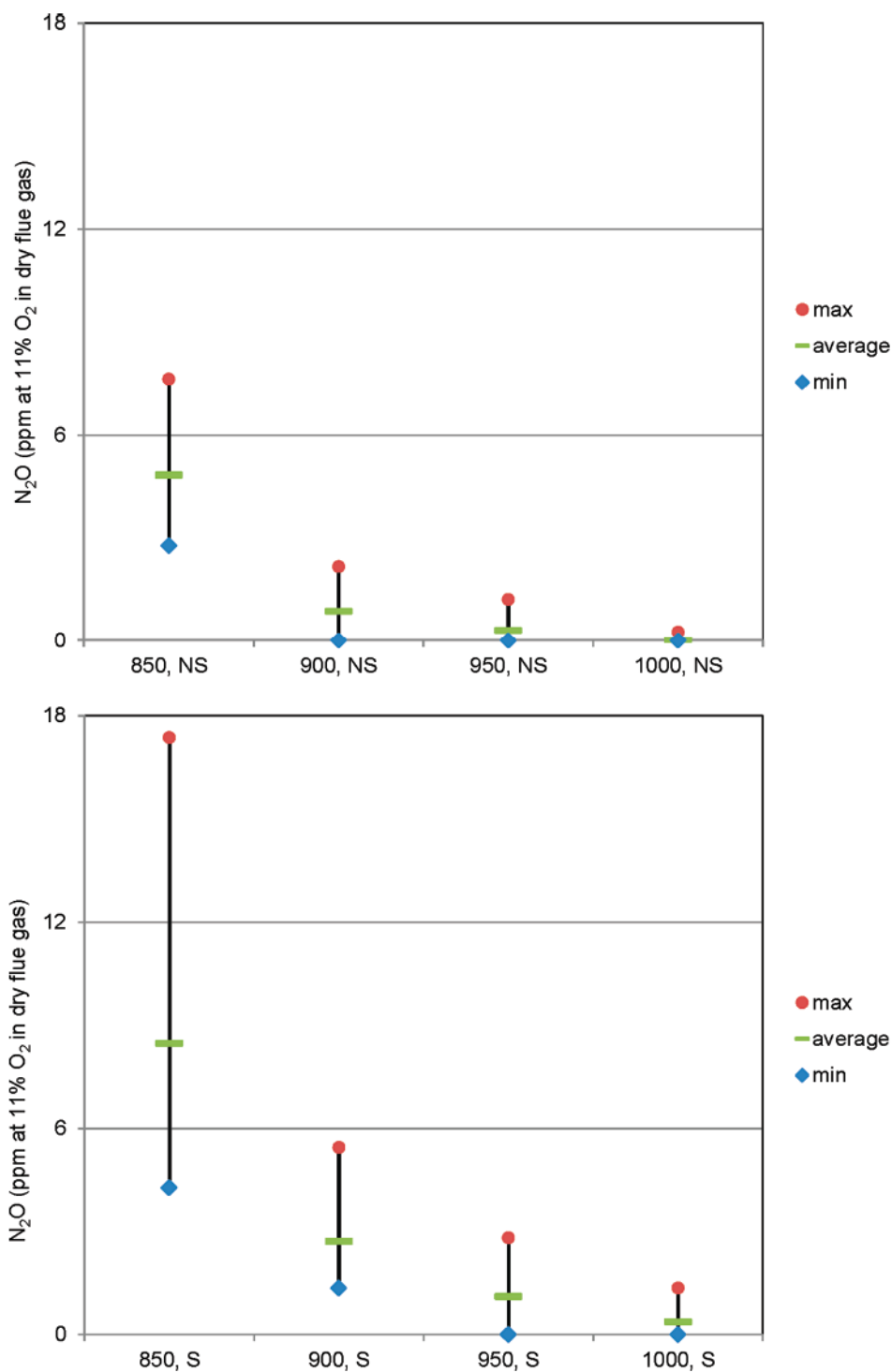
Figure 10. Average, minimum, and maximum value of N_2O as ppm corrected to 11% O_2 in dry flue gas for staged air combustion (S) and nonstaged combustion (NS) at the different temperature levels.

primary excess air ratio, fuel-N content, differences in residence times, and mixing conditions may also have an effect on the fuel nitrogen conversion. The optimum condition for maximum conversion of fuel-N to molecular nitrogen, N_2, is highly affected by the mentioned parameters. However, since only one fuel was tested, the primary excess air ratio is the only important variable in addition to the potential temperature effect regarding the NOx emission level. The NOx/Fuel-N and TFN/Fuel-N ratios, as

shown in Figure 11, were checked and showed good consistency, always well below unity,[8] since the values for TFN (TFN = NO + NO_2 + $2N_2O$ + HCN + NH_3) is calculated after complete burnout where the residence time has been several seconds. Residence time in the reduction zone is of importance for nitrogen conversion, however up to a certain value, beyond which it does not significantly influence TFN/Fuel-N.[18,46] In this work, the residence time is well above the expected needed time
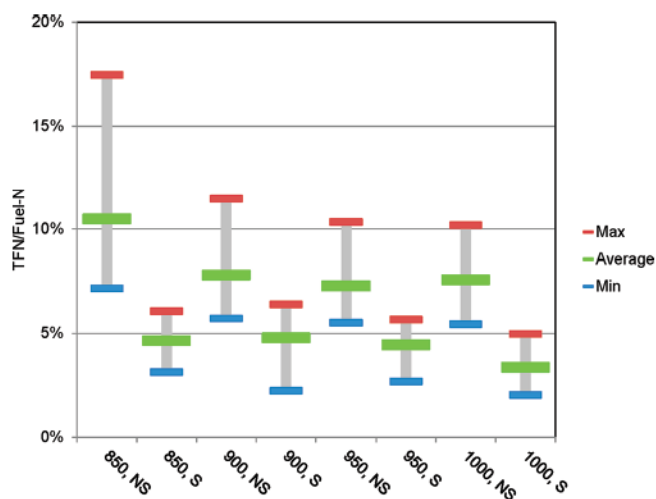
Figure 11. Average, minimum and maximum values of TFN/Fuel-N for staged air combustion (S) and nonstaged combustion (NS) at the different temperature levels.

(below 2 s) and, hence, the results are not influenced by the residence time. After the reduction zone, the combustion is completed by injection of the secondary air. Of course, good mixing of secondary air and the combustible gases are important. In average, a large amount of the TFN is composed of NOx (96%) and is varying between 81 and 100% depending on the temperature and the combustion scenario. Therefore the mentioned values in the last figure, Figure 11, can be regarded as approximate values for NOx/Fuel-N.

4. CONCLUSIONS

From the experimental studies carried out in the present work, using demolition wood pellets as fuel, the following conclusions can be drawn: The primary excess air ratio is the most important parameter which can be optimized for maximum conversion of fuel-N to N_2, hence reducing the NOx level. The effect of two-stage combustion of biomass is significant for reduction of NOx emission levels. Staged air combustion, in this case, can reduce the emission level by 50−75% and even up to 85% at the optimum conditions. The maximum NOx reduction happens when the primary air is injected at a primary excess air ratio of 0.8−0.95 and the total excess air ratio is 1.6−1.9 for staged air combustion. The experiments show that also the total excess air ratio has an important effect on the NOx emission.

The N_2O level has an inverse effect for staged air combustion, i.e., increasing for staged air combustion. The average N_2O level increase for the different temperatures is 75−1660% but with a low amount of N_2O at high temperatures.

However, the experimental results show that the NOx emission level is not affected significantly by temperature neither in nonstaged or staged air combustion when temperatures are kept below 1000 °C in the reactor. Yet, the effect of temperature on the N_2O level is considerable. This study shows, as expected, that at high temperatures, N_2O emissions almost disappear. The results point to that the effects of temperature and staged air combustion are counteractive for N_2O, meaning a negative influence on N_2O for staged air combustion and a desirable N_2O reduction effect with increasing temperature. Therefore to

minimize N_2O emissions and reduce emissions of unburnt, temperatures of above 900 °C are beneficial.

Hydrocarbons emission, C_xH_y, is almost independent of the combustion condition whether it is staged air combustion or nonstaged combustion. In both cases, the emission levels of hydrocarbons are below 4 ppm at 11% O_2 in dry flue gas. CO emissions increase for staged air combustion compared to nonstaged combustion by a factor of about 1.5 at a given temperature. Increasing temperature decreases the CO emission level in the whole temperature range of 850−1000 °C.

■ AUTHOR INFORMATION

Corresponding Author

*E-mail: ehsan.houshfar@ntnu.no. Phone: +47-73593896. Fax: +47-73593580.

■ ACKNOWLEDGMENT

■ REFERENCES

(1) REN21. *Renewables 2010 Global Status Report*, Paris, REN21 Secretariat, 2010.

(2) Rodrigues, M.; Faaij, A. P. C.; Walter, A. Techno-economic analysis of co-fired biomass integrated gasification/combined cycle systems with inclusion of economies of scale. *Energy* 2003, 28 (12), 1229−1258.

(3) Kessler, F. M.; Knechtle, N.; Frischknecht, R. *Heizenergie aus Heizöl, Erdgas oder Holz*; Umwelt Schrift Nr. 315; Bern, 2000.

(4) Nussbaumer, T. Combustion and co-combustion of biomass: fundamentals, technologies, and primary measures for emission reduction. *Energy Fuels* 2003, 17 (6), 1510−1521.

(5) Miller, J. A.; Bowman, C. T. Mechanism and modeling of nitrogen chemistry in combustion. *Prog. Energy Combust. Sci.* 1989, 15 (4), 287−338.

(6) Jenkins, B. M.; Baxter, L. L.; Miles, T. R. Combustion properties of biomass. *Fuel Process. Technol.* 1998, 54 (1−3), 17−46.

(7) Houshfar, E.; Løvås, T.; Skreiberg, Ø. Detailed chemical kinetics modeling of NOx reduction in combined staged fuel and staged air combustion of biomass. *18th European Biomass Conference & Exhibition (EU BC&E)*, Lyon, France, 2010; pp 1128−1132.

(8) Salzmann, R.; Nussbaumer, T. Fuel Staging for NOx Reduction in Biomass Combustion: Experiments and Modeling. *Energy Fuels* 2001, 15 (3), 575−582.

(9) Kicherer, A.; Spliethoff, H.; Maier, H.; Hein, K. R. G. The effect of different reburning fuels on NOx-reduction. *Fuel* 1994, 73 (9), 1443−1446.

(10) Zabetta, E. C.; Hupa, M.; Saviharju, K. Reducing NOx Emissions Using Fuel Staging, Air Staging, and Selective Noncatalytic Reduction in Synergy. *Ind. Eng. Chem. Res.* 2005, 44 (13), 4552−4561.

(11) Skreiberg, Ø.; Kilpinen, P.; Glarborg, P. Ammonia chemistry below 1400 K under fuel-rich conditions in a flow reactor. *Combust. Flame* 2004, 136 (4), 501−518.

(12) Kilpinen, P.; Hupa, M. Homogeneous N2O chemistry at fluidized bed combustion conditions: A kinetic modeling study. *Combust. Flame* 1991, 85 (1−2), 94−104.

(13) Kilpinen, P.; Glarborg, P.; Hupa, M. Reburning chemistry: a kinetic modeling study. *Ind. Eng. Chem. Res.* 1992, 31 (6), 1477−1490.

(14) Hämäläinen, J. P.; Aho, M. J.; Tummavuori, J. L. Formation of nitrogen oxides from fuel-N through HCN and NH3: a model-compound study. *Fuel* 1994, 73 (12), 1894–1898.

(15) Becidan, M.; Skreiberg, Ø.; Hustad, J. E. NOx and N2O Precursors (NH3 and HCN) in Pyrolysis of Biomass Residues. *Energy Fuels* 2007, 21 (2), 1173–1180.

(16) Hansson, K.-M.; Samuelsson, J.; Tullin, C.; Åmand, L.-E. Formation of HNCO, HCN, and NH3 from the pyrolysis of bark and nitrogen-containing model compounds. *Combust. Flame* 2004, 137 (3), 265–277.

(17) Nussbaumer, T. Primary and secondary measures for the reduction of nitric oxide emissions from biomass combustion. In *Developments in Thermochemical Biomass Conversion*, Banff, Canada, 1996; Bridgwater, A. V.; Boocock, D. G. B., Eds. Blackie Academic & Professional: 1997; pp 1447–1461.

(18) Skreiberg, Ø.; Glarborg, P.; Jensen, A. D.; Dam-Johansen, K. Kinetic NOx modelling and experimental results from single wood particle combustion. *Fuel* 1997, 76 (7), 671–682.

(19) Lin, W.; Jensen, P. A.; Jensen, A. D. Biomass Suspension Combustion: Effect of Two-Stage Combustion on NOx Emissions in a Laboratory-Scale Swirl Burner. *Energy Fuels* 2009, 23 (3), 1398–1405.

(20) Stubenberger, G.; Scharler, R.; Zahirovic, S.; Obernberger, I. Experimental investigation of nitrogen species release from different solid biomass fuels as a basis for release models. *Fuel* 2008, 87 (6), 793–806.

(21) Johansson, L. S.; Leckner, B.; Gustavsson, L.; Cooper, D.; Tullin, C.; Potter, A. Emission characteristics of modern and old-type residential boilers fired with wood logs and wood pellets. *Atmos. Environ.* 2004, 38 (25), 4183–4195.

(22) Dagaut, P.; Glarborg, P.; Alzueta, M. U. The oxidation of hydrogen cyanide and related chemistry. *Prog. Energy Combust. Sci.* 2008, 34 (1), 1–46.

(23) Sørum, L.; Skreiberg, Ø.; Glarborg, P.; Jensen, A.; Dam-Johansen, K. Formation of NO from combustion of volatiles from municipal solid wastes. *Combust. Flame* 2001, 124 (1–2), 195–212.

(24) Wendt, J. O. L.; Sternling, C. V.; Matovich, M. A. Reduction of sulfur trioxide and nitrogen oxides by secondary fuel injection. *Symp. (Int.) Combust.* 1973, 14 (1), 897–904.

(25) Chen, S. L.; McCarthy, J. M.; Clark, W. D.; Heap, M. P.; Seeker, W. R.; Pershing, D. W. Bench and pilot scale process evaluation of reburning for in-furnace NOx reduction. *Symp. (Int.) Combust.* 1988, 21 (1), 1159–1169.

(26) Pershing, D, W.; Berkau, E, E., The Chemistry of Nitrogen Oxides and Control through Combustion Modifications. In *Pollution Control and Energy Needs*, Jimeson, R. M.; Spindt, R. S., Eds.; American Chemical Society: Washington, DC, 1974; Vol. 127, pp 218–240.

(27) Svoboda, K.; Pohořelý, M.; Hartman, M. Effects of Operating Conditions and Dusty Fuel on the NOx, N2O, and CO Emissions in PFB Co-combustion of Coal and Wood. *Energy Fuels* 2003, 17 (4), 1091–1099.

(28) Bauer, R.; Gölles, M.; Brunner, T.; Dourdoumas, N.; Obernberger, I. Modelling of grate combustion in a medium scale biomass furnace for control purposes. *Biomass Bioenergy* 2010, 34 (4), 417–427.

(29) Zhou, H.; Jensen, A. D.; Glarborg, P.; Kavaliauskas, A. Formation and reduction of nitric oxide in fixed-bed combustion of straw. *Fuel* 2006, 85 (5–6), 705–716.

(30) Houshfar, E.; Skreiberg, Ø.; Todorović, D.; Skreiberg, A.; Løvås, T.; Jovović, A.; Sørum, L. NOx emission reduction by staged combustion in grate combustion of biomass fuels and fuel mixtures. *Fuel* 2011, submitted for publication.

(31) Berndes, G.; Baxter, L.; Coombes, P.; Delcarte, J.; Evald, A.; Hartmann, H.; Jansen, M.; Koppejan, J.; Livingston, W.; Loo, S. v.; Madrali, S.; Moghtaderi, B.; Nägele, E.; Nussbaumer, T.; Obernberger, I.; Oravainen, H.; Preto, F.; Skreiberg, Ø.; Tullin, C.; Thek, G. *The Handbook of Biomass Combustion and Co-firing*; Earthscan: London, 2008.

(32) Glarborg, P.; Jensen, A. D.; Johnsson, J. E. Fuel nitrogen conversion in solid fuel fired systems. *Prog. Energy Combust. Sci.* 2003, 29 (2), 89–113.

(33) Nussbaumer, T. *Biomass Combustion in Europe Overview on Technologies and Regulations*; Report 08-03; prepared by Verenum Switzerland for New York State Energy Research and Development Authority: Albany, NY, 2008.

(34) Johansson, L. S.; Tullin, C.; Leckner, B.; Sjövall, P. Particle emissions from biomass combustion in small combustors. *Biomass Bioenergy* 2003, 25 (4), 435–446.

(35) Eskilsson, D.; Rönnbäck, M.; Samuelsson, J.; Tullin, C. Optimisation of efficiency and emissions in pellet burners. *Biomass Bioenergy* 2004, 27 (6), 541–546.

(36) Kozinski, J. A.; Saade, R. Effect of biomass burning on the formation of soot particles and heavy hydrocarbons. An experimental study. *Fuel* 1998, 77 (4), 225–237.

(37) Becidan, M. l.; Houshfar, E.; Khalil, R. A.; Skreiberg, Ø.; Løvås, T.; Sørum, L. Optimal mixtures to reduce the formation of corrosive compounds during straw combustion: a thermodynamic analysis. *Energy Fuels* 2011, 25 (7), 3223–3234.

(38) Khalil, R. A.; Houshfar, E.; Musinguzi, W.; Becidan, M.; Skreiberg, Ø.; Goile, F.; Løvås, T.; Sørum, L. Experimental investigation on corrosion abatement in straw combustion by fuel-mixing. *Energy Fuels* 2011, 25 (6), 2687–2695.

(39) Skreiberg, Ø.; Hustad, J. E.; Karlsvik, E. Empirical NOx-modelling and experimental results from wood stove combustion. In *Developments in Thermochemical Biomass Conversion*, Banff, Canada, 1996; Bridgwater, A. V.; Boocock, D. G. B., Eds. Blackie Academic & Professional: London, UK, 1997; pp 1462–1478.

(40) Mahmoudi, S.; Baeyens, J.; Seville, J. P. K. NOx formation and selective non-catalytic reduction (SNCR) in a fluidized bed combustor of biomass. *Biomass Bioenergy* 2010, 34 (9), 1393–1409.

(41) Skreiberg, Ø.; Becidan, M.; Hustad, J. E.; Mitchell, R. E. Detailed chemical kinetics modelling of NOx reduction by staged air combustion at moderate temperatures. In *The Science in Thermal and Chemical Biomass Conversion Conference*, Victoria, BC, Canada, 2004, Bridgwater, A. V., Boocock, D. G. B., Eds. CPL Press: Newbury, Berkshire, UK, 2006, pp 40–54.

(42) Kristensen, P. G.; Glarborg, P.; Dam-Johansen, K. Nitrogen chemistry during burnout in fuel-staged combustion. *Combust. Flame* 1996, 107 (3), 211–222.

(43) Liu, H.; Gibbs, B. M. Modelling of NO and N2O emissions from biomass-fired circulating fluidized bed combustors. *Fuel* 2002, 81 (3), 271–280.

(44) Aho, M. J.; Hämäläinen, J. P.; Tummavuori, J. L. Importance of solid fuel properties to nitrogen oxide formation through HCN and NH3 in small particle combustion. *Combust. Flame* 1993, 95 (1–2), 22–30.

(45) Winter, F.; Wartha, C.; Hofbauer, H. NO and N2O formation during the combustion of wood, straw, malt waste and peat. *Bioresour. Technol.* 1999, 70 (1), 39–49.

(46) Padinger, R.; Leckner, B.; Åmand, L.-E.; Thunman, H.; Ghirelli, F.; Nussbaumer, T.; Good, J.; Hassler, P.; Salzmann, R.; Winter, F.; Wartha, C.; Löffler, G.; Wargadalam, V. J.; Hofbauer, H.; Saastamoinen, J.; Oravainen, H.; Heiskanen, V. P.; Hämäläinen, J. P.; Taipale, R.; Bilbao, R.; Alzueta, M. U.; Millera, A.; Oliva, M.; Ibáñez, J. C.; Kilpinen, P. Reduction of nitrogen oxide emissions from wood chip grate furnaces, Final report for the EU-JOULE III project JOR3-CT96-0059, *1st World Conference on Biomass for Energy and Industry*, Sevilla, Spain, 2000, Kyritsis, S., Beenackers, A. A. A. M., Helm, P., Grassi, A., Chiaramonti, D., Eds.; James & James (Science Publishers) Ltd.: Sevilla, Spain, 2000; pp 1457–1463.

Ash related behaviour in staged and non-staged combustion of biomass fuels and fuel mixtures

Michaël Becidan [a,*], Dusan Todorovic [b], Øyvind Skreiberg [a], Roger A. Khalil [a], Rainer Backman [a], Franziska Goile [a], Alexandra Skreiberg [a], Aleksandar Jovovic [b], Lars Sørum [a]

[a] SINTEF Energy Research, Kolbjørn Hejes vei 1A, NO-7465 Trondheim, Norway
[b] University of Belgrade, Faculty of Mechanical Engineering, 11000 Belgrade, Serbia

ARTICLE INFO

ABSTRACT

The fate of selected elements (with focus on the important players in corrosion i.e. Na, K, Pb, Zn, Cl and S) are investigated for three biomasses (wood, demolition wood and coffee waste) and six mixtures of these as pellets both with and without air staging in a laboratory reactor. In order to get a complete overview of the combustion products, both online and offline analytical methods are used. Information is collected about: flue gas composition, particle (fly ash) size distribution and composition, bottom ash composition and melting properties. The main findings are: (1) complex interactions are taking place between the mixed fuels during combustion; (2) the mode of occurrence of an element as well as the overall structure of the fuel are important for speciation; (3) the pelletisation process, by bringing chemical elements into intimate contact, may affect partitioning and speciation; (4) staging and mixing might simultaneously have positive and negative effects on operation; (5) staging affects the governing mechanisms of fly ash (aerosols) formation.

1. Introduction

The European Council has set two key targets for the EU energy strategy: (1) a reduction of at least 20% in GHG emissions by 2020 and (2) a 20% share of renewable energies in EU energy consumption by 2020 [1]. In 2007, the EU met 8.5% of its final energy consumption by renewable energy [2]. Biomass is accounting for 2 thirds of renewable energy sources in Europe and the current trends seem to confirm this predominant position. This means that a considerable growth is to be expected in this sector to meet the EU goals.

Less than 3% of the biomass are converted to produce transport biofuels while respectively 2 thirds and 1 third of the remaining biomass are used to produce heat and electricity [3]. The majority of heat and electricity from biomass is produced in thermal systems using combustion. However, this is not without challenges with corrosion, deposit build-up, slagging/fouling, polluting emissions (NOx, SOx, trace metals) being amongst the major issues. Many of these problems are ash-related and a variety of methods exist to mitigate them including use of corrosion-resistant alloys and coatings, improved design, improved combustion process and control, better cleaning methods and the use of additives.

Additives are chemicals that can mitigate corrosion and deposition. Extensive tests, both lab- and full-scale, and calculations have been performed on several classes of chemicals, especially AlSi-, Ca-, S- and P-containing substances [4–10]. Some additives are part of patented

systems [11], however, it is a disputed field because of often inconclusive or installation-specific results. Furthermore, even though some additives show good abilities, far from everything is understood about their action.

Corrosion is mainly associated with alkali (Na, K) and Cl but also Pb and Zn [12]. Rather than using expensive additives, wastes or by-products containing high enough concentrations of corrosion-fighting chemical elements can be added. These materials are cheaper than standard additives and it can allow the combustion of an otherwise low-quality and/or unused fuel. A possible problem is that, contrary to dedicated chemicals, these materials have a complex chemical make-up which may include chemical elements interfering with and diluting the action of the corrosion-fighting elements. One example is the reaction of Ca with S which would otherwise prevent the formation of corrosive alkali chlorides by forming alkali sulphates. They may contain problematic elements (trace metals) when it comes to final disposal. On the other hand, the complex structure of these fuels might also lead to synergy effects. The literature concerning "additional" fuels focuses on three materials: coal [8,13], ash [14] and sludge [14–16].

The reactions involved are complex and only partly identified but a general consensus is that three mechanisms may take place (M is Na or K) [4,5,10,17,18]:
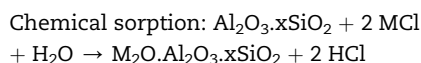
Chemical sorption: $Al_2O_3.xSiO_2 + 2\ MCl + H_2O \rightarrow M_2O.Al_2O_3.xSiO_2 + 2\ HCl$

Physical sorption: Cl and alkalis are bound to $Al_2O_3.xSiO_2$ by Van der Waals forces

Chemical reaction: $MCl + S$ (as sulphate or dioxide) $\rightarrow M_2SO_4$
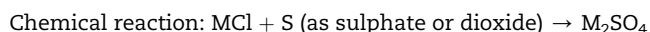
Experimental studies have shown that the predominating mechanism is dependent on the additive but also on temperature [4,5,10,17,18]. During chemical sorption, the alkali is strongly associated to the aluminosilicate while Cl is released as harmless HCl. The strong association means that the aluminosilicate cannot be recycled and reused but also that there is no risk of the alkali to be released because of, for example, concentrations or temperature variations as might happen with physical adsorption. However, physical adsorption has a higher capture capacity (several layers of alkali chlorides may be captured) and the additive may be reused after washing.

Combustion air staging is a common practice used to reduce NOx emissions [19,20]. Combustion air is separated into primary air and secondary air. Typically 70–90% of the stoichiometric air ratio is added in the primary combustion zone producing a fuel-rich environment with low temperatures followed by an oxygen-rich secondary combustion zone to complete oxidation. The main goal is to reduce oxygen availability in areas critical to NOx formation. However, reducing conditions may also affect the ash components speciation and partitioning and therewith corrosion and deposition. Little attention has been given to alkalis and reducing conditions in thermal systems, except for a few theoretical results [21,22]. Trace metals have been studied to

a larger extent [23–28]. These studies show that advanced air distribution can modify the phase distribution and speciation of chemical elements [29,30].

This study is focusing on experiments in a lab-scale reactor with a good control and overview of the operational parameters (temperature, feedstock and air inputs) and the combustion products (flue gas, fly and bottom ash) in order to study the influence of (a) the mixing of biomass fuels in pellets; (b) air staging. Seven parameters have been chosen to evaluate the effects of mixing and staging: (1) HCl & SO_2 emissions; (2) fly ash size distribution; (3) bottom ash composition; (4) bottom ash fusion properties; (5) fly ash composition; (6) Cl-conversion; (7) S-conversion.

2.   Materials and methods

The reactor used has a ceramic inner tube with a diameter of 100 mm. The altogether 2 m high vertical tube consists of two such ceramic tubes, each 1 m long, which are connected with a ceramic socket. The ceramic tubes are made of non-porous and non-catalytic alumina.

The reaction section, located above the grate, is 1.6 m long, while the section below the grate is 0.4 m long. The inlet air is preheated to the reactor temperature. The primary air is added under the grate and the secondary air is added above the grate.

Two types of experiments are carried out: (1) experiments with air staging and (2) experiments without air staging. Only isothermal experiments were performed with a reactor temperature of 850 °C. The primary air and secondary air were also preheated to this temperature. The total excess air ratio was about 1.6, and the primary excess air ratio was about 0.8 in the staged air experiments. Pellets are fed from a rotating battery of fuel containers using a water-cooled piston at a feeding rate of 400 g h^{-1}.

The experimental set-up with its advanced monitoring and control systems as well as the online and offline analytical methods gives a very accurate picture of the thermal process and all its products. Gas analysis was carried out using GC and FTIR. Particle size distribution and concentration in the flue gas were measured online by an ELPI in a particle size range of 0.03–10 μm. Speciation in the ELPI samples is estimated with the help of SEM-EDX using a series of assumptions described in detail by Rainer et al. [31]. The chemical composition of the bottom ash is determined by ICP-AES and ICP-SFMS.

Staged and non-staged experiments are carried out with four kinds of pellets: (1) wood (WP), (2) demolition wood (DW), (3) coffee waste (CW) and (4) six mixtures of these.

The WP is a Norwegian mixed timber of pine and spruce obtained through Felleskjøpet, Norway. DW is from houses/buildings in Sweden (obtained through Vattenfall, Sweden). CW was received from Kjeldsberg Kaffe, Norway. This substance consists of skin, silverskin, pulp, parchment, and broken beans that are lost during the roasting process. The beans used were almost exclusively from Brazil. All the samples were collected in 2009–2010.

The pellets are cylindrical extrudates, with a fixed diameter of 6 mm and a length of 5–15 mm and are air-dried before

the experiments. The proximate analysis of the pellet samples are shown in Table 1.

The ultimate analyses of the pellets, including ashes, are shown in Table 2. The fuels also have different chemical structures [32]. CW has the highest ash content but it is still relatively low (58 g kg^{-1} on dry basis). DW has the highest Cl-content while CW has the highest S-content. DW has the highest Si and Al but also Na contents. CW has both the highest Ca and K concentrations.

3. Results and discussion

3.1. HCl & SO$_2$ emission levels

For pure biomass fuels, staging leads to a reduction in HCl emissions while no clear trend is observed for the mixtures (three are unaffected, two display increasing emissions and one a decrease). This might be due to accuracy issues as HCl is difficult to quantify. However the somewhat consistent results (all pure fuels exhibit a decrease in HCl while mixtures exhibit varying trends) might reveal complex synergies between mixed fuels.

The experimental results (both staged and non-staged) show that increasing fuel-Cl lead to increasing HCl emissions during combustion. The resulting emissions for the mixtures indicate an unexpected effect of mixing on HCl emissions: in most cases, the resulting emissions are lower than the average of the pure biomass emissions, including for the ternary mixtures. No explanation can be given except synergy effects between the mixed fuels. Such complex (i.e. non-linear) interactions between chemical elements are actually not uncommon in biomass combustion [33].

Increasing S-fuel is leading to increasing SO$_2$ emissions. Contrary to HCl, the mixing effect can generally be described "as expected" with the resulting mixtures emissions in between those of the involved pure biomass samples. For DW and DW/WP (WP has a very low S concentration) no effect from staging is visible while the other fuels and mixtures show a little increase of SO$_2$ with staging.

The opposite effects of mixing and staging on the chemistries of S and Cl show that the same methods cannot be used to reduce the circulation of both S and Cl.

3.2. Particle (fly ash) size distribution

The particles formed during fixed bed biomass incineration are of two groups [34]: (a) coarse fly ash particles with a diameter between 1 and 250 μm; (b) aerosols with a diameter below 1 μm. The fly ash size distribution from fixed bed combustion of biomass is therefore bimodal. While the large particles are physically entrained from the bed by the flue gas and mainly made of Ca, Al and Si, the aerosols are originating from the release of volatile compounds (such as alkali chlorides) followed by nucleation and condensation of these vapours and subsequent coagulation of particles [34]. Other processes (condensation of vapours onto large particles) may also occur. The release behaviour and governing mechanisms are not well known yet and are affected by a variety of operating and feedstock parameters [34].

Fig. 1 presents the particle size distribution of the fly ash up to 10 μm (which is the most corrosive fraction) for the pure fuels and mixtures for non-staged and staged experiments. The curves are an average of all experiments as the same trend is observed for all fuels and mixtures. It is clear that staging leads to a displacement towards larger particles from less than 0.1 μm to over 0.1 μm (but under 1 μm) indicating a change in release behaviour and mechanisms. The total number of particles emitted appears little affected by staging meaning that the total weight of particles emitted is increased by staging.

3.3. Bottom ash composition

The main bottom ash constituents for all fuels are Si, Al, Ca, Fe, K and Mg. The main components of fly ash are K, S, Cl and Na but also significant levels of Pb and Zn (see also 3.5). K in the bottom ash is most certainly forming (alumino)silicates [35] or is already part of non-volatile structures.

The most interesting result concerning the effect of staging is that K is (relatively) more retained in the bottom ash than Na when staging is used with pure biomass fuels while staging has no measurable effect on Na and K chemistries in mixtures. This strongly infers that mixed fuels in pellets interact together and that these interactions lead to non-linear effects on overall chemistry. This is not uncommon as indicated in 3.1 and [33].

Table 1 – Proximate analysis and heating value of pellets (g kg^{-1}, dry basis).					
	Ash	Volatile	Fixed C	Moisture	HHV (MJ kg^{-1})
Wood (WP)	2.1	854.3	143.7	65.1	20.63
Demolition wood (DW)	37.3	772.7	190.0	81.2	20.54
Coffee waste (CW)	58.2	761.7	180.7	175.3	22.20
1/2 WP-1/2 DW[a]	19.7	813.5	166.9	67.8	20.62
1/2 WP-1/2 CW[a]	30.0	808.0	162.2	87.6	21.36
1/2 DW-1/2 CW[a]	47.7	767.2	185.4	127.2	21.24
2/3 WP-1/3 CW[a]	20.7	823.4	156.0	113.5	21.08
1/3 WP-2/3 CW[a]	39.3	792.6	168.4	80.2	21.55
1/3 WP-1/3 DW-1/3 CW[a]	32.4	796.2	171.5	245.3	21.04
a Calculated except moisture.					

Table 2 – Ultimate analysis of pellets, including ash elements (g kg^{-1}, dry basis).						
	C	H	O	N	S	Cl
Wood (WP)	512.2	60.7	425.4	1.4	0.30	0.2
Demolition wood (DW)	505.9	60.9	416.5	15.9	0.75	1.13
Coffee waste (CW)	529.0	64.7	376.4	28.2	1.87	0.38
1/2 WP-1/2 DW	509.1	60.8	421.1	8.5	0.52	0.65
1/2 WP-1/2 CW	519.8	62.5	403.3	13.4	1.01	0.28
1/2 DW-1/2 CW	520.1	60.6	392.1	25.8	1.37	0.85
2/3 WP-1/3 CW	519.3	60.6	408.1	11.4	0.81	0.27
1/3 WP-2/3 CW	527.9	60.4	386.8	23.5	1.41	0.36
1/3 WP-1/3 DW-1/3 CW	517.2	60.7	404.5	16.7	0.97	0.61

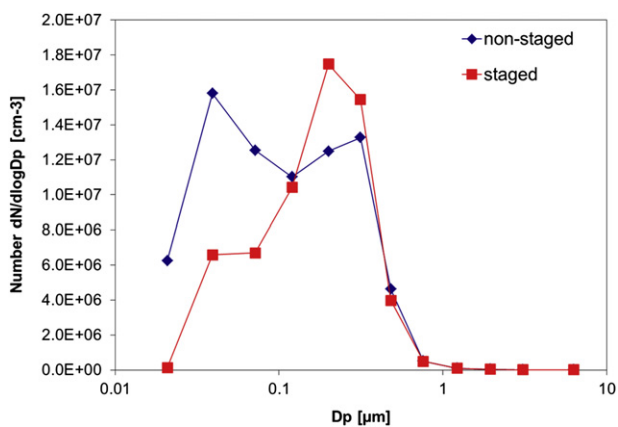|	WP	DW	CW	WP/DW	WP/CW	DW/CW	WP(2/3)/CW(1/3)	WP(1/3)/CW(2/3)	WP/DW/CW
Si	0.394	12.33	1.93	8.96	0.831	17.05	3.58	6.98	7.97
Al	0.085	1.94	0.80	1.13	0.399	4.16	2.14	4.85	2.91
Ca	1.195	7.00	16.37	3.99	8.080	10.22	4.61	8.19	6.57
Fe	0.064	5.49	1.26	2.96	1.222	5.04	2.09	7.50	5.32
K	0.579	1.13	19.80	0.89	9.474	14.61	9.48	20.11	10.00
Mg	0.251	1.11	6.45	0.68	3.083	3.82	2.19	4.43	2.52
Mn	0.135	0.14	0.10	0.14	0.114	0.14	0.14	0.14	0.14
Na	0.093	1.32	0.17	0.69	0.112	0.91	0.14	0.15	0.58
P	0.120	0.37	2.03	0.24	0.986	1.73	1.09	2.27	1.22
Ti	0.003	2.23	0.08	1.22	0.029	1.96	0.33	0.70	1.22

3.4. Bottom ash fusion properties

The four ash fusion temperatures represent transitional states between solid and fluid ash. These temperatures give an indication of the softening and melting behaviour of the ash. Despite the shortcomings inherent to this empirical method and a relatively weak record of correlation with slagging and fouling (especially for fuels other than coal), fusion temperatures are valuable guides to the high temperature behaviour of the fuel inorganic elements and can give useful information regarding the fouling and slagging propensities of ashes [36]. The initial deformation temperature (IDT) is for example a guidance criterion for the prevention of severe superheater fouling: plant design should limit the temperature of the flue gas entering the superheater section to a value below IDT. The fusion temperatures are related to the composition but also structure of the ashes.

Fig. 1 – Particle (fly ash) size distribution. Average for all fuels and mixtures.

For the non-staged experiments, the IDT of the pure fuels are all around 1100 °C (+/−50 °C). This is also true for the mixtures except for WP(1/3)/CW(2/3) and the ternary mixture. Wood pellets (WP) and demolition wood pellets (DW) fusion temperatures are almost not affected by staging, while CW fusion temperatures are increasing from under 1100 to over 1200 °C. The four transitional temperatures are very close for DW.

No obvious trends concerning the influence of mixing and staging are observed as presented in Fig. 2.

However, two main behaviours may be envisioned: (a) there are interactions between the chemical elements of the fuels (as suggested in 3.3) during incineration therewith forming an ash with a new structure and with properties difficult to predict and/or correlate; this might be promoted by pellets, more compact and denser than loose biomass, in which ash compounds are more intimately in contact; (b) the resulting ash might be a mixture of the two pure fuels ash (no interactions).

3.5. Fly ash composition

The method used to estimate speciation and concentrations is described by [31]. The main components in the fly ash are K, S, Cl and Na (see Fig. 3(a) and (b)).

In average 700 g kg^{-1} of the O-free samples (excluding C and Al) consisted of these elements. Zn and Pb represent on average 200 g kg^{-1} whereas the portion of the inert oxide forming elements Si, Ca, Fe, P, Mg and Cr is 100 g kg^{-1}. P and Mg compositions are low in all samples.

The portion of inert metals is generally higher in the bigger particle size fractions than in the smaller fractions, indicating that the compounds of these metals (oxides) originate from the original fuel ash and have not been vaporized during combustion.
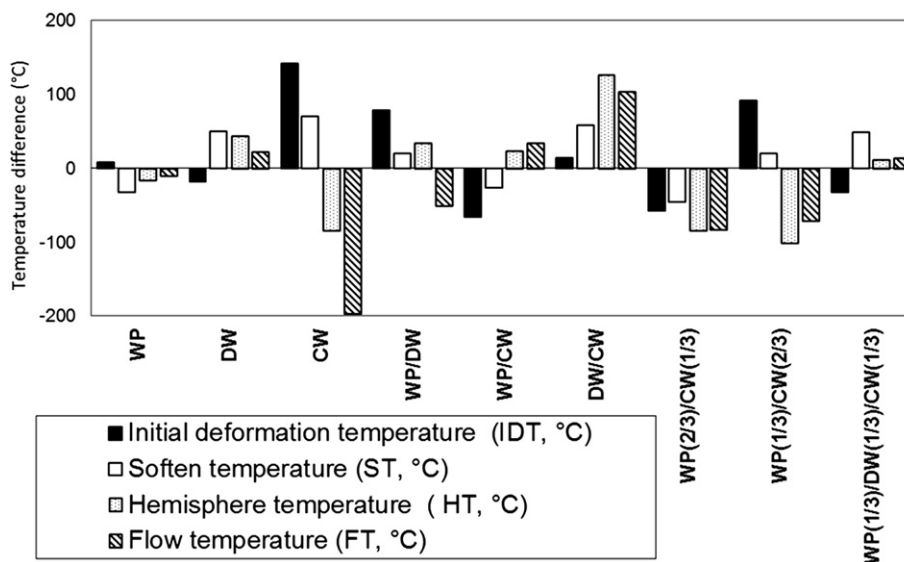
Fig. 2 – Temperature difference (°C) between non-staged and staged experiments for four characteristic temperatures in the various fuels and fuel mixtures.

Pb and Zn are partly in oxide form, partly in salt form. The oxides are most probably ZnO and PbO. The salt part is made of sulphate and chloride of K, Na, Zn and Pb.

The Cl content of the salt part of the WP sample is 50–200 g kg^{-1} with the staged samples showing slightly higher values than the non-staged samples. The DW sample has 500–600 g kg^{-1} Cl in both non-staged and staged samples, whereas the CW samples have no Cl.

CW composition shows no trends as a function of particle size. K constitutes some 700 g kg^{-1} of the metals, Zn 250 g kg^{-1} and Na 50 g kg^{-1}. Non-staged and staged samples are similar except for significantly higher Zn in the staged samples.

In WP, K decreases with increasing particles size. Zn is low in the smaller fractions and higher in the bigger ones. The staged samples have higher Na than the non-staged.

The DW samples show significant trends in the metal content as a function of particle size. In the staged runs, K decreases from 400 g kg^{-1} in the 0.1 μm sample to 200 g kg^{-1} in the 1.5 μm sample. In the non-staged sample, K is 200 g kg^{-1} in the small particles and 150 g kg^{-1} in the larger ones. Zn increases correspondingly from smaller to bigger particles. Pb shows a slight decrease. There is significantly higher Na in the non-staged samples, but in neither runs Na showed any trend as a function of particle size.

The salt part of WP/DW consists of 600 g kg^{-1} Cl both in non-staged and staged runs. Some 500 g kg^{-1} of the metals are Zn and Pb with a slight increase of Zn as a function of particle size.

The WP/CW samples show small amounts of Cl, almost no in the non-staged samples and below 100 g kg^{-1} in the staged samples. K is the dominating metal with 700 g kg^{-1} in the non-staged samples and around 500 g kg^{-1} in the staged ones. In staged samples, Zn increases with the particle size while there are no trends in composition of the non-staged samples.

The DW/CW samples contain very small amounts of Cl, slightly more in the non-staged samples. In the staged run, K shows a small decreasing trend with particle size and Zn

a corresponding increase. This trend is not seen in the non-staged run.

The samples from runs with mixtures of WP and CW (2/3WP+1/3CW) and (1/3WP+2/3CW) are very similar. The non-staged samples show no compositional changes as a function of particle size, while K is decreasing and Zn is increasing in the two air-staged runs. Na shows no trend as function of particle size.

The samples from the run with mixture WP/DW/CW show higher Cl-content than the other ones. The staged samples have some 100 g kg-1 and the non-staged some 50 g kg^{-1} Cl. The Zn content is somewhat higher in the staged samples and increases in bigger particles. K shows a corresponding decrease. Na is, again, not affected by particle size.

3.6. Cl-chemistry

Fig. 4 presents the phase distribution of Cl in the three biomass samples and six biomass mixtures both for non-staged and staged combustion experiments. Experimental challenges make it difficult to reach satisfying mass balances in some experiments but the interpretation of the overall trends, i.e. qualitative rather than quantitative results, still brings valuable knowledge.

The three biomass samples (non-staged combustion experiments) can be said to belong to two groups: (1) fuels in which most of Cl is converted to HCl represented here by wood pellets (WP); (2) fuels in which Cl is distributed equally in both phases. Such grouping has also been reported in thermodynamic equilibrium calculations for waste fractions (including biomass) [37].

Staging has the same effect on all fuels but with different strengths: it displaces Cl from the gas to the solid phase. The differences in the magnitude of the effect may be partly attributable to the fuel-Cl content but the chemical make
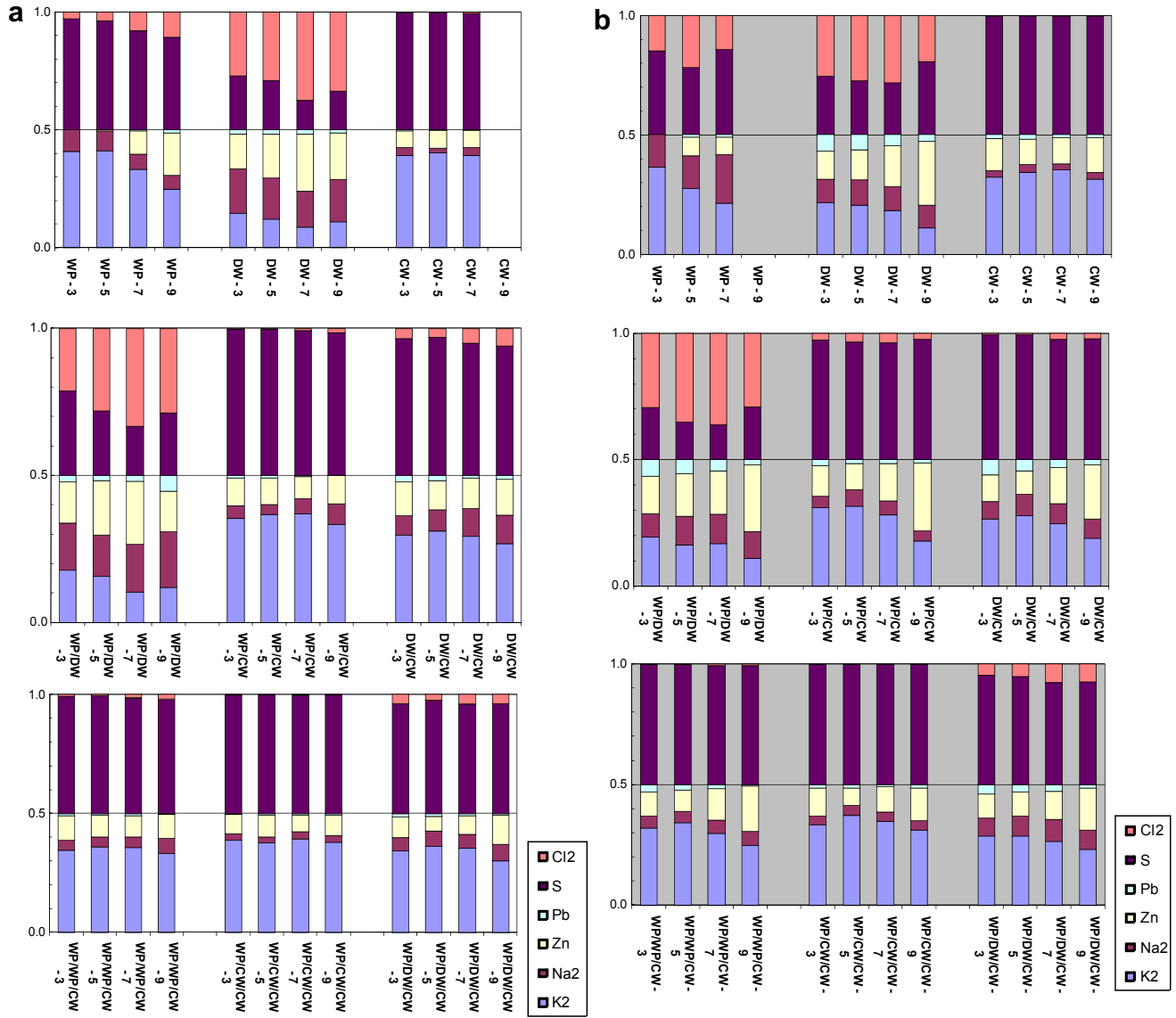
Fig. 3 − (a). Calculated composition (mass fraction) of the salt part of fly ash samples from the runs with different fuel mixtures at non-staged primary air conditions. Upper: Pure fuels. Middle: Binary mixtures. Lower: Ternary mixtures.(b). Calculated composition (mass fraction) of the salt part of fly ash samples from the runs with different fuel mixtures at staged primary air conditions. Upper: Pure fuels. Middle: Binary mixtures. Lower: Ternary mixtures.
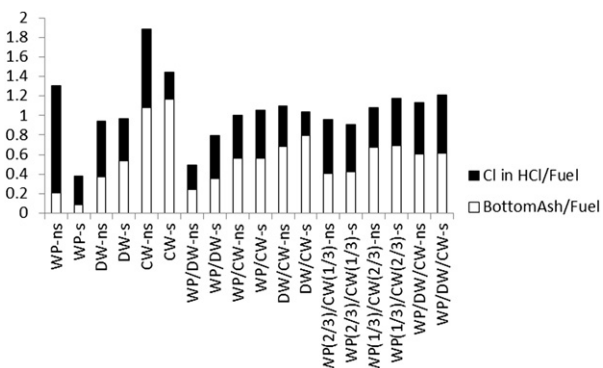
Fig. 4 − Cl-phase distribution (conversion factors) for staged (s) and non-staged (ns) combustion conditions.

up of the fuels (modes of occurrence) is most probably another important factor.

When looking at the (non-staged) results for the three 50/50 mixtures (see Fig. 4), it appears that the resulting retention in the bottom ash is at the high end of the values of the respective mixed fuels. This behaviour can not be explained but seems to prove that complex interactions between the mixed fuels are occurring. Air staging does not have a significant effect for WP/DW and WP/CW.

Mixtures in which one fuel is dominating (WP(2/3)/CW(1/3) and WP(1/3)/CW(2/3)) offer clearer trends when it comes to Cl-distribution (for non-staged experiments): increasing the share of CW increases the share of Cl in bottom ash. This result is in good correlation with the results for the single-fuel
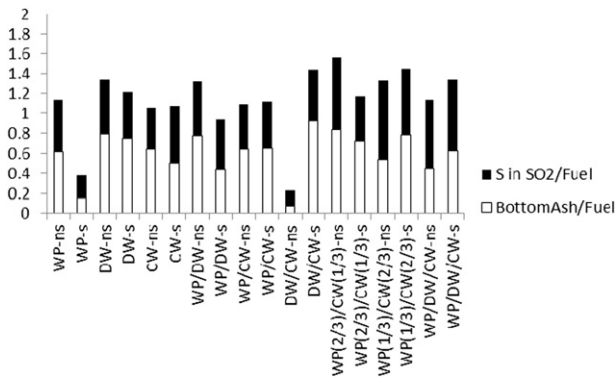
Fig. 5 − S-phase distribution (conversion factors) for staged (s) and non-staged (ns) combustion conditions.

pellets. As observed previously, the effect of air staging is almost non-existent in mixtures.

3.7.   S-chemistry

Fig. 5 shows the phase distribution of S in the three pure biomass fuels and the mixtures. S partitioning is between the gas phase (as SO_2) and the solid phase (bottom ash). Experimental challenges make it difficult to reach satisfying mass balances in some experiments but the interpretation of the overall trends, i.e. qualitative rather than quantitative results, still brings valuable knowledge.

In non-staged experiments, it appears that for all fuels and fuel mixtures studied, about half of S is found in the bottom ash. The distribution does not seem to be affected by S concentration or its modes of occurrence which most certainly vary in the different fuels. This is in good accordance with both experimental results [28], where it is measured that from about one fourth to one half of biomass-S is released to the gas phase from 500 °C for woody biomass, and with thermodynamic calculations [37] which predict that about half of biomass-S is released to the gas phase (average at 600−1200 °C). Staging does not appear to have an influence on S-phase distribution.

4.   Conclusions

The fate of selected ash elements are investigated for three biomasses (wood, demolition wood and coffee waste) and six mixtures of these as pellets both with and without air staging in a grate fired laboratory reactor. Data is collected about: flue gas composition, fly ash size distribution and composition, bottom ash composition and melting properties.

A very large quantity of data is presented and discussed. The main overall findings are: (1) experimental results (see the effect of staging on Na and K in bottom ash) indicate that complex interactions are taking place between the mixed fuels; (2) the same ash-forming element may react differently to staging and/or mixing in different fuels, indicating the importance of the mode of the overall structure of the fuel; (3) several results infer that pelletisation, by bringing chemical elements into more intimate contact than in loose biomass, affects their overall chemistry (partitioning and speciation); (4) staging and mixing might simultaneously have positive and negative effects; (5) staging affects the governing mechanisms of fly ash (aerosols) formation. The central practical implications of the aforementioned findings may be summarised as such: (1) mixing of different biomass may be an efficient method to affect the overall chemistry of specific chemical elements and therewith operational challenges such as fouling, deposition or slagging; (2) pelletisation may enhance the chemical effects of mixing; (3) staging, by influencing aerosols formation, may be a promising way of reducing the problems associated with them, especially corrosion.

REFERENCES

[1] EU Green Paper. Towards a European strategy for the security of energy supply; 29.11.2000.
[2] Communication from the Commission. 20 20 by 2020 Europe's climate change opportunity. COM; 2008. 30 final (23.01.08).
[3] European Environment Agency. http://www.eea.europa.eu/ articles/if-bioenergy-goes-boom. Published: Nov 15, 2008. Last modified: Apr 13, 2011. Cited date: Dec 20, 2011.
[4] Punjak WA, Uberoi M, Shadman F. High-temperature adsorption of alkali vapors on solid sorbents. AIChE J 1989; 35(7):1186−94.
[5] Turn SQ, Kinoshita CM, Ishimura DM, Zhou J, Hiraki TT, Masutani SM. "An experimental Investigation of alkali removal from biomass Producer gas using a fixed bed of solid Sorbent. J I Energy 1998;71(9):163−77.
[6] Aho M. Reduction of chlorine deposition in FB boilers with aluminium-containing additives. Fuel 2001;80(13):1943−51.
[7] Iisa K, Salmenoja YL. Sulfation of potassium chloride at combustion conditions. Energ Fuel 1999;13(6):1184−90.
[8] Aho M, Ferrer E. Importance of coal ash composition in protecting the boiler against chlorine deposition during combustion of chlorine-rich biomass. Fuel 2005;84(2-3): 201−12.
[9] Punjak WA, Shadman F. Aluminosilicate sorbents for control of alkali vapors during coal combustion and gasification. Energ Fuel 1988;2(5):702−8.
[10] Kyi S, Chadwick BL. Screening of potential mineral additives for use as fouling preventatives in Victorian brown coal combustion. Fuel 1999;78(7):845−55.
[11] Andersson C, inventor; Vattenfall AB, applicant. A method for operating a heat-producing plant for burning chlorine-containing fuels. Worldwide patent WO 2002059526. 2002 Jan 24.
[12] Nielsen HP, Frandsen FJ, Dam-Johansen K, Baxter LL. The implications of chlorine-associated corrosion on the operation of biomass-fired boilers. Prog Energ Combust 2000; 26(3):283−98.

[13] Ferrer E, Aho M, Silvennoinen J, Nurminen RV. Fluidized bed combustion of refuse-derived fuel in presence of protective coal ash. Fuel Process Technol 2005;87(1):33–44.

[14] Coda B, Aho M, Berger R, Hein KRG. Behavior of chlorine and enrichment of risky elements in bubbling fluidized bed combustion of biomass and waste assisted by additives. Energ Fuel 2001;15(3):680–90.

[15] Aho M, Silvennoinen J. Preventing chlorine deposition on heat transfer surfaces with aluminium–silicon rich biomass residue and additive. Fuel 2004;83(10):1299–305.

[16] Johansson L, Leckner B, Tullin C, Åmand L, Davidsson K. Properties of particles in the fly ash of a biofuel-fired Circulating Fluidized Bed (CFB) boiler. Energ Fuel 2008;22(5): 3005–15.

[17] Escobar I, Oleschko H, Wolf KJ, Müller M. Alkali removal from hot flue gas by solid sorbents in pressurized pulverized coal combustion. Powder Technol 2008;180(1-2):51–6.

[18] Uberoi M, Punjak W, Shadman F. The kinetics and mechanism of alkali removal from flue gases by solid sorbents. Prog Energ Combust 1990;16(4):205–11.

[19] Li S, Xu T, Hui S, Zhou Q, Tan H. Optimization of air staging in a 1 MW tangentially fired pulverized coal furnace. Fuel Process Technol 2009;90(1):99–106.

[20] Khan AA, de Jong W, Jansens PJ, Spliethoff H. Biomass combustion in fluidized bed boilers: potential problems and remedies. Fuel Process Technol 2009;90(1):21–50.

[21] Nielsen HP. Deposition and high-temperature corrosion in biomass-fired boilers[dissertation]. Lyngby: Technical University of Denmark; 1998.

[22] Knudsen J, Jensen P, Lin W, Frandsen F, Dam-Johansen K. Sulfur transformations during thermal conversion of herbaceous biomass. Energ Fuel 2004;18(3):810–9.

[23] Elled A-L, Åmand L-E, Leckner B, Andersson B-A. The fate of trace elements in fluidised bed combustion of sewage sludge and wood. Fuel 2007;86(5-6):843–52.

[24] Sørum L, Frandsen FJ, Hustad JE. On the fate of heavy metals in municipal solid waste combustion Part I: devolatilisation of heavy metals on the grate. Fuel 2003; 82(18):2273–83.

[25] Boman C, Ohman M, Nordin A. Trace element enrichment and behavior in wood pellet production and combustion processes. Energ Fuel 2006;20(3):993–1000.

[26] Elled A-L, Åmand L-E, Eskilsson D. Fate of zinc during combustion of demolition wood in a fluidized bed boiler. Energ Fuel 2008;22(3):1519–26.

[27] Abanades S, Flamant G, Gagnepain B, Gauthier D. Fate of heavy metals during municipal solid waste incineration. Waste Manage Res 2002;20(1):55–68.

[28] Van Lith S. Release of inorganic elements during wood-firing on a grate.[dissertation]. Lyngby: CHEC Research Centre, Technical University of Denmark; 2005.

[29] Dahl J, Obernberger I, Brunner T, Biedermann F. Results and evaluation of a new heavy metal fractionation technology in grate-fired biomass combustion plants as a basis for an improved ash utilisation. In: ETA-renewable energy, editor. Proceedings of the 12th European conference and technology exhibition on biomass for energy, industry and climate protection; 2002 Jun 17-21. Amsterdam; The Netherlands: ETA-Florence; 2002. p. 690–4. Italy and WIP-Munich, Germany.

[30] European Commission. Integrated pollution prevention and control reference document on the best available techniques for waste incineration. Seville, Spain: Directorate-General JRC Joint Research Centre Institute for Prospective Technological Studies; 2006 Aug. 638 pp.

[31] Backman R, Khalil RA, Todorovic D, Skreiberg Ø, Becidan M, Goile F, et al. The effect of peat ash addition to demolition wood on the formation of alkali, lead and zinc compounds at staged combustion conditions. Fuel Process Technol. in press.

[32] Becidan M, Skreiberg Ø, Hustad JE. NOx and N_2O Precursors (NH_3 and HCN) in pyrolysis of biomass residues. Energ Fuel 2007;21(2):1173–80.

[33] Hupa M. Interaction of fuels in co-firing in FBC. Fuel 2005; 84(10):1312–9.

[34] Obernberger I. Fly ash and aerosol formation in biomass combustion processes – an introduction. International seminar on aerosols in biomass combustion, Graz, Austria, 2005 Mar 18. www.ieabcc.nl/meetings/task32_Graz_aerosols/01_Obernberger.pdf. Cited 2011 Dec 20.

[35] Nielsen H, Baxter L, Sclippab G, Morey C, Frandsen FJ, Dam-Johansen K. Deposition of potassium salts on heat transfer surfaces in straw-fired boilers: a pilot-scale study. Fuel 2000; 79(2):131–9.

[36] Raask E. Mineral impurities in coal combustion: behaviour, problems, and remedial measures. Washington: Hemisphere Publishing Corporation; 1985.

[37] Becidan M, Sørum L, Lindberg D. Impact of Municipal Solid Waste (MSW) quality on the behavior of alkali metals and trace elements during combustion: a thermodynamic equilibrium analysis. Energ Fuel 2010;24(6):3446–55.

The effect of peat ash addition to demolition wood on the formation of alkali, lead and zinc compounds at staged combustion conditions

Rainer Backman [a], Roger A. Khalil [a,*], Dusan Todorovic [b], Øyvind Skreiberg [a], Michaël Becidan [a], Franziska Goile [a], Alexandra Skreiberg [a], Lars Sørum [a]

[a] SINTEF Energy Research, Energy Processes, NO-7465 Trondheim, Norway
[b] University of Belgrade, Faculty of Mechanical Engineering, Kraljice Marije 16, Belgrade, Serbia

ABSTRACT

Combustion experiments were performed in a multi-fuel reactor with continuous feed of pellets by applying staged air combustion. Total characterization of the elemental composition of the fuel, the bottom ash and some particle size stages of fly ash was performed. This was done in order to follow the fate of some of the problematic compounds in demolition wood as a function of peat-ash addition and other combustion related parameters. A method was developed to estimate the composition and speciation of the salt part of aerosols based on SEM/EDX analysis. The results show that the concentrations of zinc and lead account for 40–50% of the salts produced for the small particles (0.093 μm) and up to 90% for the larger particles (1.59 μm). A considerable part of these metals are chemically bound to chlorides and sulfates together with potassium and sodium indicating extensive volatilization of zinc and lead. The experiments show that the reactions of potassium, zinc and lead are the most affected. This gives rise to higher concentrations of zinc and lead in the aerosols. The chloride content in the aerosols decreases with increased peat ash addition. This will have an inhibiting effect on corrosion, but the higher Zn and especially Pb concentrations will lead to a lower first melting point of the aerosol particles. This may promote deposition and cause corrosion.

© 2011 Elsevier B.V. All rights reserved.

1. Introduction

One of the purposes for biomass utilization, besides the sustainability aspects, is to replace fossil fuel and decrease the greenhouse gas emission from the energy conversion. The increased biomass consumption has resulted in higher prices of virgin wood up to a range where it is no longer profitable to operate power stations based on combustion of wood alone [1]. This has lead to increased utilization of alternative fuels that are cheaper but have different properties compared to virgin wood, which can make combustion more problematic. This is also true for small power units that usually rely on indigenous fuel supply delivered at a minimal transport costs. Alternative fuels that are solely combusted or co-combusted such as peat, agricultural waste, different grass types and fast growing species all have one thing in common, a high ash content compared to wood. The higher ash content in such fuels may cause severe problems resulting in unscheduled and expensive shutdown periods in power plants. In fixed bed combustors, the alkali metals in particular can become volatile and stick on heat transfer surfaces downstream in the process. This process has been found in many cases to be accelerated by the presence of zinc and lead in the fuel, which both are even more volatile than alkali metal compounds. Such depositions are difficult to remove and cause lower efficiencies due to a decrease in heat transfer. They can also bridge between the tubes and cause flue gas flow restriction which results in higher pressure drops. The deposits themselves have a composition which make them quite aggressive resulting in attacks on the metallic surface of the heating tubes. For example, the chlorine in the ash facilitates the mobility of alkalis and trace metals, forming chlorides which have a low melting temperature. During combustion of fuels with high alkali content, the mobility of present chlorine is greatly enhanced. These alkali-chlorine compounds leave the bottom ash as different gaseous volatiles passing through the process along with the reacting gas and finally the flue gas. However, the capture of alkalis (and/or alkali chlorides in some cases) through the use of additives has helped lowering the alkali chlorides concentration in the flue gas and by that decreasing substantially corrosion in boilers. Similar possibilities to capture zinc and lead are highly interesting. When additives are used, chlorine is usually released as HCl, a compound that is corrosive on its own but lacks the sticky property that metal chlorides have. In addition, HCl is easily cleaned from the flue gas in a post-combustion stage by scrubbing it with lime stone or by dry-sorption with $Ca(OH)_2$ [2]. Additives can be either mixed with the fuels prior to combustion, they can be added to the bed material in case of fluidized bed or they can be sprayed at critical stages directly into the flue gas. Depending on their

* Corresponding author. Tel.: + 47 73590596; fax: + 47 73592889.
E-mail addresses: rainer.backman@sintef.no (R. Backman), Roger.A.Khalil@Sintef.no (R.A. Khalil), oyvind.skreiberg@sintef.no (Ø. Skreiberg), Michael.becidan@sintef.no (M. Becidan), franziska.goile@sintef.no (F. Goile), info@sintef.no (A. Skreiberg), lars.sorum@sintef.no (L. Sørum).

elemental composition, additives can be separated into groups containing calcium, phosphorous, sulfur, aluminum or aluminum-silicate [3]. For liquid-based additives, the so-called ChlorOut system developed by Vattenfall has shown good results in substantially decreasing the alkali chlorides and possibly also trace metal chlorides in the flue gas [4,5]. ChlorOut is based on spraying a solution of ammonium sulfate prior to the superheater section in the boiler. Other sulfate solutions like aluminum and ferric sulfates have also shown to have a similar effect to the ChlorOut system [6]. Additives in the form of solid particles can also be mixed with the bio-fuel prior to combustion. Sulfur rich additives such as peat or pure sulfur are expected to chemically react with potassium, sodium, zinc and lead to form $MxSO_4$. Sulfur addition to agricultural waste has shown promising results in decreasing the potential of corrosion in boilers [7,8]. Calcium–phosphorous and Aluminum–silicate based additives were tested in a full scale straw pellet boiler at the Amager power station in Denmark [9]. Among the tested additives were sand, dicalciumfosfat, chalk and bentonite. In addition, kaolin as an additive is studied in a related experimental work [10].

A special group is addition of fuel ash from other fuels or by co-combustion [11,12]. Dedicated chemicals are not the only possible additives, other materials/fuels such as biomass, sludge, coal or coal ash may also have a positive effect on alkali chemistry. For example, fly ash from peat may potentially absorb alkali and possibly some trace elements (Pb, Zn). The chemistry of peat ash is complicated due to its complex and varying composition. Many studies, mainly from co-combustion of peat with problematic fuels show the many possible reactions between peat ash and other ash constituents [13–16]. Peat also contains inert ash components like silicate and oxides which do not interact chemically with other components. The physical effect of this inert ash may, however, be significant. It has been shown to have a cleaning effect on superheater deposits by mechanical wearing effects. Part of the oxide ash has been found to have an alkali absorbing ability and high calcium content may promote formation of Ca-compounds which dissolve potassium and possibly also zinc and lead. Peat is also relatively rich in sulfur and promotes the formation of alkali sulfates instead of chlorides, which lowers both deposition and corrosion risks.

The objective of this study is to investigate which influence peat fly ash has on the distribution of ash components in biomass combustion. Demolition wood is used as the main fuel. Demolition wood has high contents of zinc and lead and has been shown to be quite problematic from a corrosion point of view. In the present work, the first attempts are made to determine which chemical effects of peat ash addition in demolition wood combustion are detectable on the bottom ash, fly ash and gas composition in carefully controlled combustion experiments.

2. Materials and methods

Demolition wood was provided by Vattenfall from the combustion plant at Nyköping, Sweden. The proximate analysis of the sample was carried out according to the ASTM standards ASTM E871, ASTM E872 and ASTM D1102, respectively for the moisture content, volatile matter and ashes. The fixed carbon was calculated by difference to 100%. The results of both the proximate and ultimate analysis are presented in Table 1. A chemical analysis of the ash content of the primary fuel and all the blends was determined by the ICP-AES (inductive coupled plasma equipped with an atomic emission spectrometry analyzer) and ICP-SFMS (inductive coupled plasma equipped a mass spectrometry analyzer) methods. The metal composition of the ash for the different fuel mixtures are presented in Table 2 recalculated on dry fuel basis.

The experiments were carried out in an electrically heated high temperature multi-fuel reactor. The reaction section, located above

the grate is 1.6 m long, while the section below the grate is 0.4 m long. The reactor heating system is fitted inside the insulation shell and consists of four separate 0.5 m high heating zones of 4 kW each (16 kW in total) that enclose the ceramic tube. The combustion air is preheated to the reactor temperature in external pre-heaters. The primary air is added under the grate and the secondary air is added above the grate. The lower part of the multi-fuel reactor is the section containing 2-grate system (10 cm apart): a primary grate and a final burnout grate and an ash collection system. Both the reactor flue gas composition and the composition of the fuel gas after the primary zone as well as the particle emission size distribution were continuously monitored.

For gas analysis in the primary zone a Varian CP-4900 micro gas chromatograph (GC) was used. The exhaust gases were quantified online with two different FTIRs, a Bomem 9100 and a Gasmet DX-4000. In order to detect instabilities during combustion a gas analyzer with a fast response time (HORIBA PG-250) was used.

The fly ash samples measured by means of a 13 stage low-pressure impactor where collected on aluminum plates [17]. The plates were covered by a thin layer of Vaseline to provide a sticky surface. The chemical analysis of the samples was made by energy-dispersive X-ray analysis connected to a scanning electron microscope, SEM/EDX

Table 1
Ultimate and proximate analysis of the demolition wood wt.%, db.

Proximate analysis			
Volatiles (dry basis)	Fixed carbon (dry basis)	Ash (dry basis)	Moisture (as received)
77.13	19.00	3.87	7.98

Ultimate Analysis (oxygen calculated by difference)					
C	H	N	O	S	Cl
50.53	6.09	1.59	41.60	0.08	0.11

Table 2
Chemical composition of the ash of demolition wood and the generated mixtures recalculated on wt.% dry fuel basis.

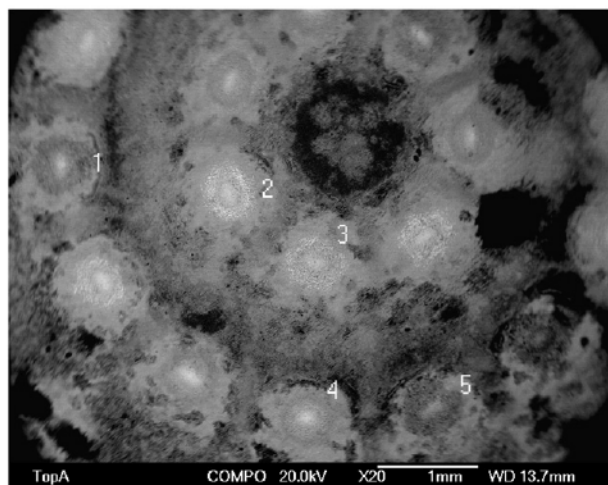| Peat ash %	0	1	5	10
Ash content [%]	3.9	5.2	8.9	13.4
Si [%]	1.2	1.9	2.4	3.6
Al [%]	0.2	0.3	0.3	0.5
Ca [%]	0.7	1.1	1.7	3.7
Fe [%]	0.5	0.4	2.5	1.2
K [%]	0.1	0.1	0.1	0.1
Mg [%]	0.1	0.3	0.7	1.8
Mn [%]	0.01	0.02	0.03	0.03
Na [%]	0.1	0.1	0.1	0.1
P [%]	0.04	0.05	0.05	0.10
Ti [%]	0.2	0.3	0.2	0.2
As [mg/kg]	4	3	4	5
Ba [mg/kg]	319	367	274	379
Be [mg/kg]	0.04	0.06	0.13	0.25
Cd [mg/kg]	1.31	1.02	0.97	0.55
Co [mg/kg]	1.36	2.21	1.37	1.46
Cr [mg/kg]	59	50	55	96
Cu [mg/kg]	166	275	29	29
Mo [mg/kg]	0.89	1.43	0.82	2.56
Nb [mg/kg]	0.60	0.68	0.60	0.90
Ni [mg/kg]	2.7	2.3	3.1	2.8
Pb [mg/kg]	426	447	637	258
Sc [mg/kg]	0.11	0.19	0.21	0.54
Sn [mg/kg]	1.89	2.99	5.40	2.11
Sr [mg/kg]	25	30	28	45
V [mg/kg]	1.57	2.12	3.14	3.57
W [mg/kg]	12	75	12	15
Y [mg/kg]	0.49	1.05	2.11	5.10
Zn [mg/kg]	679	606	421	346
Zr [mg/kg]	9	12	10	13

Fig. 1. SEM image of the pattern on particles collected on the ELPI-plates.

[18]. The particles on each plate formed a pattern of piles as seen in Fig. 1. The total mass of the particles on each plate was around 10–100 μg. For each run, four plates with the particle sizes (D50%) 0.093, 0.26, 0.611 and 1.59 μm were chosen for SEM/EDX analysis. Five EDX spot analyzes were taken from different locations on each plate (see Fig. 1). After standard ZAF-correction the analysis was normalized to 100% by weight. The analysis of the aluminum plates was made directly on the foil. The signals for carbon, oxygen and aluminum cannot be used for quantitative information due to several reasons. The carbon signal can originate from possible unburned residue in the samples, but also from the adhering Vaseline. The oxygen signal can come from, besides the particles, from the Vaseline and from the oxide layer covering the aluminum plate. The aluminum signal comes mainly from the plate beneath the samples. It was seen that the aluminum signal was stronger for bigger particles, probably due a lower coverage of the aluminum than with small particles. Peat ash contains aluminum so the effect of those additions on the fly ash could not be studied.

All experiments in this work were carried out with demolition wood and demolition wood with peat ash employing staged air combustion. The peat ash originates from the combustion plant owned by Vattenfall in Uppsala. The peat ash was mixed with lime from the plant's deSO$_x$ stage. The lime addition was unavoidable since it is part of the gas cleaning system at the Vattenfall plant in Uppsala. Only isothermal experiments were performed, the reactor was preheated to the required temperature which was held constant during the experiment. The total excess air ratio was about 1.6, and the primary air stoichiometry was about 0.8 for most of the experiments but was also varied in order to study the effect of lean O$_2$ condition in the primary zone on the volatility of chlorine and other alkali compounds. The reference experiment was run at a reactor temperature of 850 °C and with no addition of peat ash. Three other experiments were run at the same operational conditions with the exception of the peat ash addition of respectively 1, 5 and 10% to the demolition wood. Another two were run with 5% peat ash addition at different reactor temperatures of 800 and 900 °C. And finally two experiments were performed with lower (marked as LP) and higher (HP) air supply to the primary zone compared to the reference experiment. The secondary air combustion was changed respectively in order to obtain a total air excess ratio of 1.6.

3. Assumptions made for aerosol characterization

The first step of the data treatment was to recalculate the analysis to 100 wt.% discarding C, O and Al-signals. The variation among the five analyses of each plate was fairly small, indicating that the particles in the piles are homogeneous. This is illustrated in Fig. 2 which shows the normalized analyzes for the smallest (0.1 μm) and the biggest (1.6 μm) particle fraction analyzed. Note the significantly higher concentrations of Si, Ca and Fe in the bigger fractions. In the following calculations arithmetical average for the five analyzes are used. The second step of the data treatment was to estimate in which compounds the elements studied are in the samples. This consideration is based on several recently published studies on aerosol formation in combustion, as well as on thermodynamic considerations and own field experience. The following assumptions regarding the speciation are made: (i) Potassium and sodium are as chlorides or sulfates, (ii) Silicon, calcium, iron, magnesium and chromium are as oxides, (iii) Zinc and lead can be both as oxides and/or chlorides and sulfates. The first assumption is well established for fuels containing sulfur and chlorine. Alkali is volatilized as hydroxides or chlorides. Some of the alkali is sulfated at high temperatures and the first aerosol particles to form are sulfate. At lower temperatures alkali chlorides start to condense, probably mainly by a heterogeneous nucleation mechanism on sulfate or other submicron particles. The second assumption is based on the fact that Si, Ca, Fe, Mg and Cr are non-volatile. All these elements, except Ca, do not form sulfates or chlorides at higher temperatures. Thus they are transported downstream mainly as particles with a somewhat uncertain formation mechanism. Some of them may act as seed particles for alkali compound nucleation. Ca forms easily sulfate, but in the present case the calcium content in the samples are so low that this formation is not critical. Probably the non-sulfated part of Ca is in the form of carbonate at lower temperatures. Ca can also form phosphates at high temperatures, usually calcium hydroxyapatite. However, the content of P is so low in the present samples that this reaction can be neglected. The third
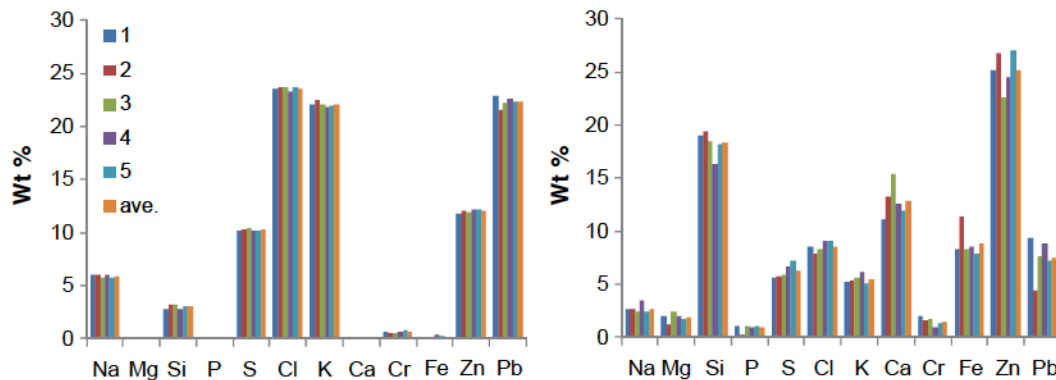

Fig. 2. Normalized concentrations (wt.%) calculated from C–O–Al free SEM/EDX analyzes of the five spots of the ELPI-samples for the reference run with demolition wood at 850 °C. Left: 0.1 μm plate. Right: 1.6 μm plate.
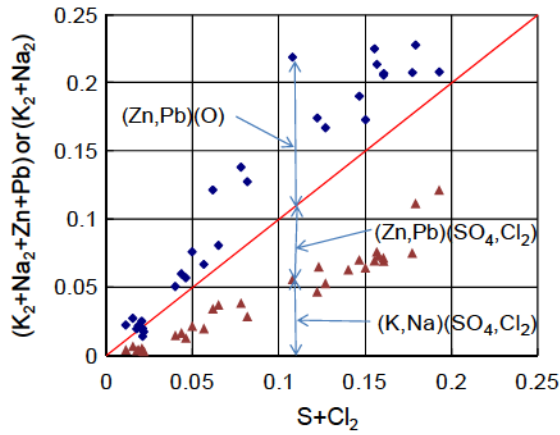
Fig. 3. Equivalent cations plotted against equivalent anions for fly ash samples from runs with peat ash addition. The upper points are for $K_2 + Na_2 + Zn + Pb$ and the lower for $K_2 + Na_2$. Indicated with arrows are the portions of different compounds in a given sample.

Fig. 5. Lead and zinc concentrations in the bottom ash samples (LP/HP; Low/High primary air amounts compared to the reference experiment).

assumption is the most critical one. In combustion conditions zinc and lead are partly volatile depending on the local chlorine content. These metals do not have similar chemistry although they are often treated together. Lead is much more volatile than zinc, but mainly in the form of gaseous PbO, which condensates at temperatures around 400 °C. Partly the oxide can react with chlorine and condensates as $PbCl_2$ at temperatures below 300 °C. At higher SO_2 concentrations lead can condensate as sulfates or as oxy-sulfate. Several sulfate-oxide compounds are possible. Solid zinc oxide is very stable in combustion conditions, but at lower temperatures both chlorides and sulfate can form. Probably zinc oxide is transported as small solid particles. It has been suggested that zinc inside the reducing fuel particle can form Zn gas which rapidly oxidizes to ZnO particles when it reaches oxygen rich location in an around the burning fuel particle [19,20]. This can explain the submicron size of the ZnO particles. We define two chemical different fractions in the fly ash samples: an "inert" part which constitutes of SiO_2, CaO, Fe_2O_3, MgO, P_2O_5, Cr_2O_3, ZnO and PbO, and a "salt" part consisting of sulfates and chlorides of potassium, sodium, zinc and lead. The inert part is assumed not to chemically interact with the
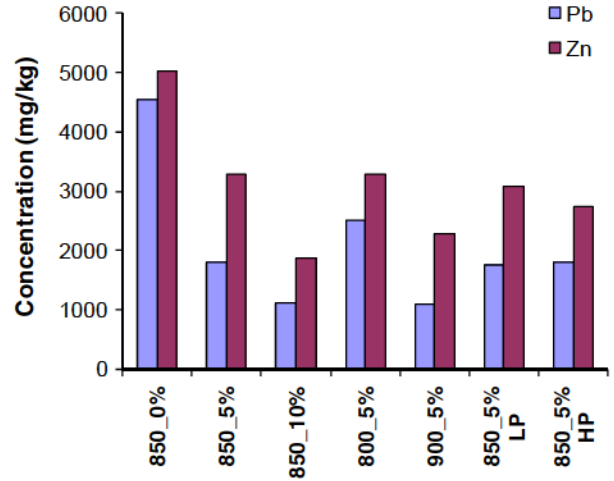
salt part. It consists of high melting oxides and may be silicates as well as free oxides. The portion of the inert part increases with particles size indicating that these particles have their origin in the fuel ash. The salt part can be denoted $(K, Na, Zn, Pb)(Cl_2, SO_4)$ and all its constituents are probably formed via the gas phase in a condensation/sublimation process. In this chemical system both solid and liquid solubility can exist between the components. Potassium and sodium chloride can form a solid solution, as can the sulfates of the two metals. Several double salts exist, both Zn and Pb form compounds with potassium chlorides. All four metals form a common chloride and sulfate melt with its lowest first melting point at around 200 °C [21]. The definition "salt" is somewhat inaccurate, but refers here to a low-melting water soluble fraction in contrast to the high melting insoluble inert oxide fraction. The salt fraction is the one causing deposition problems in the superheater area of steam boilers. The submicron particles which are transported to the heat transfer surfaces by thermophoresis can both initiate and further promote deposit build up if they contain a molten fractions above 15 wt-% [21]. The water solubility as such is not important for the deposition mechanisms, but it indicates an important property that can be used to determine the portion of Zn and Pb present
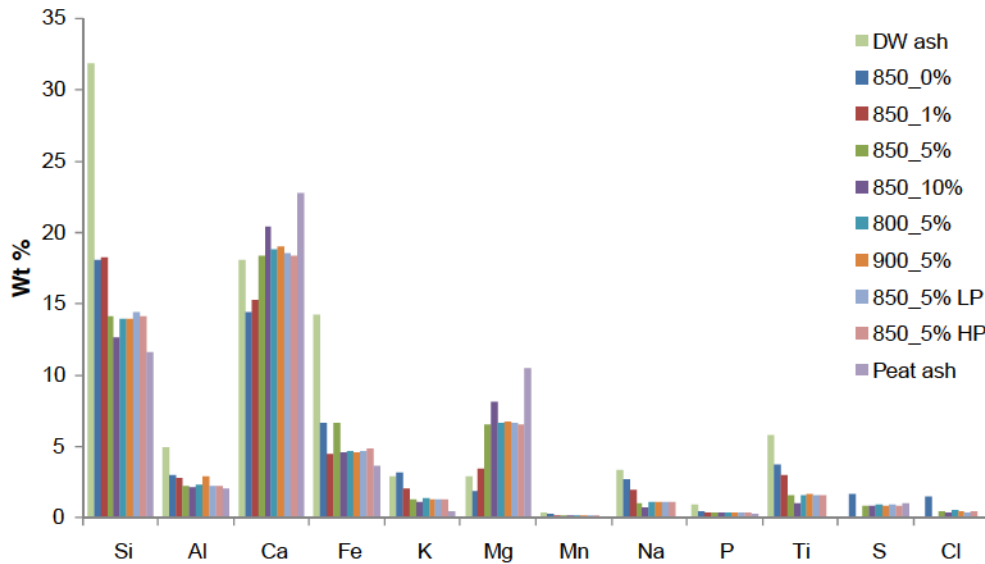

Fig. 4. Major composition of bottom ash from all experiments of Si, Al, Ca, Fe, K, Mg, Mn, Na, P, Ti, S and Cl using ICP-AES. Recalculated on dry ash. Oxygen not included in the analysis. First column gives the demolition wood ash (DW), the last one the peat ash.

in the salt part. It is evident that the salt part must have a balance between cations and anions. Thus, because we know, based on the chemical analysis of the fly-ash samples, the amount of Cl, S (as SO_4), K and Na, we can determine by difference the portion of Zn and Pb. It is not possible to distinguish in which form the specific metals are (chloride or sulfate), only the sum of metals can be balanced against the sum of anions. Fig. 3 shows as plot of the equivalent cations vs. equivalent anions (molar basis) for fly-ash samples from a run with kaolin addition. The notation K_2, Na_2 and Cl_2 are used for consistency with $ZnCl_2$ and $PbCl_2$. "S" should be read as "SO_4". It can be seen that the amount of K_2 and Na_2 cannot fill up all sulfate and chloride in the samples. Thus, a part of Zn and Pb are expected to be present as sulfate and chloride, too. Subsequently a diagram with normalized equivalent fractions of the cations and anions are used to compare the compositions of the salt part of fly-ash samples taken in different running conditions.

4. Results and discussion

4.1. Bottom ash analysis

To determine the fate of some of the ash elements during combustion and the effect of peat ash, the chemical composition of the bottom ash was determined by the ICP-AES and ICP-SFMS methods. The concentrations of the main elements for all the experiments are shown graphically in Fig. 4. The figure shows that the peat ash is richer in calcium and magnesium than the demolition wood (DW) ash, which, hold more silicon, potassium, sodium, aluminum and titanium. The ash content of DW is around 4%, i.e. an addition of 5% peat ash would approximately double the amount of incoming ash. The results show a clear trend of decreasing Si, K, Na, Al and Ti with increasing peat ash addition as expected. Similarly Ca and Mg increase with peat ash addition. No clear trends are seen between the samples for the other major elements. Differences between the samples at different temperatures (800–900 °C) are small, as are they for the samples taken during different air staging at 850 °C and 5% peat ash addition. As seen in Fig. 5, the concentration of both lead and zinc decrease linearly with peat ash addition. The decrease corresponds fairly well with the dilution effect due to added peat ash. It was not possible to close the mass balance for lead and zinc accurately enough to determine if there is an enrichment or depletion of these metals in the bottom ash due to peat ash addition. On the other hand, a clear trend for both lead and zinc can be seen in the samples at different temperatures with 5% peat ash addition. The concentration of both metals decrease as a function of temperature indicating higher devolatilization at higher temperatures.
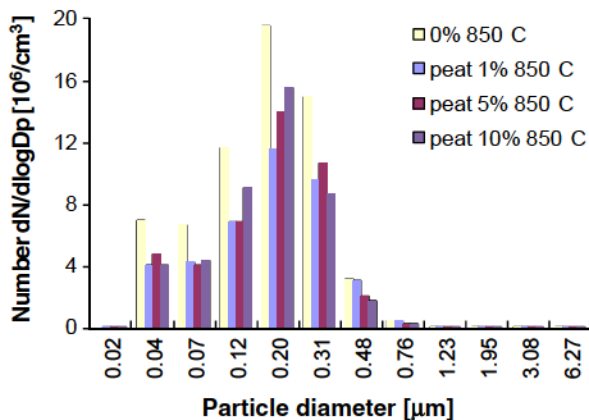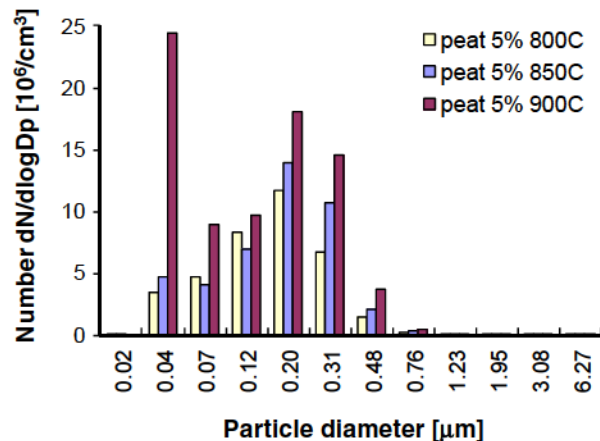

Fig. 7. The partide size distribution in the fly ash + lime for different reactor temperatures.

4.2. Aerosol size distribution

The particle size distribution in the flue gas was monitored with an ELPI for the aerosols in the range of 0.03–10 μm. It is acknowledged by the authors that larger particles belonging to the coarse fly ash range might exist in addition to the size range discussed in this study. It is however believed that these particles are most likely found in moderate quantities because of a low probability of entrained particles. This is due to the straight reactor geometry and the extremely low flow velocity (0.03–0.07 m/s). The results of the particle size distribution are shown in Figs. 6–8. There is not a clear trend showing how increasing addition of peat ash influences the particle size distribution (Fig. 6). In the reference sample without ash addition, the amount of smaller particles are considerably higher than in the experiments with peat ash addition, which show a slight increase of particles smaller than 0.2 μm with increased peat ash addition. For larger particles a decrease in the amount of particles is seen. Higher temperatures give increased amount of all particle fractions (Fig. 7). The load of 0.04 μm particles is exceptionally high at 900 °C. For the other size fractions the amount of particles is 50–100% higher at 900 °C that at 800 °C. The results indicate that a low level primary air-staging give higher particle loads, especially for smaller particles (Fig. 8), whereas the high level air-staging seems to promote formation of particles in the range 0.3–1.2 μm.

Fig. 6. The particle size distribution in the fly ash for different peat ash + lime additions.
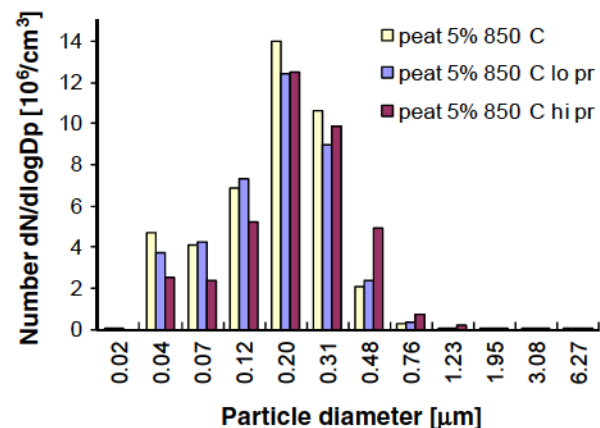

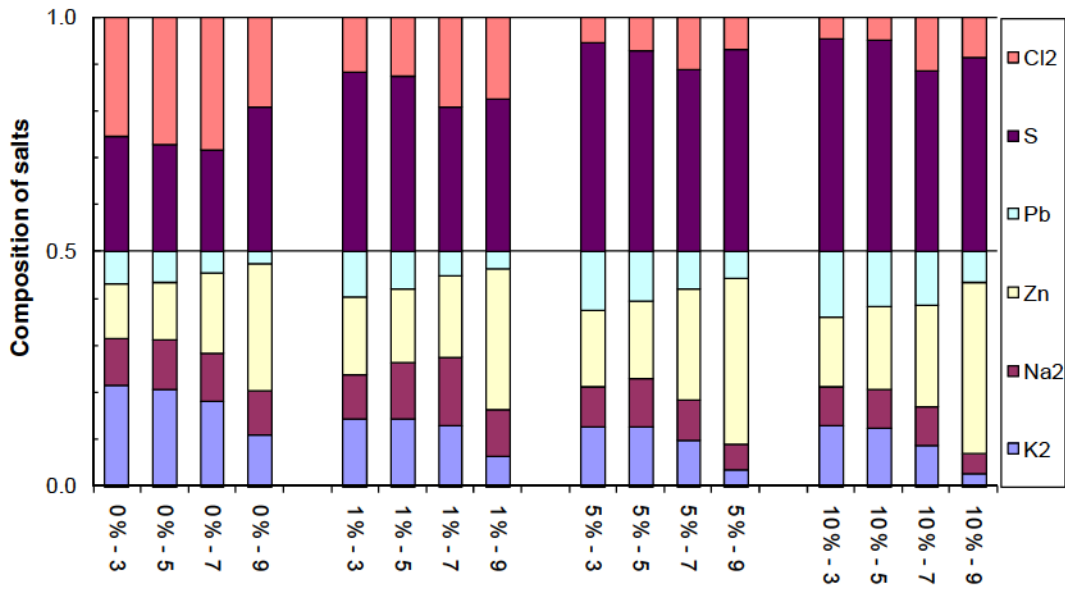Fig. 8. The particle size distribution in the fly ash + lime for different primary air amounts.

Fig. 9. The chemical composition of the impactor stages 3, 5, 7 and 9 corresponding to the sizes 0.093; 0.26; 0.611; 1.59 μm of the fly ash taken by the ELPI in the exhaust of the reactor as a function of peat ash + lime addition.

4.3. Chemical composition of particles

The composition of the salt part of the samples collected in the ELPI measurements are given in Figs. 9–11. The samples are dominated by Zn and Pb. In average 50 wt.% of the oxygen-free samples (excluding carbon and aluminum) consisted of these elements. The portion of K, S, Cl and Na where in average 35 wt.%, whereas the portion of the inert oxide forming elements Si, Ca, Fe, P, Mg and Cr was 15 wt.%. P and Mg were very low in all samples. The portion of inert metals was generally higher in the bigger particle size fractions than in the smaller fractions, indicating that the compounds of these metals (oxides) originate from the original fuel ash and have not been devolatilized. Lead and zinc are partly in oxide form, partly in salt form. The oxides are most probably ZnO and PbO. The salt part constitutes of sulfate and chloride of K, Na, Zn and Pb. For peat ash addition at 850 °C (Fig. 9), the salt part was richest in chloride for the reference run (50%) and decreased at peat ash addition to 20–30% chloride at 1%,

and to 5–10% chloride at 5 and 10% ash addition, respectively, the latter two being very similar in composition. Potassium decreased significantly with increasing peat ash addition, being 40–50% in the reference run and 5–10% at 10% ash addition. A corresponding decrease in the Na content is not observed. Zinc increased with increasing ash addition, indicating formation of zinc sulfate. The zinc content was higher in big particles compared to smaller particles. Lead, again, showed the opposite trend decreasing with particle size. The composition of the salt part for the different temperatures is very similar for the runs at 800 °C and 850 °C, chloride being some 20% in all samples (Fig. 10). At all three temperatures the zinc content is dominating. The concentrations of zinc (and lead) account for about 40–50% of the salts produced for the small particles (0.093 μm) and up to 90% for the larger particles (1.59 μm). It shows an increasing trend with increasing particle size. In contrast, both potassium and lead decrease with particle size while the trends in sodium content are weak. No clear trend can be seen in the composition of the salt part as
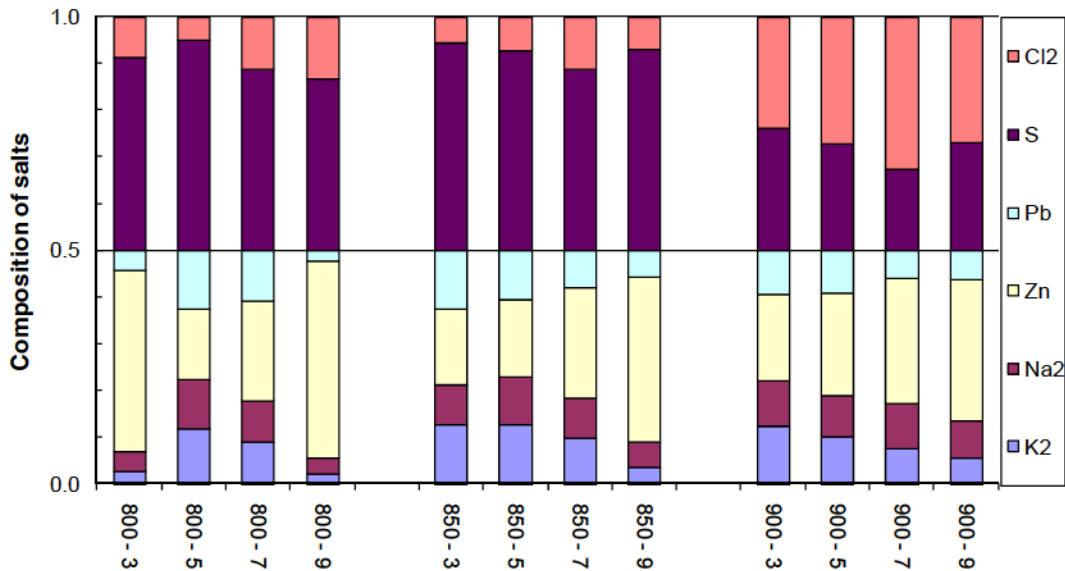

Fig. 10. The chemical composition of the impactor stages 3, 5, 7 and 9 corresponding to the sizes 0.093; 0.26; 0.611; 1.59 μm of the fly ash taken by the ELPI in the exhaust of the reactor as a function of temperature.
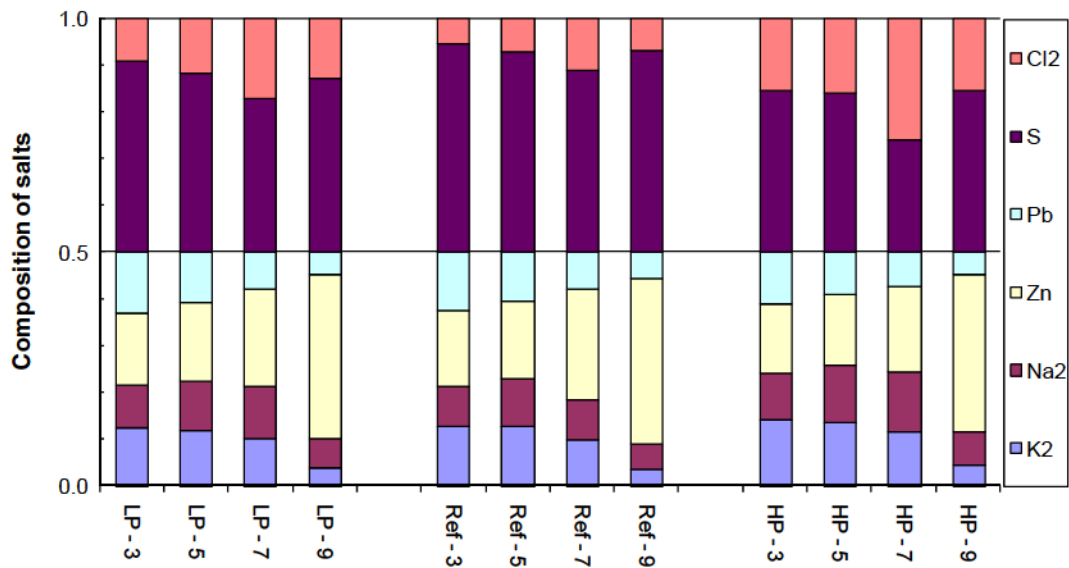
Fig. 11. The chemical composition of the impactor stages 3, 5, 7 and 9 corresponding to the sizes 0.093; 0.26; 0.611; 1.59 μm of the fly ash taken by the ELPI in the exhaust of the reactor as function of different air distribution between primary and secondary stages (LP/HP; Low/High primary air amounts compared to the reference experiment).

a function of primary air level (Fig. 11). Low and normal primary air are very similar. They have a chloride content of 10–20% and show all an increase of zinc and decrease of potassium and lead with increasing particle size. The high primary air sample has slightly higher chloride content (20–40%) for all size fractions. To sum up, lower alkali chloride concentrations could have an inhibiting effect on corrosion, but high Zn and especially Pb concentrations may lead to a lower first melting point of the aerosol particles. This, again, may promote deposition on heat transfer surfaces in the flue gas channel.

4.4. The fate of chlorine

The chlorine distribution between the bottom ash and the gas phase relative to the chlorine input in the fuel is shown in Fig. 12. Note that bottom ash analysis could not be made for the sample with 1% peat ash addition. The figure does not include the chlorine in the fly
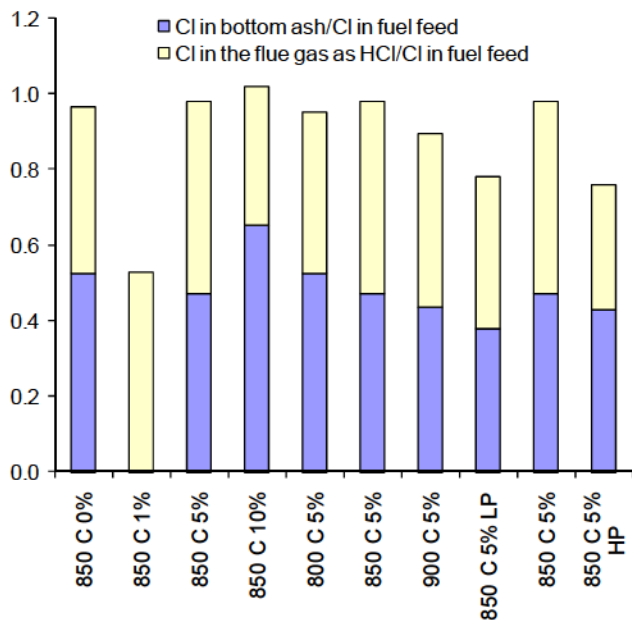

Fig. 12. Distribution of chlorine between gas phase (as measured HCl) and bottom ash.

ash because not all of the impactor stages were chemically analyzed. However, the chlorine in the fly ash is assumed to have a minor influence on the total mass balance due to the relatively small amounts of fly ash compared to bottom ash. It can be noticed that the chlorine distribution is somewhat unbalanced probably due to uncertainties in the chemical analysis of the raw fuel, the bottom ash and measurements in the gas phase. However, some interesting trends can be extracted from the results. Generally, the portion of chlorine in the bottom ash is 40–50% of total chlorine. This is a high value, which may be due to the relatively high amount of unburned char in the bottom ash samples. It is expected based on thermodynamic considerations and experience that the chlorine is in the form of alkali chlorides in completely burned ash fractions. Some chlorine can probably dissolve into molten silicates but the amount of this is expected to be low compared to alkali chlorides. The chlorine in the bottom ash seems to increase with increased peat ash addition. Comparing the 5% and 10% additions at 850 °C, show considerably higher Cl in the bottom ash at 10% addition. This indicates that the retention of Cl is strongly affected by the presence of peat ash in the fuel pellet. The calcium content of the peat ash used is rather high, which could promote $CaCl_2$ formation, but taking into consideration the high sulfur content in the bottom ash, the stable form of calcium not bound to silicate, should be calcium sulfate. The peat ash seems to be facilitating chlorine mobility at higher temperatures. A slight trend in seen for the different reactor temperatures with less chlorine in the bottom ash at higher temperatures, However, a clear corresponding increase of HCl is not seen in these samples. No clear trends on the Cl-distribution of different air-staging could be detected.

4.5. The fate of sulfur

The distribution of sulfur between bottom ash and SO_2 in the gas is shown in Fig. 13. The ratios for sulfur in gas to total sulfur and the ratio in bottom ash to total sulfur are rather near to unity, indicating that the mass balance for sulfur is fairly well closed based on these two fractions. Thus, the amount of sulfur of the fly ash is small compared to the total amount. Some 60–80% of the total sulfur is found in the bottom ash for all samples. No clear trends can be detected between the different running conditions indicating that the sulfur chemistry for the demolition wood is not significantly affected by the ash addition. This could be expected due to the rather low sulfur content in the peat ash used.
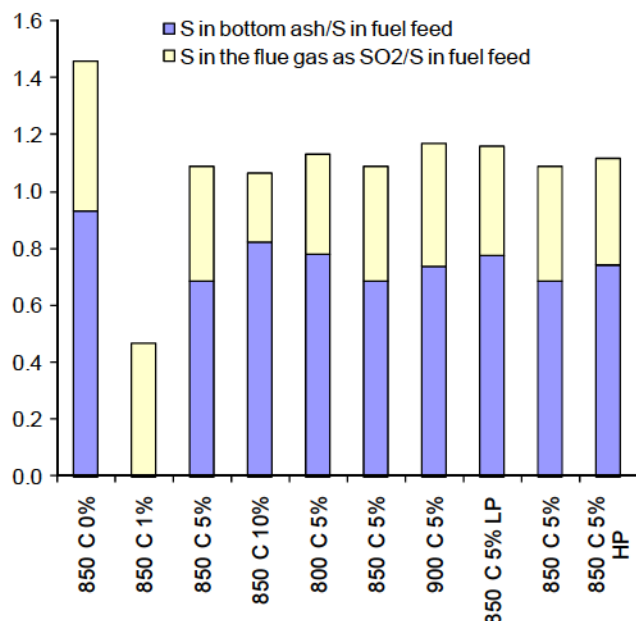
Fig. 13. Distribution of sulfur between gas phase (as measured SO_2) and bottom ash.

5. Conclusions

Experiments were made to understand how an addition of peat ash affects the composition of ash fractions and gas in combustion of demolition wood with variations in reactor temperature, combustion air distribution and amount of peat ash addition. The gas phase was monitored with several gas analyzers both in the primary zone and in the stack. Complete characterization of the raw fuel and the bottom ash was performed for all the experiments. The fly ash particle size distribution was monitored and in addition a chemical analysis of the fly ash from four impactor stages was performed. The following conclusions were made base on the interpretations of the measured data:

- The bottom ash composition changed as peat ash was added. Enrichment of the main elements more abundant in the peat ash (Ca and Mg) was observed indicating that the added ash generally followed the bottom ash.
- Zinc and lead which originate from the demolition wood showed the same behavior, i.e. their concentration in the bottom ash decreased with peat ash addition. As a function of temperature Zn and Pb decrease in the bottom ash indicating more extensive mobility of these metals at higher temperatures. 60–80% of the total sulfur and 40–50% of the total chlorine retain in the bottom ash.
- A method was developed to estimate the composition and speciation of the salt part of fly ash samples based on SEM/EDX analysis. The results show that the concentrations of zinc and lead are very high in the fly ash samples. A considerable part of these metals are chemically bound to chlorides and sulfates together with potassium and sodium indicating extensive volatilization of both zinc and lead.
- Potassium volatilization decreased with peat ash addition, which may be due to reactions between peat ash and alkali. The zinc content was higher in big particles (0.4–1.3 μm) compared to smaller particles. Lead, again, showed the opposite trend decreasing with particle size.

- Although it was not possible to determine quantitatively the effect of peat addition, the experiments show that the inorganic reactions are influenced in several ways. Potassium, zinc and lead are the metals most affected. Probably an absorption effect of potassium gives rise to higher concentrations of zinc and lead in the aerosols. Simultaneously the chloride content in the aerosols decreases with increased peat ash addition.

References

[1] L.L. Baxter, T.R. Miles, T.R. Miles, B.M. Jenkins, T. Milne, D. Dayton, R.W. Bryers, L.L. Oden, The behavior of inorganic material in biomass-fired power boilers: field and laboratory experiences, Fuel Process. Technol. 54 (1998) 47–78.
[2] C. Yin, L.A. Rosendahl, S.K. Kær, Grate-firing of biomass for heat and power production, Prog. Energy Combust. 34 (2008) 725–754.
[3] L.S. Bäfver, M. Rönnbäck, B. Leckner, F. Claesson, C. Tullin, Particle emission from combustion of oat grain and its potential reduction by addition of limestone or kaolin, Fuel Process. Technol. 90 (2009) 353–359.
[4] M. Broström, H. Kassman, A. Helgesson, M. Berg, C. Andersson, R. Backman, A. Nordin, Sulfation of corrosive alkali chlorides by ammonium sulfate in a biomass fired CFB boiler, Fuel Process. Technol. 88 (2007) 1171–1177.
[5] P. Henderson, P. Szakálos, R. Pettersson, C. Andersson, J. Högberg, Reducing superheater corrosion in wood-fired boilers, Mater. Corros. 57 (2006) 128–134.
[6] M. Aho, P. Vainikka, R. Taipale, P. Yrjas, Effective new chemicals to prevent corrosion due to chlorine in power plant superheaters, Fuel 87 (2008) 647–654.
[7] M. Aho, J. Silvennoinen, Preventing chlorine deposition on heat transfer surfaces with aluminium-silicon rich biomass residue and additive, Fuel 83 (2004) 1299–1305.
[8] B.J. Skrifvars, T. Laurén, M. Hupa, R. Korbee, P. Ljung, Ash behaviour in a pulverized wood fired boiler — a case study, Fuel 83 (2004) 1371–1379.
[9] L. Tobiasen, R. Skytte, L.S. Pedersen, S.T. Pedersen, M.A. Lindberg, Deposit characteristic after injection of additives to a Danish straw-fired suspension boiler, Fuel Process. Technol. 88 (2007) 1108–1117.
[10] R. Khalil, D. Todorovic, Ø. Skreiberg, M. Becidan, R. Backman, F. Goile, A. Skreiberg, L. Sørum, The effect of kaolin on the combustion of demolition wood under well controlled conditions, submitted to Waste Manage. Res. (2011).
[11] B. Coda, M. Aho, R. Berger, K.R.G. Hein, Behavior off chlorine and enrichment of risky elements in bubbling fluidized bed combustion of biomass and waste assisted by additives, Energ Fuel 15 (2001) 680–690.
[12] M. Theis, B.J. Skrifvars, M. Zevenhoven, M. Hupa, H.H. Tran, Fouling tendency of ash resulting from burning mixtures of biofuels. Part 2: Deposit chemistry, Fuel 85 (2006) 1992–2001.
[13] L. Pommer, M. Öhman, D. Broström, J. Burvall, R. Backman, I. Olofsson, A. Nordin, Mechanisms behind the positive effects on bed agglomeration and deposit formation combusting forest residue with peat additives in fluidized beds, Energ Fuel 23 (2009) 4245–4253.
[14] B.J. Skrifvars, R. Backman, M. Hupa, G. Sfiris, T. Abyhammar, A. Lyngfelt, Ash behaviour in a CFB boiler during combustion of coal, peat or wood, Fuel 77 (1998) 65–70.
[15] B.J. Skrifvars, M. Zevenhoven, R. Backman, M. Hupa, Predicting the ash behavior of different fuels in fluidized bed combustion, Proceedings of the 16th International Conference on Fluidized Bed Combustion Paper No. FBC01-113, 2001.
[16] M. Zevenhoven-Onderwater, J.P. Blomquist, B.J. Skrifvars, R. Backman, M. Hupa, The prediction of behaviour of ashes from five different solid fuels in fluidised bed combustion, Fuel 79 (2000) 1353–1361.
[17] http://dekati.com/ 2010.
[18] http://www.topanalytica.com/ 2010.
[19] S. Abanades, G. Flamant, B. Gagnepain, D. Gauthier, Fate of heavy metals during municipal solid waste incineration, Waste Manage. Res. 20 (2002) 55–68.
[20] I. Obernberger, Ash related problems in biomass combustion plants, Inaugural lecture presented on May 20, 2005 at Technische Universiteit Eindhoven, 2005, available at, www.alexandria.tue.nl/extra2/redes/obernberger2005.pdf.
[21] R. Backman, B.J. Skrifvars, P. Yrjas, The influence of aerosol particles on the melting behaviour of ash deposits in biomass fired boilers, Aerosols in Biomass Combustion Series Thermal Biomass Utilization, Graz, Volume 6, 2005, pp. 119–132.

Original Article

The effect of kaolin on the combustion of demolition wood under well-controlled conditions

Roger A Khalil,[1] Dusan Todorovic,[2] Øyvind Skreiberg,[1] Michael Becidan,[1] Rainer Backman,[1] Franziska Goile,[1] Alexandra Skreiberg[1] and Lars Sørum[1]

Abstract

In an attempt to look at means for reduction of corrosion in boilers, combustion experiments are performed on demolition wood with kaolin as additive. The experiments were performed in a multi-fuel reactor with continuous feed of pellets and by applying staged air combustion. A total characterization of the elemental composition of the fuel, the bottom ash and some particle size stages of fly ash was performed. This was done in order to follow the fate of some of the problematic compounds in demolition wood as a function of kaolin addition and other combustion-related parameters. In particular chlorine and potassium distribution between the gas phase, the bottom ash and the fly ash is reported as a function of increased kaolin addition, reactor temperature and air staging. Kaolin addition of 5 and 10% were found to give the least aerosol load in the fly ash. In addition, the chlorine concentration in aerosol particles was at its lowest levels for the same addition of kaolin, although the difference between 5 and 10% addition was minimal. The reactor temperature was found to have a minimal effect on both the fly ash and bottom ash properties.

Keywords

Demolition wood, combustion, kaolin additive, bottom ash, fly ash, gas composition

Date received: 21 January 2011; accepted: 21 September 2011

Introduction

Biomass is receiving increased interest from decision makers which has resulted in more utilization over recent years. Different final products originating from biomass are produced nowadays and include biofuel for the transport sector, chemicals, power and heat. The purpose of biomass utilization is to replace fossil fuel and thereby decrease greenhouse gas emissions which are contributing to global warming. The increased biomass consumption has resulted in higher prices of virgin wood up to a range at which it is no longer profitable to operate power stations based on combustion of wood alone (Baxter et al., 1998). This has resulted in the increased utilization of alternative fuels that are less expensive to acquire but have different properties in comparison with virgin wood, which makes combustion more problematic. This also holds true for small power units that usually rely on indigenous fuel supply delivered at minimal transport costs. Alternative fuels such as peat, agricultural waste, different grass types and fast-growing species, which are solely combusted or co-combusted, all have one thing in common, namely a high ash content. The higher ash content in such fuels may cause severe problems resulting in unscheduled and expensive shutdown periods in power plants. In fixed bed combustors, the alkali metals in particular can become volatile and stick on heat transfer surfaces downstream in the process. Such deposits are difficult to remove and cause lower

efficiencies due to a decrease in heat transfer and a higher flue gas temperature. They can also bridge between the tubes and restrict flue gas flow which results in higher pressure drops. The deposits themselves have a composition which make them quite aggressive resulting in attacks on the metallic surface of the heating tubes. For example, the chlorine in the ash facilitates the mobility of alkalis such as potassium, forming KCl which has a low melting temperature. During combustion there is not much one can do to prevent chlorine compounds from leaving the bottom ash as different gaseous volatiles passing through the process along with the flue gas. However, the capture of alkalis through the use of additives has helped to lower the alkali chlorides concentration in the flue gas and thereby decrease corrosion in boilers substantially. Chlorine having to compete for the alkalis during chemical reactions is usually released as HCl, a compound that is corrosive

[1]SINTEF Energy Research, Department of Energy Processes, Trondheim, Norway
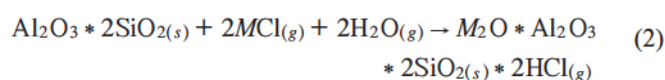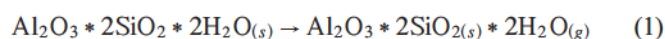[2]Faculty of Mechanical Engineering, University of Belgrade, Belgrade, Serbia

Corresponding author:
Roger A. Khalil, SINTEF Energy Research, Department of Energy Processes, NO-7465, Trondheim, Norway
Email: roger.a.khalil@sintef.no

on its own but lacks the sticky property that alkali chlorides have. In addition, HCl is easily cleaned from the flue gas in a post-combustion stage by scrubbing it with limestone or by dry-sorption with Ca(OH)$_2$ (Yin et al., 2008). In fluidized bed combustion systems, agglomeration can become a serious problem for fuels containing high amounts of potassium oxides (K$_2$O). The K$_2$O and other alkali oxides react with silicate (Si) found in the sand that is usually used as bed material and form compounds with low melting points (760–875 °C) (Werther et al., 2000). Furthermore, in such cases the role of additives has been shown to have a positive effect on abating agglomeration by forming compounds that can withstand the high temperature environment (Bartels et al., 2008; Davidsson et al., 2007, 2008; Khan et al., 2009; Llorente et al., 2006; Pettersson et al., 2009; Vamvuka et al. 2008, 2008). Additives can be either mixed with the fuels prior to combustion, they can be added to the bed material in case of fluidized bed combustor or they can be sprayed at critical stages directly into the flue gas at an optimized gas temperature. Depending on their elemental composition, additives can be separated into groups containing calcium, phosphorous, sulfur, aluminium or aluminium–silicate (Bäfver et al., 2009). For liquid-based additives, the so-called ChlorOut system developed by Vattenfall has shown some promising results in substantially decreasing the alkali chlorides in the flue gas (Broström et al., 2007; Henderson et al. 2006). ChlorOut is based on spraying a solution of ammonium sulfate prior to the superheater section in the boiler. Other sulfate solutions such as aluminium and ferric sulfates have also shown to have a similar effect to the ChlorOut system (Aho et al., 2008). Additives in the form of solid particles can also be mixed with the bio-fuel prior to combustion. Sulfur-rich additives such as peat or pure sulfur are expected to chemically react with potassium and sodium to form M$_2$SO$_4$, where M can be either K or Na. Sulfur addition to agricultural waste has shown promising results in decreasing the potential of corrosion in boilers (Aho and Silvennoinen, 2004; Skrifvars et al., 2004). Calcium–phosphorous and aluminium–silicate-based additives were tested in a full-scale straw pellet boiler at the Amager power station in Denmark (Tobiasen et al., 2007). Among the tested additives were sand, dicalcium phosphate, chalk and bentonite. The work concluded by picking sand and bentonite as having favourable properties for combating deposits in the boiler.

In this study, kaolin was chosen as the additive to demolition wood in order to study in detail its effectiveness in capturing the alkalis from the gas phase. Kaolin reactivity with gaseous alkalis has already been shown to be quite effective (Tran et al., 2004, 2005) and many publications applying kaolin as additive in full-scale applications have shown good tendencies towards benefits in preventing agglomeration, fouling and corrosion (Coda et al., 2001; Davidsson et al., 2007; Vamvuka et al., 2008). However, in this work a laboratory-scale reactor with good control over temperature, fuel and air inputs in addition to gas and particle measurement was used to study some parameter variations on the reactivity of kaolin. The aluminium silicates in kaolin can react with alkalis and form compounds with higher melting point (Davidsson et al., 2008). The reactions between alkali chlorides and aluminium silicates are expected to follow mechanisms presented in Equation (1) and Equation (2) (Coda et al., 2001).

$$Al_2O_3 * 2SiO_2 * 2H_2O_{(s)} \rightarrow Al_2O_3 * 2SiO_{2(s)} * 2H_2O_{(g)} \quad (1)$$

$$Al_2O_3 * 2SiO_{2(s)} + 2MCl_{(g)} + 2H_2O_{(g)} \rightarrow M_2O * Al_2O_3 \\ * 2SiO_{2(s)} * 2HCl_{(g)} \quad (2)$$

where M can be either K or Na.

As reactions in Equation (1) and (2) show the alkalis are captured by the kaolin while the chlorine is released as HCl.

Materials and methods

Demolition wood was provided by Vattenfall from the combustion plant at Nyköping, Sweden. The demolition wood was ground in a mill to produce a maximum particle size of 2–3 mm. The particles were then mixed with appropriate amounts of kaolin to produce fuels with 1, 5 and 10 wt.% kaolin relative to the fuel. The additives were mixed manually while spraying approximately 8% water relative to the total mass into the blend. The water was necessary in order to produce pellets of adequate quality which was performed in a laboratory scale pellet machine. The produced pellets had a diameter of 6 mm and a of length 5–15 mm and were air dried to an average moisture content of 12 wt.% before they were used in experiments. The proximate analysis of the sample was carried out according to the ASTM standards ASTM E871, ASTM E872 and ASTM D1102, respectively, for the moisture content, volatile matter and ashes. The fixed carbon was calculated by difference to 100%. The results of both the proximate and ultimate analysis are presented in Table 1. A chemical analysis of the ash content of the primary

Table 1. Ultimate and proximate analysis of the demolition wood wt-% (db).

Proximate analysis			
Volatiles (dry basis)	Fixed carbon (dry basis)	Ash (dry basis)	Moisture (as received)
77.13	19.00	3.87	7.98

Ultimate analysis (oxygen calculated by difference)					
C	H	N	O	S	Cl
50.53	6.09	1.59	41.60	0.08	0.11

fuel and all the blends was determined by the inductive coupled plasma equipped with an atomic emission spectrometry analyser (ICP-AES) and inductive coupled plasma equipped a mass spectrometry analyser (ICP-SFMS) methods. The element composition of the ash for the different fuel mixtures are presented in Table 2.

Experimental setup

The experiments were carried out in an electrically heated high-temperature multi-fuel reactor. Its schematic drawing is presented in Figure 1. The reaction section, located above the grate is 1.6 m long, while the section below the grate is 0.4 m long. The reactor heating system is fitted inside the insulation shell and consists of four separate 0.5 m high heating zones of 4 kW each (16 kW in total) that enclose the ceramic tube. The combustion air is pre-heated to the reactor temperature in external pre-heaters. The primary air is added under the grate and the secondary air is added above the grate. The lower part of the multi-fuel reactor is the section containing two-grate system (10 cm apart): a primary grate and a final burnout grate and an ash collection system. Both

the reactor flue gas composition and the composition of the fuel gas after the primary zone as well as the particle emission size distribution were continuously monitored.

For gas analysis in the primary zone a Varian CP-4900 micro gas chromatograph (GC) was used. The exhaust gases were quantified online with two different Fourier transform infrared spectrometers (FTIRs), a Bomem 9100 and a Gasmet DX-4000. In order to detect instabilities during combustion a gas analyser with a fast response time (HORIBA PG-250) was used. Particle size distribution and concentration in the flue gas were measured by an electrical low pressure impactor (ELPI). The ELPI measures airborne particle size distribution in a range of 0.03–10 μm with twelve stages and a time resolution of 2 to 3 s. The nominal air flow is 10 L min^{-1} and the lowest stage pressure is 100 mbar. The aerosol samples measured by means of a 13-stage low-pressure impactor were collected on aluminium plates. The chemical analyses of the samples were made by energy-dispersive X-ray analysis connected to a scanning electron microscope (SEM/EDX). The total mass of the particles on each plate was around 10 to 100 μg. For each run, four plates with the particle sizes ($D_{50\%}$) 0.093, 0.26, 0.611 and 1.59 μm were chosen for analysis.

Table 2. Chemical composition (dry basis) of the ash of demolition wood and the generated mixtures.

| Kaolin %	0	1	5	10	100
Ash content (%)	3.9	4.3	7.9	11.7	100
Si (%)	1.2	1.7	3.7	5.5	21.9
Al (%)	0.2	0.7	1.9	3.2	18.9
Ca (%)	0.7	0.7	0.7	0.7	0.07
Fe (%)	0.5	0.3	0.5	0.5	0.6
K (%)	0.1	0.1	0.2	0.2	1.3
Mg (%)	0.1	0.1	0.1	0.1	0.1
Mn (%)	0.01	0.01	0.01	0.01	0.005
Na (%)	0.1	0.1	0.1	0.1	0.04
P (%)	0.04	0.04	0.04	0.04	0.03
Ti (%)	0.2	0.2	0.3	0.3	0.3
Cl (%)	0.11	0.12	0.11	0.09	–
S (%)	0.07	0.11	0.13	0.12	0.02
As (mg kg^{-1})	4	4	10	3	–
Ba (mg kg^{-1})	319	332	285	336	192
Be (mg kg^{-1})	0.04	0.20	0.69	1.25	14
Cd (mg kg^{-1})	1.31	0.78	1.22	0.88	0
Co (mg kg^{-1})	1.36	1.20	1.37	1.86	1.08
Cr (mg kg^{-1})	59	33	39	56	34
Cu (mg kg^{-1})	166	358	40	81	7.82
Mo (mg kg^{-1})	0.89	0.70	0.67	0.94	0
Nb (mg kg^{-1})	0.60	0.90	2.47	3.38	37.4
Ni (mg kg^{-1})	2.7	13.0	2.0	17	4.99
Pb (mg kg^{-1})	426	233	361	415	69.1
Sc (mg kg^{-1})	0.11	0.14	0.35	0.57	4.17
Sn (mg kg^{-1})	1.89	1.81	1.76	2.20	10.3
Sr (mg kg^{-1})	25	26	26	28	37.2
V (mg kg^{-1})	1.57	1.93	3.35	4.86	39.3
W (mg kg^{-1})	12	21	11	55	0
Y (mg kg^{-1})	0.49	0.63	1.36	2.15	18.8
Zn (mg kg^{-1})	679	1030	333	908	34.1
Zr (mg kg^{-1})	9	10	16	20	103
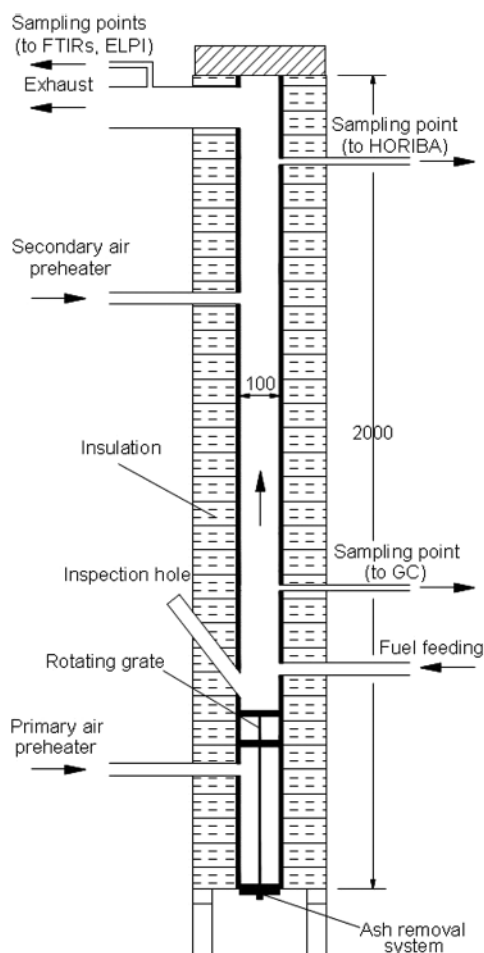
Figure 1. Schematic drawing of the reactor.

Five EDX spot analyses were taken from different locations on each plate. After standard ZAF-correction the analysis was normalized to 100% by weight. The signals for carbon, oxygen and aluminium cannot be used for quantitative information for several reasons. The carbon signal can originate from possible unburned residue in the samples, but also from the adhering Vaseline. These same sources can also disturb the oxygen signal. The aluminium signal comes mainly from the plate beneath the samples. As kaolin contains aluminium, the effect of those additions on the fly ash could not be studied. The assumptions made for the data treatment of the aerosol concentrations are explained elsewhere (Backman et al., 2011). Temperature was measured in the reactor at several heights and in the flue gas channel. All experiments in this work were carried out with demolition wood and demolition wood with kaolin employing staged air combustion and isothermal conditions. The total excess air ratio was about 1.6, and the primary air stoichiometry was about 0.8 for most of the experiments but was also varied in order to study the effect on the volatility of chlorine and other alkali compounds of a lean O_2 condition in the primary zone. The reference experiment was run first at a reactor temperature of 850 °C and with no addition of kaolin. Three other experiments were run under the same conditions with the exception of

the kaolin addition of 1, 5 and 10% of weight, respectively, to the demolition wood. Another two were run with 5% of kaolin addition but with different reactor temperatures of 800 and 900 °C. Finally two experiments were performed with lower (marked as LP) and higher (HP) air supply to the primary zone in comparison with the reference experiment. The secondary air combustion was changed, respectively, in order to obtain a total air excess ratio of 1.6. The feeding frequency was set to ensure a feeding rate of $400\,\mathrm{g\,h^{-1}}$. The pellets were primarily combusted on the upper grate. The pellets were gradually moved from the fuel-feeding inlet to a slot leading to the second grate by rotating blades. Each grate had two rotating blades moving at a speed of 3 min per round. Final burnout took place on the second grate before the ash was moved to a slot from where it fell into the ash bin. Due to small variation in pellet size, it was not possible to feed the target rate of $400\,\mathrm{g\,h^{-1}}$ exactly. Accordingly, the supply of primary air could not be regulated accurately to attain the under stoichiometric condition of 0.8, although the variations were within an acceptable range. The primary air supply was adjusted so that the CO concentration from the primary zone was approximately 3%. The combustion time for each experiment was dependent on whichever of the following two events occurred first: (i) minimum stable combustion conditions of 2 h; or (ii) a 90% fill signal of aerosols in the impactor.

Results

Due to the relatively long reactor residence time (30–60 s) and the high reactor temperature (800–900 °C), the amount of unburnt gases were very low (typically below 50 ppm CO at 11% O_2 in dry flue gas). However, during an initial stabilization period and short periods of high fluctuation in the fuel feeding, the air excess ratio deviated from the target value of 1.6. During such periods the CO emission level increased to typically 200 ppm at 11% O_2 in dry flue gas. The combined emission levels of hydrocarbons were typically below 5 ppm at 11% O_2 in dry flue gas. The average concentration and standard deviation (in brackets) were 8.2% (1.0), 28 ppm (30) and 11.5% (0.9), respectively, for O_2, CO and CO_2. These are average values for all the measured data points and for all the conducted experiments.

Bottom ash analysis

In order to be able to check the fate of some of the ash elements during combustion and the effect of kaolin, the chemical composition of the bottom ash was determined by the ICP-AES and ICP-SFMS methods. The concentrations of the most important elements for all the experiments are shown graphically in Figure 2. The increase of silicon and aluminium due to increased kaolin content is noticeable in the bottom ash. The potassium and chlorine also decrease as kaolin increases, although from this figure alone it is difficult to conclude whether this is due to chemical reactions or a dilution effect.

The ash fusion temperature for the bottom ash was determined in an oxidizing atmosphere in a carbolite ash fusion analyser according to the international test standard (ISO 540:1995). The ash samples from each experiment were shaped into three duplicates of cube pellets with a size of 3 mm. The ash cubes were put on a tile and placed inside the furnace that was programmed to increase the temperature at a rate of 8 °C min^{-1} and up to 1500 °C. The changes of the shape of the ash cubes were recorded with a high resolution video system. The initial deformation temperature (IDT), the softening temperature (ST), the hemisphere temperature (HT), and the fluid temperature (FT) were determined after a visual observation of the recorded video. The average values of the four characteristic temperatures are shown in Figure 3.

As this method for determining the fusion characteristics for ash depends on visual observation of the ash deformation, some uncertainties can be expected due to the human error factor. With the exception of the experiment with 10% kaolin, all the different temperature characteristics seemed to increase with increasing kaolin share in the bottom ash. Increasing kaolin share also resulted in greater scatter among the different characteristics. Some irregular tendencies were also found, mostly for the initial deformation temperature and to some extent for the soften temperature. These two ash temperature characteristics were the most difficult to determine by visual observation. The results of these temperatures could vary by a 100 °C depending on the person interpreting the deformation of ash cube pellets.
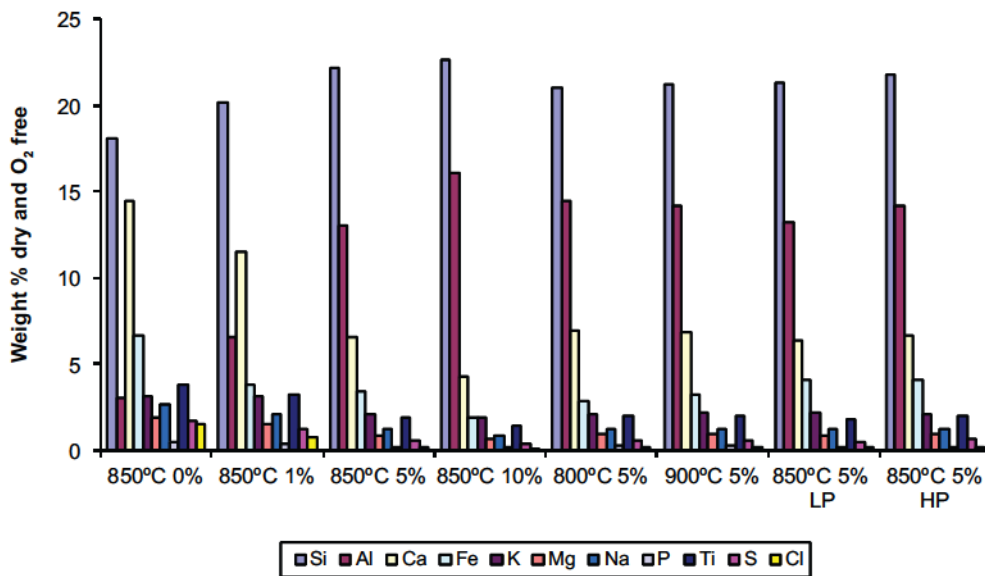

Figure 2. Major composition of bottom ash from all experiments of Si, Al, Ca, Fe, K, Mg, Na, P, Ti, S, and Cl using ICP-AES. Recalculated on dry ash. Oxygen not included in the analysis.
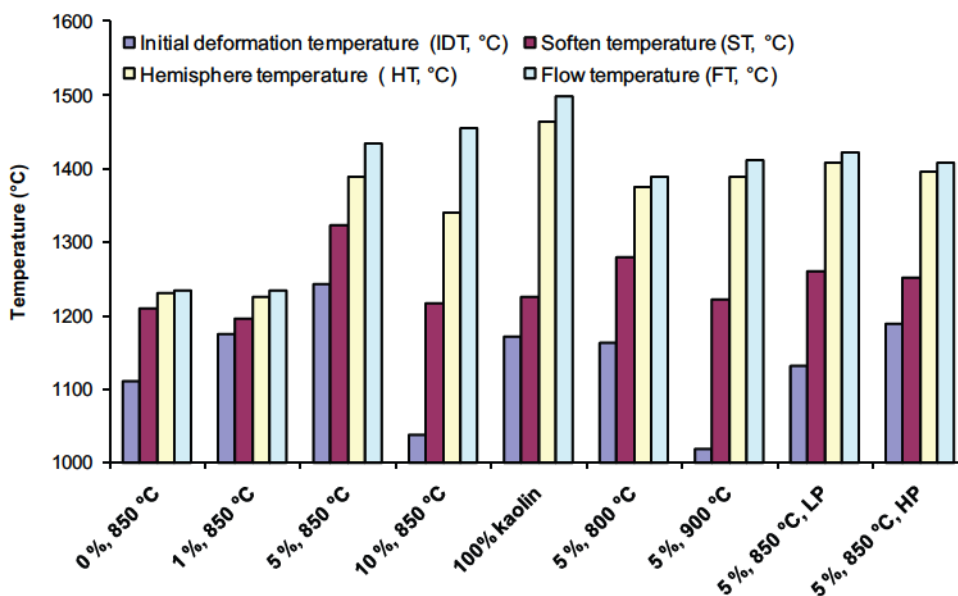

Figure 3. The bottom ash fusion temperature.

Aerosol size distribution

The particle size distribution in the flue gas was monitored with an ELPI for the aerosols in the range of 0.03–10 μm. It is acknowledged by the authors that larger particles belonging to the coarse fly ash range might exist in addition to the size range discussed in this study. It is however believed that these particles are most likely found in moderate quantities because of a low probability of entrained particles. This is due to the straight reactor geometry and the extremely low flow velocity (0.03–0.07 m/s). The results of the particle size distribution are shown in Figures 4, 5 and 6.

In general, it can be concluded that the addition of kaolin to demolition wood decreased the particle load in the flue gas (Figure 4). This holds true for all the particle size ranges with the exception of the range 0.07–0.12 μm for which the trends were more or less constant. In comparison with the work performed by Bäfver et al. (2009) on oat grain in a residential boiler with a kaolin addition of 2 and 4%, the particle size distribution range and shape was quite similar to the ones shown in this study. The only exception was a higher particle load for the smallest particles for experiments with kaolin. This difference could be attributed to totally different reactor geometry and air flow pattern between the two reactors. The influence of reactor temperature on the fly ash load in the flue gas can be observed in Figure 5. For particles smaller than 0.2 μm the particle load was highest for a reactor temperature of 850°C. For higher particle sizes, increasing temperature gave increased particle load. The same trends can also be found for the experiment with different primary air conditions (Figure 6). For particles smaller than 0.31 μm, the highest particle load was obtained for a primary air stoichiometry of 0.8 after the primary zone (the middle series). The load for larger particles increased with increased combustion air through the primary zone.

Aerosol composition

The main components in the analysed particles were K, S, Cl and Na. On average 50 wt.% of the oxygen-free samples (excluding carbon and aluminium) consisted of these elements. Zn and Pb

constituted on average 35 wt.% whereas the portion of the inert oxide forming elements Si, Ca, Fe, P, Mg and Cr was 15 wt.%. P and Mg were very low in all samples. The portion of inert metals were generally higher in the larger particle size fractions than in the smaller fractions, indicating that the compounds of these metals (oxides) originate from the original fuel ash and were not devolatilized. Lead and zinc were partly in oxide form, partly in salt form. The oxides were most probably ZnO and PbO. The salt part was constituted by sulfate and chloride of K, Na, Zn and Pb and calculated from the elemental composition according to the following assumptions: (i) potassium and sodium are as chlorides or sulfates; (ii) silicon, calcium, iron, magnesium and chromium are as oxides; (iii) zinc and lead can be both as oxides and/or chlorides and sulfates. Only the salt formation in the aerosols is shown in Figures 7, 8 and 9. For kaolin addition at 850°C (Figure 7), the salt part was richer in chloride for the reference run and at 1% kaolin addition (30–40% as chloride) than for the runs with higher kaolin addition (5–10% chloride), the rest being sulfate. There is no big differences between smaller (0.1 μm) and bigger (1.6 μm) particles. The ratio between sodium and potassium was quite constant (1:2). However, in the reference sample the portion of potassium decreased with increasing particle size and zinc
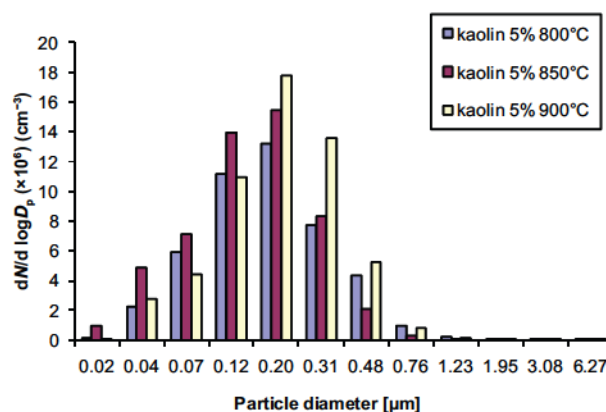

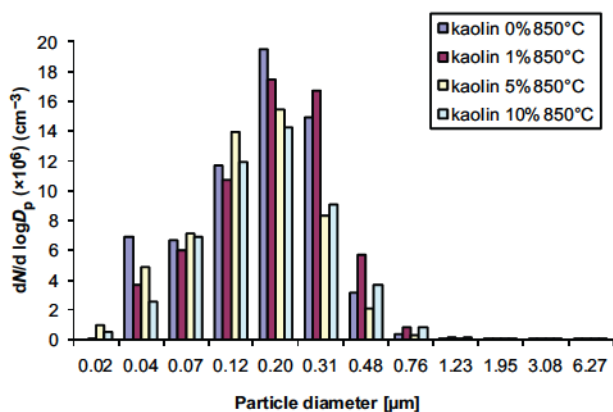**Figure 5.** The particle size distribution of the fly ash for different reactor temperatures.

Figure 4. The particle size distribution of the fly ash for increasing kaolin addition.
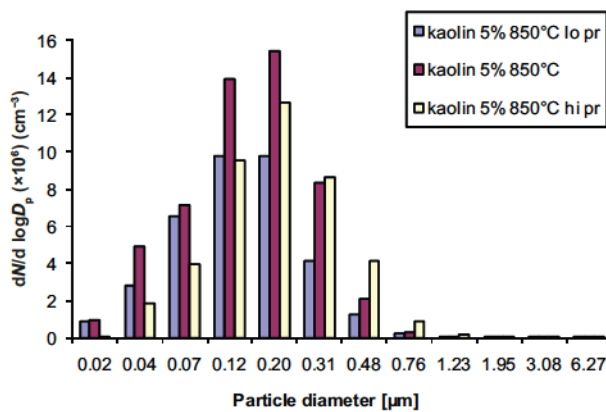

Figure 6. The particle size distribution of the fly ash for different primary air amounts.

increases. A similar trend can be observed in the samples with 5 and 10% kaolin addition. The Pb content decreased slightly with increasing particle size.

For the temperature effect at 5% kaolin addition (Figure 8), the portion of chloride was higher at 900°C (20–50%) than at 800°C and 850°C (10–20%). A slight decrease in both Zn and Pb was observed with increasing particle size. The results indicate that the smaller particles had less chloride than the larger ones.

For primary air variations (Figure 9), no clear trends can be seen in the composition of the salt part as a function of primary air level. Low and normal primary air are very similar. They have a chloride content of 5–10% and show a slight increase of zinc and decrease of lead with increasing particle size. The high primary air sample has constant chloride content (10%) for all size fractions.

The fate of chlorine

The chlorine distribution among the bottom ash phase and the gas phase relative to the chlorine input in the fuel is shown in Figure 10. This figure does not include the chlorine part found in the fly ash because not all of the impactor stages were chemically analysed. However, the chlorine part belonging to the fly ash was assumed to have a minor influence on the total mass balance due to the relatively small amounts of fly ash compared to bottom ash.
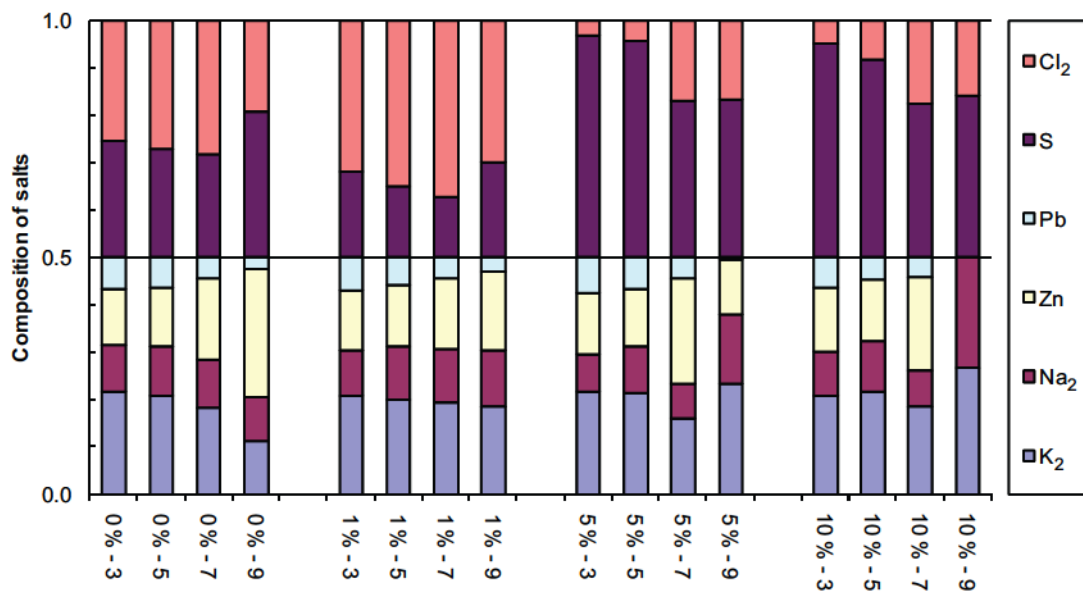

Figure 7. The chemical composition impactor stages 3, 5, 7 and 9 corresponding to the sizes 0.093; 0.26; 0.611; 1.59 μm of the fly ash taken by the ELPI in the exhaust of the reactor as a function of kaolin addition.
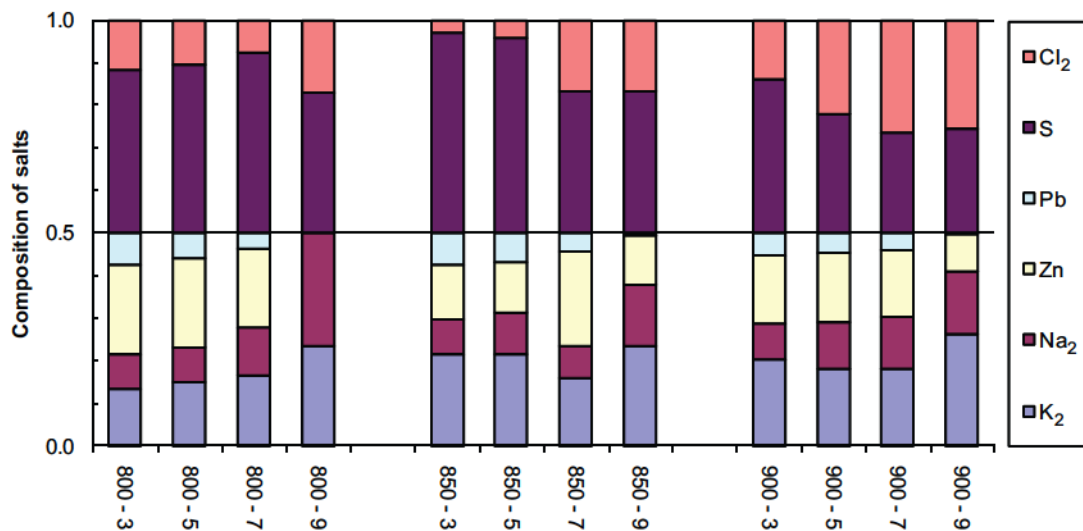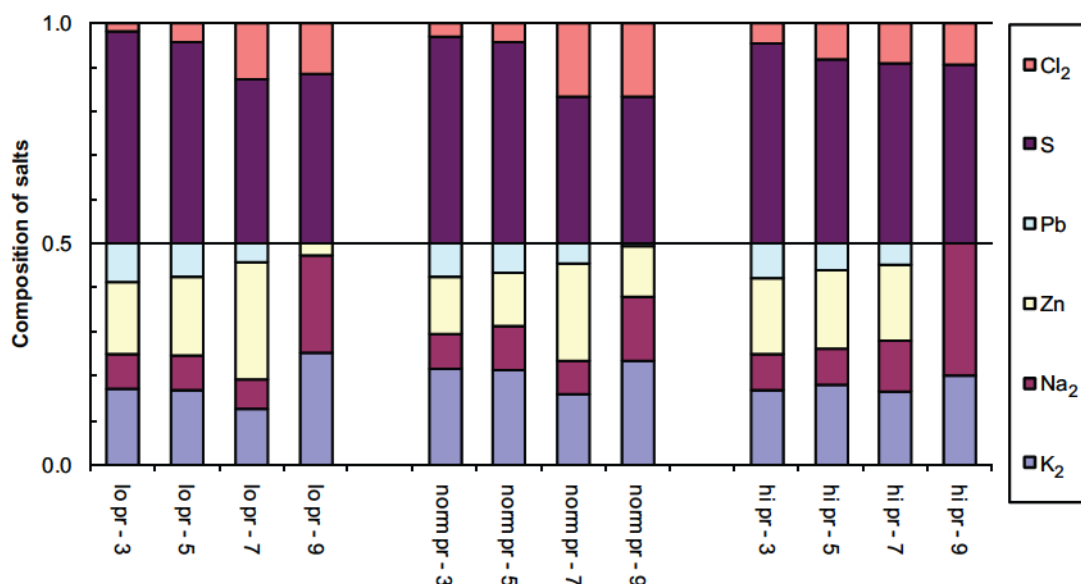

Figure 8. The chemical composition impactor stages 3, 5, 7 and 9 corresponding to the sizes 0.093; 0.26; 0.611; 1.59 μm of the fly ash taken by the ELPI in the exhaust of the reactor as a function of temperature.

Figure 9. The chemical composition impactor stages 3, 5, 7 and 9 corresponding to the sizes 0.093; 0.26; 0.611; 1.59 μm of the fly ash taken by the ELPI in the exhaust of the reactor as a function of different air distribution between primary and secondary stages.
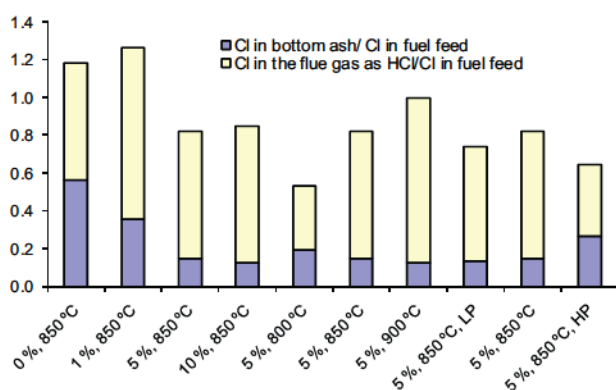
Figure 10. Distribution of chlorine between gas phase (as measured HCl) and bottom ash.

From Figure 10 it can be seen that the chlorine distribution was somewhat unbalanced due to uncertainties in the chemical analysis of the raw fuel, the bottom ash and measurements in the gas phase. Nevertheless, the figure gives important information about trends that influence the chlorine distribution as a function of increased kaolin, temperature, and combustion air distribution. The chlorine in the bottom ash decreased with increased kaolin amounts and reactor temperature. Leaner conditions in the primary zone seem also to decrease the chlorine content in the bottom ash. The kaolin seemed to be facilitating the chlorine mobility although this was not detected as increased amounts in the gas phase throughout the entire range of the kaolin addition. The trends were clearer for the different reactor temperatures in which less chlorine in the bottom ash, due to increased temperature, translated into more HCl release. As has been described earlier (Equations (1) and (2)), the effect of kaolin on abating the

chlorine release in the fly ash is done by capturing the potassium and sodium in the bottom ash. This should translate into increased potassium and sodium for increased amounts of the additive in the raw fuel. However, this is not the case as a similar mass balance to that for chlorine shows that the ratios for K and Na (bottom ash to input fuel) were close to unity for all experiments.

Conclusions

An experimental attempt was made to understand the behaviour of the corrosive chlorine compounds for variations in reactor temperature, combustion air distribution and kaolin addition. The gas phase was monitored with several gas analysers in both the primary zone and in the stack. A complete characterization of the raw fuel and the bottom ash was also performed for all the experiments. Kaolin was found to facilitate the mobility of chlorine by decreasing its concentration in the bottom ash by 37, 74 and 78%, respectively, for 1, 5, and 10% kaolin addition. The fly ash particle size distribution was also monitored and in addition a chemical analysis of the fly ash from four impactor stages was performed. Kaolin was found to be effective at reducing the chlorine concentration in the fly ash. The optimal addition was 5% and a further increase to 10% did not result in a noticeable chlorine reduction (Figure 7). The addition of 5% has almost eliminated the chlorine content for the impactor stages 3 and 5. For fuels with high chlorine content, one can conclude that an addition of 5% kaolin could lead to reduced corrosion potential due to a significant reduction of chlorine in the fly ash. The effect of reactor temperature was not clear in terms of the chlorine content in the fly ash (Figure 8). This is probably because the reactor temperature does not influence the temperature close to the combusting fuel greatly. On the other hand, leaner air conditions in

the primary stage, which should mean lower temperature in the reacting region between the solid and the gas phase, resulted in decreased chlorine content in the fly ash (Figure 9). The addition of kaolin clearly changed the composition of the bottom ash as well. The chlorine content in the bottom ash decreased as kaolin increased (Figure 10). Kaolin also influenced the melting behaviour of the bottom ash as can be seen in Figure 3 in which the fusion temperature characteristics increased with increased addition of kaolin.

Funding

References

Aho M and Silvennoinen J (2004) Preventing chlorine deposition on heat transfer surfaces with aluminium-silicon rich biomass residue and additive. *Fuel* 83: 1299–1305.

Aho M, Vainikka P, Taipale R, et al. (2008) Effective new chemicals to prevent corrosion due to chlorine in power plant superheaters. *Fuel* 87: 647–654.

Backman R, Khalil R, Todorovic D, et al. (2011) The effect of peat ash addition to demolition wood on the formation of alkali, lead and zinc compounds at staged combustion conditions. *Fuel Processing Technology* doi:10.1016/j.fuproc.2011.04.035 (in press).

Bartels M, Lin WG, Nijenhuis J, et al. (2008) Agglomeration in fluidized beds at high temperatures: mechanisms, detection and prevention. *Progress in Energy and Combustion Science* 34: 633–666.

Baxter LL, Miles TR, Jenkins BM, et al. (1998) The behavior of inorganic material in biomass-fired power boilers: field and laboratory experiences. *Fuel Processing Technology* 54: 47–78.

Broström M, Kassman H, Helgesson A, et al. (2007) Sulfation of corrosive alkali chlorides by ammonium sulfate in a biomass fired CFB boiler. *Fuel Processing Technology* 88: 1171–1177.

Bäfver LS, Rönnbäck M, Leckner B, et al. (2009) Particle emission from combustion of oat grain and its potential reduction by addition of limestone or kaolin. *Fuel Processing Technology* 90: 353–359.

Coda B, Aho M, Berger R, et al. (2001) Behavior off chlorine and enrichment of risky elements in bubbling fluidized bed combustion of biomass and waste assisted by additives. *Energy & Fuels* 15: 680–690.

Davidsson KO, Steenari BM and Eskilsson D (2007) Kaolin addition during biomass combustion in a 35 MW circulating fluidized-bed boiler. *Energy & Fuels* 21: 1959–1966.

Davidsson KO, Åmand LE, Steenari BM, et al. (2008) Countermeasures against alkali-related problems during combustion of biomass in a circulating fluidized bed boiler. *Chemical Engineering Science* 63: 5314–5329.

Henderson P, Szakálos P, Pettersson R, et al. (2006) Reducing superheater corrosion in wood-fired boilers. *Materials and Corrosion-Werkstoffe Und Korrosion* 57: 128–134.

Khan AA, de Jong W, Jansens PJ, et al. (2009) Biomass combustion in fluidized bed boilers: Potential problems and remedies. *Fuel Processing Technology* 90: 21–50.

Llorente MJF, Cuadrado RE, Laplaza JMM, et al. (2006) Combustion in bubbling fluidised bed with bed material of limestone to reduce the biomass ash agglomeration and sintering. *Fuel* 85: 2081–2092.

Pettersson A, Åmand LE and Steenari BM (2009) Chemical fractionation for the characterisation of fly ashes from co-combustion of biofuels using different methods for alkali reduction. *Fuel* 88: 1758–1772.

Skrifvars BJ, Laurén T, Hupa M, et al. (2004) Ash behaviour in a pulverized wood fired boiler – a case study. *Fuel* 83: 1371–1379.

Tobiasen L, Skytte R, Pedersen LS, et al. (2007) Deposit characteristic after injection of additives to a Danish straw-fired suspension boiler. *Fuel Processing Technology* 88: 1108–1117.

Tran KQ, Iisa K, Hagström M, et al. (2004) On the application of surface ionization detector for the study of alkali capture by kaolin in a fixed bed reactor. *Fuel* 83: 807–812.

Tran KQ, Iisa K, Steenari BM, et al. (2005) A kinetic study of gaseous alkali capture by kaolin in the fixed bed reactor equipped with an alkali detector. *Fuel* 84: 169–175.

Vamvuka D, Pitharoulis M, Alevizos G, et al. (2009) Ash effects during combustion of lignite/biomass blends in fluidized bed. *Renewable Energy* 34: 2662–2671.

Vamvuka D, Zografos D and Alevizos G (2008) Control methods for mitigating biomass ash-related problems in fluidized beds. *Bioresource Technology* 99: 3534–3544.

Werther J, Sänger M, Hartge EU, et al. (2000) Combustion of agricultural residues, *Progress in Energy and Combustion Science* 26; 1–27.

Yin C, Rosendahl LA and Kær SK (2008) Grate-firing of biomass for heat and power production. *Progress in Energy and Combustion Science* 34: 725–754.

BIOGRAPHY

Name and Surname:	Dušan Todorović
Date of Birth:	06.06.1983.
Place of Birth:	Kraljevo, Republic of Serbia

EDUCATINAL:

1990-1998	Primary school "Živan Maričić" in Žiča, Kraljevo
1998-2002	Gymnasium, Kraljevo
2002-2007	Faculty of Mechanical Engineering Kraljevo University of Kragujevac, Department for Heat Technique and Environmental Protection. Awarded for extraordinary success achieved during the study (grade point average: 9.37 out of 10.00).

EMPLOYMENT RECORD:

2008-2013	University of Belgrade Faculty of Mechanical Engineering, Department of Process Engineering, **Associate**
2013-2015	University of Belgrade Faculty of Mechanical Engineering, Department of Process Engineering, **Research Associate**
2015-	University of Belgrade Faculty of Mechanical Engineering, Department of Process Engineering, **Teaching Assistant**

Прилог 1.

Изјава о ауторству

Потписани: Душан М. Тодоровић

број индекса: D2/07

Изјављујем

да је докторска дисертација под насловом

EFFECT OF BIOMASS CHARACTERISTICS AND COMBUSTION PROCESS ON
FLUE GASEOUS COMPOSITION AND ASH RELATED PROPERTIES
(УТИЦАЈ ОДАБРАНИХ ВРСТА БИОМАСЕ И ПРОЦЕСА САГОРЕВАЊА НА
САСТАВ И КАРАКТЕРИСТИКЕ ГАСОВИТИХ И ЧВРСТИХ ПРОДУКАТА)

- резултат сопственог истраживачког рада,
- да предложена дисертација у целини ни у деловима није била предложена за добијање било које дипломе према студијским програмима других високошколских установа,
- да су резултати коректно наведени и
- да нисам кршио ауторска права и користио интелектуалну својину других лица.

Потпис докторанда

У Београду, 12.06.2015.

Прилог 2.

Изјава о истоветности штампане и електронске верзије докторског рада

Име и презиме аутора: Душан М. Тодоровић

Број индекса: D2/07

Студијски програм: Докторске академске студије-Машинско инжењерство

Наслов рада: EFFECT OF BIOMASS CHARACTERISTICS AND COMBUSTION PROCESS ON FLUE GASEOUS COMPOSITION AND ASH RELATED PROPERTIES
(УТИЦАЈ ОДАБРАНИХ ВРСТА БИОМАСЕ И ПРОЦЕСА САГОРЕВАЊА НА САСТАВ И КАРАКТЕРИСТИКЕ ГАСОВИТИХ И ЧВРСТИХ ПРОДУКАТА)

Ментор проф. др Александар Јововић, дипл. инж. маш.

Потписани Душан М. Тодоровић

Изјављујем да је штампана верзија мог докторског рада истоветна електронској верзији коју сам предао/ла за објављивање на порталу **Дигиталног репозиторијума Универзитета у Београду.**

Дозвољавам да се објаве моји лични подаци везани за добијање академског звања доктора наука, као што су име и презиме, година и место рођења и датум одбране рада.

Ови лични подаци могу се објавити на мрежним страницама дигиталне библиотеке, у електронском каталогу и у публикацијама Универзитета у Београду.

Потпис докторанда

У Београду, 12.06.2015.

Прилог 3.

Изјава о коришћењу

Овлашћујем Универзитетску библиотеку „Светозар Марковић" да у Дигитални репозиторијум Универзитета у Београду унесе моју докторску дисертацију под насловом:

EFFECT OF BIOMASS CHARACTERISTICS AND COMBUSTION PROCESS ON FLUE GASEOUS COMPOSITION AND ASH RELATED PROPERTIES (УТИЦАЈ ОДАБРАНИХ ВРСТА БИОМАСЕ И ПРОЦЕСА САГОРЕВАЊА НА САСТАВ И КАРАКТЕРИСТИКЕ ГАСОВИТИХ И ЧВРСТИХ ПРОДУКАТА)

која је моје ауторско дело.

Дисертацију са свим прилозима предао/ла сам у електронском формату погодном за трајно архивирање.

Моју докторску дисертацију похрањену у Дигитални репозиторијум Универзитета у Београду могу да користе сви који поштују одредбе садржане у одабраном типу лиценце Креативне заједнице (Creative Commons) за коју сам се одлучио/ла.

1. Ауторство

2. Ауторство - некомерцијално

③ Ауторство – некомерцијално – без прераде

4. Ауторство – некомерцијално – делити под истим условима

5. Ауторство – без прераде

6. Ауторство – делити под истим условима

(Молимо да заокружите само једну од шест понуђених лиценци, кратак опис лиценци дат је на полеђини листа).

Потпис докторанда

У Београду, 12.06.2015.